

Environmental Fate and Transport of a New Energetic Material, CL-20 SERDP Project ER 1256

Performing Organization

Biotechnology Research Institute, National Research Council of Canada,
6100 Royalmount Ave., Montreal (Quebec) H4P 2R2, Canada.

Prepared by

Jalal Hawari, Ph D Chemistry
Principal Investigator

Final Technical Report, March 2006

REPORT DOCUMENTATION PAGE				<i>Form Approved OMB No. 0704-0188</i>	
<small>The public reporting burden for this collection of information is estimated to average 1 hour per response, including the time for reviewing instructions, searching existing data sources, gathering and maintaining the data needed, and completing and reviewing the collection of information. Send comments regarding this burden estimate or any other aspect of this collection of information, including suggestions for reducing the burden, to the Department of Defense, Executive Services and Communications Directorate (0704-0188). Respondents should be aware that notwithstanding any other provision of law, no person shall be subject to any penalty for failing to comply with a collection of information if it does not display a currently valid OMB control number.</small>					
PLEASE DO NOT RETURN YOUR FORM TO THE ABOVE ORGANIZATION.					
1. REPORT DATE (DD-MM-YYYY)		2. REPORT TYPE		3. DATES COVERED (From - To)	
4. TITLE AND SUBTITLE				5a. CONTRACT NUMBER	
				5b. GRANT NUMBER	
				5c. PROGRAM ELEMENT NUMBER	
6. AUTHOR(S)				5d. PROJECT NUMBER	
				5e. TASK NUMBER	
				5f. WORK UNIT NUMBER	
7. PERFORMING ORGANIZATION NAME(S) AND ADDRESS(ES)				8. PERFORMING ORGANIZATION REPORT NUMBER	
9. SPONSORING/MONITORING AGENCY NAME(S) AND ADDRESS(ES)				10. SPONSOR/MONITOR'S ACRONYM(S)	
				11. SPONSOR/MONITOR'S REPORT NUMBER(S)	
12. DISTRIBUTION/AVAILABILITY STATEMENT					
13. SUPPLEMENTARY NOTES					
14. ABSTRACT					
15. SUBJECT TERMS					
16. SECURITY CLASSIFICATION OF:			17. LIMITATION OF ABSTRACT	18. NUMBER OF PAGES	19a. NAME OF RESPONSIBLE PERSON
a. REPORT	b. ABSTRACT	c. THIS PAGE			19b. TELEPHONE NUMBER (Include area code)

This report was prepared under contract to the Department of Defense Strategic Environmental Research and Development Program (SERDP). The publication of this report does not indicate endorsement by the Department of Defense, nor should the contents be construed as reflecting the official policy or position of the Department of Defense. Reference herein to any specific commercial product, process, or service by trade name, trademark, manufacturer, or otherwise, does not necessarily constitute or imply its endorsement, recommendation, or favoring by the Department of Defense.

Project Participants

Jalal Hawari,	Ph.D. Chemistry, <i>PI</i>
Vimal Balakrishnan,	Ph.D. Chemistry
Ghalib Bardai,	M.Sc. Biochemistry
Bharat Bhushan,	Ph.D. Microbiology
Sabine Dodard,	M.Sc. Biochemistry
Diane Fournier,	Ph.D. Microbiology
Carl Groom,	M.Sc. Biochemistry
Annamaria Halasz,	M.Sc. Chemistry
Fanny Monteil-Rivera,	Ph.D. Chemistry
Pierre Yves Robidoux,	Ph.D. Ecotoxicology
Sylvie Rocheleau,	M.Sc.A. Environmental Engineering
Manon Sarrazin,	B.Sc. Chemistry
Kathleen Savard,	B.Sc. Biology
Geoffrey Sunahara,	Ph.D. Toxicology

Table of content

I	Project Background	1
II	Global Objectives	4
III	Summary of Accomplishments	4
IV	Analytical methods for the determination of CL-20 in water and soil	7
	<i>Introduction</i>	7
	<i>Material and Methods</i>	7
	<i>Accomplishments</i>	8
V	QC/QA Interlaboratory study	11
VI	Physico-chemical measurements of CL-20	13
	<i>Introduction</i>	13
	<i>Material and Methods</i>	13
	<i>Accomplishments</i>	14
VII	Hydrolysis of CL-20 in aqueous solution	17
	<i>Introduction</i>	17
	<i>Material and Methods</i>	17
	<i>Accomplishments</i>	18
VIII	Photodegradation of CL-20 in aqueous solutions	20
	<i>Introduction</i>	20
	<i>Material and Methods</i>	20
	<i>Accomplishments</i>	21
	<i>Conclusion</i>	31
IX	Degradation of CL-20 by iron (0)	32
	<i>Introduction</i>	32
	<i>Material and Methods</i>	32
	<i>Accomplishments</i>	35
	<i>Conclusion</i>	41
X	Sorption-desorption of CL-20 on soil	42
	<i>Introduction</i>	42
	<i>Material and Methods</i>	42
	<i>Accomplishments</i>	45
	<i>Conclusion and Perspectives</i>	54
XI	Microbial and enzymatic degradation of CL-20	56
XII	Aerobic degradation of CL-20	58
XII.1	Biotransformation of CL-20 by <i>P. chrysosporium</i>	58

<i>Introduction</i>	58
<i>Material and Methods</i>	58
<i>Accomplishments</i>	60
<i>Conclusion</i>	64
XII.2 Biotransformation of CL-20 with the soil isolate <i>Pseudomonas</i> sp FA1	65
<i>Material and Methods</i>	65
<i>Accomplishments</i>	67
<i>Conclusion</i>	75
XIII Anaerobic degradation of CL-20.....	76
XIII.1 Biotransformation of CL-20 with <i>Clostridium</i> sp. strain EDB2.....	76
<i>Introduction</i>	76
<i>Materials and Methods</i>	77
<i>Accomplishments</i>	79
<i>Conclusion</i>	82
XIV Enzymatic degradation of CL-20: determination of reaction pathways	84
XIV.1 Biotransformation of CL-20 by salicylate 1-monooxygenase.....	84
<i>Introduction</i>	84
<i>Material and Methods</i>	84
<i>Accomplishments</i>	86
<i>Conclusion</i>	95
XIV.2 Nitroreductase catalyzed biotransformation of CL-20.....	97
<i>Introduction</i>	97
<i>Material and Methods</i>	97
<i>Accomplishments</i>	98
<i>Conclusion</i>	103
XIV.3 Stereo-specificity for pro-(<i>R</i>) hydrogen of NAD(P)H during enzyme-catalyzed hydride transfer to CL-20.....	104
<i>Introduction</i>	104
<i>Materials and Methods</i>	104
<i>Accomplishments</i>	106
XV Aquatic toxicity studies	110
XVI Terrestrial toxicity studies	111
XVI.1 Higher plant toxicity tests	111
XVI.2 Earthworm survival and reproduction tests	111
XVI.3 Enchytraeid survival and reproduction tests	112

<i>Introduction</i>	112
<i>Material and Methods</i>	112
<i>Accomplishments</i>	115
<i>Conclusion</i>	122
XVII Avian reproduction toxicity tests	123
<i>Introduction</i>	123
<i>Material and Methods</i>	123
<i>Accomplishments</i>	127
<i>Discussion</i>	134
XVIII Bioaccumulation of CL-20 in plants and earthworms.....	136
XVIII.1 Optimization of bioaccumulation test using ryegrass	136
XVIII.2 Optimization of bioaccumulation test using earthworm <i>Eisenia andrei</i>	136
XIX CL-20 metabolic products in plants, earthworms and quail.....	137
XIX.1 Toxicity of CL-20 metabolic products on earthworms	137
XIX.2 Biotransformation of CL-20 in quail liver	138
<i>Abstract</i>	138
<i>Introduction</i>	139
<i>Materials and Methods</i>	139
<i>Accomplishments</i>	142
XIX.3 Toxicity and bioaccumulation of CL-20 in ryegrass <i>Lolium perene</i> as compared to RDX and HMX.....	153
<i>Abstract</i>	153
<i>Introduction</i>	154
<i>Materials and Methods</i>	155
<i>Accomplishments</i>	157
XX Action item.....	164
XXI Acknowledgements	164
XXII References	165
XXIII Appendix: Output.....	179
XXIV Appendix: Publications.....	186

List of Figures

Figure 1 Structures of cyclic nitramine explosives RDX, HMX and CL-20. The three heterocyclic nitramines contain characteristic N-NO ₂ functional groups that may determine their physicochemical, microbial and toxic properties.	2
Figure 2 A typical HPLC chromatogram showing separation of CL-20 from RDX and HMX (column: LC-CN; mobile phase: 30 % water-70% methanol; Flow rate: 1 mL/min; Detector: PDA (λ = 230 nm)).	9
Figure 3 Effect of acidification and temperature on the stability of CL-20 in water/acetonitrile media.	9
Figure 4 Solubility of CL-20 in water as a function of temperature.	14
Figure 5 Compared solubilities of RDX, HMX and CL-20 in water.	15
Figure 6 Solubility of CL-20 in water in presence of cyclodextrines.	16
Figure 7 Time course for the alkaline hydrolysis (pH 10) of CL-20 at 30°C and formation of nitrite (NO ₂ ⁻), nitrous oxide (N ₂ O), ammoniac (NH ₃) and formate (HCOO ⁻). Note that NO ₂ ⁻ is present at t = 0.	19
Figure 8 A time course study for the photolysis of CL-20 (1.20 μ mole) at 300 nm and 25 °C in CH ₃ CN/water solutions (50 % v/v) showing formation of nitrite (NO ₂ ⁻), nitrate (NO ₃ ⁻), ammonium (NH ₄ ⁺) and formic acid (HCOOH).	22
Figure 9 LC/UV (230 nm) (A) and LC/MS (ES-) extracted ion chromatograms of CL-20 and its products after 30 s of photolysis at 254 nm. Extracted mass ion adducts [M + NO ₃ ⁻] were 500 Da (B, I), 484 Da (C, II) and deprotonated mass ion [M – H] were 408 Da (D, III and IV) and 345 Da (E, V and VI).	23
Figure 10 LC/MS (ES-) spectra of CL-20 (I) and its initial intermediates (II to VI) observed during photolysis at 254 nm in MeCN/H ₂ O (50 % v/v), (a) from non-labeled and (b) from uniformly ring labeled ¹⁵ N-[CL-20].	24
Figure 11 Postulated photorearrangement route of CL-20 at 300 nm in CH ₃ CN/water (50 % v/v). Bracketed compounds were not observed.	26
Figure 12 Postulated photodenitration route of CL-20 at 300 nm in an aqueous acetonitrile solution. Bracketed compounds were not observed.	27
Figure 13 Postulated secondary decomposition routes following initial denitration of CL-20. Bracketed compounds were not observed.	28
Figure 14 Photolysis of aqueous solutions of CL-20 with sunlight. Error bars represent standard	

deviation of duplicate experiment. Average temperature and average UV index are also reported for each day of exposure to interpret the variation of rates in the degradation.....	30
Figure 15 Time course of the Fe ⁰ -mediated anaerobic degradation of CL-20 in water. (A) Carbon-containing compounds. (B) Nitrogen-containing compounds. Data points are the mean and error bars the average deviation (<i>n</i> = 2).....	35
Figure 16 LC/UV chromatograms at 250 nm showing the detection of glyoxal. (A) CL-20/Fe ⁰ reaction solution after derivatization. (B) Glyoxal standard solution after derivatization with pentafluorobenzylhydroxylamine. (C) MS (ES+) obtained for both the standard and the sample.	36
Figure 17 Typical LC/MS chromatograms of intermediates Ia and II formed upon the double denitration of CL-20 in the Fe ⁰ -mediated reaction. (A) Extracted Ion Chromatogram (EIC) of <i>m/z</i> = 345 Da (Ia and Ib) and 381 Da (II). (B) Mass spectra and structures of Ia and II. .	39
Figure 18 Typical LC/MS chromatograms of early intermediates III and IV in the Fe ⁰ -mediated decomposition of CL-20. (A) Extracted Ion Chromatogram (EIC) of <i>m/z</i> = 484 Da (III) and 468 Da (IV). (B) Mass spectra and structures of III and IV.....	40
Figure 19 Typical LC/MS chromatograms of intermediates V and VI in the Fe ⁰ -mediated decomposition of CL-20. (A) Extracted Ion Chromatogram (EIC) of <i>m/z</i> = 455 Da (V) and 376 Da (VI). (B) Mass spectra and structures of V and VI.....	41
Figure 20 Sorption and desorption kinetics for CL-20 with VT and GS soils (Error bars represent the standard deviation of 3 replicates).	46
Figure 21 Sorption-desorption isotherms for CL-20 in non-sterile SSL, VT, FSB, GS and FS soils at ambient temperature (sorption: filled symbols, solid lines; desorption: hollow symbols, dashed lines; for clarity, data obtained with soils having a high affinity for CL-20 are presented separately from data obtained with soils having a low affinity for CL-20). ...	47
Figure 22 Percent recovery of CL-20 upon agitation at different pHs and ambient temperature, in presence or not of non-sterile VT soil.....	52
Figure 23 Stability of CL-20 in sterile soils having various pHs (CSS and SAC = pH 8.1; VT = pH 5.6) (Error bars represent the standard deviation of 3 replicates).	53
Figure 24 Time-course study of abiotic transformation of CL-20 in sterilized SAC soil (pH 8.1). Bars indicate standard deviation (<i>n</i> = 2).	54
Figure 25 Degradation of CL-20 (3.6 mg L ⁻¹) in a N-limited medium with (Δ) and without (□) the addition of <i>P. chrysosporium</i> spores. Bars indicate standard deviation (<i>n</i> = 3).....	60
Figure 26 Time-course study of bio-transformation of CL-20 by MnP purified from <i>Nemalotoma frowardii</i>	61

- Figure 27 Mineralization of [^{14}C]-glyoxal added to a spore suspension of *P. chrysosporium* prepared in N-limited medium. Bars indicate standard deviation from triplicate experiments. 62
- Figure 28 Liberation of $^{14}\text{CO}_2$ from [^{14}C]-CL-20 added to a spore suspension of *P. chrysosporium* (non-ligninolytic) (Δ), and [^{14}C]-CL-20 added to 7-day old ligninolytic fungal culture (\square). Experiments were performed in N-limited medium. Bars indicate standard deviation from triplicate experiments..... 63
- Figure 29 Degradation of CL-20 pre-sorbed on VT soil (1.33 g) by *P. chrysosporium* in N-limited medium (10 mL). Glucose was supplemented on day 21 (Δ). Bars indicate standard deviation ($n = 3$)..... 64
- Figure 30 Growth of *Pseudomonas* sp. FA1 at various concentrations of CL-20 (\circ) and $(\text{NH}_4)_2\text{SO}_4$ (\bullet). The viable-cell count in early-stationary-phase-culture (16 h) was determined for each nitrogen concentration. Linear regression curve for $(\text{NH}_4)_2\text{SO}_4$ has a gradient of 0.122 and an r^2 of 0.990. Linear regression curve for CL-20 has a gradient of 0.224 and an r^2 of 0.992. Data are means of results from duplicate experiments, and error bars indicate standard error. Some error bars are not visible due to their small size..... 68
- Figure 31 Effect of alternate cycle of aerobic and anaerobic growth conditions on biotransformation of CL-20 by *Pseudomonas* sp. FA1. Symbols: growth (\blacktriangle) and CL-20 degradation (\bullet) under aerobic conditions. Open triangles and circles show the levels of growth and CL-20 biotransformation, respectively, under aerobic conditions (for the first 9 h) and then under anaerobic conditions. Data are mean of results from triplicate experiments, and error bars indicate standard error. Some error bars are not visible due to their small size. 69
- Figure 32 Time-course study of NADH-dependent biotransformation of CL-20 by a membrane-associated enzyme(s) from *Pseudomonas* sp. FA1 under anaerobic conditions. Symbols indicate the levels of CL-20 (\bullet), NADH (\blacksquare), nitrite (\circ), nitrous oxide (\blacktriangledown). Data are means of results from triplicate experiments, and error bars indicate standard errors. Some error bars are not visible due to their small size..... 72
- Figure 33 Time-course study of NADH-dependent reduction of nitrite to nitrous oxide by a membrane-associated enzyme(s) from *Pseudomonas* sp. FA1 under anaerobic conditions. Symbols indicate the levels of nitrite (\bullet), nitrous oxide (\circ), NADH (\blacktriangle). Data are means of results from triplicate experiments, and error bars indicate standard errors. Some error bars are not visible due to their small size..... 72
- Figure 34 Schematic representation of the technique used to isolate chemotactic bacteria. A 5- μL micro-capillary containing an explosive solution and sealed at outer end is inserted into an air-tight 10-mL glass vial containing 5 mL of enriched culture under anaerobic conditions. 78
- Figure 35 Transmission electron micrograph of negatively stained cell of strain EDB2. Bar

indicates 1 μ m.	80
Figure 36 Qualitative chemotaxis assay with strain EDB2 by agarose-plug method. Bright ring of bacterial cells around the plug indicated chemotaxis.	81
Figure 37 Biotransformation of RDX (●), HMX (○) and CL-20 (▼) by strain EDB2 as a function of its growth (■). Data are mean \pm SD ($n = 3$). Some error bars are not visible due to their small size.	82
Figure 38 Progress curve demonstrating CL-20 biotransformation as a function of salicylate 1-monooxygenase concentration. The linear-regression curve has a gradient of 15.42 and a r^2 of 0.99. Data are means of results from the triplicate experiments, and error bars indicate standard errors. Some error bars are not visible due to their small size.	86
Figure 39 Time-course study of NADH-dependent biotransformation of CL-20 by salicylate 1-monooxygenase (1 mg) under anaerobic conditions. Residual CL-20 (●), NADH (○), nitrite (▼), and nitrous oxide (▽). Data are means of results from triplicate experiments, and error bars indicate standard errors. Some error bars are not visible due to their small size.	88
Figure 40 A, Concentration-dependent inhibition of salicylate 1-monooxygenase catalyzed biotransformation of CL-20 by diphenyliodonium. B, Biotransformation of CL-20 by the native- (1), deflavo- (2) and reconstituted- salicylate 1-monooxygenase (3). One hundred percent CL-20 biotransformation activity was equivalent to 15.36 ± 0.66 nmol h ⁻¹ mg of protein ⁻¹ . Data are mean percentages of CL-20 biotransformation activity \pm standard errors ($n = 3$).	90
Figure 41 (A) LC/MS (ES-) extracted ion-chromatogram of CL-20 ($m/z = 500$ Da) and its metabolite (Ia) ($m/z = 345$ Da) produced by the reaction of CL-20 with salicylate 1-monooxygenase; (B-E): LC/MS (ES-) spectra of non-labeled CL-20 (B), and its metabolite Ia (C), amino-labeled [¹⁵ N]-CL-20 (D), and its metabolite Ia (E).	92
Figure 42 Proposed pathway of initial biotransformation of CL-20 catalyzed by salicylate 1-monooxygenase followed by secondary decomposition. Nitrogen atoms shown in bold were amino-nitrogens and were uniformly labeled in [¹⁵ N]-CL-20. Secondary decomposition of intermediate Ia is shown, whereas Ib might also decompose like Ia. Intermediate shown between brackets was not detected.	93
Figure 43 (A) Time course of formation and disappearance of key metabolites Ia and Ib during biotransformation of CL-20 by nitroreductase. Chromatograms corresponding to numbers 1-3 indicate increasing formation of metabolite Ia at times 5, 15 and 30 min, respectively, whereas chromatograms 4-6 indicate disappearance of Ia at times 60, 90 and 150 min, respectively. Proposed molecular structures of Ia and Ib are shown in Figure 42; (B) Formation and disappearance of Ia in terms of HPLC-UV-area as a function of time.	100
Figure 44 Time-course study of NADH-dependent biotransformation of CL-20 by nitroreductase under anaerobic conditions. CL-20 (●), nitrite (○), nitrous oxide (▼) and formate (■). Data are mean \pm SE ($n = 2$). Some error bars are not visible due to their small size.	101

Figure 45 HPLC-UV chromatogram of CL-20 (I) and N-denitrohydrogenated product (II) obtained during CL-20 reaction with diaphorase from <i>Clostridium kluyveri</i> at pH 7.0 and 30°C.....	108
Figure 46 Proposed hydride transfer reaction of CL-20, and possible hydrogen-deuterium exchange between ND-group of product II and water.	108
Figure 47 Standard Lineweaver-Burk plots of CL-20 concentration <i>versus</i> its enzymatic biotransformation rate; A, plots using dehydrogenase enzyme from <i>Clostridium</i> sp. EDB2 in the presence of either NADH (○), (S)NADD (▼), or (R)NADD (●); B, plots using diaphorase enzyme from <i>Clostridium kluyveri</i> in the presence of either NADPH (○), (S)NADPD (▼) or (R)NADPD (●). Data are mean of the triplicate experiments, and the standard deviations were within 8 % of the mean values.	109
Figure 48 Adult survival and juvenile production by <i>Enchytraeus crypticus</i> exposed to CL-20 in freshly amended SSL soil.....	116
Figure 49 Adult survival and juvenile production by <i>Enchytraeus crypticus</i> exposed to CL-20 in freshly amended RacAg2002 soil.	116
Figure 50 Adult survival and juvenile production by <i>Enchytraeus crypticus</i> exposed to CL-20 in freshly amended Rac50-50 soil.....	117
Figure 51 Effects of CL-20 (nominal concentrations) or RDX on juvenile production by <i>Enchytraeus albidus</i> in freshly amended Rac50-50 soil.	119
Figure 52 Schedule for the two CL-20 exposure studies: subacute study (A) and subchronic study (B).....	124
Figure 53 Changes in body weight of juvenile Japanese quail gavaged with CL-20 for 5 days (subacute study). Exposure schedule is shown in Figure 52. Each value is the mean \pm SD (standard deviation)(n = 44 birds). * Above bars denotes value is statistically different from the control ($p \leq 0.05$).	128
Figure 54 Somatic index of selected organs of juvenile Japanese quail gavaged with CL-20 for 5 days followed by 10 days of vehicle only (no CL-20). Data are expressed as mean \pm SD (n = 44 birds). Study design is shown in Fig. 52. * Above bars denotes value is statistically different from the control ($p \leq 0.05$).....	129
Figure 55 Effects of 42 days dietary exposure of CL-20 on Japanese quail embryo weights. Data are mean embryo weight \pm SD. (n = number of embryos evaluated). * Above bars denotes values statistically different from the control ($p \leq 0.05$)......	132
Figure 56 Effects of 42 d dietary exposure of CL-20 on the mean number of eggs produced per hen. These exposure effects were not significant compared to controls ($p > 0.05$)......	132
Figure 57 Recovery of CL-20 using spiked tissue samples (Δ , Brain; \diamond , Spleen; \blacksquare , Heart) and	

the modified USEPA Method 8330A (USEPA, 1997). Inset shows CL-20 recovery at spiked concentrations less than 0.8 µg CL-20/g tissue dry weights. R ² value was determined by linear regression using least-squares method.....	133
Figure 58 Recovery of CL-20 from spiked liver tissue using modified USEPA Method 8330A (USEPA, 1998).	133
Figure 59 Concentration of CL-20 in soil exposed and not exposed to <i>Eisenia andrei</i> (ongoing experiment).	136
Figure 60 Silver stain of SDS-PAGE purification of quail and rabbit hepatic cytosolic CL-20 degrading enzyme. Lane 1, molecular weight markers from top to bottom (97 kDa Phosphorylase b, 66 kDa Serum albumin, 45 kDa Ovalbumin, 31 kDa anhydrase, 21.5 kDa Trypsin, 14.4 kDa Lysozyme); Lane 2, total rabbit proteins eluted from the Glutathione affinity column; Lane 3, total quail proteins (QL1 and QL2) eluted from the Glutathione affinity column.	145
Figure 61 Time course study of enzyme dependent biotransformation of CL-20 under aerobic conditions. Symbols indicate concentration of CL-20 remaining (-●-), nitrite (-▲-), or GSH (-■-). Incubation conditions: 37°C, 2 h under aerobic conditions. Data are the means of triplicates, and error bars represent SE.	147
Figure 62 Time course study of enzyme dependent biotransformation of CL-20 under aerobic conditions. Symbols indicate concentration of CL-20 remaining (-●-), nitrite (-▲-), or GSH (-■-). Incubation conditions: 37°C, 2 h under aerobic conditions. Data are the means of triplicates, and error bars represent SE.	148
Figure 63 Extracted ion chromatogram of CL-20 and its intermediates M and M' (A) obtained by LC-MS of a mixture of CL-20 incubated for 20 minutes with GSH and cytosolic enzymes of quail. The UV spectrum of M (inset B) and M' (inset C) are indicated. The mass spectrum of M' obtained for intermediate of non labeled CL-20 (D), intermediate of ¹⁵ N ring labeled CL-20 (E) and intermediate of ¹⁵ NO ₂ labeled CL-20 (F).....	149
Figure 64 Proposed biotransformation pathway of CL-20 with GSH.	152
Figure 65 Effects of CL-20 in SSL soil (A), CL-20 in DRDC soil (B), and RDX or HMX in SSL soil (C) on ryegrass <i>Lolium perenne</i> shoot growth compared to carrier (acetone) control. Significant ($p \leq 0.05$, Fisher's LSD) change from carrier control is indicated by [*]. Negative values indicate reduction in shoot growth.	158
Figure 66 Effects of CL-20 in SSL soil (A) and in DRDC soil (B) on ryegrass <i>Lolium perenne</i> root growth compared to carrier (acetone) control. Significant ($p \leq 0.05$, Fisher's LSD) change from carrier control is indicated by [*]. Negative values indicate reduction in shoot growth.	159
Figure 67 Bioaccumulation of CL-20 in ryegrass <i>Lolium perenne</i> shoots exposed to SSL (A) and RDDC (B) amended soils.	160

Figure 68 Bioaccumulation of CL-20 in ryegrass <i>Lolium perenne</i> roots exposed to SSL (A) and RDDC (B) amended soils.	161
--	-----

List of Tables

Table 1 Single laboratory study: recovery data for soil samples spiked with different concentrations of CL-20 at BRI.	10
Table 2 Recovery data for SSL soil samples spiked with CL-20: Interlaboratory study.	12
Table 3 Aqueous solubilities (S) of RDX, HMX and CL-20 as a function of temperature and log K_{ow} values measured at ambient temperature.	16
Table 4 Normalized molar yields for the products obtained upon alkaline hydrolysis (pH 10) of CL-20. ^a	18
Table 5 Characterization of soils ^a used in this study.	43
Table 6 Isotherm parameters, K_{oc} , and recoveries for CL-20 sorption and desorption by various soils.	48
Table 7 Sorption and stability of CL-20 with minerals.....	50
Table 8 Isotherm parameters and K_{oc} for CL-20 sorption and desorption by various soils.	51
Table 9 K_{oc} extracted from sorption isotherms with different fractions of soil organic matter ...	52
Table 10 Effect of flavin contents in native- and deflavo-enzyme preparations on the CL-20 biotransformation activities of various enzyme fractions from <i>Pseudomonas</i> sp. FA1 under anaerobic conditions ^a	71
Table 11 Stoichiometry of reactants and products during biotransformation of CL-20 ^a	73
Table 12 Effects of enzyme inhibitors on the CL-20 biotransformation activity of membrane-associated enzyme(s) ^a	74
Table 13 Quantitative chemotaxis assay with strain EDB2 by micro-capillary method.....	81
Table 14 Comparative stoichiometries of reactants and products during biotransformation of CL-20 by the salicylate 1-monooxygenase from <i>Pseudomonas</i> sp. ATCC 29352 and the membrane-associated enzyme(s) from <i>Pseudomonas</i> sp. FA1.....	89
Table 15 Properties of metabolites detected and identified by LC/MS (ES-) during biotransformation of CL-20 catalyzed by salicylate 1-monooxygenase from <i>Pseudomonas</i> sp. ATCC 29352.	94
Table 16 Stoichiometry and mass-balance of reactants and products after 3 h of reaction between CL-20 and nitroreductase under anaerobic conditions at pH 7.0 and 30°C.	102

Table 17 Time-course of H \leftrightarrow D exchange between ND-group of N-denitrohydrogenated product and water as followed with a LC-MS during dehydrogenase catalyzed hydride transfer from (R)NADD to CL-20.	107
Table 18 Physical and chemical characteristics of soil used in the study.	113
Table 19 Toxicological benchmarks (mg kg ⁻¹) for CL-20 determined in freshly amended soils using the Enchytraeid Survival and Reproduction Test with <i>Enchytraeus crypticus</i> and <i>Enchytraeus albidus</i> ^a	118
Table 20 Effects of RDX or HMX on adult survival and juvenile production (means \pm standard deviation) by two enchytraeid species in a freshly amended composite soil Rac50-50.	120
Table 21 Selected plasma biochemical parameters of adult Japanese quail exposed to CL-20 by gavage for 5 d followed by 10 days exposure with no CL-20	130
Table 22 Selected plasma biochemical parameters of adult Japanese quail fed CL-20 in the diet for 42 d.....	131
Table 23 Lethal effects of CL-20, glyoxal and formic acid on earthworm <i>Eisenia andrei</i> in freshly amended Sassafras sandy loam (SSL) soil.....	137
Table 24 Purification of hepatic glutathione S-transferase from quail or rabbit.....	143
Table 25 Effects of enzyme inhibitors and incubation conditions on CL-20 biotransformation activity in quail liver whole cytosol.....	144
Table 26 N-Terminal Amino Acid Sequences of Glutathione S-Transferases	146
Table 27 Selected physico-chemical characteristics of the test soils.....	156
Table 28 Bioaccumulation factor of CL-20, RDX and HMX in ryegrass <i>Lolium perenne</i>	162

I Project Background

The present SERDP funded project (CP 1256) responds directly to the original SERDP research solicitation on “Environmental Fate and Transport of the New Energetic Material, CL-20” (CPSON-02-01) under the Broad Agency Announcement (BAA). This SON identified the need to determine the transport, fate and environmental effects of CL-20 (2,4,6,8,10,12-hexanitro-2,4,6,8,10,12-hexaazaisowurtzitane) (Figure 1).

CL-20, which was initially synthesized by Nielsen *et al.* (1987, 1990) and later adopted by Thiokol for pilot scale production (Wardle *et al.*, 1996), is a high-density polynitro compound that is currently under consideration for military application. Indeed CL-20 is envisaged to deliver 10 to 20% higher performance than octahydro-1,3,5,7-tetranitro-1,3,5,7-tetrazocine (HMX) and better performance than hexahydro-1,3,5-trinitro-1,3,5-triazine (RDX) (Nielsen *et al.* 1998; Geetha *et al.* 2003, Giles *et al.* 2004) (Figure 1). However, it is recognized that the potential environmental fate and impact of this compound must be understood prior to its adoption as a commonly used energetic material. The provision of scientifically sound environmental data on the chemical and microbial reactivities of CL-20 and its interactions with soil and potential receptors is important because it will help understand and predict the fate and environmental impact of this powerful energetic compound.

Previous practices involving explosives such as RDX and HMX including manufacturing, waste discharge, testing and training, demilitarization and open burning/open detonation (OB/OD) have resulted in severe soil and groundwater contamination (Haas *et al.*, 1990; Myler and Sisk, 1991). Thus, in spite of their low solubility in water, the monocyclic nitramines RDX (45 mg/L at 25°C) and HMX (5 mg/L, at 25°C) (Talmage *et al.*, 1999) have exhibited an ability to migrate through subsurface soil and cause groundwater contamination. CL-20 being a cyclic nitramine might also migrate from surface soil to groundwater. Since both RDX and HMX are toxic to aquatic organisms (Sunahara *et al.*, 1999, 2001; Talmage *et al.*, 1999), earthworms (Robidoux *et al.*, 2000, 2001), and indigenous soil microorganisms (Gong *et al.*, 2001; Sunahara *et al.*, 2001), it is important to limit the potential adverse environmental consequences of the widespread usage of CL-20 by thoroughly investigating its transport, transformation and impact in soil.

While both RDX and HMX are cyclic oligomers of methylenenitramine, $\text{CH}_2\text{-N-NO}_2$, ($(\text{CH}_2\text{NNO}_2)_3$ for RDX and $(\text{CH}_2\text{NNO}_2)_4$ for HMX), CL-20 contains the repeating unit CH-NNO_2 (Wardle *et al.*, 1996; Nielsen *et al.*, 1998). The presence of C-bonded nitramine groups in all three chemicals could result in similarities in the chemical and enzymatic reactions and reactivities. However, in contrast to RDX and HMX, which are monocyclic nitramines, CL-20 is a rigid polycyclic nitramine characterized by having a three dimensional cage structure. This structural difference could result in drastic differences in the course of the chemical and biochemical reactions and the type of breakdown products. In particular, the presence of a relatively long (weak) C-C bond in CL-20 (bond denoted *a* in Figure 1) could play a significant role in differentiating its degradation pathway(s) from those of the two monocyclic nitramines RDX and HMX.

McCormick *et al.* (1981) first reported the transformation of RDX to nitroso derivatives prior to ring cleavage to produce hydrazines, dimethyl nitrosamines and methanol. Subsequent work in our laboratory demonstrated that initial denitration of these nitramines is also an

important step that can easily lead to ring cleavage and decomposition to nitrous oxide, nitrogen, formaldehyde and carbon dioxide (Hawari *et al.*, 2000a,b; Hawari, 2000; Halasz *et al.*, 2002; Fournier *et al.*, 2002). It would thus be worthwhile to ascertain whether our hypotheses drawn for the (bio)degradation of RDX and HMX are applicable to CL-20.

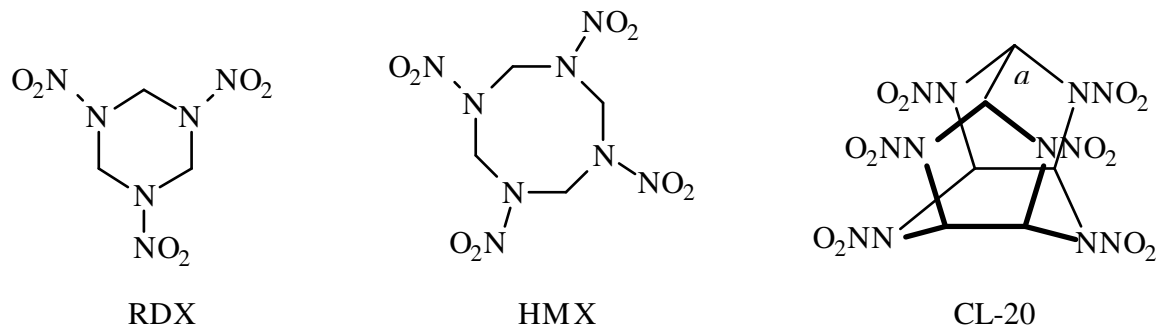
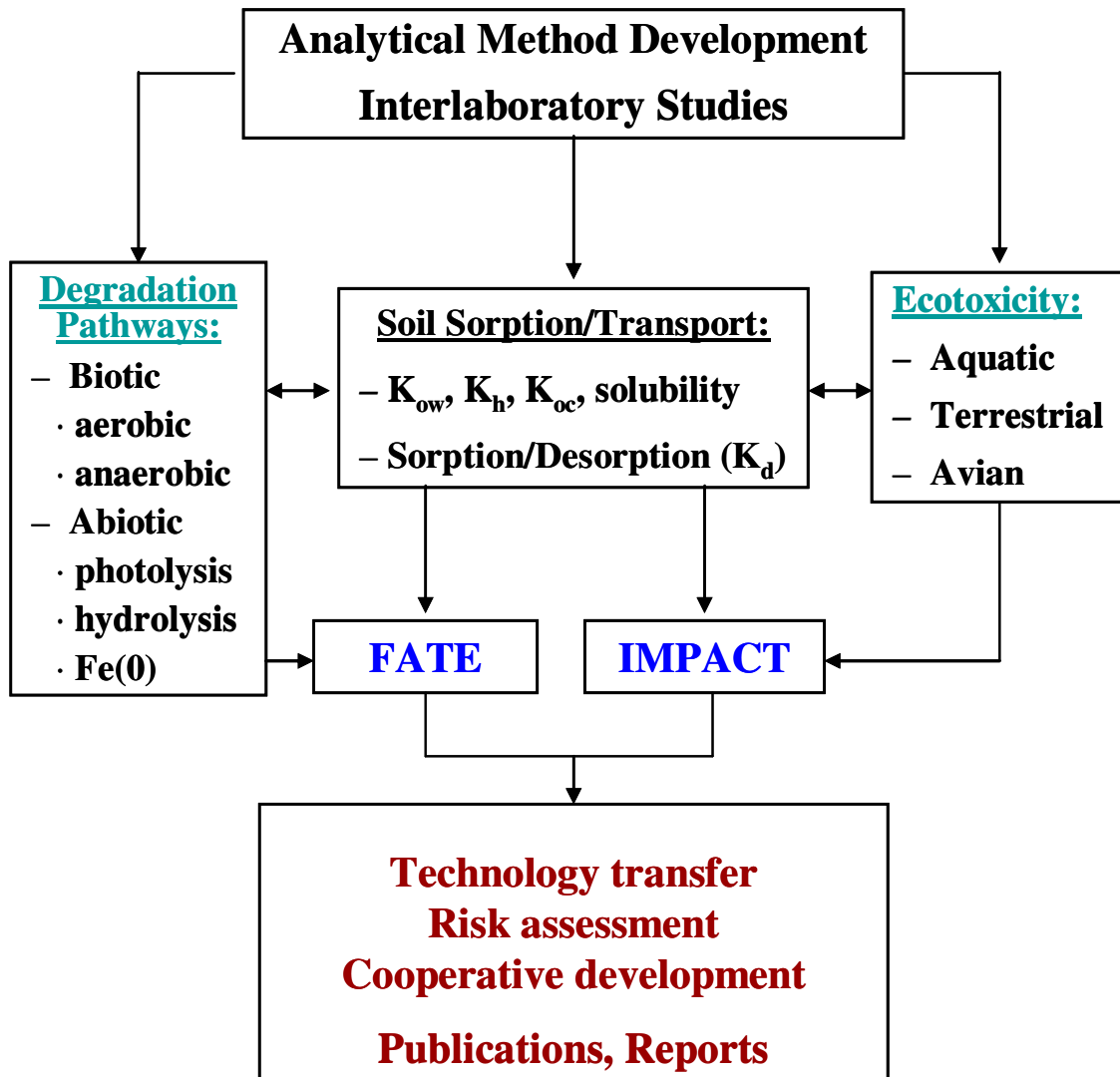


Figure 1 Structures of cyclic nitramine explosives RDX, HMX and CL-20. The three heterocyclic nitramines contain characteristic N-NO₂ functional groups that may determine their physicochemical, microbial and toxic properties.

We believe that the knowledge we discovered earlier on the chemical and microbial transformation of the two cyclic nitramines RDX and HMX (Hawari, 2000) and on their interactions with soils (Sheremata and Hawari, 2000a; Monteil-Rivera *et al.*, 2003) will be very helpful in designing laboratory experiments to determine transport and transformation of CL-20 in various soil/water systems.

The following chapters thus summarize laboratory findings of a comprehensive research strategy that was undertaken to determine environmental fate and impact of CL-20 in response to SERDP needs (ER 1256). We first measured important physicochemical parameters of CL-20 including water solubility (S), water/octanol partition coefficient (K_{ow}) and sorption (K_d) onto various types of soil. Then we determined its stability in aged soil under different conditions (pH, organic matter, micro flora) and degradability with zero valent iron (ZVI), and towards light. Other laboratory experiments were conducted to determine biotic (microbial and enzymatic) degradation of CL-20 in water / soil systems using soil indigenous microorganisms or specific isolates (*Pseudomonas* sp., *Clostridium* sp., *Phanerochaete chrysosporium*, *Irpex lacteus*) and enzymes (dehydrogenase, nitroreductase). In parallel we conducted several biological biochemical and biological assays to determine toxicity of the explosive towards various terrestrial, aquatic and avian receptors (see Project Overview, page 9). The knowledge gained on the transport and transformation routes and toxicity of CL-20 can then be used to help understand and predict fate and impact (toxicity mechanisms) of the chemical.

Project Overview



II Global Objectives

The present project addresses the objectives set forth in CPSON-02-0 to determine environmental fate and impact of the emerging high energetic chemical CL-20. The objectives were specifically outlined to:

1. Develop analytical methods to measure CL-20 as well as its potential intermediate and end degradation products.
2. Determine physicochemical properties (S , K_{ow} , K_d , K_{oc}) of CL-20.
3. Determine aerobic and anaerobic biodegradation of CL-20 in soil/water.
4. Determine enzymes responsible for initiating the degradation of CL-20.
5. Conduct a battery of ecotoxicological tests to determine the toxic effects of CL-20 on selected ecological receptors, e.g. terrestrial plants, soil invertebrates, soil microorganisms, and avian and aquatic species.
6. Determine sorption of CL-20 onto soil and its effect on biodegradation kinetics and toxicity mechanisms.

III Summary of Accomplishments

We first developed an SOP (Standard Operating Procedure) HPLC method for the analysis of CL-20 in soil and water and forwarded the method to the two PIs of the other two projects on CL-20 (ER 1254, ER1255). During the year 2003, an interlaboratory study was conducted between the three laboratories involved in the CL-20 projects (ER 1254, ER1255) to validate the HPLC method for the analysis of CL-20 in water and soil. Reasonably low RSD values were observed among the three laboratories ($10 \leq \%$), indicating reliability of the method in evaluating CL-20 concentrations in soil/water systems.

To provide insight on the fate (transport) of CL-20 in the environment (sorption and migration through subsurface soil) we determined the solubility of the chemical in water at different temperatures (5 to 60 °C). Also we measured its octanol/water partition coefficient ($K_{ow} = 82.6$). Subsequently we determined the sorption behavior of the chemical in several soils differing in pH, mineral phases and organic content. We found that CL-20 was highly retained by the organic fraction of soils, and that the sorption was governed more by the type of organic matter rather than its amount. Also the chemical exhibits a higher affinity for more condensed and/or reduced organic matter than for soil humic acids. In general sorption onto soils was found to be reversible and did not prevent abiotic or biotic transformations, or transport through subsurface soils.

The stability of CL-20 was investigated in aqueous solutions under a range of pH conditions. The chemical hydrolyzes readily under alkaline conditions with initial denitration followed by ring cleavage and decomposition to nitrite, nitrous oxide, ammonia, formic acid and glyoxal. When the chemical is subjected to light (300 nm and using solar irradiation) it also decomposes with the concurrent formation of nitrite to produce nitrous oxide, ammonia, formic acid and glyoxal. Similarity in product distribution of both hydrolysis and photolysis lead us to

conclude that following denitration the resulting intermediate(s) decompose spontaneously in water. Interestingly, when CL-20 was treated with Fe^0 in water the chemical degraded *via* at least two initial routes: one involving denitration and the second involving sequential reduction of the N- NO_2 groups to the corresponding nitroso (N-NO) derivatives prior to denitration and ring cleavage. Also the reaction mixture CL-20/ Fe^0 produced glyoxal, glycolic acid, formic acid, nitrous oxide and ammonium. The resemblance of product distribution in all tested abiotic reactions support the hypothesis that initial denitration of CL-20 leads to the spontaneous decomposition of the molecule in water.

Under biotic conditions CL-20 was found to degrade under both aerobic and anaerobic conditions. We found that the aerobic soil isolate, *Pseudomonas* sp. FA1, was capable of utilizing CL-20 as sole nitrogen source. Subsequent work showed that an NADH-dependent, membrane-associated flavoenzyme was responsible for CL-20 biotransformation. Also we isolated an obligate anaerobic bacterium, *Clostridium* sp. EDB2, from sediment obtained from Halifax Harbour for its ability to degrade CL-20 and demonstrated a chemotactic response towards the nitramine. Several fungi were also found capable of degrading the chemical, with *P. Chrysosporium* being the most efficient degrader. Once again we identified that disappearance of the energetic chemical was accompanied with the liberation of nitrite in most cases. The product distribution basically indicated the formation of NO_2 , N_2O , NH_3 , HCHO , $(\text{COOH})_2$ and CO_2 . Using LC/MS with UL ring labeled [^{15}N]-CL-20 and UL NO_2 labeled [$^{15}\text{NO}_2$ -CL-20] we were able to identify several initial intermediates from the (bio)decomposition of CL-20 and thus were able to discover several initial degradation routes leading to its decomposition, most notably denitration, denitrohydrogenation and reduction of the N- NO_2 to the corresponding N-NO group(s).

Finally, we obtained definitive data on the toxicity of the energetic chemical towards various aquatic (algae, microorganisms), terrestrial (earthworms, plants, microbes) and avian (Japanese quail) receptors. For the aquatic toxicity, CL-20 showed no adverse effects on the marine bacteria *Vibrio fischeri* and the freshwater green algae *Selenastrum capricornutum*, up to its water solubility (ca. 3.6 mg L^{-1}). In the case of terrestrial toxicity, CL-20 was not acutely toxic to the plants tested (alfalfa (*Medicago sativa*) and perennial ryegrass (*Lolium perenne*)), and had no statistically significant effects on microbial communities measured as DHA or on the ammonium oxidizing bacteria determined as PNA in two soil types, but definitive toxicity tests of three soil invertebrates (earthworm *Eisenia andrei*, and enchytraeids *Enchytraeus albidus* and *Enchytraeus crypticus*) showed the chemical to act as a reproductive toxicant to the earthworm and enchytraeids, with lethal effects observed at higher concentrations. We investigated the toxicity of CL-20 on an avian species, the Japanese quail (*Coturnix coturnix japonica*) using test methods modified from standard toxicity test guidelines. Several physiological parameters were monitored in both studies. In the acute dosing studies, CL-20 caused no overt toxicity to the birds and elicited few effects in treated adult individuals. Treatment-related effects were on the liver as evidenced by increased liver weight and elevated enzyme activity. In the subchronic study we also observed treatment-related effects suggesting possible reproductive and developmental effects. In an effort to understand the mechanism of CL-20 toxicity, we purified and identified a hepatic enzyme capable of biotransforming CL-20. Subsequently, we identified possible conjugated metabolites that could explain the adverse effects we observed.

Experimental findings of this project (SERDP ER1256) are discussed in the following chapters and in the publications (22) that are annexed at the end of the report.

TECHNICAL APPROACH
AND
ACCOMPLISHMENTS

IV Analytical methods for the determination of CL-20 in water and soil

Research conducted under this task was published in:

1. Groom CA, Halasz A, Paquet L, D'Cruz P, Hawari J. (2003) Cyclodextrin assisted capillary electrophoresis for determination of the cyclic nitramine explosives RDX, HMX and CL-20: a comparison with high performance liquid chromatography (HPLC). *J. Chromatogr. A* 999:17-22.
2. Monteil-Rivera F, Paquet L, Deschamps S, Balakrishnan VK, Beaulieu C, Hawari J. (2004) Physico-chemical measurements of CL-20 towards environmental applications: comparison with RDX and HMX. *J. Chromatogr. A* 1025:125-132.
3. Groom C, Halasz A, Paquet L, Thiboutot S, Ampleman G, Hawari J. (2005) Detection of nitroaromatic and cyclic nitramine compounds by cyclodextrin assisted electrophoresis quadrupole ion trap mass spectrometry. *J. Chromatogr. A* 1072: 73-82.

Introduction

An SOP (standard operating procedure) HPLC method describing the analysis of CL-20 in water and soil was first developed and shared with the other two labs working on projects ER 1254 and ER1255. This method (preparation of soil and water samples, extraction, recovery, detection limits, accuracy and precision) is described in a paper published in *J Chromatogr. A* (Monteil-Rivera *et al.*, 2003) attached at the end of the report. In addition a capillary electrophoresis / mass spectrometry methods were developed to rapidly resolve and detect CL-20, HMX and RDX and their related degradation intermediates in environmental samples and published in *J. Chromatogr. A* (Groom *et al.*, 2003 and 2005).

Material and Methods

Chemicals and sample preparation. CL-20 was obtained from A.T.K. Thiokol Propulsion (Brigham City, UT, USA) with a purity of 99.3 % (determined by HPLC). IR showed that 95 % of the chemical was present in the ϵ -form. Acetonitrile (CH_3CN , HPLC grade) and methanol (CH_3OH , HPLC grade) were from J.T. Baker, acetone (CH_3COCH_3 , HPLC grade) was from Fisher.

Aqueous samples were diluted with acidified ($250\ \mu\text{L conc. H}_2\text{SO}_4\ \text{L}^{-1}$) CH_3CN to give a 50:50 (v:v) $\text{CH}_3\text{CN}:\text{H}_2\text{O}$ mixture. If analysis could not be performed on the day of preparation, samples were stored at 4°C away from light.

For soil samples, U.S. EPA SW-846 method 8330 (USEPA, 1997) was used with a slight modification. Dried soil (2.0 g) was weighed into 16-mL glass tubes with PTFE-lined caps. Samples and associated quality-control samples were spiked with surrogate (RDX) and CL-20 solutions in acetone to obtain concentrations of CL-20 in soil ranging from 1 to 10,000 mg kg^{-1} . The solvent was allowed to evaporate overnight in a fume-hood before subsequent extraction by CH_3CN (10 mL / tube) using sonication at 20°C for 18 h. After centrifugation at $1170 \times g$ for 30 min, a volume of supernatant (5 mL) was combined with 5 mL of a $\text{CaCl}_2/\text{NaHSO}_4$ aqueous solution (5 and $0.2\ \text{g L}^{-1}$, respectively) instead of the usual solution of calcium chloride. The

resulting sample was shaken, allowed to stand for 30 min and filtered through a 0.45 μm -Millipore PTFE filter. After discarding the first 3 mL, the filtrate was analyzed by HPLC. In order to assess the effect of water on the extraction efficiency, some samples were supplemented with water (15 % or 50 % wt/wt water) following acetone evaporation. One third of the samples were extracted immediately, a second third after being stored at 10 °C and in the dark for 7 days, and the final third after being stored for 21 days under similar conditions.

Analytical methods. The CL-20 concentration was analysed by HPLC using a chromatographic system (ThermoFinnigan, San Jose, CA) composed of a Model P4000 pump, a Model AS3000 injector, including temperature control for the column, and a Model UV6000LP Photodiode-Array Detector. The separation was completed on a Supelcosil LC-CN column (25 cm, 4.6 mm, 5 μm ; Supelco, Oakville, ON) maintained at 35° C. The mobile phase (70 % aqueous methanol) was run isocratically at 1 mL/min for the entire run time of 14 min. The detector was set to scan from 200 to 350 nm. Chromatograms were extracted at a wavelength of 230 nm with quantification taken from peak areas of external standards. Peaks were identified by comparison with elution times for external standards and UV spectra. The injection volume was 50 μL . Calibration standards (0.05 – 25 mg of CL-20 L^{-1}) were prepared by diluting (50:50 (v:v)) intermediate acetonitrile solutions in acidified water (0.2 g L^{-1} sodium bisulfate).

Accomplishments

Because explosives are often applied as mixtures, it was important to establish analytical conditions that permit a good separation amongst CL-20 and other energetic chemicals. Analysis by HPLC of a mixture containing RDX, HMX and CL-20 using the previously mentioned conditions gave a well-resolved chromatogram with retention times of 4.8 min, 5.9 min and 8.3 min, respectively (Figure 2). Peak areas were used to quantify chromatographic signals and excellent linearity was obtained over the entire range of CL-20 concentrations used (0.05 – 25 mg L^{-1}) ($y = 6.4864 \times 10^5 x$; $R^2 = 0.99996$). The instrumental detection limit (IDL) and the instrumental quantification limit (IQL) were found to be 3 and 9 $\mu\text{g L}^{-1}$, respectively (RSD = 3.8 % n = 10).

Larson *et al.* (2002) recently published an HPLC method for analyses of CL-20 in water and soil samples but the susceptibility of CL-20 to decomposition was not reported. We found that CL-20 degrades significantly in aqueous acetonitrile media and that degradation was more rapid at 21°C (65 % after 7 days) than at 10°C (8 % after 7 days) (Figure 3). We also found that decomposition can be avoided by acidifying the medium to pH 3 (Figure 3). Therefore, in order to avoid a possible degradation of CL-20, all aqueous samples should be analyzed after a 50:50 (v:v) dilution with acidified CH_3CN . CL-20 is a weak acid that, upon losing one of its labile protons, can undergo decomposition. It hydrolyses in water under rather mild alkaline conditions. Since acetonitrile is known to be a more powerful proton acceptor than water (Buncel and Dust, 2003), it may favor the initial deprotonation of CL-20 and hence cause decomposition even in neutral media. Acidification of the media prevents the removal of the labile proton from CL-20, thereby stabilizing the chemical.

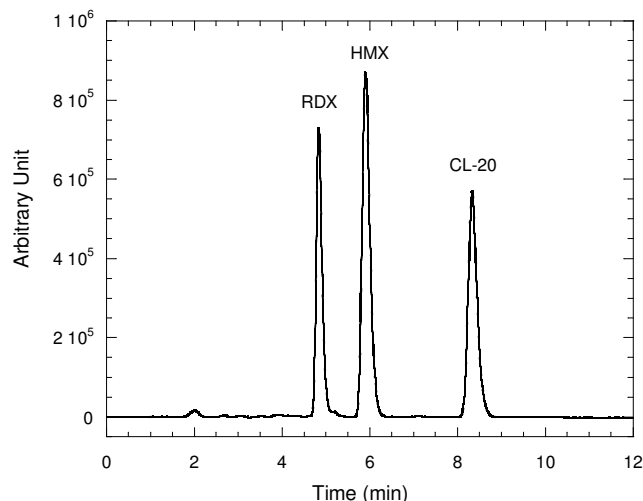


Figure 2 A typical HPLC chromatogram showing separation of CL-20 from RDX and HMX (column: LC-CN; mobile phase: 30 % water-70% methanol; Flow rate: 1 mL/min; Detector: PDA ($\lambda = 230$ nm)).

As a consequence of the instability of CL-20 observed in aqueous acetonitrile media, the U.S. EPA SW-846 method 8330 (USEPA, 1997) was slightly modified and the extract was added to a solution of CaCl_2 containing 0.2 g L^{-1} of sodium bisulfate to bring the solution pH to 3. The method detection limit (MDL) and the method quantification limit (MQL) were determined and found to be 0.06 and 0.20 mg kg^{-1} , respectively ($n=10$; $\text{RSD} = 10.7 \%$). CL-20 recoveries were found to stand within the interval: $83 \% < R < 113 \%$ ($n=20$, $\text{SD} = 4.9 \%$, average = 97.9%).

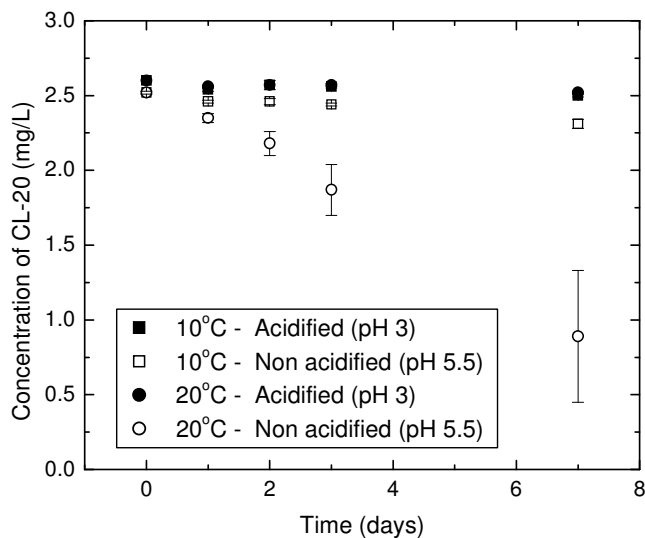


Figure 3 Effect of acidification and temperature on the stability of CL-20 in water/acetonitrile media.

Table 1 Single laboratory study: recovery data for soil samples spiked with different concentrations of CL-20 at BRI.

Nominal Conc. (mg kg ⁻¹)	% water	Meas. Conc. (mg kg ⁻¹)	SD ^a (n=3)	% RSD ^b	Mean % Recovery
1.00	0	1.040	0.156	14.99	104.0
	15	1.015	0.021	2.041	101.5
	50	1.000	0.028	2.771	100.0
5.00	0	5.107	0.535	10.477	102.1
	15	5.166	0.062	1.202	103.3
	50	5.300	0.080	1.508	106.0
10.00	0	10.373	0.211	2.037	103.7
	15	10.156	0.188	1.855	101.6
	50	10.400	0.126	1.212	104.0
100.00	0	99.247	1.385	1.396	99.2
	15	99.354	1.078	1.085	104.0
	50	101.656	0.321	0.315	101.7
1,000.00	0	978.733	6.481	0.662	97.9
	15	994.578	11.404	1.147	99.5
	50	1,001.720	15.574	1.555	100.2
10,000.00	0	10,261.667	137.114	1.336	102.6
	15	9,669.702	394.638	4.081	96.7
	50	9,978.400	334.422	3.351	99.8

^a SD = Standard Deviation; ^b RSD = Relative Standard Deviation.

Single laboratory precision method and data recoveries are gathered in Table 1 for soil samples spiked with different concentrations of CL-20. Precision was good for replicate analyses and excellent recoveries (96-106 %) were obtained over a wide range of concentrations. The addition of water (0, 0.353, or 2 mL of water, corresponding to soils containing 0, 15 or 50 % moisture, respectively) did not affect the extracted amounts of CL-20. No degradation of CL-20 occurred when 2 mL of water were added to the 10 mL of acetonitrile and sonicated for 18 h at 20 °C, thus demonstrating the applicability of the method to both dry and wet samples. Aging (21 days) of spiked samples with 0 or 15 % water showed that CL-20 extractability was not affected and that irreversible binding did not occur within this period of time.

V QC/QA Interlaboratory study

In order to validate the SOP method developed in our laboratory, a QC/QA study was conducted between the three groups involved in the CL-20 SERDP projects: CP 1254, 1255, 1256. Dried SSL soil (Sassafras Sandy Loam sampled in uncontaminated open grassland on the property of US Army Aberdeen Proving Ground, (Edgewood, MD)) was spiked at the ECBC (Edgewood Chemical Biological Center, Edgewood, MD) with four different concentrations of CL-20. The four samples were then shipped to the two other groups (PNNL (Pacific Northwest National Laboratory and BRI) in coolers containing ice blocks. Samples were received at BRI, around 10 days after shipment. The method described above was then applied in triplicate at BRI to determine the concentration in each sample. Results were sent to ECBC for compilation. The results obtained in the three different laboratories are gathered in Table 2. The reasonably low RSD values observed among the three labs ($10 \leq \%$) are indicative of a reliable analytical method to evaluate CL-20 concentrations in soil. Moreover, the 10 days spent at room temperature during the shipping does not seem to have caused degradation.

Table 2 Recovery data for SSL soil samples spiked with CL-20: Interlaboratory study.

	ECBC ^a	BRI ^b	PNNL ^c	Results from the 3 laboratories			
Target Conc. (µg/g)	Conc. in soil (± SD ^d)(µg/g)	Conc. in soil (± SD ^d)(µg/g)	Conc. in soil (± SD ^e)(µg/g)	Mean Conc. in soil (µg/g)	SD Conc. in soil (µg/g)	% RSD	Mean %Recovery
0.10	N.d.	0.112 (0.005)	0.129 (0.013)	0.120	0.012	10.09	120.41
0.50	0.483 (0.032)	0.525 (0.014)	0.448 (0.071)	0.486	0.039	7.97	97.11
1.00	0.996 (0.105)	1.129 (0.055)	1.130 (0.094)	1.085	0.077	7.07	108.50
10.00	9.387 (1.333)	10.381 (0.498)	10.89 (0.401)	10.219	0.0765	7.48	102.19

^a ECBC = Edgewood Chemical Biological Center; ^b BRI = Biotechnology Research Institute; ^c PNNL = Pacific Northwest National Laboratory; ^d n=3; ^e n=2.

VI Physico-chemical measurements of CL-20

Results obtained in this task have been published in:

Monteil-Rivera F, Paquet L, Deschamps S, Balakrishnan VK, Beaulieu C, Hawari J. (2003) *Physico-chemical measurements of CL-20 towards environmental applications: comparison with RDX and HMX. J. Chromatogr. A.* 1025: 125-132

Introduction

To be able to understand the environmental fate of the emerging explosive CL-20 we must first determine essential physico-chemical parameters (aqueous solubility, octanol-water partition coefficient, stability in water under stirring) for the chemical. Aqueous solubility (S) and octan-1-ol/water partition coefficient (K_{ow}) values are needed to predict potential migration of CL-20 through subsurface soil. The aqueous solubility (S) and the octanol/water partition coefficient (K_{ow}) of CL-20 have been determined at various temperatures and at room temperature, respectively. Since CL-20 is a cyclic nitramine, both S and K_{ow} have also been measured for the two other known cyclic nitramines RDX and HMX under similar conditions for comparative purposes. Soil adsorption/desorption parameters were also determined, and are presented and discussed latter in the present report.

Material and Methods

Characterization. CL-20 (purity 99.3 % determined by HPLC) was obtained from Thiokol Propulsion (Thiokol Utah 84302 USA), as an ϵ -form with ≥ 95 % as determined by IR. Elemental composition was determined on a Carlo Erba EA 1108 analyzer and was found to be C 16.84 %, N 37.52 %, H 1.06 % (calculated values for $C_6H_6N_{12}O_{12}$: C 16.45 %, N 38.36 %, H 1.38 %).

Nuclear magnetic resonance (NMR) spectra were collected in deuterated acetone: 1H NMR (600.13 MHz, CD_3COCD_3) δ 8.34 (s, 4H), 8.20 (s, 2H), ^{13}C NMR (150.91 MHz, CD_3COCD_3) δ 75.16 (s, 2C), 72.18 (s, 4C), ^{15}N NMR (60.84 MHz, CD_3COCD_3) δ 339.5 (s, 4N) 336.4 (s, 2N), 200.3 (s, 4N), 180.8 (s, 2N).

Unidentified impurities were detected during 1H NMR analysis (δ 7.9, 7.7, 3.3, 2.9, 1.3), but no such impurities were detected in the ^{13}C -NMR spectrum, suggesting that their concentrations are low. The impurities are most probably low molecular weight compounds.

Determination of aqueous solubility (S) of CL-20. The solubility (S) of CL-20 was determined in water at temperatures (T) of 5, 10, 15, 20, 25, 40 and 60 °C. An excess amount of CL-20 (0.015 g) was added to 100 mL of deionized water in a glass bottle. The samples were stirred at the required temperature in a thermostated bath. After a 24 h stirring period, the suspension was allowed to set for 1h and an aliquot of supernatant was taken from the middle of the solution (without filtration) and diluted 1:1 in methanol. The resulting solution was analyzed by HPLC.

Octanol/water partition coefficient (K_{ow}) of CL-20. The octan-1-ol/water partition coefficient, K_{ow} , of CL-20 was determined at room temperature (21 ± 1 °C) according to OECD guideline

107 (OECD, 1981) with slight modifications. OECD guideline requires the use of solvents saturated with each other, but due to the low solubility of CL-20 in water it was not possible to use octan-1-ol-saturated water. Experiments were thus performed with non-saturated water and octan-1-ol solutions. Known volumes of a filtered aqueous solution of CL-20 (3.5 mg/L) were added to octan-1-ol in a 16-mL PTFE-lined capped glass tube. The resulting mixtures were equilibrated by periodical shaking (4 cycles of 10 min) and centrifuged (2700 rpm). Each phase was analyzed for its content of CL-20 using HPLC. However, the octanol phase was diluted (1:3) with a solution containing 70 % methanol in water prior to analysis. Experiments were run in triplicate using different ratios of octanol to water and different amounts of CL-20. K_{ow} was calculated as the ratio (CL-20 concentration in the aqueous phase / CL-20 concentration in the octanol phase).

Accomplishments

Solubility of CL-20 in water is presented in Figure 4 as a function of temperature. We found that a slight change in temperature can drastically affect solubility of CL-20 in water. In general, water solubility of CL-20 at room temperature (20°C) was found to be around 3.5 mg/L.

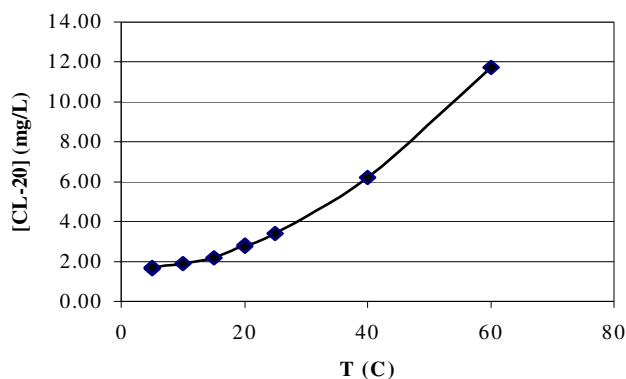


Figure 4 Solubility of CL-20 in water as a function of temperature.

For ideal solutions, the amount of a compound present in solution at saturation can be estimated using equation (1).

$$\ln x_B = - \left(\frac{\Delta_{fus}H}{R} \right) \left(\frac{1}{T} - \frac{1}{T^*} \right) \quad (1)$$

where x_B = mole fraction of solute, $\Delta_{fus}H$ = enthalpy of fusion of solute, R = ideal gas constant, T = temperature at which equilibrium is considered, T^* = melting temperature of solute. Aqueous solutions of explosives are not ideal, but the S-T relationship can follow equation (2) as described by Lynch *et al.* (2001).

$$\ln S = A - \frac{B}{T} \quad (2)$$

Where S = solubility and A and B = arbitrary constants.

Data were plotted as $\ln S$ vs. $1/T$ (K) and linear regression was performed as shown in Figure 5. For comparison, solubility data measured under similar conditions for RDX and HMX were also plotted (Figure 5). The solubility of CL-20 was found to follow equation (2) (with A and B equal to 13.54 and 3578, respectively). Figure 5 clearly demonstrates that the solubility of CL-20 is much lower than that of RDX. The comparison with the solubility of HMX is more complex since CL-20 is more soluble than HMX at lower temperatures but the trend is reversed at temperatures above 20°C.

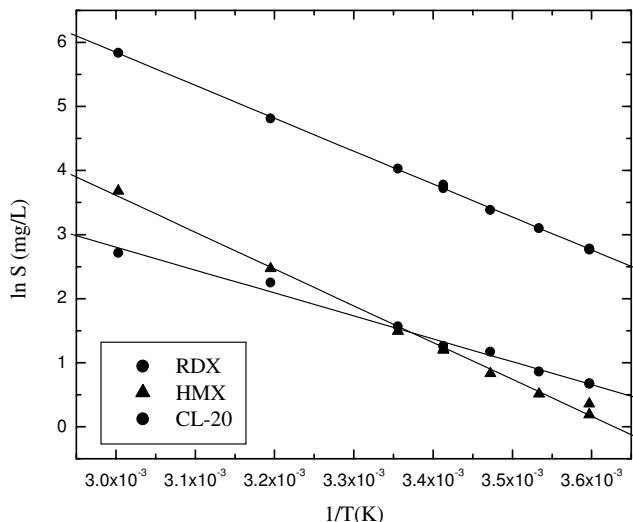


Figure 5 Compared solubilities of RDX, HMX and CL-20 in water.

In an effort to enhance the solubility of CL-20 in water, we used cyclodextrins (CDs) and measured their binding constants. Two CDs were used: Hydroxypropyl- β -cyclodextrin (HP- β -CD) and heptakis-2,6-di-O-methyl- β -cyclodextrin (DM- β -CD). An excess of CL-20 (300 mg/L) was combined with increasing concentrations of CD (0 – 5 % w/v), CL-20 solubility was measured after 18 hours of equilibration at room temperature (21 ± 1 °C) and the value was compared to the solubility measured without cyclodextrine ($[CL-20]_0$) (Figure 6).

As with RDX and HMX, the aqueous solubility of CL-20 increases with temperature, but to a lesser extent. The solubility of CL-20 is much lower than that of RDX, whereas the comparison with HMX is more complex: CL-20 is more soluble than HMX at lower temperatures but the trend is reversed at temperatures above 20°C.

Three different sets of conditions were used for each explosive and each set was run in triplicate. The average of the nine measurements is reported in Table 3. Regardless of the octanol/water ratios used, K_{ow} values remained basically constant and a value of 82.6 ± 0.9 ($\log K_{ow} = 1.92 \pm 0.02$) was obtained for CL-20, significantly higher than the partition coefficients for RDX (8.0 ± 0.6) and HMX (1.46 ± 0.02). This finding suggests that CL-20 will sorb onto soils more strongly than RDX and HMX and that this hydrophobic interaction will be particularly important in soils containing high amounts of organic matter.

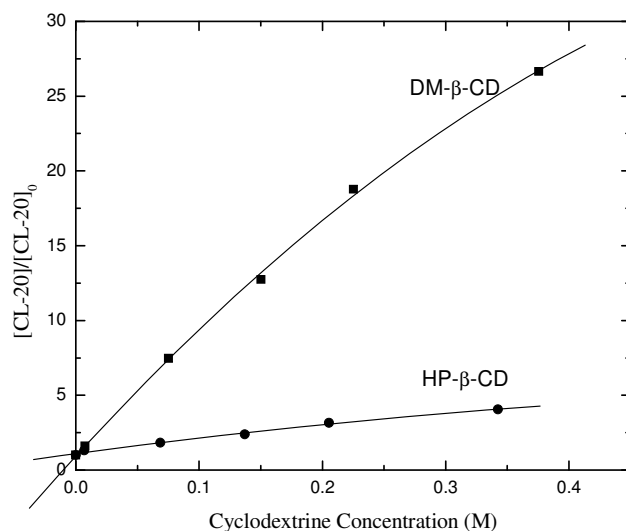


Figure 6 Solubility of CL-20 in water in presence of cyclodextrines.

Table 3 Aqueous solubilities (S) of RDX, HMX and CL-20 as a function of temperature and log K_{ow} values measured at ambient temperature.

T (°C)	Aqueous Solubility (mg L ⁻¹) (± SD; n=3)		
	RDX	HMX	CL-20
5	16.01 (0.16)	1.32 (0.16)	1.97 (0.08)
10	22.19 (0.12)	1.67 (0.14)	2.12 (0.04)
15	29.67 (0.57)	2.27 (0.09)	2.48 (0.02)
20	42.58 (1.32)	3.34 (0.12)	3.16 (0.04)
25	56.35 (1.79)	4.46 (0.03)	3.65 (0.04)
30	n.d. ^a	n.d.	4.89 (0.03)
40	122.94 (0.94)	11.83 (0.09)	7.39 (0.06)
50	n.d.	n.d.	11.62 (0.01)
60	342.71 (3.25)	39.69 (2.24)	18.48 (0.80)
T (°C)	Log K_{ow} (± SD; n=9)		
	RDX	HMX	CL-20
21	0.90 (0.03)	0.165 (0.006)	1.92 (0.02)

^a n.d.: Non determined.

VII Hydrolysis of CL-20 in aqueous solution

This work was published in:

Balakrishnan VK, Halasz A, Hawari J. (2003) Alkaline hydrolysis of the cyclic nitramine explosives RDX, HMX and CL-20: New insights into degradation pathways obtained by the observation of novel intermediates. *Environ. Sci. Technol.* 37: 1838-1843.

Introduction

Since the end products of the mono cyclic nitramine RDX decomposition during enzymatic biodegradation with strain DN22 (Fournier *et al.*, 2002) were similar to those obtained via both alkaline hydrolysis (Hoffsommer *et al.*, 1997; Heilmann *et al.*, 1996) and photodenitration (Hawari *et al.*, 2002), we hypothesize that following initial denitration of the cyclic nitramine, ring cleavage and subsequent decomposition is largely dictated by the aqueous chemistry of the resulting intermediates. Therefore, if other cyclic nitramines such as CL-20 produce end products similar to those of RDX, then one may assume that their decomposition mechanisms resemble those described for RDX. Hence, our objectives in the present study were: 1) to determine whether CL-20 hydrolyzes in aqueous, alkaline (pH 10) solutions; 2) to identify end products and compare them to RDX and HMX end-products; and 3) to increase CL-20 concentrations in aqueous acetonitrile solutions to observe and identify early intermediates that could give insight into initial steps involved into the hydrolysis mechanism.

Material and Methods

Hydrolysis in aqueous solution. To a series of dry 20 mL vials (each wrapped in Aluminum foil) was added an aliquot (100 μ L) of CL-20 stock solution prepared in acetone (10,000 mg/L). The acetone was evaporated in a fume hood, followed by the addition of 10 mL of a NaOH solution (pH 10) to give a final CL-20 concentration of 100 mg L⁻¹. The initial concentration was kept well in excess of the maximum solubility of CL-20 in water (ca. 3.5 mg L⁻¹) in an attempt to generate sufficient amounts of intermediates to allow detection. The vials were sealed with Teflon coated serum caps and placed in a thermostated benchtop shaker at 30°C and 200 rpm. Some vials were sparged with argon for 2 hours to allow analysis for N₂. We used a gas-tight syringe to measure gaseous products (N₂O and N₂) in the head space but for the analysis of the liquid medium we first quenched the reaction by adding HCl in a CH₃CN solution (10 mL) (pH 4.5). Acetonitrile was used to solubilize unreacted starting material for subsequent analysis. The quenched vials were then stored in a refrigerator at 4°C until analyzed.

Hydrolysis in aqueous acetonitrile. A dry 100-mL vial (wrapped in Aluminum foil) was charged with approximately 0.5 g (1.14 mmol) CL-20, 50 mL HPLC grade acetonitrile, and 0.1 N NaOH (50 mL). The resulting solution had an initial CL-20 concentration of 50 mg L⁻¹ and a pH of 12.7. The vial was sealed with a Teflon coated serum cap, and placed in a thermostated benchtop shaker at 30°C and 200 rpm. The reaction was quenched by bubbling CO₂ (an acid) into the solution until the pH decreased to 6 (approximately 3 minutes of bubbling time).

required). The mixture was then concentrated under reduced pressure (18 mm Hg), and lyophilized for subsequent analysis (see below).

Analytical Procedures. The concentration of CL-20 was determined using HPLC as described in section V. Formaldehyde (HCHO) (Summers, 1990) and nitrous oxide (N₂O) (Sheremata and Hawari, 2000b) were analyzed as described previously. Nitrate (NO₃⁻), formate (HCOO⁻) and ammonium (NH₄⁺) were performed by capillary electrophoresis on a Hewlett-Packard 3D-CE equipped with a Model 1600 photodiode array detector and a HP capillary part number 1600-61232. The total capillary length was 64.5 cm, with an effective length of 56 cm and an internal diameter of 50 µm. For nitrite, nitrate and formate, analyses were performed using sodium borate (25 mM) and hexamethonium bromide (25 mM) electrolytic solution at pH 9.2 (Okemgbo et al., 1999). The ammonium cation was analyzed using a formic acid (5 mM), imidazole (10 mM) and 18-crown-6 (50 mM) electrolytic solution at pH 5. In all cases, UV detection was performed at 215 nm (Beck, 1994).

A Micromass bench-top single quadrupole mass detector attached to a Hewlett Packard 1100 Series HPLC system equipped with a PDA detector was used to analyze for CL-20 ring cleavage intermediates. The samples were injected into a 4 µm-pore size Supelcosil CN column (4.6 mm ID by 25 cm; Phenomenex, Torrance, Ca) at 35°C. The solvent system was composed of 20% acetonitrile: 80 % water (v/v). For mass analysis, ionization was performed in a negative electrospray ionization mode, ES(-), producing mainly the deprotonated molecular mass ions [M-H]. The mass range was scanned from 30 to 400 Da with a cycle time of 1.6 s, and the resolution was set to 1 Da (width at half height).

Accomplishments

Briefly, we hydrolyzed CL-20 in aqueous solution and the resulting time profile of CL-20 disappearance and products appearance is shown in Figure 7. We found that the removal of the nitramine was accompanied by the formation of two molar equivalents of nitrite and the formation of nitrous oxide, formate and ammonium (Table 4). 4-nitro-2,4-diazabutanal (4-NDAB), an important end-product detected with RDX and HMX, was not formed here due to the presence of C-C bonds (elongated) in the rigid caged polycyclic CL-20 that are absent in the case of RDX and HMX (see structures Figure 1).

Table 4 Normalized molar yields for the products obtained upon alkaline hydrolysis (pH 10) of CL-20.^a

NO ₂ ⁻	N ₂ O	NH ₄ ⁺	HCHO	HCOO ⁻
1.91 ± 0.09	0.91 ± 0.10	0.79 ± 0.05	Not formed	0.493 ± 0.007

^a Stoichiometries are calculated based on the number of moles of product observed for each mole of CL-20 consumed. Standard deviations result from duplicate measurements.

CL-20 disappeared at a faster rate ($1.09 \times 10^{-2} \text{ h}^{-1}$) than did either RDX ($7.21 \times 10^{-3} \text{ h}^{-1}$) or HMX ($\sim 1 \times 10^{-4} \text{ h}^{-1}$) under similar conditions. Our findings indicate that, as we observed with RDX and HMX, initial denitration appears to play a critical role in initiating the decomposition of this polycyclic nitramine.

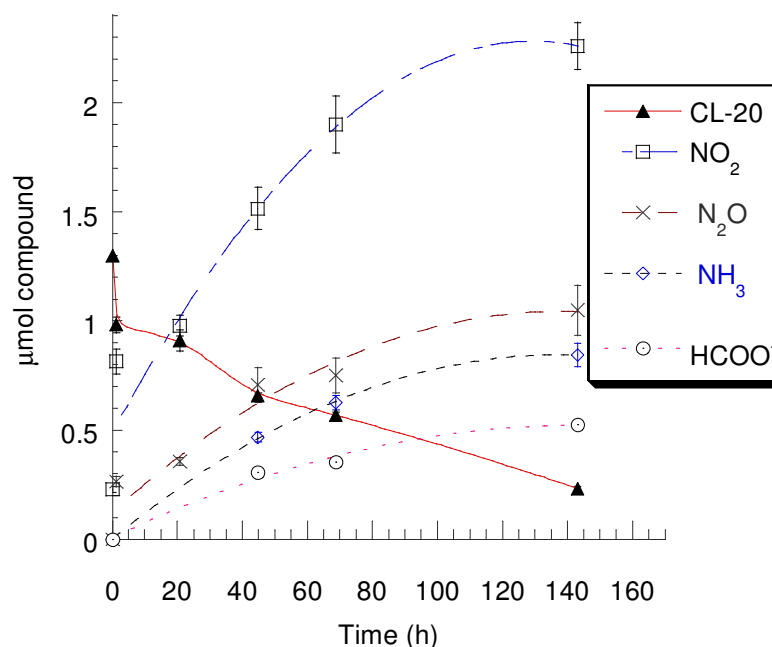


Figure 7 Time course for the alkaline hydrolysis (pH 10) of CL-20 at 30°C and formation of nitrite (NO_2^-), nitrous oxide (N_2O), ammoniac (NH_3) and formate (HCOO^-). Note that NO_2^- is present at $t = 0$.

VIII Photodegradation of CL-20 in aqueous solutions

The work conducted under this task was published in:

Hawari J, Deschamps S, Beaulieu C, Paquet L, Halasz A. (2004) Photodegradation of CL-20: insights into the mechanisms of initial reactions and environmental fate. *Water Res.* 38: 4055-4064.

Introduction

The understanding of the photodegradation mechanisms of a chemical is a necessary step to predict its fate and its impact in natural environment. As far as we are aware little information is available on the photodegradation of CL-20 in solution. Pace and Kalyanaraman (1993) reported the cleavage of an N-NO₂ bond during CL-20 photolysis by trapping the generated ·NO₂ radical in DMSO and detecting the spin adduct using ESR spectroscopy. No other information on the identity of the degradation products was provided. On the other hand, solid-state photochemistry of the energetic chemical has been reported by Pace (1991) and Ryzhkov and McBride (1996) and was suggested to proceed *via* the initial cleavage of an N-NO₂ bond. Recently we discovered that initial denitration of RDX by photolysis (Hawari *et al.*, 2002) led to ring cleavage and effective decomposition with a product distribution including HCHO, HCOOH, NH₂CHO, NH₃, NO₂⁻, NO₃⁻, and N₂O. Since CL-20 is also a cyclic nitramine with C-N-NO₂ linkages, we assumed that it could undergo decomposition following a similar initial denitration reaction in water. Our objective in the present study was thus to test this hypothesis. In order to do so, we photolyzed CL-20 in aqueous and CH₃CN/H₂O solutions using a Rayonet photoreactor (254 - 350 nm) and sunlight and attempted to identify intermediate products that could provide insight into the initial photodegradation step mechanism.

Material and Methods

Chemicals. Acetonitrile, formic acid, formaldehyde, D₂O, H₂¹⁸O and ¹⁸O₂ were obtained from Aldrich, Canada.

Irradiation Experiments. A Rayonet RPR-100 photoreactor fitted with a merry-go-round apparatus (Southern New England Co, Hamden, CT) equipped with either sixteen 254 nm (35 watts), 300 nm (21 watts) or 350 nm (24 watts) fluorescent lamps were used as light sources. In some experiments photolysis was conducted using sunlight. Photolysis was conducted in 20 mL quartz tubes each charged with a 10 mL of aqueous or aqueous acetonitrile solutions (50 % v/v) of CL-20 (3.5 mg/L and 50 mg/L, respectively). Acetonitrile was used to increase solubility of CL-20 in an attempt to generate sufficient amounts of intermediates to allow detection.

Photolysis was carried out in either degassed (Ar bubbling) or non-degassed (with O₂ or ¹⁸O₂ bubbling) tubes sealed with Teflon coated mininert valves. Controls containing CL-20 were kept in the dark during the course of the experiment. To determine the role of water in the photolysis process we photolyzed CL-20 (3.5 mg/L) in the presence of D₂O and H₂¹⁸O. The temperature of the reactor was maintained at 25 °C.

Analytical methods. A Bruker bench-top ion trap mass detector attached to a Hewlett Packard 1100 Series HPLC system equipped with a PDA detector was used to analyze for CL-20 and its intermediates. The samples were injected into a 5 μ m-pore size Zorbax SB-C18 capillary column (0.5 mm ID by 150 mm; Agilent, CA) at 25°C. The solvent system was composed of a CH₃CN/Water gradient (30 % v/v to 70 % v/v) at a flow rate of 15 μ L/min. For mass analysis, ionization was performed in a negative electrospray ionization mode, ES(-), producing mainly the deprotonated molecular mass ions [M-H]. The mass range was scanned from 40 to 550 Da.

The concentration of CL-20 was followed by HPLC as described earlier. Formic acid (HCOOH), nitrite (NO₂⁻) and nitrate (NO₃⁻) were measured using an HPLC from Waters (pump model 600 and auto-sampler model 717 plus) equipped with a conductivity detector (model 430). The acetonitrile content of the sample was removed under a high flow of helium before injection. The separation was made on a Dionex IonPac AS15 column (2 x 250 mm). The mobile phase was 30 mM KOH at a flow rate of 0.4 mL/min and 40°C. The detection of anions was enhanced by reducing the background with an autosuppressor from Altech (model DS-Plus). Detection limits were 100 ppb for formate and nitrate and 250 ppb for nitrite. Ammonium cation was analyzed using a SP 8100 HPLC system equipped with a Waters 431 conductivity detector and a Hamilton PRP-X200 (250 mm x 4.6 mm x 10 μ m) analytical cation exchange column as described earlier (Hawari *et al.*, 2001). Analysis of N₂ and N₂O was carried as previously described (Fournier *et al.*, 2002). Formaldehyde (HCHO) was analyzed as described by Summers (1990) and Hawari *et al.* (2002).

Accomplishments

Photodegradation of CL-20 in aqueous solutions. We found that photolysis of CL-20 in aqueous (3.5 mg/L) or CH₃CN/water (50 mg/L) solutions (50 % v/v) at 300 nm led to the disappearance of the energetic chemical, but the presence of CH₃CN increased solubility of the energetic chemical and consequently led to the accumulation of sufficient amounts of products that facilitated detection. The removal of CL-20 at 300 nm was accompanied with the concurrent formation and accumulation of nitrite (NO₂⁻), nitrate (NO₃⁻), ammonia (NH₃) and formic acid (HCOOH) (Figure 8). Nitrogen (N₂) and nitrous oxide (N₂O) were detected in trace amounts. Apparently NO₃⁻ was produced from photo-oxidation of NO₂⁻. Bose *et al.* (1998) reported that photo-oxidation of the cyclic nitramine RDX with ozone at 230 nm also produced nitrate.

Photolysis of CL-20 at either 350 nm or with sunlight gave a similar product distribution but at rates much lower than those observed using the Rayonet photoreactor at shorter wavelengths. In dark controls containing CL-20 in either water or CH₃CN/water, no appreciable reduction in the concentration of the energetic chemical was observed within the time course of the experiment.

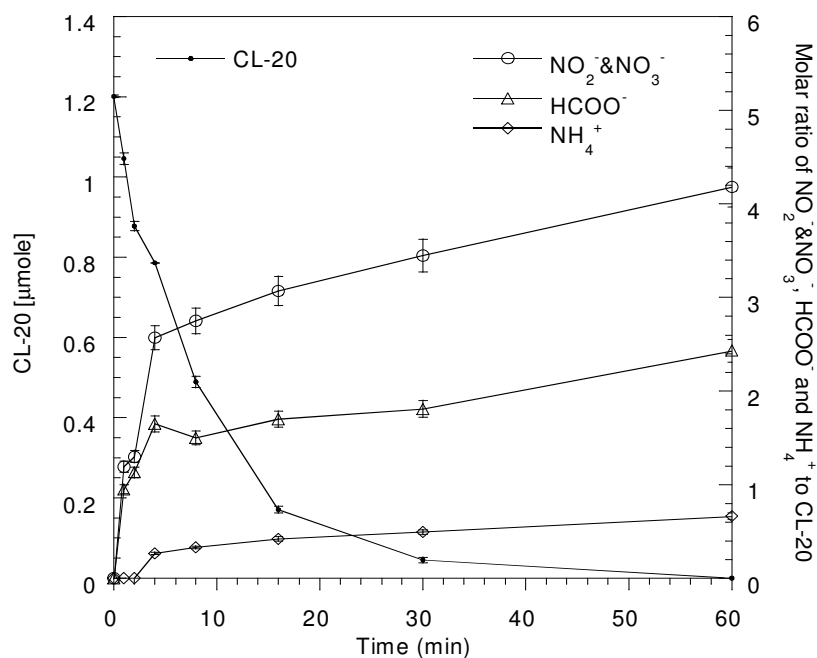


Figure 8 A time course study for the photolysis of CL-20 (1.20 μmole) at 300 nm and 25 $^{\circ}\text{C}$ in CH_3CN /water solutions (50 % v/v) showing formation of nitrite (NO_2^-), nitrate (NO_3^-), ammonium (NH_4^+) and formic acid (HCOOH).

In general we found that the present photodegradation of the caged structure polycyclic nitramine CL-20 was much more rapid than RDX (Hawari *et al.*, 2002). The extreme reactivity of CL-20 as compared to monocyclic nitramines has also been noted during their thermal decomposition (Oxley *et al.*, 1994, Korsounskii *et al.*, 2000). Korsounskii *et al.* (2000) found that the thermal decomposition of HMX and CL-20 in solution proceeded *via* N- NO_2 cleavage with first order rate constants (k) of 1.6×10^{-5} and $4.4 \times 10^{-3} \text{ s}^{-1}$, respectively. The increased ring strain in CL-20 was suggested to accelerate the decomposition of the energetic chemical as compared to the less strained monocyclic nitramines (Oxley *et al.*, 1994).

Intermediates and insight into the mechanisms of initial reactions. Figure 9A is a typical LC/UV chromatogram of a photolyzed mixture of CL-20 in acetonitrile/water solution taken after 30 s of photolysis at 254 nm, and Figures 9 B-E represent the extracted ion chromatogram of CL-20 (I) and various suspected intermediates (II to VI) detected as their adduct mass ($[\text{M} + \text{NO}_3^-]$) or deprotonated molecular ($[\text{M} - \text{H}]^-$) mass ions. The LC/MS (ES-) spectra of CL-20 (I) and its initial intermediates (II to VI) are presented in Figures 10 I-VI, respectively.

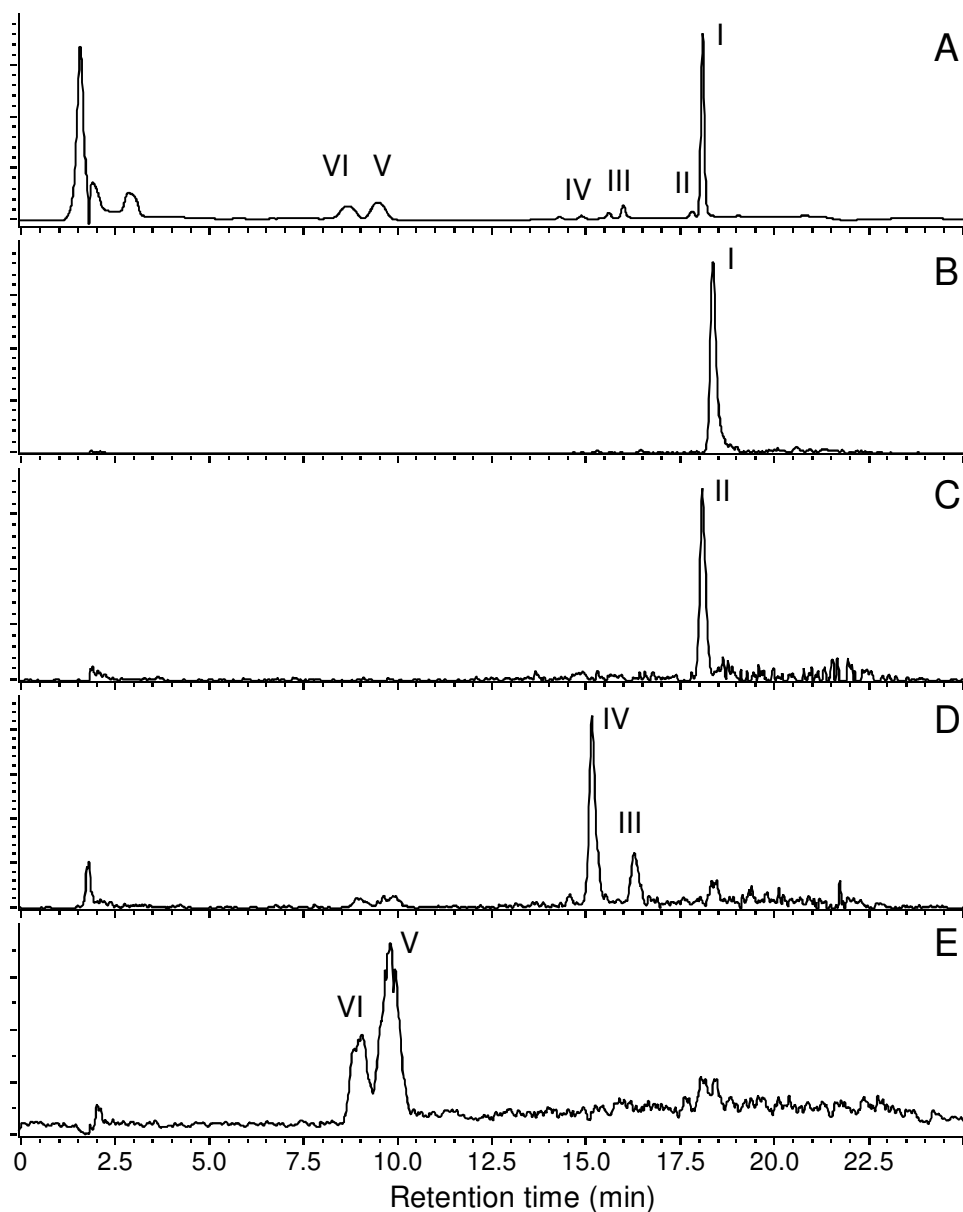


Figure 9 LC/UV (230 nm) (A) and LC/MS (ES-) extracted ion chromatograms of CL-20 and its products after 30 s of photolysis at 254 nm. Extracted mass ion adducts $[M + NO_3^-]$ were 500 Da (B, I), 484 Da (C, II) and deprotonated mass ion $[M - H]$ were 408 Da (D, III and IV) and 345 Da (E, V and VI).

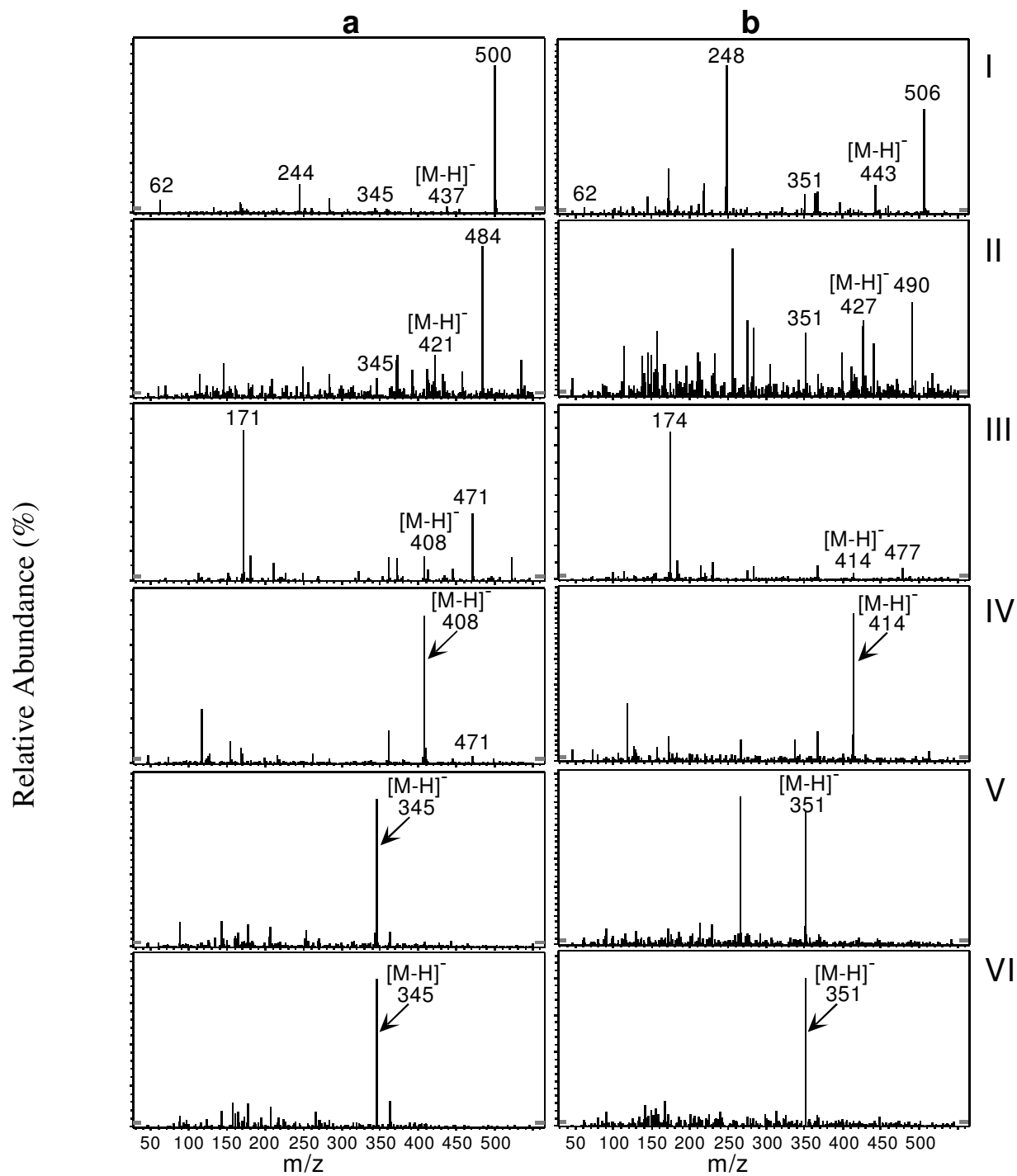


Figure 10 LC/MS (ES-) spectra of CL-20 (I) and its initial intermediates (II to VI) observed during photolysis at 254 nm in MeCN/H₂O (50 % v/v), (a) from non-labeled and (b) from uniformly ring labeled ¹⁵N-[CL-20].

Photorearranged product. Peak I with a retention time (r.t.) of 18.2 min was that of CL-20 which appeared as a nitrate adduct $[M + NO_3^-]$ at 500 Da (Figures 9 B and 10-Ia). Such adducts have been detected during the LC/MS (ES-) analysis of RDX (Zhao and Yinon, 2002), while peaks II to VI represented the intermediate products of I. Peak II, appearing at 18 min., was only detected in trace amounts and showed a $[M - H]$ molecular mass ion at 421 Da, matching a molecular formula of $C_6H_6N_{11}O_{11}$. The mass spectrum of II showed another characteristic mass ion at 484 Da representing the nitrated mass ion adducts $[M + NO_3^-]$. Using the ring labeled ^{15}N -CL-20 the previously detected mass ions (421 and 484 Da) for II were observed at 427 and 490 Da (an increase of 6 amu), respectively, suggesting the involvement of the 6 ring ^{15}N atoms in the intermediate (Figure 10-b). We tentatively identified II as the mononitroso derivative of CL-20 (Fig. 9C and 10-IIa, and b). It has been reported that thermolysis (Shu *et al.*, 2002) and photolysis (Peyton *et al.*, 1999) of RDX can lead to the formation of the nitroso product *via* homolysis of an N- NO_2 bond followed by a secondary reaction that involved the generated N centered species and nitric oxide (NO). Also RDX (Zuckermann *et al.*, 1987; Capellos *et al.*, 1989) and HMX (Zuckermann *et al.*, 1987) have been reported to photodissociate to produce 'OH radical *via* a five membered ring intermediate formed by a transfer of H from a α -CH to one of the two oxygens in a N- NO_2 (1,5-H shift) bond in the molecule. The subsequent loss of OH from the five membered ring would yield a product with a nitroso functionality.

We presume that both rearrangements described above for monocyclic nitramines RDX and HMX might also be applicable to polycyclic nitramines such as CL-20.

The other two small peaks III and IV, which appeared at r.t. of 16.2 and 15.3 min, respectively, each showed a $[M - H]$ at 408 Da matching a molecular formula of $C_6H_7N_{11}O_{11}$ (Figures 9 D and 10-IIIa,IVa). Also a characteristic mass ion at 471 Da appeared for each of the two products (III and IV), representing a nitrate molecular mass ion adducts $[M + NO_3^-]$. When we photolyzed the ring labeled ^{15}N -[CL-20] the previously detected mass ions for III and IV were observed at 414 Da (an increase of 6 amu), suggesting once again the presence of the 6 ^{15}N ring atoms in each of the two intermediates (Figure 10b). We tentatively identified the intermediates as either a photorearranged carbinol (III) or a rearranged ketone (IV) formed *via* initial loss of 1NO from CL-20 and the gain of 1H from water (Figure 11). Bulusu *et al.* (1970) reported similar rearrangements during electron impact - spectrometric analysis of cyclic nitramines.

When photolysis was conducted in either $H_2^{18}O$ or D_2O the 408 Da intermediate was observed at 408 and 409 Da, respectively, suggesting that water acted as H (or D) donor during its reaction with CL-20 (Figure 11). The presence of $^{18}O_2$ during photolysis did not affect the detected mass ions, but we detected the labeled ^{18}O in nitrate ($N^{18}O^{16}O_2^-$) only.

Cleavage of N- NO_2 . The two LC/MS peaks V and VI, with retention times at 9.0 and 9.9 min, respectively, showed the same $[M - H]^+$ at 345 Da and matched a molecular formula of $C_6H_6N_{10}O_8$ (Figures 9 E and 10-V,VI). Once again when we photolyzed the ring labeled ^{15}N -[CL-20] the two intermediates V and VI showed their $[M-H]$ at 351 Da (an increase of 6 amu), suggesting the involvement of 6 ^{15}N atoms in the formation of each product (Figure 10b). We tentatively identified V and VI as a pair of isomers of the diene products formed after the successive loss of two nitro groups from CL-20 (Figure 12).

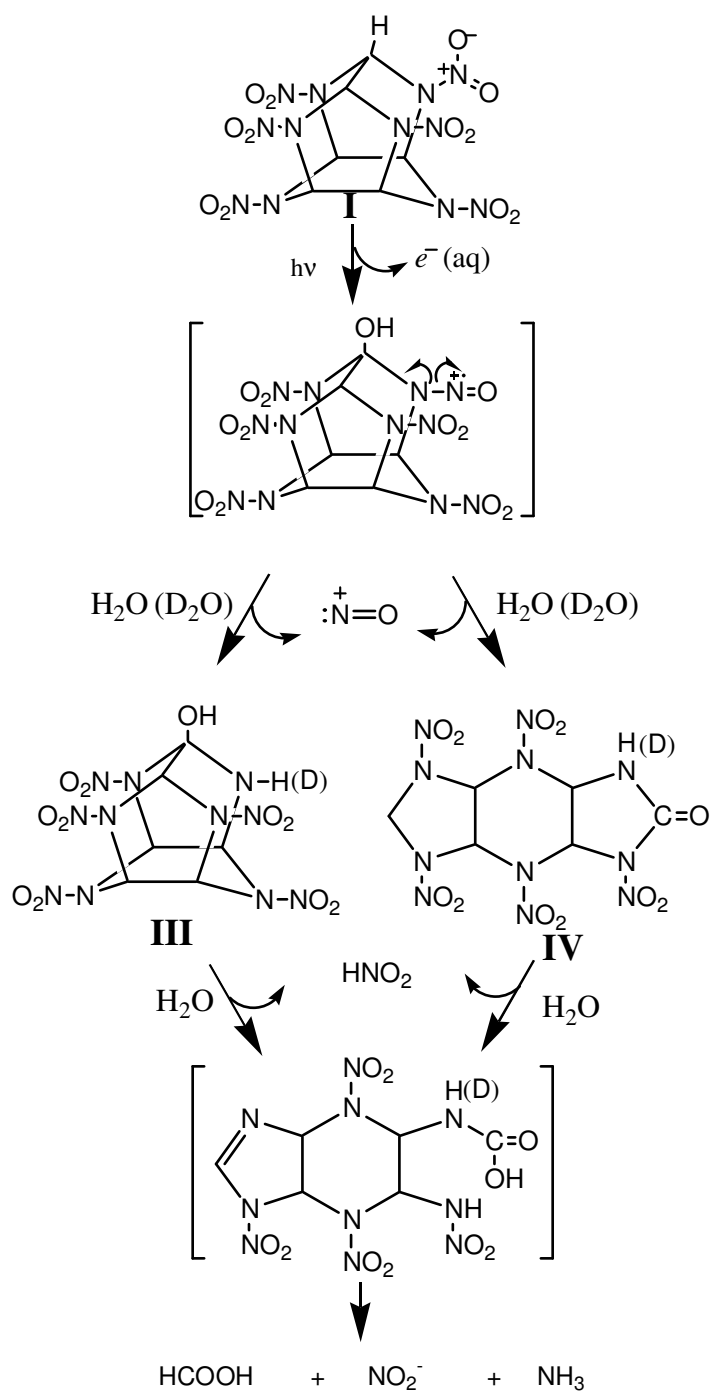


Figure 11 Postulated photorearrangement route of CL-20 at 300 nm in CH₃CN/water (50 % v/v). Bracketed compounds were not observed.

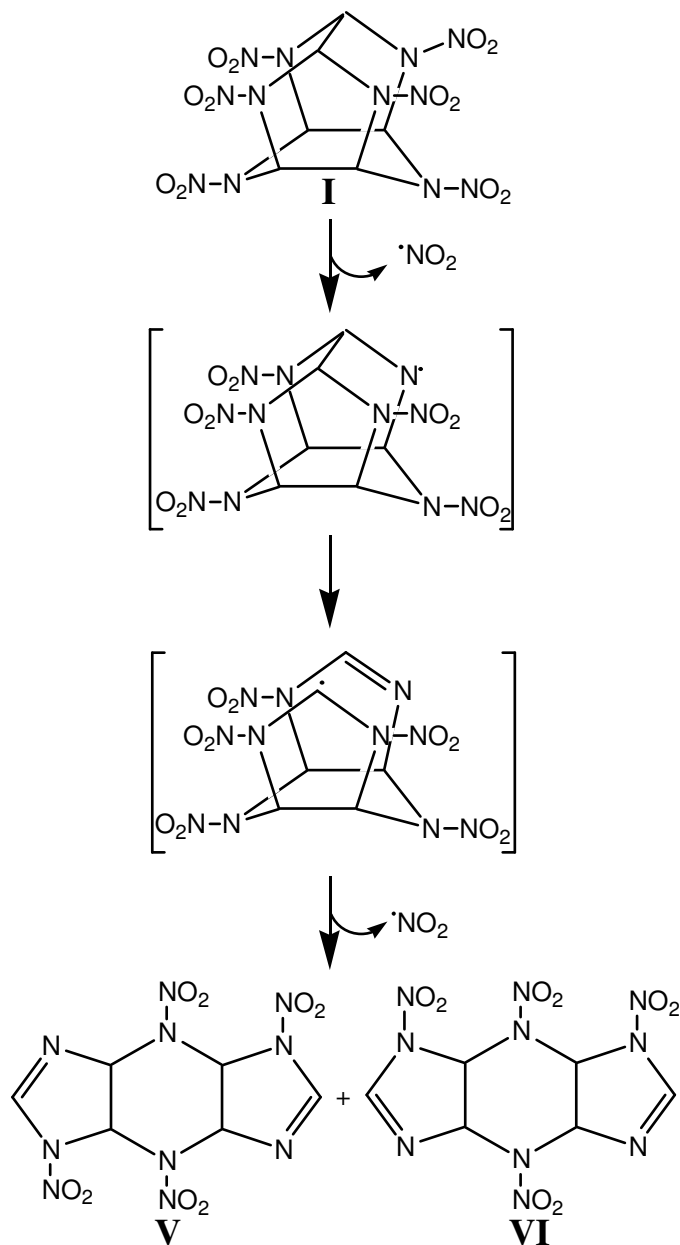


Figure 12 Postulated photodenitration route of CL-20 at 300 nm in an aqueous acetonitrile solution. Bracketed compounds were not observed.

We also detected an intermediate with a r.t. at 2.0 min. and a $[\text{M} - \text{H}]^-$ at 381 Da with a characteristic mass ion fragment at 190 Da, matching a molecular formula of $\text{C}_6\text{H}_{10}\text{N}_{10}\text{O}_{10}$. When conducting photolysis of CL-20 in either H_2^{18}O or D_2O the 381 Da products appeared at 385 Da and its mass ion fragment appeared at 192 Da, suggesting that 2 H_2O molecules reacted

with the former product (V) (Figure 13). We presume that both rearrangements described above for monocyclic nitramines RDX and HMX might also be applicable to polycyclic nitramines such as CL-20.

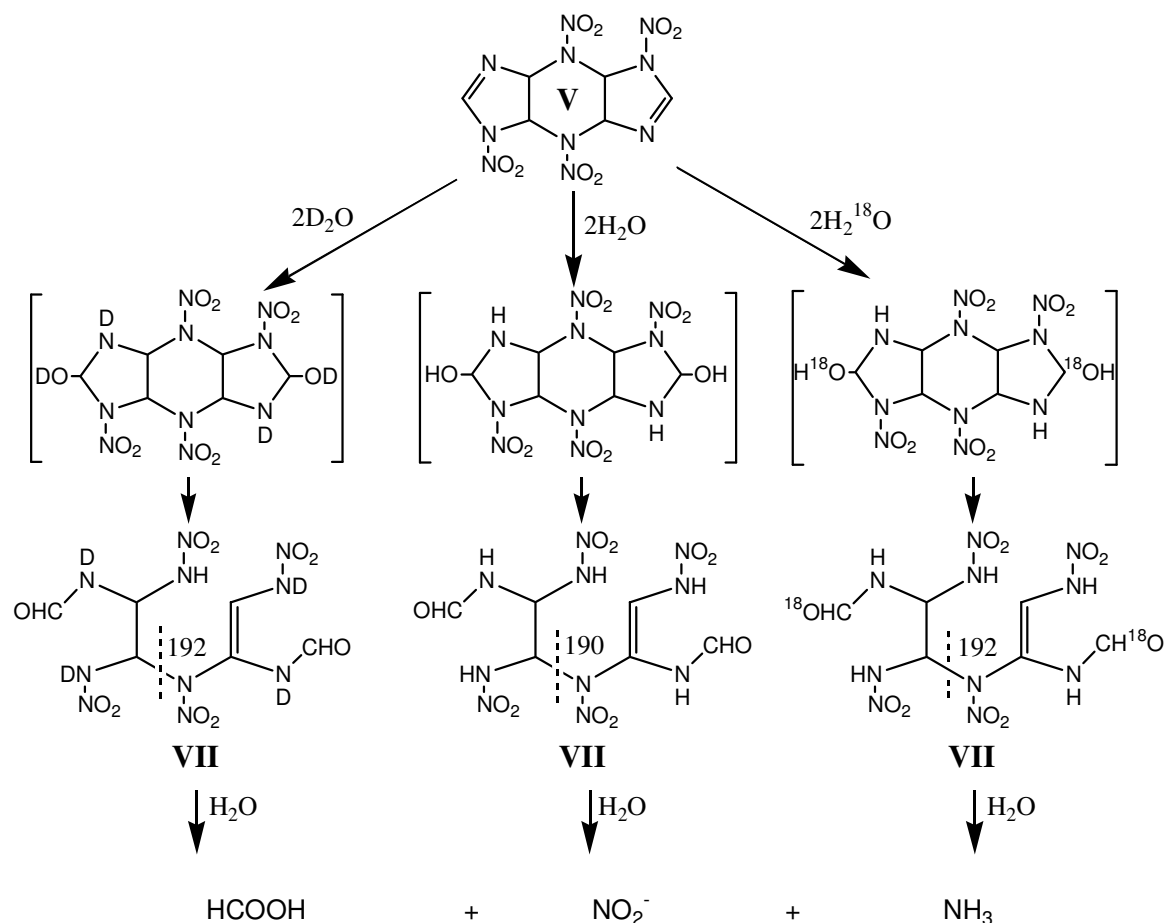


Figure 13 Postulated secondary decomposition routes following initial denitration of CL-20. Bracketed compounds were not observed.

When photolysis was repeated in the presence of $^{18}\text{O}_2$ no ^{18}O was detected in either intermediate. The intermediate was tentatively identified as the hydrolytic ring cleavage product (VII) of the diene V (or VI) (Figure 13). Previously we found that following RDX photodenitration H_2O reacts with the generated enamine bond ($-\text{C}=\text{N}-$) to produce an unstable carbinol that dissociates rapidly in water to HCHO , N_2O and 4-nitro-2,4-diazabutanal (Hawari *et al.*, 2002). We thus suggest that a similar pathway might be responsible for the formation of VII during the photolysis of the polycyclic nitramine CL-20 (Figure 13).

Reaction stoichiometry and regioselectivity of denitration. Figure 8 shows that the initial disappearance of the energetic chemical at 300 nm ($0.168 \mu\text{mol} \cdot \text{min}^{-1}$) was accompanied with the

formation of NO_2^- ($0.237 \mu\text{mol}\cdot\text{min}^{-1}$), HCOOH ($0.219 \mu\text{mol}\cdot\text{min}^{-1}$) and NH_3 ($0.011 \mu\text{mol}\cdot\text{min}^{-1}$). The formation of NO_2^- and HCOOH was concurrent with the disappearance of CL-20, but NH_3 seemed to appear only after 5 min of photolysis. The delay in the detection of NH_3 as shown in Figure 8 suggested the involvement of an inner aza N in its formation which first necessitated ring cleavage following denitration.

After 16 h, the reaction stoichiometry for the reacted CL-20 ($1.2 \mu\text{mol}$) was $6.11 \mu\text{mole}$ for NO_2^- and NO_3^- , $1.65 \mu\text{mole}$ for NH_3 and $6.34 \mu\text{mole}$ for HCOOH , suggesting that approximately 5 of 6 peripheral NO_2 and 5.3 carbon atoms in CL-20 were detected in the form of NO_2^- and HCOOH , respectively. The remaining nitrogen (mainly ring aza) was involved in the production of N_2O ($0.267 \mu\text{mol}$), N_2 (trace) and unidentified products.

The rapid initial formation of nitrite and most importantly HCOOH was more likely attributed to an initial denitration step followed by a rapid ring cleavage possibly at the elongated C-C bond bridging the two cyclopentane rings (Figure 12). We suggested that following homolysis of an N- NO_2 bond, the resulting N-centered free radical would undergo a rapid rearrangement to get rid of the strained rigid structure with the loss of another $\cdot\text{NO}_2$ radical to give the diene V (or its isomer VI) (Figure 12). Patil and Brill (1991) reported that following N- NO_2 homolytic cleavage of CL-20 the molecule could undergo rapid ring opening to rid itself from the strained rigid structure. The diene V (Figure 12) has two reactive allylic N- NO_2 bonds that might also undergo rapid homolytic cleavage with light, supporting the rapid release of 4 NO_2^- as nitrite ion during the first 10 min of photolysis (Figure 8). Several researchers studied the regioselectivity of cleaving the N- NO_2 bond during photolysis of CL-20 in the solid phase (Pace, 1991; Ryzhkov and McBride, 1996) and concluded that one of the N- NO_2 bonds located at one of the two five-member rings in CL-20 are preferentially cleaved. The formation of NO_2^- during photolysis of CL-20 can be achieved by either concerted elimination of HONO or direct homolysis of an N- NO_2 bond. Such reactions have been frequently reported to occur during photolysis of RDX and HMX (Zuckermann *et al.*, 1987; Capellos *et al.*, 1989; Peyton *et al.*, 1999; Hawari *et al.*, 2002). The energy associated with 254 and 300 nm is 472 and 400 kJ mol^{-1} , respectively, and therefore either wavelength should be sufficient to cleave the N- NO_2 bond(s) (BDE $204.9 \text{ kJ mol}^{-1}$; Behrens and Bulusu, 1991) in CL-20.

The secondary reactions responsible for the formation of products such as HCOOH , NH_3 and N_2 are not clear yet. However, we presumed that the decomposition of the unstable diols (VII) (Figure 13) of the diene V (or its isomer VI) would lead to their formation. Likewise the hydrolytic decomposition of either intermediate III or IV (Figure 11) could lead to HCOOH , NH_3 and NO_2^- . Interestingly, when we hydrolyzed CL-20 at pH 10 we found that the removal of the nitramine was accompanied by the formation of 2, 1 and 0.5 molar equivalents of NO_2^- , NH_3 and HCOOH , respectively (Balakrishnan *et al.*, 2003). We also showed that a denitrifying bacterium (*Pseudomonas* strain FA1) could degrade the energetic chemical *via* initial enzymatic denitration to produce nitrite, nitrous oxide and HCOOH (Bhushan *et al.*, 2003a). The striking similarity in the product distribution of the present photolysis study and those of the alkaline hydrolysis and biodegradation of CL-20 suggests that initial denitration whether chemical, photochemical or enzymatic is sufficient to decompose the energetic chemical to produce almost similar products.

Photodegradation of CL-20 with sunlight. Quartz tubes (20 mL) charged with 15 mL of an aqueous solution of CL-20 (2.8 mg/L) were placed perpendicular to soil and exposed to sunlight during daytime and kept inside overnight. At the end of each exposure day, the number of

exposure hours was reported along with the average temperature and the UV index of the day, and an aliquot of solution was collected for analysis of CL-20 by HPLC. Two of the tubes were covered with white paper and subjected to same exposure periods, for controls. Experiments were conducted in duplicate.

Photolysis of CL-20 with sunlight was tested in October, in Montreal (QC, Canada), when temperatures do not exceed 15°C to avoid thermal decomposition (Monteil-Rivera *et al.*, 2004). Data presented in Figure 14 clearly indicate degradability of CL-20 upon exposure to sunlight.

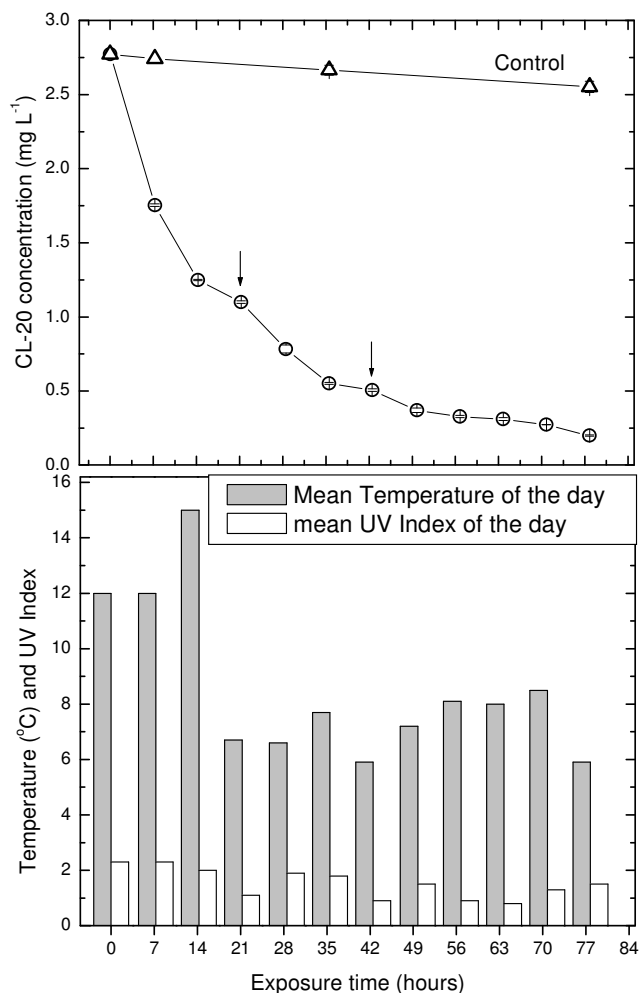


Figure 14 Photolysis of aqueous solutions of CL-20 with sunlight. Error bars represent standard deviation of duplicate experiment. Average temperature and average UV index are also reported for each day of exposure to interpret the variation of rates in the degradation.

While a loss of 8 % was measured in the covered controls after almost 80 h of exposure, 93 % of CL-20 disappeared in the uncovered tubes during the same period. A decrease of the degradation rate was noticed at the end of days 3 (21 h) and 6 (42 h). The decrease in degradation

rate coincided with a lower mean UV index. Variations of both the temperature and the UV index over the exposure time prevented us from applying a kinetics model to the data. However, the initial degradation rate was calculated and CL-20 was found to decompose at a rate of $2.1 \mu\text{g h}^{-1}$ (4.8 nmol h^{-1}). With the aim to limit thermal decomposition, the period of the year selected to run this experiment gave rise to low UV indexes (1 to 3) on a scale that can exceed 11. We demonstrated degradability of CL-20 despite prevailing cloudy days in October. We thus expect that during summer and/or in regions that are more UV-exposed than Montreal, photolysis of CL-20 would occur at a higher rate.

Conclusion

Photolysis of CL-20 at 300 nm led to rapid decomposition and to the formation of nitrite and HCOOH in almost stoichiometric amounts after 16 h. Reaction at shorter wavelengths (λ_{254} nm) was much more rapid, but reaction at longer wavelengths (λ_{350} nm or sunlight) was much slower. Following the detection of several transient intermediates we suggested that initial photorearrangement and homolysis of one of the *N*-NO₂ bond(s) might have been responsible for the decomposition of CL-20. However, we were unable to quantify the relative importance of each route in the decomposition process. The discovery of several CL-20 intermediates and the knowledge gained on their reactions should provide insight into the mechanism of CL-20 photodecomposition and thus help predict the environmental fate and impact of the energetic chemical. Future experiments conducted with ¹⁵N-labeled CL-20 will be very useful to understand the secondary reactions routes leading to HCOOH and NH₃.

IX Degradation of CL-20 by iron (0)

This work was published in;

Balakrishnan VK, Monteil-Rivera F, Halasz A, Corbeanu A, Hawari J. (2004) *Decomposition of the polycyclic nitramine explosive, CL-20, by Fe⁰*. *Environ. Sci. Technol.* 38: 6861-6866, attached at the end of the present report.

Introduction

With the anticipated wide use of the emerging explosive CL-20 and the recent demonstration of its toxicity towards certain soil invertebrates (Robidoux *et al.*, 2004) there is the potential for soil and groundwater contamination. In this context, applying cost effective remediation technologies to remove the chemical from contaminated environments may become necessary. Earlier we showed that CL-20 was highly unstable in alkaline solutions (Balakrishnan *et al.*, 2003) but applying alkaline hydrolysis on site by changing soil pH may disturb local populations and therefore cause some damages. We thus decided to investigate a different technology that could be applied in a contaminated site without generating excessive adverse effects.

Zerovalent iron has been widely used to degrade a variety of oxidized chemicals. For instance, Fe⁰ was found to degrade inorganic compounds like nitrate ion (Alowitz and Scherer, 2002; Westerhoff and James, 2003; Su and Puls, 2004), chlorinated solvents such as perchloroethylene (PCE) and carbon tetrachloride (CCl₄) (Helland *et al.*, 1995; Scherer *et al.*, 2000; Rosenthal *et al.*, 2004), emerging contaminants in drinking water like N-Nitrosodimethylamine (NDMA) (Gui *et al.*, 2000; Odziemkowski *et al.*, 2000), and munitions wastes such as trinitrotoluene (TNT) (Hundal *et al.*, 1997). Recent studies showed that the monocyclic nitramine explosive, RDX, could be readily degraded by Fe⁰ (Hundal *et al.*, 1997; Singh *et al.*, 1998, Oh *et al.*, 2001) or Fe^{II} (Gregory *et al.*, 2004), and that permeable reactive barriers containing zerovalent iron may be effective for remediation of RDX-contaminated sites (Hundal *et al.*, 1997; Singh *et al.*, 1998, Comfort *et al.*, 2003). With six N-NO₂ groups, CL-20 is also a good candidate for transformation *via* reductive processes and zerovalent iron could be seen as a potential treatment technology applicable to the energetic chemical. In the present study, Fe⁰ was employed to degrade CL-20 and LC/MS was used to detect new degradation products and therefore gain insight into its degradation routes. Understanding the degradation pathways of CL-20 will contribute to the development of effective remediation strategies.

Material and Methods

Chemicals. ε-CL-20, [¹⁵N]-amino labeled CL-20, and [¹⁵N]-nitro labeled CL-20 were provided by A.T.K. Thiokol Propulsion (Brigham City, UT). Fe⁰ powder (100 mesh) having a surface area of 0.9821 m²/g (determined by BET analysis, Micromeritics, Norcross, GA, USA) and oxygen and carbon contents of 0.54 and 0.28 %, respectively, was obtained from Anachemia Chemicals (Montreal, QC, Canada), as was glycolic acid. Glyoxal (ethanedial), O-(2,3,4,5,6-pentafluorobenzyl)hydroxylamine hydrochloride (PFBHA), ferrozine (3-(2-pyridyl)-5,6-

diphenyl-1,2,4-triazine-p,p'-disulfonic acid, monosodium salt), and iron (II) sulfate were obtained from Aldrich Chemicals. All other chemicals used in this study were of reagent grade, and used without further purification.

Degradation of CL-20 by Fe^0 . A series of 20 mL vials wrapped in aluminum foil and containing 10 mL of deionized water and 0.1 g Fe^0 powder were sealed with Teflon coated serum caps and sparged with argon for 20 minutes. The redox potential of the solution was occasionally measured after sparging and found to be -225 mV, demonstrating the anaerobic atmosphere of the medium. An aliquot of CL-20 stock solution (1 % w/v) prepared in acetonitrile was then added to the vials, giving an initial amount of CL-20 of $2.4 \mu\text{mol}$. The initial CL-20 concentration (100 mg L^{-1}) was kept well in excess of its maximum water solubility (ca. 3.6 mg L^{-1} at 25°C (Monteil-Rivera *et al.*, 2004)) in an attempt to generate sufficient amounts of reaction intermediates to allow detection. The vials were agitated at 50 rpm in a rotary shaker.

The following eight controls were prepared as described above: 1) Fe^0 , CL-20, water, in air; 2) Fe^0 , CL-20, dry acetonitrile, under argon; 3) Fe^0 , CL-20, dry acetonitrile and H_2 gas; 4) $Fe(SO_4)$, CL-20, water, under argon; 5) Fe^0 , $HCOO^-$, water, under argon; 6) Fe^0 , glyoxal, water, under argon; and 7) Fe^0 , NO_2^- , water, under argon; 8) Fe^0 , N_2O , water, under argon.

Abiotic degradation of CL-20 in SAC soil (pH 8.1). Gamma-irradiated SAC soil (1.5 g) was added to 10 mL of an aqueous solution of CL-20 ($500 \mu\text{g}$ or $1.14 \mu\text{mol}$) in a 60-mL serum bottles. The bottles were sealed with Teflon coated septa and aluminum caps and covered with aluminum foil. The soil slurries were then shaken (400 rpm) at room temperature. At a given time, three samples were sacrificed and 10 mL of acetonitrile were added to the whole reaction mixture to solubilize any undissolved CL-20. The resulting solution was filtered through a $0.45\text{-}\mu\text{m}$ syringe filter and CL-20 was analyzed by HPLC connected to a photodiode array (PDA) detector as described previously (Monteil-Rivera *et al.*, 2004). Degradation products were analyzed as described in section VI.

Analytical Techniques. A gas-tight syringe was used to sample gaseous products from the headspace for subsequent analysis of nitrous oxide by GC-ECD as described by Sheremata and Hawari (2000b). Meanwhile, at the end of each reaction 10 mL of acetonitrile (CH_3CN) were added to the whole reaction mixture to solubilize any undissolved CL-20. The resulting solution was filtered through a $0.45\text{-}\mu\text{m}$ syringe filter and CL-20 was analyzed by HPLC connected to a photodiode array (PDA) detector as described previously (Annual report 2002; Monteil-Rivera *et al.*, 2004).

Analyses of nitrite (NO_2^-), nitrate (NO_3^-), formate ($HCOO^-$), and glycolate ($HOCH_2COO^-$) were performed by ion chromatography (IC) equipped with a conductivity detector after evaporating acetonitrile and removing the glyoxal by precipitation with *O*-(2,3,4,5,6-pentafluorobenzyl)hydroxylamine hydrochloride (PFBHA). The Waters IC system consisted of a Model 600 Pump, a Model 717 Autosampler Plus, and a Model 430 Conductivity Detector. Separation was performed on a DIONEX IonPac AS15 column ($2 \times 250 \text{ mm}$). The mobile phase was 30 mM KOH for nitrite and nitrate and 5 mM KOH for formate and glycolate, at a flow rate of 0.4 mL/min and 40°C . The detection of anions was enhanced by reducing the background with a Model DS-Plus autosuppressor from ALTECH (Guelph, ON, Canada). Ammonia was determined by ion chromatography (IC). The IC system consisted of a resin based Hamilton

PRP-X200 cation chromatography column (250 mm \times 2.1 mm), a TSP Model P4000 pump, an AS3000 Autosampler, and a Waters Millipore Model 431 conductivity detector. The mobile phase was 4 mM nitric acid with 30% methanol at a flow rate of 0.75 mL/min at 40°C.

In order to provide insight into the role of iron in catalyzing CL-20 degradation, the presence of Fe²⁺ and Fe³⁺ was determined using Stookey's Ferrozine method (Stookey, 1970). Briefly, 100 μ L of a 0.05 M solution of ferrozine was added to 2 mL of the filtered CL-20 / Fe⁰ reaction mixture, and heated to ca. 80°C for 10 min. The solution was cooled to 2 °C and ammonium hydroxide/ammonium acetate buffer (pH 9) was added to achieve a solution pH of 6. The absorbance of the resulting magenta colored solution of Fe^{II} complex was measured at 562 nm, and the concentration of Fe^{II} in the sample was determined by comparison against a standard curve prepared using ferrous ammonium sulfate. To determine Fe^{III}, hydroxylamine hydrochloride (10 % v/v) was added to the filtered CL-20/Fe⁰ reaction mixture in order to reduce Fe^{III} to Fe^{II}. The converted Fe^{II} was then determined by the same procedure, and [Fe^{III}] was calculated by subtracting the amount of Fe^{II} found in the CL-20/Fe⁰ reaction mixture prior to the addition of hydroxylamine hydrochloride from the amount of Fe^{II} found after the addition of the amine.

Glyoxal (CHO-CHO) was determined as its derivatized product with PFBHA (Bao *et al.*, 1998). A solution of PFBHA (15 g L⁻¹; 20 μ L) was added to 0.5 mL of aqueous sample and the pH was adjusted to 3 with 5% HCl. After 1 h of reaction in the dark and at room temperature, 1 mL of acetonitrile was added to the mixture, and the resulting solution was analyzed by HPLC/UV-MS. The derivatized compound was analyzed in the positive electrospray mode (ES+) using a Micromass bench-top single quadrupole mass detector attached to a Hewlett Packard 1100 Series HPLC system equipped with a DAD detector. Separation was performed on a Supelcosil C8 column (25 cm \times 4.6 mm, 5 μ m) at 35°C using 1 mL/min of acetonitrile/water gradient (60 % of acetonitrile to 90 %, 10 min, 90% to 60%, 2 min, and 60 %, 6 min). The identity of the derivatized compound was confirmed by comparing the mass spectrum obtained with that obtained with glyoxal and quantification was done by UV at 250 nm.

Intermediate products of CL-20 were analyzed by LC/MS using a Bruker bench-top ion trap mass detector attached to a Hewlett Packard 1100 Series HPLC system equipped with a DAD detector. The samples were injected into a 5 μ m-pore size Zorbax SB-C18 capillary column (0.5 mm ID by 150 mm; Agilent, CA) at 25°C. The solvent system was composed of a CH₃CN/H₂O gradient (30 to 70 % v/v) at a flow rate of 15 μ L/min. For mass analysis, negative electrospray ionization was used to produce deprotonated molecular ions [M-H]⁻ or nitrate adducts ions [M+NO₃]⁻. The mass range was scanned from 40 to 550 Da. The identity of the intermediates was confirmed using [¹⁵N]-amino and [¹⁵N]-nitro labeled CL-20.

Nitrogen gas (¹⁵N¹⁴N and ¹⁵N¹⁵N) and nitrous oxide (¹⁵N¹⁴NO and ¹⁵N¹⁵NO) were analyzed using a Hewlett-Packard 6890 GC (Mississauga, ON, Canada), coupled with a 5973 quadrupole mass spectrometer. A GS-gas Pro capillary column (30 m \times 0.32 mm) (J & W Scientific, Folsom, CA) was used under splitless condition. The injector and mass spectrometer interface (MSD) were maintained at 150°C and 250°C, respectively. The column was set at -25°C for 1.5 min and then raised to -10°C at a rate of 10°C/min which was held for 5 min. The MSD was used in the scan mode (electron impact) between 10 to 50 Da.

Accomplishments

Degradation of CL-20 with iron. Figure 15 shows that CL-20 (2.4 μmol) completely degraded within 10 h of reaction with Fe^0 (under anaerobic conditions) to form HCOO^- , NO_2^- , NH_4^+ , and N_2O . These products are the same as those reported in previous studies on the alkaline hydrolysis (Balakhishnan *et al.*, 2003), photolysis (Hawari *et al.*, 2004), and microbial degradation (Bhushan *et al.*, 2003a) of CL-20. Formaldehyde, which is a common degradation product of RDX and HMX, was not detected here. However, while RDX and HMX are cyclic oligomers of methylene nitramine, $\text{CH}_2\text{-NNO}_2$, CL-20 contains the repeating unit CH-NNO_2 where each carbon atom is bound to another carbon (Figure 1). Moreover, whereas RDX and HMX are both synthesized from formaldehyde, glyoxal (CHO-CHO) is used as the starting material in the synthesis of CL-20 (Wardle *et al.*, 1996; Sikder *et al.*, 2002). We thus investigated the presence of glyoxal as a possible degradation product of CL-20.

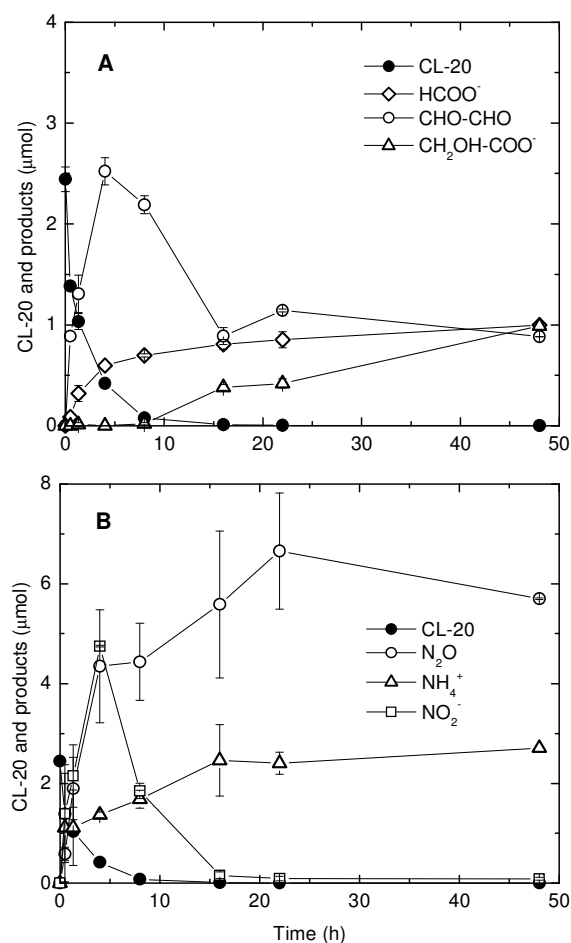


Figure 15 Time course of the Fe^0 -mediated anaerobic degradation of CL-20 in water. (A) Carbon-containing compounds. (B) Nitrogen-containing compounds. Data points are the mean and error bars the average deviation ($n = 2$).

Figure 16 shows the chromatograms obtained upon separately derivatizing the reaction mixture and a reference standard of glyoxal with PFBHA. The exact match between the sample and the standard conclusively proved that glyoxal was a product of CL-20 degradation, and to the best of our knowledge, this is the first such report. Glyoxal was analyzed throughout the reaction (Figure 15A) as the derivatized product of PFBHA.

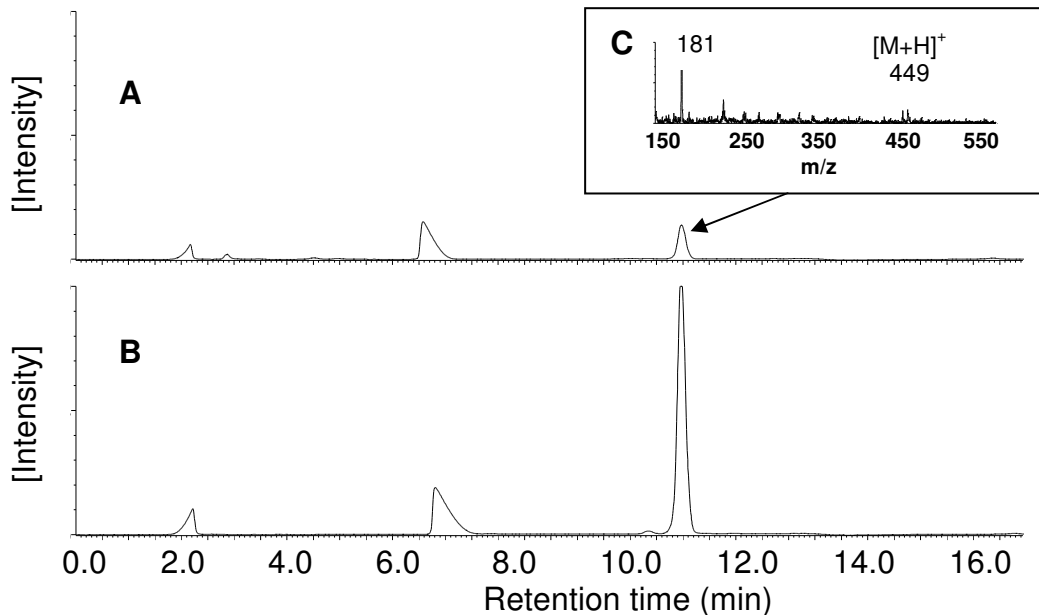


Figure 16 LC/UV chromatograms at 250 nm showing the detection of glyoxal. (A) CL-20/Fe⁰ reaction solution after derivatization. (B) Glyoxal standard solution after derivatization with pentafluorobenzylhydroxylamine. (C) MS (ES+) obtained for both the standard and the sample.

Since Figure 15A clearly shows that glyoxal (CHOCHO) was a transient species, we analyzed for its potential decomposition product(s). It has been reported that glyoxal in the presence of multivalent metal ions including Fe^{II} can be transformed into glycolic acid (Kiyoura and Kogure, 1997). A control containing glyoxal (2.67 μ mol) and iron (0.1 g) led to the production of glycolic acid (CH₂OHCOOH) (1.16 μ mol), demonstrating the transformation of glyoxal into glycolic acid under the present conditions. As a consequence, glycolic acid was also measured in the reaction medium (Figure 15A). Unlike glyoxal, formate did not react with iron under the current conditions.

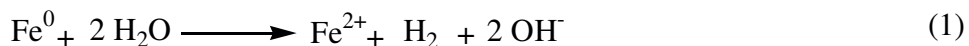
Figure 15B summarizes the nitrogen-containing products of CL-20. Of the nitrogen-containing products N₂O and ammonia (detected as NH₄⁺) appeared to be stable as demonstrated by stirring Fe⁰ (0.1 g) with 2 μ mol of NH₄Cl or 0.11 μ mol of N₂O. The transformation of nitrite after 16 h is consistent with the findings of other researchers who observed that Fe⁰ could chemically reduce nitrite to ammonium (Scherer *et al.*, 2000; Kielemoes *et al.*, 2000; Alowitz

and Scherer, 2002). An experiment was specifically designed to evaluate the transformation of nitrite with iron under the present conditions. After contacting Fe⁰ (0.1 g) with an aqueous solution of nitrite (2.4 µmol) for 16 h, NH₄⁺ (0.6 µmol), N₂O (0.12 µmol), and N₂ (not quantified) were observed along with unreacted nitrite (0.9 µmol). A fraction of the ammonium and nitrous oxide detected at the end of the reaction likely resulted from the reduction of nitrite ions, as supported by the detection of ¹⁵N¹⁵NO (46 Da) when using ¹⁵N-nitro labeled CL-20.

After 4 h of reaction, 83 % of CL-20 was transformed to give a carbon mass balance of 46.5 % that was distributed between HCOO⁻ (formate, 4.9 %) and CHO-CHO (glyoxal, 41.6 %). Analysis of the reaction medium by LC/MS at this time confirmed the presence of several intermediates in the system (see next section). At the end of the reaction (48 h) the carbon mass balance decreased to 32.4 % and was distributed as follows: HCOO⁻ (formate, 6.8 %), CHO-CHO (glyoxal, 12.1 %), and CH₂OH-COO⁻ (glycolate, 13.5 %). The amount of glyoxal significantly decreased between 4 and 48 h to produce glycolate. However, the decrease in total C mass balance shows that glycolate was not the only product of glyoxal. The latter is a highly reactive dialdehyde (Vyas *et al.*, 2001) that can readily condense with alcohols and amines, which are suspected products in the system.

As for the nitrogen mass balance, it was 60.7 % after 4 h, distributed amongst NO₂⁻ (19.6 %), N₂O (35.5 %), and NH₃ (5.6 %). The use of [¹⁵N]-amino labeled CL-20 led to the detection of a mass ion of 29 Da corresponding to ¹⁵N-¹⁴N, confirming that N₂ was a product of CL-20, but we were unable to quantify it.

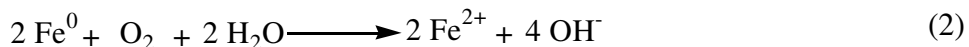
Insights into the role of Fe⁰ in initiating the decomposition of CL-20. Oxidation of Fe⁰ to Fe^{II} in water is concomitant with a release of hydroxide ions in solution (Equation 1), so that one might expect a pH increase as the reaction evolves. Since hydrolysis of CL-20 has been observed under alkaline conditions (Balakrishnan *et al.*, 2003), a possible initiator for CL-20 decomposition was the OH⁻ resulting from oxidation of iron. The pH was thus measured at the end of each reaction and was found to remain constant at approximately 5.5, even after 120 h of reaction. The formation of formic and glycolic acids as products of CL-20 may be responsible for the pH stabilization. Hydrolysis of CL-20 was therefore excluded as a potential degradation route.



In the Fe⁰-H₂O system, there are three main reductants present upon the anaerobic corrosion of the metal: Fe⁰, Fe^{II}, and H₂ (Matheson and Tratnyek, 1994). Neither iron powder in dry CH₃CN nor iron powder in dry CH₃CN in the presence of H₂ were able to degrade CL-20 (data not shown), suggesting that Fe⁰ or H₂ would not be responsible for CL-20 decomposition. This observations added to the formation of Fe^{III} upon reduction of CL-20 led us to attribute the reductive process to Fe^{II}. For instance, we found that after 6 h of contact between CL-20 and Fe⁰ approximately 5 ppm (0.89 µmol) of Fe^{III} was detected. By contrast, an oxygen-free control solution containing only Fe⁰ and water (*i.e.* no CL-20) produced a negligible quantity of Fe^{III} ion in the same time span. When CL-20 (2.3 µmol) was mixed with FeSO₄ (3.56 µmol, 200 ppm in Fe^{II} as measured by Stookey's method) degradation did not occur, indicating that Fe²⁺ ions in solution were not responsible for the degradation of CL-20. Since dissolved Fe²⁺ ion had no

impact on CL-20 degradation, the e⁻ transfer to the energetic chemical that caused its degradation must have involved surface-bound Fe²⁺. The involvement of surface bound Fe²⁺ was noted earlier for the destruction of a wide variety of environmental organic contaminants including CCl₄ (Helland *et al.*, 1995; Scherer *et al.*, 2000), trifluralin (Klupinski and Chin, 2003), nitrobenzenes (Klausen *et al.*, 1995; Charlet *et al.*, 1998) and the nitramine, RDX (Gregory *et al.*, 2004).

Note that in the presence of oxygen, Fe⁰ can still form Fe²⁺ (equation 2), but the electrons generated from Fe²⁺ oxidation are trapped by triplet oxygen, ^TO₂ (a diradical in the ground state), instead of initiating CL-20 destruction. As a result, CL-20 degradation was not observed when the experiment was conducted in air.



Thus, in the absence of air, the oxidation of surface-bound Fe^{II} to Fe^{III} and the subsequent transfer of a single electron to CL-20 were likely responsible for the degradation of the energetic chemical. The resulting CL-20 anion radical is expected to rapidly denitrate to undergo spontaneous decomposition as observed by Bhushan *et al.* (2004b) when challenging CL-20 with salicylate 1-monooxygenase (see section XI). According to the crystal structure analysis of CL-20 (Zhao and Shi, 1996), the elongated C-C bond at the top of the molecule (bond denoted *a* in Figure 1) is the weakest bond and should cleave first.

Potential initial decomposition routes of CL-20

Note: Throughout the present report, structures of CL-20 intermediates are tentatively identified based on LC/MS data and our previous experience in analyzing nitramines compounds. However, isomeric structures could also be possible.

Several intermediates were observed during biodegradation (Bhushan *et al.*, 2004a & 2004b) and photolysis (Hawari *et al.*, 2004) of CL-20. Among them, the imine (**Ia**) and its dicarbinol (**II**) intermediates with retention times of 8.6 and 14.0 min, respectively (Figure 17A), and [M-H]⁻ ions at 345 and 381 Da, respectively (Figure 17B), also appeared when reacting CL-20 with Fe⁰. Imine **Ia** can be readily hydrated in water (March, 1985) and form the α-hydroxyalkylnitramine **II**. The resulting α-hydroxynitramines are unstable (March, 1985), and are expected to undergo a rapid ring cleavage (across the O₂NN-COH bond) to ultimately produce formate from the elongated C-C bond and glyoxal from the remaining two C-C bonds in CL-20.

We were also able to detect two new intermediates (**III** and **IV**) with retention times at 16.8 and 16.3 min, respectively (Figure 18A). The two intermediates had their [M-H]⁻ at 421 and 405 Da each matching an empirical formula of C₆H₆N₁₂O₁₁ or C₆H₆N₁₂O₁₀, respectively (Figure 18B). The corresponding nitrate adduct ions [M+NO₃]⁻ were detected at 484 and 468 Da, respectively. Using ¹⁵N ring labeled and ¹⁵NO₂ labeled CL-20, **III** and **IV** were detected at 427 and 411 Da, respectively, representing an increase of 6 amu in each case due to the presence of six ¹⁵N atoms. In the case of ¹⁵N-amino labeled CL-20 the adduct mass ions of the **III** and **IV** appeared at 490 and 474 Da, respectively also showing an increase of 6 amu. However, in the case of ¹⁵NO₂ labeled CL-20, the adduct mass ions of **III** and **IV** appeared at 491 and 475 Da, respectively, representing an increase of 7 amu.

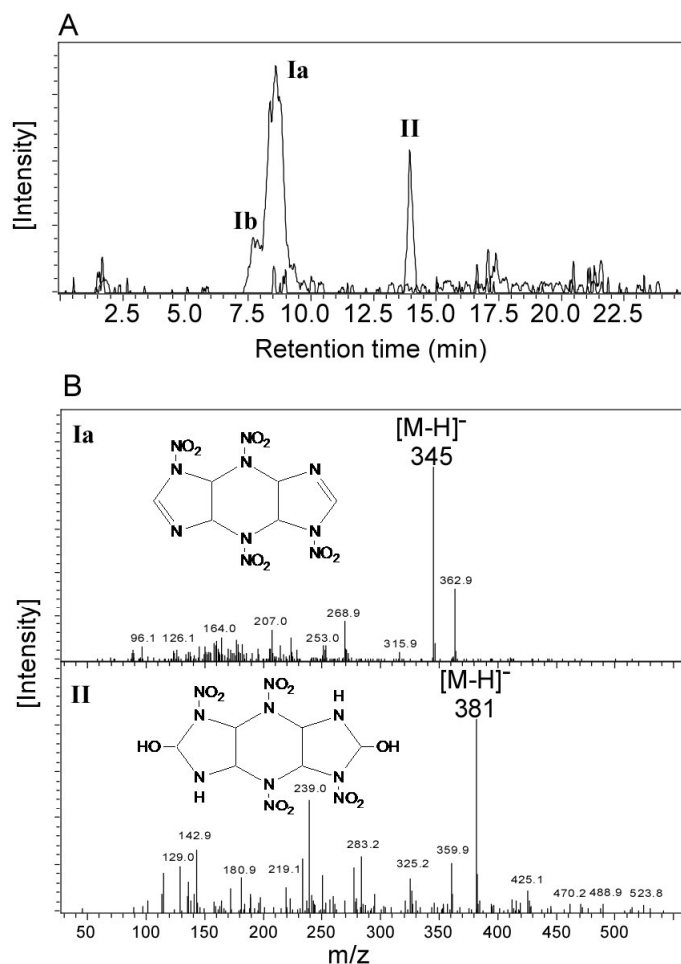


Figure 17 Typical LC/MS chromatograms of intermediates Ia and II formed upon the double denitration of CL-20 in the Fe^0 -mediated reaction. (A) Extracted Ion Chromatogram (EIC) of $m/z = 345$ Da (Ia and Ib) and 381 Da (II). (B) Mass spectra and structures of Ia and II.

The extra 1 amu was attributed to the involvement of $^{15}\text{NO}_3^-$ originated from the $^{15}\text{NO}_2$ labeled CL-20. A similar nitrate adduct was detected during LC/MS analysis of CL-20 (500 Da) (Hawari et al., 2004). We tentatively identified **III** and **IV** as the mononitroso and the dinitroso derivatives of CL-20 (Figure 18B). As far as we are aware this is the first observation of nitroso products of CL-20. The transient observation of initially reduced nitroso products **III** and **IV** highlights the potential occurrence of second initial degradation route for CL-20, *i.e.* the sequential reduction of N- NO_2 groups to the corresponding N-NO derivatives. Similar reduction has been reported for RDX with iron (Oh *et al.*, 2001; Gregory *et al.*, 2004), but no such reactions were known with CL-20.

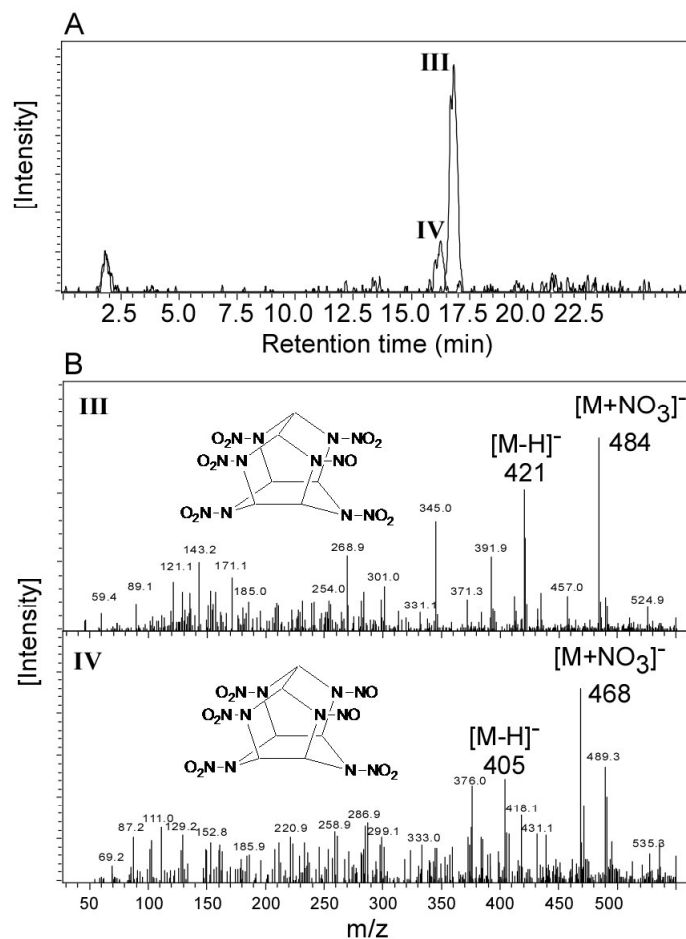


Figure 18 Typical LC/MS chromatograms of early intermediates III and IV in the Fe⁰-mediated decomposition of CL-20. (A) Extracted Ion Chromatogram (EIC) of m/z = 484 Da (III) and 468 Da (IV). (B) Mass spectra and structures of III and IV.

Finally, Figure 19 shows the presence of two other key intermediates (**V** and **VI**) of CL-20 with their LC/MS peaks appearing at retention times of 13.9 and 13.4 min and their deprotonated molecular mass ions at 392 Da and 376 Da, respectively. The two intermediates showed their nitrate adduct ions [M+NO₃)⁻ at 455 and 439 Da, respectively (Figure 19B). The use of ¹⁵NO₂ labeled CL-20 led to the observation of **V** and **VI** at 397 and 381 Da, respectively, suggesting the loss of one NO₂ from CL-20. Intermediate **V** (Figure 19B) was tentatively identified as the denitrohydrogenated intermediate while intermediate **VI** (Figure 19B) was tentatively identified as its denitrohydrogenated mononitroso product of CL-20. The formation of the last two intermediates resembles the known pathway of the reductive dechlorination of polychlorinated compounds by zerovalent iron (dehalohydrogenation) (Helland *et al.*, 1995; Scherer *et al.*, 2000) where there is an apparent substitution of hydride for the leaving group (Cl⁻ or NO₂⁻). While the finding that CL-20 can degrade *via* multiple pathways is important, the absence of reference standards for these newly-detected intermediates prevented us from determining the quantitative contribution of each route in the decomposition of CL-20.

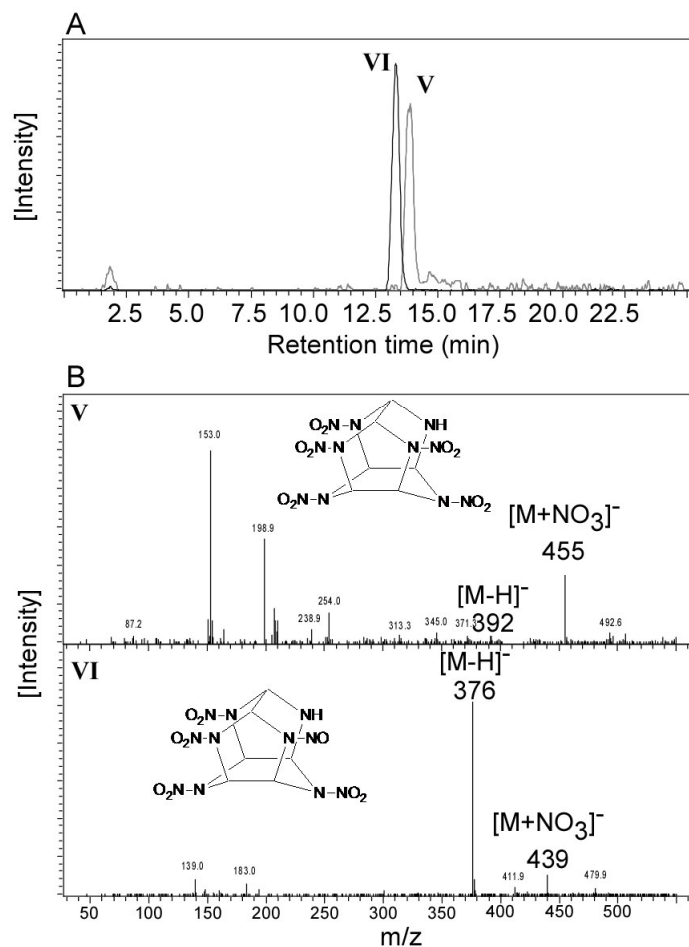


Figure 19 Typical LC/MS chromatograms of intermediates V and VI in the Fe⁰-mediated decomposition of CL-20. (A) Extracted Ion Chromatogram (EIC) of m/z = 455 Da (V) and 376 Da (VI). (B) Mass spectra and structures of V and VI.

Conclusion

This study demonstrates that elevated concentrations of CL-20 (100 mg/L) can be efficiently decomposed within a few hours in the presence of zerovalent iron in water in the absence of oxygen. The technology of permeable reactive barriers composed of Fe⁰ therefore holds great promise to rapidly remediate this potential emerging contaminant from anaerobic subsurface soils. While nitrous oxide and ammonium constitute the major nitrogen-containing products, formate, glyoxal and glycolic acid were discovered as important products contributing to the carbon mass balance. Glyoxal is a known toxic chemical (Shangari *et al.*, 2003) and its formation as a product of CL-20 will require investigating its fate under natural conditions.

X Sorption-desorption of CL-20 on soil

This work was published in:

Balakrishnan VK, Monteil-Rivera F, Gautier MA, Hawari J. (2004) Sorption and Stability of the polycyclic nitramine explosive CL-20 in soil. *J. Environ. Qual.* 33: 1362-1368.

Introduction

Sorption of organic chemicals to soil is a major process that can affect their mobility, degradation and toxicity by reducing their availability. A fundamental understanding of sorption and desorption mechanisms is therefore essential for the accurate prediction of the fate and impact of organic contaminants in soils and groundwater. Previous studies performed with the monocyclic nitramine RDX (Leggett, 1985; Sheremata *et al.*, 2001) and HMX (Brannon *et al.*, 2002; Monteil-Rivera *et al.*, 2003) revealed that both nitramines had a very low tendency to sorption and that this sorption was governed by the clay rather than the organic content of soil. To our knowledge, the sorption/desorption behavior of CL-20 in soils has never been reported in the literature. We therefore measured sorption/desorption isotherms for CL-20 with five slightly acidic soils of varying organic content and then measured the extent of sorption on minerals to evaluate the respective contribution of organic matter and minerals in immobilizing the explosive. Since we showed that CL-20 readily undergoes denitration under alkaline conditions in water (pH 10) (see section VII), we also found it useful to investigate the role of sorption/desorption on CL-20 hydrolysis in alkaline soils. In particular, one issue needed to be addressed: does sorption of CL-20 onto soil affect its hydrolysis kinetics?

Further work was conducted to (1) determine whether the high affinity of CL-20 towards certain soils was attributable to the physical structure or to the chemical composition of the organic matter and to study the effect of aging on CL-20 availability; and (2) determine CL-20 degradation products in soil under both biotic and abiotic conditions and (3). The results of this research are presented in this section. To distinguish between the affinity of CL-20 with the amorphous or the more condensed organic matter in soil, three of the above soils (VT, FSB and FS, Table 5) were washed several times with 0.1 M NaOH. The extracted organic matter was precipitated using HCl. Both the alkali-washed residue (adjusted to pH ~ 5) and the extracted organic matter were analyzed for CHNS and O, and subjected to sorption experiments to assess their respective affinity for CL-20.

Material and Methods

Chemicals. Silica (grade 60, 60-200 mesh), Iron (III) oxide (5 μ m, > 99 % pure), Kaolinite and Montmorillonite K10 were obtained from Aldrich and used as received. Monoclinic illite shale $\{(K, H_3O)(Al, Mg, Fe)_2 (Si, Al)_4 O_{10} [(OH)_2, H_2O]\}$ was obtained from Ward's Natural Science Establishment, Inc. (Rochester, NY), ground and passed through a 2-mm sieve. The pH of the powdered illite (initially 8.60) was adjusted to 5.4 using HCl in the sorption experiments. All other chemicals were of reagent grade and used without purification. CL-20 (in ϵ -form) and [^{14}C]-CL-20 were provided by A.T.K. Thiokol Propulsion (Brigham City, UT). A standard soil

humic acid was obtained from the International Humic Substances Society (IHSS) (<http://www.ihss.gatech.edu/>) and sterilized by gamma irradiation. All other chemicals used in this study were of reagent grade.

Soil characteristics. Seven soils were used in this study: 1) a Sassafras sandy loam (SSL) sampled in an uncontaminated open grassland on the property of US Army Aberdeen Proving Ground, (Edgewood, MD); vegetation and the organic horizon were removed to just below the root zone and the top 15 cm of the A-horizon was collected; 2) a sandy agricultural topsoil (VT) originating from Varennes (QC, Canada) with a total nitrogen and phosphorus of 1100 and 400 mg.kg⁻¹, respectively; 3) a sandy forest soil from Boucherville, QC, Canada (FSB); 4) a sandy forest soil provided by a local supplier (FS), 5) a sandy garden soil (GS) obtained from a local supplier; 6) a clay soil from St. Sulpice, QC, Canada (CSS); and, 7) a sandy soil provided by agriculture Canada (SAC). Soils were passed through a 2 mm sieve and air dried prior to use. The soils differ with respect to total organic carbon, pH levels, and sand, silt and clay content (Table 5). A portion of the VT, CSS and SAC soils was sterilized as described elsewhere (Sheremata *et al.*, 2001), by gamma irradiation from a ⁶⁰Co source at the Canadian Irradiation Center (Laval, QC) with a dose of 50 kGy over 2 h.

To distinguish between the affinity of CL-20 with the amorphous or the more condensed organic matter in soil, three of the above soils (VT, FSB and FS, Table 5) were washed several times with 0.1 M NaOH. The extracted organic matter was precipitated using HCl. Both the alkali-washed residue (adjusted to pH ~ 5) and the extracted organic matter were analyzed for CHNS and O, and subjected to sorption experiments to assess their respective affinity for CL-20.

Table 5 Characterization of soils^a used in this study.

Soil	Granulometry			TOC (%)	pH
	% Sand	% Silt	% Clay		
VT	83	12	4	2.3	5.6
SSL	71	18	11	0.33	5.1
FSB	99.3		0.7 ^b	16	5.7
FS	89.8	9.1	1.2	20	6.9
GS	99.4		0.6 ^b	34	6.1
CSS	2.3	53.2	44.5	0.31	8.1
SAC	98.6	1.3	0.1	0.08	8.1

^a VT = Varennes Topsoil; SSL = Sassafras Sandy Loam; FSB = Forest Soil Boucherville; GS = Garden Soil; FS = Forest soil; CSS = Clay St. Sulpice; SAC = Soil Agriculture Canada. ^b Value denotes % silt + clay.

Sorption/desorption procedure. Batch sorption experiments were conducted at ambient temperature (21 ± 2°C) in 16-mL borosilicate centrifuge tubes fitted with a Teflon coated screw cap. Aqueous CL-20 solutions were prepared to give initial CL-20 concentrations ranging from 0.5 to 3.5 mg/L. The ratio solid/solution was varied so that an adsorption rate of 25 to 75 % of CL-20 was obtained. The tubes were wrapped in aluminum foil and agitated for 2 weeks on a Wrist Action[®] shaker. They were then centrifuged for 30 min at 1170 × g, and the supernatant

was filtered through a Millex-HV 0.45 µm filter (Millipore Corp., Bedford, MA). The filtrate collected after discarding the first 3 mL was analyzed by HPLC, as described earlier (Annual report 2002; Monteil-Rivera *et al.*, 2004).

Desorption experiments were conducted by adding deionized water (10 mL) to the pellet remaining in the tube after removing the supernatant, and agitating the suspensions for 1 week. Samples were then centrifuged, filtered and analyzed as described for sorption experiments. The solution volumes that remained in the soil at the end of the sorption and desorption phases were determined by weight and corrections were made to account for CL-20 present in these volumes.

Sorbed CL-20 was extracted with acetonitrile from the solid recovered after sorption or desorption as described in the EPA SW-846 Method 8330 (USEPA, 1997), modified to use an acidic calcium chloride solution (CaCl₂: 5 g/L; NaHSO₄: 0.23 g/L; pH 3) in the sedimentation step.

Six replicates were used for each concentration: three were extracted with acetonitrile immediately after sorption, the other three were extracted after desorption. Blanks, containing the same amount of sorbent and volume of water, were subjected to the same test procedure for all soils, and no interfering peaks were detected.

Sorption and desorption data were fitted to the linear equation ($x/m = K_d C$) where x/m is the mass of solute sorbed per unit mass at equilibrium (mg kg⁻¹), C is the aqueous phase concentration of solute at equilibrium (mg L⁻¹) and K_d is the distribution coefficient (L kg⁻¹). The organic normalized distribution coefficient K_{oc} was then calculated as: $K_{oc} = K_d/f_{oc}$, where f_{oc} represents the fraction of organic carbon.

Sorption and Desorption Kinetics. For sorption experiments, an aqueous solution of CL-20 (3 mg/L) was shaken with soil over a period ranging from 1 h to 14 days. For desorption experiments, the soils were first shaken with a 3 mg/L CL-20 solutions for 72 h. After centrifugation, the supernatant was removed and the pellet was contacted with fresh deionized water during periods varying from 1 h to 6 days. Sorbed CL-20 was extracted from the recovered solid using acetonitrile as described above. The kinetics experiments were conducted in triplicate.

Sorption/Desorption isotherms. Aqueous CL-20 solutions were prepared to give initial CL-20 concentrations ranging from 0.5 to 3.5 mg/L. Isotherms were measured using SSL, VT, FSB, FS and GS soils. Sorption experiments were conducted over a period of 65 h for SSL, FS and VT soils, and 72 h for FSB and GS soils, while desorption experiments were conducted over a period of 24 h (SSL and VT soils) and 48 hours (FSB, FS and GS soils). Following the general procedure described above, six replicates were used for each concentration: three were extracted with acetonitrile immediately after sorption, the other three were extracted after desorption. Blanks containing the same amount of soil and volume of water were subjected to the same test procedure for all soils, and no interfering peaks were detected.

All sorption and desorption data were fitted to the linear [1] and Freundlich [2] equations:

$$\frac{x}{m} = K_d C \quad [1]$$

$$\frac{x}{m} = K_f C^{1/n} \quad [2]$$

where x/m is the mass of solute sorbed per unit mass at equilibrium (mg kg⁻¹), C is the aqueous

phase concentration of solute at equilibrium (mg L^{-1}), K_d is the distribution coefficient (L kg^{-1}), K_F is the Freundlich constant that gives a measure of the adsorbent capacity ($\text{mg}^{1-1/n} \text{kg}^{-1} \text{L}^{1/n}$), and $1/n$ gives a measure of the intensity of sorption. Because the value of K_F depends on the value of $1/n$ for a given sample, K_F values cannot be compared between different isotherms. Therefore, the extent of sorption and desorption will be compared using the K_d constants, which will be denoted K_d^S for sorption and K_d^D for desorption. Although the K_d values vary with sorbate concentration for samples that exhibit a high level of non-linearity, we will treat the linear model as providing average K_d constants that are representative of the sorption processes for each soil. These average values will be used to determine the K_{oc} values ($K_{oc} = K_d^S/f_{oc}$, where f_{oc} represents the fraction of organic carbon).

Behavior of CL-20 in alkaline soils. The effect of pH on the stability of CL-20 in soil was studied either by artificially adjusting the pH of VT soil suspensions or by using naturally alkaline soils. In the case of VT soil, the soil (1.34 g) was contacted for 2 h with 5 mL of water containing the amount of HCl or NaOH required obtaining a final pH ranging from 3 to 9. After adding 5 mL of an aqueous solution of CL-20 (3.5 mg/L), the slurries were agitated for 65 h. They were then centrifuged for 30 min at $1170 \times g$ and the pH was measured in the supernatant before filtration through a Millex-HV 0.45- μm filter, dilution using acetonitrile acidified to pH 3 (with H_2SO_4), and analysis by HPLC. Potential CL-20 products (nitrite, nitrate, and formate ions) were quantified in the most alkaline samples as described below. All the soil pellets were extracted with CH_3CN in order to calculate a total percent recovery of CL-20.

In the naturally alkaline soils, 10 mL of a CL-20 solution (3.5 mg/L) and 1.34 g of the sterile SAC (pH 8.1) soil or sterile CSS (pH 8.1) soil were agitated in borosilicate centrifuge tubes, using a Wrist Action Shaker at 430 rpm. At various time intervals, tubes were removed and after centrifugation for 30 min at $1170 \times g$, the pH was measured in the supernatant and the latter was filtered. The filtrates collected after discarding the first 3 mL were diluted using acidified acetonitrile, and analyzed by HPLC. Nitrite, nitrate and formate ions were quantified in the 14-d samples as well as in controls (sterile soil and water without CL-20) stirred for 14 d under similar conditions. The soils were extracted with acetonitrile, and a total recovery was calculated for CL-20. For comparison, a similar experiment was conducted with sterile VT soil (pH 5.6).

Analytical Methods. All CL-20 standards and samples were prepared in acidified (pH 3) mixtures of 50:50 $\text{CH}_3\text{CN}:\text{H}_2\text{O}$. Dissolved soil organic matter or clay mineral that precipitated from solution at pH 3 were separated by centrifugation for 10 min. at $16\,000 \times g$ (Eppendorf Centrifuge 5415D), and the supernatant was subsequently analyzed by HPLC.

CL-20, nitrate (NO_3^-) and formate (HCOO^-) ions were quantified as described in previous sections. Analysis of nitrite (NO_2^-) ions was performed colorimetrically as described in EPA Method 354.1 (USEPA, 1979).

Accomplishments

Sorption/desorption Kinetics. Kinetics experiments were performed using VT (2.3 % TOC) and GS (34 % TOC) soils in order to determine the minimum time required to reach sorption and desorption equilibria. The sorption experiments revealed differing behavior in both soils (Figure

20).

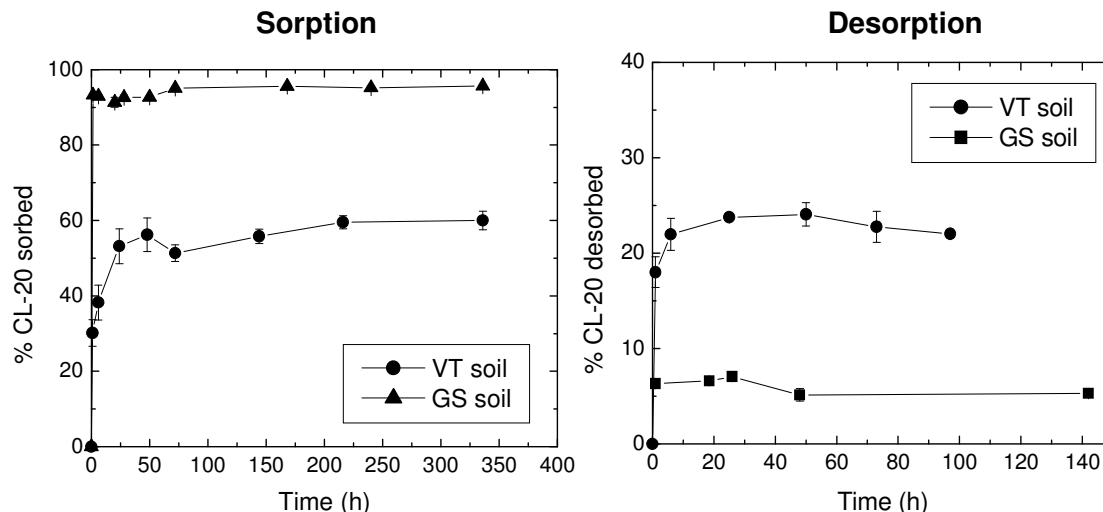


Figure 20 Sorption and desorption kinetics for CL-20 with VT and GS soils (Error bars represent the standard deviation of 3 replicates).

For GS soil, a rapid sorption occurred with maximal sorption (94 %) reached within 1.5 h, while VT soil yielded a slower sorption, with approximately 200 hours being required to attain sorption equilibrium (60 % sorption). In the case of VT, a fast initial adsorption is followed by a slower migration and diffusion of the CL-20 into the organic matter matrix and mineral structure. These results show that the sorbing sites present in GS soil are easier to reach than those present in VT soil, suggesting that different types of sites are involved in CL-20 immobilization by soils. No information is yet available on the sorption and desorption kinetics of CL-20 onto soils, but for the monocyclic nitramines RDX and HMX, a rapid sorption was reported to occur in less than 24 h for each compound in different soils, including VT soil (Xue *et al.*, 1995; Myers *et al.*, 1998; Sheremata *et al.*, 2001; Monteil-Rivera *et al.*, 2003). The slower sorption of CL-20 onto the VT soil is indicative of a different sorption mechanism operating for CL-20 than for RDX and HMX.

Desorption equilibria were achieved in less than 1 h and 20 h for GS and VT soils, respectively (Figure 20). As was the case for sorption, desorption of CL-20 from VT soil is probably delayed by the need for the chemical to diffuse through the soil structure.

CL-20 sorption/desorption isotherms. Sorption and desorption isotherms of CL-20 in soils are presented in Figure 21 for the SSL, VT, FSB, FS and GS soils. Since no microbial growth inhibitor was added to the media and non-sterile soils were used, some degradation of CL-20 was observed (2 to 16 % depending on the soil employed (Table 6) during the time frame of the sorption/desorption isotherms (about one week). In order to account for CL-20 degradation, the amount of sorbed CL-20 was determined by extracting the soil with acetonitrile, rather than estimating it by difference from the aqueous concentration.

Non linear regression procedures using Microcal Origin software were utilized for fitting Freundlich and linear ($1/n$ set equal to 1) isotherms to the sorption data. Values of the resulting

parameters for the two models along with the R^2 values are presented in Table 6 and theoretical curves resulting from the Freundlich model are presented in Figure 21. From the data presented, it is evident that all sorbents exhibited nonlinear isotherms, with $1/n$ values ranging from 0.49 to 0.94. The R^2 values show that the Freundlich model fits the equilibrium sorption data better than the linear model. Moreover, the linear model is not appropriate for describing FSB and GS soils ($R^2 < 0.7$). The general nonlinearity of the isotherms observed in this study indicates that CL-20 sorption to soil occurs through interactions with different classes of sites having different sorption energies (Weber and DiGiano, 1996).

Sorption was significantly higher in the FS ($K_d = 311 \text{ L kg}^{-1}$), GS ($K_d = 187 \text{ L kg}^{-1}$) and FSB ($K_d = 37 \text{ L kg}^{-1}$) soils than in the VT ($K_d = 15.1 \text{ L kg}^{-1}$) and SSL ($K_d = 2.4 \text{ L kg}^{-1}$) soils. The higher K_d (and K_F) values obtained in soils with higher organic content suggest that soil organic matter plays a determining role in CL-20 sorption. This result demonstrates a major difference in behavior between CL-20 and the two monocyclic nitramines, RDX and HMX, whose sorption onto soil was previously demonstrated to be independent of organic content (Leggett, 1985; Sheremata *et al.*, 2001; Brannon *et al.*, 2002; Monteil-Rivera *et al.*, 2003).

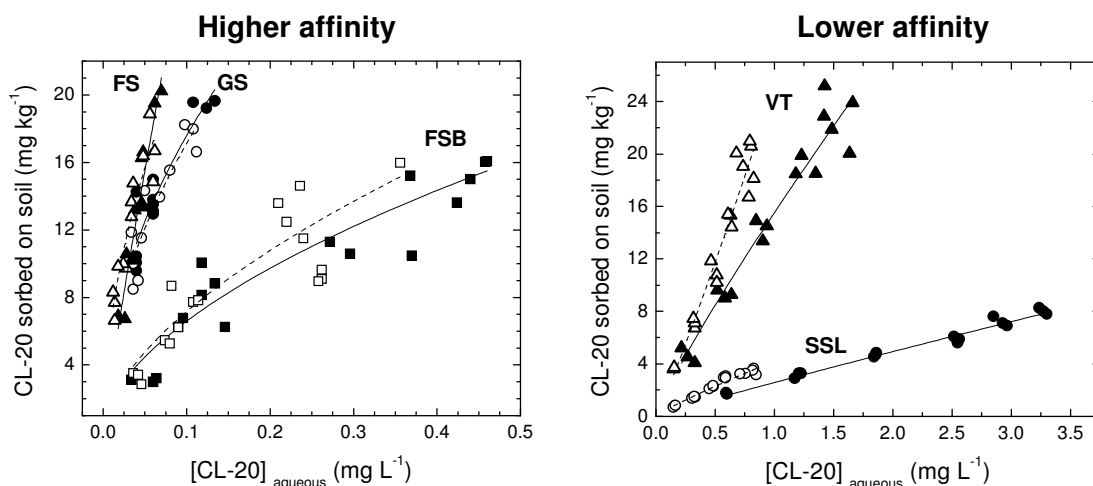


Figure 21 Sorption-desorption isotherms for CL-20 in non-sterile SSL, VT, FSB, GS and FS soils at ambient temperature (sorption: filled symbols, solid lines; desorption: hollow symbols, dashed lines; for clarity, data obtained with soils having a high affinity for CL-20 are presented separately from data obtained with soils having a low affinity for CL-20).

Table 6 Isotherm parameters, K_{oc} , and recoveries for CL-20 sorption and desorption by various soils.

Soil	Freundlich Fitting			Linear Fitting		K_{oc}^c	% Recovery ^d
	K_F^a	1/n	r^2	K_d^b	r^2		
SSL	sorption	2.57 ± 0.11^e	0.94 ± 0.04^e	0.983	2.43 ± 0.04^e	0.981	736 97.0 ± 2.3
	desorption	4.22 ± 0.15	0.89 ± 0.07	0.956	4.43 ± 0.11	0.947	
VT	sorption	15.53 ± 0.50	0.87 ± 0.08	0.948	15.06 ± 0.42	0.928	655 97.3 ± 2.8
	desorption	25.09 ± 1.27	1.09 ± 0.11	0.932	24.14 ± 0.65	0.929	
FSB	sorption	23.76 ± 2.03	0.57 ± 0.06	0.884	36.86 ± 2.26	0.667	230 98.5 ± 8.2
	desorption	27.86 ± 5.27	0.59 ± 0.11	0.716	48.81 ± 3.38	0.569	
GS	sorption	54.83 ± 8.57	0.49 ± 0.06	0.867	187.43 ± 13.73	-0.027	551 92.6 ± 5.8
	desorption	54.31 ± 11.07	0.50 ± 0.08	0.834	190.59 ± 13.71	0.150	
FS	sorption	232.52 ± 71.31	0.90 ± 0.10	0.904	310.83 ± 9.37	0.895	1554 84.3 ± 11.0
	desorption	75.98 ± 16.47	0.53 ± 0.07	0.873	330.84 ± 21.95	0.402	

^a Freundlich coefficient in $\text{mg}^{1-1/n} \text{kg}^{-1} \text{L}^{1/n}$. ^b Distribution coefficient in L kg^{-1} . ^c Organic carbon-normalized sorption coefficient in L kg^{-1} . ^d Average percent recovery of CL-20 for all sorption-desorption samples in one soil, as determined by adding the amount of sorbed CL-20 to the amount of CL-20 present in the aqueous phase. Error denotes standard deviation ($n = 36$ for SSL, VT, and FSB soils; $n = 24$ for GS soil; $n = 29$ for FS soil). ^e Standard error.

The higher $\log K_{ow}$ measured for CL-20, compared to that of RDX and HMX (see Table 3) demonstrates a higher hydrophobicity of the former, which is likely responsible for its superior affinity towards soils with high organic content. Numerous relationships based on Equation 3 have been developed between soil sorption coefficients (K_{oc}) and n-octanol/water coefficients (K_{ow}):

$$\text{Log } K_{oc} = m \log K_{ow} + b \quad [3]$$

where m and b are parameters extracted from linear regressions. To predict a K_{oc} value from a K_{ow} value, a reasonable similarity should be ensured between the solute molecule of interest and the family of compounds used to establish the data set upon which m and b are based (Sabljic *et al.*, 1995). No correlation is currently available in the literature for nitramines, but by applying the general model given by Sabljic *et al.* (1995) for non-hydrophobic chemicals (defined as chemicals containing atoms other than C, H, and halogens ($m = 0.52$; $b = 1.02$)), a K_{oc} value of 104 L kg^{-1} was found for CL-20. The fact that this theoretical value is inferior to all those measured in the present study (see Table 6), coupled with the fact that the K_{oc} values measured varied by almost one order of magnitude confirms that CL-20 adsorption onto organic matter is not limited to a pure physical distribution process, as already suggested by the non-linear isotherms. It is thus the type of organic matter present in soils, rather than its amount, which will be a determining factor in the immobilization of CL-20.

A sorption-desorption hysteresis ($K_d^D > K_d^S$) was observed for the SSL and VT soils (Figure 21, Table 6), while sorption to the FS and GS soils appears to be fully reversible ($K_d^D \sim K_d^S$). Meanwhile, the large divergence observed on the measurements performed with FSB soil makes it hard to ascertain whether or not this soil gave rise to sorption hysteresis. Hysteresis phenomena can be caused by organic matter or mineral constituents of soil. We assessed the sorption of CL-20 onto silica, ferric oxide and three different clays (Table 7). Clays have been shown to play a determining role in the sorption of RDX and HMX (Brannon *et al.*, 2002); moreover when HMX was adsorbed on montmorillonite under similar conditions, a K_d^S value of 15.6 L kg^{-1} was measured. It is clear from the data presented in Table 7 that CL-20 has a low tendency to adsorb on any of the mineral phases, and that it adsorbs much less on clay than do RDX and HMX.

Based on FTIR measurements, Boyd *et al.* (2001) suggested that nitro-containing compounds are strongly retained by complexation between metals in clay minerals (e.g., K^+) and $-\text{NO}_2$ groups. With 6 $-\text{NO}_2$ groups, CL-20 contains more sites capable of interacting with such metals compared to RDX (3 $-\text{NO}_2$) and HMX (4 $-\text{NO}_2$). However, its polycyclic caged structure makes it a bulkier compound ($\sim 6\text{-}7 \text{ \AA}$ diameter, as estimated from crystallographic data (Zhao and Shi, 1996)) that is unable to migrate into the clay layers ($3\text{-}9 \text{ \AA}$ for a montmorillonite, $\sim 5 \text{ \AA}$ for a smectite (Brindley, 1981)). Given the small contribution of mineral phases in CL-20 retention, the hystereses observed with VT and SSL soils are likely caused by the organic content of soil.

Table 7 Sorption and stability of CL-20 with minerals.

Mineral	pH	K_d^S ^a (\pm SD, n=3) (L kg ⁻¹)	% Recovery ^b (\pm SD, n=3)
Silica	6.0	0.35 ± 0.05	89.4 ± 0.9
Fe ₂ O ₃	5.9	~ 0	93.6 ± 1.0
Montmorillonite	2.4	0.62 ± 0.07	99.9 ± 1.6
Kaolinite	5.4	0.14 ± 0.04	95.7 ± 0.3
Illite	5.4 ^c	0.30 ± 0.04	97.8 ± 0.5

^a Distribution coefficient for sorption. ^b Average percent recovery of CL-20 determined after adding the amount of sorbed CL-20 to the amount of CL-20 present in the aqueous phase. ^c After adjustment with HCl.

The full CL-20 recoveries we obtained upon sonicating the sorbed soils in acetonitrile rules out the formation of covalent bonds between CL-20 and organic matter as the reason for the hysteresis. Weber *et al.* (1998) previously suggested that the form of the soil organic matter played a critical role in the hysteresis observed in the sorption-desorption behavior of HOCs such as phenanthrene. Humic acids, with their large microporosities, allow for fast interaction with water, thus producing a reversible sorption. In contrast, condensed organic matter presents physically rigid zones that interact poorly with water and tend to trap any molecules sorbed within it, producing a sorption-desorption hysteresis (Weber *et al.*, 1998). It is possible that the hysteresis observed in the present study was due to an entrapment of CL-20 in condensed organic matter. However, a matrix change that could occur from the sorption to the desorption step to give access to sites with higher sorbing capacity in the desorption batch is not excluded.

Interaction of CL-20 with organic matter (OM). As reported in the annual report of 2003, CL-20 sorption was significantly higher in soils with higher organic content thus suggesting that soil organic matter played a determining role in the sorption (Table 8).

This result demonstrated a major difference in behavior between CL-20 and the two monocyclic nitramines, RDX and HMX, the sorption of which was previously demonstrated to be independent of organic content (Leggett, 1985; Sheremata *et al.*, 2001; Brannon *et al.*, 2002; Monteil-Rivera *et al.*, 2003). The higher log K_{ow} measured for CL-20 (1.92), compared to that of RDX (0.90) and HMX (0.16) (Monteil-Rivera *et al.*, 2004) demonstrates a higher hydrophobicity of the former, which was likely responsible for its superior affinity towards soils with high organic content. However, as seen in Table 6, the K_{oc} values varied by almost one order of magnitude from soil to soil, which suggested that CL-20 adsorption onto organic matter was not limited to a pure physical distribution process.

In order to better understand the role of organic matter (OM) in the sorption of CL-20, three of the above soils were washed with an NaOH solution to extract the amorphous organic matter and sorption isotherm experiments were conducted with (1) the three sterile soils, (2) the three sterile alkali-washed soils and (3) the three sterile corresponding extracted OM. Organic matter that is not extracted in alkaline solution is known to be more condensed and more reduced than the extractable fraction, which is usually composed of humic acids, *i.e.* amorphous OM (Ran

et al., 2002). Analysis of the three extracted OM samples by solid CP-MAS ^{13}C -NMR gave three spectra similar to each other and typical of soil humic acid (Monteil-Rivera *et al.*, 2000). Sorption data presented in table 9 show that CL-20 exhibited a higher affinity for the unextractable OM (condensed and/or reduced OM) than for the extractable organic matter (humic acids).

Table 8 Isotherm parameters and K_{oc} for CL-20 sorption and desorption by various soils.

Soil	TOC (%)	Linear Fitting			K_{oc}^b
			K_d^a	r^2	
SSL	0.33	sorption	2.43 ± 0.04^e	0.981	736
		desorption	4.43 ± 0.11	0.947	
VT	2.3	sorption	15.06 ± 0.42	0.928	655
		desorption	24.14 ± 0.65	0.929	
FSB	16	sorption	36.86 ± 2.26	0.667	230
		desorption	48.81 ± 3.38	0.569	
GS	34	sorption	187.43 ± 13.73	-0.027	551
		desorption	190.59 ± 13.71	0.150	
FS	20	sorption	310.84 ± 9.37	0.895	1554
		desorption	330.84 ± 21.95	0.402	

^a Distribution coefficient in L kg^{-1} . ^b Organic carbon-normalized sorption coefficient in L kg^{-1} .

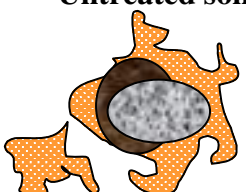
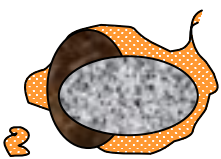
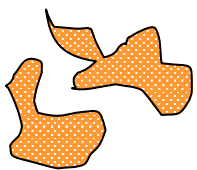
The K_{oc} value was also measured with a standard soil humic acid obtained from the International Humic Substances Society and a value of 386 L kg^{-1} was obtained in agreement with the three values measured with the extracted OM samples. Soil humic acids thus led to relatively low K_{oc} values ($\sim 200\text{-}400 \text{ L kg}^{-1}$) compared to the K_{oc} of unextracted OM ($400\text{-}2200 \text{ L kg}^{-1}$). However, the high variations of the latter demonstrate that several types of organic matter may remain in the soil after extracting the humic acids. More work is still necessary to further understand the different sorbing behaviors of unextracted OM.

In conclusion, these data demonstrate that adsorption of CL-20 is lower on amorphous humic acid than on more condensed soil organic fraction. The adsorption of CL-20 on a soil will then be function of the amount of each organic fraction in the soil. Consequently, estimating CL-20 adsorption coefficient for a given soil based on the sole organic content will not be possible. Experiments are presently ongoing to study the effect of aging on the sorption extent and reversibility.

Behavior of CL-20 in alkaline soils. We have just demonstrated that CL-20 can be significantly sorbed to soils, provided that the latter contains organic matter. Given that CL-20 undergoes rapid hydrolysis under alkaline conditions (pH 10) (section VII), it would now be worthwhile to

determine how the presence of soils affects the hydrolysis of CL-20. In order to generate a pH-profile of CL-20 stability in soil, we adjusted the pH of VT soil and contacted it with CL-20 solution for 65 hours. Below pH 7.5, percent recoveries remained approximately constant at ca. 100 %, while above pH 7.5, CL-20 degraded (Figure 22).

Table 9 K_{oc} extracted from sorption isotherms with different fractions of soil organic matter

	$K_{OC} (L\ kg^{-1})$		
	Untreated soil	Alkali-washed soil	Amorphous OM
Soil			
VT	681	753	339
FSB	334	475	227
FS	1383	2212	162

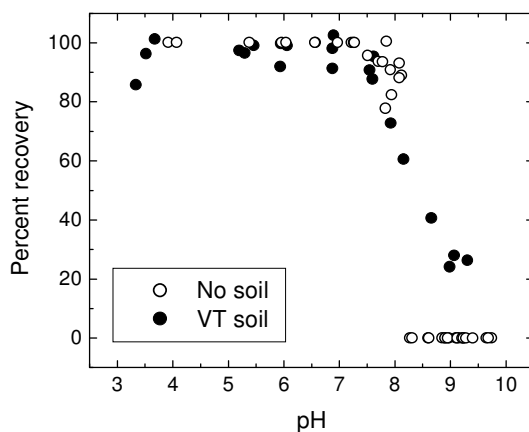


Figure 22 Percent recovery of CL-20 upon agitation at different pHs and ambient temperature, in presence or not of non-sterile VT soil.

The disappearance of CL-20 was accompanied by the formation of NO_2^- and $HCOO^-$. The fact that degradation was observed in soils with $pH > 7.5$ indicates that CL-20 will not persist in

naturally alkaline soil environments. In aqueous control samples of CL-20 (Figure 22), degradation was observed at pH > 7.5 and was complete at pH > 8.1. The greater extent of degradation observed in the control solutions than in the soils at pH > 8 suggests that to a certain extent, the presence of soil protects CL-20 against decomposition.

Given the significant degradation of CL-20 observed when we increased the pH of VT suspensions, the behavior of CL-20 was followed over time in two sterile, naturally alkaline soils. After 14 days of contact with sterile SAC and sterile CSS soils (pH 8.1), 100 % and 82 % of the CL-20 degraded, respectively, compared to only 8 % loss in sterile VT soil (pH 5.6) (Figure 23). Clearly, CL-20 is not stable in alkaline soils. In fact, degradation in the naturally alkaline soils produced 2 equivalents of nitrite (NO_2^-) for each mole of CL-20 reacted, exactly as observed for the aqueous alkaline hydrolysis of CL-20 at pH 10. Despite the equivalent pH values of both soils, CL-20 degraded faster in SAC soil than it did in CSS soil. SAC soil contains very low amounts of the two most active sorbents in soils (0.1 % clay and 0.08 % TOC), whereas CSS soil contains clay (44.5 %) and organic carbon (0.31 %). As a result, CL-20 does not sorb onto SAC soil ($K_d^S \sim 0 \text{ L kg}^{-1}$) and is thus not protected from degradation. In contrast, the slight sorption to CSS soil ($K_d^S = 1.0 \pm 0.3 \text{ L kg}^{-1}$, $n = 24$) retards CL-20 hydrolysis. The minor increase of K_d^S from 0.97 (after 1 d) to 1.26 (after 14 d) L kg^{-1} throughout the degradation experiment indicates a progressive desorption of CL-20 from the soil. Therefore, sorption retards the hydrolysis of the energetic chemical but it does not prevent it.

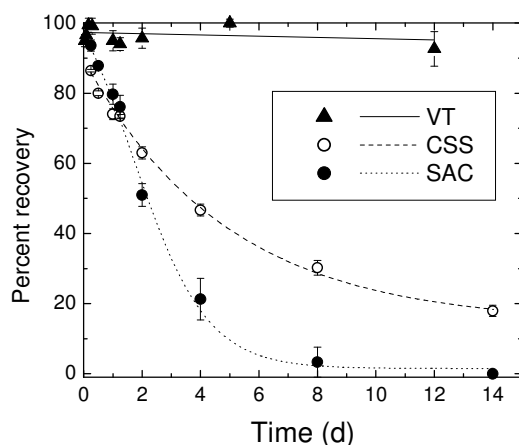


Figure 23 Stability of CL-20 in sterile soils having various pHs (CSS and SAC = pH 8.1; VT = pH 5.6) (Error bars represent the standard deviation of 3 replicates).

Abiotic degradation of CL-20 in SAC soil (pH 8.1). Following the demonstration that CL-20 could be abiotically degraded in slightly alkaline soils (Balakrishnan *et al.*, 2004b) and the recent advances we made by discovering the formation of glyoxal in both abiotic and biotic processes, we used one of the sterilized alkaline soils and determined the product distributions over time (Figure 24). Disappearance of CL-20 was concomitant with the formation of NO_2^- (2.3 equ.),

N_2O (4.2 equ.), HCOO^- (1.2 equ.), and NH_3 (0.9 equ.) with a stoichiometry closely similar to that observed in water at pH 10, except for N_2O (NO_2^- : ~ 1.9 equ.; N_2O : 0.9 equ.; HCOO^- : 0.5 equ.; NH_3 : 0.8 equ.) (Balakrishnan *et al.*, 2003). Besides these products, glyoxal was formed with a maximum concentration (0.35 equ.) being reached after 45 h. Glyoxal was transformed further to partially produce glycolate (0.2 equ.). When a control was done with glyoxal in the same soil, 70 % loss was measured after 48 h of contact time. Glyoxal, with its two aldehyde groups, is a very reactive molecule that can either degrade to yet unidentified products or be covalently bound to the soil matrix. More work is still necessary to identify products of glyoxal in soil.

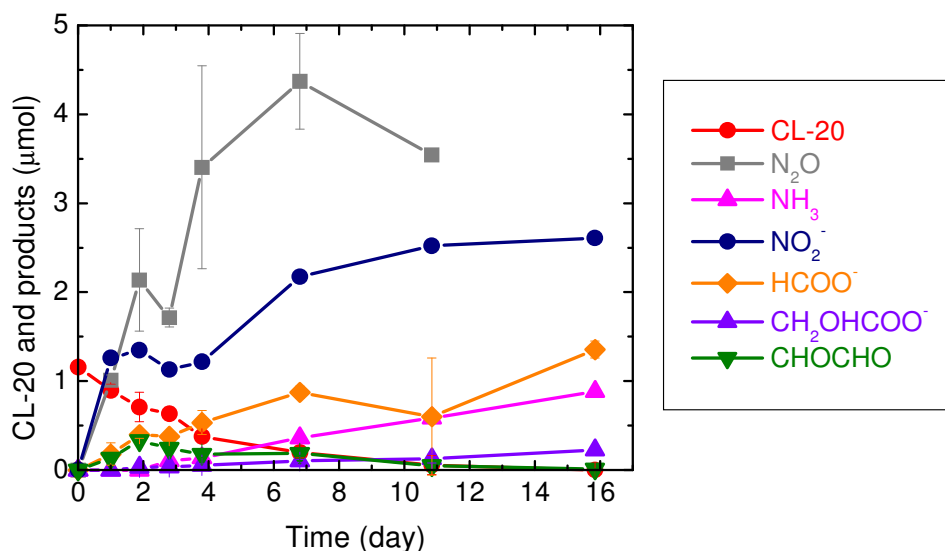


Figure 24 Time-course study of abiotic transformation of CL-20 in sterilized SAC soil (pH 8.1). Bars indicate standard deviation ($n = 2$).

Conclusion and Perspectives

This study reveals that CL-20 can be highly retained by soils (a K_d as high as 300 L kg^{-1} was measured). In contrast to the monocyclic nitramines, RDX and HMX, that were mainly adsorbed by the clay fraction of soil, CL-20 affinity for soil is governed by the organic content of soil, and only a small fraction of the energetic chemical is actually bound to the mineral phase. The type of organic matter rather than its amount appeared determining in the immobilization of CL-20 onto soils, thus indicating that the exclusive use of the $\log K_{ow}$ value will not be sufficient for predicting sorption of CL-20 to soil. Further work is underway to determine whether the high affinity of CL-20 towards certain soils is attributable to the physical structure or to the chemical composition of the organic matter and to study the effect of aging on CL-20 availability.

The present study showed that CL-20 sorption to soil retards its hydrolysis but does not eliminate this process. Even when sorbed, the chemical readily decomposes in natural soils with $\text{pH} > 7.5$ suggesting that, unlike RDX and HMX, CL-20 will not be a persistent organic pollutant in even slightly alkaline soils. Degradation of CL-20 in a sterilized soil gave products similar to those observed with either Fe^0 or enzymes. Glyoxal transformed further to partially produce

glycolate but more work is necessary to understand the fate of the dialdehyde in soil. While an excellent N mass balance was obtained (98 % of N recovered), uncertainty remains on the fate of carbon-containing compounds (27 % of C recovered).

We showed that CL-20 could be highly retained by soils (a K_d as high as 300 L kg⁻¹ was measured). In contrast to the monocyclic nitramines, RDX and HMX, that were mainly adsorbed by the clay fraction of soil, CL-20 affinity for soil is governed by the organic content of soil, and only a small fraction of the energetic chemical is actually bound to the mineral phase. The type of organic matter rather than its amount appeared determining in the immobilization of CL-20 onto soils, thus indicating that the exclusive use of the log K_{ow} value was not sufficient for predicting sorption of CL-20 to soil. CL-20 sorption to soil was also shown to retard abiotic degradation of the chemical in alkaline soils.

XI Microbial and enzymatic degradation of CL-20

Results from these tasks were published in:

1. Bhushan B, Halasz A, Hawari J. **2006**. Effect of iron (III), humic acid, and anthraquinmone-2, 6-disulphonate on biodegradation of cyclic-nitramines by *Clostridium* sp. EBD2. *J. Appl. Microbiology* 100: 555-563.
2. Fournier D, Monteil-Rivera F, Halasz A, Bhatt M, Hawari J. **2005**. Degradation of CL-20 by white-rot fungi. *Chemosphere* (**In press**)
3. Bhushan, B., A. Halasz, Hawari J. **2005**. Biotransformation of CL-20 by a dehydrogenase enzyme from *Clostridium* sp. EDB2. *Appl. Microbiol. Biotech.* 69: 448-455.
4. Bhushan B, Halasz A, Hawari J. **2005**. Stereo-specificity for pro-(R) hydrogen of NAD(P)H during enzyme-catalyzed hydride transfer to CL-20. *Biochem. Biophys. Res. Commun.* 337: 1080-1083.
5. Bhushan B, Halasz A, Hawari J. **2004**. Nitroreductase catalyzed biotransformation of CL-20. *Biochem. Biophys. Res. Commun.* 322:271-276.
6. Bhushan B, Halasz A, Thiboutot S, Ampleman G, Hawari J. **2004**. Chemotaxis-mediated biodegradation of cyclic nitramine explosives RDX, HMX and CL-20 by *Clostridium* sp. EDB2. *Biochem. Biophys. Res. Commun.* 316:816-821.
7. Bhushan B, Halasz A, Spain JC, Hawari J. **2004**. Initial reaction(s) in biotransformation of CL-20 is catalyzed by salicylate 1-monooxygenase from *Pseudomonas* sp. strain ATCC 29352. *Appl. Environ. Microbiol.* 70:4040-4047.
8. Trott S, Nishino SF, Hawari J, Spain J. **2003**. Biodegradation of the nitramine explosive CL-20. *Appl. Environ. Microbiol.* 69:1871-1874.
9. Bhushan B, Paquet L, Spain JC, Hawari J. **2003**. Biotransformation of 2,4,6,8,10,12-hexanitro-2,4,6,8,10,12-hexaazaisowurtzitane (CL-20) by denitrifying *Pseudomonas* sp. Strain FA1. *Appl. Environ. Microbiol.* 69:5216-5221.

PREFACE

In order to determine whether biodegradation affects the fate and transport of CL-20 in terrestrial and aquatic ecosystems, we evaluated the ability of several microorganisms, bacteria and fungi, to biodegrade CL-20 in laboratory microcosms. A CL-20 degrading bacterial strain, *Agrobacterium* sp. JS71, was first isolated from enrichment cultures containing garden soil (from Panama City, Florida) as inoculum, succinate as carbon source, and CL-20 as nitrogen source.

In another study, a facultative CL-20 degrading bacterium, strain *Pseudomonas* sp. Strain FA1 FA1, was isolated from a Canadian garden topsoil. Strain FA1 appeared to be a gram-negative, motile denitrifying bacteria that was found to biotransform under both anaerobic as well as aerobic conditions, but favorably under anaerobic conditions in the presence of an electron donor [NAD(P)H]. Several other bacterial species capable of degrading CL-20 were isolated from a variety of microbial sources, namely municipal garbage dumping site, explosive-contaminated soil and garden soil of the institute campus. In subsequent chapters we will discuss in more details biotransformation of CL-20 with several isolates and enzymes under both aerobic and anaerobic conditions. We will determine reaction kinetics, reaction stoichiometry, carbon and nitrogen mass balances and attempt to elucidate initial and secondary biotransformation routes involved in the degradation for the energetic chemicals.

XII Aerobic degradation of CL-20

Results from these tasks were published in:

1. Trott S, Nishino SF, Hawari J, Spain J. (2003) Biodegradation of the nitramine explosive CL-20. *Appl. Environ. Microbiol.* 69:1871-1874.
2. Bhushan B, Paquet L, Spain JC, Hawari J. (2003) Biotransformation of 2,4,6,8,10,12-hexanitro-2,4,6,8,10,12-hexaazaisowurtzitane (CL-20) by denitrifying *Pseudomonas* sp. Strain FA1. *Appl. Environ. Microbiol.* 69:5216-5221.
3. Fournier D, Monteil-Rivera F, Halasz A., Bhatt M, Hawari J. (2005) Degradation of CL-20 by white-rot fungi. *Chemosphere (In press)*

XII.1 Biotransformation of CL-20 by *P. chrysosporium*

Introduction

In the present study, we use the fungus *P. chrysosporium* to determine the degradation products of CL-20. Because our previous studies performed with HMX (Fournier *et al.*, 2004a) revealed that the use of the whole fungus could prevent the detection of some early or transient metabolites, the purified ligninolytic enzyme manganese peroxidase (MnP, EC 1.11.1.13) from *Nematospora frowardii* was thus used in the present study to degrade CL-20 in an attempt to identify products of degradation. The radiotracer [^{14}C]-CL-20 was employed to conduct mineralization experiments and thereby improve the carbon mass balance. Moreover, since the degradation of CL-20 with Fe^0 led to the formation of important amounts of glyoxal that further degraded to glycolate (Balakrishnan *et al.*, 2004a), we will also measure mineralization of the dialdehyde to investigate its role in the mineralization process.

Material and Methods

Chemicals. CL-20 (in ϵ -form), [^{15}N]-amino labeled CL-20, [^{15}N]-nitro labeled CL-20, and [^{14}C]-CL-20 were provided by A.T.K. Thiokol Propulsion (Brigham City, UT). [^{14}C]-glyoxal was purchased from American Radiolabeled Chemicals (Saint-Louis, MO). All other chemicals used in this study were of reagent grade.

Soil characteristics. An agricultural topsoil from Varennes (Quebec, Canada) designated as VT soil, was used in the present study. The VT soil granulometry was the following (% w/w): sand (83), silt (12), and clay (4). The total organic carbon was (2.3%) and the total nitrogen and phosphorus were 1100 and 400 mg.kg^{-1} , respectively. VT soil had a pH of 5.6. Prior to usage, the soil was passed through a 2 mm sieve and residual moisture was removed by air-drying in a fume-hood.

Bio-transformation of CL-20 with *P. chrysosporium*. The strain ATCC 24725 was maintained on Yeast Peptone Dextrose (YPD) plates and was cultivated in the modified Kirk's nitrogen-limited medium (pH 4.5) as previously described (Tien and Kirk, 1988; Fournier *et al.*, 2004b). Bio-transformation experiments were performed in the N-limited mineral medium (10 mL in 125 mL serum bottle) supplemented with CL-20 at its maximum water solubility (ca. 3.6 mg L^{-1} at

25°C). Cultures were started with the addition of 2×10^6 fungal spores. Un-inoculated bottles containing the sterile CL-20 solution were incubated as controls for possible abiotic degradation. The bottles were sealed with Teflon coated serum septa and aluminum caps. The cultures were incubated statically in the dark at $37 \pm 2^\circ\text{C}$, and were aerated every 3 to 4 days.

Bio-transformation of CL-20 with MnP of *Nemalotoma frowardii*. The MnP from a high potential fermentation strain of *Nemalotoma frowardii* was purchased from JenaBIOS GmbH (Jena, Germany). The enzymatic reactions were performed in 6-mL vials in a total volume of 1 mL: 50 mM sodium malonate (pH 4.5), 1 mM MnCl_2 , H_2O_2 (0.33 mM), MnP (1.5 U) and CL-20 (approximately 38 mg/L in an attempt to generate sufficient amounts of reaction intermediates to allow detection). The vials were sealed with Teflon coated serum septa and aluminum caps. Reactions were carried out at $37 \pm 2^\circ\text{C}$ under agitation at 150 rpm.

Mineralization of CL-20 and glyoxal with fungi: Carbon mass balance. Mineralization of CL-20 was performed by adding to a spore suspension or to 7 day-old mycelium (see above) either [^{14}C]-CL-20 (0.048 μCi) or [^{14}C]-glyoxal (0.26 μCi). Formation of $^{14}\text{CO}_2$ was monitored as described previously (Fournier *et al.*, 2002). Microcosms were aerated every 3 to 4 days.

Bio-transformation of CL-20 pre-adsorbed on VT soil with *P. chrysosporium*. Gamma-irradiated VT soil (1.33 g) was added to 10 mL of a CL-20 solution (ca. 3.6 mg L^{-1}) prepared in N-limited medium in 125-mL serum bottles. The bottles were sealed with Teflon coated septa and aluminum caps. The soil slurries were then shaken for 2 weeks at $37 \pm 2^\circ\text{C}$ under agitation at 200 rpm to allow sorption equilibrium to be reached, as previously determined for CL-20 and VT soil (Balakrishnan *et al.*, 2004b). After 2 weeks of pre-equilibration, cultures were started with the addition of 2×10^6 fungal spores. Three samples were sacrificed for each selected time and analyses of CL-20 and products were done as described in section VI.

Un-inoculated bottles containing the sterile CL-20 solution were incubated as controls for possible abiotic degradation. The sorption obtained after fourteen days of incubation was measured as described in the previous paragraph to estimate the fraction of sorbed CL-20 when starting the biodegradation experiment.

Analytical Techniques. At the end of each enzymatic or microbiological reaction acidified acetonitrile (0.25 mL of H_2SO_4 per liter of acetonitrile) was added to the reaction mixture to solubilize any undissolved CL-20. The samples were then submitted to sonication at 20°C for 18 h. The resulting solution was filtered through a 0.45- μm membrane (Millipore PTFE) and CL-20 was analyzed by HPLC as described previously (Monteil-Rivera *et al.*, 2004). Analyses of nitrate (NO_3^-), formate (HCOO^-), glycolate ($\text{HOCH}_2\text{COO}^-$), ammonia (NH_3), glyoxal, and intermediate products of CL-20 were performed as previously described (section IX; Balakrishnan *et al.*, 2004a). Nitrite (NO_2^-) was analyzed using the US EPA Method 354.1 (1979).

Accomplishments

Bio-transformation of CL-20 with *P. chrysosporium*. In the liquid cultures inoculated with fungal spores, the initial concentration of CL-20 (3.6 mg L^{-1}) started to degrade after 2 days of incubation (Figure 25). A rapid degradation phase started after 2 days of incubation and led to 100 % removal of CL-20 after 5 days (Figure 25). With 7-day old cultures, no lag was observed and almost all of the CL-20 (11.5 mg L^{-1}) was depleted within 2 days of incubation (Annual report 2003). No degradation of CL-20 was observed in the non-inoculated controls.

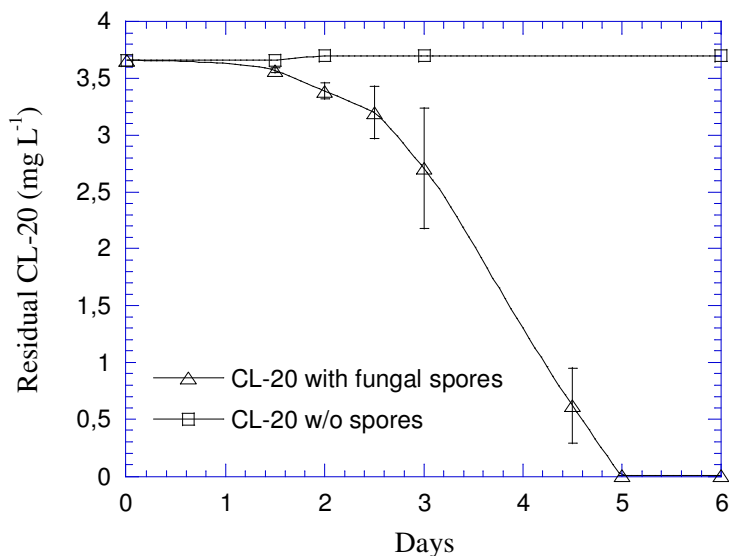


Figure 25 Degradation of CL-20 (3.6 mg L^{-1}) in a N-limited medium with (Δ) and without (\square) the addition of *P. chrysosporium* spores. Bars indicate standard deviation ($n = 3$).

Metabolites formed during the degradation of CL-20. Degradation of CL-20 by *P. chrysosporium* led to N_2O (Annual report 2003). When ring labeled [^{15}N]- CL-20 was used, GC-MS analysis revealed the presence of the masses 44 ($^{14}\text{N}_2\text{O}$) and 45 ($^{14}\text{N}^{15}\text{NO}$) meaning that N_2O originated from both nitro ($^{14}\text{NO}_2$) and nitramine ($^{15}\text{N}-^{14}\text{NO}_2$) groups in the energetic chemical.

Because no early intermediates were observed when the whole fungus was used, MnP was employed to determine the distribution and stoichiometry of CL-20 metabolites. We previously observed that the culture conditions used for the growth of *P. chrysosporium* allowed the production of MnP, with only traces of LiP. The concentration and the amounts of commercially available MnP from *P. chrysosporium* were not sufficient to allow the study of CL-20 transformation. Therefore, in order to detect all possible metabolites from CL-20 decomposition we used a commercial MnP purified from another ligninolytic white-rot fungus, *Nematoloma frowardii*. It should be noted however that most of the MnPs described so far seem to follow a similar catalytic mechanism, i.e. oxidation of the substrate by a 1-electron transfer (Hofrichter, 2002), so that MnPs from different basidiomycetes should attack CL-20 in a similar way.

No mononitroso derivative of CL-20 was observed during the incubation with *P. chrysosporium*, which was in contrast to what had been observed during incubation of HMX with the fungus *P. chrysosporium* (Fournier *et al.*, 2004a). Similarly, incubation with MnP did not generate any CL-20 nitroso-derivative. Instead of the reductive attack reported for biotransformation of TNT, RDX, or HMX by *P. chrysosporium* (Hawari *et al.*, 1999; Sheremata and Hawari, 2000b; Fournier *et al.*, 2004a), we thus hypothesized that one or several fungal extracellular enzymes such as MnP participated in the oxidation of CL-20 molecule.

The use of MnP enabled the detection of an HPLC peak showing a mass ion $[M-H]^-$ at 345 Da identical to the intermediate **Ia** (Figure 17) detected during reaction with iron and photolysis of CL-20. The LC/MS peak matched a molecular formula of $C_6H_6N_{10}O_8$ that likely corresponded to the doubly denitrated CL-20 molecule. Like in the photolysis process, the use of nitrogen ring-labeled $[^{15}N]$ -CL-20 gave a mass ion $[M-H]^-$ at 351 Da, in agreement with the formation of this doubly denitrated intermediate.

Nitrous oxide (N_2O), nitrite ion (NO_2^-), and glyoxal were detected and quantified throughout the enzymatic reaction (Figure 26).

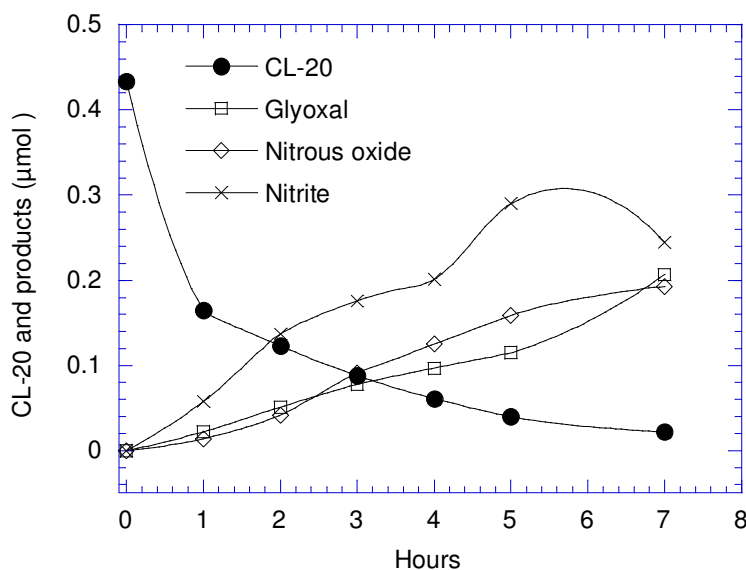


Figure 26 Time-course study of bio-transformation of CL-20 by MnP purified from *Nematotoma frowardii*.

The nitrite formation, which was concomitant with CL-20 removal, supported the occurrence of a denitration process. The formation of glyoxal confirmed the occurrence of ring cleavage and decomposition of intermediate **Ia**, as was the case when reacting Fe^0 with CL-20 (Balakrishnan *et al.*, 2004a). Therefore we concluded that CL-20 underwent a double denitration followed by ring cleavage as shown in Figures 12 and 13.

From each mole of CL-20 degraded, approximately 0.5 mole was transformed into NO_2^- , and 0.5 mole was transformed into N_2O , corresponding to 5 and 8 % of total N, respectively. Several assays aimed at detecting ammonium (NH_4^+) were not successful because of the presence of an

important analytical interference. Ammonium might have been present in the MnP commercial preparation and another enzymatic assay will be performed with washed MnP. In terms of carbon stoichiometry, we experienced again a major analytical interference during the determination of formate (HCOO^-). It is clear that formate was produced from CL-20, but quantification of the metabolite was not possible. It will be repeated with washed MnP. As reported in the degradation of CL-20 with Fe^0 , significant amounts of glyoxal were produced. The ratio of glyoxal over CL-20 degraded after 7 h of reaction indicated that around 15 % of C was transformed into the dialdehyde.

Because glyoxal is a known toxic chemical (Shangari *et al.*, 2003), its formation as a product of CL-20 required investigating its degradability using MnP and the whole fungus. In a separate experiment, we tested the biodegradability of glyoxal with MnP. The dialdehyde remained intact during more than 18 hours of incubation (result not shown). Subsequently, we measured the degradability of glyoxal by the whole fungus *P. chrysosporium*, known to produce many other enzymes than MnP (*i.e.* glyoxal oxidase, several isoforms of LiP and MnP, membrane-linked cytochrome P-450, glutathione S transferase, ...). Figure 12 shows the mineralization of glyoxal with *P. chrysosporium*. As hypothesized, the enzymes produced by the complex fungal culture allowed the mineralization of glyoxal. The transformation of glyoxal to CO_2 began after 1 day of incubation and produced 87 % of CO_2 after 43 days of incubation (Figure 27).

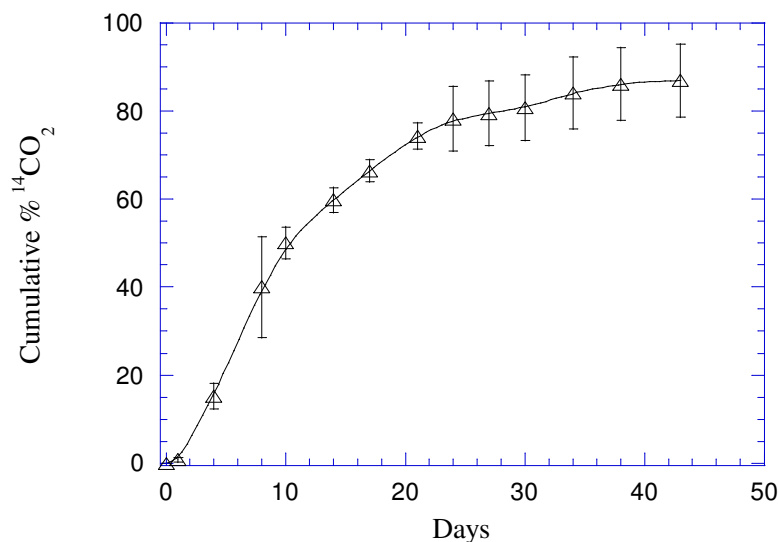


Figure 27 Mineralization of [^{14}C]-glyoxal added to a spore suspension of *P. chrysosporium* prepared in N-limited medium. Bars indicate standard deviation from triplicate experiments.

Mineralization of CL-20 using *P. chrysosporium* cultures. Two mineralization experiments

were started by adding [^{14}C]-CL-20 (4.75 mg L^{-1}) to the microcosms: one involved addition of CL-20 to a 7-day old culture of *P. chrysosporium*, and another involved simultaneous addition of CL-20 and non-ligninolytic fungal spores. During the first 20 days of incubation, no significant difference was observed between the two culture systems (Figure 28). The production of CO_2 began after 5 days of incubation and occurred at a similar rate whether CL-20 was added to spores or to mycelium. However, after 20 days of incubation, the ligninolytic cultures (spiked with [^{14}C]-CL-20 on day 7) seemed to be slightly more performant.

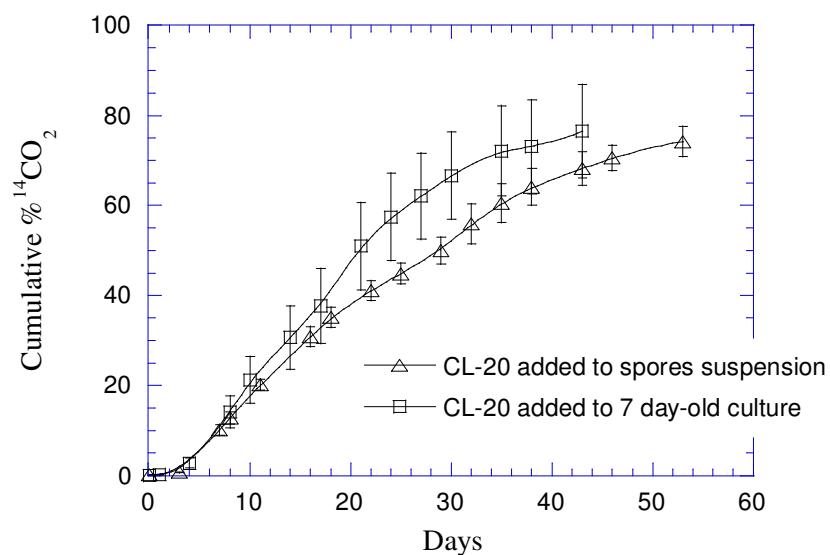


Figure 28 Liberation of $^{14}\text{CO}_2$ from [^{14}C]-CL-20 added to a spore suspension of *P. chrysosporium* (non-ligninolytic) (Δ), and [^{14}C]-CL-20 added to 7-day old ligninolytic fungal culture (\square). Experiments were performed in N-limited medium. Bars indicate standard deviation from triplicate experiments.

Biotransformation of CL-20 pre-adsorbed on VT soil. Since we showed that CL-20 sorption to soil could retard its abiotic degradation but did not stop it (Annual report 2003, Balakrishnan *et al.*, 2004b), we investigated the effect of sorption on biotic degradation of the energetic chemical. VT soil, which demonstrated a sorption coefficient of 15 L kg^{-1} (Balakrishnan *et al.*, 2004b), was chosen for this study. The nitramine was first allowed to sorb on sterilized soil in N-limited medium and the fungal spores were added after 14 days of pre-equilibration. The degradation of CL-20 in soil slurries was measured and compared to the one in N-limited medium to determine the effect of sorption on the biotransformation kinetics.

In the soil slurries where 80 % of the CL-20 was found to be associated with the soil particles, degradation occurred at a slower rate (Figure 29) than in the liquid cultures (Figure 26). After 6 days of slow degradation, a more rapid degradation phase was observed, which lasted 12 days and led to 80 % removal of CL-20, before a new decrease of degradation rate was observed. Carbon supplementation by addition of glucose on day 21 led to almost complete degradation after 35 days (Figure 29). Sorption of CL-20 on VT soil did not prevent degradation of the

chemical by *P. chrysosporium*. As compared to the degradation in liquid medium, presorption of CL-20 on soil retarded the beginning of degradation and decreased the degradation rate by a factor of 6.4. However, sorption of CL-20 on soil was reversible and did not prevent biotransformation by *P. chrysosporium*.

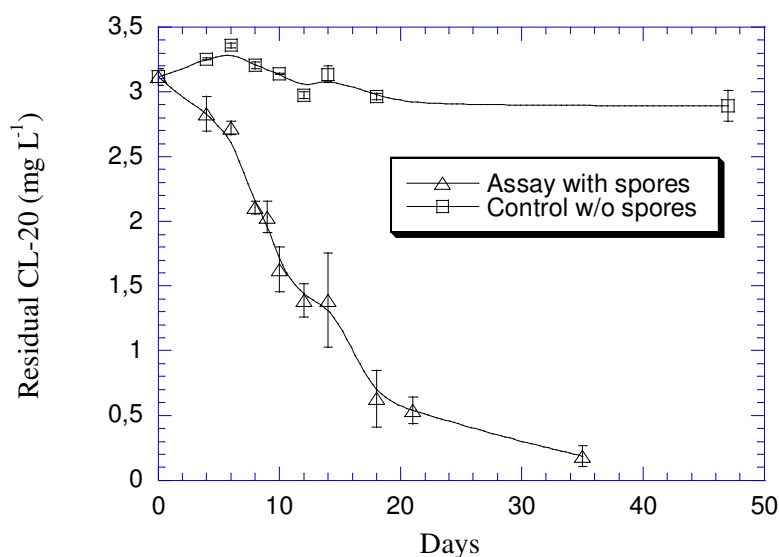


Figure 29 Degradation of CL-20 pre-sorbed on VT soil (1.33 g) by *P. chrysosporium* in N-limited medium (10 mL). Glucose was supplemented on day 21 (Δ). Bars indicate standard deviation ($n = 3$)

Conclusion

Both ligninolytic and non-ligninolytic *P. chrysosporium* can transform CL-20. The enzymatic mechanism involved in the first attack of the molecule was not yet identified. However because no nitroso-CL-20 was observed, the mechanism seems to differ from the one involved in the fungal degradation of RDX, HMX or TNT. CL-20 degraded more rapidly when ligninolytic culture conditions (known to favor the production of MnP and LiP) were applied. The use of commercial MnP allowed us to determine that CL-20 was transformed *via* initial denitration followed by ring cleavage, producing nitrite ion, nitrous oxide, glyoxal, and formate. The latter products were also observed during photolysis and iron reduction of CL-20.

In addition, *P. chrysosporium* was found to extensively mineralize radio labeled CL-20 and glyoxal indicating that the compounds are not recalcitrant toward the fungus. C and N mass balances will be completed in the near future.

P. chrysosporium was also able to degrade CL-20 in soil, but at a slower rate. Our previous studies have indicated that sorption of CL-20 was reversible (Balakrishnan *et al.*, 2004b) and the bio-degradation kinetics observed here was likely controlled by the desorption rate.

In addition to the present soil experiment, where an exogenous microorganism was added to the microcosms, other experiments will be carried out to determine the potential of indigenous microorganisms in soil to degrade CL-20.

XII.2 Biotransformation of CL-20 with the soil isolate *Pseudomonas* sp FA1

Material and Methods

Chemicals. NADH, NADPH, diphenyliodonium chloride (DPI), FMN, FAD, NaNO₂, dicumarol, 2,2-dipyridyl, 2-methyl-1,2-di-3-pyridyl-1-propanone (metyrapone) and phenylmethanesulfonyl fluoride (PMSF) were purchased from Sigma chemicals, Canada. Nitrous oxide (N₂O) was purchased from Scott specialty gases, Sarnia, ON, Canada. Carbon monoxide (CO) was purchased from Aldrich chemical company, Milwaukee, WI, USA. All other chemicals were of the highest purity available.

Isolation and identification of CL-20 degrading strains. One gram of garden soil was suspended in 20 mL of minimal medium (ingredients per liter of deionized water: K₂HPO₄, 1.22 g; KH₂PO₄, 0.61 g; NaCl, 0.20 g; MgSO₄, 0.20 g; succinate, 8.00 g; pH 7.0) supplemented with CL-20 at a final concentration of 4.38 mg L⁻¹ added from a 10,000 mg L⁻¹ stock solution made in acetone. The inoculated medium was incubated under aerobic conditions at 30°C on an orbital shaker (150 rpm) in the dark. The disappearance of CL-20 was monitored over several days. The enriched culture was plated periodically onto the same medium with 1.8 % agar (Difco, Becton Dickinson and Co., Sparks, MD, USA) and surface of solidified agar plates were layered with 10 µM CL-20. The isolated colonies were sub-cultured three times using the same agar plates and were tested for their ability to biotransform CL-20 in liquid medium. Of the few isolated bacterial strains, a denitrifying strain FA1 capable of utilizing CL-20 as a sole nitrogen source was selected for further study.

For identification and characterization of strain FA1, standard biochemical techniques were used according to Bergey's manual of systematic bacteriology (Palleroni, 1984). Total cellular fatty acids (fatty acid methyl esters, FAME) analysis and 16S ribosomal RNA gene analysis were performed and analyzed by MIDI labs, DL, USA.

CL-20 was added to the medium in concentrations above saturation levels (*i.e.* ≥ 10 µM or 4.38 mg L⁻¹) from a 10,000 mg L⁻¹ stock solution made in acetone. Saturated solutions were used in order to detect and quantify the metabolites, which are otherwise produced in trace amounts during biotransformation. To determine the residual CL-20 during biotransformation studies, the total CL-20 content in one serum bottle was solubilized in 50 % aqueous acetonitrile and analyzed by HPLC.

The following minimal medium (MM) was used for the CL-20 biotransformation studies and was composed of (ingredients per liter deionized water): K₂HPO₄, 1.22 g; KH₂PO₄, 0.61 g; NaCl, 0.20 g; MgSO₄, 0.20 g; succinate, 8.00 g; trace elements, 10 mL; pH 7.0. Modified Wolfe's mineral solution was used as trace elements solution and was composed of (ingredients per liter deionized water): MnSO₄ · H₂O, 0.20 g; CaCl₂ · 2 H₂O, 0.10 g; CoCl₂ · 6 H₂O, 0.10 g; ZnCl₂, 0.15 g; CuSO₄ · 5 H₂O, 0.01 g; FeSO₄ · 7 H₂O, 0.10 g; Na₂MoO₄, 0.05 g; NiCl₂ · 6 H₂O, 0.05 g; Na₂WO₄ · 2 H₂O, 0.05 g.

A comparative growth experiment was performed between (NH₄)₂SO₄ and CL-20 as sole nitrogen sources to determine the number of nitrogen atoms from CL-20 that were incorporated

into biomass. Cells were grown in MM containing increasing concentrations of either $(\text{NH}_4)_2\text{SO}_4$ or CL-20 as a sole nitrogen source, at 30°C under aerobic conditions on an orbital shaker (150 rpm) in the dark for 16 h. After incubation period the microbial growth yield in the form of total viable cell counts were determined by standard plate count method. In this method, the cultures were serially diluted in sterile phosphate buffer saline (PBS) and spread plated onto LB agar plates (per liter of deionized water composed of tryptone 10 g, yeast extract 5 g, NaCl 10 g, Agar 15 g). All ingredients, except NaCl, were purchased from Becton Dickinson and company, Sparks, MD, USA. The plates were incubated at 30°C overnight. After incubation, the numbers of bacterial colonies grown in the plates were considered to determine the total viable cell count per mL of culture.

In order to determine the effect of alternate cycles of aerobic and anaerobic growth conditions on CL-20 biotransformation by the isolate FA1, cells were grown in MM containing 10 mM of $(\text{NH}_4)_2\text{SO}_4$ and 25 μM of CL-20 in two serum bottles under aerobic conditions up to a late-log phase ($\text{OD}_{600\text{ nm}} \sim 0.60$) and then anaerobic conditions were created in one of the two growing cultures by flushing the headspace with argon for 30 min. The cultures were further grown till stationary phase. Growth and CL-20 disappearance were monitored in both serum bottles over the course of experiment.

To determine whether the enzyme system responsible for CL-20 biotransformation was induced or constitutive, two batches of cells were grown in MM containing 10 mM of $(\text{NH}_4)_2\text{SO}_4$ in the presence and absence of CL-20 (10 μM). At mid-log phase, the cells were harvested by centrifugation at 4°C and washed thrice with phosphate buffer saline (PBS), pH 7.0. The washed cells (5 mg wet biomass/mL) were tested for their ability to biotransform CL-20 under aerobic and anaerobic conditions.

Preparation of cytosolic and membrane-associated enzymes. Bacterial cells were cultured in two liters of MM containing 10 mM of $(\text{NH}_4)_2\text{SO}_4$ up to a mid-log phase (8-9 h, $\text{OD}_{600\text{ nm}}$ of 0.45) at 30°C and then induced with 10 μM CL-20. After induction, the cells were further incubated up to 12-16 h ($\text{OD}_{600\text{ nm}}$ of 0.95). Cells were harvested by centrifugation, washed thrice with phosphate buffer saline (PBS), pH 7.0 and then suspended in 50 mM potassium phosphate buffer (pH 7.0) containing 1 mM PMSF and 100 mM NaCl. The washed cell biomass (0.2 g/mL) was subjected to disruption with French press at 20,000 p.s.i. The disrupted cell suspension was centrifuged at $9000 \times g$ for 30 min at 4°C to remove cell debris and undisrupted cells. The supernatant was centrifuged at $165,000 \times g$ for 1 h at 4°C. The pellet (membrane protein fraction) and supernatant (soluble protein fraction) thus obtained were separated, mixed with 10 % glycerol, aliquots were prepared and stored at -20°C till further use. The protein content was determined with a bicinchoninic acid protein assay kit from Pierce Chemicals Company, Rockford, Ill.

Total flavin (FMN and FAD) contents in the crude extract, the membrane fraction and the soluble-protein fractions were determined by a spectrophotometric method described by Aliverti et al. (1999). Deflavo-enzyme(s) and reconstitution of deflavo-enzyme(s) were prepared as described before (Bhushan *et al.*, 2002).

Biotransformation assays. Enzyme catalyzed biotransformation assays were performed under aerobic as well as anaerobic conditions in 6-mL glass vials. Anaerobic conditions were created by purging all the solutions with argon gas three times (10 min each time at 10 min intervals) and

replacing the headspace air with argon in sealed vials. Each assay vial contained, in 1 mL of assay mixture, CL-20 (25 μ M), NADH or NADPH (150 μ M), soluble or membrane-enzyme preparation (1.0 mg) and potassium phosphate buffer (50 mM, pH 7.0). Reactions were performed at 30°C. Different controls were prepared by omitting enzyme, CL-20 or NADH from the assay mixture. Boiled enzyme was also used as a negative control. Residual NADH or NADPH was measured as described before (Bhushan *et al.*, 2002). Samples from liquid and gas phase in the vials were analyzed for residual CL-20 and biotransformed products. CL-20 biotransformation activity of enzyme(s) was expressed as nmol h⁻¹ mg protein⁻¹ unless otherwise stated.

Bioconversion of nitrite to nitrous oxide was determined by incubating 20 μ M NaNO₂ with a membrane-enzyme(s) preparation using NADH as electron donor. Disappearance of nitrite and formation of nitrous oxide were measured periodically. Results were compared with a control without NaNO₂.

Enzyme inhibition studies. Inhibition with diphenyliodonium chloride (DPI), an inhibitor of flavoenzymes that act by forming flavin-phenyl adduct (Chakraborty and Massey, 2002), was assessed by incubating the enzyme preparation with DPI at different concentrations (0 - 2.0 mM) at room temperature for 30 min before CL-20 biotransformation activities were determined. Other enzyme inhibitors such as dicumarol, carbon monoxide (60 s bubbling through the enzyme solution), metyrapone and 2,2-dipyridyl were incubated with enzyme preparation at different concentrations for 30 minutes at room temperature. Thereafter, CL-20 biotransformation activity of the treated enzyme was determined.

Analytical procedures. CL-20, nitrite (NO₂⁻), nitrous oxide (N₂O), formaldehyde (HCHO) and formic acid (HCOOH) were analyzed as described in the previous sections.

Accomplishments

Isolation and identification of CL-20 degrading strain FA1. The standard enrichment techniques were used to isolate CL-20 degrading strains from garden soil samples. The enrichment experiments were carried out over a period of three weeks and four CL-20 degrading strains designated as FA1 to FA4 were isolated. Strain FA1 biotransformed CL-20 at a higher rate compared to the other isolates (data not shown) and was capable of utilizing CL-20 as a sole nitrogen source and therefore it was selected for further study.

Strain FA2 was identified as a *Bacillus* sp. by 16S ribosomal RNA gene analysis while strains FA3 and FA4 remained unidentified. FA1 was characterized by standard biochemical tests mentioned in the Bergey's manual of systematic bacteriology (Palleroni, 1984). Strain FA1 was a non-spore forming, gram-negative, motile bacterium with small rod structure (approx. 1.5 – 2.0 μ m). Biochemically, it showed positive results for oxidase, catalase and nitrite reductase and utilized succinate, fumarate, acetate, glycerol and ethanol as sole carbon sources. It utilized CL-20, ammonium sulfate, ammonium chloride and sodium nitrite as sole nitrogen sources. Total cellular fatty acids methyl esters analysis (FAME) of strain FA1 showed a similarity index of 0.748 with *Pseudomonas putida* biotype A. On the other hand, 16S ribosomal RNA gene analysis showed a 99 % similarity of strain FA1 with a *Pseudomonas* sp. C22B (GenBank

accession number AF408939) isolated from a soil sample in a shipping container. No published data is available in regard to strain C22B. On the basis of above data we identified and named the strain FA1 as *Pseudomonas* sp. FA1.

Nucleotide sequence accession number. The 16S rRNA gene sequence of *Pseudomonas* sp. FA1 was deposited in GenBank under an accession number AY312988.

Growth of strain FA1 on CL-20 as a nitrogen source. As mentioned above strain FA1 was capable of utilizing CL-20, ammonium sulfate, ammonium chloride and sodium nitrite as sole nitrogen sources. In order to determine the number of nitrogen atoms from CL-20 that were incorporated into biomass, cells were grown in MM containing different concentrations of either $(\text{NH}_4)_2\text{SO}_4$ or CL-20. After incubation, the growth yield in form of total viable cell counts was determined. The growth yield using CL-20 as nitrogen source was about 1.83-fold higher compared to that observed with $(\text{NH}_4)_2\text{SO}_4$ (Figure 30). No growth was observed in the control experiment without any nitrogen source. The ratio of growth yields in $(\text{NH}_4)_2\text{SO}_4$ versus CL-20 (Figure 30) indicated that of the 12 nitrogen atoms per CL-20 molecule, approx. 4 nitrogen atoms were assimilated into the biomass. The soil isolate *Agrobacterium* sp. JS71 utilized CL-20 as a sole nitrogen source and assimilated 3 moles of nitrogen per mole of CL-20.

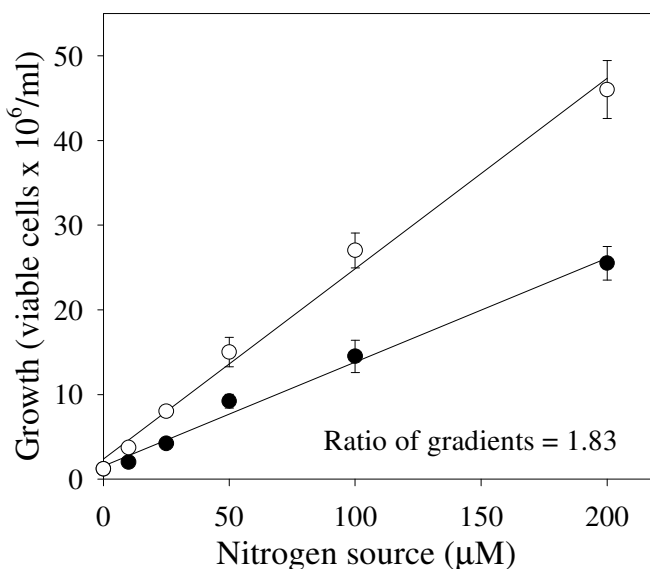


Figure 30 Growth of *Pseudomonas* sp. FA1 at various concentrations of CL-20 (○) and $(\text{NH}_4)_2\text{SO}_4$ (●). The viable-cell count in early-stationary-phase-culture (16 h) was determined for each nitrogen concentration. Linear regression curve for $(\text{NH}_4)_2\text{SO}_4$ has a gradient of 0.122 and an r^2 of 0.990. Linear regression curve for CL-20 has a gradient of 0.224 and an r^2 of 0.992. Data are means of results from duplicate experiments, and error bars indicate standard error. Some error bars are not visible due to their small size.

Biotransformation of CL-20 by intact cells. In a study of the effect of alternate cycle of aerobic and anaerobic growth conditions on CL-20 biotransformation, we observed that after creating anaerobic conditions in one of the two growing cultures at 9 h of growth, most of the CL-20 was biotransformed in the subsequent 2 h of incubation but that under aerobic conditions it took more than 20 h to biotransform the same amount of CL-20 (Figure 31). This experimental finding indicated that the growth of *Pseudomonas* sp. FA1 was faster under aerobic conditions while CL-20 biotransformation by the mid-log phase culture (8-9 h) was more rapid under anaerobic conditions.

An experiment with uninduced and CL-20 (10 μM)-induced cells showed CL-20 biotransformation activities of 1.4 ± 0.05 and $3.2 \pm 0.1 \text{ nmol h}^{-1} \text{ mg of protein}^{-1}$, respectively, indicating that CL-20 was biotransformed at a 2.2-fold faster rate by the induced cells than by the uninduced cells. This experimental finding indicated that there could be an up-regulation of an enzyme in the induced cells that might be responsible for CL-20 biotransformation. In addition, the increase in activity could be due to an improved uptake of CL-20 following induction of the cells with CL-20

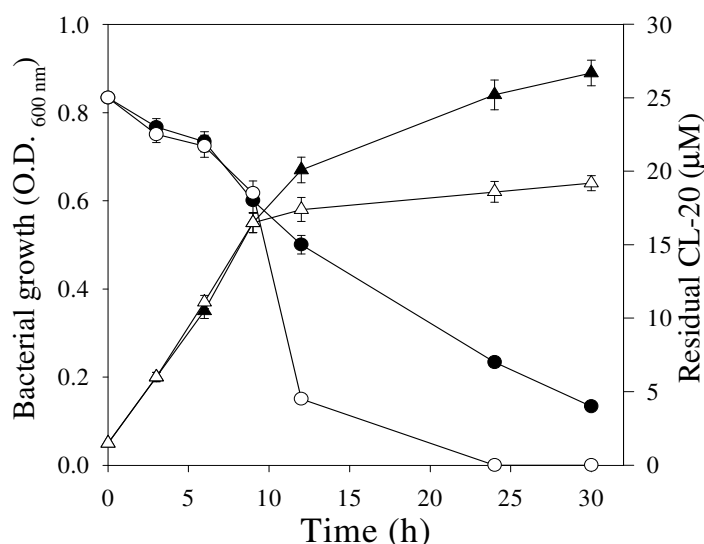


Figure 31 Effect of alternate cycle of aerobic and anaerobic growth conditions on biotransformation of CL-20 by *Pseudomonas* sp. FA1. Symbols: growth (▲) and CL-20 degradation (●) under aerobic conditions. Open triangles and circles show the levels of growth and CL-20 biotransformation, respectively, under aerobic conditions (for the first 9 h) and then under anaerobic conditions. Data are mean of results from triplicate experiments, and error bars indicate standard error. Some error bars are not visible due to their small size.

Localization of enzyme(s) responsible for CL-20 biotransformation. The CL-20 biotransformation activities of cell-free crude extract, cytosolic soluble enzyme(s) and membrane-enzyme(s) were determined under aerobic as well as anaerobic conditions. We found that all the three enzyme(s) fractions exhibited higher activities under anaerobic conditions

(Table 10) than those observed under aerobic conditions (data not shown). In case of membrane-enzyme(s), CL-20 biotransformation was about 5-fold higher under anaerobic conditions ($11.5 \pm 0.4 \text{ nmol h}^{-1} \text{ mg of protein}^{-1}$) than under aerobic conditions ($2.5 \pm 0.1 \text{ nmol h}^{-1} \text{ mg of protein}^{-1}$), indicating the involvement of an initial oxygen sensitive step during biotransformation of CL-20. As a result, the subsequent study was carried out under anaerobic conditions.

CL-20 biotransformation activities of membrane-enzyme(s) using NADH or NADPH as an electron-donor were 11.5 ± 0.4 or $2.1 \pm 0.1 \text{ nmol h}^{-1} \text{ mg of protein}^{-1}$, respectively, indicating that the responsible enzyme was mainly NADH-dependent.

The CL-20 biotransformation activities of membrane and soluble enzyme(s) fractions were 11.5 ± 0.4 and $2.3 \pm 0.05 \text{ nmol h}^{-1} \text{ mg of protein}^{-1}$, respectively (Table 10), which clearly indicated that the enzyme(s) responsible for CL-20 biotransformation was membrane-associated. The CL-20 biotransformation activities observed in the soluble enzyme(s) fraction presumably leached out from the membrane-enzyme(s) fraction during cell-disruption process.

Enzymatic biotransformation of CL-20 and product stoichiometry. The membrane-enzyme(s) catalyzed the biotransformation of CL-20 optimally at pH 7.0. Activity remained unchanged between pH 6.0 and 7.5 but higher or lower pHs caused reduction in activity (data not shown). A time course study carried out with membrane-enzyme(s) showed that CL-20 disappearance was accompanied by the formation of nitrite and nitrous oxide at the expense of the electron-donor NADH (Figure 32). After 2.5 h of reaction, each reacted CL-20 molecule produced about 2.3 nitrite ions, 1.5 molecules of nitrous oxide and 1.7 molecules of formic acid (Table 11). Of the total 12 nitrogen atoms (N) and 6 carbons (C) per reacted CL-20 molecule, we recovered approximately 5 N (as NO_2^- and N_2O) and 2 C (as HCOOH), respectively. The remaining 7 N and 4 C may be present in unidentified intermediate(s).

Pseudomonas sp. FA1 was a denitrifying bacterium; hence, nitrite was observed as a transient intermediate during CL-20 biotransformation and was partially converted to nitrous oxide. This observation was proved by incubating membrane-enzyme(s) with inorganic NaNO_2 under the same reaction conditions as those used for CL-20. The results showed an NADH-dependent reduction of nitrite (used as NaNO_2) to nitrous oxide (Figure 33).

In biological systems, the enzymatic conversion of nitrite to nitrous oxide occurs via a transient formation of nitric oxide (NO) and this process involves two enzymes *i.e.* nitrite reductase (converts nitrite to nitric oxide) and nitric oxide reductase (converts nitric oxide to nitrous oxide). Since *Pseudomonas* species are known to produce these two reductase enzymes (Forte *et al.*, 2001; Arese *et al.*, 2003), we assume that the membrane preparation from strain FA1 may contain these two enzymes.

Table 10 Effect of flavin contents in native- and deflavo-enzyme preparations on the CL-20 biotransformation activities of various enzyme fractions from *Pseudomonas* sp. FA1 under anaerobic conditions^a.

Localization of enzyme(s)	Total Flavin content in native-enzyme(s) (nmol/mg of protein)	CL-20 biotransformation activity of native-enzyme(s) (nmol h ⁻¹ mg of protein ⁻¹)	Total Flavin content in deflavo-enzyme(s) (nmol/mg of protein)	CL-20 biotransformation activity of deflavo-enzyme(s) (nmol h ⁻¹ mg of protein ⁻¹)
1. Cell-free crude extract	22.6 ± 1.3	15.6 ± 0.7	N.D.	N.D.
2. Cytosolic soluble enzyme(s)	5.5 ± 0.2	2.3 ± 0.05	1.2 ± 0.2	0.5 ± 0.05
3. Membrane-associated enzyme(s)	12.6 ± 0.6	11.5 ± 0.4	3.8 ± 0.3	2.7 ± 0.1

^a Data are means ± standard errors from triplicate experiments. N.D., not determined

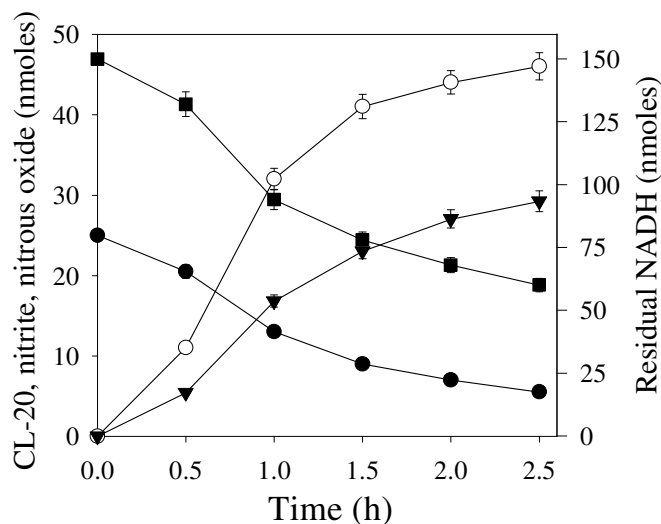


Figure 32 Time-course study of NADH-dependent biotransformation of CL-20 by a membrane-associated enzyme(s) from *Pseudomonas* sp. FA1 under anaerobic conditions. Symbols indicate the levels of CL-20 (●), NADH (■), nitrite (○), nitrous oxide (▼). Data are means of results from triplicate experiments, and error bars indicate standard errors. Some error bars are not visible due to their small size.

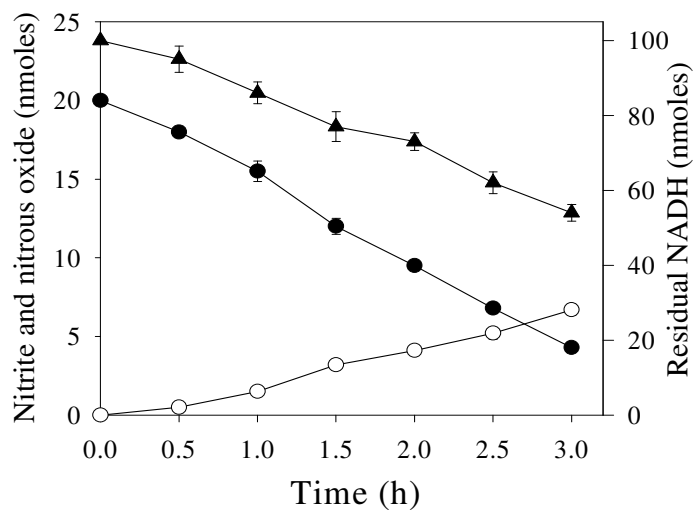


Figure 33 Time-course study of NADH-dependent reduction of nitrite to nitrous oxide by a membrane-associated enzyme(s) from *Pseudomonas* sp. FA1 under anaerobic conditions. Symbols indicate the levels of nitrite (●), nitrous oxide (○), NADH (▲). Data are means of results from triplicate experiments, and error bars indicate standard errors. Some error bars are not visible due to their small size.

Table 11 Stoichiometry of reactants and products during biotransformation of CL-20^a.

Reactants or Products	Amount (nmol)	Molar ratio of reactants to products per reacted CL-20 molecule
Reactants		
1. CL-20	20	1.0
2. NADH	90	4.5
Products		
1. Nitrite (NO ₂ ⁻)	46	2.3
2. Formate (HCOOH)	34	1.7
3. Nitrous oxide (N ₂ O)	29	1.5

^aCL-20 was biotransformed by a membrane-associated enzyme(s) (1 mg/mL) from *Pseudomonas* sp. FA1 at pH 7.0, 30 °C for 2.5 h under anaerobic conditions. The data are means of results of triplicate experiments.

Involvement of flavoenzyme(s) in the biotransformation of CL-20. The total flavin contents were measured in crude extract, cytosolic soluble enzymes and membrane- enzymes. The membrane-enzyme(s) contained about 56 % of the total flavin content and retained about 74 % of the total CL-20 biotransformation activity present in the crude extract (Table 10). In the deflavoenzyme(s) preparation there was a corresponding decrease in flavin content as well as CL-20 biotransformation activity (Table 10), which indicated the involvement of a flavin moiety in CL-20 biotransformation. Furthermore, the CL-20 biotransformation activity of deflavoenzyme was restored up to 75 % after reconstitution with equimolar concentrations of FAD and FMN (100 µM each). The comparison of CL-20 biotransformation activities of the native enzyme (11.5 ± 0.4 nmol h⁻¹ mg of protein⁻¹), deflavoenzyme (2.7 ± 0.1 nmol h⁻¹ mg of protein⁻¹) and reconstituted-enzyme(s) (8.90 ± 0.5 nmol h⁻¹ mg of protein⁻¹) clearly showed the involvement of a flavoenzyme(s) in biotransformation of CL-20 by *Pseudomonas* sp. FA1. The free FAD and FMN also biotransformed CL-20 in the presence of NADH, however, the biotransformation rate was about 5-fold lower than that of the native membrane-enzyme(s). This finding additionally supported the involvement of a flavin-containing enzyme in CL-20 biotransformation and also indicated that the flavin-moieties have to be in an enzyme-bound form in order to function efficiently.

Study with diphenyliodonium chloride (DPI) showed a 62 % inhibition of CL-20 biotransformation (Table 12). Analogously with previous reports, which proved that DPI targets flavin-containing enzymes that catalyze one-electron transfer reactions (Chakraborty and Massey, 2002; O'Donnell *et al.*, 1994), the present study suggested the involvement of such an enzyme during biotransformation of CL-20 by strain FA1. The involvement of a flavoenzyme in biotransformation of RDX (Bhushan *et al.*, 2002) and HMX (Bhushan *et al.*, 2003b) via one-electron transfer has already been established. In our previous study with diaphorase (a FMN containing flavoenzyme from *Clostridium kluyveri*), we reported an oxygen-sensitive one-

electron transfer reaction that caused N-denitration of RDX leading to its decomposition (Bhushan *et al.*, 2002). Moreover, a xanthine oxidase catalyzed an oxygen-sensitive, initial single N-denitration of HMX at the FAD site, leading to the spontaneous decomposition of the molecule (Bhushan *et al.*, 2003b).

Table 12 Effects of enzyme inhibitors on the CL-20 biotransformation activity of membrane-associated enzyme(s)^a

Inhibitor (2 mM)	% CL-20 biotransformation activity ^b
1. Without inhibitor (control)	100 ± 1.7
2. Diphenyliodonium	38 ± 2.3
3. Dicumarol	86 ± 3.5
4. Metyrapone	91 ± 2.8
5. Carbon monoxide ^c	87 ± 2.2
6. 2,2-dipyridyl	92 ± 3.4

^a the CL-20 biotransformation activity of the membrane-associated enzymes (1 mg/mL) was determined at pH 7.0 and 30°C after 1 h under anaerobic conditions. ^b 100 % CL-20 biotransformation activity was equivalent to 11.5 nmol h⁻¹ mg of protein⁻¹. Data are mean percentages of CL-20 biotransformation activity ± standard errors (*n* = 3). ^c Carbon monoxide was bubbled through the aqueous phase and headspace for 60 s in sealed vials.

On the other hand, enzyme inhibitors such as dicumarol (a DT-diaphorase inhibitor) (Tedeschi *et al.*, 1995), metyrapone and CO (cytochrome P450 inhibitors) (Bhushan *et al.*, 2003c), and 2,2-dipyridyl (metal chelator) did not show effective inhibition of CL-20 biotransformation activity of membrane-enzyme(s) from strain FA1 (Table 10). The inhibition study ruled out the possibility of involvement of above mentioned or similar type of enzymes during biotransformation of CL-20 by *Pseudomonas* sp. FA1.

Proposed initial reaction of CL-20 biotransformation. According to the time-course study described above, the disappearance of CL-20 was accompanied by the formation of nitrite (Figure 32) and this reaction was oxygen-sensitive. Additionally, the DPI-mediated inhibition of CL-20 degradation activity (Table 12) showed the involvement of a flavoenzyme catalyzing one-electron transfer. The evidence suggests that CL-20 molecule undergoes enzyme catalyzed one-electron reduction to form an anion radical of CL-20. This anion radical undergoes denitration to form a free-radical, which eventually undergoes spontaneous ring-cleavage and decomposition to produce nitrous oxide, nitrite and formic acid. Previously, we reported a one-electron transfer reaction catalyzed by a diaphorase, a flavoenzyme from *Clostridium kluyveri*, which caused N-

denitration of RDX leading to its decomposition (Bhushan *et al.*, 2002). The present study analogously with the initial biotransformations of other cyclic nitramine compounds, such as RDX (Bhushan *et al.*, 2002) and HMX (Bhushan *et al.*, 2003b) supports an initial enzymatic N-denitration of CL-20 prior to ring-cleavage.

Nitrite ions probably come from the four nitro-groups bonded to the two five-member rings in the CL-20 structure. Nitrous oxide can be produced in two different ways: first, by enzymatic reduction of nitrite and second, during secondary decomposition of the CL-20 free-radical as it was previously suggested by Patil and Brill (1991). Nitrous oxide was also produced during secondary decomposition of RDX (Bhushan *et al.*, 2002) and HMX (Bhushan *et al.*, 2003b, Hawari *et al.*, 2001). Formic acid was presumably formed following denitration and the cleavage of the C-C bond bridging the two five-member rings in CL-20 structure. Indeed, this bond is relatively longer (Xinqi and Nicheng, 1996) and thus weaker than the other C-C bonds. Formaldehyde (HCHO), a major carbon compound produced during biotransformation of RDX and HMX (Bhushan *et al.*, 2002, 2003a,c; Halasz *et al.*, 2002; Hawari, 2000; Hawari *et al.*, 2000b, 2001), was not observed in the present study.

Conclusion

A *Pseudomonas* sp. FA1, capable of utilizing CL-20 as sole nitrogen source, was isolated and identified from a soil sample. Strain FA1 grew well under aerobic conditions but biotransformed CL-20 under anaerobic conditions to produce nitrite, nitrous oxide and formic acid. Studies with deflavo-form of enzyme and its subsequent reconstitution, and the inhibition of holoenzyme by DPI evidently support the involvement of a flavoenzyme in CL-20 biotransformation. The enzyme responsible for biotransformation of CL-20 by strain FA1 is a NADH-dependent, membrane-associated flavoenzyme.

The present study has provided the insights into the initial microbial and enzymatic biotransformation of CL-20 and some of its products that were not known before. Further work is now necessary to identify the intermediates and end-products from CL-20 to supplement the mass balance study, which would help in determining the complete biodegradation pathway of CL-20. The continuation of the work will thus involve the use of ^{14}C and ^{15}N labeled CL-20.

A vast literature available online (<http://www.ncbi.nlm.nih.gov>) revealed that *Pseudomonas* and the bacteria belonging to family Pseudomonadaceae are prevalent in almost all types of environments e.g. soils, marine and fresh water sediments. The present study would therefore help in understanding the environmental fate (biotransformation, biodegradation and/or natural attenuation) of cyclic nitramine explosive compounds such as CL-20.

XIII Anaerobic degradation of CL-20

Results obtained from this task was published in:

1. Bhushan B, Paquet L, Spain JC, Hawari J. (2003) Biotransformation of 2,4,6,8,10,12-hexanitro-2,4,6,8,10,12-hexaazaisowurtzitane (CL-20) by denitrifying *Pseudomonas* sp. Strain FA1. *Appl. Environ. Microbiol.* 69:5216-5221
2. Bhushan B, Halasz A, Thiboutot S, Ampleman G, Hawari J. (2004) Chemotaxis-mediated biodegradation of cyclic nitramine explosives RDX, HMX and CL-20 by *Clostridium* sp. EDB2. *Biochem. Biophys. Res. Commun.* 316:816-821
3. Bhushan, B, A. Halasz and J. Hawari. (2006) Effect of iron (III), humic acid, and anthraquinmone-2, 6-disulphonate on biodegradation of cyclic-nitramines by *Clostridium* sp. EBD2. *J. Appl. Microbiology* 100: 555-563.

XIII.1 Biotransformation of CL-20 with *Clostridium* sp. strain EDB2

Introduction

Cyclic nitramines such as RDX, HMX and CL-20 lack the electronic stability of aromatic compounds like TNT so that an initial attack, whether biological or chemical, can lead to decomposition of these molecules in aqueous media (Hawari, 2000; Hawari *et al.*, 2000a). However, with respective water solubilities of 40.0, 6.6 and 3.6 mg/L at 25 °C (Monteil-Rivera *et al.*, 2004), RDX, HMX and CL-20 may be preferentially attached to solid surfaces and/or trapped in pores when present in marine and terrestrial environments. CL-20, with its higher ability to adsorb on matrix containing organic matter (Balakrishnan *et al.*, 2004b) may be even more strongly bound to the sediment. Rates of biodegradation of such chemicals are limited by the rates of their mass-transfer from non-aqueous phase.

In order to degrade the explosive, the potential microorganism(s) must come in contact with the molecule. Bacterial chemotaxis is one such process that brings microbes closer to the contaminated sites and thus enhance the rate of biodegradation (Marx and Aitken, 2000; Law and Aitken, 2003). Motile and chemotactic microorganisms have advantage over non-motile and non-chemotactic ones by having the ability of sensing the explosive and thus move to form high-population densities around the chemical (Park *et al.*, 2003). The dense microbial population can tolerate higher concentration of toxic chemicals (Greenberg, 2003) and reproduce more rapidly thus stimulating a rapid cleanup. Bacterial chemotaxis to a variety of organic pollutants and their subsequent degradation has been studied extensively (Marx and Aitken, 2000; Samanta *et al.*, 2000; Parales *et al.*, 2000; Parales and Hardwood, 2002; Pandey and Jain, 2002; Law and Aitken, 2003) however no report was available with regard to cyclic nitramine explosives.

In the present study, we isolated an obligate anaerobic bacterium *Clostridium* sp. strain EDB2 from a marine sediment collected from a shipwreck site near Halifax Harbor in Canada. The strain demonstrated chemotaxis response towards the three cyclic nitramine explosives,

RDX, HMX and CL-20, and successfully degraded them. The present study is thus a model system to understand the environmental significance of chemotactic bacteria in accelerating the biodegradation of cyclic nitramine explosives under *in situ* conditions.

Materials and Methods

Chemicals and sediment. Commercial grade RDX, HMX (chemical purity > 99 % for both explosives), [UL-¹⁴C]-RDX (chemical purity > 98 %, radiochemical purity 97 %, specific radioactivity 28.7 $\mu\text{Ci.mmol}^{-1}$), [UL-¹⁴C]HMX (chemical purity > 94 %, radiochemical purity 91 %, specific radioactivity 101.0 $\mu\text{Ci.mmol}^{-1}$) and Hexahydro-1,3,5-trinitroso-1,3,5-triazine (TNX) were provided by Dr. G. Ampleman, Defense Research and Development Canada (DRDC-DND), Valcartier, QC, Canada. Hexahydro-1-nitroso-3,5-dinitro-1,3,5-triazine (MNX) and 4-nitro-2,4-diazabutanal were obtained from SRI International (Menlo Park, CA). Methylenedinitramine (MDNA) was obtained from the rare chemical department of Aldrich, Oakville, ON, Canada. ϵ -CL-20 (99.3 % purity) was provided by ATK Thiokol Propulsion, Brigham City, UT, USA. Micro-capillaries (1 and 5 μL), low-melting-point agarose and NADH were purchased from Sigma chemicals, Canada.

Marine sediment samples were collected from a shipwreck site (200 meters deep sea bed) at 50 nautical miles east of the Halifax harbor, Canada. Chemical analysis showed that sediment was composed of silt, clay, sand and total organic matter at a concentration of 90.45, 8.25, 1.30 and 1.90 %, w/w, respectively. Major metals were Fe, Ca, Al, and Na at a concentration of 40, 24, 15 and 10 g/kg, respectively, and pH of sediment was 7.7.

Media composition. Medium M1 was composed of (per liter): NaCl, 10.0 g; NaHCO₃, 2.5 g; NaH₂PO₄, 0.6 g; KCl, 0.2 g; NH₄Cl, 0.5 g; and Fe(III)-citrate, 12.25 g. Ingredients were mixed in hot water. pH was adjusted to 7.0 with 10 N NaOH. One liter medium was bubbled with N₂:CO₂ (80:20) for 45 min. After autoclaving at 121°C for 20 min, we added filter-sterilized anaerobic solutions of lactate and glucose, 25 mM each; peptone, 1.0 g; trace elements, 10 mL; and vitamin mixture, 10 mL. Trace elements and vitamin mixture were same as reported (Lovley *et al.*, 1984). Medium M2 was composed of (per liter): Peptone 8 g; yeast extract 2 g; NaCl, 10 g; glucose and lactate 25 mM each. For making solid agar slants or plates, 1.8 % agar powder (Difco) was added to the medium.

Isolation of chemotactic bacteria. Enrichments were carried out by adding RDX, HMX and CL-20 together (30 μM each) and sediment (1 % w/v) to medium M1 followed by incubation at room temperature for about 2 weeks under strict anaerobic conditions (N₂:CO₂, 80:20). The enriched culture (2.0 mL) was suspended in 3.0 mL of phosphate buffer saline (PBS) (100 mM, pH 7.0) supplemented with glucose (5 mM) as carbon and energy source. The cell-suspension was sealed in 10-mL vials under strict anaerobic conditions. Micro-capillaries, sealed at one end, were then charged with 5 μM solution of either RDX, HMX or CL-20 and inserted into the above sealed vials by piercing through the butyl rubber septum and partly dipped into the enriched culture as shown in Figure 34. After every 24 h of incubation, one capillary was taken out and plated onto the agar slants of both media M1 and M2 and incubated at room temperature under anaerobic conditions. This exercise was repeated every 24 h for about two weeks to allow isolation of a motile and chemotactic bacterial strain. The isolated strain formed small, black colonies (≤ 1 mm

diameter) on solidified medium M1, and small, white, shining colonies (≤ 1 mm diameter) on solidified medium M2.

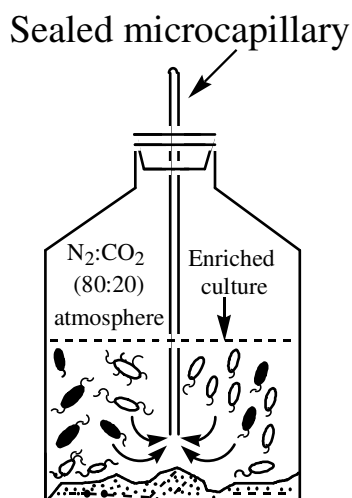


Figure 34 Schematic representation of the technique used to isolate chemotactic bacteria. A 5- μ L microcapillary containing an explosive solution and sealed at outer end is inserted into an air-tight 10-mL glass vial containing 5 mL of enriched culture under anaerobic conditions.

Bacterial Identification. Morphological, physiological and biochemical characterization of the isolated strain were performed by standard methods described for gram-staining, spore-staining, catalase, oxidase, H₂S production, nitrate- and nitrite-reduction, in the manual of methods for general bacteriology (Gerhardt, 1981). 16S rRNA gene analysis (1200 bases) and mol % G+C content of the strain were performed by laboratory services division, University of Guelph, ON, Canada. The strain was named EDB2 (EDB stands for explosive degrading bacterium).

Following microscopy techniques were performed to determine morphology, motility, flagella and cell-count: 1) Phase contrast microscopy was used to observe cell-motility by hanging drop method (Gerhardt, 1981) using standard microscope glass slides with cavity. It was also used for bacterial cell count with Petroff-Hausser counter (Hausser Scientific, Horsham, PA, USA); 2) Transmission electron microscopy (TEM) was used to observe bacterial morphology and type of flagella. For TEM, bacterial cells were negatively stained as follows: a 20 μ L of mid-log-phase culture was placed onto a formvar (polyvinyl formaldehyde) coated grid of mesh size 400. After 4 min of incubation at room temperature the excess fluid was drained off with whatman filter paper. The culture sticking to the grid was stained with 2 % ammonium molybdate for about 30 seconds. Excess stain was drained and grid was washed with double distilled water. The grid was air-dried and observed under a transmission electron microscope (Hitachi H7500).

Chemotaxis assays

Qualitative agarose-plug assay. This assay was conducted as described by Childers *et al.* (2002) with some modifications using low-melting-point agarose (1.6 % w/v, Sigma chemicals, Canada). Briefly, a chemotaxis chamber of dimensions 20 \times 20 \times 1.5 mm was made with two

plastic strips glued to a glass slide. A drop of low-melting-point agarose containing an explosive compound was placed on a glass coverslip and inverted onto the plastic strips. Bacterial cells, grown anaerobically in 100 mL of medium M2 supplemented with RDX, HMX and CL-20 together (15 μ M each), were washed once with PBS buffer and resuspended in 8 mL of PBS buffer containing 1 mM glucose as energy source before transferring to the chemotaxis chamber. The latter was then transferred to a plastic tube sealed with a rubber stopper followed by flushing with N₂:CO₂ (80:20) to create anaerobic conditions and then incubated at 30°C. Bacterial ring formation around the agarose-drop was observed for 60 min. Two separate controls were used for comparison; the first contained agarose-drop with buffer alone, and the second contained autoclaved killed cells against a test chemical(s).

Quantitative micro-capillary assay. A modified version of previously described method (Samanta et al., 2000) was used. The cyclic nitramines, at a defined concentration, were charged into 1- μ L micro-capillaries (Drummond scientific company, Broomall, PA, USA). The latter were inserted into a U-shaped chamber (similar to the chemotaxis chamber as mentioned above but without agarose-drop) already flooded with cell suspension of strain EDB2. The U-shaped chamber was then incubated under anaerobic conditions for 30 min. Micro-capillaries were removed from the chamber and the cells sticking outside the capillaries were washed away with PBS buffer. Cells accumulated inside the capillaries were counted by Petroff-Hausser counter following serial dilutions. Controls were same as mentioned above.

Biotransformation assays for RDX, HMX and CL-20. Biotransformation assays were performed in 6-mL air-tight glass vials under strict anaerobic conditions by purging the reaction mixture with argon for 20 min. Each assay vial contained (one ml of assay mixture) either RDX (20 μ M), HMX (20 μ M) or CL-20 (20 μ M) and resting-cells preparation (5 mg wet biomass/ml) in a potassium phosphate buffer (50 mM, pH 7.0). To determine the effect of NADH on rate of biotransformation of explosive(s), NADH (200 μ M) was added to the reaction vial(s) and incubated at 30°C. Three different controls were prepared by omitting either resting-cells, NADH or both from the assay mixture. Residual NADH was measured as described before (Bhushan *et al.*, 2002). The energetic chemicals and their biotransformed products were analyzed as previously described (Hawari *et al.*, 2001; Hawari *et al.*, 2002; Monteil-Rivera *et al.*, 2004). Explosive degradation activity of the cells was expressed as nmol h⁻¹ mg cell biomass⁻¹ unless otherwise stated.

Accomplishments

Isolation and identification of strain EDB2. We used a new technique devised to isolate chemotactic bacteria (Figure 35) to isolate an obligate anaerobic bacterial strain EDB2, from a marine sediment. Strain EDB2 was small rods of length 1.8 – 3.5 μ m and diameter 0.7–1.0 μ m, and exhibited gram-variable character. Spores were not seen in a stationary-growth-phase culture. The temperature and pH optima for the growth were 30 °C and 7.0, respectively. Strain EDB2 was motile with help of numerous peritrichous flagella (Figure 35). It was catalase and oxidase negative, and produced H₂S from S₂O₃²⁻. Also, it reduced nitrate and nitrite to N₂O using NADH as electron-donor. 16S rRNA gene analysis of 1200 bases (GenBank accession number AY510270) showed that strain EDB2 was 97 % similar to *Clostridium xylanolyticum* (GenBank

accession number X76739) and *Clostridium* strain DR7 (GenBank accession number Y10030). Strain EDB2 differed from *C. xylanolyticum* for having higher mol % G+C content of 53.6 compared to 40 %, and for its potential to reduce nitrite and nitrate. No published description was available for *Clostridium* strain DR7. The results showed that strain EDB2 belonged to genus *Clostridium* however it did not match with any closely related species.

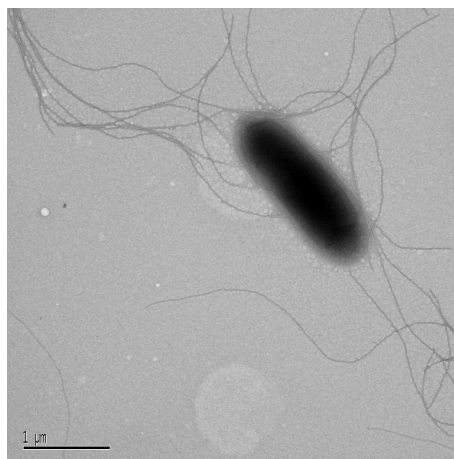


Figure 35 Transmission electron micrograph of negatively stained cell of strain EDB2. Bar indicates 1 μm .

Chemotaxis response of strain EDB2 towards cyclic nitramines including CL-20. Agarose-plug assays showed qualitative chemotaxis of strain EDB2 in form of visible bright rings around the agarose-plug(s) containing RDX, HMX, CL-20 or nitrite. Control agarose-plug containing only buffer did not show chemotaxis response (Figure 36).

Micro-capillary assays showed quantitative chemotaxis response of strain EDB2 towards the three explosives and the nitrite ion (Table 13). Since we found that biotransformation of RDX, HMX and CL-20 occurred via an initial N-denitration (discussed below), we presumed that nitrite released from the explosive molecules was responsible for eliciting a chemotaxis response in strain EDB2. Hexahydro-1-nitroso-3,5-dinitro-1,3,5-triazine (MNX), a RDX metabolite that also released nitrite on reaction with strain EDB2, elicited a chemotaxis response in strain EDB2 (Figure 36 and Table 13). On the other hand, HMX, being the most recalcitrant (discussed below), elicited the least chemotaxis response (Table 13). Our hypothesis was strengthened when hexahydro-1,3,5-trinitroso-1,3,5-triazine (TNX), a RDX metabolite without a nitro group, did not elicit chemotaxis response (Table 13). Additionally, methylenedinitramine and 4-nitro-2,4-diazabutanal, both ring-cleavage metabolites from RDX and/or HMX (Halasz *et al.*, 2002; Fournier *et al.*, 2002), neither released nitrite during their reaction with resting cells of strain EDB2 nor they elicited chemotaxis response in strain EDB2. Other known carbon products of cyclic nitramines *i.e.* HCHO and HCOOH, which lack NO_2^- , elicited a poor chemotaxis response in bacterium (data not shown). The above data confirmed that nitrite released from the explosives was primarily responsible for inducing chemotaxis response in strain EDB2. Once

gathered around the contaminated site, strain EDB2 may form high population density and reproduce more rapidly as did other bacteria (Park *et al.*, 2003; Greenberg, 2003). As a result, higher degradation rates of energetic chemicals can be achieved by strain EDB2 as previously reported with regard to bacterial degradation of naphthalene (Marx and Aitken, 2000; Law and Aitken, 2003).

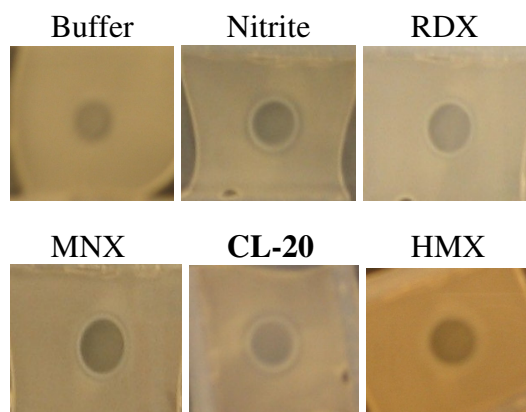


Figure 36 Qualitative chemotaxis assay with strain EDB2 by agarose-plug method. Bright ring of bacterial cells around the plug indicated chemotaxis.

Table 13 Quantitative chemotaxis assay with strain EDB2 by micro-capillary method.

Compound	Conc. (μM)	Chemotaxis index ^a
1. Buffer ^b	—	1.0 ± 0.1
2. RDX	10	5.0 ± 0.4
3. HMX	10	2.4 ± 0.2
4. CL-20	8	7.2 ± 0.5
5. MNX	10	5.9 ± 0.4
6. TNX	10	1.3 ± 0.1
7. Nitrite	10	7.9 ± 0.6
	100	18.5 ± 1.3

^a ratio of number of cells accumulated inside the capillary containing test compound to the number of cells accumulated inside the capillary containing only buffer (*i.e.* 850 ± 90 cells); data are mean \pm SD ($n = 3$).

^b negative control without compound.

Biodegradation of cyclic nitramine explosives including CL-20. Growing-culture of strain EDB2 biotransformed the three explosives, in medium M2, as a function of its growth with the following order *i.e.* CL-20 > RDX > HMX (Figure 37). In resting cells study, biotransformation

rates of RDX, HMX and CL-20 by strain EDB2 were 1.8 ± 0.2 , 1.1 ± 0.1 and 2.6 ± 0.2 nmol h⁻¹ mg biomass⁻¹ (mean \pm SD; $n = 3$), respectively, whereas, in the presence of 100 μ M NADH, the biotransformation rates of the three explosives enhanced to 4.5 ± 0.3 , 2.5 ± 0.3 and 7.2 ± 0.6 nmol h⁻¹ mg biomass⁻¹ (mean \pm SD; $n = 3$), respectively. In contrast, a negligible response was observed upon addition of 100 μ M NADPH indicating the involvement of unidentified NADH-dependent enzyme(s). No degradation was observed in control experiments without resting cells within one hour of assay time. We found that biotransformation of RDX or HMX was accompanied by the formation of NO₂⁻, N₂O, HCHO and HCOOH, while biotransformation of CL-20 produced NO₂⁻, N₂O and HCOOH.

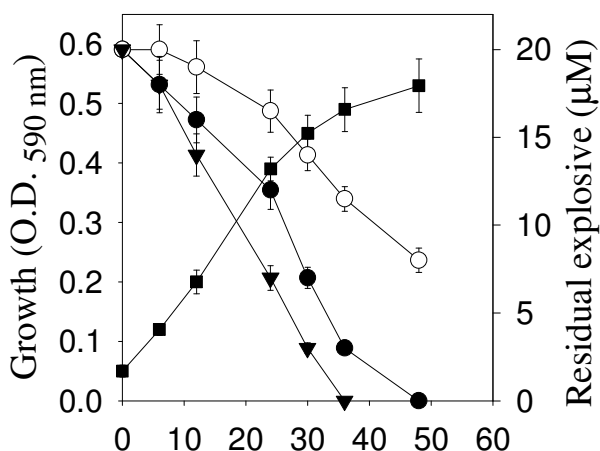


Figure 37 Biotransformation of RDX (●), HMX (○) and CL-20 (▼) by strain EDB2 as a function of its growth (■). Data are mean \pm SD ($n = 3$). Some error bars are not visible due to their small size.

Resting-cells of strain EDB2 also catalyzed NADH-dependent biotransformation of HCHO to HCOOH which did not accumulate (data not shown). In a subsequent experiment, strain EDB2 mineralized 40 % of H¹⁴CHO (of the total 340 μ g H¹⁴CHO/L medium) with evolution of ¹⁴CO₂ after 4 days of incubation in medium M1 suggesting an intermediary formation of HCOOH.

Conclusion

In the present study, we isolated an obligate anaerobic bacterium *Clostridium* sp. strain EDB2 from a marine sediment. Strain EDB2, motile with numerous peritrichous flagella, demonstrated chemotactic response towards RDX, HMX, CL-20 and NO₂⁻. The three explosives were biotransformed by strain EDB2 via N-denitration with concomitant release of nitrite ion (NO₂⁻). The NO₂⁻ thus produced attracted other distantly located bacterial cells to help accelerating the biodegradation process. Biotransformation rates of RDX, HMX and CL-20 by the resting cells of strain EDB2 were 1.8 ± 0.2 , 1.1 ± 0.1 and 2.6 ± 0.2 nmol h⁻¹ mg wet biomass⁻¹

(mean \pm SD; $n = 3$), respectively. In comparison to the conventional microbial degradation where microorganism(s) fortuitously come in contact with the energetic chemicals, the present study emphasizes the use of chemotactic bacteria for efficient removal of explosives in contaminated sites. This is the first report, which showed that a pure bacterial culture (strain EDB2) accessed the three hydrophobic cyclic nitramine explosives by chemotaxis and degraded them to innocuous products. The properties demonstrated by strain EDB2 renders it useful for the cleanup of sites contaminated with cyclic nitramines.

XIV Enzymatic degradation of CL-20: determination of reaction pathways

XIV.1 Biotransformation of CL-20 by salicylate 1-monooxygenase

The findings of the research performed under this section have been published in:

Bhushan B, Halasz A, Spain JC, Hawari J. (2004) Initial reaction(s) in biotransformation of CL-20 catalyzed by salicylate 1-monooxygenase from *Pseudomonas* sp. ATCC 29352. *Appl. Environ. Microbiol.* 70:4040-4047. Copy attached at the end of the present report.

Introduction

We reported earlier aerobic biodegradation of CL-20 by the soil isolate *Agrobacterium* sp. JS71, which utilized CL-20 as a sole nitrogen source and assimilated 3 moles of nitrogen per mole of CL-20 (Trott *et al.*, 2003) and anaerobic biodegradation of the same chemical by the soil isolate *Pseudomonas* sp. strain FA1 (Bhushan *et al.*, 2003a). In both cases, no information was provided on the initial enzymatic reactions involved in the biodegradation of CL-20. Flavoenzyme(s) from *Pseudomonas* sp. FA1 might have been responsible for the biotransformation of CL-20 via an initial N-denitration mechanism (Bhushan *et al.*, 2003a), however, we did not detect initial metabolite(s) to support our hypothesis.

Previous reports on biotransformation and biodegradation of RDX and HMX by a variety of microorganisms and enzymes have shown that initial N-denitration led to ring cleavage and decomposition (Bhushan *et al.*, 2002, 2003c; Halasz *et al.*, 2002; Fournier *et al.*, 2002). We also reported CL-20 biotransformation products such as nitrite, nitrous oxide and formate (Bhushan *et al.*, 2003a).

Salicylate 1-monooxygenase (EC 1.14.13.1), a flavin adenine dinucleotide (FAD)-containing enzyme from *Pseudomonas* sp. (ATCC 29352), is capable of catalyzing a variety of biochemical reactions (Kamin *et al.*, 1978). The physiological role of salicylate 1-monooxygenase is to biotransform salicylate to catechol (Katagiri *et al.*, 1965). However, it demonstrates activity against many other substrates such as o-halogenophenol and o-nitrophenol (Suzuki *et al.*, 1991), benzoates and variety of other compounds (Kamin *et al.*, 1978). We hypothesized that CL-20, being an oxidized chemical, might act as a substrate of salicylate 1-monooxygenase by accepting electron(s).

In the present study, we used salicylate 1-monooxygenase as a model flavoenzyme to understand the initial enzymatic reaction(s) involved in the biodegradation of CL-20 and to gain insights into how flavoenzyme(s) producing bacteria biotransform CL-20. Uniformly ring-labeled [¹⁵N]-CL-20 and ¹⁸O-labeled water (H₂¹⁸O) were used to identify the intermediate(s) produced during the course of reaction by LC/MS. Additionally, we studied the involvement of the FAD-site of salicylate 1-monooxygenase in CL-20 biotransformation.

Material and Methods

Chemicals. CL-20 in ε-form and 99.3 % purity, and uniformly ring-labeled [¹⁵N]-CL-20 (ε-form and 90.0 % purity) were provided by ATK Thiokol Propulsion, Brigham City, UT, USA. NADH, diphenyliodonium chloride (DPI) and flavin adenine dinucleotide (FAD) were purchased from

Sigma chemicals, Oakville, ON, Canada. ^{18}O -labeled water (95 % normalized ^{18}O atoms) was purchased from Aldrich Chem. Co., Milw, WI, USA. All other chemicals were of the highest purity grade.

Enzyme preparation and modification. Salicylate 1-monooxygenase (EC 1.14.13.1) from *Pseudomonas* sp. ATCC 29352 was purchased as a lyophilized powder (protein approx. 45 % by Biuret method) from Sigma chemicals, Oakville, ON, Canada. Native enzyme activity against salicylate was determined as per company guidelines. The enzyme was washed with phosphate buffer (pH 7.0) at 4°C using Biomax-5K membrane centrifuge filter units (Sigma chemicals, Oakville, ON) to remove preservatives and then resuspended in the same buffer. The protein content was determined by Pierce BCA (bicinchoninic acid) protein assay kit from Pierce chemicals company, Rockford, IL, USA. Apoenzyme (deflavo-form) was prepared by removing FAD from salicylate 1-monooxygenase using a previously reported method (Wang *et al.*, 1984). Reconstitution was carried out by incubating the apoenzyme with 100 μM of FAD in a potassium phosphate buffer (50 mM, pH 7.0) for 1 h at 40°C. The unbound FAD was removed by washing the enzyme with the same buffer using Biomax-5K membrane centrifuge filter units.

Biotransformation assays. Enzyme catalyzed biotransformation assays were performed under aerobic as well as anaerobic conditions in 6-mL glass vials. Anaerobic conditions were created by purging the reaction mixture with argon gas for 20 min and by replacing the headspace air with argon in sealed vials. Each assay vial contained, per mL of assay mixture, CL-20 or uniformly ring-labeled [^{15}N]-CL-20 (25 μM or 11 mg L^{-1}), NADH (100 μM), enzyme preparation (250 μg) and potassium phosphate buffer (50 mM, pH 7.0). Higher CL-20 concentrations than its aqueous solubility of 3.6 mg L^{-1} (Monteil-Rivera *et al.*, 2004), were used in order to allow detection and quantification of the intermediate(s). Reactions were performed at 30°C. Three different controls were prepared by omitting either enzyme, CL-20 or NADH from the assay mixture. Boiled enzyme was also used as a negative control. NADH oxidation was measured spectrophotometrically at 340 nm as described before (Bhushan *et al.*, 2002). Samples from the liquid and gas phase in the vials were analyzed for residual CL-20 and biotransformed products.

To determine the residual CL-20 concentrations during biotransformation studies, the reaction was performed in multiple identical vials. At each time point, the total CL-20 content in one reaction vial was solubilized in 50 % aqueous acetonitrile and analyzed by HPLC (see below).

To demonstrate the effect of enzyme concentration on CL-20 biotransformation, a progress curve was made under anaerobic conditions by incubating salicylate 1-monooxygenase at an increasing concentration (0.25 to 2.0 mg/mL) with 45 μM CL-20 and 100 μM NADH. The reactions conditions were the same as described above.

To determine the incorporation of water into CL-20 metabolite(s), H_2^{18}O was mixed with potassium phosphate buffer (100 mM; pH 7.0) at a ratio of 8:2. All other reaction ingredients and conditions were the same as those described above for the biotransformation of CL-20.

Enzyme inhibition studies. Inhibition with diphenyliodonium chloride (DPI), an inhibitor of flavoenzymes that acts by forming flavin-phenyl adduct (Chakraborty and Massey, 2002), was assessed by incubating salicylate 1-monooxygenase (1 mg) with DPI (0 to 0.5 mM) at room temperature for 15-20 min. After incubation, CL-20 biotransformation activities of the enzyme

were determined by monitoring the residual CL-20 as described above.

Analytical procedures. CL-20 and its degradation products were detected and analyzed as described in section IX. Formaldehyde (HCHO) was analyzed by HPLC after derivatization with 2,4-pentanedione as previously reported (Halasz *et al.*, 2002).

Accomplishments

Salicylate 1-monooxygenase catalyzed biotransformation of CL-20. Biotransformation of CL-20 with a purified salicylate 1-monooxygenase, from *Pseudomonas* sp. ATCC 29352, was found to be NADH-dependent and optimal at pH 7.0 and 30°C under dark conditions. A progress curve demonstrated a linear increase in CL-20 biotransformation as a function of enzyme concentration (Figure 38). The rates of CL-20 biotransformation were 15.36 ± 0.66 and 2.58 ± 0.18 nmol h⁻¹ mg of protein⁻¹ under anaerobic and aerobic conditions, respectively, indicating the involvement of an initial oxygen-sensitive process. On the other hand, salicylate 1-monooxygenase activity against the physiological substrate salicylate was 3,480 nmol min⁻¹ mg of protein⁻¹ under aerobic conditions. The low activity of enzyme against CL-20 might be due to three reasons: (1) biotransformation rate of the poorly soluble CL-20 is limited by the rate of mass transfer from solid to aqueous phase. In comparison, the aqueous solubility of salicylate is about 2000 mg/L at 20°C (The Merck Index, 2001) and would be higher at 30°C. (2) CL-20 is not a physiological substrate of salicylate 1-monooxygenase hence its interaction with this enzyme is expected to be rather slow. (3) CL-20 was biotransformed under anaerobic conditions in contrast to the aerobic biotransformation of salicylate.

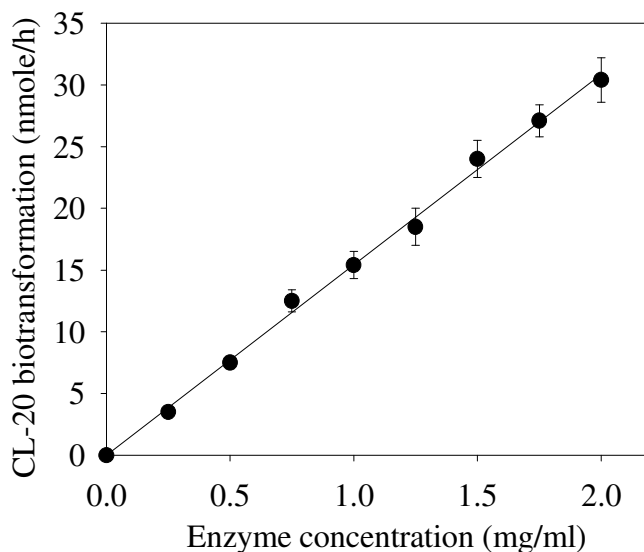


Figure 38 Progress curve demonstrating CL-20 biotransformation as a function of salicylate 1-monooxygenase concentration. The linear-regression curve has a gradient of 15.42 and a r^2 of 0.99. Data are means of results from the triplicate experiments, and error bars indicate standard errors. Some error

bars are not visible due to their small size.

In a previous study, the rates of CL-20 biotransformation with flavoenzyme(s) from *Pseudomonas* sp. FA1, under anaerobic and aerobic conditions, were 11.46 ± 0.36 and 2.46 ± 0.06 nmol h⁻¹ mg protein⁻¹, respectively (Bhushan *et al.*, 2003a), which appear to be similar to those we observed in the present study. The total flavin contents in salicylate 1-monooxygenase and flavoenzyme(s) from *Pseudomonas* sp. FA1 were 20.5 and 12.6 nmol mg protein⁻¹, respectively. Hence, under anaerobic conditions, CL-20 biotransformation by the two enzymes in terms of their flavin contents were 0.72 and 0.90 nmol h⁻¹ (nmol flavin moiety)⁻¹, respectively. In all controls, we found that abiotic degradation of CL-20 was negligible in one hour of reaction time. The maximum abiotic degradation of CL-20 (0.60 ± 0.06 nmol h⁻¹) was seen in a control with NADH under anaerobic conditions, which was only 5 % of the CL-20 degradation catalyzed by salicylate 1-monooxygenase.

Molecular oxygen (O₂) inhibits CL-20 biotransformation in two possible ways: first, by competing with CL-20 for accepting electron(s) at the FAD-site since O₂, in the absence of substrate, is known to accept electrons from the reduced salicylate 1-monooxygenase to produce H₂O₂ (Kamin *et al.*, 1978); second, by quenching an electron from the CL-20 anion-radical (described below) converting it back to the parent molecule (CL-20) and thus enforcing a futile redox-cycling. Analogously, O₂-mediated inhibition of RDX anion-radical formation was observed during biotransformation of RDX catalyzed by diaphorase (Bhushan *et al.*, 2002). Due to the inhibitory effect of oxygen, the subsequent experiments were carried out under anaerobic conditions.

Time-course studies showed a gradual disappearance of CL-20 at the expense of the electron-donor NADH with concomitant release of nitrite (NO₂⁻) and nitrous oxide (N₂O) (Figure 39). We found that N₂O, although produced at later steps of CL-20 biotransformation (described below), appeared before NO₂⁻ in the assay medium as shown in Figure 39. This could be explained by two facts, first, there was a large difference in stoichiometries of nitrite (1.7) and nitrous oxide (3.2); second, nitrous oxide detection method (GC-electron capture detector) was much more sensitive (lowest detection limit 0.022 nmol) than the nitrite detection method (HPLC-conductivity detector) (lowest detection limit 5.434 nmol/ml). Hence, nitrous oxide was detected as early as 20 min after the beginning of reaction, whereas nitrite was detected only after 30 min (Figure 39). After 2 h of reaction, each reacted CL-20 molecule consumed about 1.9 NADH molecules and produced 1.7 nitrite ions, 3.2 molecules of nitrous oxide, 1.5 molecules of formic acid and 0.6 molecule of ammonium (Table 14). Of the total 12 nitrogen atoms (N) and 6 carbons (C) per reacted CL-20 molecule, we recovered approximately 9 N (as NO₂⁻, N₂O and NH₄⁺) and 2 C (as HCOOH), respectively. The remaining 3 N and 4 C were probably present in yet unidentified product(s). In comparison, a membrane-associated flavoenzyme(s) from *Pseudomonas* sp. FA1 produced 2.3 nitrite ions, 1.5 molecules of nitrous oxide and 1.7 molecules of formic acid from each reacted CL-20 molecule (Table 14). Furthermore, during photodegradation of CL-20 at 300 nm in acetonitrile-aqueous solution which was also initiated by N-denitration, the product distribution was similar to the present study, but the stoichiometry was different *i.e.* each reacted molecule of CL-20 produced 5.0, 5.3, 1.4 and 0.3 molecules of NO₂⁻, HCOOH, NH₃ and N₂O, respectively (Hawari *et al.*, 2004). The probable reason for the higher yields of NO₂⁻ and HCOOH in photolysis of CL-20 was attributed to the intense action of

the high energy wavelength $\lambda_{300\text{ nm}}$ (energy 400 kJ/mol) which caused rapid cleavage of N-NO₂ and -HC-NNO₂ bonds in CL-20.

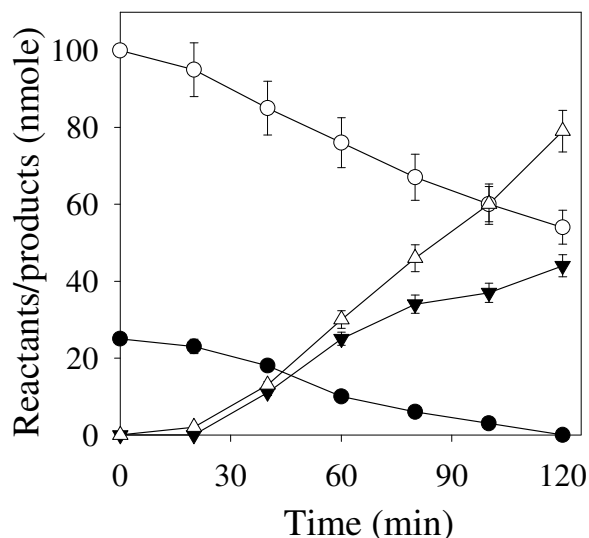


Figure 39 Time-course study of NADH-dependent biotransformation of CL-20 by salicylate 1-monooxygenase (1 mg) under anaerobic conditions. Residual CL-20 (●), NADH (○), nitrite (▼), and nitrous oxide (▽). Data are means of results from triplicate experiments, and error bars indicate standard errors. Some error bars are not visible due to their small size.

Involvement of flavin-moiety (FAD) in CL-20 biotransformation. Salicylate 1-monooxygenase from *Pseudomonas* sp. is a dimeric protein with two identical subunits where each subunit has an approximate mol. wt. of 45.5 kDa and contains one molecule of FAD (White-Stevens and Kamin, 1972). Diphenyliodonium (DPI) inhibited the biotransformation of CL-20 in a concentration-dependent manner (Figure 40A). It is known that DPI inhibits flavoenzymes by the formation of flavin-phenyl adduct (Chakraborty and Massey, 2002) which indicated the involvement of FAD in CL-20 biotransformation. Furthermore, DPI targets flavin-containing enzymes that catalyze one-electron transfer reactions (O'Donnell *et al.*, 1994; Chakraborty and Massey, 2002), which provided strong circumstantial evidence that a one-electron transfer process was involved in the initial reaction that might have caused N-denitration of CL-20.

Table 14 Comparative stoichiometries of reactants and products during biotransformation of CL-20 by the salicylate 1-monooxygenase from *Pseudomonas* sp. ATCC 29352 and the membrane-associated enzyme(s) from *Pseudomonas* sp. FA1.

Reactant or product	<i>Pseudomonas</i> sp. ATCC 29352 ^a		<i>Pseudomonas</i> sp. FA1 ^b	
	Amount (nmol)	Molar ratio of reactant to product per reacted CL-20 molecule	Amount (nmol)	Molar ratio of reactant to product per reacted CL-20 molecule
Reactants				
CL-20	25 ± 1.4	1.0 ± 0.05	20 ± 1.2	1.0 ± 0.06
NADH	48 ± 2.7	1.9 ± 0.10	90 ± 7.1	4.5 ± 0.35
Products				
Nitrite (NO ₂ ⁻)	43 ± 2.5	1.7 ± 0.09	46 ± 3.2	2.3 ± 0.16
Nitrous oxide (N ₂ O)	79 ± 5.3	3.2 ± 0.21	29 ± 1.6	1.5 ± 0.08
Formate (HCOOH)	37 ± 2.4	1.5 ± 0.09	34 ± 2.8	1.7 ± 0.13
Ammonium (NH ₄ ⁺)	15 ± 0.9	0.6 ± 0.04	N.D.	N.D.

^a reaction was performed at pH 7.0, 30°C for 2 h under anaerobic conditions; ^b data are from Bhushan et al., 2003a; all the data are mean ± SE (*n* = 3); N.D., not determined.

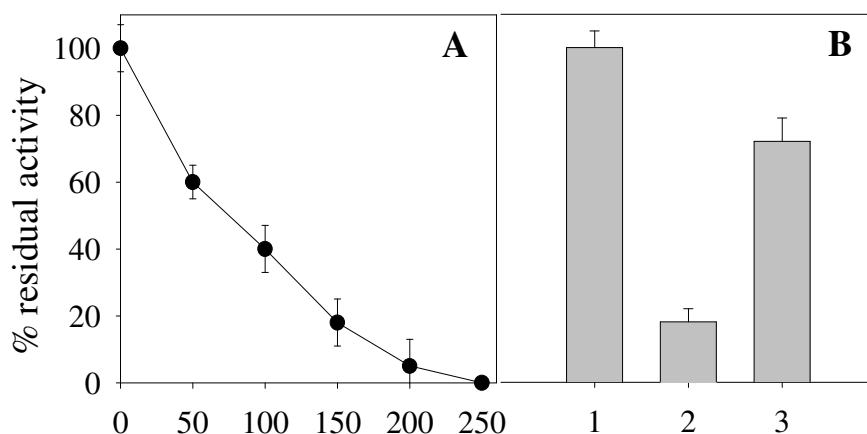


Figure 40 A, Concentration-dependent inhibition of salicylate 1-monooxygenase catalyzed biotransformation of CL-20 by diphenyliodonium. B, Biotransformation of CL-20 by the native- (1), deflavo- (2) and reconstituted- salicylate 1-monooxygenase (3). One hundred percent CL-20 biotransformation activity was equivalent to $15.36 \pm 0.66 \text{ nmol h}^{-1} \text{ mg of protein}^{-1}$. Data are mean percentages of CL-20 biotransformation activity \pm standard errors ($n = 3$).

The involvement of FAD was additionally confirmed by assaying deflavo- and reconstituted-form of salicylate 1-monooxygenase against CL-20. The specific activities of the native-, deflavo- and reconstituted-form of salicylate 1-monooxygenase against CL-20 were 15.36 ± 0.66 , 2.70 ± 0.18 and $10.98 \pm 0.18 \text{ nmol h}^{-1} \text{ mg of protein}^{-1}$, respectively, revealing that deflavo-enzyme lost about 82 % of its activity compared to the native-enzyme (Figure 40B). The remaining 18 % activity observed in deflavo-enzyme was due to incomplete removal of FAD (data not shown). On the other hand, the reconstituted enzyme, prepared by reconstitution of deflavo-enzyme with FAD, restored the CL-20 biotransformation activity up to 72 % (Figure 40B). The above results indicate the direct involvement of FAD in biotransformation of CL-20. Free FAD (100 μM) also transformed CL-20 in the presence of NADH (100 μM) at a rate of $2.10 \pm 0.18 \text{ nmol h}^{-1}$, corresponding to 14 % of the bound-FAD present in native salicylate 1-monooxygenase. This finding not only supports the involvement of FAD in CL-20 biotransformation but also suggests that the flavin-moiety has to be enzyme-bound in order to function efficiently. The involvement of flavoenzyme(s) in biotransformation of RDX (Bhushan *et al.*, 2002) and HMX (Bhushan *et al.*, 2003b) via a one-electron transfer process has previously been reported. In a study with flavin mononucleotide (FMN) containing diaphorase from *Clostridium kluyveri*, we reported an oxygen-sensitive one-electron transfer reaction that caused an initial N-denitration of RDX followed by spontaneous decomposition (Bhushan *et al.*, 2002). On the other hand, a FAD containing xanthine oxidase also catalyzed a similar reaction with HMX (Bhushan *et al.*, 2003b).

Detection and identification of metabolites. The metabolites obtained by reaction between salicylate 1-monooxygenase and CL-20 were detected by their deprotonated molecular mass ions

[M-H]⁻ in LC/MS (ES⁻) studies and summarized in Table 15. Intermediates **Ia** and **Ib** appeared simultaneously with retention times (R_t) of 8.2 and 7.5 min, respectively (Figure 41A), but with the same [M-H]⁻ at 345 Da (Figure 41C) corresponding to an empirical formula of C₆H₆N₁₀O₈. When ring-labeled [¹⁵N]-CL-20 was used in the reaction, both **Ia** and **Ib** showed a deprotonated molecular mass ion [M-H]⁻ at 351 Da (Table 15, Figure 41E) indicating that each intermediate included the six nitrogen atoms from the CL-20 ring. Moreover, the use of [¹⁸O]-labeled-H₂¹⁸O did not affect the mass of intermediates **Ia** and **Ib**. The intermediates **Ia** and **Ib**, previously observed during photolysis of CL-20 (Hawari *et al.*, 2004), were tentatively identified as isomers resulting from the loss of two -NO₂ groups that occurred during the initial reaction(s) between CL-20 and salicylate 1-monooxygenase. In the present study, we describe the secondary decomposition of intermediate **Ia** (Figure 23). Intermediate **Ib**, being an isomer of intermediate **Ia**, might also decompose in a similar way.

Several other products including **II**, **IX**, and **X** were also detected with R_t at 12.5, 1.9 and 1.7 min, respectively, and with [M-H]⁻ at 381, 381, and 293 Da corresponding to empirical formulae of C₆H₁₀N₁₀O₁₀, C₆H₁₀N₁₀O₁₀, and C₆H₁₀N₆O₈, respectively (Table 15). Likewise, when amino-labeled [¹⁵N]-CL-20 was used, the [M-H]⁻ of products **II**, **IX**, and **X** were observed at 387, 387, and 297 Da, respectively, indicating the incorporation of six [¹⁵N]-atoms in **II** and **IX** and only four [¹⁵N]-atoms in **X** (Table 15). When the experiment was repeated with ¹⁸O-labeled water (H₂¹⁸O), the [M-H]⁻ of products **II**, **IX**, and **X** were observed at 385, 385, and 301 Da, respectively, indicating the incorporation of two [¹⁸O]-atoms into **II** and **IX**, and four [¹⁸O]-atoms into **X** (Table 15). Based on above data, the intermediate **II** was tentatively identified as a carbinol adducts (C₆H₁₀N₁₀O₁₀), whereas intermediates **IX** (C₆H₁₀N₁₀O₁₀) and **X** (C₆H₁₀N₆O₈) were sequential ring cleavage products (Table 15 and Figure 42). All above metabolites were transient and completely disappeared after 2.5 h of reaction.

To determine the source of N₂O, experiments were performed with uniformly-ring-labeled [¹⁵N]-CL-20. ¹⁵N¹⁴NO was detected in GC-MS analysis with a molecular mass of 45 Da which confirmed that of the two nitrogen atoms in N₂O one nitrogen was from the CL-20 ring and the second was from the peripheral nitro (-NO₂) group. We found that all of the N₂O, in the present study, was labeled and produced from N-NO₂ groups released from the CL-20 as previously suggested by Patil and Brill (1991). Analogously, N₂O generation from N-NO₂ has also been reported during biodegradation of RDX (Halasz *et al.*, 2002) and HMX (Bhushan *et al.*, 2003b). In a previous study, we reported that N₂O, besides being produced from N-NO₂, was also produced via nitrite reduction catalyzed by an enzyme preparation from *Pseudomonas* sp. FA1 (Bhushan *et al.*, 2003a). In contrast, the present study did not show N₂O production through nitrite reduction. For instance, when we incubated NaNO₂ (1 mM) with salicylate 1-monooxygenase and NADH under similar reaction conditions as used for CL-20 biotransformation, N₂O was not detected during 2 h of reaction which additionally supported that N-NO₂ was the only source of N₂O in the present study.

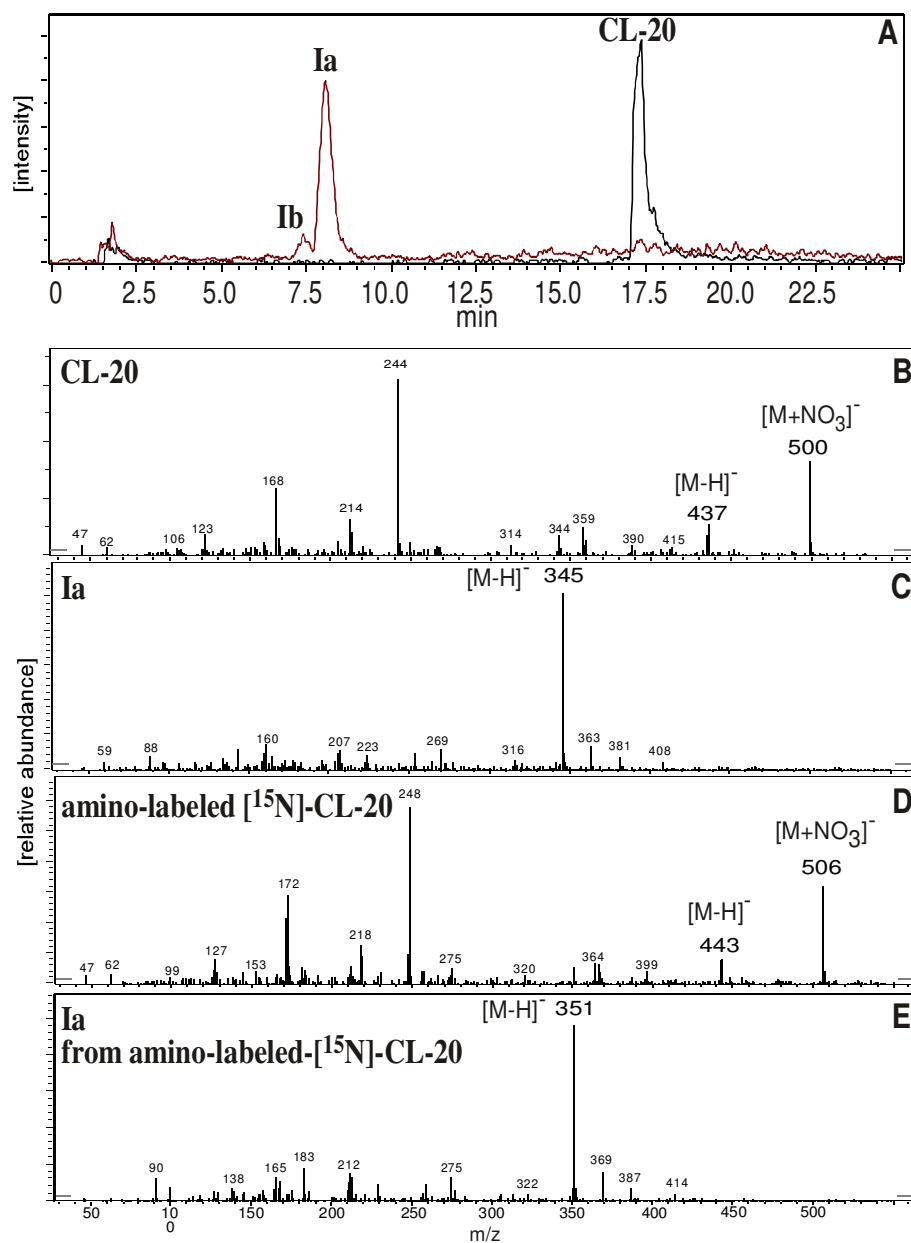


Figure 41 (A) LC/MS (ES-) extracted ion-chromatogram of CL-20 ($m/z = 500$ Da) and its metabolite (Ia) ($m/z = 345$ Da) produced by the reaction of CL-20 with salicylate 1-monooxygenase; (B-E): LC/MS (ES-) spectra of non-labeled CL-20 (B), and its metabolite Ia (C), amino-labeled [¹⁵N]-CL-20 (D), and its metabolite Ia (E).

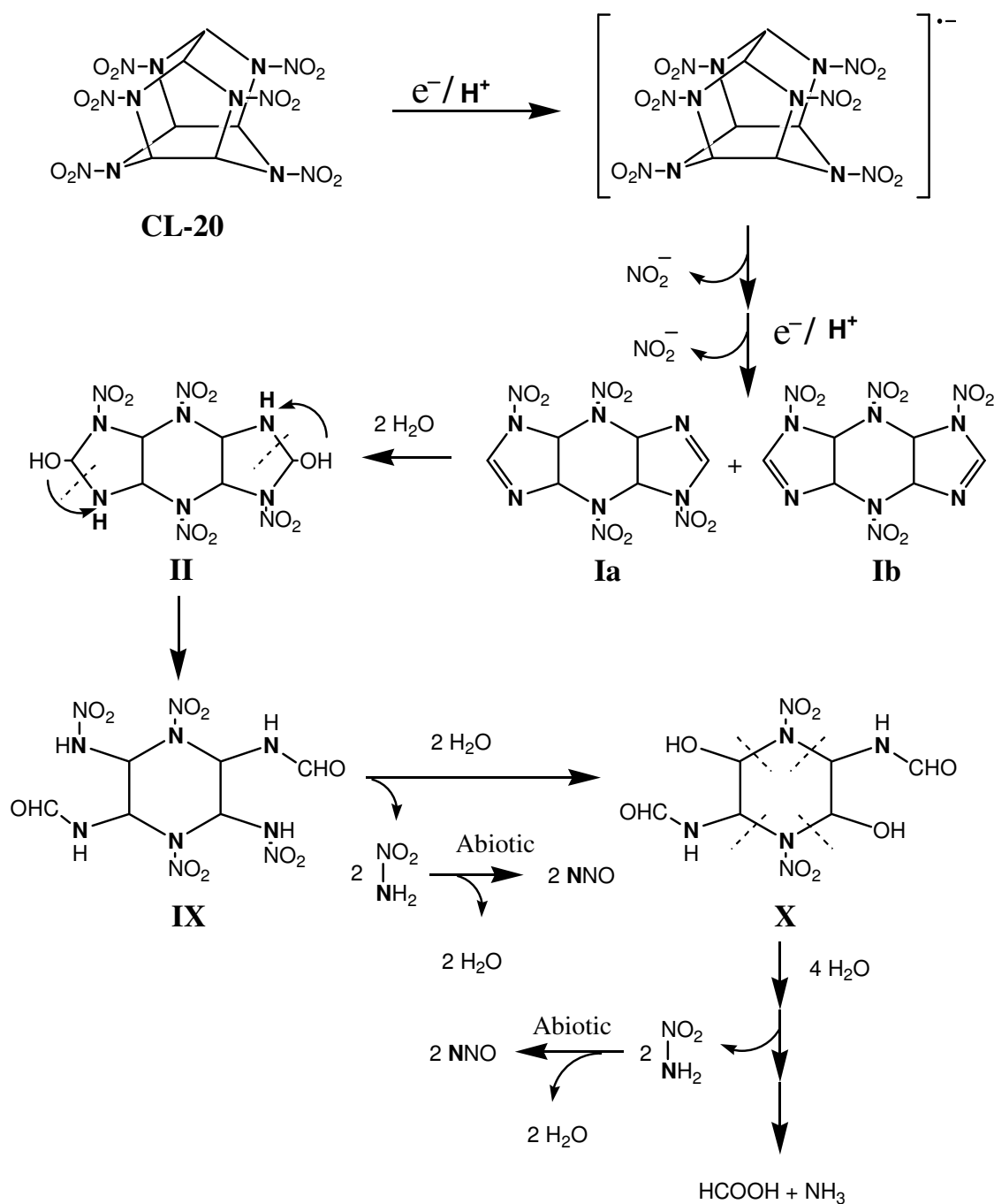


Figure 42 Proposed pathway of initial biotransformation of CL-20 catalyzed by salicylate 1-monooxygenase followed by secondary decomposition. Nitrogen atoms shown in bold were amino-nitrogens and were uniformly labeled in [^{15}N]-CL-20. Secondary decomposition of intermediate **Ia** is shown, whereas **Ib** might also decompose like **Ia**. Intermediate shown between brackets was not detected.

Table 15 Properties of metabolites detected and identified by LC/MS (ES-) during biotransformation of CL-20 catalyzed by salicylate 1-monooxygenase from *Pseudomonas* sp. ATCC 29352.

Metabolite ^a	Retention time (R _t) (min.)	Relative peak area in LC/MS (ES-) extracted ion-chromatogram ^b	[M-H] ⁻ (Da) ^c	Number of nitrogen atoms from labeled-[¹⁵ N]-CL-20 ring	Number of oxygen atoms from H ₂ ¹⁸ O	Proposed empirical formula
Ia	8.2	207980	345	6	0	C ₆ H ₆ N ₁₀ O ₈
Ib^d	7.5	26089	345	6	0	C ₆ H ₆ N ₁₀ O ₈
II	12.5	11092	381	6	2	C ₆ H ₁₀ N ₁₀ O ₁₀
IX	1.9	71672	381	6	2	C ₆ H ₁₀ N ₁₀ O ₁₀
X	1.7	7637	293	4	4	C ₆ H ₁₀ N ₆ O ₈

^a tentative structures of these metabolites are shown in Figure 42; ^b all peaks persisted for about 1.5 h and then gradually disappeared after 2.5 h of reaction; ^c deprotonated mass ions; ^d **Ib**, an isomer of **Ia**, was a minor intermediate as shown in Figure 41A.

Proposed mechanism(s) of initial reaction(s) followed by secondary decomposition of CL-20.

Based on the gradual appearance of nitrite (Figure 39), reaction inhibition by oxygen and DPI, detection of initial intermediate(s) (Figure 41), and analogy with other systems (Bhushan *et al.*, 2002, 2003b), we propose that salicylate 1-monooxygenase catalyzed a single-electron transfer to the CL-20 molecule to produce an anion-radical (Figure 42). Spontaneous N-denitration of the radical (*i.e.* release of first NO_2^-) would produce a transient N-centered free-radical as previously proposed during biotransformation (Bhushan *et al.*, 2003a), thermolysis (Patil and Brill, 1991), and photodegradation of CL-20 (Hawari *et al.*, 2004). The N-centered free-radical, being unstable, must undergo rapid rearrangement by cleaving at the weaker C—C bond bridging the two 5-member rings in CL-20 (Figure 42) (Xinqi and Nicheng, 1996). The rearranged molecule would accept a second electron in order to release a second NO_2^- to produce two isomeric intermediates **Ia** and **Ib** (Table 15, Figures 41 and 42). Stoichiometrically, two N-denitration steps would require an obligatory transfer of two electrons (equivalent to one NADH molecule), however, we found that 1.9 NADH molecules were consumed for each reacted CL-20 molecule (Table 14). The excess of NADH utilized (*i.e.* 0.9 molecule) could be due to either binding of NADH to the enzyme and hence lack of detection or utilization by yet unidentified CL-20 metabolite(s).

Intermediate **Ia**, produced as a result of two N-denitration steps, underwent hydrolysis by the addition of two H_2O molecules across the two imine bonds ($-\text{C}=\text{N}-$) to produce an unstable carbinol derivative **II** as confirmed by ^{18}O -labeled water experiment. Compound **II** might then cleave at $\text{O}_2\text{NN}-\text{CH}(\text{OH})$ bond following rearrangement to produce intermediate **IX** which has a similar $[\text{M}-\text{H}]^-$ of 381 Da as that of **V** (Table 15 and Figure 42). Addition of a water molecule across a $-\text{C}=\text{N}-$ bond followed by ring-opening has previously been reported during photolysis of CL-20 (Hawari *et al.*, 2004) and RDX (Hawari *et al.*, 2002), and cytochrome P450 catalyzed biotransformation of RDX (Bhushan *et al.*, 2003c). Stoichiometric addition of two H_2O molecules to **IX**, confirmed by ^{18}O -labeled water experiment, produced intermediate **X** with concomitant release of two nitramide molecules ($\text{NH}_2\text{-NO}_2$) (Table 15 and Figure 42). Intermediate **X**, being an α -hydroxyalkyl nitramine was unstable in water (Druckrey, 1973) and therefore decomposed to finally produce nitrous oxide, formic acid and ammonia as quantified in Table 14 and shown in Figure 42.

Conclusion

In the present study, salicylate 1-monooxygenase, a flavin adenine dinucleotide (FAD)-containing purified enzyme from *Pseudomonas* sp. ATCC 29352, biotransformed CL-20 at rates of 15.36 ± 0.66 and $2.58 \pm 0.18 \text{ nmol h}^{-1} \text{ mg of protein}^{-1}$ under anaerobic and aerobic conditions, respectively. We provided the first biochemical evidence of initial reaction(s) involved in the transformation of CL-20 catalyzed by salicylate 1-monooxygenase under anaerobic conditions. The mechanism described here is consistent with our previous enzymatic studies with RDX and HMX (Bhushan *et al.*, 2002, 2003b), which also suggested that one-electron transfer is necessary and sufficient to cause N-denitration of RDX and HMX leading to their advanced decomposition. Some of the CL-20 products observed in the present study are consistent with those reported previously with respect to alkaline hydrolysis (Balakrishnan *et al.*, 2003), biotransformation

(Bhushan *et al.*, 2003a) and photolysis (Hawari *et al.*, 2004). However, in these previous studies neither initial metabolite(s) nor the involvement of any specific enzyme(s) was described. The present study thus advances our understanding of the initial steps involved in biotransformation of CL-20 by flavoenzymes(s)-producing bacteria. *Pseudomonas* sp., being the source of salicylate 1-monooxygenase and other flavoenzymes, seems to be a promising degrader of CL-20. Ubiquitous presence of *Pseudomonas* and similar bacteria in the environments such as soil, marine and fresh water sediments, and estuaries would therefore help in understanding the fate of CL-20 in such environments.

XIV.2 Nitroreductase catalyzed biotransformation of CL-20

These results have been published in the manuscript:

Bhushan B, Halasz A, Hawari J. (2004) Nitroreductase catalyzed biotransformation of CL-20. *Biochem. Biophys. Res. Commun.* 322: 271-276. Copy attached at the end of the present report.

Introduction

In the previous sections, we showed that biodegradation of CL-20 produced HCOOH as a carbon-product in addition to several nitrogen-containing products such as nitrite, nitrous oxide and ammonium (Bhushan *et al.*, 2003a, 2004b). Only formic acid (2 moles per mole of CL-20) was confirmed as a carbon product of CL-20, and carbon mass-balance were far to be complete due to the missing four mole equivalents of carbon in CL-20.

Recently, a new carbon-containing product, glyoxal, was detected and quantified (1 mol glyoxal/mol CL-20) during CL-20 reaction with Fe⁰ under anaerobic conditions (section I; Balakrishnan *et al.*, 2004a). Since we hypothesized that an oxygen-sensitive enzyme should also biotransform CL-20 *via* an initial denitration to eventually give a similar product distribution as the one obtained with Fe⁰, we used a nitroreductase from *E. coli* to catalyze biotransformation of CL-20 to gain more insight into the initial enzymatic steps involved in the decomposition of the chemical.

Material and Methods

Chemicals. CL-20 (ϵ -form and 99.3 % purity) and uniformly ring-labeled [¹⁵N]-CL-20 (ϵ -form and 90.0 % purity) were provided by ATK Thiokol Propulsion, Brigham City, UT, USA. NADH, flavin mononucleotide (FMN), glyoxal (40 % solution), superoxide dismutase (SOD, EC 1.15.1.1, from *Escherichia coli*) and cytochrome c (from horse heart, MW 12,384 Da, purity 90 %) were purchased from Sigma chemicals, Oakville, ON, Canada. All other chemicals were of the highest purity grade.

Enzyme preparation and modification. Nitroreductase (purity 90 % by SDS-PAGE), from *Escherichia coli*, was purchased from Sigma chemicals, Oakville, ON, Canada. The enzyme was washed with phosphate buffer (pH 7.0) at 4°C using Biomax-5K membrane centrifuge filter units (Sigma chemicals, Oakville, ON) to remove preservatives and then re-suspended in the same buffer. Native enzyme activity was determined as per company guidelines. The protein content was determined by Pierce BCA (bicinchoninic acid) protein assay kit from Pierce chemicals company, Rockford, IL, USA.

Apoenzyme (deflavo-form) was prepared by removing FMN from the holoenzyme using a previously reported method (Koder *et al.*, 2002). Reconstitution was carried out by incubating the apoenzyme with 100 μ M of FMN in a potassium phosphate buffer (50 mM, pH 7.0) for 1 h at 4°C. The unbound FMN was removed by washing the enzyme with the same buffer using Biomax-5K membrane centrifuge filter units.

Biotransformation assays. Enzyme catalyzed biotransformation assays were performed under aerobic as well as anaerobic conditions in 6 mL-glass vials. Anaerobic conditions were created by purging the reaction mixture with argon gas for 20 min and by replacing the headspace air with argon in sealed vials. Each assay vial contained, per mL of assay mixture, CL-20 or uniformly ring-labeled [^{15}N]-CL-20 (25 μM or 11 mg L^{-1}), NADH (100 μM), enzyme preparation (50 μg) and potassium phosphate buffer (50 mM, pH 7.0). Reactions were performed at 30°C. Three different controls were prepared by omitting either enzyme, CL-20 or NADH from the assay mixture. Heat inactivated enzyme (90°C for 30 min) was also used as a negative control. NADH oxidation was measured spectrophotometrically at 340 nm as described before (Bhushan *et al.*, 2004b). Samples from the liquid and gas phase in the vials were analyzed for residual CL-20 and biotransformed products.

To determine the residual CL-20 concentrations during biotransformation studies, the reaction was performed in multiple identical vials. At each time point, the total CL-20 content in one reaction vial was solubilized in 50 % aqueous acetonitrile and analyzed by HPLC (see below).

To demonstrate the effect of enzyme concentration on CL-20 biotransformation, a progress curve was made under anaerobic conditions by incubating nitroreductase at an increasing concentration (25 to 150 $\mu\text{g/ml}$) with CL-20 (45 μM) and NADH (200 μM). The reactions conditions were the same as described above.

The effect of molecular oxygen (O_2) on CL-20 biotransformation activity of nitroreductase was determined by performing the assays under aerobic conditions at pH 7.0 and 30°C. Formation of anion-radical $\text{CL-20}^{\bullet-}$ was determined by incubating CL-20 with nitroreductase in the presence of NADH, cytochrome c (75 μM) and superoxide dismutase (SOD: 150 $\mu\text{g/mL}$) as described previously (Anusevicius *et al.*, 1998). Inhibition of cytochrome c reduction in the presence of SOD was monitored at 550 nm.

Analytical procedures. CL-20 and its degradation products, N_2O ($^{14}\text{N}^{14}\text{NO}$ and $^{15}\text{N}^{14}\text{NO}$), HCOOH , NO_2^- , NH_4^+ and glyoxal were analyzed as described in section VI.

Accomplishments

Nitroreductase catalyzed biotransformation of CL-20. A purified nitroreductase, from *Escherichia coli*, biotransformed CL-20 in a NADH-dependent manner at pH 7.0 and 30°C under anaerobic conditions. A progress curve demonstrated a linear increase in CL-20 biotransformation as a function of enzyme concentration (data not shown). The rates of CL-20 biotransformation were 204.0 ± 1.2 and $15.0 \pm 0.6 \text{ nmol h}^{-1} \text{ mg of protein}^{-1}$ (mean \pm SD; $n = 3$) under anaerobic and aerobic conditions, respectively, indicating the involvement of an oxygen-sensitive process. In all controls, we found a negligible abiotic removal of CL-20 during one hour of reaction time.

Oxygen-sensitivity of the reaction suggested that nitroreductase catalyzed a one-electron transfer to CL-20 to first produce an anion radical ($\text{CL-20}^{\bullet-}$) before N-denitration as previously reported during biotransformation of CL-20 with salicylate 1-monooxygenase (Bhushan *et al.*, 2004b). Subsequently, we found that under aerobic conditions, superoxide dismutase (SOD) inhibited 30 % of reduction of cytochrome c, which suggested the formation of oxygen free-

radical ($\text{O}^{\bullet-}$) during the reaction. Hence, molecular oxygen (O_2) inhibited CL-20 biotransformation by quenching an electron from the CL-20 anion-radical and converting it back to the parent molecule (CL-20), and thus enforcing a futile redox-cycling. Control experiments without nitroreductase showed that CL-20 was neither auto-oxidized nor it directly reduced cytochrome c. Analogously; O_2 -mediated inhibition of RDX anion-radical formation was previously reported during biotransformation of RDX with diaphorase (Bhushan *et al.*, 2002). Furthermore, the phenomenon of regeneration of parent nitro-compound during reaction of nitro anion-radical with molecular oxygen (O_2) in aerobic systems is well established (Wardman and Clarke, 1976; Orna and Mason, 1989; Anusevicius *et al.*, 1998; Koder *et al.*, 2001). Due to the inhibitory effect of oxygen, the subsequent experiments were carried out under anaerobic conditions.

Time-course of formation of initial metabolite ($\text{C}_6\text{H}_6\text{N}_{10}\text{O}_8$). In LC/MS (ES-) studies, we found two isomeric key intermediates, which appeared simultaneously as early as 5 min of the reaction with retention times (R_t) of 8.2 and 7.5 min, respectively (Figure 43A). A time-course, considering the relative HPLC-UV areas, showed that both intermediates reached their maximum level after 30 min and then gradually declined during the course of reaction (Figures 43A and 43B). As reported in previous sections (section VIII, Hawari *et al.*, 2004; section XIV.1, Bhushan *et al.*, 2004b), the two isomers had their deprotonated molecular mass ion $[\text{M}-\text{H}]^-$ at 345 Da corresponding to an empirical formula of $\text{C}_6\text{H}_6\text{N}_{10}\text{O}_8$ that was further confirmed by using uniformly ring-labeled ^{15}N -CL-20. These products corresponded to the doubly denitrated product of CL-20, **Ia** and **Ib** of Figure 42.

Detection and quantification of end-products. Time-course studies showed a gradual disappearance of CL-20 at the expense of the electron-donor NADH with concomitant release of nitrite (NO_2^-), nitrous oxide (N_2O) and formate (Figure 44). After 3 h of reaction, each reacted CL-20 molecule consumed about 1.3 NADH molecules and produced 1.8 nitrite ions, 3.3 molecules of nitrous oxide, 1.6 molecules of formic acid, 1.3 ammonium ions and 1.0 molecule of glyoxal (Table 16). Of the total 12 nitrogen atoms (N) and 6 carbons (C) per reacted CL-20 molecule, we recovered approximately 10 N (as NO_2^- , N_2O and NH_4^+) and 4 C (as HCOOH and glyoxal), respectively. The product distribution gave carbon and nitrogen mass-balance of 60 and 81 %, respectively (Table 16).

The products obtained in the present study were similar, though produced in different relative yields, to those observed previously during photolysis of CL-20 (section VIII; Hawari *et al.*, 2004) and reaction of CL-20 with Fe^0 (section IX; Balakrishnan *et al.*, 2004.a). The similar products obtained biotically or abiotically suggest that once CL-20 undergoes initial N-denitration, the subsequent reactions in water are basically similar.

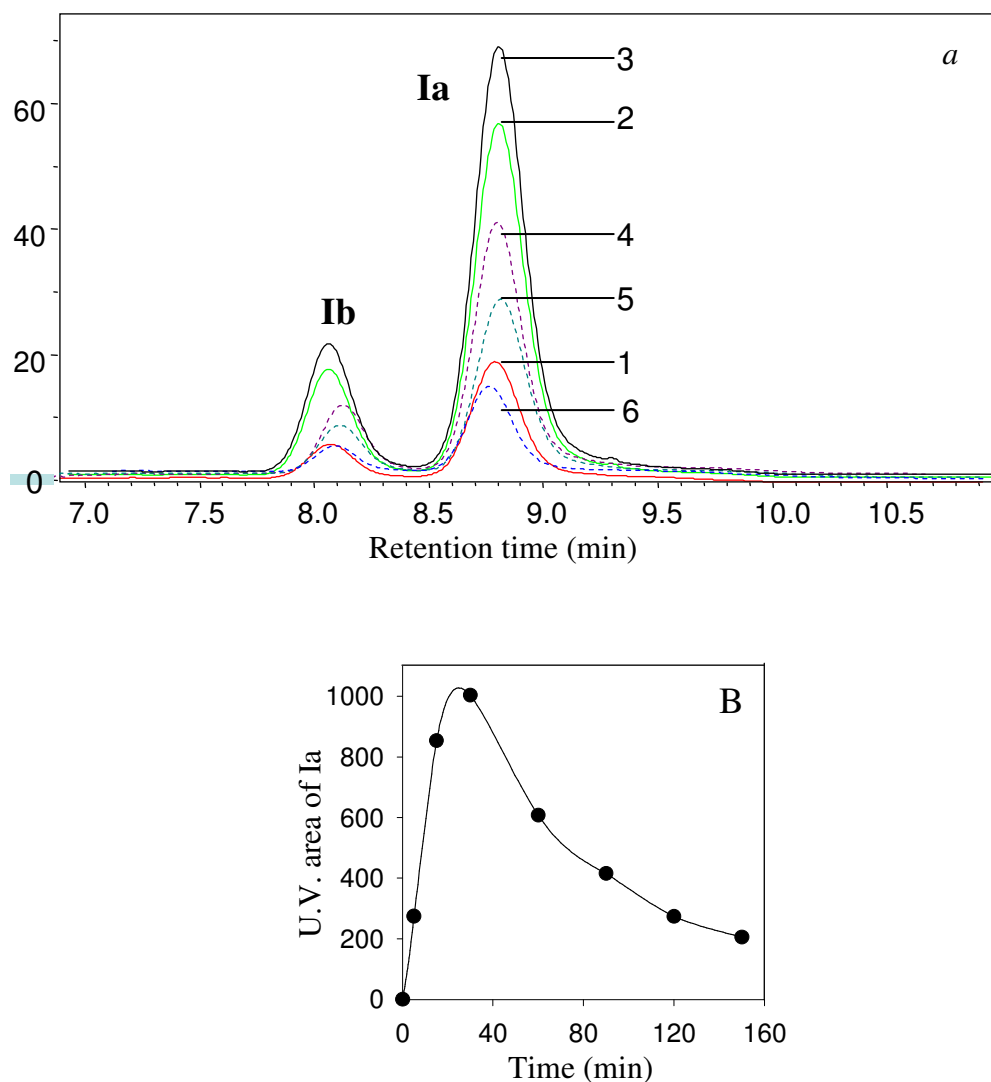


Figure 43 (A) Time course of formation and disappearance of key metabolites Ia and Ib during biotransformation of CL-20 by nitroreductase. Chromatograms corresponding to numbers 1-3 indicate increasing formation of metabolite Ia at times 5, 15 and 30 min, respectively, whereas chromatograms 4-6 indicate disappearance of Ia at times 60, 90 and 150 min, respectively. Proposed molecular structures of Ia and Ib are shown in Figure 42; (B) Formation and disappearance of Ia in terms of HPLC-UV-area as a function of time.

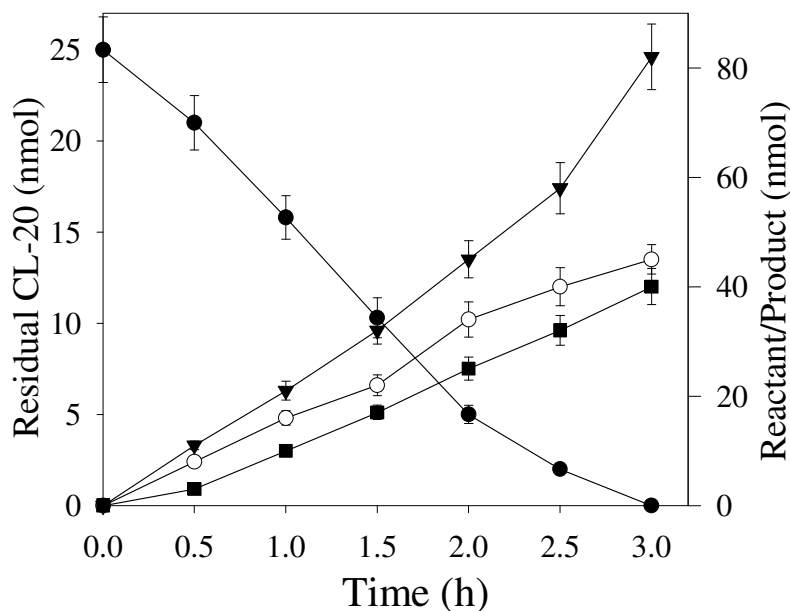


Figure 44 Time-course study of NADH-dependent biotransformation of CL-20 by nitroreductase under anaerobic conditions. CL-20 (●), nitrite (○), nitrous oxide (▼) and formate (■). Data are mean \pm SE ($n = 2$). Some error bars are not visible due to their small size.

A comparative study between [^{14}N]-CL-20 and amino-labeled [^{15}N]-CL-20 using GC-MS analysis showed that, like with salicylate 1-monooxygenase (section XIV.1, Bhushan *et al.*, 2004b), N-NO₂ groups in CL-20 were the source of N₂O, detected as $^{14}\text{N}^{14}\text{NO}$ (44 Da) and $^{15}\text{N}^{14}\text{NO}$ (45 Da), respectively.

Formate appeared earlier in the assay medium compared to glyoxal (data not shown) which indicated that formate might have been originated from the initial denitration followed by rapid cleavage of the weakest C-C bond (Figure 1.) In contrast, glyoxal probably comes from the other two C-C bonds in CL-20. We recovered 1 molar equivalent of glyoxal per reacted CL-20, as found previously during CL-20 reaction with Fe⁰ (section IX; Balakrishnan *et al.*, 2004a).

However, when we incubated glyoxal (35 μM) with enzyme (50 μg nitroreductase) in 1 mL of buffer for 2 days, about 44 % of glyoxal disappeared and could not be recovered either by heating (80 °C for 1 h) or by denaturing the enzyme with acetonitrile. This finding suggests that more glyoxal could have formed and may have bound to the proteins *via* a non-enzymatic process called glycation (Shangari *et al.*, 2003).

In the presence of Fe⁰, glyoxal further converted to glycolic acid (Balakrishnan *et al.*, 2004a) while in the present study glyoxal was accumulated as an end-product. Under biological conditions, further conversion of either glyoxal (OHC-CHO) or glycolic acid (HOH₂C-COOH) to glyoxylic acid (HOOC-CHO) requires involvement of glyoxal oxidase or glycolate oxidase, respectively (Whittaker *et al.*, 1996; Yadav and Gupta, 2000). The formation of glyoxal as a CL-20 product is environmentally significant since glyoxal is a reactive α -oxoaldehyde and its biological toxicity are well known (Shangari *et al.*, 2003). Glyoxal is also produced in biological

systems as a result of glucose auto-oxidation, DNA oxidation by oxygen free-radicals and lipid oxidation (Murata-Kamiya *et al.*, 1997; Shangari *et al.*, 2003). It reacts with proteins and nucleic acids by forming covalent bonds via a non-enzymatic process called glycation thus leading to a variety of clinical manifestations (Shangari *et al.*, 2003). It is a known mutagen (Shangari *et al.*, 2003) and an important allergen (Uter *et al.*, 2001). Thus, glyoxal produced from CL-20 may significantly contribute to the biological toxicity of CL-20.

Table 16 Stoichiometry and mass-balance of reactants and products after 3 h of reaction between CL-20 and nitroreductase under anaerobic conditions at pH 7.0 and 30°C.

Reactant/Product	Amount (nmol)	Molar ratio per mole of reacted CL-20	% Carbon recovery	% Nitrogen recovery
Reactants				
CL-20	25 ± 1.8	1.0 ± 0.07	100	100
NADH	34 ± 2.3	1.3 ± 0.08	N.A.	N.A.
Products				
Nitrite	45 ± 2.7	1.8 ± 0.10	N.A.	15.0
Nitrous oxide	82 ± 6.4	3.3 ± 0.25	N.A.	55.0
Ammonium	33 ± 2.5	1.3 ± 0.05	N.A.	10.8
Formic acid	40 ± 3.3	1.6 ± 0.13	26.6	N.A.
Glyoxal	25 ± 1.3	1.0 ± 0.05	33.3	N.A.
Total mass-balance			59.9	80.8

Data are mean ± standard errors ($n = 2$).

Involvement of flavin-moiety (FMN) in CL-20 biotransformation. Nitroreductase, from *Escherichia coli*, is a monomeric protein with a mol. wt. of 24 kDa and contains one molecule of FMN per enzyme monomer (Parkinson *et al.*, 2000). The involvement of FMN in CL-20 biotransformation was determined by assaying deflavo- and reconstituted-form of nitroreductase against CL-20. The specific activities of the native-, deflavo- and reconstituted-form of nitroreductase against CL-20 were 204 ± 12 , 24.0 ± 1.8 and 165 ± 12 nmol h⁻¹ mg of protein⁻¹, respectively, revealing that deflavo-enzyme lost about 88 % of its activity compared to the native-enzyme. The remaining 12 % activity observed in deflavo-enzyme was due to incomplete

removal of FMN (data not shown). The reconstituted enzyme, prepared by reconstitution of deflavo-enzyme with FMN, restored the CL-20 biotransformation activity up to 81 %. The above results suggested the involvement of FMN in biotransformation of CL-20. Furthermore, the free FMN (100 μ M) also transformed CL-20 in the presence of NADH (200 μ M) at a rate of 10.2 ± 1.2 nmol h⁻¹, however, the biotransformation rate was only 5 % of the enzyme-bound-FMN present in native nitroreductase. This finding additionally supported the involvement of FMN in CL-20 biotransformation and also suggested that flavin-moiety functions more efficiently in enzyme-bound form.

Conclusion

In the present study, we found that nitroreductase from *Escherichia coli* catalyzed a one-electron transfer to CL-20 to form a radical anion (CL-20^{•-}) which upon initial N-denitration also produced metabolites **Ia** and **Ib** from Figure 23. The latter decomposed spontaneously in water to produce nitrous oxide (N₂O), ammonium (NH₄⁺), glyoxal (OHC-CHO) and formic acid (HCOOH). The present study provided the first biochemical evidence for the quantitative formation of glyoxal and HCOOH during enzymatic biotransformation of CL-20. This study supported the previous finding of glyoxal production during chemical degradation of CL-20 with Fe⁰ (Balakrishnan *et al.*, 2004a). In the latter case, however, glyoxal was further converted to glycolic acid and other unidentified product(s). Detection and quantification of glyoxal provided a better understanding of the products and mass-balance of CL-20 reaction with nitroreductase(s)- or similar enzyme(s)-producing bacteria. Further work, however, is required to determine the fate and impact of glyoxal, a known toxic compound, in the environment.

XIV.3 Stereo-specificity for pro-(R) hydrogen of NAD(P)H during enzyme-catalyzed hydride transfer to CL-20

Research findings published in:

Bhushan B, Halasz A, Hawari J. (2005) Stereo-specificity for pro-(R) hydrogen of NAD(P)H during enzyme-catalyzed hydride transfer to CL-20. *Biochem Biophys Research Communication* 337: 1080-1083. A copy can be found at the end of the report.

Introduction

Several previous studies have shown that CL-20 can be degraded by microorganisms such as *Pseudomonas* sp. FA1, *Clostridium* sp. EDB2, *Agrobacterium* sp. strain JS71, and white-rot fungi (Bhushan *et al.*, 2003a, 2004c; Trott *et al.*, 2003; Fournier *et al.*, 2005), by enzymes e.g. monooxygenase, nitroreductase, and dehydrogenase (Bhushan *et al.*, 2004a,b, 2005a), and by indigenous degraders present in soils and sediments (Szecsody *et al.*, 2004; Strigul *et al.*, 2005). However, none of these reports has emphasized on the mechanism of hydride-transfer to CL-20. Previously, a DT-diaphorase from rat liver catalyzed a hydride transfer from NADPH to a nitramine compound, 2,4,6-trinitrophenyl-N-methylnitramine (Tetryl), to produce a corresponding N-denitrohydrogenated product (Anusevicius *et al.*, 1998). In another report, a diaphorase from *Clostridium kluyveri* catalyzed a hydride transfer to a cyclic nitramine compound, RDX, followed by N-denitration (Bhushan *et al.*, 2002). Based on the stoichiometry of NADH consumed per reacted RDX molecule, Bhushan *et al.* (2002) proposed the formation of a corresponding N-denitrohydrogenated product. The latter, however, could not be detected probably due to its very short half-life. More recently, a dehydrogenase enzyme from *Clostridium* sp. EDB2 degraded CL-20 via the formation of the N-denitrohydrogenated product (Bhushan *et al.*, 2005a). None of the above studies elaborated on the enzyme's stereo-specificity for either pro-R or pro-S hydrogens of NADH.

In the present study, we employed two enzymes, a dehydrogenase from *Clostridium* sp. EDB2, and a diaphorase from *Clostridium kluyveri*, to study the enzyme-catalyzed hydride transfer to CL-20, and to gain insights into the enzyme's stereo-specificity for either pro-R or pro-S hydrogens of NAD(P)H. We used LC-MS (ES-) to detect a mass-shift in the N-denitrohydrogenated product following CL-20 reactions with NAD(P)H and NAD(P)D as a hydride-source. Hydrogen-deuterium exchange between the ND-group of N-denitrohydrogenated product and the water was also examined during the reaction.

Materials and Methods

Enzymes preparation. NAD⁺, NADP⁺, ATP, 2-propanol-*d*8, ethanol-*d*5, alcohol dehydrogenase, D-glucose-*d*1, glucose-6-phosphate dehydrogenase, and hexokinase were purchased from Sigma-Aldrich chemicals, Oakville, ON, Canada. All other chemicals were of the highest purity grade. A dehydrogenase enzyme was isolated and purified from *Clostridium* sp. EDB2 as described before (Bhushan *et al.*, 2005a). A diaphorase (EC 1.8.1.4) from *Clostridium kluyveri* was obtained as a lyophilized powder from Sigma chemicals, Oakville, ON, Canada. The enzyme was suspended in 50 mM potassium phosphate buffer (pH 7.0) and filtered through a Biomax-5K

membrane filter (Sigma chemicals) before resuspending into the same buffer. The native enzyme activity of diaphorase was estimated spectrophotometrically at 340 nm (as per company guidelines) as the rate of oxidation of NADH using 2,6-dichlorophenol-indophenol as an electron acceptor.

Synthesis of deuterated and non-deuterated pyridine nucleotides. (R)NADD was synthesized by the method described by Ganzhorn and Plapp (Ganzhorn et al., 1988) with some modifications. A total of 25 mM of NAD⁺, 200 mM of ethanol-*d*5, and 75 units of alcohol dehydrogenase were dissolved in 5 mL of 50 mM Tris-buffer, pH 9.0. The reaction was allowed to proceed at 37°C, and the formation of (R)NADD was monitored by following the increase in absorbance at 340 nm. When no further increase in the OD₃₄₀ was observed, the enzyme was separated from the reaction mixture using 10 kDa molecular weight cutoff filter (Centriprep YM10, Amicon Bioseparations, Bedford, MA).

(S)NADD was synthesized by the modified method described by Sucharitakul et al. (2005). The reaction mixture was composed of: 25 mM NAD⁺, 35 mM of D-glucose-*d*1, 80 mM ATP, 75 units each of hexokinase and glucose-6-phosphate dehydrogenase in 4 mL of 100 mM phosphate-buffer at pH 8.0. The reaction was allowed to proceed at room temperature until a maximum absorbance was achieved at 340 nm. Enzymes were removed with 5 kDa molecular weight cutoff filter. For proper controls, non-deuterated (S)NADH and (R)NADH were also synthesized by utilizing the non-deuterated components, and by using the identical procedures that were used for (S)NADD and (R)NADD, respectively.

Furthermore, (R)NADPD and (S)NADPD were synthesized by the methods described by Pollock and Barber (2001). Non-deuterated (S)NADPH and (R)NADPH were also synthesized by utilizing the non-deuterated components, and by using the identical procedures that were used for (S)NADPD and (R)NADPD, respectively.

Biotransformation assays. Enzyme catalyzed biotransformation assays were performed under anaerobic conditions in 6 ml glass vials. Anaerobic conditions were created by purging the reaction mixture with argon gas for 20 min in sealed vials. Each assay vial contained, in one ml of assay mixture, CL-20 (25 µM or 11 mg liter⁻¹), NADH(D) or NADPH(D) (200 µM), enzyme preparation (250 µg) and potassium phosphate buffer (50 mM, pH 7.0). Reactions were performed at 30°C. Three different controls were prepared by omitting either enzyme, CL-20, or NAD(P)H(D) from the assay mixture. Heat-inactivated enzyme was also used as a negative control. NAD(P)H(D) oxidation was measured spectrophotometrically at 340 nm as described before (Bhushan *et al.*, 2002). Samples from the liquid phase in the reaction vials were analyzed periodically for the residual CL-20, and the N-denitrohydrogenated product.

For enzyme kinetics, enzyme and CL-20 reactions were performed at increasing CL-20 concentrations in the presence of NADH(D) in case of dehydrogenase, and NADPH(D) in case of diaphorase. The data thus obtained were used to generate standard Lineweaver-Burk plots (Double reciprocal plots).

Analytical techniques. CL-20 was analyzed with a LC-MS using a negative electro-spray ionization mode (ES-) to produce deprotonated molecular mass ion as described previously (Bhushan *et al.*, 2005a; Hawari *et al.*, 2004; Balakrishnan *et al.*, 2004a). Whereas, N-denitrohydrogenated product was detected, with a LC-MS, as an [M+TFA]⁻ adduct at m/z 506 Da

following addition of trifluoroacetic acid (TFA) in the mobile phase. Protein concentrations were estimated by bicinchoninic acid (BCA) kit (Pierce Chemicals, Rockford, IL) using bovine serum albumin as standard.

Accomplishments

Two purified enzymes, a dehydrogenase from *Clostridium* sp. EDB2 and a diaphorase from *Clostridium kluyveri*, biotransformed CL-20 (I) at rates of 18.5 and 24 nmol/h/mg protein, using NADH and NADPH as a hydride-source, respectively, to produce a denitrohydrogenated product (II) (Fig. 45 and 46). The latter had a HPLC-retention time and a molecular mass of 11.8 minute and 393 Da (detected as $[M+TFA]^-$ adduct mass at m/z 506 Da), respectively. Product II was produced as a result of an obligate transfer of a hydride ion at N-NO₂ group of CL-20 with concomitant release of a nitro-group (Fig. 46). The product II, as reported in our previous study, was unstable in water, and therefore readily decomposed to finally produce NO₂⁻, N₂O, and HCOOH (Bhushan *et al.*, 2005a). Product II was previously detected during photolysis, and Fe(0)-mediated degradation of CL-20 however in these reactions NAD(P)H was not used as reducing agent (Hawari *et al.*, 2004; Balakrishnan *et al.*, 2004a). On the contrary, in enzyme catalyzed reduction reactions, the reduced pyridine nucleotides such as NADH or NADPH mainly serve as the source of hydride (Ganzhorn and Plapp, 1988; Sucharirakul *et al.*, 2005; Pollock *et al.*, 2001; You, 1982).

To understand the stereo-specific effect of pro-*R* and pro-*S* hydrogens on hydride transfer reactions, both enzymes, dehydrogenase and diaphorase, were reacted with CL-20 in the presence of either deuterated or non-deuterated reduced pyridine nucleotides. In case of dehydrogenase enzyme, when Lineweaver-Burk plots of (*S*)NADD and (*R*)NADD were compared with NADH, we found a 2-fold deuterium isotopic effect with (*R*)NADD (i.e. V_{max} was 2-fold less with (*R*)NADD) compared to NADH, whereas results with (*S*)NADD were similar to those of NADH (Fig. 47A). This study revealed that dehydrogenase stereo-specifically utilized pro-(*R*)-hydride of NADH for CL-20 reduction, and that the isotope effect is due to the cleavage of (4*R*)-deuterium-carbon bond in NADH.

Furthermore, in case of diaphorase, when Lineweaver-Burk plots of (*S*)NADPD and (*R*)NADPD were compared with NADPH, we found a 1.5-fold deuterium isotopic effect with (*R*)NADPD compared to NADPH, whereas results with (*S*)NADPD were closely identical to those obtained with NADPH (Fig. 47B). This study showed that diaphorase stereo-specifically transferred a pro-(*R*)-hydride of NADPH to CL-20 in order to produce denitrohydrogenated product II, and that the isotope effect is due to the cleavage of (4*R*)-deuterium-carbon bond in NADPH.

In order to confirm the presence of hydride, from NAD(P)H, in product II (MW 393 Da), we performed enzymatic reactions with CL-20 in the presence of either NADD or NADPD containing deuterated pro-*R* or deuterated pro-*S* hydrogens. In a comparative study with LC-MS, using dehydrogenase, we found a positive mass-shift of 1 Da in product II using (*R*)NADD compared to either NADH or (*S*)NADD suggesting the involvement of a deuteride (D⁻) transfer from (*R*)NADD. Surprisingly, the mass signal, corresponding to mono-deuterated product II with MW 394 Da (detected as $[M+TFA]^-$ adduct mass at m/z 507 Da), rapidly decreased with time with a concomitant increase in the non-deuterated mass signal corresponding to MW 393 Da (detected as $[M+TFA]^-$ adduct mass at m/z 506 Da) (Table 17). Similar results were obtained

when diaphorase was reacted with CL-20 in the presence of (*R*)NADPD (data not shown). The above experimental evidence suggested that the deuterium at ND-group of the product II might be labile, and therefore we detected a rapid exchange of $D \leftrightarrow H$ between ND-group and water (Fig. 46) as marked by the rapidly decreased mass signal of mono-deuterated product II during the course of reaction (Table 17).

Table 17 Time-course of $H \leftrightarrow D$ exchange between ND-group of N-denitrohydrogenated product and water as followed with a LC-MS during dehydrogenase catalyzed hydride transfer from (*R*)NADD to CL-20.

Reaction time (minute)	Mass signal intensity of N-denitrohydrogenated product	
	Non-deuterated [$M_{h7} + TFA^{\dagger}$] ⁻	Deuterated [$M_{h6,d1} + TFA$] ⁻
	m/z 506 Da	m/z 507 Da
Control*	216211	0
0	0	0
5	74759	2440
10	104799	578
20	120673	342

[†] Molecular mass of N-denitrohydrogenated product of CL-20 as an adduct with TFA (trifluoroacetic acid). *CL-20 was reacted with dehydrogenase in the presence of NADH for 20 minutes.

Several enzymes have previously been reported to be stereo-specific towards either (*R*)- or (*S*)-hydrogens of NAD(P)H for a hydride transfer to a variety of substrates (Ganzhorn and Plapp, 1988; Sucharirakul *et al.*, 2005; Pollock *et al.*, 2001; You, 1982). However, the present study is the first one that showed stereo-specificity of two enzymes, dehydrogenase and diaphorase from *Clostridium* species, toward (*R*)-hydrogens of NAD(P)H for a hydride transfer to an environmentally significant cyclic nitramine compound, CL-20. Taken together, the data presented here extend our fundamental knowledge about the role of enzyme-catalyzed hydride transfer reactions in CL-20 biotransformation.

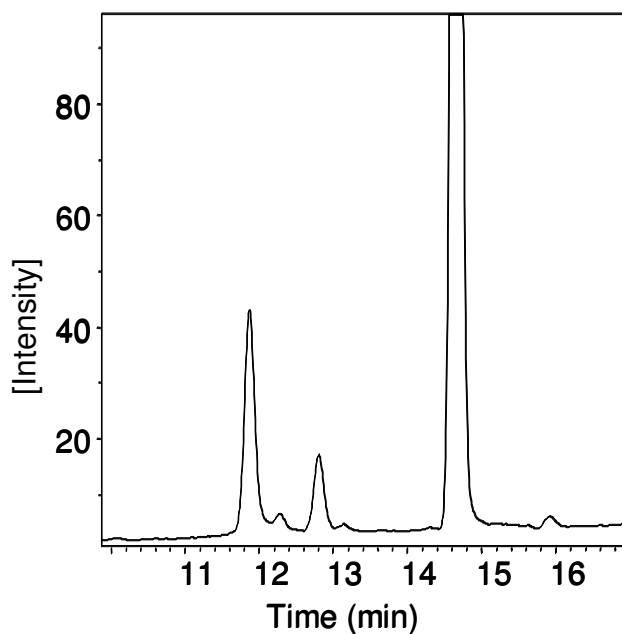


Figure 45 HPLC-UV chromatogram of CL-20 (I) and N-denitrohydrogenated product (II) obtained during CL-20 reaction with diaphorase from *Clostridium kluyveri* at pH 7.0 and 30°C.

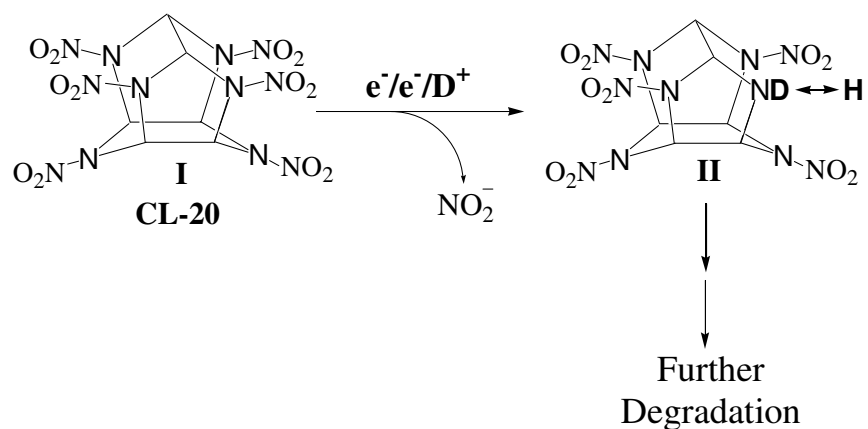


Figure 46 Proposed hydride transfer reaction of CL-20, and possible hydrogen-deuterium exchange between ND-group of product II and water.

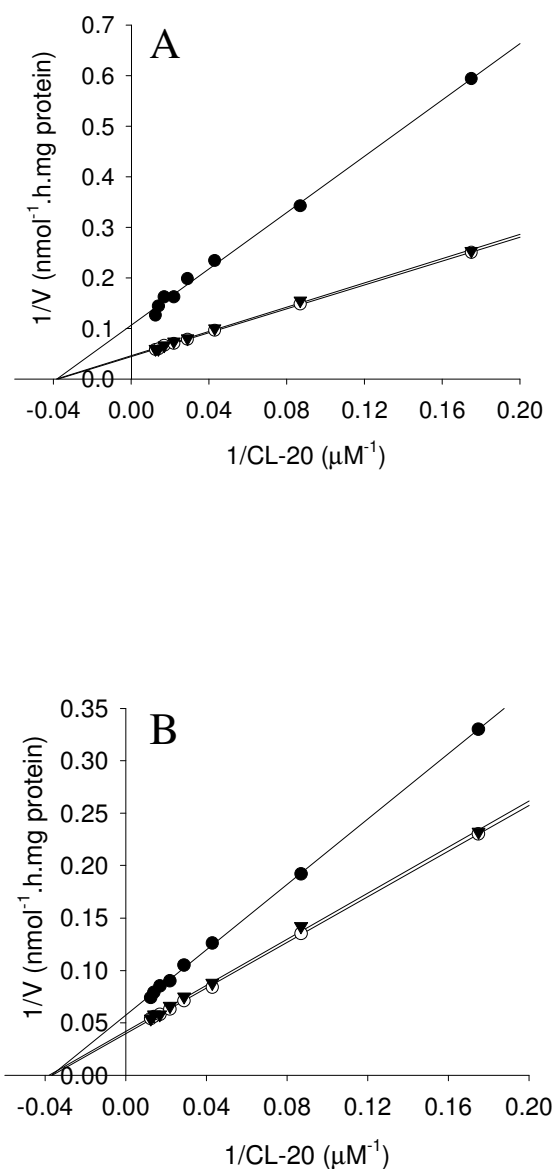


Figure 47 Standard Lineweaver-Burk plots of CL-20 concentration *versus* its enzymatic biotransformation rate; A, plots using dehydrogenase enzyme from *Clostridium* sp. EDB2 in the presence of either NADH (\circ), (S)NADD (\blacktriangledown), or (R)NADD (\bullet); B, plots using diaphorase enzyme from *Clostridium kluyveri* in the presence of either NADPH (\circ), (S)NADPD (\blacktriangledown) or (R)NADPD (\bullet). Data are mean of the triplicate experiments, and the standard deviations were within 8 % of the mean values.

XV Aquatic toxicity studies

The work performed under this milestone was published in 2004.

Gong P, Sunahara GI, Rocheleau S, Dodard SG, Robidoux PY, Hawari, J. (2004) Preliminary Ecotoxicological Characterization of a New Energetic Substance, CL-20. *Chemosphere* 56:653-658.

For further details, the paper is attached in annex at the end of the report.

Abstract

CL-20 (ϵ -polymorph) was amended to soil or deionized water to construct concentration gradients and to test its toxicities to various ecological receptors. Results of Microtox (15-min contact) and 96-h algae growth inhibition tests indicate that CL-20 showed no adverse effects on the bioluminescence of marine bacteria *Vibrio fischeri* and the cell density of freshwater green algae *Selenastrum capricornutum* respectively, up to its water solubility (ca. 3.6 mg L⁻¹). CL-20 and its possible biotransformation products did not inhibit seed germination and early seedling (16 - 19 d) growth of alfalfa (*Medicago sativa*) and perennial ryegrass (*Lolium perenne*) up to 10,000 mg kg⁻¹ in a Sassafras sandy loam soil (SSL). Indigenous soil microorganisms in SSL and a garden soil were exposed to CL-20 for one or two weeks before dehydrogenase activity (DHA) or potential nitrification activity (PNA) were assayed. Results indicate that up to 10,000 mg kg⁻¹ soil of CL-20 had no statistically significant effects on microbial communities measured as DHA or on the ammonium oxidizing bacteria determined as PNA in both soils. Data indicates that CL-20 was not acutely toxic to the species or microbial communities tested and that further studies are required to address the potential long-term environmental impact of CL-20 and its possible degradation products.

XVI Terrestrial toxicity studies

XVI.1 Higher plant toxicity tests

The work performed under this milestone was published in 2004 together with the aquatic toxicity studies. See Section XV for the abstract of the paper.

Gong, P, Sunahara, GI, Rocheleau, S, Dodard, SG, Robidoux, PY, and Hawari, J. (2004) Preliminary Ecotoxicological Characterization of a New Energetic Substance, CL-20. *Chemosphere* 56:653-658.

XVI.2 Earthworm survival and reproduction tests

The work performed under this milestone was published in 2004.

Robidoux PY, Sunahara GI, Savard K, Berthelot Y, Leduc F, Dodard S, Martel M, Gong P, Hawari J. (2004) Acute and chronic toxicity of the new explosive CL-20 in the earthworm (*Eisenia andrei*) exposed to amended natural soils. *Environ Toxicol Chem.* 23:1026-1034.

For further details, the paper is attached in annex at the end of the report.

Abstract

Monocyclic nitramine explosives RDX and HMX are known to be toxic to a number of ecological receptors including earthworms. The polycyclic nitramine CL-20 being a powerful explosive may replace RDX and HMX, but its toxicity is not known. In the present study, the lethal and sublethal toxicities of CL-20 to the earthworm (*Eisenia andrei*) were evaluated. Two natural soils, a natural sandy forest soil (designated RacFor2002) taken in the Montreal area (QC, Canada; 20% organic carbon, pH 7.2) and a Sassafra sandy loam soil (SSL) taken on the property of US Army Aberdeen Proving Ground (Edgewood, MD; 0.33 % organic carbon, pH 5.1) were used in this study. Results showed that CL-20 was not lethal at concentrations ≤ 125 mg CL-20/ kg in the RacFor2002 soil, but lethal at concentrations ≥ 90.7 mg CL-20/ kg in the SSL soil. Effects on the reproduction parameters, such as a decrease in the number of juveniles after 56 days of exposure, were observed at the initial concentration ≥ 1.6 mg CL-20/ kg in the RacFor2002 soil compared to ≥ 0.2 mg CL-20/ kg in the SSL soil. Moreover, low concentrations of CL-20 in SSL soil (ca. 0.1 mg CL-20/ kg; nominal concentration) were found to reduce the fertility of earthworms. Taken together, this study shows that CL-20 is reproductive toxicant to the earthworm, with lethal effects at higher concentrations. Its toxicity can be decreased in soils favoring CL-20 adsorption (high organic carbon content).

XVI.3 Enchytraeid survival and reproduction tests

Research under this task is published in:

Dodard S. G., G. I. Sunahara, M. Sarrazin, P. Gong, R.G. Kuperman, G. Ampleman, S. Thiboutot, and J. Hawari (2005) *Survival and reproduction of enchytraeid worms (Oligochaeta) in different soil types amended with cyclic nitramine explosives. Environmental Toxicology and Chemistry*. 24(10): 2579-2587

Introduction

Wide use of CL-20 could cause hazardous environmental effects. Limited information is available on the effects of CL-20 on soil microorganisms, terrestrial plants and aquatic biota (Gong *et al.*, 2004). Recently, Robidoux *et al.* (2004) found that CL-20 significantly decreased adult earthworm *Eisenia andrei* survival at 90.7 mg kg⁻¹ soil and juvenile production at 0.01 mg kg⁻¹ soil (nominal concentration), but there is no published information available on the effects of CL-20 on enchytraeids. More information is presently necessary to predict the ecotoxicological impact of CL-20 in the terrestrial environment. Enchytraeid worms have been increasingly used in ecotoxicological studies because they are sensitive to many chemicals, including trace metals, organics and some energetic materials (Posthuma *et al.*, 1997; Puurtinen and Martikainen, 1997; Collado *et al.*, 1999; Schäfer and Achazi, 1999; Dodard *et al.*, 2003, 2004; Kuperman *et al.*, 1999, 2004a, b).

To improve our understanding of ecotoxicity of CL-20 and to generate ecotoxicological data that can be used in the ecological risk assessments in case of its accidental release, the objectives of the present study were to characterize the lethal and sublethal effects of CL-20 on enchytraeids in three different freshly amended soil types. Due to the presence of the same characteristic N-NO₂ groups in RDX, HMX and CL-20, we thought that similar effects could be observed on soil invertebrates such as enchytraeids. Assessments of RDX or HMX toxicity for the same enchytraeid species were conducted in parallel with the CL-20 studies to enable direct comparisons of ecotoxicological data determined under similar experimental conditions.

Material and Methods

Chemicals and reagents. CL-20 was obtained from ATK Thiokol Propulsion (Brigham City, UT). RDX and HMX were obtained from Produits Chimiques Expro (Valleyfield, QC, Canada). All energetic compounds used were ≥ 99% pure. All other chemicals, including carbendazim (methyl benzimidazol-2-yl carbamate; CAS 10605-21-7), were of ACS reagent grade or higher, and were obtained from either BDH (Toronto, Ontario, Canada) or Aldrich Chemical (Milwaukee, WI, USA). Deionized water (ASTM Type I) was obtained using a Millipore Super-Q water purification system (Nepean, ON, Canada) and was used throughout this study. All glassware was washed with phosphate-free detergent, rinsed with acetone, and acid-washed before a final and thorough rinse with deionized water.

Preparation of test soils. The soils used for this study were Sassafra sandy loam (SSL; Fine-

loamy, siliceous), an agricultural soil (RacAg2002; Fine-sandy, composite) and a 50:50 mixture of forest and agricultural soils (Rac50-50; Fine-sandy, composite). The SSL soil was collected from uncontaminated open grassland on the property of Aberdeen Proving Ground (APG, MD, USA). The RacAg2002 and Rac50-50 were obtained from a local supplier (Racicot, Boucherville, QC, Canada). The soil was sieved through a 5-mm mesh screen, air-dried for at least 72 h, passed through a 2-mm sieve, and stored at room temperature until use. The pH of the soils was measured before and after each test, using the CaCl_2 method (ISO/10390, 1994). The soil moisture content and water holding capacity were measured according to the enchytraeid reproduction test guidelines (ISO/16387, 2001). Selected soil properties are summarized in Table 18.

Table 18 Physical and chemical characteristics of soil used in the study.

Parameters	SSL ^a	RacAg2002	Rac50-50
pH	5.5	8.2	7.9
Water Holding Capacity (% v w^{-1})	21	320	93
CEC ^b (cmol kg^{-1})	5.5	69.6	20.3
Organic matter (% w w^{-1})	0.33	42	23
Texture ^c			
Sand, 50 – 2000 μm	71	90	87
Silt, 2 – 50 μm	18	9	11
Clay, < 2 μm	11	1	2

^a Soils used: SSL, Sassafra sandy loam; RacAg2002, agricultural soil; Rac50-50, composite mixture of forest and agricultural soils. ^b CEC = cation exchange capacity. ^c Values are expressed as % (w w^{-1}), and include organic matter contents.

Different dilutions of test compound were prepared separately using 10 mL of stock solutions of RDX, HMX or CL-20 in acetone, and were added separately to individual 400-g batches of air-dried soils to obtain nominal concentrations (mg kg^{-1} , dry soil mass) ranging from 175 to 700 for RDX, 200 to 1000 for HMX, and 0.001 to 10 for CL-20. Solvent controls for soil treatments were amended with acetone only (1% v w^{-1}). All soil samples were left for at least 16 h in a darkened chemical hood to allow the evaporation of the solvent vehicle (1% v w^{-1}). Final concentrations of CL-20 in all soils were confirmed by HPLC after 24-h equilibration, and were: 0, 0.001, 0.050, 0.10, 0.50, 2.98, and 9.79 mg kg^{-1} for SSL; and 0, 0.001, 0.01, 0.05, 0.10, 0.50, and 1.0 mg kg^{-1} for both RacAg2002 or Rac50-50. Selection of RDX and HMX concentrations in soil used in the present experiments were based on earlier studies (Phillips *et al.*, 1993; Jarvis *et al.*, 1998; Schäfer and Achazi, 1999; Robidoux *et al.*, 1999, 2000; Simini *et al.*, 2004). The soil samples were stored at 4°C until further analyses. All samples were prepared in triplicate and were analyzed within one week.

Culturing and handling of test species. Laboratory cultures of *Enchytraeus albidus* Henle

(1837) and *Enchytraeus crypticus* were originally provided by Dr. J. Römcke (Frankfurt, Germany) and the U.S. Army Edgewood Chemical Biological Center (APG, MD, USA), respectively. Enchytraeids were cultured separately in a mixture (1:1, w w⁻¹) of garden soil (designated GS1) and OECD Standard Artificial Soil (OECD, 1984a) adjusted to 60% water holding capacity, according to Römcke and Moser (1999). GS1 was a sandy loam soil that was passed through a 2 mm sieve, and consisted of 70% sand, 7% clay, and 23% silt, with a pH of 6.9, water holding capacity of 76%, total organic carbon of 11.2% and Kjeldahl N (K-N) of 0.38%. The OECD artificial soil had the following constituents, 70 % sand, 20 % kaolin clay and 10 % of grounded peat, and pH was adjusted to 6.0 ± 0.5 °C with CaCO₃. The potworms were fed once a week with commercially available oats (Pablum[®] Oat cereal, H.J. Heinz Company of Canada, North York, Ontario, Canada). Mature *E. albidus* with visible eggs in the clitellum region were acclimated in RacAg2002, SSL or Rac50-50 soils for 24 h before testing. Cultures of *E. crypticus* were maintained in the test soils for 2-3 months prior to testing; therefore, no acclimating was required.

Enchytraeid Reproduction and Survival Test. The Enchytraeid Reproduction and Survival Test (ERST) used in the present study were adapted from the ISO bioassay ISO/16387 (ISO, 2001). Briefly, 20 g dry weight of each soil type was placed into separate 200-mL glass jars, and was hydrated to 85-100% of their respective water holding capacity. After the 24-h equilibration period, each jar received different amounts (depending on the species) of lyophilized oats that was mixed into the soil. *E. albidus* and *E. crypticus* were fed with 40 and 50 mg of oats, respectively. Ten acclimated enchytraeids were then added to each test container. Each toxicity test was appropriately replicated (n = 3) and included negative (no chemicals added, n = 3), carrier (acetone, n = 3), and positive (reference toxicant, n = 3) controls. Each jar was covered with a glass Petri dish to prevent moisture loss during the incubation period. All containers were placed in an environment-controlled incubator at 20°C and 16:8 h (light: dark period). The containers were weighed once a week and the weight loss was replenished with the appropriate amount of water. Lyophilized oats (20 mg for *E. albidus* and 50 mg for *E. crypticus*) were added weekly to each test container. Adult survival was assessed on day 21 of the tests for *E. albidus*, and on day 14 for *E. crypticus*. All surviving adults were removed from the soil and were counted. The soil (containing cocoons and juveniles) was then returned to the same test container, and the soil moisture was re-adjusted to 60% water holding capacity, before incubation for an additional 21 d for *E. albidus*, and 14 d for *E. crypticus*. Juvenile production by both species was assessed by counting the number of hatched juveniles on day 42 (*E. albidus*) or day 28 (*E. crypticus*) of the test. For this, 5 mL of 95% ethanol was added to each soil sample as a preservative, and approximately 250 µL of Bengal Rose biological stain (1% solution in ethanol) was also added to each container. Water was added into each container at the soil level followed by 30% AM-30 Ludox colloidal silica (Sigma-Aldrich Canada, Oakville) in order to have a depth of 1 to 2 cm of liquid above the soil. Ludox allowed soil particles to stay at the bottom while enchytraeids float; this method for extracting enchytraeids from soil is rapid and highly efficient (Phillips and Kuperman, 1999).

Quality control. Carbendazim (methyl benzimidazol-2-yl carbamate; CAS 10605-21-7) was used

as the reference toxicant (positive control) in SSL soil for *E. crypticus*, and OECD Standard Artificial soil for both *E. crypticus* and *E. albidus*. Nominal carbendazim concentrations tested were 10, 25, 50, 75, and 100 mg kg⁻¹ soil for *E. crypticus*, and 1.0, 2.5, 5.0, 10.0, and 50 mg kg⁻¹ soil for *E. albidus*. Validity criteria for the positive controls were based on in-house control data and published reports (Dodard *et al.*, 2003). The test validity criteria for negative controls included 80% or higher adult potworms survival, an average of 25 or higher for number of juveniles produced, and a coefficient of variation of 50% or less (ISO, 2001).

All definitive tests with *E. crypticus*, and with *E. albidus* in Rac50-50 soil complied with the validity criteria of the ISO/16387 guideline. The EC50 value for juvenile production by *E. albidus* in the positive control (carbendazim) using OECD standard soil was 1.6 mg kg⁻¹ and was consistent with Römcke and Moser (1999). The EC50 value for juvenile production by *E. crypticus* were 44 mg kg⁻¹ in OECD standard soil and 8.5 mg kg⁻¹ in SSL soil, and were within the baseline values established for our laboratory culture of *E. crypticus*. Mean adult survival in negative controls ranged from 84 to 97% in tests with *E. crypticus*, and was 99% in test with *E. albidus*. Mean number of juveniles produced by *E. crypticus* in negative controls ranged from 117 to 856, and was 45 for *E. albidus* in Rac50-50 soil. The coefficients of variation in all tests ranged from 10.1 to 29.8 percent. It should be noted that the reproduction of *E. albidus* was not supported in SSL and RacAg2002 soils that had properties (pH and organic matter content) outside optimal requirements for this species (Römcke and Moser, 1999). Accordingly, data for CL-20 toxicity for *E. albidus* in EM-amended SSL should be used with caution.

Chemical analysis of cyclic nitramines. Acetonitrile extractions of RDX, HMX or CL-20 from amended soils were performed according to USEPA Method 8330A (USEPA, 1998). For each treatment group, 2-g soil samples were weighed in triplicate into separate 50-mL screw-top glass test tubes, 10 mL acetonitrile was added and the samples were vortexed for 1 min, before sonication at 60 KHz in the dark for 18 h at 21°C. Five mL of sample was then transferred to a glass tube, to which 5 mL of CaCl₂ solution (5 g L⁻¹) was added. The tightly closed glass vial was left to precipitate in the dark. Supernatant was filtered through a 0.45 µm membrane (Millipore). The energetic chemicals in the soil extracts were analyzed and quantified using an HPLC-UV system as described elsewhere (Robidoux *et al.*, 2002, 2004). The limit of detection of the energetic chemicals in the liquid samples (µg L⁻¹) was approximately 50 for RDX, 100 for HMX and 50 for CL-20. Precision was ≥ 95% (standard deviation < 2%, signal to noise ratio = 10). The limit of quantification in SSL soil was 0.25 mg kg⁻¹ for both RDX and CL-20, and 0.5 mg kg⁻¹ for HMX. Both RacAg2002 and Rac50-50 soils showed background signals changing the quantification limit for CL-20 to 2.0 and 0.5 mg kg⁻¹, respectively. Therefore, only nominal values are reported for all concentrations below 2 mg kg⁻¹.

Accomplishments

The development of ecotoxicological benchmarks for energetic contaminants in soil has become a critical need in recent years (Talmage *et al.*, 1999). These benchmarks are required for use in ecological risk assessment of contaminated sites associated with military operations, which commonly produce elevated levels of explosives in soil. Our toxicity studies designed to address this need, used enchytraeids an ecologically relevant soil invertebrate species exposed to CL-20

in freshly amended soil types with contrasting properties that could affect its bioavailability. Toxicity tests with RDX or HMX were also conducted to allow a direct comparison of their effects with CL-20 using the same enchytraeid species.

Toxicity of CL-20 to enchytraeid. Both adult survival and juvenile production by *E. crypticus* were affected by exposure to soils initially spiked with CL-20, within the concentration ranges tested in definitive tests (Figures 48 to 50).

The order of toxicity of CL-20 spiked soils (from greatest to least) for *E. crypticus* was RacAg2002 \geq SSL $>$ Rac50-50 soils.

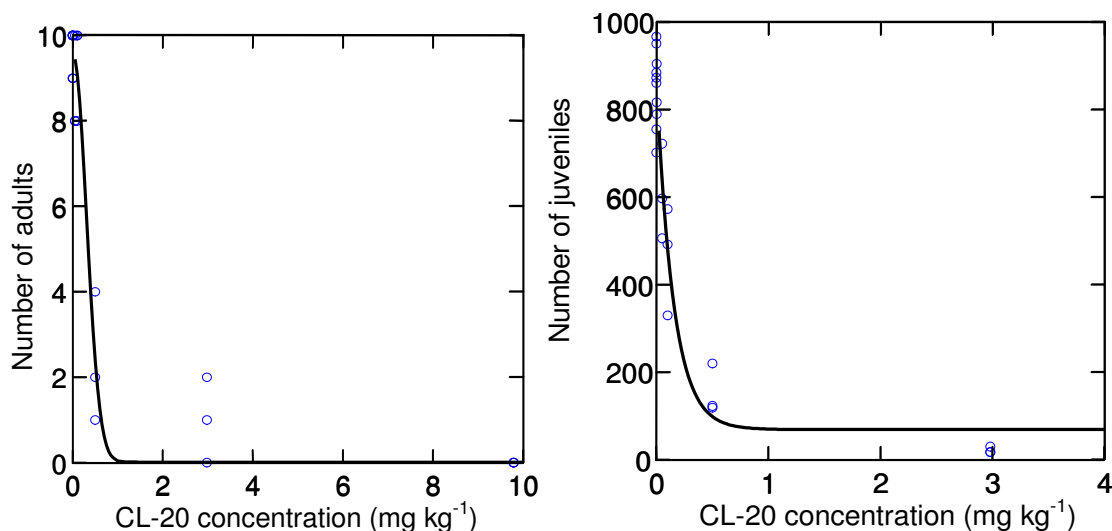


Figure 48 Adult survival and juvenile production by *Enchytraeus crypticus* exposed to CL-20 in freshly amended SSL soil.

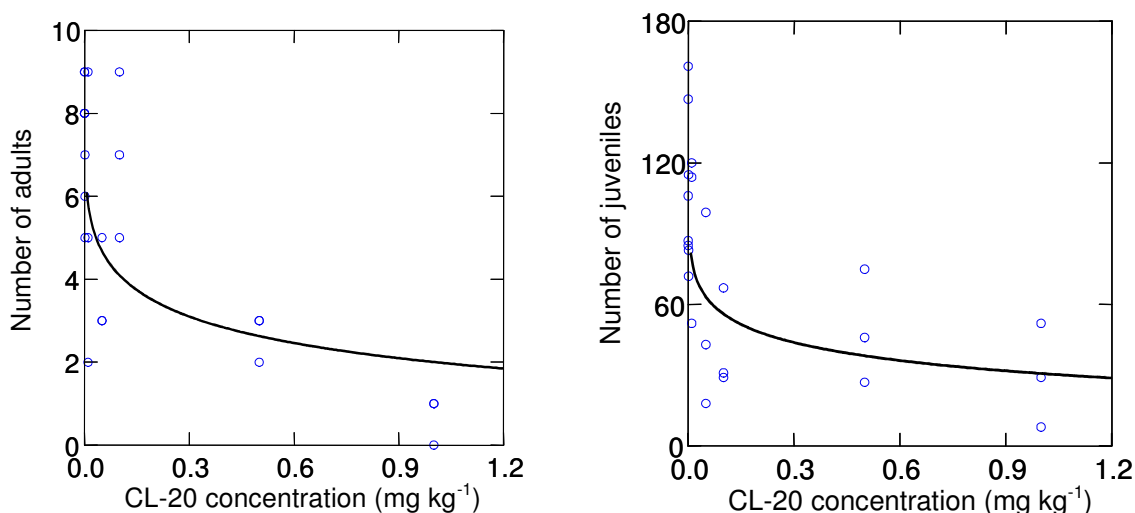


Figure 49 Adult survival and juvenile production by *Enchytraeus crypticus* exposed to CL-20 in freshly amended RacAg2002 soil.

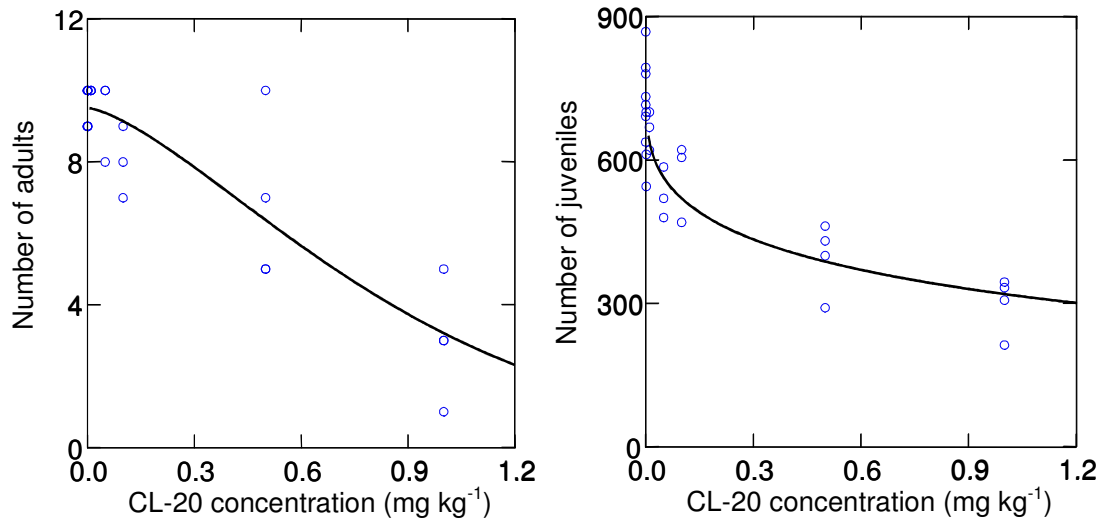


Figure 50 Adult survival and juvenile production by *Enchytraeus crypticus* exposed to CL-20 in freshly amended Rac50-50 soil.

In contrast to its effects on *E. crypticus*, CL-20 did not adversely affect adult *E. albidus* survival in RacAg2002 soil at concentrations up to and including 1 mg kg⁻¹. Toxicity of CL-20 for adult survival of both species was similar in Rac50-50 soil based on NOEC or LOEC values, and was greater in SSL soil for *E. albidus* compared with *E. crypticus* (Table 19). CL-20 caused a concentration-dependent decrease in juvenile production by *E. albidus* in the Rac50-50 soil (Figure 51, Table 19) producing the EC20 and EC50 values, which were not statistically different (on the 95% CI basis) from those determined for *E. crypticus*. No concentration-response relationships could be ascertained for juvenile production in RacAg2002 soils that did not support *E. albidus* reproduction.

Ecotoxicological benchmarks summarized in Table 19 show that CL-20 in soil was highly toxic to *E. crypticus* in the three soil types tested, with LC50 and EC50 values ranging from 0.1 to 0.7, and from 0.08 to 0.62 mg kg⁻¹ soil, respectively. Reproduction was a more sensitive assessment endpoint compared with adult mortality in all soil types tested (Table 19).

Table 19 Toxicological benchmarks (mg kg⁻¹) for CL-20 determined in freshly amended soils using the Enchytraeid Survival and Reproduction Test with *Enchytraeus crypticus* and *Enchytraeus albidus*^a.

Species / Soil	Adult Survival				Juvenile Production			
	LC20 (95% CI)	LC50 (95% CI)	LOEC	NOEC	EC20 (95% CI)	EC50 (95% CI)	LOEC	NOEC
<i>E. crypticus</i>								
SSL	0.2 (0.06 – 0.35)	0.4 (0.2 – 0.5)	0.5	0.1	0.04 (0.02 – 0.05)	0.12 (0.07 – 0.16)	0.05	0.001
RacAg2002	0.003 (0 – 0.02)	0.1 (0 – 0.3)	0.05 ^b	0.01 ^b	0.001 (0 – 0.01)	0.08 (0 – 0.24)	0.05	0.01
Rac50-50	0.3 (0.14 – 0.53)	0.7 (0.6 – 0.9)	0.5	0.1	0.03 (0 – 0.08)	0.62 (0.26 – 0.98)	0.05 ^b	0.01 ^b
<i>E. albidus</i>								
SSL	0.006 (0 – 0.02)	0.2 (0 – 0.4)	0.05	0.001	ND	ND	ND	ND
RacAg2002	> 1.0	> 1.0	> 1.0	1.0	ND	ND	ND	ND
Rac50-50	> 0.5	> 0.5	0.5	0.1	0.05 (0 – 0.13)	0.19 (0.04 – 0.34)	0.5 ^b	0.1 ^b

^a Mortality was tested on day 14 for *E. crypticus*, and on day 21 for *E. albidus*, by counting the number of surviving adult enchytraeids.

Reproduction was tested on day 28 for *E. crypticus*, and on day 42 for *E. albidus*, by counting the number of juvenile enchytraeids.

Soils used: SSL, Sassafras sandy loam soil; RacAg2002, agricultural soil; Rac50-50, composite mixture of forest and agricultural soil.

ND: Not determined because SSL and RacAg2002 soils do not support the growth and reproduction of *E. albidus*.

^b Based on Bonferroni adjusted comparison probabilities.

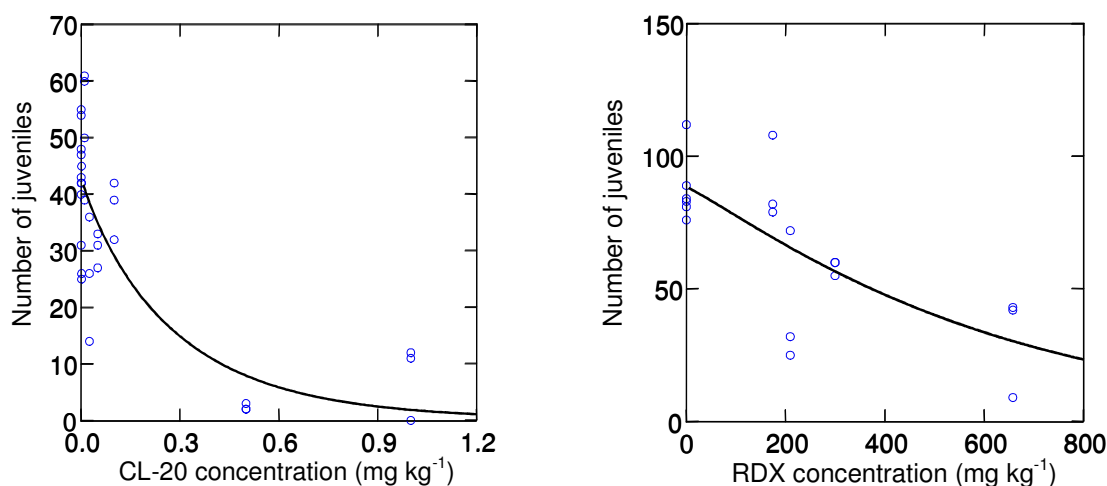


Figure 51 Effects of CL-20 (nominal concentrations) or RDX on juvenile production by *Enchytraeus albidus* in freshly amended Rac50-50 soil.

Comparison of the toxic effects of CL-20, RDX, and HMX. Exposure of *E. crypticus* or *E. albidus* test species to RDX or HMX in Rac50-50 soil, did not affect adult survival up to their respective highest concentrations of 658 and 918 mg kg⁻¹ (Table 20). Juvenile production by either species was unaffected by HMX in all treatment concentrations tested in Rac50-50 soil. In contrast to HMX, exposure of *E. albidus* to RDX significantly ($p \leq 0.05$) decreased juvenile production at 209 mg kg⁻¹ (bounded LOEC) and elicited a concentration dependent response producing the EC50 value of 444 mg kg⁻¹. Experimentally determined toxicological benchmark data for the enchytraeid worm *E. albidus* in Rac50-50 soil showed that contrary to our earlier hypothesis that CL-20, RDX, and HMX should exhibit similar toxicities, the toxicity of CL-20 was three orders of magnitude greater compared with RDX, with EC50 values for reproduction of 0.19 and 444 mg kg⁻¹, respectively. The difference in toxicity between these two explosives was even greater for *E. crypticus*, which was not affected by exposure to RDX up to the highest concentration of 658 mg kg⁻¹ when tested in Rac50-50 soil. These data agree with results by Schäfer and Achazi (1999) who reported that RDX did not affect *E. crypticus* up to 1,000 mg kg⁻¹ in standard LUFA 2.2 soil aged for 1 month prior to the exposure. Studies by Kuperman *et al.* (2004b) using higher RDX concentrations for *E. crypticus* exposures in SSL soil (similar to that used in our studies), produced EC50 value of 51,413 mg kg⁻¹, five orders of magnitude difference compared with CL-20 effects on this species determined in our study (EC50 of 0.12 mg kg⁻¹).

The greatest contrast in CL-20 toxicity for both enchytraeid species was observed using HMX. This explosive did not adversely affect either adult survival or reproduction up to 918 mg kg⁻¹. These results are consistent with findings by Kuperman *et al.* (2004b), who reported no adverse effects of HMX on *E. crypticus* in freshly amended SSL soil up to 21,750 mg kg⁻¹. Based on the results of our present studies and those reported in the reviewed literature, the order of toxicity of cyclic nitramine explosives to enchytraeids in freshly amended soils is (from greatest to least) CL-20 > RDX > HMX.

Table 20 Effects of RDX or HMX on adult survival and juvenile production (means \pm standard deviation) by two enchytraeid species in a freshly amended composite soil Rac50-50.

Test Groups	Concentrations (mg kg ⁻¹) ^a	Adult survival		Number of juveniles produced	
		<i>E. albidus</i>	<i>E. crypticus</i>	<i>E. albidus</i>	<i>E. crypticus</i>
Negative control	0	9.3 \pm 0.6	9.7 \pm 0.6	83 \pm 7	622 \pm 50
Solvent control	0	10.0 \pm 0.0	10.0 \pm 0.0	92 \pm 17	569 \pm 85
RDX	174	9.0 \pm 1.0	9.3 \pm 0.6	90 \pm 16	512 \pm 81
	209	10.0 \pm 0.0	9.3 \pm 0.6	43* \pm 25	515 \pm 168
	299	9.7 \pm 0.6	9.3 \pm 0.6	58* \pm 3	460 \pm 103
	658	9.7 \pm 0.6	10.0 \pm 0.0	31* \pm 19	474 \pm 34
HMX	205	10.0 \pm 0.0	9.7 \pm 0.6	98 \pm 21	522 \pm 61
	484	9.0 \pm 1.0	9.7 \pm 0.6	88 \pm 8	476 \pm 40
	918	9.7 \pm 0.6	10.0 \pm 0.0	75 \pm 0.6	572 \pm 115

^a expressed as measured concentrations

* Significant difference from the respective solvent control ($p \leq 0.05$).

Both CL-20 and RDX are known to degrade more easily than does HMX. In fact, when soil samples where past and present practices involving the extensive use of the melt-cast explosive Octol (HMX: 70 w/w %; TNT: 30 w/w %; RDX: <1 w/w %) were characterized, only HMX was detected as the principal soil contaminant (Groom *et al.*, 2002; Dubé *et al.*, 1999; Jenkins *et al.*, 1998). HMX was also found intact when up taken by plants (Groom *et al.*, 2002; Yoon *et al.*, 2002). CL-20 was also found to biotransform faster than RDX under similar conditions (Figure 37; Bhushan *et al.*, 2004c). The order of toxicity of the three energetic chemicals seemingly follows their order of chemical and biochemical reactivities, thus suggesting that these chemicals may exert their toxic effects, at least in part, through their degradation products. It should be noted however that the toxicity order also follows the order of log K_{ow} values (CL-20: 1.92 > RDX: 0.90 > HMX: 0.16; Monteil-Rivera *et al.*, 2004) and that the toxicity could be favored by a higher log K_{ow} and thereby a higher solubility in the receptor tissues.

Earlier studies with TNT (Lachance *et al.*, 2004) showed that this energetic chemical and its transformed products (2-amino-dinitrotoluene and 4-amino-dinitrotoluene) were responsible for causing toxic effects to earthworms. In the case of CL-20, the chemical can be degraded in non-sterile soils (Trott *et al.*, 2003), under alkaline conditions (Balakrishnan *et al.*, 2003), or in the presence of zero valent iron (Balakrishnan *et al.*, 2004a) to produce nitrite (NO_2^-), nitrous oxide (N_2O), ammonia (NH_3), formic acid (HCOOH), or glyoxal (HCOCHO). The higher pH of RacAg2002 compared with SSL and Rac50-50 soils (Table 18) may have contributed to accelerated hydrolysis of CL-20 and the concomitant formation of greater quantities of potentially toxic byproducts such as glyoxal or formic acid. The presence of these transformation products may explain, at least in part, the observed CL-20 toxicity in our enchytraeid toxicity studies, as well as others using earthworms (Robidoux *et al.*, 2004). Preliminary studies (described in more details in section XIX.1) were thus conducted with glyoxal and formic acid amended in SSL soil at varying concentrations (1, 10 and 100 mg kg^{-1} dry soil), which showed no lethal effects of either chemical to the earthworm at the concentrations tested. Therefore, CL-20 degradation products other than glyoxal or formic acid, such as the early reactive intermediates including free radicals (Hawari *et al.*, 2004) may lead to cell organelle injury.

Influence of soil types on CL-20 toxicity to enchytraeids. Soil properties can influence the bioavailability and toxicity of energetic contaminants to soil invertebrates (Phillips *et al.*, 1993; Robidoux *et al.*, 2002, 2004; Schäfer, 2002; Kuperman *et al.*, 2004b; Simini *et al.*, 2004). CL-20 is highly immobilized by soils rich in organic matter (OM), and its bioavailability (and subsequent toxicity) could vary depending on the amount and quality of OM (Balakrishnan *et al.*, 2004b). In the present study, we assessed toxicity of different cyclic nitramines including CL-20 to enchytraeid worms using three soil types that have contrasting properties (pH, OM, and clay contents, as shown in Table 18).

Results indicate that the soil with highest pH, CEC, and organic matter content (RacAg2002) (Table 18) sustained the greatest CL-20 toxicity to *E. crypticus* adult survival and reproduction based on LC50 or EC50 values (Table 19). The effect of pH was discussed when comparing the toxicity of CL-20 with that of RDX and HMX. Clay was shown to have no effect on the availability of CL-20 (Balakrishnan *et al.*, 2004b). As for the organic matter, the SSL soil used in the present study has a low OM content that supports relatively high bioavailability of CL-20 in soil ($K_d = 2.43 \text{ L kg}^{-1}$, Table 6). Although K_d coefficients were not measured for the

composite soils RacAg2002 and Rac50-50, a lower availability of CL-20 is expected in these soils due to the higher fraction of OM they contain (42 and 23 %, respectively). Indeed, high content of OM should favor both sorption and microbial degradation. Based on the availability of the chemical, CL-20 in freshly amended SSL soil should thus sustain a higher toxicity compared to the composite RacAg2002 and Rac50-50. Results of definitive tests showed that this was not the case (Table 19), and that RacAg2002 soil sustained the greatest CL-20 toxicity to *E. crypticus* adult survival and reproduction based on LC50 and EC50 values, followed by SSL and Rac50-50 soils. These results indicate that differences in CL-20 toxicity to enchytraeids between test soils cannot be interpreted solely on the basis of the ability of the energetic chemical to bind onto soil. More soils should be tested to further understand the differences in CL-20 toxicity observed in different soils.

Conclusion

The present study showed clearly that CL-20 (and possibly its degradation products) was highly toxic to *E. crypticus* and *E. albidus*. This effect is orders of magnitude more pronounced compared with the currently used explosives RDX and HMX. Identification of all intermediate and final products of the degradation of CL-20 is necessary before its ecological risks and impacts in the soil vadose zone can be more clearly understood.

XVII Avian reproduction toxicity tests

Work conducted under this task was published in:

Bardai, G., Sunahara, G. I., Spear, P. A., Martel, M., Gong, P., and Hawari, J. (2005) Effects of Dietary Administration of CL-20 on the Japanese Quail (*Coturnix coturnix japonica*), *Archives of Environmental Contamination and Toxicology* 49: 215-222

Introduction

CL-20 is being considered as a potential replacement for existing explosive materials such as RDX and HMX. The toxicity of the latter to terrestrial vertebrate species such as mammals, amphibians and birds is becoming better known (Schneider *et al.*, 1976; Levine *et al.*, 1981; Talmage *et al.*, 1999; Gogal *et al.*, 2003; Johnson *et al.*, 2004). Gogal *et al.* (2003) found the approximate lethal dose of acute oral RDX exposure in northern bobwhite (*Colinus virginianus*) to be 280 mg/kg body weight (BW) for males, and 187 mg/kg BW for females. The dose-dependent effects of RDX also included a decrease in food intake, body weight, and spleen and liver mass for 14 days but not for 90 days of exposure. Although the effects of CL-20 in plant and soil invertebrate species have been recently reported (Gong *et al.* 2004; Robidoux *et al.* 2004), there is presently a lack of data describing the toxic effects of CL-20 on avian species.

CL-20 is a polycyclic nitramine characterized by having N-NO₂ bonds, similar to the two monocyclic nitramines RDX and HMX. Based on these structural similarities, we hypothesized that the effects of CL-20 to birds may be similar to those of RDX. In the present study, we thus investigated the toxic effects of CL-20 on the gallinaceous test species, the Japanese quail (*Coturnix coturnix japonica*). We selected this species because it is amenable to laboratory toxicity testing, and species of this order can have significant dietary exposure to soil based on their foraging and behavioral habits. This species are used in many standard toxicity testing regimes for standard avian toxicity testing (ASTM 1997; USEPA 1996a,b; OECD 1984b,c). Data generated using these standardized toxicity test methods will be useful for the ecotoxicological risk assessment of birds exposed to CL-20.

The effect of CL-20 on Japanese quail were studied using two standard toxicity tests: firstly, a 14-day subacute assay using repeated gavages doses (0, 307, 964, 2439, 3475 or 5304 mg CL-20/kg body weight (BW)/d) for 5 d followed by no CL-20 exposure (vehicle only) for 10 d; and secondly, a subchronic feeding assay (0, 11, 114, or 1085 mg CL-20/kg feed) for 42 d.

Material and Methods

Chemicals and reagents. CL-20 in the ϵ form (purity > 95%) was obtained from ATK Thiokol Propulsion (Brigham City, Utah, USA). Acetonitrile and acetone (HPLC grade) were obtained from EM Science (Darmstadt, Germany). All other chemicals and reagents were of the highest grades of purity available, and were obtained from Anachemia (Milwaukee, WI, USA). Deionized water was obtained using a Zenopure Mega-90 water purification system. All glassware was washed with phosphate-free detergent, rinsed with acetone, and acid-washed

before a final rinse with deionized water.

Raising of test species. Fertilized Japanese quail (*Coturnix coturnix japonica*) eggs (n= 70 for subacute study, and n= 120 for subchronic study) obtained from a local breeder (Couvoir Simetin, Mirabel, QC, Canada) were placed in an environment-controlled incubator at $37 \pm 1^\circ\text{C}$, $65 \pm 5\%$ relative humidity, and turned 180° every fourth hour. Three days before hatching, rotation of eggs was stopped and the relative humidity raised to 70%. Eggs were grouped at the center of the incubator, on a 5-mm mesh until they hatched. When dry, quail chicks were transferred to a heated brooder (35°C achieved using an electric resistance element), under constant illumination with red incandescent light to prevent eye damage. Birds were fed a diet of powdered Turkey Starter (Purina Mills, St Louis, MO, USA) and tap water *ad libitum*, until 14 days of age. Quail were then maintained under controlled conditions of temperature ($22.0 \pm 3.0^\circ\text{C}$), relative humidity ($50.0 \pm 6.0\%$), and lighting (14:10 h, light:dark cycle).

Experimental design. The subacute study (Figure 52A) described in this article was designed according to the USEPA (1996a) and OECD (1984b) protocols. Forty-four 2-week old quail were weighed, banded, and observed for any abnormalities. A blood sample (1 mL) was taken from the jugular vein (described below) and each bird was then randomly assigned to six groups (n = 7-8 per group, 44 total).

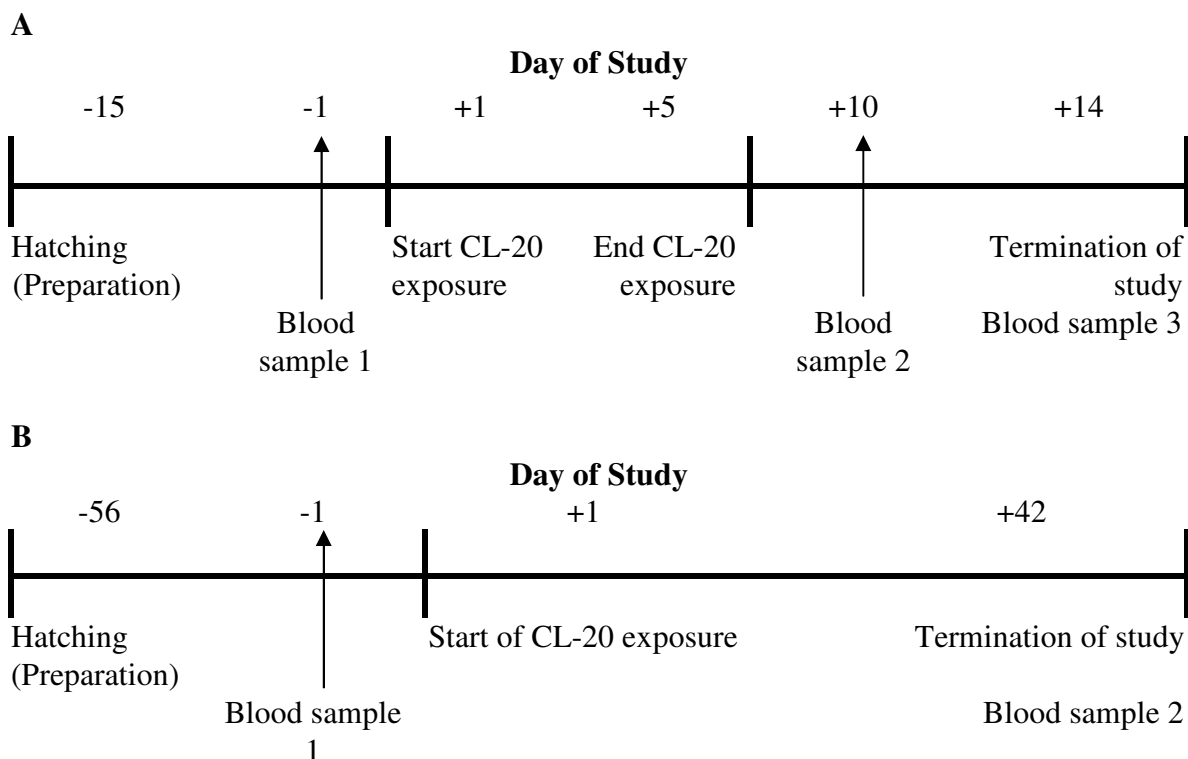


Figure 52 Schedule for the two CL-20 exposure studies: subacute study (A) and subchronic study (B).

Animals were housed together in stainless steel cages (61 cm width \times 76 cm length \times 41 cm high; 10-mm mesh floor) (2-3 individuals per cage) and were uniquely identified by a leg band. Two days later, birds were gavaged daily for 5 d with pulverized commercial feed (Ralston Purina Turkey Grower) containing CL-20.

Briefly, the feed was pulverized using a hand-held blender until a granular consistency was formed, before the addition of CL-20. The CL-20 contaminated feed was prepared daily, and the doses were adjusted to the body weight that was taken daily during the dosing period (1% of BW). To deliver the contaminated feed, the desired quantity was transferred into a 5-mL syringe, and then 1 mL of water was added to the syringe to form a slurry. A 10-gauge stainless steel curved feeding tube equipped with a Luer Lock fitting (Becton Dickinson, Canada) onto the syringe was inserted down the esophagus to the crop. The slurry was administered gently to ensure minimal regurgitation. The calculated doses delivered (mg CL-20/kg BW) were: 307 ± 1 , 964 ± 8 , 2439 ± 12 , 3475 ± 5 , and 5304 ± 53 . A second blood sample (from 1 to 1.5 mL) was collected 5 d after completion of the dosing. At the end of the experiment (Day 14 of study), a third blood sample (5 mL) was procured and the organs (heart, brain, liver, and spleen) were weighed and were frozen at -80°C for residual CL-20 analysis. The somatic index (%) was calculated as the wet organ weight (g) per 100 g body weight.

In the subchronic study (Figure 52B), when the quail reached 2 weeks of age, the lighting period was changed (16:8 h light: dark cycle) to provide optimal reproductive conditions, and the birds ($n = 48$) were randomly assigned to each of the four dose groups (described below) in triplicate. Each exposure was conducted in triplicate; each group of 3 females and 1 male were housed together in stainless steel cages (described above). Quail were uniquely identified by a leg band. During this period, close surveillance was required to monitor any signs of increased aggression. Individuals injured or demonstrating incompatible behavior relative to the group were replaced. Eggs were collected and incubated during the pre-exposure period to verify fertility and thus ensure that only proven breeders were included in this study. Two days prior to the start of feeding CL-20 diets when quail were 54 d old, a blood sample (2 mL) was taken from each bird. The diets were prepared by mixing CL-20 (previously dissolved in acetone) with commercial feed (Ralston Purina Turkey Grower) to achieve nominal concentrations of 10, 100, and 1000 mg CL-20/kg feed. The vehicle control diets were treated with similar quantities of acetone without CL-20 as described above. Acetone was allowed to evaporate, and the CL-20 feed mixture was then placed in glass jars and stored at $4.0 \pm 2.0^{\circ}\text{C}$ in the absence of light. Measured concentrations of CL-20 in the feed were analyzed using HPLC (11 ± 1 , 114 ± 26 , and 1085 ± 52 mg CL-20/kg feed corresponding to the target exposure groups of 10, 100, and 1000 mg/kg BW, respectively), and were found to be consistent throughout the study. All feed was provided daily *ad lib*. Daily feed consumption was estimated as the difference between initial and final feed weight plus the quantity of unconsumed pellets recovered from the litter pans, which was determined daily for the first 2 weeks of the study, and then every alternate day.

Subsamples of eggs (based on total eggs collected, $n = 15$ -20 per day) were collected and frozen at -80°C ; the remaining eggs ($n = 10$ -12 collected per day) were stored in a refrigerator ($16 \pm 1^{\circ}\text{C}$ and 60-70% humidity) for 5 d. Eggs of the latter group were then incubated at 37.8°C and 60% relative humidity. Following eight days of incubation, the eggs were cooled to 4°C , and embryos were then removed and weighed. Embryos were then preserved in capped vials containing 10% formalin, and were stored at room temperature in the dark until further

evaluation of developmental effects. Embryos were evaluated according to the Hamburger-Hamilton system (1951) for normal stages of chick embryo development. At the end of the 6-week exposure period, the adult birds were sacrificed and examined for gross lesions. Liver, spleen, heart, and brain were excised, weighed, frozen in liquid nitrogen, and then stored at -80°C prior to residual CL-20 analyses.

For both studies, birds were monitored daily for changes in health or disposition (*i.e.*, alertness, appearance). For the subchronic study, body weight gain was measured daily for the duration of the gavage phase, and then at study days 10 and 14. Body weight and feed consumption for the subacute study were measured daily for a 2 week period, and then every alternate day. At the end of the experiments, birds were anesthetized (2-5% isoflurane), and euthanized (90% CO₂ / 10% O₂). Moribund animals were treated in the same fashion. Manipulation and handling were in accordance with the Canadian Council on Animal Care guidelines (1984).

Blood collection and analysis. For clinical chemistry and hematological analyses, female quail blood was collected from the jugular vein with a 27-gauge needle and a 3-mL syringe containing 100 µL of a 1% EDTA solution in saline. Males were not considered for this study because of the low number of males per exposure group (1 male per 3 females per replicate, 3 replicates per exposure group). Blood was thoroughly mixed and 250 µL was removed for whole blood analysis. Plasma was prepared in 1.5 mL Eppendorf tubes centrifuged at 13,000 × *g* for 5 min, and was used either fresh for clinical chemistry analysis to screen for biochemical and pathological abnormalities, or was stored at -80°C for plasma residual CL-20 analysis. Quail plasma was analyzed to determine its clinical chemistry profile (Beckman LX20 Pro, Rochester, NY) which included sodium (Na), potassium (K), chloride (Cl), glucose (Glu), creatinine (Cre), total protein (TP), phosphorus (PO₄), total bilirubin (Tbili), direct bilirubin (Dbili), uric acid (Uric), magnesium (Mg), cholesterol (Chol), alanine aminotransferase (ALT), aspartate aminotransferase (AST), alkaline phosphatase (ALP), amylase (AMY), lactate dehydrogenase (LDH), and triglycerides (TG). For hematological analysis, a drop of anticoagulated blood was placed on a microscope slide and a smear was made. The blood smear was fixed in methanol, stained with modified Wright-Giemsa and the leukocyte differential was performed where 100 leukocytes (lymphocytes, heterophils, monocytes, basophils, and eosinophils) were enumerated. Heterophil to lymphocyte ratios were calculated to investigate stress. For hematocrit (HCT) determination, a non-heparinized hematocrit capillary tube was filled with anticoagulated blood. The bottom of the capillary tube was sealed with a clay plug, and centrifuged for 5 min at 3000 rpm, and the HCT was determined as the ratio between total capillary volume and the packed cell volume (PCV).

CL-20 extraction from quail tissue. CL-20 extractions were performed according to USEPA Method 8330A (USEPA, 1997) with the following modifications. For CL-20 exposure studies, whole organs taken from test animals were immediately homogenized on ice in 7 mL cold acetonitrile using a Polytron tissue homogenizer (30 s for brain and spleen, or 1 min for heart and liver) in Teflon tubes. Following overnight sonication in the dark at 8°C (60 Hz; Branson 3200, Danbury, CT, USA), samples were centrifuged at 4°C for 10 min at 10,000 × *g*. To 5 mL of the decanted supernatant was added an equal volume of a CaCl₂ (90 mM)-NaHSO₄ (1.6 mM) solution, and the resulting mixture was vortexed for 30 s and stored at 4°C for 2 h to precipitate

proteins. The resulting solution was filtered through a 0.45- μ m membrane prior to HPLC analysis. To increase the sensitivity of the above method, the supernatants of different tissue samples (liver, heart, brain, and kidney) were also concentrated. Each supernatant (5 mL) was evaporated to dryness in a Speed Vac (Savant, Hicksville, NY, USA). To the precipitate was added 500 μ L acetonitrile and vortexed for 1 min, after which the CaCl_2 - NaHSO_4 solution was added as described above. For the control recovery studies, whole organs (liver, brain, spleen, or heart) were taken from non-treated quail and were spiked with varying concentrations of CL-20 prior to being immediately frozen at -80°C for 24 h. The organs were then thawed in cold acetonitrile, and CL-20 was extracted as described above.

Extraction of CL-20 from the test diet. Acetonitrile extractions of test diet were also performed using the USEPA Method 8330A (USEPA, 1997). One mL of 1.6 mM NaHSO_4 prepared in water was added to two grams of feed and vortexed for 10 s. To this was added 10 mL (for feed containing 10 mg CL-20/kg feed) or 20 mL of acetonitrile (for feed containing 100-1000 mg CL-20/kg feed), prior to vortexing for 1 min.

Analytical procedures. CL-20 was analyzed as described in section VI.

Statistical analysis. The data were evaluated by two-way and repeated measures analysis of variance (ANOVA). Statistical comparisons between exposure groups were performed by Dunnett's test ($p \leq 0.05$). Statistical analysis was performed using JMPIN (Version 4, SAS[®] Institute, Cary, NC, USA).

Accomplishments

Subacute study. No clinical or overt toxic symptoms were observed during the 5-d exposure period to CL-20. The change in average weight gain for each exposure group is shown in Figure 53. Data indicate that a dose-dependent decrease in body weight gain occurred during the first 5 days of this study ($p \leq 0.05$). On study days 1 to 3, the CL-20 quail exposure groups ≥ 964 mg/kg BW/d gained less weight than the control group ($p \leq 0.05$). However, this effect was not detected by the end of the study (day 14, or 10 d of no CL-20 exposure).

Liver weights were significantly elevated in the highest dose group (5304 mg/kg BW/d), whereas other organ weights (brain and spleen) were not significantly different between CL-20 treated and control groups (Figure 54). Increases in plasma sodium and creatinine levels were found in birds treated with 5304 mg CL-20/kg BW/d, compared with controls (Table 21). Hematological parameters (heterophil to lymphocyte ratios, and hematocrit) in the subacute study were not statistically different between exposure groups when compared to controls (data not shown).

Subchronic study No clinical or overt toxic symptoms were observed during the 42-d exposure period in this study. Aggressive behavior was noted in one individual who was subsequently isolated from the control group. Another bird from a different control group had to be euthanized due to injuries inflicted by an aggressive control bird (that was hence removed from the triplicate). These observations were not related to exposure. Based on feed consumption (feed consumed per number of individuals in each dose group) and the mean body weight, the

calculated daily doses to quail consuming the CL-20 diet were 0, 0.96, 10, and 94 mg CL-20/kg BW, for the measured 0, 11, 114, and 1085 mg CL-20/kg feed exposure groups, respectively. Throughout this study, no differences in feed consumption or body weight were observed between exposure groups (data not shown). Clinical chemistry analysis of quail blood taken from the subchronic study (Table 22) revealed that the aspartate aminotransferase (AST) level was increased by 1.25 times in the birds of the highest measured feed dose level (1085 mg CL-20/kg) relative to controls ($p \leq 0.05$).

Embryo weight was found to decrease significantly and in a dose-dependent manner (Figure 55). Based on the measured exposure concentration, the unbounded lowest observed adverse effect level (LOAEL) for this effect was 11 mg/kg feed. Some of the embryos in the storage vials dehydrated making these samples unsuitable for further analysis. In the 114 mg/kg feed exposure group, two of the 6 embryos had multiple (both cranial and facial) deformities. Whereas in the highest dose group (1085 mg/kg feed), three of the 9 embryos experienced beak curvatures, possible mid brain enlargement, and classical one sided development with micro-opthalmia. These CL-20 exposure-related deformities were not observed in the control group; however, two of the nine control embryos showed very slight ocular asymmetric deviations. No decrease in the rate of development was detected, all embryos being at stages 30-31 (Hamburger and Hamilton, 1951). In addition, CL-20 exposure tended to decrease the number of eggs laid per female ($p > 0.05$) compared to controls (Figure 56).

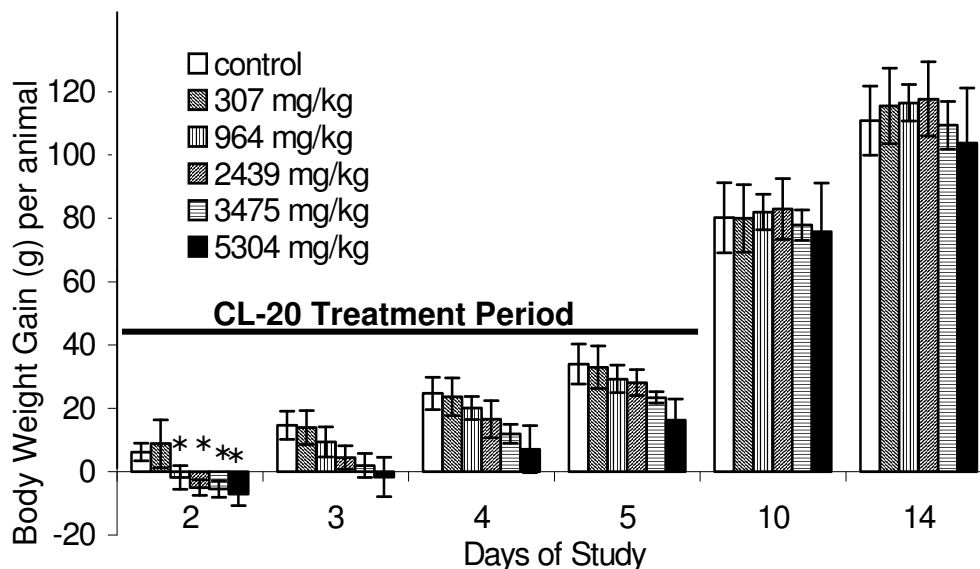


Figure 53 Changes in body weight of juvenile Japanese quail gavaged with CL-20 for 5 days (subacute study). Exposure schedule is shown in Figure 52. Each value is the mean \pm SD (standard deviation)(n = 44 birds). * Above bars denotes value is statistically different from the control ($p \leq 0.05$).

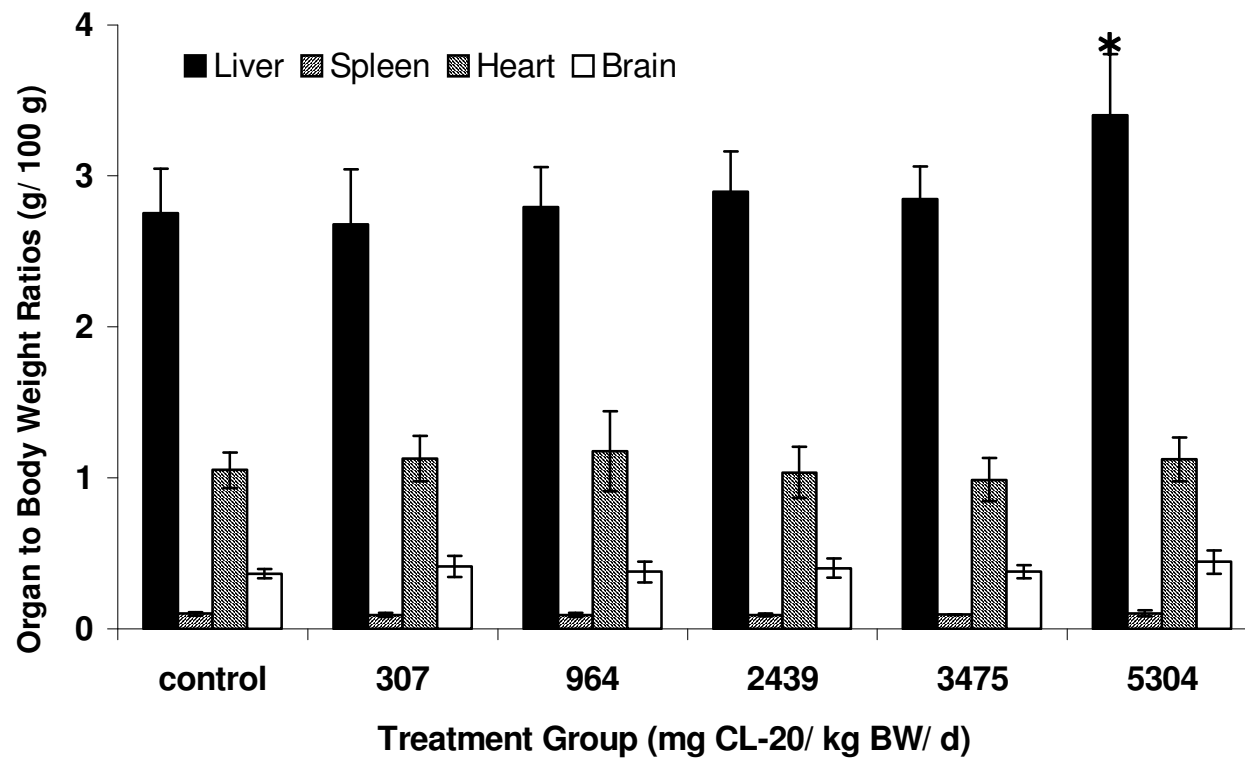


Figure 54 Somatic index of selected organs of juvenile Japanese quail gavaged with CL-20 for 5 days followed by 10 days of vehicle only (no CL-20). Data are expressed as mean \pm SD (n = 44 birds). Study design is shown in Fig. 52. * Above bars denotes value is statistically different from the control ($p \leq 0.05$)

Table 21 Selected plasma biochemical parameters of adult Japanese quail exposed to CL-20 by gavage for 5 d followed by 10 days exposure with no CL-20

Parameters	CL-20 Exposure Groups (mg CL-20 per kg body weight per d) ^a					
	0	307	964	2439	3475	5304
PO ₄ (mmol/L) ^b	3.22 ± 0.21 ^c	2.89 ± 0.26	2.91 ± 0.26	2.53 ± 0.21	2.73 ± 0.24	2.96 ± 0.39
TP (g/L)	19.2 ± 3.6	22.0 ± 2.6	22.3 ± 2.9	18.4 ± 2.9	20.8 ± 2.8	21.63 ± 3.25
Glu (mmol/L)	16.3 ± 1.0	17.0 ± 0.7	16.7 ± 1.0	16.4 ± 1.2	17.1 ± 1.3	16.36 ± 1.45
Cre (μmol/L)	20.0 ± 2.6	18.6 ± 3.2	20.3 ± 4.0	18.2 ± 5.4	21.8 ± 4.4	25.00 ± 3.16 [*]
Na (mmol/L)	143.9 ± 0.8	145.5 ± 1.0	144.0 ± 0.8	144.6 ± 2.7	149.5 ± 1.6	151.7 ± 2.70 [*]
ALP (IU/L)	592 ± 327	711 ± 253	1056 ± 301	485 ± 396	328 ± 275	509 ± 230
ALT (IU/L)	4.25 ± 1.50	4.20 ± 1.30	5.00 ± 0.82	4.80 ± 0.84	4.50 ± 1.05	4.50 ± 0.76
Uric (μmol/L)	201.3 ± 53.3	239.2 ± 78.1	269.0 ± 134.8	195.0 ± 37.6	216.0 ± 101.8	300.6 ± 68.5
AMY (IU/L)	336 ± 71	460 ± 190	377 ± 197	178 ± 60	436 ± 136	377 ± 193
AST (IU/L)	101.3 ± 11.7	87.3 ± 10.0	94.0 ± 10.1	107.2 ± 21.9	95.5 ± 13.5	101.9 ± 11.8
Chol (mmol/L)	5.32 ± 0.74	4.06 ± 0.91	5.17 ± 1.52	5.63 ± 2.50	4.67 ± 0.98	5.38 ± 1.44
Dbili (μmol/L)	1.25 ± 0.24	0.95 ± 0.21	0.78 ± 0.31	1.40 ± 0.50	0.83 ± 0.27	1.16 ± 0.49
Tbili- (μmol/L)	2.8 ± 0.5	2.6 ± 1.6	4.0 ± 1.2	2.2 ± 1.3	2.3 ± 1.1	3.5 ± 0.9
GGT (IU/L)	6.5 ± 4.5	8.8 ± 2.3	8.0 ± 1.4	8.4 ± 0.9	7.5 ± 2.2	10.0 ± 2.2
LDH (IU/L)	59.8 ± 13.0	48.8 ± 8.4	47.0 ± 9.5	49.2 ± 12.8	41.0 ± 12.7	56.4 ± 28.8
TG (mmol/L)	1.84 ± 0.20	1.42 ± 0.32	2.05 ± 0.91	2.04 ± 0.52	1.49 ± 0.36	2.06 ± 0.78
Mg (mmol/L)	0.15 ± 0.50	0.20 ± 0.01	0.28 ± 0.05	0.11 ± 0.14	0.10 ± 0.04	0.13 ± 0.7

^a Measured concentrations of CL-20 intake by gavaged quails. ^b Abbreviations used: Phosphate (PO₄), Total Proteins (TP), Glucose (Glu), Creatinine (Cre), Alkaline phosphatase (ALP), Alanine aminotransferase (ALT), Amylase (AMY), Aspartate aminotransferase (AST), Cholesterol (Chol), Direct Bilirubin (Dbili), Total Bilirubin (Tbili), γ-glutamyltransferase (GGT), Lactate dehydrogenase (LDH), Triglycerides (TG), Magnesium (Mg) ^c Data are expressed as mean ± SD (standard deviation) (n = 4-8 birds per exposure group). ^{*} Exposure group is significantly different from control using Dunnett's test (*p* ≤ 0.05).

CL-20 recovery from tissue. CL-20 was not detected in the plasma or selected organs (brain, spleen, heart and liver) of quail treated with CL-20 (data not shown), despite the excellent recovery of the chemical (99-105 %) using different spiked tissues (Figures 57 and 58).

Table 22 Selected plasma biochemical parameters of adult Japanese quail fed CL-20 in the diet for 42 d

Parameters	CL-20 Exposure Groups (mg CL-20/kg feed) ^a			
	0	11	114	1085
PO ₄ (mmol/L) ^b	2.87 ± 0.63 ^c	2.56 ± 0.39	3.03 ± 0.84	2.11 ± 0.71
TP (g/L)	31.6 ± 4.0	30.1 ± 2.3	33.5 ± 1.7	28.3 ± 3.2
Glu (mmol/L)	15.1 ± 0.99	15.4 ± 1.29	14.5 ± 0.8	14.4 ± 0.9
Cre (μmol/L)	30.3 ± 9.6	32.4 ± 4.7	24.4 ± 6.1	27.0 ± 9.6
Na (mmol/L)	144.4 ± 3.6	142.3 ± 1.3	139.8 ± 3.5	142.3 ± 1.3
ALT (IU/L)	5.16 ± 1.60	4.83 ± 2.22	6.00 ± 1.63	6.50 ± 1.51
Uric (μmol/L)	213.4 ± 58.7	303.0 ± 147.0	136.8 ± 71.2	232.3 ± 131.5
AMY (IU/L)	507 ± 179	368 ± 222	643 ± 304	472 ± 154
AST (IU/L)	133.3 ± 11.6	144.8 ± 23.5	154.6 ± 27.4	167.2 ± 23.2 *
Chol (mmol/L)	6.27 ± 2.06	4.84 ± 1.76	7.39 ± 3.85	4.63 ± 1.34
Tbili- (μmol/L)	7.65 ± 1.97	6.94 ± 1.45	8.12 ± 1.39	6.98 ± 0.96
GGT (IU/L)	5.88 ± 1.64	6.57 ± 1.13	6.13 ± 2.41	6.43 ± 1.90
LDH (IU/L)	54.8 ± 59.0	31.3 ± 27.0	34.8 ± 51.0	74.2 ± 39.0
TG (mmol/L)	11.7 ± 2.4	9.8 ± 2.7	10.8 ± 2.2	9.2 ± 2.7
Mg (mmol/L)	1.63 ± 0.33	1.36 ± 0.23	1.48 ± 0.29	1.34 ± 0.25
K (mmol/L)	2.9 ± 0.5	3.2 ± 0.3	2.7 ± 0.3	2.9 ± 0.4
Cl (mmol/L)	110.1 ± 4.2	107.8 ± 3.9	107.1 ± 3.5	110.3 ± 3.2

^a Measured concentration in feed using USEPA Method 8330A (USEPA, 1997).

^b Abbreviations used: Phosphate (PO₄), Total Proteins (TP), Glucose (Glu), Creatinine (Cre), Alanine aminotransferase (ALT), Amylase (AMY), Aspartate aminotransferase (AST), Cholesterol (Chol), Total Bilirubin (Tbili), γ-glutamyltransferase (GGT), Lactate dehydrogenase (LDH), Triglycerides (TG).

^c Data are expressed as mean ± SD (standard deviation) (n= 7-9 birds per group).

* denotes exposure group is significantly different from control using Dunnett's test ($p \leq 0.05$).

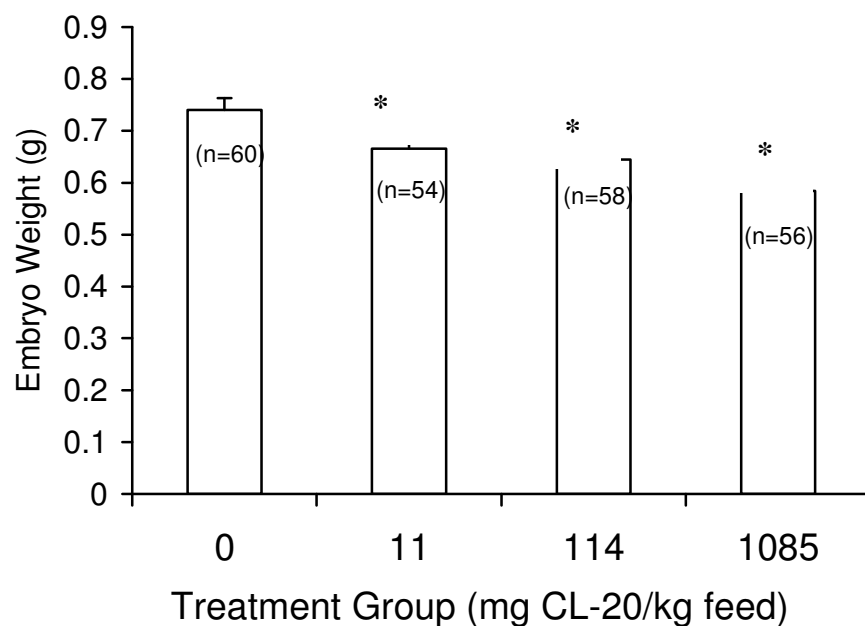


Figure 55 Effects of 42 days dietary exposure of CL-20 on Japanese quail embryo weights. Data are mean embryo weight \pm SD. (n = number of embryos evaluated). * Above bars denotes values statistically different from the control ($p \leq 0.05$).

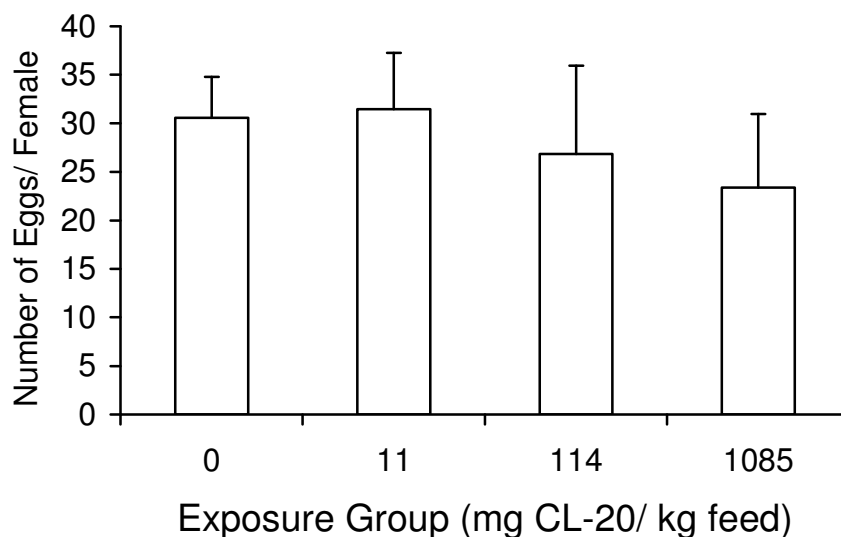


Figure 56 Effects of 42 d dietary exposure of CL-20 on the mean number of eggs produced per hen. These exposure effects were not significant compared to controls ($p > 0.05$).

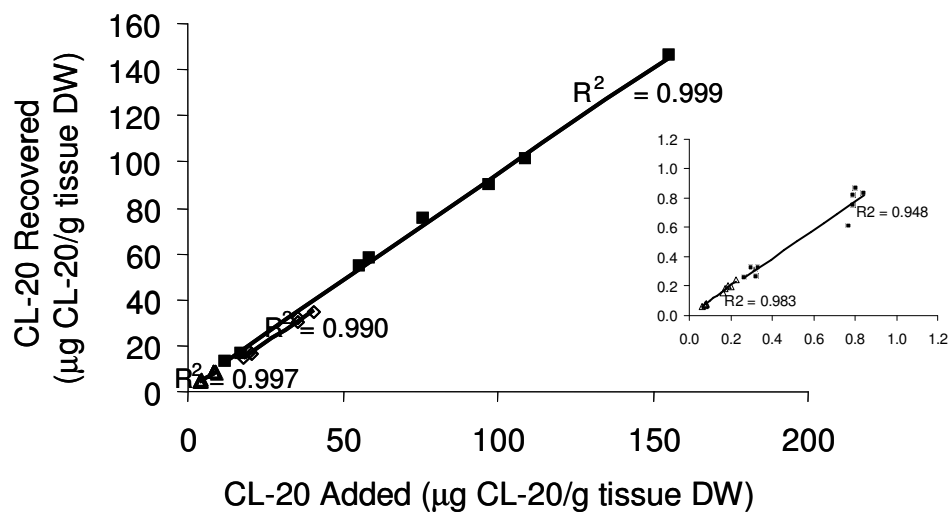


Figure 57 Recovery of CL-20 using spiked tissue samples (△, Brain; ◇, Spleen; ■, Heart) and the modified USEPA Method 8330A (USEPA, 1997). Inset shows CL-20 recovery at spiked concentrations less than 0.8 µg CL-20/g tissue dry weights. R^2 value was determined by linear regression using least-squares method.

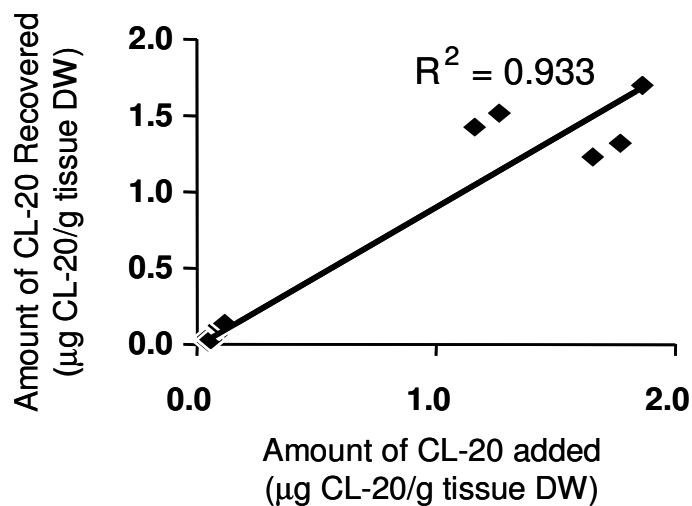


Figure 58 Recovery of CL-20 from spiked liver tissue using modified USEPA Method 8330A (USEPA, 1998).

Discussion

Few acute and subchronic effects were found from oral CL-20 exposures to adult Japanese quail in this study. However, our 42-d subchronic study indicates that CL-20 exposure led to significant decreases in embryo weight without a corresponding effect on developmental stage. This would suggest an effect on energy metabolism rather than a decrease in the rate of embryonic development, *per se*. Although we have evidence that CL20 exposure caused abnormal developmental effects, these results should be considered preliminary until a more rigorous teratological evaluation is done. Bushan *et al.* (2004a, b) reported the formation of nitrite (NO_2^-), nitrous oxide (N_2O), ammonia, formic acid, ammonium or glyoxal from the enzymatic biodegradation of CL-20 by the flavin containing enzymes, nitroreductase and salicylate 1-monooxygenase. Quail have been found to possess both Phase I and II biotransformation enzymes (Gregus *et al.*, 1983). It is possible that quail may possess similar enzymes capable of degrading CL-20, and that the presence of the resulting degradation products may be related to the observed CL-20 toxicity in our present studies. A preliminary survey of the avian toxicity literature failed to identify studies characterizing the toxic effects of the latter CL-20 degradation products to quail. To further characterize the reported effect of embryo malformation by CL-20 and gain more information about the mechanism of CL-20 toxicity (direct and indirect effects of CL-20 on the embryo), *in vitro* approaches are recommended.

Earlier studies have shown that exposure to the monocyclic nitramine explosive RDX causes central nervous system (CNS) disturbances in birds (northern bobwhite), terrestrial salamanders and mammals (rats and miniature swine) (Schneider *et al.*, 1976; Levine *et al.*, 1981; Gogal *et al.*, 2003; Johnson *et al.*, 2004). Rats injected intraperitoneally with 500 mg RDX/kg BW had seizures prior to death. Miniature swine treated intravenously with RDX showed convulsions from 12 to 24 h after exposure. A recent study reported that red-backed salamanders (*Plethodon cinereus*) exposed to 5,000 mg RDX/kg soil in laboratory microcosms for 28 days showed signs of neuromuscular effects, including lethargy, convulsions, rolling and gaping motions, hyperactivity, as well as a marked weight loss (Johnson *et al.*, 2004). In contrast to these earlier studies using RDX, none of the CL-20 treated birds in our present studies exhibited signs of neurotoxicity.

Earlier studies by Gogal *et al.* (2003) showed that RDX in a water vehicle was lethal to the northern bobwhite at a single dose (≥ 187 mg RDX/kg BW) after 72 h exposure. In our subacute study, CL-20 caused no mortality in adult Japanese quail gavaged with up to 5304 mg CL-20/kg BW. These data suggest that CL-20 is not as lethal to galliform species as RDX. Physico-chemical differences between RDX (aqueous solubility at 20°C = 42.58 mg/L, $\log K_{ow}$ = 0.90) and CL-20 (aqueous solubility at 20°C = 3.16 mg/L, $\log K_{ow}$ = 1.92) (Monteil-Rivera *et al.*, 2004) may favor the absorption or bioavailability of RDX relative to CL-20, and may help to explain the differences in acute toxicity. Increased liver to BW ratios were observed in the highest dose group (5304 mg CL-20/kg BW/d), 10 d post CL-20 exposure, whereas the spleen- and heart- to body weight ratios were not significantly altered compared to controls. This effect contrasts with the earlier results showing decreased liver to BW ratios observed for northern bobwhite exposed to RDX in feed (Gogal *et al.*, 2003). Birds exposed to RDX for 14 days caused significant increases in the hematological parameters such as heterophil counts, and the heterophil/lymphocyte ratio, as well as an increase in the packed cell volume (PCV) (Gogal *et*

al., 2003). In contrast, our study using CL-20 did not show an effect of exposure on the heterophil/lymphocyte ratio or on PCV, suggesting that CL-20 is not an immunotoxicant or a mitogen at least during this period of exposure. It is possible that immunological effects may have occurred but were reversed during our exposure schedule that allowed 10-d of no exposure with CL-20.

Conclusion Although CL-20 has certain structural similarities to the monocyclic nitramine RDX (Figure 1), this polycyclic nitramine does not appear to demonstrate the same profile of toxicities as RDX in quail. Our present study has provided basic toxicity data, and suggests that further research should be carried out to study the developmental effects of CL-20 in birds.

XVIII Bioaccumulation of CL-20 in plants and earthworms

XVIII.1 Optimization of bioaccumulation test using ryegrass

Optimization of plant bioaccumulation tests including the determination of: 1) the optimal number of seeds to obtain maximal growth of shoots and roots, 2) the maximal duration of the bioaccumulation test, and 3) the minimal frequency of aeration necessary to maintain optimal growth (every two days, twice a week, once a week) was conducted. Preliminary results indicate that 50 seeds of ryegrass should be sown per 4 inch-pot, plant bioaccumulation test should be done over 42 days, and samples should be taken every week. Based on range-finding and limit tests performed earlier in the project, a first bioaccumulation test using unlabelled CL-20 was initiated in October 2004 with ryegrass seeds exposed to 10, 100, 1000 and 10000 mg CL-20 per kg SSL amended soil.

XVIII.2 Optimization of bioaccumulation test using earthworm *Eisenia andrei*

A first bioaccumulation study using unlabelled CL-20 was initiated with the earthworm *Eisenia andrei* exposed to 10, 25, 50 and 200 mg CL-20 / kg SSL amended soil. Uptake kinetics were monitored for 28 days. Preliminary results presented in Figure 59 indicate that no CL-20 was degraded in the soil exposed to earthworms except at the highest concentration (200 mg/kg soil) where less than 10% was degraded after 7 days of exposure. No detectable CL-20 was bioaccumulated in earthworm tissue, which is consistent with earlier results obtained in our laboratory (Robidoux *et al.*, 2004). Interestingly, exposure to all concentrations of CL-20 rendered their body more rigid. Recently we received [^{14}C]-CL-20 and thus bioaccumulation tests using the radiolabeled substrate will be performed in air-tight transparent desiccators designated as mesocosms.

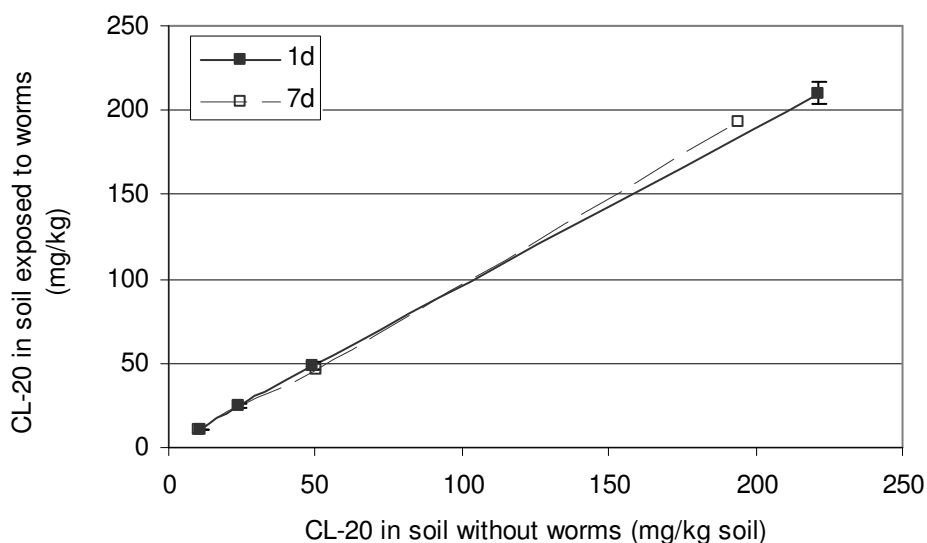


Figure 59 Concentration of CL-20 in soil exposed and not exposed to *Eisenia andrei* (ongoing experiment).

XIX CL-20 metabolic products in plants, earthworms and quail

Part of the work under this task was published in:

1. Dodard S. G., G. I. Sunahara, M. Sarrazin, P. Gong, R.G. Kuperman, G. Ampleman, S. Thiboutot, and J. Hawari (2005). Survival and reproduction of enchytraeid worms (*Oligochaeta*) in different soil types amended with cyclic nitramine explosives. *Environmental Toxicology and Chemistry*. 24(10): 2579-2587
2. Bardai, G, Sunahara, G.I., Spear, P. A., Grosz, S., and Hawari, J (2006) Purification of a cytosolic GST from Japanese quail(*Coturnix coturnix japonica*) capable of biotransforming CL-20 (submitted: *Toxicological Sciences*)

In order to understand the mechanisms of CL-20 toxicity we are conducting experiments to determine degradation products of the energetic chemical in various tissue samples of quail, earthworms and plants.

XIX.1 Toxicity of CL-20 metabolic products on earthworms

The toxic effects of glyoxal and formic acid, two CL-20 products detected under both abiotic and biotic conditions, were measured in freshly amended SSL soil. Toxicity to the earthworm (*Eisenia andrei*) was evaluated using the USEPA earthworm survival test method (1989) at concentrations of 1, 10 and 100 mg/kg dry soil. Our results showed that glyoxal and formic acid were not lethal to *E. andrei* after a 14-d exposure (Table 23).

Table 23 Lethal effects of CL-20, glyoxal and formic acid on earthworm *Eisenia andrei* in freshly amended Sassafras sandy loam (SSL) soil

	CL-20 ¹		Glyoxal ²	Formic acid ²
	(mg / kg)		(mg / kg)	(mg / kg)
Toxicological endpoint	7 d Mortality ³	14 d Mortality ³	14 d Mortality ³	14 d Mortality ³
NOEC	100	10	100	100
LOEC	1000	100	> 100	> 100
LC ₂₀ (95% CI)	490	67	> 100	> 100
LC ₅₀ (95% CI)	> 1000	331	> 100	> 100

¹ Based on measured concentrations. ² Based on nominal concentrations.

³ Based on the number of surviving adult earthworms on days 7 and 14 of the experiment.

XIX.2 Biotransformation of CL-20 in quail liver

Work conducted under this task was submitted in:

Ghalib K. Bardai, Halasz A, Sunahara G I, Dodard S, Spear PA, Grosse S, Hoang J, Hawari J. (2006). *In vitro Degradation of 2,4,6,8,10,12-Hexanitro-2,4,6,8,10,12-Hexaazaisowurtzitane (CL-20) by Cytosolic Enzymes of Japanese Quail and the Rabbit.* (to Environ. Toxicol. Chem, Jan 2006)

Our earlier *in vivo* studies (reported in Section XVII) showed that subacute and subchronic CL-20 exposure to adult quail had no observable effects on these individuals. Analysis of quail plasma and organs (liver, brain, heart and spleen) showed that CL-20 was not present. It is possible that the adult quail may possess an enzymatic mechanism to biotransform CL-20. In the adult quail, the liver is the primary organ for Phases I and II xenobiotic biotransformation reactions (Gregus *et al.*, 1983). CL-20, an electrophilic molecule, is a possible substrate for nucleophilic reactions. Nucleophilic conjugation reactions with thiols, formed via the glutathione S-transferases (GST) enzyme and reduced glutathione (GSH) are well documented (Klaassen, 1996). We hypothesize that the quail liver may contain a GST type enzyme capable of biotransforming CL-20 with glutathione as a required substrate. To test this hypothesis we incubated cytosol (100 K \times g supernatant) from quail liver with CL-20, and found a time-dependent and significant decrease in the quantity of CL-20 *in vitro*. Using two known inhibitors of GST (ethacrynic acid or S-octylglutathione, a glutathione analogue) the biotransformation of CL-20 was significantly inhibited *in vitro*. Furthermore, if liver cytosol is passed through a GSH-Affinity column, and the resulting eluate is incubated with CL-20, we observed that the ability to biotransform CL-20 was lost. Diphenyliodonium (DPI), an inhibitor of flavin-containing enzymes, or carbon monoxide, a cytochrome P450 inhibitor, did not inhibit the biotransformation of CL-20. These preliminary studies indicate that CL-20 can be metabolized by bird liver through a mechanism related to glutathione S-transferase. Studies using purified enzyme preparations and ¹⁴C-labeled CL-20 will be carried out to test this hypothesis.

Abstract

Earlier studies show that exposure of adult quail to 2,4,6,8,10,12-hexanitro-2,4,6,8,10,12-hexaazaisowurtzitane (CL-20) increased liver weights and elevated plasma aspartate aminotransferase activities in treated animals. Analysis of plasma and tissue samples (liver, brain, heart, or spleen) indicated that CL-20 was not detectable in treated animals. We hypothesized that the liver was the organ of toxicity. The present *in vitro* study was then undertaken to determine if the quail liver could biotransform CL-20, using rabbit liver as a comparison. Results indicate that the biotransformation of CL-20 was inhibited by ethacrynic acid (93%), and by the glutathione (GSH) analogue, S-octylglutathione (80%), suggesting the involvement of glutathione S-transferase (GST). Partially purified cytosolic α and μ type GST (requiring presence of GSH as a cofactor) from either quail or rabbit liver was capable of CL-20 biotransformation. The degradation of CL-20 (0.30 ± 0.05 and 0.40 ± 0.02 nmol/min/mg protein for quail and rabbit, respectively) was accompanied with the formation of nitrite and consumption of GSH. Using LC/MS we detected two intermediates with the same deprotonated

molecular mass ion $[M-H]^-$ at 700 Da, suggesting their presence as two isomeric species with the empirical formula $C_{16}H_{24}N_{14}O_{16}S$. Further LC/MS analysis using ring labeled $[^{15}N]$ CL-20 and the nitro group-labeled $[^{15}NO_2]$ CL-20 the $[M-H]^-$ of the two intermediates appeared at 706 and 705 Da, respectively, suggesting that the metabolite (and its isomer) is a GS-monodenitrated CL-20 adduct. We concluded that the in vitro denitration of CL-20 by GST should also be a key initial step in the in vivo biotransformation of the chemical in quail.

Introduction

As we mentioned previously CL-20, an emerging energetic chemical, is a high-density caged polycyclic nitramine compound that is currently being considered for military application. Recently our laboratory (Bardai *et al.*, 2005) investigated the toxic effects of this chemical on the gallinaceous test species, the Japanese quail (*Coturnix coturnix japonica*) and demonstrated that subchronic feeding CL-20 in the diet to adult quail (up to 1085 mg/kg BW for 42 d) increased liver weights and elevated plasma aspartate aminotransferase activities in treated animals, and led to significant developmental effects on embryos. However, no overt toxicological effects were observed in the CL-20 treated birds. This study also reported the absence of CL-20 in quail plasma and other major organs such as liver, brain, heart, and spleen, suggesting that CL-20 might have been in these organs, particularly in liver. The above hypothesis necessitates the identification and purification of possible enzymes capable of CL-20 biotransformation.

The presence of highly oxidized NO_2 groups in CL-20 makes the molecule a potential electrophilic substrate in many nucleophilic reactions (Armstrong, 1997; Eaton and Bammler, 1999). Nucleophilic conjugation reactions with thiols on electrophilic substrates, formed via the glutathione S-transferases (GST) enzyme and glutathione (GSH) are well documented (Chasseaud, 1979; Jakoby, 1978). In the present study, we hypothesized that CL-20 might react with a nucleophile such as glutathione (GSH) in the presence of a GST type enzyme(s) in the liver. In the present study we report the purification of an avian GST from quail liver capable of biotransforming CL-20. Insights into the biotransformation of CL-20 in liver was studied using LC/MS in the presence of uniformly ring labeled $[^{15}N]$ CL-20 and nitro labeled $[^{15}NO_2]$ CL-20. For confirmatory purposes, we also report the purification of GST enzyme from rabbit (*Sylvilagus floridanus*) capable of biotransforming CL-20.

Materials and Methods

Chemicals and reagents. CL-20 in the ϵ -form (purity > 95%), uniformly ring-labeled $[UL-^{14}C]$ CL-20 (96.7% chemical purity, 95.7% radiochemical purity, and specific activity of 294.5 $\mu Ci/mmol$), $[UL-^{15}N]$ CL-20 (87.6% purity) and $[UL-^{15}NO_2]$ CL-20 (99.4% purity) were obtained from ATK Thiokol Propulsion (Brigham City, Utah, USA). Reduced glutathione (GSH), 1-chloro-2,4-dinitrobenzene (CDNB), diphenyliodonium chloride (DPI), allopurinol, ethacrynic acid (EA) and S-octylglutathione (Oct-GSH) were purchased from Sigma Chemicals (Oakville, Ontario, Canada). Carbon monoxide (CO) was purchased from Aldrich Chemical Company (Milwaukee, WI). Sephadex G-25 and GSH-Sepharose affinity columns were obtained from Amersham Pharmacia Biotech (Uppsala, Sweden). All other chemicals and reagents were

the highest grades of purity available and were obtained from Sigma Chemicals. Deionized water was obtained using a Zenopure Mega-90 water purification system. All glassware was washed with phosphate-free detergent, rinsed with acetone, and acid-washed before a final rinse with deionized water.

Enzyme purification. All procedures including FPLC™ (Amersham Pharmacia Biotech, Uppsala, Sweden) were performed at 4°C unless otherwise stated, and according to the method described by Dai *et al.* (1996) with the following modifications. Protein purification columns used in this study were pre-equilibrated in Buffer A (PBS; 140 mM NaCl, 2.7 mM KCl, 10 mM Na₂HPO₄, 1.8 mM KH₂PO₄, pH 7.4) at 4°C. Adult female quails (9 weeks old) and adult rabbits were obtained from a local farm (Ferme Bourgois, Mirabel, PQ, Canada). Animals were sacrificed by decapitation, livers were then removed, washed with ice-cold isotonic saline, and minced (2-mm thickness). Seven quail livers (wet weight 35 g), or rabbit liver (wet weight 40 g) were pooled and rapidly homogenized in 50 ml of phosphate buffered saline (Buffer A) using a Polytron tissue grinder. The homogenate was centrifuged at 10,000g for 30 min, and the supernatant was further centrifuged at 100,000g for 60 min. The 100,000g supernatant (containing cytosol) was filtered through glass wool and used for further purification. A 50-ml aliquot of cytosol was then applied to a Pharmacia XK-50 desalting column. The desalted crude cytosolic fraction was then passed three times through a XK-16 column containing 15 ml of GSH Sepharose at 1 ml/min. Following each pass of crude cytosol, the column was washed extensively with Buffer A, and the bound GST was eluted with 50 mM Tris-HCl (pH 8.0) containing 10 mM GSH. Protein was monitored at 280 nm, and active fractions (those having high CDNB conjugating activity as described below) were collected. The buffer was then exchanged to Buffer A, and the protein was concentrated using Amicon centrifugal filter units (15 ml; 10,000 MW cut off). Aliquots (300 µl) of the above concentrated fractions were applied onto a Sepharose 12 column (previously equilibrated with Buffer A) and eluted with the same buffer at a flow rate of 0.5 ml/min. Active fractions were collected and pooled. Protein concentration was determined with a bicinchoninic acid protein assay kit from Pierce Chemical Company (Rockford, IL) using bovine serum albumin (BSA) as the standard.

Sodium dodecyl sulphate – polyacrylamide gel electrophoresis (SDS-PAGE) and N-terminal sequencing. The SDS-PAGE was performed on 12% gels containing 0.1% SDS (Lammeli, 1970) using a BioRad Mini Protean II electrophoresis system. The loading volume was 10 µl (containing 1 µg protein) per well. Molecular weights were determined from R_f values of standard marker proteins (BioRad Hercules, CA), and protein bands were visualized using a silver stain. Gel analysis was carried out using the Biorad Quantity One Analysis software. The N-terminal microsequencing was performed as described previously (Bhushan *et al.*, 2005a).

Glutathione-S-Transferase (GST) Assay. The GST assays were performed in a microtiter plate reader (Bio-Tek KC4; Bio-Tek® Instruments Inc, Winooski, VT) which measures absorbance (340 nm) in a 96-well microtiter plate. The GST activity was measured with CDNB as the substrate and reduced GSH as the cofactor. Solutions of CDNB (20 mM) dissolved in 95% ethanol, and GSH (20 mM) were prepared fresh daily in a sodium phosphate buffer (100 mM, pH 6.5). The reaction mixture (250 µl) contained: 100 mM sodium phosphate buffer (pH 6.5), 1 mM GSH, and 1 mM CDNB. The ethanolic concentration was less than 5% unless otherwise stated. The increase in absorbance was recorded for 5 min to ensure that the reaction was completed.

The initial linear portion of the response curve (i.e., between 5 and 35 seconds after the initiation of the reaction) was used to determine the rate of product formed. Measurements were taken every 3 sec. Nonenzymatic base catalyzed conjugation of GSH with CDNB was subtracted from all assays, by including a blank (buffer only) consisting of all of the assay components except the active protein. One unit (U) of transferase activity was defined as the formation of one micromole of product (S-2,4-dinitrobenzene-glutathione) per minute, measured at 340 nm using an extinction coefficient of 9.6 mM^{-1} for the conjugate (Habig *et al.*, 1974). Initial-velocity studies of the purified enzyme were performed using the GST assay described above, except that varying concentrations of CDNB (from 0.02 to 5 mM) and GSH (from 0.07 to 5 mM) were used. Apparent enzyme kinetic constants (app. V_{\max} and app. K_m) were calculated according to the Michaelis-Menten equation using the Eadie-Hofstee plot. Specific activities were defined as $\mu\text{mol}/\text{min}/\text{mg}$ protein (U/mg).

CL-20 Biotransformation Assay. Enzyme-catalyzed CL-20 biotransformation assays and inhibition studies were performed under anaerobic (i.e., samples purged with argon for 15 min) or aerobic conditions (air), using 6-ml glass septum-sealed vials with constant agitation in the dark at 37°C for 2 h. Each 1-ml test unit contained: CL-20 (25 μM), enzyme preparation (0.50 mg protein) or cytosol (5 mg protein), reduced glutathione (200 μM) and Buffer A (described above). The CL-20 was used in excess to its water solubility (8.2 μM) to allow detection of trace amounts of intermediate(s). Inhibition studies were assessed by incubating cytosol or pure enzyme preparation, with the following inhibitors: diphenyliodonium chloride (DPI), allopurinol, ethacrynic acid (EA), S-octylglutathione (Oct-GSH), and carbon monoxide (CO). The reaction was stopped by addition of 1 ml acetonitrile, vortexed and placed in the dark at 4°C for 1 h to allow for protein precipitation. The solution was subsequently filtered through a 0.45 μm membrane. The CL-20 concentrations were measured by high-pressure liquid chromatography (HPLC), as described below. Activity of the enzymatic biotransformation of CL-20 was defined as nmole CL-20 per min per mg protein. Controls included: PBS only, GSH only, enzyme preparation (EP) only, EP + GSH, GSH + CL-20, EP + CL-20, and CL-20 with and without NADPH. Other CL-20 biotransformation assays were carried out as described above using [^{14}C]CL-20, [^{15}N]CL-20, [$^{15}\text{NO}_2$]CL-20, to help identify reaction intermediates.

Analytical Procedures. Nitrite and nitrate concentrations were quantified using a reverse polarity capillary electrophoretic method described by Okemgbo *et al.* (1999) and used by Balakrishnan *et al.* (2003). Briefly, an Agilent 3D CE system was fitted with a bare silica bubble capillary (total length 64.5 cm, effective length 56 cm, internal diameter 50 μm). The separation buffer (pH 9.2) contained 25 mM sodium tetraborate and 25 mM hexamethonium bromide. Injections were performed hydrodynamically (25 sec, 50 mbar, injection volume 34 nl). The separation voltage was -30 kV (cathode at inlet). Quantification was obtained by peak area using direct absorbance at 220 nm. Using commercial external standards (Alltech Assoc., Deerfield, IL, USA), the instrumental quantification limit was 0.2 ppm ($N = 10$, peak area 4.5 mAU-s, RSD 3.9%). The GSH was quantified according to Hissin and Hilf (1976). Glyoxal was quantified as previously described (Bhushan *et al.*, 2004b). Analyses of formate (HCOO^-), glycolate ($\text{HOCH}_2\text{COO}^-$) and oxalate were performed by ion chromatography (IC) equipped with a conductivity detector as previously described (Balakrishnan *et al.*, 2004a).

CL-20 was quantified by HPLC-UV as previously described (Bardai *et al.*, 2005). For the determination of [UL-¹⁴C]CL-20 and its biotransformation products, an HPLC system composed of a Waters 717 Plus autosampler, a Model 128 Beckman pump, LCN column (25 cm x 4.6 mm ID, 5 µm particles; Supelco, Bellefonte, PA, USA), a Beckman UV detector (λ =230 nm), and a radioisotope detector (In/Us) were used. The column heater was set to 27°C. The mobile phase consisted of acetonitrile/water (70/30, v/v) delivered at 1.0 ml/min. The sample volume injected was 100 µl with a 50-min run time. Radioactivity counts were performed in a liquid scintillation counter (Tri-Carb 2100TR; Canberra, Concord, Ontario). The [¹⁴C]CL-20 mass balance was calculated by determining the radioactivity collected in eluate fractions (3 ml) for the entire analysis period compared to total [¹⁴C]CL-20 activity.

A Bruker bench-top ion trap mass detector attached to a Hewlett Packard 1100 Series HPLC system equipped with a PDA detector was used to identify reaction intermediates. The samples were injected into a 3-5 µm-pore size Intersil CN capillary column (0.5 mm ID by 150 mm; Alltech, IL) at 25°C. The solvent system was composed of a MeCN/Water gradient (10 % v/v to 70 % v/v) at a flow rate of 12 µl/min. For mass analysis, ionization was performed in a negative electrospray ionization mode ES(-), producing mainly the deprotonated molecular mass ions [M-H]⁻ or adduct mass ions [M+NO₃]⁻ for CL-20 and [M-2H +Na]⁻ for intermediate products. The mass range was scanned from 100 to 800 Da.

Statistical Analysis. Differences between the test and control samples were considered significant at $P \leq 0.05$, using the Student's t-test for unpaired data. Statistical analysis was performed using JMPIN (Version 4, SAS[®] Institute, Cary, NC, USA). The GST kinetic constants (K_m and V_{max}) were determined by Eadie-Hofstee plots, and were compared to the K_m and V_{max} constants generated by the Michelis-Menten equation using Kaleidagraph[®] (Reading, PA).

Accomplishments

Enzyme purification studies. Table 24 shows the CDNB and CL-20 specific activities, distribution and recovery from the purification of hepatic glutathione *S*-transferase for both quail and rabbit. The specific CL-20 biotransformation rate in quail liver increased from 0.006 to 0.017 nmol/min/mg protein, with each successive supernatant fraction (10,000g or 100,000g), while the specific GST activity remained the same. However, for rabbit both the GST activity (10 times quail) and removal rate of CL-20 remained the same in both the 10,000g or 100,000g fractions (Table 24). Furthermore, the amount of CL-20 biotransformed under anaerobic conditions was greater than that under aerobic conditions in the cytosol fractions (Table 25). To identify the possible enzymes capable of CL-20 biotransformation in the cytosol, we tested several nonspecific and specific enzymes inhibitors to enzymes known to biotransform CL-20. Such enzymes include diphenyliodonium chloride (DPI, an inhibitor of flavoenzymes) (Bhushan *et al.*, 2003a), carbon monoxide (a cytochrome P450 inhibitor), allopurinol (a xanthine oxidase inhibitor) (Bhushan *et al.*, 2003b), ethacrynic acid (EA, a GST inhibitor) (Cameron *et al.*, 1995; Poleman *et al.*, 1993; Schultz *et al.*, 1997), and S-octylglutathione (Oct-GSH, a glutathione analogue). Only EA and Oct-GSH was found to cause a significant decrease in the biotransformation of CL-20 in the crude liver cytosol of quail (Table 25) and rabbit (data not shown).

Table 24 Purification of hepatic glutathione S-transferase from quail or rabbit

Purification Step	Total Protein (mg)	Total Activity (U)	GST Specific activity ^a	CL-20 Specific activity ^b	Purification (-fold)	Recovery (%)	Ratio ^c
Quail							
1. Crude Homogenate	6422	1416	0.22	0.004	1.0		52
2. 10,000g supernatant	3845	1060	0.27	0.006	1.5	74	39
3. 100,000g supernatant	1921	508	0.26	0.017	4.3	36	15
4. GST-Affinity Chromatography	12	245	20.5	0.30	75	17	68
Rabbit							
1. Crude Homogenate	10226	26106	2.6	0.008	1.0		325
2. 10,000g supernatant	5378	12611	2.3	0.012	1.5	48	192
3. 100,000g supernatant	3545	10657	3.0	0.014	1.8	41	214
4. GST-Affinity Chromatography	99	3001	30	0.40	50	11.5	75

^a Specific activity measured according to Habig *et al.* (1974), using 1-chloro-2,4-dinitrobenzene (CDNB) as substrate (U/mg protein)

^b Specific activity of CL-20 disappearance (nmol/min/mg protein)

^c Calculated as Specific activity of CDNB (U/mg protein)/Specific activity of CL-20 (nmol/min/mg protein)

Table 25 Effects of enzyme inhibitors and incubation conditions on CL-20 biotransformation activity in quail liver whole cytosol

inhibitor (100 μ M) or Incubation Condition	% CL-20 biotransformed *	% Activity
Anaerobic	37.1 ± 1.3^a	100
Aerobic	19.8 ± 3.2	53
Diphenyliodonium (DPI)	34.4 ± 2.1^{ns}	93
Carbon monoxide (CO)	35.8 ± 1.9^{ns}	96
Ethacrynic acid (EA)	2.5 ± 1.6^b	7
Allopurinol	40.3 ± 1.3^{ns}	108
S-octylglutathione (Oct-GSH)	7.5 ± 0.9^b	20

* Mean \pm SE. (n=3). Hundred percent activities was equivalent to 0.01 nmol CL-20 transformed per mg protein per min. ^a Significantly different from control (Aerobic incubation) at $P \leq 0.05$. ^b Significantly different from control (Anaerobic incubation) at $P \leq 0.05$. ^{ns} denotes no significant difference vs. control (Anaerobic incubation) ($P > 0.05$)

Enzyme identification studies. The SDS-PAGE analysis of the proteins (quail) eluted from the GSH affinity column resolved two bands, which were identified as, QL1 and QL2 (Figure 60, Lane 3) and were estimated to be ~ 27 and ~ 28 kDa, respectively, within the range of the molecular masses reported for avian GSTs (24-30 kDa) (Chang *et al.*, 1990; Hsieh *et al.*, 1999; Yeung and Gidari, 1980). The bands from the rabbit preparation were estimated to be ~ 28 and 29 kDa. Partial N-terminal amino acid sequence analysis of QL1 and QL2 is listed in Table 26. An alignment of the N-terminal amino acid sequence of QL1 with the corresponding chicken and quail class (QL2) μ sequences shows 100% homology for the first 9 amino acids. Alignment of QL2 (class α and μ) with the corresponding chicken sequence, shows 100% homology for the first 12 amino acids, indicating that two different GSTs were retained on the affinity column. This confirms that the enzymes responsible for CL-20 biotransformation are GST type enzymes, and were used for CL-20 biotransformation assays.

Time course of CL-20 biotransformation in vitro. Biotransformation of CL-20 only occurred when CL-20 was incubated in the presence of both the partially purified enzyme and GSH. This reaction was completely inhibited in the presence of ethacrynic acid for quail and rabbit (data not shown) and yielded results that were consistent with those obtained using whole cytosol (Table 25). The incubation of CL-20 with only GSH (i.e., no enzyme added) did not cause biotransformation of CL-20.

Also, no CL-20 biotransformation was observed when CL-20 was incubated with other stronger reducing agents such as β -mercaptoethanol (BME), dithiothreitol (DTT), or NADPH, (data not shown). Time course studies for both quail and rabbit purified GST incubated with CL-20 under aerobic conditions, showed that the disappearance of CL-20 (0.30 ± 0.05 and 0.40 ± 0.02 nmol/min/mg protein for quail and rabbit, respectively) was accompanied by a decrease in GSH (Figure 61) and the formation of nitrite using the quail or rabbit GSTs (Figure 61). The accumulation of nitrate (NO_3^-) was not detected in significant amounts when compared to controls (data not shown).

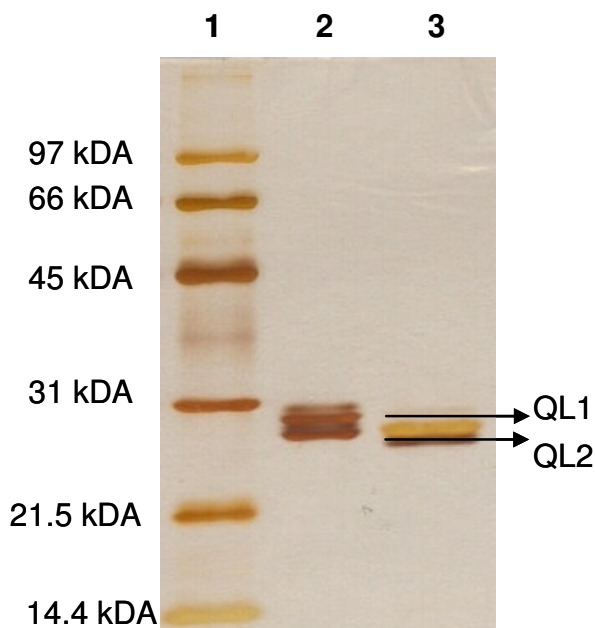


Figure 60 Silver stain of SDS-PAGE purification of quail and rabbit hepatic cytosolic CL-20 degrading enzyme. Lane 1, molecular weight markers from top to bottom (97 kDa Phosphorylase b, 66 kDa Serum albumin, 45 kDa Ovalbumin, 31 kDa anhydase, 21.5 kDa Trypsin, 14.4 kDa Lysozyme); Lane 2, total rabbit proteins eluted from the Glutathione affinity column; Lane 3, total quail proteins (QL1 and QL2) eluted from the Glutathione affinity column.

Carbon Recovery and Metabolite Identification. To determine the carbon recovery of CL-20 biotransformation, we carried out time course studies using [UL- ^{14}C]CL-20. We detected two peaks that eluted with retention times (R_t) of 4 and 5 min (Figure 62). The sum of radioactivity obtained from these peaks and the remaining radioactivity in unreacted CL-20 (27 min), accounted for 100% of original radioactivity in the munition compound (inset Figure 62).

Degradation products of CL-20 were identified by their deprotonated molecular mass ion $[\text{M}-\text{H}]^-$ using LC/MS (ES-). The two peaks, M and M' detected with R_t at 2.5 and 4.9 min, respectively (Figure 63A), showed the same $[\text{M}-\text{H}]^-$ at 699 Da (Figure 63D), each matching a molecular formula of $\text{C}_{16}\text{H}_{24}\text{N}_{14}\text{O}_{16}\text{S}$. Using uniformly ring labeled ^{15}N -[CL-20] and uniformly labeled $^{15}\text{NO}_2$ -[CL-20] the two intermediates M and M' showed their $[\text{M}-\text{H}]^-$ at 705 Da (an increase of 6 amu, Figure 63E) and at 704 Da (an increase of 5 amu, Figure 63F), respectively, suggesting the involvement of six ^{15}N atoms from the ring and five ^{15}N atoms from NO_2 in the formation of each intermediate. Insets 63B and 63C show the UV spectra of both metabolites.

Table 26 N-Terminal Amino Acid Sequences of Glutathione S-Transferases

Transferase	Alignment of N-terminal amino acid sequences	GenBank primary accession number	Reference
Quail GST QL1 (class-mu)	NH ₂ -VVT ¹ LG ² YWD ³ I		This study
Chicken GST (class-mu)	-VVT ¹ LG ² YWD ³ IRGLA ⁴ HA	<u>S18464</u>	(Chang <i>et al.</i> , 1990)
Mouse GST (class-mu 6)	MPV ¹ TLG ² YWD ³ IRGLA ⁴ HA	<u>CAA04060</u>	(DeBruin <i>et al.</i> , 1998)
Quail GST QL2 (class mu)	VVT ¹ LG ² YWD ³ IRGLA ⁴ A		(Dai <i>et al.</i> , 1996)
Quail GST QL2 (class alpha)	NH ₂ -SGK ¹ PRL ² TYLN ³ GR		This study
Chicken GST (class alpha)	-SGK ¹ PRL ² TYVN ³ GRGRMESIR	<u>NP990149</u>	(Hsieh <i>et al.</i> , 1999)

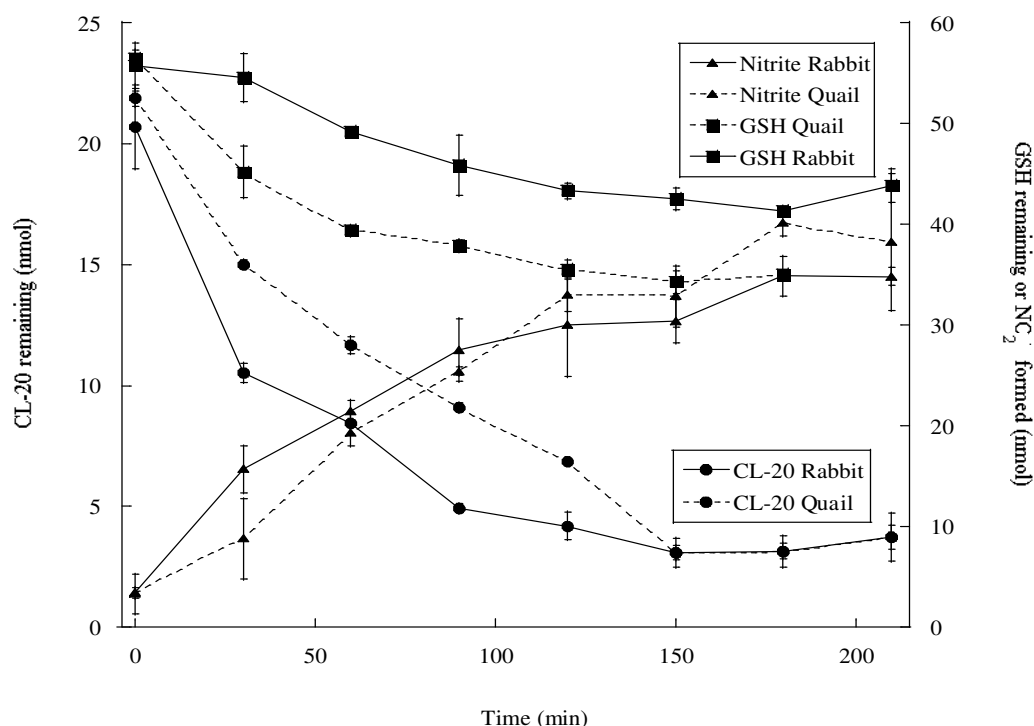


Figure 61 Time course study of enzyme dependent biotransformation of CL-20 under aerobic conditions. Symbols indicate concentration of CL-20 remaining (●), nitrite (▲), or GSH (■). Incubation conditions: 37°C, 2 h under aerobic conditions. Data are the means of triplicates, and error bars represent SE.

We have shown earlier that 15-d subacute and 42-d subchronic treatment of CL-20 to adult quail led to increased liver weights and elevated plasma aspartate transferase activities in treated birds, and significant developmental effects on embryos (Bardai *et al.*, 2005). Despite these effects, CL-20 was not detected in the plasma or in selected organs (brain, spleen, heart, and liver) of CL-20-treated birds. We therefore carried out a series of experiments to test the possibility that CL-20 can be biotransformed *in vitro* using hepatic subcellular fractions and partially purified enzyme preparations taken from untreated birds.

Results of the present studies indicate that GST is involved in the biotransformation of CL-20 *in vitro*. The GST from quail and rabbit liver were isolated from crude cytosol using GSH affinity chromatography (Table 24). The quail GST type enzyme that was eluted from the affinity column (Figure 61) had a specific activity of 20.5 U/mg protein, which is comparable to that of the purified quail GST (24.8 U/mg) described by Dai *et al.* (1996). The rabbit GST type enzyme had a specific activity of 30 μ mol/min/mg protein (Table 24). The similar ratios of CDNB/CL-20 specific activity for crude extract and purified GST for quail (Table 24) show that all of the important CL-20 biotransformation activity was purified from the crude extract.

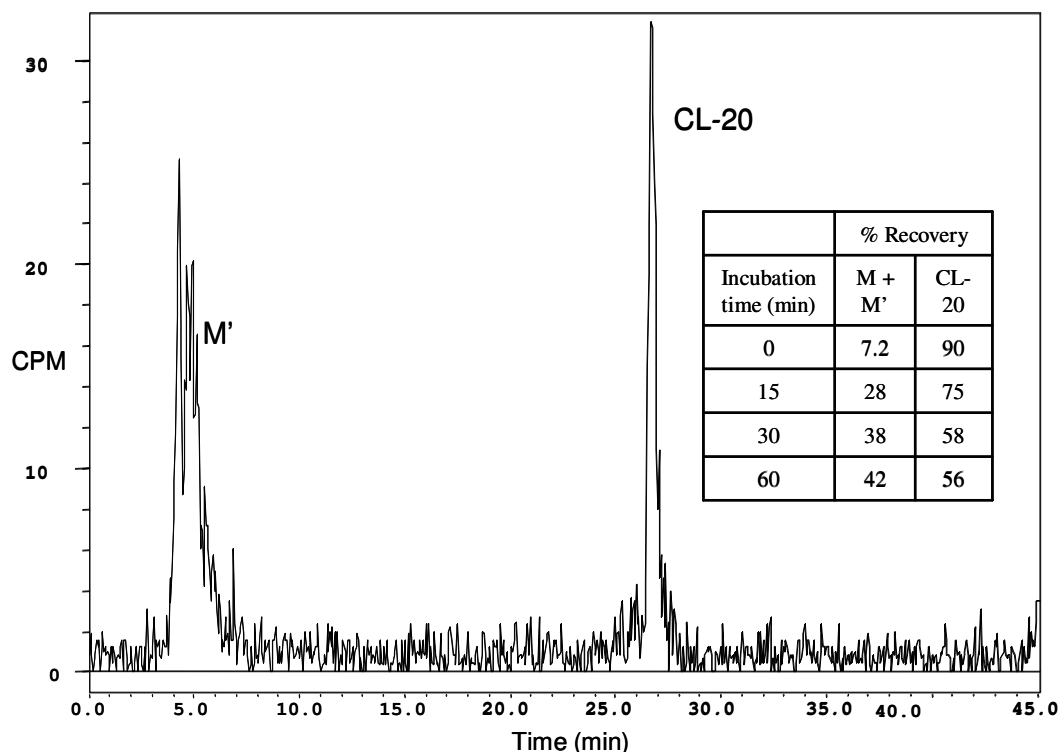


Figure 62 Time course study of enzyme dependent biotransformation of CL-20 under aerobic conditions. Symbols indicate concentration of CL-20 remaining (-●-), nitrite (-▲-), or GSH (-■-). Incubation conditions: 37°C, 2 h under aerobic conditions. Data are the means of triplicates, and error bars represent SE.

When CL-20 was incubated with purified GST in the presence of other stronger reducing agents such as BME, DTT, or NADPH, we found that no CL-20 biotransformation occurred. These results indicate that even though it is a highly oxidized molecule, CL-20 can not be biotransformed by simple reduction without the presence of both enzyme and GSH. The absolute requirement of both GSH and enzyme for the biotransformation of CL-20 offers further evidence that the enzyme responsible for the biotransformation of CL-20 may be a GST enzyme. The diuretic drug ethacrynic acid (EA), an α,β -unsaturated ketone, and the glutathione analogue S-octylglutathione both inhibited the biotransformation of CL-20 (Table 25). Glutathione analogues bearing hydrophobic R groups are effective inhibitors of cytosolic GSTs via simultaneous occupation of the peptide and substrate binding site. For example, Poleman *et al.* (1993) and Cameron *et al.* (1995) reported that EA may bind to the active site of GST when it is used both as a substrate and as a competitive inhibitor of GST.

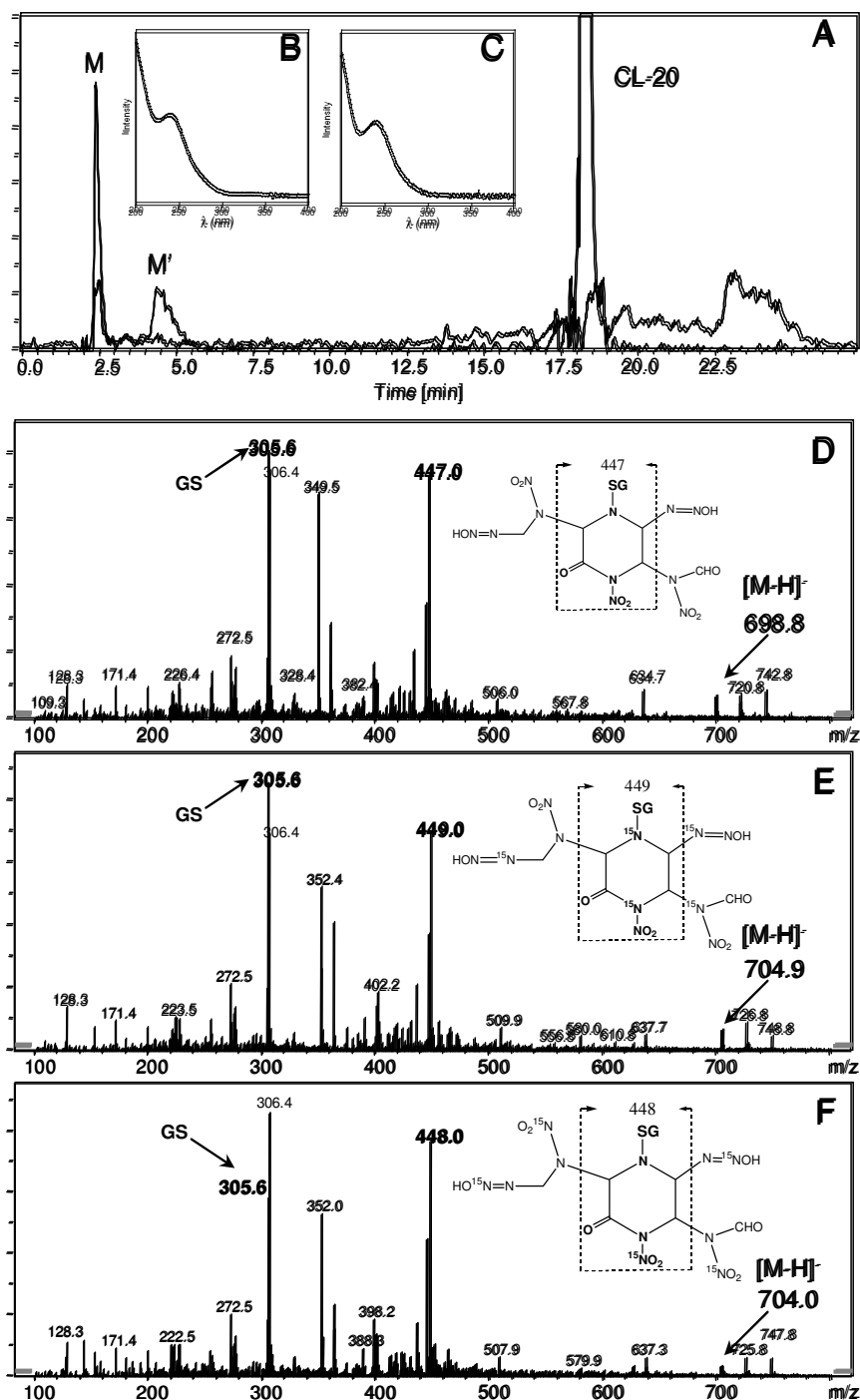


Figure 63 Extracted ion chromatogram of CL-20 and its intermediates M and M' (A) obtained by LC-MS of a mixture of CL-20 incubated for 20 minutes with GSH and cytosolic enzymes of quail. The UV spectrum of M (inset B) and M' (inset C) are indicated. The mass spectrum of M' obtained for intermediate of non labeled CL-20 (D), intermediate of ¹⁵N ring labeled CL-20 (E) and intermediate of ¹⁵NO₂ labeled CL-20 (F).

Thus far only bacterial enzymatic biotransformation of CL-20 under anaerobic conditions has been reported (Bhushan *et al.*, 2003a, 2004a,b, 2005a). In these studies biotransformation is suggested to proceed via initial formation of a CL-20 radical anion by the transfer of an electron from NADH to CL-20 followed by rapid denitration. However, under aerobic conditions molecular oxygen (O₂) quenches the electron from the CL-20 anion radical, converting it back to the parent molecule. In the present study, we found that CL-20 was preferably biotransformed in crude hepatic cytosol under anaerobic conditions (Table 25) whereas the partially purified enzyme biotransformed CL-20 at the same rate under either aerobic or anaerobic conditions. A possible explanation for this observation is that under aerobic conditions, certain cellular oxidases including lipoxygenase, cyclooxygenase, xanthine oxidase, etc. within the liver cytosol may form reactive oxygen species (ROS) or radicals that would normally be removed by the GSH antioxidant system (Matés *et al.*, 2000; Meister and Anderson, 1983). It is thus possible that the amount of GSH available to participate in the biotransformation of CL-20 in crude cytosol under aerobic conditions would be decreased. However, under anaerobic conditions, the rate of ROS formation decreases in the cytosol and amount of GSH available to participate in the biotransformation of CL-20 increases. Therefore, the use of a pure enzyme should not show differences in activity. We observed that the biotransformation of CL-20 using the partially purified enzyme preparation was not affected by ambient conditions (data not shown).

Figure 61 shows that the disappearance of CL-20 is accompanied with the formation of nitrite, suggesting the initial occurrence of denitration. Biotransformation of CL-20 via an initial denitration has been observed in both biotic and abiotic systems (Balakrishnan *et al.*, 2003; Bhushan *et al.*, 2004a). Ogawa *et al.* (1995a, b) demonstrated that the biotransformation of the organic nitrate esters, nitroglycerin and isosorbide dinitrate occurred in rabbit cytosol. These authors also demonstrated that the denitration of these compounds was potentiated by the presence of GSH, and was inhibited by S-alkyl GSH, a glutathione analogue similar to S-octylglutathione used in the present study. Also, we detected glyoxal (data not shown) indicating the occurrence of complete ring cleavage. This is in line with the formation of glyoxal following denitration of CL-20 under both abiotic (Balakrishnan *et al.* 2004a) and biotic conditions (Bhushan *et al.* 2004a, b). The formation of glyoxal may explain the decrease in GST enzyme activity (Fig. 2) because glyoxal can react with amino acids, specifically arginine residues present in proteins (Odani *et al.*, 1998). Recently, Bhushan *et al.* (2004a, b; 2005a) demonstrated that a model flavin containing enzymes and a dehydrogenase can biodegrade CL-20 under anaerobic conditions via initial denitration to eventually produce glyoxal, formic acid, and ammonia.

To determine the biotransformation intermediates of CL-20 we conducted in vitro biotransformation assays using [¹⁴C]CL-20 and [¹⁵N]CL-20. Data indicates that CL-20 was biotransformed into two polar intermediates, as evidenced by the two radioactive peaks obtained with R_t at 4 and 5 min. (Figure 62 and inset). Using LC/MS we also detected two intermediates with the same [M-H]⁻ at 699 Da and a characteristic fragment ion 447 Da, therefore presumed to be isomers of the same empirical formula C₁₆H₂₄N₁₄O₁₆S (Figure 63). Figures 63B and 64C show that the metabolites while having identical masses also show identical UV spectra, offering further evidence that both intermediates may share similar structures and functional groups. When we used the uniformly ring-labeled [¹⁵N]CL-20 the [M-H]⁻ of M and M' were observed at 705, indicating an increase in mass by 6 Da, showing the presence of all six [¹⁵N]-ring atoms in the metabolites. Whereas the characteristic fragment ion, previously shown at 447 Da (Figure

63D) increased to 449 Da, indicating the presence of two ^{15}N -ring atoms in the fragment (Figure 63E). Experiments performed with $[\text{}^{15}\text{NO}_2]\text{CL-20}$ yielded $[\text{M-H}]^-$ products at 704 Da, indicating the incorporation of five $[\text{}^{15}\text{NO}_2]$ in the metabolite. The mass change observed for the fragment ion was 448 Da, an increase of 1, corresponding to the presence of one $^{15}\text{NO}_2$ atom in the fragment (Figure 63F). The involvement of GSH in these intermediates is confirmed by the detection of the mass ion fragment 306, 272, and 128 Da are characteristics of GS involvement (Figure 63D, E and F). The deprotonated mass of GSH (306) and the fragmentation masses of 128 and 272 have been observed in other GSH conjugated products (Dieckhaus *et al.* 2005). The two peaks were thus tentatively identified as a pair of isomers of a product formed after the loss of one nitro group from CL-20 and conjugated with GSH (Figure 64).

Figure 64 shows a proposed pathway of CL-20 biotransformation with a proposed intermediate and the structure of the two possible isomers. The biotransformation of hydrophobic compounds, such as CL-20, into more polar and excretable derivatives is a physiological role of the liver. One of the consequences of biotransformation by the liver is the propensity of a molecule to form a chemically reactive metabolites usually electrophiles. Glutathione conjugation reactions involving GST are typical examples of biotransformation reactions that may lead to the production of chemically reactive metabolites (Armstrong, 1997). Results presented in this article indicate that the quail liver contains GST capable of transforming CL-20 *in vitro* into a CL-20 glutathione conjugate. It is possible that the increase in hepatic liver enzymes and liver weights which we previously observed in CL-20 treated animals (Bardai *et al.*, 2005), could have been as a result of cellular damage of hepatocytes caused by the reactive glutathione CL-20 conjugate.

The conjugated structures proposed in the present article (Figure 64) have reactive functional groups, such as aldehydes and a diazoniumhydroxide moiety (R-N=N-OH) that may react with biological receptors causing damage. For example NHOH containing molecules, although are not completely identical to N=N-OH have been reported to cause embryonic cytotoxicity induced via a free radical mechanism (DeSesso *et al.*, 2000). The embryonic cytotoxicity induced required the presence of a terminal hydroxylamine group for initiation (DeSesso *et al.*, 2000) and may be implicated in the developmental toxicity we previously observed (Bardai *et al.*, 2005). Whether the possible CL-20 metabolic product(s) may lead to adverse health effects in exposed individuals or non-target receptors is not presently known.

In summary, we report the partial purification of avian and mammalian enzymes that are capable of significantly degrading CL-20. The enzyme preparation from quail described in this article contained a mixture of both α and μ type GSTs that showed 100% homology to the first 12 amino acids on similar chicken GST. Biotransformation of CL-20 was accompanied with the release of nitrite and the removal of glutathione as demonstrated by the observation of two key intermediates that were tentatively identified as GS conjugate adducts with denitrated CL-20.

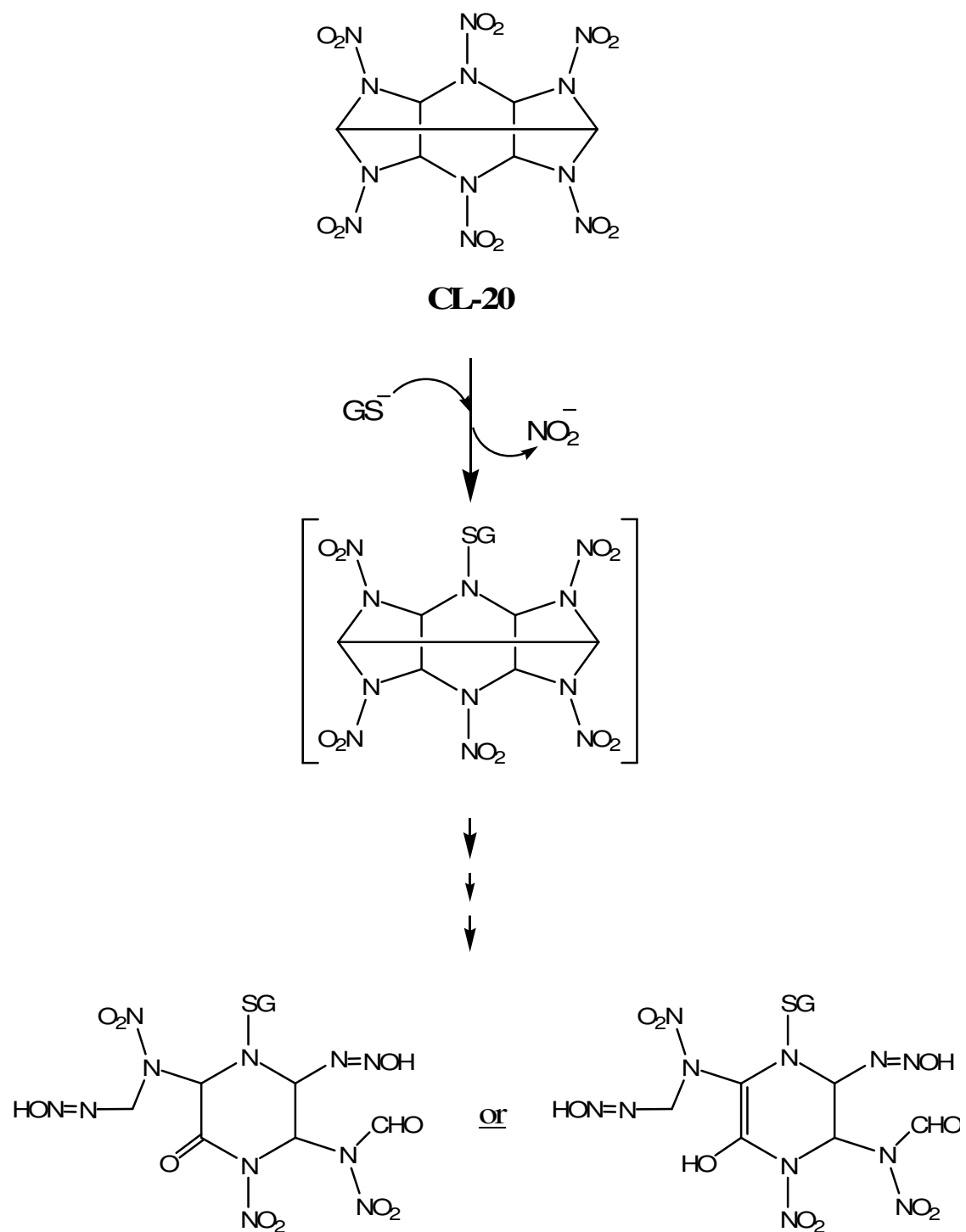


Figure 64 Proposed biotransformation pathway of CL-20 with GSH.

XIX.3 Toxicity and bioaccumulation of CL-20 in ryegrass *Lolium perenne* as compared to RDX and HMX

Research findings in from this task is in the following manuscript.

*Sylvie Rocheleau, Majorie Martel, Geneviève Bush, Roman G. Kuperman, Jalal Hawari, and Geoffrey I. Sunahara. Toxicity and bioaccumulation of CL-20, RDX and HMX in ryegrass *Lolium perenn* (In preparation)*

Abstract

Some studies are available on the toxicity of CL-20 but very few address the bioaccumulation potential of CL-20 to soil organisms. The objectives of this study were to evaluate the toxicity and the bioaccumulation potential of CL-20 as compared to RDX and HMX in perennial ryegrass *Lolium perenne* L. exposed to a Sassafras sandy loam (SSL) soil and a sandy soil (DRDC) containing different clay content (11% and 0.3%, respectively) and using multiple concentrations. In the SSL soil, CL-20 inhibited shoot growth at concentration at and below 960 mg kg⁻¹, stimulated shoot growth at 9604 mg kg⁻¹ and inhibited root growth at 9604 mg kg⁻¹. In DRDC soil, the only significant deleterious effect of CL-20 was established for shoot growth at 9810 mg kg⁻¹ after 42 days of exposure. Greater CL-20 ryegrass tissue concentrations were found when grown in DRDC soil with lower clay content suggests that this sandy soil can sustain greater bioavailability of CL-20, as compared with the SSL soil. At the greater exposure concentrations ranging between 9604 and 10411 mg kg⁻¹, the bioaccumulation factor (BAF) for RDX (0.14) was 7- and 14-times greater than BAFs for HMX (0.02) or CL-20 (0.01), respectively. The greater bioaccumulation of RDX in ryegrass tissue may be due to the greater solubility of this compound as compared to CL-20 and HMX. The BAFs greater than one (1.5, 8.4 and 19.2) for ryegrass exposed to low CL-20 concentrations (9-11 mg kg⁻¹) indicate that CL-20 can bioaccumulate in plants and that CL-20 may potentially biomagnify across the food chain.

Introduction

Hexanitrohexaazaisowurtzitane or CL-20 is a newly developed energetic compound which has enhanced performance in detonation velocity as compared to hexahydro-1,3,5-trinitro-1,3,5-triazine (RDX) and octahydro-1,3,5,7-tetranitro-1,3,5,7-tetrazocine (HMX) (Larson *et al.*, 2002). Information on the environmental impacts of CL-20 is limited. Gong *et al.* (2004) determined that CL-20 has no toxic effect on the bioluminescence of marine bacteria *Vibrio fischeri* (Microtox) and on the cell density of fresh water algae *Selenastrum capricornutum*, up to CL-20 water solubility level (3.2 mg l^{-1}). At concentrations up to $10,000 \text{ mg kg}^{-1}$, Gong *et al.* (2004) also determined that CL-20 had no toxic effect on the activity of soil ammonium oxidizing bacteria, and on growth of alfalfa *Medicago sativa* L. and perennial ryegrass *Lolium perenne* L. in a Sassafras sandy loam soil. Robidoux *et al.* (2004) showed that CL-20 was lethal to earthworm *Eisenia andrei* at concentrations of 91 mg kg^{-1} in Sassafras sandy loam soil (SSL) and had deleterious effect on its reproduction at concentrations of 0.2 and 1.6 mg kg^{-1} in SSL and in forest sandy soil, respectively. Dodard *et al.* (2005) showed that CL-20 amended in three types of soil (SSL, agricultural, and composite agricultural-forest soils) was lethal and inhibited the reproduction of enchytraeid worms (*Enchytraeus crypticus* Westheide & Graefe 1992 and *E. albidus* Hence 1837), with EC_{50} values ranging from 0.1 to 0.7 and 0.08 to 0.62 mg kg^{-1} , respectively. Similar toxicity of CL-20 to *E. crypticus* was reported by Kuperman *et al.* (2006). In Japanese quail (*Coturnix coturnix japonica*) sub-acute and sub-chronic feeding studies, Bardai *et al.* (2005) demonstrated that CL-20 decreased the adult body weight, increased the adult liver weight, plasma sodium and creatin levels, and impacted the embryo development.

The ecotoxicity of RDX and of HMX has been more extensively studied. Bentley *et al.* (1984) determined that HMX was not lethal to the water flea *Daphnia magna* and to the fathead minnow *Pimephales promelas* up to its water solubility (3.3 mg l^{-1}). Bentley *et al.* (1977) also determined that RDX and HMX were toxic to the fish *Lepomis macrochirus*, with $\text{LC}_{50-96\text{h}}$ of 3.6 mg l^{-1} and 0.015 mg l^{-1} , respectively. HMX did not affect the lettuce *Lactuca sativa* L. and barley *Hordeum vulgare* growth at concentrations up to 1866 and 3320 mg kg^{-1} in silica artificial soil and sandy forest soil, respectively (Robidoux *et al.*, 2003). In a comparative study on the toxicity of RDX to fifteen terrestrial plants exposed to concentrations up to $4,000 \text{ mg kg}^{-1}$, Winfield *et al.* (2004) determined that the sunflower *Helianthus annuus* L. was the most sensitive plant exhibiting several adverse developmental effects, while RDX caused only yellow spots on ryegrass *Lolium perenne* L. leaves. RDX or HMX had no adverse effect in freshly amended SSL soil on potworm *E. crypticus* adult survival and juvenile production at concentrations up to 1,194 and $21,750 \text{ mg kg}^{-1}$, respectively (Kuperman *et al.*, 2003). RDX or HMX had no effect on earthworm *Eisenia fetida* adult survival, but respective EC_{20} values of 1.2 and 2.7 mg kg^{-1} for decreased cocoon production were established for exposures in freshly amended SSL soil. Toxicity data to cyclic nitramines by most soil test species reviewed above does not provide information on their bioaccumulation potential in ecological receptors. Such bioaccumulation potential requires investigation to assess ecological risks of food chain transfer of CL-20, RDX, and HMX to higher trophic levels (Major *et al.*, 2002).

The objectives of these studies were to evaluate the toxicity and the bioaccumulation potential of CL-20 as compared to RDX and HMX in perennial ryegrass *L. perenne* exposed to two types of

sandy and sandy loam soils with different bioavailability characteristics using multiple concentrations. Perennial ryegrass was chosen because of its relative sensitivity to EMs, such as 2,4,6-trinitrotoluene (TNT), 1,3,5-trinitrobenzene (TNB), 2,4-dinitrotoluene (2,4-DNT), and 2,6-dinitrotoluene (2,6-DNT), as compared to corn, lettuce, alfalfa, and millet (Rocheleau *et al.*, 2006). Ryegrass has also been extensively used in uptake studies of other energetic compounds (TNT, RDX, and HMX) and other chemicals, such as trifluralin, lindane, ethofumesate, copper and cadmium (Kohler and Branham, 2002; Li *et al.*, 2002; Sidoli O'Connor *et al.*, 2003). Finally, ryegrass is used as turf and foraging grass, therefore making it a relevant ecological receptor.

Materials and Methods

Chemicals and reagents. Energetic materials RDX (CAS: 121-82-4; purity: 99%), and HMX (CAS: 2691-41-0; purity: 99%) were obtained from the Defense Research and Development of Canada (Val Bélair, QC, Canada). CL-20 (CAS: 135285-90-4; purity: 99.3%) was obtained from ATK Thiokol Propulsion (Brigham City, UT). Certified standards of the energetic materials (AccuStandard, Inc., New Haven, CT) were used for HPLC determinations. Boric acid (H_3BO_3 ; CAS: 10043-35-3; purity: 99.9%) was used as the positive control for the phytotoxicity tests. American Society for Testing and Materials (ASTM) type I water (ASTM, 2004) was obtained using the Millipore® Super Q water purification system (Millipore®, Nepean, ON, Canada) and was used throughout the studies. All other chemicals were either analytical or certified grade. Glassware was washed with phosphate-free detergent, followed by rinses with tap water, ASTM type I water, acetone, analytical reagent grade nitric acid 1% (v/v), then with ASTM type I water.

Test Soil. Two types of soil were used to assess the phytotoxicity and the bioaccumulation of EMs. Sassafras Sandy Loam (SSL) was collected from an open grassland field on the property of the U.S. Army Aberdeen Proving Ground (Maryland, USA), and a sandy soil (DRDC) representative of soil found on Canadian army sites was collected at the Defence Research and Development Canada in Val Bélair (Quebec, Canada). These soils were selected because of their relatively high bioavailability of EMs, *i.e.* low organic matter (1.2% in both soils) and relatively low clay contents (11% and 0.3%, respectively). Selected physico-chemical characteristics of the test soils are presented in Table 27. Vegetation and the organic horizon were removed to just below the root zone, and the top 15 cm of the A-horizon was then collected. The SSL and DRDC soils were air-dried, sieved through 5-mm² and 2-mm² mesh screens, respectively, and then stored at room temperature before use in testing. Soil analyses showed that no EM compound was present above analytical detection limits. Total concentrations of metals and nutrients in both soils were within regional background ranges.

Soils were separately and independently amended with CL-20, RDX, or HMX. Individual EMs were dissolved in acetone and transferred evenly across the soil surface, ensuring that the volume of solution added at any one time did not exceed 15% (volume mass⁻¹) of the dry mass soil. The acetone was allowed to volatilize (minimum of 18 h) in a darkened chemical hood, and then mixed overnight (18 ± 2 h) using a three-dimensional rotary mixer. ASTM type I water was added to adjust the soil moisture to a level equivalent to 75% of the water holding capacity (WHC, see Table 27).

Table 27 Selected physico-chemical characteristics of the test soils

Parameters	SSL ¹	DRDC ²
pH	5.5	4.9
Water holding capacity (% v/w)	18	23
Organic matter (% w/w) ³	1.2	1.2
Texture	Sandy loam	Sandy
Sand, 50-2000 µm	71	98
Silt, 2-50 µm	18	1.7
Clay, < 2 µm	11	0.3
K _D for sorption ⁴	2.43 ± 0.04 ⁵	0.84 ± 0.08 ⁶
K _D for desorption ⁴	4.43 ± 0.11 ⁵	0.09 ± 0.29 ⁶

¹ SSL: Sassafras sandy loam soil from Aberdeen Proving Ground, MD, USA.; ² DRDC: sandy soil from Defence Research and Development Canada, Val Bélair, QC, Canada.; ³ values are expressed as % w/w and include organic matter contents.; ⁴ distribution coefficient.; ⁵ values obtained by Balakrishnan *et al.* (2004b).; ⁶ Distribution coefficient determined as described in Balakrishnan *et al.* (2004b).

Plant toxicity tests. The plant toxicity tests were performed following ASTM (1998) and United States Environmental Protection Agency, USEPA (1982) standard protocols. Based on the results of our previous studies (Rocheleau *et al.*, 2006), perennial ryegrass *Lolium perenne* L. “Express” (Pickseed Canada Inc., St-Hyacinthe, Quebec, Canada) was selected for testing because it has relatively high sensitivity to EMs. Nominal treatment concentrations for each EM included 10, 100, 1000, and 10000 mg kg⁻¹. Control treatments included a negative (ASTM type I water), a carrier (acetone), and a positive (boric acid at concentrations of 50, 80, 110, 150 and 200 mg kg⁻¹). All treatments were replicated (n = 3). Ryegrass shoot biomass exposed to RDX or HMX was measured after 19 d. Shoot and root biomass exposed to CL-20 were measured after 21 and 42 d. Roots were separated from soil using a 2-mm sieve, soil was washed away from roots with ASTM type 1 water, and excess water was absorbed with a paper towel. Shoots and roots were kept at -80°C until chemical extraction. Dry mass was determined after lyophilizing the plant tissue for 24 h.

Chemical extractions and analyses. For each soil treatment, triplicates of 2-g soil aliquots were weighed into 50-ml glass centrifuge tubes. Ten ml acetonitrile containing the appropriate recovery standard (2,4-DNT for RDX or HMX extractions; RDX for CL-20 extractions) was

added and the samples were vortexed for 1 min, then sonicated in the dark for 18 ± 2 h at 20°C (modified USEPA Method 8330A; USEPA, 1998). Five ml of supernatant was transferred to a glass tube, to which 5 ml of CaCl_2 solution (5 g l^{-1}) was added. For soil samples amended with CL-20, NaHSO_4 was added to the CaCl_2 solution to prevent CL-20 degradation. Supernatants were filtered through $0.45 \mu\text{m}$ Millex-HV syringe cartridges. Extraction was repeated if internal standard recovery was lower than 90 percent.

Lyophilized plant tissue was grinded and at least 0.02 g was transferred to a glass conical tube, to which a volume of internal standard / acetonitrile solution equivalent to 25 times dry biomass was added. Plant extracts were sonicated in the dark at 20°C for $18 \text{ h} \pm 2 \text{ h}$ and then centrifuged at 1500 rpm ($360 \times g$) for one hour. Supernatants were transferred in glass vials, to which an equivalent volume of ASTM type I water was added and kept at 4°C for 24 h. Supernatants were filtered on $0.45 \mu\text{m}$ cartridges and analyzed by HPLC.

Soil and plant extracts were analyzed using an HPLC (Thermo Separation Products) composed of a pump (Model P4000), an auto injector (Model AS1000) and a photodiode-array detector (Model UV 6000LP). The HPLC operating conditions were as follows: column Supelcosil LC-CN ($25 \text{ cm} \times 4.6 \text{ mm}$, $5 \mu\text{m}$), mobile phase 30% water and 70% methanol, flow rate 1 ml min^{-1} , injection volume of $50 \mu\text{l}$, auto sampler temperature 10°C , wavelength scan from 200 to 350 nm. The limits of quantification were 20, 50 and $100 \mu\text{g l}^{-1}$ for CL-20, RDX and HMX, respectively.

Data analysis. Analysis of Variance (ANOVA) was used to determine the difference between shoot or root biomass of exposed plants as compared to controls, with significance level set at $p \leq 0.05$. Means separations were done using Fisher's Least Significant Difference (LSD) pairwise comparison tests. Data analyses were performed using SYSTAT 7.01 (SPSS, 1997). Bioaccumulation factors (BAFs) were calculated by dividing the EM ryegrass tissue concentration by the EM concentration in soil at the end of the exposure time.

Accomplishments

Effects of CL-20, RDX or HMX on ryegrass growth. The effect of CL-20 on ryegrass shoot and root growth depended on the type of soil and the exposure concentration of CL-20. In SSL soil (Figures 65A and 66A), CL-20 inhibited shoot growth at concentration below 960 mg kg^{-1} (up to 24% inhibition), stimulated shoot growth at 9604 mg kg^{-1} (up to 38% stimulation) and inhibited root growth at 9604 mg kg^{-1} (up to 57% inhibition). In DRDC soil (Figures 65B and 66B), the only significant deleterious effect (21% inhibition, $p < 0.05$) was established for shoot growth at 9810 mg kg^{-1} after 42 days of exposure. In a previous study, CL-20 had a stimulatory effect on shoot growth at concentrations up to 9832 mg kg^{-1} in SSL soil, but this effect was not concentration-dependent after 19 days of exposure (Gong et al., 2004). Stimulation of ryegrass growth was also observed by Strigul et al. (2005) following the exposure of CL-20 in different types of sandy and sandy loam soils.

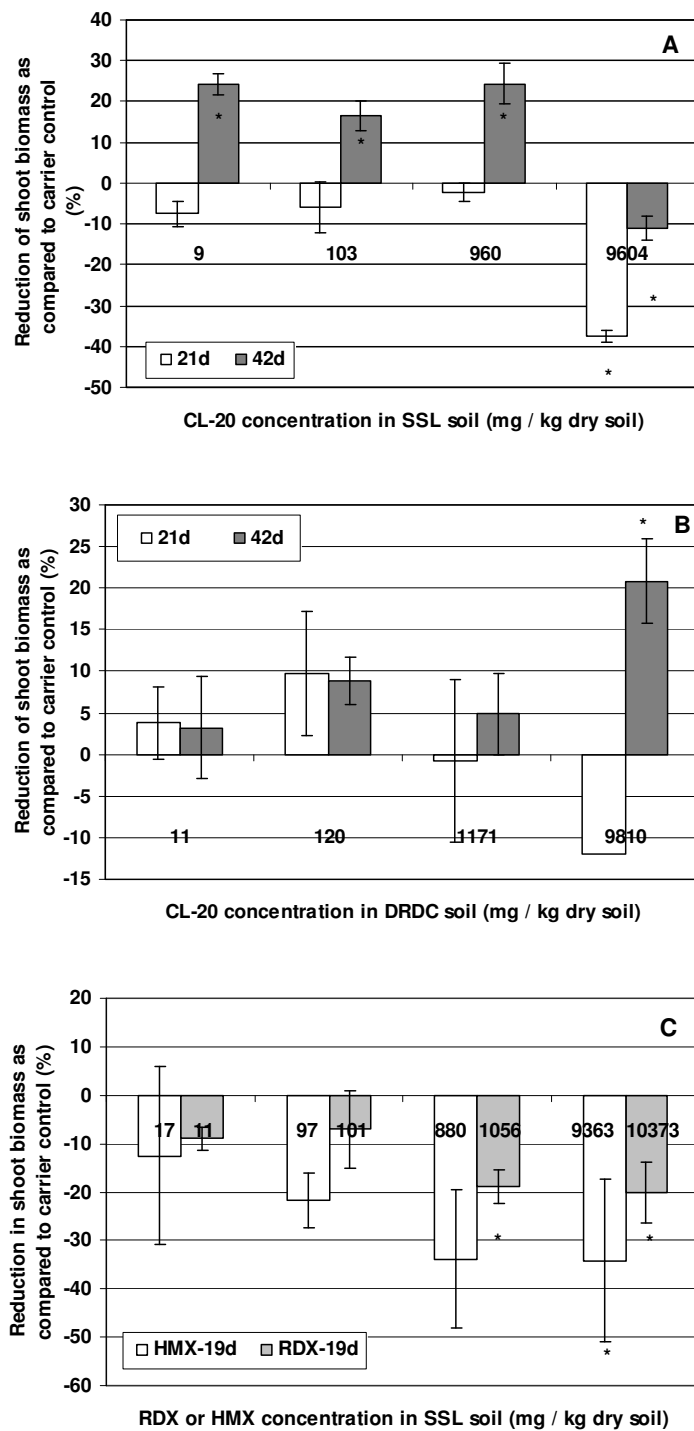


Figure 65 Effects of CL-20 in SSL soil (A), CL-20 in DRDC soil (B), and RDX or HMX in SSL soil (C) on ryegrass *Lolium perenne* shoot growth compared to carrier (acetone) control. Significant ($p \leq 0.05$, Fisher's LSD) change from carrier control is indicated by [*]. Negative values indicate reduction in shoot growth.

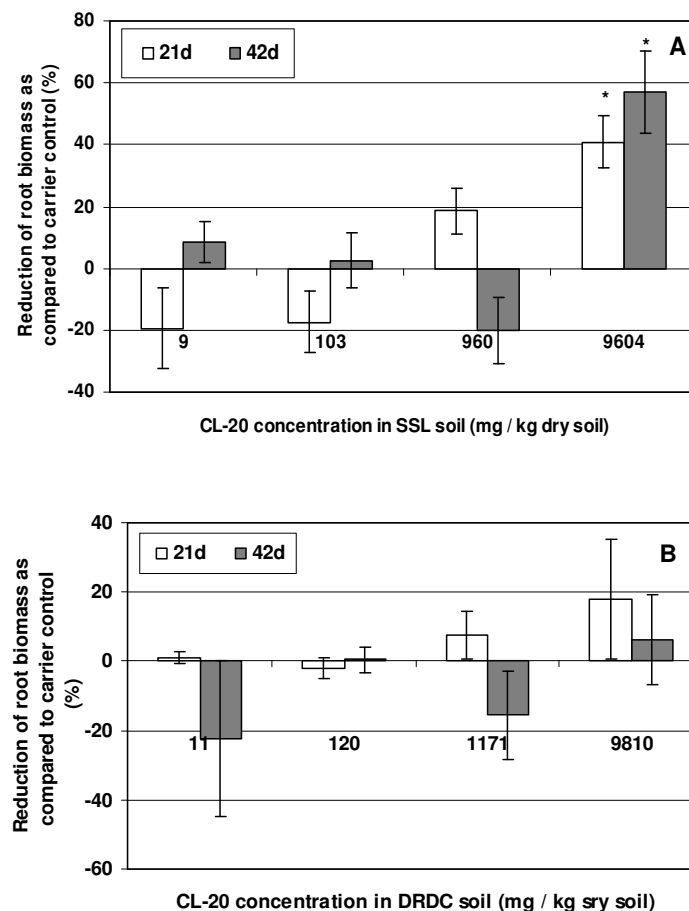


Figure 66 Effects of CL-20 in SSL soil (A) and in DRDC soil (B) on ryegrass *Lolium perenne* root growth compared to carrier (acetone) control. Significant ($p \leq 0.05$, Fisher's LSD) change from carrier control is indicated by [*]. Negative values indicate reduction in shoot growth.

The effect of RDX or HMX on ryegrass growth was assessed in SSL soil (Figure 65C). After 19 days of exposure, RDX or HMX had a stimulatory effect on ryegrass shoots at concentrations ranging from 880 to 9363 mg kg⁻¹ for RDX and at 10373 mg kg⁻¹ for HMX. These results are similar to those obtained with lettuce and barley exposed to HMX in OECD artificial and forest soils at concentrations up to 3,320 mg kg⁻¹ (Robidoux *et al.*, 2003).

Bioaccumulation of CL-20, RDX or HMX in ryegrass. CL-20 concentrations in ryegrass tissue increased with CL-20 concentrations in soil, and remained the same throughout the exposure time at the same concentration (Figures 67 and 68). The only exception was measured in the SSL soil (Figure 67A), where CL-20 ryegrass shoot concentrations decreased significantly with time when exposed to 9604 mg kg⁻¹. The highest CL-20 concentrations (95 µg g⁻¹ in the shoots and 5521 µg g⁻¹ in the roots) were measured when ryegrass was exposed to 9810 mg kg⁻¹ in the DRDC soil (Table 28). In the SSL soil, CL-20 concentrations in the ryegrass shoots were 68 µg

g^{-1} and $1655 \mu\text{g g}^{-1}$ in the roots when exposed to 9604 mg kg^{-1} in soil. In SSL soil, the highest BAFs were calculated when ryegrass was exposed to 8.6 mg kg^{-1} , with BAF values of 1.5 in shoots and 8.4 in roots, respectively (Table 28).

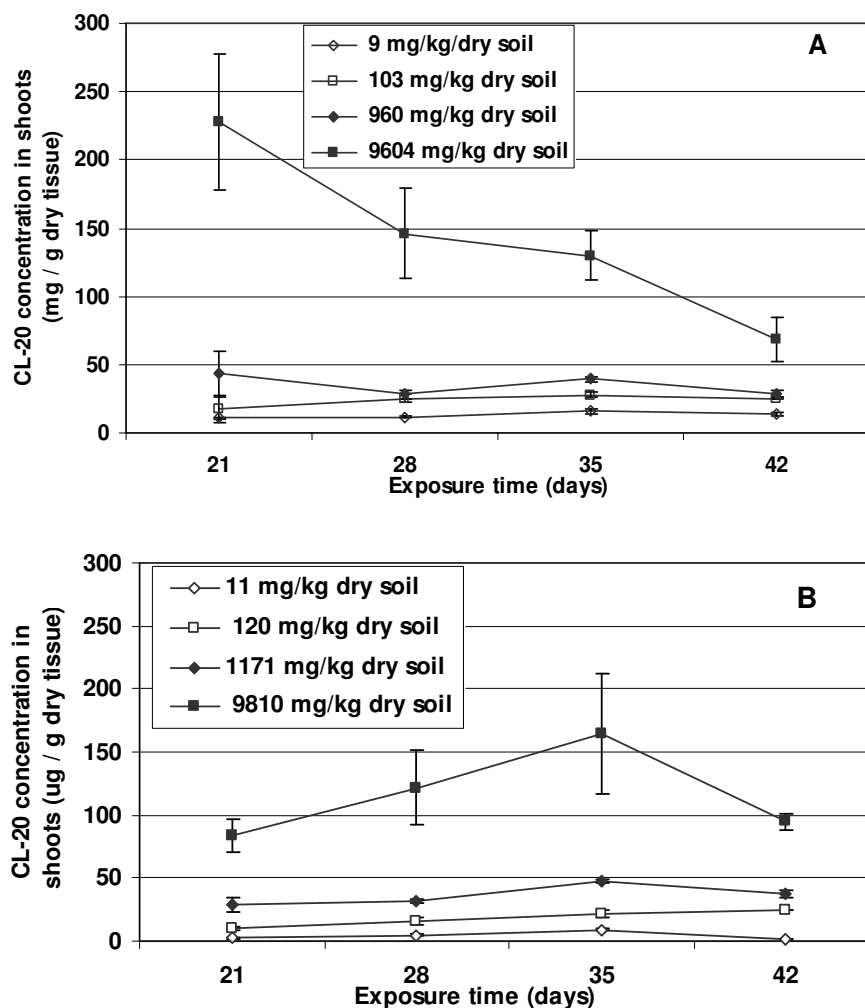


Figure 67 Bioaccumulation of CL-20 in ryegrass *Lolium perenne* shoots exposed to SSL (A) and RDDC (B) amended soils.

In DRDC soil, the highest BAFs were calculated when ryegrass was exposed to 11.2 mg kg^{-1} , with BAF values of 0.5 in shoots and 19.2 in roots, respectively. BAF values decreased with CL-20 exposure concentration in soil, indicating that the bioaccumulation in ryegrass tissue followed a non-linear increase with soil exposure concentration. CL-20 accumulated more in the roots than in the shoots in both soils (58 times in DRDC soil and 24 times in SSL soil). Higher CL-20 ryegrass tissue concentrations when grown in DRDC soil may indicate that this soil presents higher bioavailability characteristics (K_D for sorption in DRDC soil of 0.84 vs K_D for sorption in

SSL soil of 2.43; Table 27) , which may be related to the lower clay content (0.3% in DRDC vs 17% in SSL; Table 27). At median exposure concentrations of 103-120 mg kg⁻¹, CL-20 concentrations were 24-25 µg g⁻¹ in ryegrass shoots and 230-464 µg g⁻¹ in ryegrass roots. These values are comparable to those obtained by Strigul et al. (2005) in a 2-month study addressing the effect of plant growth onto CL-20 degradation in soil (100 mg kg⁻¹), during which they measured concentrations of 12 µg g⁻¹ in ryegrass leaves.

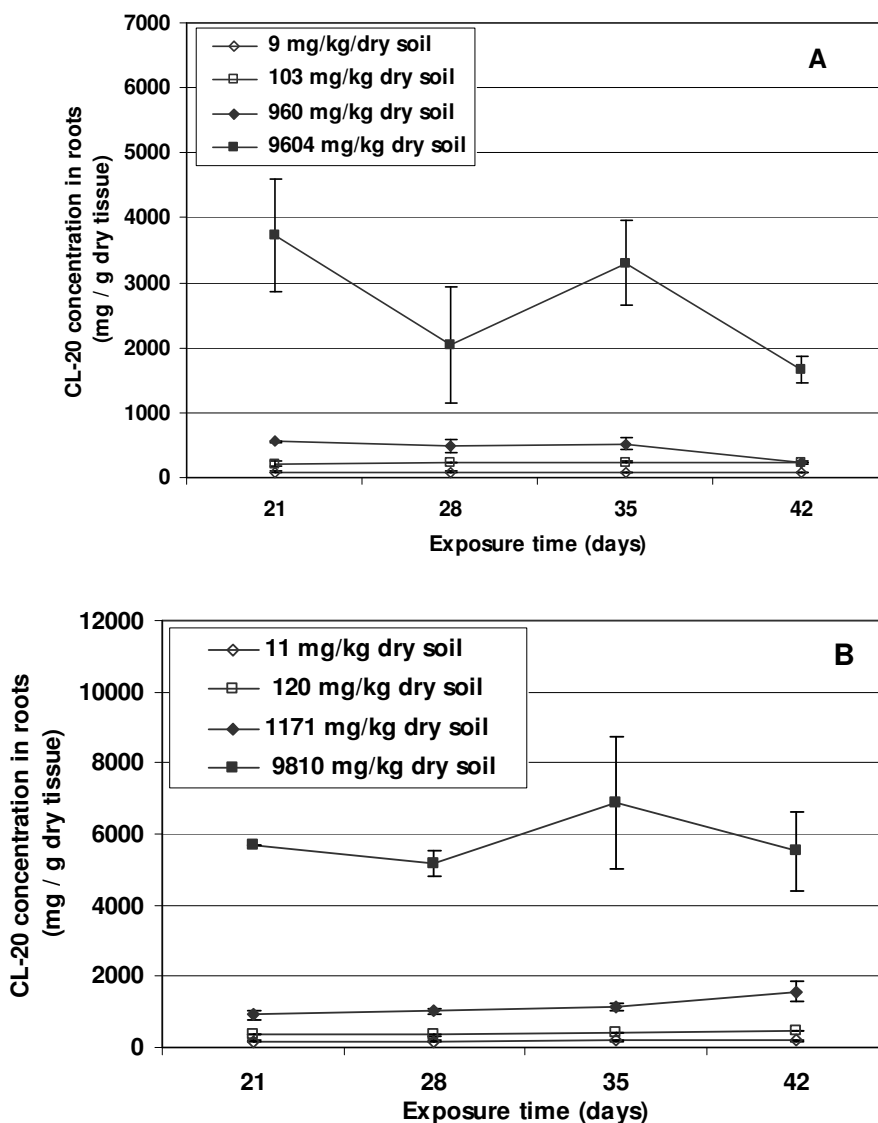


Figure 68 Bioaccumulation of CL-20 in ryegrass *Lolium perenne* roots exposed to SSL (A) and RDDC (B) amended soils.

Table 28 Bioaccumulation factor of CL-20, RDX and HMX in ryegrass *Lolium perenne*

Energetic compound	Soil	Exposure time (days)	Concentration in soil at To ¹ (mg kg ⁻¹ dry soil)	Concentration in soil at Tf ² (mg kg ⁻¹ dry soil)	Concentration in shoots (µg g ⁻¹ dry plant)	Concentration in roots (µg g ⁻¹ dry plant)	BAF ⁴ in shoots	BAF ⁴ in roots
CL-20	SSL	42	8.9 ± 0.2 ³	8.6 ± 0.2	13 ± 1	72 ± 4	1.51	8.37
CL-20	SSL	42	103 ± 13	104 ± 3	25 ± 1	230 ± 8	0.24	2.21
CL-20	SSL	42	960 ± 145	1024 ± 57	28 ± 3	222 ± 29	0.03	0.22
CL-20	SSL	42	9604 ± 1187	9457 ± 129	68 ± 16	1655 ± 202	0.01	0.18
CL-20	DRDC	42	11.2 ± 0.7	9.7 ± 0.3	5 ± 2	186 ± 14	0.52	19.18
CL-20	DRDC	42	120 ± 6	99 ± 3	24 ± 0.3	464 ± 7	0.24	4.69
CL-20	DRDC	42	1171 ± 117	1085 ± 90	38 ± 3	1558 ± 288	0.04	1.44
CL-20	DRDC	42	9810 ± 1052	10312 ± 423	95 ± 7	5521 ± 1107	0.01	0.54
RDX	SSL	19	9740 ± 267	9373 ± 569	1335 ± 218	ND ⁵	0.14	ND
HMX	SSL	19	10411 ± 1398	9064 ± 868	189 ± 19	ND ⁵	0.02	ND

¹ To: Initial concentration; ² Tf: Concentration at the end of the exposure time; ³ Average value with ± standard deviation (n =3); ⁴ BAF: Bioaccumulation factor calculated with Tf concentrations; ⁵ ND: Not determined

At exposure concentrations of 9363 and 10373 mg kg⁻¹ in SSL soil (Table 28), RDX and HMX accumulated 20 times (1335 µg g⁻¹) and 3 times (189 µg g⁻¹) more in ryegrass shoots than CL-20 (68 µg g⁻¹). BAF of RDX (0.14) was 7- and 14-times greater than BAFs in HMX (0.02) and CL-20 (0.01), respectively. This higher bioaccumulation of RDX in ryegrass tissue may be due to the higher solubility of this compound as compared to CL-20. Indeed, the water solubility of RDX, HMX and CL-20 are 43, 3.3 and 3.2 mg l⁻¹ at 20°C, respectively (Monteil-Rivera *et al.*, 2004).

For phytoremediation purposes, Groom *et al.* (2002) compared the bioaccumulation of HMX in fourteen plant species, including ryegrass *Lolium perenne*. Following a 77d-exposure to firing-range soil samples containing between 25 and 51 mg HMX kg⁻¹, the highest concentration of HMX was measured in the canola *Brassica rapa* leaf tissue (677 µg g⁻¹), while HMX concentration in ryegrass *Lolium perenne* leaves was 460 µg g⁻¹, with BAFs ranging between 8.8 and 18.0 in ryegrass tissue. These authors reported that the majority of accumulated HMX was found in the viable leaf tissue, with very low extractable HMX detected in the roots. Using different plant species, Checkai and Simini (1996) measured significant RDX uptake. When exposed to concentrations up to 100 µg l⁻¹ in irrigation water, lettuce leave, corn stover and alfalfa shoot tissue concentrations were 77, 126 and 186 µg l⁻¹, representing BAFs of 0.7, 1.26 and 1.86, respectively. Using 2-week old seedlings and embryos of sunflower *Helianthus annuus*, Winfield (2001) calculated much higher BAFs of 310.8 and 381.5 after 6-weeks of exposure to RDX at concentrations up to 100 mg kg⁻¹ of Grenada soils. Using bush bean *Phaseolus vulgaris*

Burbank exposed to 10 mg RDX kg⁻¹, Cataldo *et al.* (1990) and Harvey *et al.* (1991) reported concentrations of 75, 217 and 603 µg g⁻¹ fresh weight in roots, leaves and seeds, respectively. These studies indicate that RDX and HMX bioaccumulation in plant tissue is dependent of the plant species, and the exposure concentration.

In summary, the effects of CL-20 on ryegrass shoot and root growth depended on the type of soil and the exposure concentration of CL-20. In SSL sandy loam soil, CL-20 inhibited shoot growth at concentration below 960 mg kg⁻¹, and stimulated shoot growth and inhibited root growth at 9604 mg kg⁻¹. In DRDC sandy soil, the only significant deleterious effect of CL-20 was established for shoot growth at 9810 mg kg⁻¹. Stimulatory effect on ryegrass shoot growth was established for RDX at concentrations greater than 880 mg kg⁻¹ and for HMX at 10373 mg kg⁻¹.

CL-20 accumulated more in the roots than in the shoots, and accumulated more in the DRDC soil than in the SSL soil. Higher CL-20 ryegrass tissue concentrations when grown in DRDC soil with lower (0.3%) clay content suggests that this sandy soil can sustain greater bioavailability of CL-20, as compared with the SSL soil (11% clay). At the highest exposure concentration ranging between 9604 and 10411 mg kg⁻¹, BAF of RDX (0.14) was 7- and 14-times greater than BAFs in HMX (0.02) and CL-20 (0.01), respectively. This higher bioaccumulation of RDX in ryegrass tissue may be due to the higher solubility of this compound as compared to CL-20. BAFs of 0.5-1.5 and 8.4-19.2 in ryegrass shoots and roots exposed to 9-11 mg kg⁻¹ indicates that CL-20 may bioaccumulate in plants exposed to low concentrations of CL-20 and that CL-20 may have some potential of biomagnification across the food chain. Additional studies concurrently using several trophic levels (plants - invertebrates – mammals – birds) may be needed to confirm this potential of biomagnification of CL-20.

XX Action item

“In your Final Report, you may want to do a mass balance of CL-20 both comparatively and actually with respect to glyoxal.”

Following the reception of uniformly [^{14}C]-labeled, ring [^{15}N]-labeled and [$^{15}\text{NO}_2$]-labeled CL-20 we were first able to confirm the identity of several intermediate degradation products and second to determine the C and N mass balances of CL-20 transformations in several abiotic and biotic systems. Results are included in the following Chapters (VIII, page 31; IX, page 46; XII.1, page 81; XIV.1, page 116; and XIV.2, page 132).

XXI Acknowledgements

We would like to thank SERDP for funding, Thiokol personnel for providing the CL-20 and [^{15}N]-CL-20 samples, and for their interest. Also we would like to thank the following individuals for their excellent technical skills: Louise Paquet, BSc Chemistry; Chantale Beaulieu, BSc Chemistry; Stéphane Deschamps, BSc Biochemistry; Alain Corriveau, DEC Biology & Chemistry and France Dumas for the N-terminal analysis.. Finally, we would like to thank the project coordinators and the project managers Dr. Robin Nissan, Dr. Andrea Leeson and Dr. B. Holst.

XXII References

- Aliverti A, Curti B, Vanoni MA. **1999**. Identifying and quantifying FAD and FMN in simple and in iron-sulfur-containing flavoproteins. p. 9-23. In S. K. Chapman, and G. A. Reid (ed.), *Flavoprotein protocols: Methods in molecular biology*, vol. 131. Humana Press, Totowa, NJ.
- Alowitz MJ, Scherer MM. **2002**. Kinetics of nitrate, nitrite, and Cr(VI) reduction by iron metal. *Environ. Sci. Technol.* 36: 299-306.
- Anusevicius Z, Sarlauskas J, Nivinskas H, Segura-Aguilar J, Cenas N. **1998**. DT-diaphorase catalyzes N-denitration and redox cycling of tetryl. *FEBS Lett.* 436: 144-148.
- Arese M, Zumft WG, Cutruzzola F. **2003**. Expression of a fully functional *cd₁* nitrite reductase from *Pseudomonas aeruginosa* in *Pseudomonas stutzeri*. *Protein Expr. Purif.* 27:42-48.
- Armstrong, RN. **1997**. Structure, catalytic mechanism, and evolution of the glutathione transferases. *Chem. Res. Toxicol.* 10: 2-18.
- ASTM **1997**. Standard Practice for Conducting Subacute Dietary Toxicity Tests with Avian Species. American Society for Testing and Materials, West Conshohocken, PA, E857-05.
- ASTM **1998**. Standard guide for conducting terrestrial plant toxicity tests. American Society for Testing and Materials, West Conshohocken, PA, E1963-98.
- ASTM **2004**. Standard specification for reagent water. American Society for Testing and Materials, ASTM D 1193-99e1, In: Book of ASTM Standards, Vol. 11.01. Philadelphia, PA, USA, ASTM International: 116-118.
- Balakrishnan VK, Halasz A, Hawari J. **2003**. Alkaline hydrolysis of the cyclic nitramine explosives RDX, HMX, and CL-20: new insights into degradation pathways obtained by the observation of novel intermediates. *Environ. Sci. Technol.* 37: 1838-1843.
- Balakrishnan VK, Monteil-Rivera F, Halasz A, Corbeau A, Hawari J. **2004a**. Decomposition of the polycyclic nitramine explosive, CL-20, by Fe⁰. *Environ. Sci. Technol.* 38: 6861-6866.
- Balakrishnan VK, Monteil-Rivera F, Gautier MA, Hawari J. **2004b**. Sorption and Stability of the Polycyclic Nitramine Explosive CL-20 in Soil. *J. Environ. Qual.* 33: 1362-1368.
- Bao M, Pantani F, Griffini O, Burrini D, Santianni D, Barbieri K. **1998**. Determination of carbonyl compounds in water by derivatization-solid-phase microextraction and gas chromatographic analysis. *J. Chromatogr. A* 809: 75-87.
- Bardai G, Sunahara GI, Spear PA, Martel M., Gong P, Hawari, J. **2005**. Effects of dietary administration of CL-20 on Japanese quail *Coturnix coturnix japonica*. *Arch. Environ. Contamin. Toxicol.* 49: 215-222.
- Beck W. **1994**. In *Applications of the HP 3D Capillary Electrophoresis System*, Volume 1; Heiger, D.N., Herold, M., Grimm, R., Eds.; Hewlett Packard Company: Waldbronn, Germany, p 53.
- Behrens R Jr., Bulusu S. **1991**. Thermal decomposition of energetic materials. 2. Deuterium isotopic effects and isotopic scrambling in condensed-phase decomposition of octahydro-1,3,5,7-tetranitro-1,3,5,7-tetrazocine. *J. Phys. Chem.* 95:5838-5845.
- Bentley RE, Dean JW, Ells SJ, Hollister A, LeBlanc GA, Sauter S, Sleight BH. **1977**. Laboratory evaluation of the toxicity of cyclotrimethylene (RDX) to aquatic organisms. U.S. Army Medical Research Development Command, Frederick, MD, Index 79(7) US NTIS AD-A061 730, p 86.
- Bentley RE, Petrocelli SR, Suprenant DC. **1984**. Determination of the toxicity to aquatic organisms of HMX and related wastewater constituents. Part III. Toxicity of HMX, TAX and

- SEX to aquatic organisms. Springborn Bionomics, Wareham, MA, USA., AD-A172 385.
- Bhushan B, Halasz A, Spain JC, Hawari J. **2002**. Diaphorase catalyzed biotransformation of RDX via N-denitration mechanism. *Biochem. Biophys. Res. Commun.* 296: 779-784.
- Bhushan B, Paquet L, Spain JC, Hawari J. **2003a**. Biotransformation of 2,4,6,8,10,12-hexanitro-2,4,6,8,10,12-hexaazaisowurtzitane (CL-20) by denitrifying *Pseudomonas* sp. strain FA1. *Appl. Environ. Microbiol.* 69: 5216-5221.
- Bhushan, B., L. Paquet, A. Halasz, J. C. Spain, and J. Hawari. **2003b**. Mechanism of xanthine oxidase catalyzed biotransformation of HMX under anaerobic conditions. *Biochem. Biophys. Res. Commun.* 306: 509-515.
- Bhushan B, Trott S, Spain JC, Halasz A, Paquet L, Hawari J. **2003c**. Biotransformation of hexahydro-1,3,5-trinitro-1,3,5-triazine (RDX) by a rabbit liver cytochrome P450: Insight into the mechanism of RDX biodegradation by *Rhodococcus* sp. DN22. *Appl. Environ. Microbiol.* 69: 1347-1351.
- Bhushan B, Halasz A, Hawari J. **2004a**. Nitroreductase catalyzed biotransformation of CL-20. *Biochem. Biophys. Res. Commun.* 322: 271-276
- Bhushan B, Halasz A, Spain JC, Hawari J. **2004b**. Initial reaction(s) in biotransformation of CL-20 is catalyzed by salicylate 1-monooxygenase from *Pseudomonas* sp. strain ATCC 29352. *Appl. Environ. Microbiol.* 70: 4040-4047.
- Bhushan B, Halasz A, Thiboutot S, Ampleman G, Hawari J. **2004c**. Chemotaxis-mediated biodegradation of cyclic nitramine explosives RDX, HMX and CL-20 by *Clostridium* sp. EDB2. *Biochem. Biophys. Res. Commun.* 316: 816-821.
- Bhushan B, Halasz A, Hawari J. **2005a**. Biotransformation of CL-20 by a dehydrogenase enzyme from *Clostridium* sp. EDB2. *Appl. Microbiol. Biotechnol.* 69: 448-455.
- Bhushan B, Halasz A, Hawari J. **2005b**. Stereo-specificity for pro-(R) hydrogen of NAD(P)H during enzyme-catalyzed hydride transfer to CL-20. *Biochem. Biophys. Res. Commun.* 337: 1080-1083.
- Bose P, Glaze WH, Maddox S. **1998**. Degradation of RDX by various advanced oxidation processes: II. organic by-products. *Wat. Res.* 32:1005-1018.
- Boyd SA, Sheng G, Teppen BJ, Johnston CT. **2001**. Mechanisms for the adsorption of substituted nitrobenzenes by smectite clays. *Environ. Sci. Technol.* 35:4227-4234.
- Brannon JM, Price CB, Hayes C, Yost, SL. **2002**. Aquifer soil cation substitution and adsorption of TNT, RDX, and HMX. *Soil Sediment Contam.* 11: 327-338.
- Brindley GW. **1981**. Structures and chemical compositions of clay minerals. p. 1-21. In Longstaffe, F.J. Ed. *Short course in clays and the resource geologist*. Mineralogical Association of Canada: Edmonton, Canada.
- Bulusu S, Axenrod T, Milne GWA. **1970**. Electron-impact fragmentation of some secondary aliphatic nitramines. Migration of the nitro group in heterocyclic nitramines. *Org. Mass Spectrometry* 3:13-21.
- Buncel, E, Dust, JM. **2003**. p 8. In *Carbanion Chemistry – Structures and Mechanisms*, Oxford University Press, Inc.: New York, NY.
- Cameron AD, Sinning I, L'Hermite G, Olin B, Board PG, Mannervik B, Jones JA. **1995**. Structural analysis of human alpha-class glutathione transferase in the apo-form and in complexes with ethacrynic acid and its glutathione conjugate. *Structure* 3: 717-727.
- Canadian Council on Animal Care Guidelines **1984**. Japanese Quail. In: Guide to the Care and Use of Experimental Animals.

http://www.ccac.ca/english/gui_pol/guides/english/TOC_V2.HTM

- Capellos C, Papagiannakopoulos P, Liang Y-L. **1989**. The 248 nm photodecomposition of hexahydro-1,3,5-trinitro-1,3,5-triazine. *Chem. Phys. Lett.*, 164:533-538.
- Cataldo DA, Harvey SD, Fellows RJ. **1990**. An evaluation of the environmental fate and behavior of munitions material (TNT, RDX) in soil and plant systems. U.S. Army Biomedical Research and Development Laboratory, Frederick, MD, 88PP8853.
- Chakraborty S, Massey V. **2002**. Reaction of reduced flavins and flavoproteins with diphenyliodonium chloride. *J. Biol. Chem.* 277: 41507-41516.
- Chang LH, Chuang LF, Tsai CP, Tu CPD, Tam MF. **1990**. Characterization of glutathione S-transferases from day-old chick livers. *Biochem.* 29: 744-750.
- Charlet L, Silvester E, Liger E. **1998**. N-compound reduction and actinide immobilization in surficial fluids by Fe(II): the surface $\equiv\text{Fe}^{\text{III}}\text{OFe}^{\text{II}}\text{OH}^\circ$ species, as major reductant. *Chem. Geol.* 151: 85-93.
- Chasseaud LF. **1979**. The role of glutathione and glutathione S-transferases in the metabolism of chemical carcinogens and other electrophilic agents. *Adv. Cancer Res.* 29: 175-274.
- Checkai RT, Simini M. **1996**. Plant uptake of RDX and TNT utilizing site specific criteria for the Cornhusker Army Ammunition Plant (CAAP), Nebraska. U.S. Army ERDEC Technical report. Edgewood Research Development and Engineering Center, Aberdeen Proving Ground, MD, Project No. 56786M8AA.
- Childers SE, Ciufo S, Lovley DR. **2002**. *Geobacter metallireducens* accesses insoluble Fe(III) oxide by chemotaxis. *Nature* 416: 767-769.
- Collado R, Schmelz RM, Moser T, Römbke J. **1999**. Sublethal responses of two *Enchytraeus* species (Oligochaeta) to toxic chemicals. *Pedobiologia* 43: 625-629.
- Comfort SD, Shea PJ, Machacek TA, Satapanajaru T. **2003**. Pilot-scale treatment of RDX-contaminated soil with zerovalent iron. *J. Environ. Qual.* 32: 1717-1725.
- Dai HQ, Edens FW, Roe MR. **1996**. Glutathione S-transferase in the Japanese quail: tissue distribution and purification of the liver isozymes. *J. Biochem. Toxicol.* 11: 85-96.
- DeBruin WC, Te Morsche RH, Wagenmans MJ, Alferink JC, Townsend AJ, Wieringa B, Peters WH. **1998**. Identification of a novel murine glutathione S-transferase class mu gene. *Biochem. J.* 330: 623-626.
- DeSesso JM, Jacobson CF, Scialli AR, Goeringer GC. **2000**. Hydroxylamine moiety of developmental toxicants is associated with early cell death: A structure-activity analysis. *Teratology* 62: 346-355.
- Dieckhaus CM, Fernandez-Metzler CL, King R, Krolkowski PH, Baillie TA. **2005**. Negative ion tandem mass spectrometry for the detection of glutathione conjugates. *Chem. Res. Toxicol.* 18: 630-638.
- Dodard SG, Renoux AY, Powlowski J, Sunahara GI. **2003**. Lethal and subchronic effects of 2,4,6-trinitrotoluene (TNT) on *Enchytraeus albidus* in spiked artificial soil. *Ecotoxicol. Environ. Safety.* 54: 131-138.
- Dodard SG, Powlowski J, Sunahara GI. **2004**. Biotransformation of 2,4,6-trinitrotoluene (TNT) by enchytraeids (*Enchytraeus albidus*) in vivo and in vitro. *Environ. Pollut.* 131: 263-273.
- Dodard SG, Sunahara GI, Kuperman RG, Sarrazin M, Gong P, Ampleman G, Thiboutot S, Hawari, J., **2005**. Survival and reproduction of enchytraeid worms, oligochaeta, in different soil types amended with energetic cyclic nitamines. *Environ. Toxicol. Chem.* 24: 2579-2587.

- Druckrey, H. **1973**. Specific carcinogenic and teratogenic effects of ‘indirect’ alkylating methyl and ethyl compounds, and their dependency on stages of ontogenic development. *Xenobiotica* 3: 271-303.
- Dubé P, Ampleman G, Thiboutot S, Gagnon A, Marois A. **1999**. Report DREV –TR-1999-13. Defence Research Establishment Valcartier. Department of National Defence Canada.
- Eaton DL, Bammler TK. **1999**. Concise review of the glutathione S transferases and their significance to toxicology. *Toxicol. Sci.* 49: 156-164.
- Forte E, Urbani A, Saraste M, Sarti P, Brunori M, Giuffrè A. **2001**. The cytochrome *cbb₃* from *Pseudomonas stutzeri* displays nitric oxide reductase activity. *Eur. J. Biochem.* 268:6486-6490.
- Fournier D, Halasz A, Spain JC, Fiurasek P, Hawari J. **2002**. Determination of key metabolites during biodegradation of hexahydro-1,3,5-trinitro-1,3,5-triazine (RDX) with *Rhodococcus* sp. strain DN22. *Appl. Environ. Microbiol.* 68: 166-172.
- Fournier D, Halasz A, Thiboutot S, Ampleman G, Manno D, Hawari J. **2004a**. Biodegradation of octahydro-1,3,5,7-tetranitro-1,3,5,7-tetrazocine (HMX) by *Phanerochaete chrysosporium*: new insight into the degradation pathway. *Environ. Sci. Technol.* 38: 4130-4133.
- Fournier D, Halasz A, Spain JC, Spanggord RJ, Bottaro JC, Hawari J. **2004b**. Biodegradation of the hexahydro-1,3,5-trinitro-1,3,5-triazine ring cleavage product 4-nitro-2,4-diazabutanal (NDAB) by *Phanerochaete chrysosporium*. *Appl. Environ. Microbiol.* 70:1123-1128.
- Fournier D, Monteil-Rivera F, Halasz A, Bhatt M, Hawari J. **2005**. Degradation of CL-20 by white-rot fungi, *Chemosphere*, In Press
- Ganzhorn AJ, Plapp BV. **1988**. Carboxyl groups near the active site zinc contribute to catalysis in yeast alcohol dehydrogenase. *J. Biol. Chem.* 263: 5446-5454.
- Geetha M, Nair UR, Sarwade DB, Gore GM, Asthana SN, Singh H. **2003**. Studies on CL-20: The most powerful high energy material. *J. Therm. Anal. Calorim.* 73: 913-922.
- Gerhardt P. **1981**. Manual of methods for general bacteriology, American society for Microbiology, Washington, DC.
- Giles J. **2004**. Green explosives: collateral damage. *Nature* 427: 580-581.
- Gogal RM, Johnson MS, Larsen CT, Prater MR, Duncan RB, Ward DL, Lee RB, Salice CJ, Jortner B, Holladay SD. **2003**. Dietary oral exposure to 1,3,5-trinitro-1,3,5-triazine in the northern bobwhite (*Colinus virginianus*). *Environ. Toxicol. Chem.* 22: 381-387
- Gong P, Hawari J, Thiboutot S, Ampleman G, Sunahara GI. **2001**. Ecotoxicological effects of hexahydro-1,3,5-trinitro-1,3,5-triazine (RDX) on soil microbial activities. *Environ. Toxicol. Chem.* 20 : 947-951.
- Gong P, Sunahara GI, Rocheleau S, Dodard SG, Robidoux PY, Hawari J. **2004**. Preliminary ecotoxicological characterization of a new energetic substance, CL-20. *Chemosphere* 56: 653-658.
- Greenberg EP. **2003**. Bacterial communication: Tiny teamwork. *Nature* 424: 134-134.
- Gregory KB, Larese-Casanova P, Parkin GF, Scherer MM. **2004**. Abiotic transformation of hexahydro-1,3,5-trinitro-1,3,5-triazine by Fe^{II} bound to magnetite. *Environ. Sci. Technol.* 39: 1408-1414.
- Gregus Z, Watkins JB, Thompson TN, Harvey MJ, Rozman K, Klaassen CD. **1983**. Hepatic phase I and phase II biotransformations in quail and trout: comparison to other species commonly used in toxicity testing. *Toxicol. Appl. Pharmacol.* 67: 430-441.

- Groom CA, Halasz A, Paquet L, Morris N, Olivier L, Dubois C, Hawari J. **2002**. Accumulation of HMX (octahydro-1,3,5,7-tetranitro-1,3,5,7-tetrazocine) in indigenous and agricultural plants grown in HMX-contaminated anti-tank firing-range soil. *Environ. Sci. Technol.* 36: 112-118.
- Groom CA, Halasz A, Paquet L, D'Cruz P, Hawari J. **2003**. Cyclodextrin-assisted capillary electrophoresis for determination of the cyclic nitramine explosives RDX, HMX and CL-20: Comparison with high-performance liquid chromatography. *J. Chromatogr. A* 999: 17-22.
- Groom C, Halasz A, Paquet L, Thiboutot S, Ampleman G, Hawari J. **2005**. Detection of nitroaromatic and cyclic nitramine compounds by cyclodextrin assisted electrophoresis quadrupole ion trap mass spectrometry. *J. Chromatogr. A* 1072: 73-82.
- Gui L, Gillham RW, Odziemkowski MS. **2000**. Reduction of N-nitrosodimethylamine with granular iron and nickel-enhanced iron. 1. Pathways and kinetics. *Environ. Sci. Technol.* 34: 3489-3494.
- Haas R, Schreiber I, Low EV, Stork G. **1990**. Conception for the investigation of contaminated munitions plants. 2. Investigation of former RDX-plants and filling stations. *Fresenius' J. Anal. Chem.* 338: 41-45.
- Habig WH, Pabst MJ, Jakoby WB. **1974**. Glutathione S-transferases. The first enzymatic step in mercapturic acid formation. *J. Biol. Chem.* 249: 7130-7139.
- Halasz A, Spain J, Paquet L, Beaulieu C, Hawari J. **2002**. Insights into the formation and degradation of methylenedinitramine during the incubation of RDX with anaerobic sludge. *Environ. Sci. Technol.* 36: 633-638.
- Hamburger V, Hamilton HL. **1951**. A series of normal stages in the development of the chick embryo. *J. Morphol.* 88: 49-92.
- Harvey SD, Fellows RJ, Cataldo DA, Bean, RM. **1991**. Fate of the explosive hexahydro-1,3,5-trinitro-1,3,5-triazine (RDX) in soil and bioaccumulation in bush bean hydroponic plants. *Environ. Toxicol. Chem.* 10: 845-855.
- Hawari J, Halasz A, Beaudet S, Paquet L, Ampleman G, Thiboutot S. **1999**. Biotransformation of 2,4,6-trinitrotoluene with *Phanerochaete chrysosporium* in agitated cultures at pH 4.5. *Appl. Environ. Microbiol.* 65: 2977-2986.
- Hawari J. **2000**. Biodegradation of RDX and HMX: From basic research to field application. In *Biodegradation of Nitroaromatic Compounds and Explosives*. Spain JC, Hughes JB, and Knackmuss HJ, Eds.; CRC Press, Boca Raton: FL, pp. 277-310.
- Hawari J, Beaudet S, Halasz A, Thiboutot S, Ampleman G. **2000a**. Microbial degradation of explosives: biotransformation versus mineralization. *Appl. Microbiol. Biotechnol.* 54: 605-618.
- Hawari J, Halasz A, Sheremata T, Beaudet S, Groom C, Paquet L, Rhofir C, Ampleman G, Thiboutot S. **2000b**. Characterization of metabolites during biodegradation of hexahydro-1,3,5-trinitro-1,3,5-triazine (RDX) with municipal sludge. *Appl. Environ. Microbiol.* 66: 2652-2657.
- Hawari J, Halasz A, Beaudet S, Paquet L, Ampleman G, Thiboutot S. **2001**. Biotransformation routes of octahydro-1,3,5,7-tetranitro-1,3,5,7-tetrazocine by municipal anaerobic sludge. *Environ. Sci. Technol.* 35: 70-75.
- Hawari J, Halasz A, Groom C, Deschamps S, Paquet L, Beaulieu C, Corriveau A. **2002**. Photodegradation of RDX in aqueous solution : a mechanistic probe for biodegradation with *Rhodococcus* sp. *Environ. Sci. Technol.* 36: 5117-5123.

- Hawari J, Deschamps S, Beaulieu C, Paquet L, Halasz A. **2004**. Photodegradation of CL-20: insights into the mechanisms of initial reactions and environmental fate. *Water Res.* 38: 4055-4064.
- Heilmann HM, Wiesmann U, Stenstrom MK. **1996**. Kinetics of the alkaline hydrolysis of high explosives RDX and HMX in aqueous solution and adsorbed to activated carbon. *Environ. Sci. Technol.* 30:1485-1492.
- Helland B, Alvarez PJJ, Schnoor JL. **1995**. Reductive dechlorination of carbon tetrachloride with elemental iron. *J. Hazard. Mater.* 41: 205-216.
- Hissin PJ, Hilf R. **1976**. A fluorometric method for determination of oxidized and reduced glutathione in tissues. *Anal. Biochem.* 74: 214-226.
- Hoek B. **2004**. Military explosives and health: organic energetic compound syndrome. *Med. Confl. Surviv.* 20: 326-333.
- Hoffsommer JC, Kubose DA, Glover DJ. **1977**. Kinetic Isotope Effects and intermediate formation for the aqueous alkaline homogeneous hydrolysis of 1,3,5-triaza-1,3,5-trinitrocyclohexane (RDX). *J. Phys. Chem.* 81:380-385.
- Hofrichter M. **2002**. Review: lignin conversion by manganese peroxidase (MnP). *Enzyme Microb Tech.* 30: 454-466.
- Hsieh CH, Liu LF, Tsai CP, Tam MF. **1999**. Characterization and cloning of avian-hepatic glutathione S-transferases. *Biochem. J.* 343: 87-93.
- Hundal LS, Singh J, Bier EL, Shea PJ, Comfort SD, Powers WL. **1997**. Removal of TNT and RDX from water and soil using iron metal. *Environ. Pollut.* 97: 55-64.
- ISO (International Organization for Standardization). **1994**. *Soil Quality – Determination of pH*. ISO 10390: 1994 (E). Geneva, Switzerland.
- ISO (International Organization for Standardization). **2001**. *Soil quality: effects of pollutants on Enchytraeidae (Enchytraeus sp) – determination of effects on reproduction and survival*. ISO DIS 16387: 2001, ISO, Geneva, Switzerland.
- Jakoby WB. **1978**. The glutathione S transferases: a group of multifunctional detoxification proteins. *Adv. Enzymol. Relat. Areas Mol. Biol.* 46: 383-414.
- Jarvis SA, McFarland VA, Honeycutt ME. **1998**. Assessment of the effectiveness of composting for the reduction of toxicity and mutagenicity of explosive-contaminated soil. *Ecotoxicol Environ Safety* 39: 131-135.
- Jenkins TF, Walsh ME, Thorne PT, Miyares PH, Ranney TA, Grant CL, Esparza JR. **1998**. CRREL Special Report 98-9. Cold Regions Research and Engineering Laboratory, US Army Corps of Engineers, Office of the Chief of Engineers.
- Johnson MS, Paulus HI, Salice CJ, Checkai RT, Simini M. **2004**. Toxicologic and histopathologic response of the terrestrial salamander *Phethodon cinereus* to soil exposure of 1,3,5-trinitrohexahydro-1,3,5-triazine. *Arch. Environ. Contam. Toxicol.* 47: 496-501.
- Kamin H, White-Stevens RH, Presswood RP. **1978**. Salicylate hydroxylase. *Methods Enzymol.* 53: 527-543.
- Katagiri M, Maeno H, Yamamoto S, Hayaishi O, Kitao T, Oae S. **1965**. Salicylate hydroxylase, a monooxygenase requiring flavin adenine dinucleotide. ii. the mechanism of salicylate hydroxylation to catechol. *J. Biol. Chem.* 240: 3414-3417.
- Kielemoes J, de Boever P, Verstraete W. **2000**. Influence of denitrification on the corrosion of iron and stainless steel powder. *Environ. Sci. Technol.* 34: 663-671.
- Kiyoura, T.; Kogure, Y. **1997**. Synthesis of hydroxyacetic acid and its esters from glyoxal

- catalyzed by multivalent metal ions. *Appl. Catal. A: General* 156: 97-104.
- Klaassen CD. **1996**. *Casarett and Doull's Toxicology - The Basic Science of Poisons*. Fifth ed., Mc Graw-Hill, New York.
- Klausen J, Trober SP, Haderlein SB, Schwarzenbach RP. **1995**. Reduction of substituted nitrobenzenes by Fe(II) in aqueous mineral suspensions. *Environ. Sci. Technol.* 29: 2396-2404.
- Klupinski TP, Chin Y-P. **2003**. Abiotic degradation of trifluralin by Fe(II) : Kinetics and transformation pathway. *Environ. Sci. Technol.* 37: 1311-1318.
- Koder RL, Haynes CA, Rodgers ME, Rodgers DW, Miller AF. **2002**. Flavin thermodynamics explain the oxygen insensitivity of enteric nitroreductases, *Biochemistry*, 41: 14197-14205.
- Kohler EA, Branham BE, **2002**. Site of uptake, absorption, translocation, and metabolism of ethofumesate in three turfgrass species. *Weed Sci.* 50: 576-580.
- Korsounskii BL, Nedel'ko VV, Chukanov NV, Larikova TS, Volk F. **2000**. Kinetics of thermal decomposition of hexanitrohexaazaisowurtzitane. *Russ. Chem. Bull.* 49:812-818.
- Kuperman RG, Simini M, Phillips CT, Checkai RT. **1999**. Comparison of malathion toxicity using enchytraeid reproduction test and earthworm toxicity test in different soil types. *Pedobiologia* 43: 630-634.
- Kuperman RG, Checkai RT, Simini M, Phillips CT, Kolakowski JE, Kurnas C, Sunahara GI, **2003**. Survival and reproduction of *Enchytraeus crypticus* (Oligochaeta, Enchytraeidae) in a natural sandy loam soil amended with the nitro-heterocyclic explosives RDX and HMX. *Pedobiologia* 47: 651-656.
- Kuperman RG, Checkai RT, Simini M, Phillips CT. **2004a**. Manganese toxicity in soil for *Eisenia fetida*, *Enchytraeus crypticus* (Oligochaeta), and *Folsomia candida* (Collembola). *Ecotoxicol. Environ. Safety*. 57: 48-53.
- Kuperman RG, Simini M, Phillips CT, Checkai RT, Kolakowski JE, Kurnas CW, Sunahara GI. **2004b**. Survival and reproduction of *Enchytraeus crypticus* (Oligochaeta, Enchytraeidae) in a natural sandy loam soil amended with the nitro-heterocyclic explosives RDX and HMX. *Pedobiologia* 47: 651-656.
- Kuperman RG, Checkai RT, Simini M, Phillips CT, Anthony JS, Kolakowski JE, Davis EA. **2006**. Toxicity of emerging energetic soil contaminant CL-20 to potworm *Enchytraeus crypticus* in freshly amended or weathered and aged treatments. *Chemosphere*, **In press**.
- Lachance B, Renoux AY, Sarrazin M, Hawari J, Sunahara GI. **2004**. Toxicity and bioaccumulation of reduced TNT metabolites in the earthworm *Eisenia andrei* exposed to amended forest soil. *Chemosphere* 55: 1339-1348.
- Lammeli UK. **1970**. Cleavage of structural proteins during the assembly of the head of the bacteriophage T4. *Nature* 227: 580-685.
- Larson SL, Felt DR, Davis JL, Escalon L. **2002**. Analysis of CL-20 in environmental matrices: Water and soil. *J. Chromatographic Sci.* 40: 201-206.
- Law AMJ, Aitken MD. **2003**. Bacterial chemotaxis to naphthalene desorbing from a nonaqueous liquid. *Appl. Environ. Microbiol.* 69: 5968-5973.
- Leggett DC. **1985**. Sorption of military explosive contaminants on bentonite drilling muds. CRREL Report 85-18. US Army Cold Regions Research and Engineering Laboratory, Hanover, NH.
- Levine BS, Furedi EM, Gordon DE, Burns JM, Lish PM. **1981**. Thirteen-week toxicity study of

- hexahydro-1,3,5-trinitro-1,3,5-triazine (RDX) in Fischer 344 rats. *Toxicol. Lett.* 8: 241-245.
- Li H, Sheng G, Sheng W, Xu O. **2002**. Uptake of trifluralin and lindane from water by ryegrass. *Chemosphere* 48: 335-341.
- Lovley DR, Greening RC, Ferry JG. **1984**. Rapidly growing rumen methanogenic organism that synthesizes coenzyme M and has a high affinity for formate. *Appl. Environ. Microbiol.* 48: 81-87.
- Lynch JC, Myers KF, Brannon JM, Delfino JJ. **2001**. Effects of pH and temperature on the aqueous solubility and dissolution rate of 2,4,6-trinitrotoluene (TNT), hexahydro-1,3,5-trinitro-1,3,5-triazine (RDX), and octahydro-1,3,5,7-tetranitro-1,3,5,7-tetrazocine (HMX). *J. Chem. Eng. Data* 46: 1549-1555.
- Major MA, Johnson MS, Salice CJ. **2002**. Bioconcentration, bioaccumulation and biomagnification of nitroaromatic and nitramine explosives and their breakdown products. U.S. Army Center for Health Promotion and Preventive Medicine, Aberdeen Proving Ground, MD, 87-MA-4677-01.
- March, J. **1985**. *Advanced Organic Chemistry*. Third ed., Wiley-Interscience Publication, John Wiley and Sons: New York, pp 784-785.
- Marx, RB, Aitken MD. **2000**. Bacterial chemotaxis enhances naphthalene degradation in a heterogeneous aqueous system. *Environ. Sci. Technol.* 34: 3379-3383.
- Matés JM, Pérez-Gómez C, Blanca M. **2000**. Chemical and biological activity of free radical 'scavengers' in allergic diseases. *Clinica Chimica Acta* 296: 1-15.
- Matheson, L.J.; Tratnyek, P.G. Reductive dehalogenation of chlorinated methanes by iron metal. *Environ. Sci. Technol.* (1994) 28, 2045-2053.
- McCormick NG, Cornell JH, Kaplan AM. **1981**. Biodegradation of hexahydro-1,3,5-trinitro-1,3,5-triazine. *Appl. Environ. Microbiol.* 42: 817-823.
- Meister A, Anderson ME. **1983**. Glutathione. *Ann. Rev. Biochem.* 52: 711-760.
- Monteil-Rivera F, Brouwer EB, Masset S, Deslandes Y, Dumonceau J. **2000**. Combination of X-ray photoelectron and solid-state ^{13}C nuclear magnetic resonance spectroscopy in the structural characterisation of humic acids. *Anal. Chim. Acta* 424: 243-255.
- Monteil-Rivera F, Groom C, Hawari J. **2003**. Sorption and degradation of octahydro-1,3,5,7-tetranitro-1,3,5,7-tetrazocine in soil. *Environ. Sci. Technol.* 37: 3878-3884.
- Monteil-Rivera F, Paquet L, Deschamps S, Balakrishnan VK, Beaulieu C, Hawari J. **2004**. Physico-chemical measurements of CL-20 for environmental applications: Comparison with RDX and HMX. *J. Chromatogr. A* 1025:125-132.
- Murata-Kamiya N, Kamiya H, Kaji H, Kasai H. **1997**. Mutational specificity of glyoxal, a product of DNA oxidation, in the lacI gene of wild-type *Escherichia coli* W3110. *Mutat. Res.* 377: 255-262.
- Myers TE, Brannon JM, Pennington JC, Davis WM, Myers KF, Townsend DM, Ochman MK, Hayes CA. **1998**. Laboratory studies of soil sorption/transformation of TNT, RDX, and HMX. Technical Report IRRP-98-8. US Army Corps of Engineers, Waterways Experiment Station, Vicksburg, MS.
- Myler CA, Sisk W. **1991**. Bioremediation of explosives contaminated soils. In: *Environmental Biotechnology for Waste Treatment*, Sayler GS, Fox R, Blackburn JW. (ed.), Plenum Press, New York, NY, p 137-46.
- Nielsen AT, Christian SL, Moore DW, Gilardi RD, George CF. **1987**. Synthesis of 3,5,12-triazawurtzitane (3,5,12-triazatetracyclo[5.3.1.1^{2,6}.0^{4,9}]dodecanes). *J. Org. Chem.* 52: 1656-

1662.

- Nielsen AT, Nissan RA, Vanderah DJ, Coon CL, Gilardi RD, George CF, Flippen-Anderson J. **1990**. Polyazapolycyclics by condensation of aldehydes with amines. 2. Formation of 2,4,6,10,12-hexabenzyl-2,4,6,8,10,12-hexaazatetracyclo[5.5.0.0^{5,9}.0^{3,11}]dodecanes from glyoxal and benzylamines. *J. Org. Chem.* 55: 1495-66.
- Nielsen AT, Chafin AP, Christian SL, Moore DW, Nadler MP, Nissan RA, Vanderah DJ, Gilardi RD, George CF, Flippen-Anderson JL. **1998**. Synthesis of polyazapolycyclic caged polynitramines. *Tetrahedron* 54: 11793-11812.
- OECD **1984a**. Guidelines for Testing of Chemicals: Earthworm Acute Toxicity Test. Organization for Economic Co-operation and Development, Guideline No. 207, Paris, France.
- OECD **1984b**. Guidelines for Testing of Chemicals. Avian dietary toxicity test. Organization for Economic Co-operation and Development, Paris, France.
- OECD **1984c**. Guidelines for Testing of Chemicals. Avian reproduction test. Organization for Economic Co-operation and Development, Paris, France.
- Odani H, Shinzato T, Usami J, Matsumoto Y, Brinkmann Frye E, Baynes JW, Maeda K. **1998**. Imidazolium crosslinks derived from reaction of lysine with glyoxal and methylglyoxal are increased in serum proteins of uremic patients: evidence for increased oxidative stress in uremia. *FEBS Letters* 427: 381-385.
- O'Donnell VB, Smith GC, Jones OT. **1994**. Involvement of phenyl radicals in iodonium inhibition of flavoenzymes. *Mol. Pharmacol.* 46: 778-785.
- Odziemkowski MS, Gui L, Gillham RW. **2000**. Reduction of N-nitrosodimethylamine with granular iron and nickel-enhanced iron. 2. Mechanistic studies. *Environ. Sci. Technol.* 34: 3495-3500.
- Ogawa NO, Hirose T, Tsukamoto M, Fukushima K, Suwa T, Satoh T. **1995a**. GSH-independent denitration of organic nitrate esters in rabbit hepatic cytosol and vascular cytosol. *Res. Comm. Mol. Pathol. Pharmacol.* 88: 153-161.
- Ogawa NO, Hirose T, Tsukamoto M, Fukushima K, Suwa T, Satoh T. **1995b**. Purification and characterization of glutathione-independent denitration enzyme of organic nitrate esters in rabbit hepatic cytosol *Biol. Pharm. Bull.* 18: 1352-1355.
- Oh B-T, Just CL, Alvarez PJJ. **2001**. Hexahydro-1,3,5-trinitro-1,3,5-triazine mineralization by zerovalent iron and mixed anaerobic cultures. *Environ. Sci. Technol.* 35: 4341-4346.
- Oien N, Stenerson J. **1984**. Esterases of earthworms - III. Electrophoresis reveals that *Eisenia foetida* (Savigny) is two species. *Comp. Biochem. Physiol.* 78c, 277-282.
- Okemgbo AA, Hill HH, Metcalf SG, Bachelor MA. **1999**. Determination of nitrate and nitrite in Hanford defense waste by reverse-polarity capillary zone electrophoresis. *J. Chromatogr. A* 844: 387-394.
- Orna MV, Mason RP. **1989**. Correlation of kinetic parameters of nitroreductase enzymes with redox properties of nitroaromatic compounds. *J. Biol. Chem.* 264: 12379-12384.
- Oxley JC, Kooh AB, Szekeres R, Zheng W. **1994**. Mechanisms of nitramine thermolysis. *J. Phys. Chem.* 98: 7004-7008.
- Pace MD. **1991**. EPR spectra of photochemical NO₂ formation in monocyclic nitramines and hexanitrohexaazaisowurtzitane. *J. Phys. Chem.* 95: 5858-5864.
- Pace MD, Kalyanaraman B. **1993**. Spin trapping of nitrogen dioxide radical from photolytic decomposition of nitramines. *Free Radical Bio. Med.* 15: 337-342.

- Palleroni NJ. **1984**. Gram-negative aerobic rods and cocci: family I *Pseudomonadaceae*, p. 140-198. In N. R. Krieg, and J. G. Holt (eds.), *Bergey's manual of systematic bacteriology*, vol. 1. Williams & Wilkins, Baltimore, MD.
- Pandey G, Jain RK. **2002**. Bacterial chemotaxis toward environmental pollutants: role in bioremediation. *Appl. Environ. Microbiol.* 68: 5789-5795.
- Parales RE, Ditty JL, Harwood CS. **2000**. Toluene-degrading bacteria are chemotactic towards the environmental pollutants benzene, toluene, and trichloroethylene. *Appl. Environ. Microbiol.* 66: 4098-4104.
- Parales RE, Harwood CS. **2002**. Bacterial chemotaxis to pollutants and plant-derived aromatic molecules. *Curr. Opin. Microbiol.* 5: 266-273.
- Park S, Wolanin PM, Yuzbashyan EA, Silberzan P, Stock JB, Austin RH. **2003**. Motion to form a quorum. *Science* 301: 188.
- Parkinson GN, Skelly JV, Neidle S. **2000**. Crystal structure of FMN-dependent nitroreductase from *Escherichia coli* B: a prodrugactivating enzyme. *J. Med. Chem.* 43: 3624-3631.
- Patil, DG, Brill TB. **1991**. Thermal decomposition of energetic materials 53. Kinetics and mechanisms of thermolysis of hexanitrohexaazaisowurtzitane. *Combust. Flame* 87: 145-151.
- Peyton GR, LeFaivre MH, Maloney SW. **1999**. Verification of RDX photolysis mechanism. *CERL Technical Report 99/93*, (www.CECER.Army/TechReports).
- Phillips CT, Checkai RT, Wentsel RS. **1993**. Toxicity of Selected Munitions and Munition-contaminated Soil on the Earthworm (*Eisenia foetida*). Technical Report, U.S. Army Chemical and Biological Defense Agency, Aberdeen Proving Ground, MD, USA.
- Phillips C, Kuperman R. **1999**. A rapid and highly-efficient method for extracting enchytraeids from soil. *Pedobiologia* 43: 523-527.
- Poleman JHTM, van Ommen B, Bogaards JPP, van Bladeren PJ. **1993**. Ethacrynic acid and its glutathione conjugates as inhibitors of glutathione S-transferases. *Xenobiotica* 23: 913-923.
- Pollock VV, Barber MJ. **2001**. Kinetic and mechanistic properties of biotin sulfoxide Reductase. *Biochemistry* 40: 1430-1440.
- Posthuma L, Baerselman R, van Veen RPM, Dirven van Breemen EM. **1997**. Single and joint toxic effects of copper and zinc on reproduction of *Enchytraeus crypticus* in relationship to sorption of metals in soil. *Ecotoxicol. Environ. Safety* 38: 108-121.
- Puurtinen HM, Martikainen EAT. **1997**. Effect of soil moisture on pesticide toxicity to an enchytraeid worm, *Enchytraeus* sp. *Arch. Environ. Contam. Toxicol.* 33: 34-41.
- Ran Y, Huang W, Rao PSC, Liu D, Sheng G, Fu J. **2002**. The role of condensed organic matter in the nonlinear sorption of hydrophobic organic contaminants by a peat and sediments. *J. Environ. Qual.*: 1953-1962.
- Robidoux P-Y, Hawari J, Thiboutot S, Ampleman G, Sunahara GI. **1999**. Acute toxicity of 2,4,6-trinitrotoluene in earthworm (*Eisenia andrei*). *Ecotoxicol. Environ. Safety* 44: 311-321.
- Robidoux P-Y, Svendsen C, Caumartin J, Hawari J, Ampleman G, Thiboutot S, Weeks JM, Sunahara GI. **2000**. Chronic toxicity of energetic compounds in soil determined using the earthworm (*Eisenia andrei*) reproduction test. *Environ. Toxicol. Chem.* 19: 1764-1773.
- Robidoux P-Y, Hawari J, Thiboutot S, Ampleman G, Sunahara GI. **2001**. Chronic toxicity of octahydro-1,3,5,7-tetranitro-1,3,5,7-tetrazocine (HMX) in soil using the earthworm (*Eisenia andrei*) reproduction test. *Environ. Pollut.* 111: 283-92.
- Robidoux P-Y, Hawari J, Bardai G, Paquet L, Ampleman G, Thiboutot S, Sunahara GI. **2002**. TNT, RDX and HMX decrease earthworm (*Eisenia andrei*) life-cycle responses in a spiked

- natural forest soil. *Arch. Environ. Contam. Toxicol.* 43: 379-388.
- Robidoux P-Y, Bardai G, Paquet L, Ampleman G, Thiboutot S, Hawari J, Sunahara GI. **2003**. Phytotoxicity of 2,4,6-trinitrotoluene (TNT) and octahydro-1,3,5,7-tetranitro-1,3,5,7-tetrazocine (HMX) in amended artificial and forest soils. *Arch. Environ. Contamin. Toxicol.* 44: 198-209.
- Robidoux P-Y, Sunahara GI, Savard K, Berthelot Y, Dodard S, Martel M, Gong P, Hawari J. **2004**. Acute and chronic toxicity of the new explosive CL-20 to the earthworm (*Eisenia Andrei*) exposed to amended natural soils. *Environ. Toxicol. Chem.* 23: 1026-1034.
- Rocheleau S, Kuperman RG, Martel M, Paquet L, Bardai G, Wong S, Sarrazin M, Dodard S, Gong P, Hawari J, Checkai RT, Sunahara GI. **2006**. Phytotoxicity of nitroaromatic energetic compounds freshly amended or weathered and aged in sandy loam soil. *Chemosphere* 62: 545-558.
- Römbke J, Moser T. **1999**. *Organization and Performance of an International Ringtest for the Validation of the Enchytraeid Reproduction Test*. Research Report 296 64 906 (UBA-FB 98-104). Environmental Research of the Federal Ministry of the Environment, Nature Conservation and Nuclear Safety. German Federal Environment Agency, Berlin, Germany.
- Rosenthal H, Adrian L, Steiof M. **2004**. Dechlorination of PCE in the presence of Fe⁰ enhanced by a mixed culture containing two *Dehalococcoides* strains. *Chemosphere* 55: 661-669.
- Ryzhkov LR, McBride JM. **1996**. Low temperature reactions in single crystals of two polymorphs of the polycyclic nitramine ¹⁵N-HNIW. *J. Phys. Chem.* 100: 163-169.
- Sabljić A, Güsten H, Verhaar H, Hermens J. **1995**. QSAR modelling of soil sorption. Improvements and systematics of log K_{oc} vs. log K_{ow} correlations. *Chemosphere* 31:489-4514.
- Samanta SK, Bhushan B, Chauhan A, Jain RK. **2000**. Chemotaxis of a *Ralstonia* sp. SJ98 toward different nitroaromatic compounds and their degradation. *Biochem. Biophys. Res. Commun.* 296: 117-123.
- Schäfer RK. **2002**. Evaluation of the Ecotoxicological Threat of Ammunition Derived Compounds to the Habitat Function of Soil. Ph.D. Thesis. Free University of Berlin, Berlin, Germany.
- Schäfer R, Achazi RK. **1999**. The toxicity of soil samples containing TNT and other ammunition derived compounds in the enchytraeid and collembola-biotest. *Environ. Sci. Pollut. Res.* 6: 213-219.
- Scherer MM, Richter S, Valentine RL, Alvarez PJJ. **2000**. Chemistry and microbiology of permeable reactive barriers for *in situ* groundwater clean up. *Crit. Rev. Environ. Sci. Technol.* 26: 221-264.
- Schneider NR, Bradley SL, Andersen ME. **1976**. Toxicology of cyclotrimethylene-trinitramine (RDX): distribution and metabolism in the rat and miniature swine. AFRRRI SR76-34. Armed Forces Radiobiology Research Institute, Bethesda, MD.
- Schultz M, Dutta S, Tew KD. **1997**. Inhibitors of glutathione S-transferases as therapeutic agents. *Adv. Drug. Del. Rev.* 26: 91-104.
- Shangari N, Bruce WR, Poon R, O'Brien PJ. **2003**. Toxicity of glyoxals - role of oxidative stress, metabolic detoxification and thiamine deficiency. *Biochem. Soc. Trans.* 31: 1390-1393.
- Sheremata TW, Hawari J. **2000a**. Cyclodextrins for desorption and solubilization of 2,4,6-trinitrotoluene and its metabolites from soil. *Environ. Sci. Technol.* 34: 3462-3468.
- Sheremata TW, Hawari J. **2000b**. Mineralization of RDX by the white rot fungus *Phanerochaete*

- chrysosporium*. *Environ. Sci. Technol.* 34: 3384-3388.
- Sheremata TW, Halasz A, Paquet L, Thiboutot S, Ampleman G, Hawari J. **2001**. The fate of the cyclic nitramine explosive RDX in natural soil. *Environ. Sci. Technol.* 35: 1037-1040.
- Shu Y, Dubikhin VV, Nazin GM, Manelis G.B. **2002**. Chain and monomolecular decomposition of hexogen in solutions. *Russ. Chem. Bull., Int. Ed.* 51:1433-1440.
- Sidoli O'Connor C, Lepp NW, Edwards R, Sunderland G. **2003**. The combined use of electokinetic remediation and phytoremediation to decontaminate metal-polluted soils: a laboratory-scale feasibility study. *Environ. Monitoring Assess.* 84: 141-158.
- Sikder AK, Sikder N, Gandhe BR, Agrawal JP, Singh H. **2002**. Hexanitrohexaazaisowurtzitane or CL-20 in India: Synthesis and characterization. *Def. Sci. J.* 52: 135-146.
- Simini M, Kuperman RG, Phillips CT, Checkai RT, Kolakowski JE, Kurnas CW, Sunahara GI. **2004**. Reproduction and survival of *Eisenia andrei* in a sandy loam soil amended with the nitro-heterocyclic explosives RDX and HMX. *Pedobiologia* 47: 657-662.
- Singh J, Comfort SD, Shea PJ. **1998**. Remediating RDX-contaminated water and soil using zero-valent iron. *J. Environ. Qual.* 27: 1240-1245.
- Stookey LL. **1970**. Ferrozine – A new spectrophotometric reagent for iron. *Anal. Chem.* 42: 779-781.
- Strigul N, Braida W, Christodoulatos C, Balas W, Nicolich S. **2005**. The assessment of the energetic compound 2,4,6,8,10,12-hexanitro-2,4,6,8,10,12-hexaaisowurtzitane (CL-20) degradability in soil. *Environ. Poll.* 139: 353-361.
- Su C, Puls RW. **2004**. Nitrate reduction by zerovalent iron: effects of formate, oxalate, citrate, chloride, sulfate, borate, and phosphate. *Environ. Sci. Technol.* 38: 2715-2720.
- Sucharitakul J, Chaiyen P, Entsch B, Ballou DP. **2005**. The reductase of *p*-hydroxyphenylacetate 3-hydroxylase from *Acinetobacter baumannii* requires *p*-hydroxyphenylacetate for effective catalysis. *Biochemistry* 44: 10434-10442.
- Summers, W.R. **1990**. Characterization of formaldehyde and formaldehyde-releasing preservatives by combined reversed phase cation-exchange high performance liquid chromatography with postcolumn derivitization using Nash's reagent. *Anal. Chem.* 62: 1397-1402.
- Sunahara GI, Dodard S, Sarrazin M, Paquet L, Hawari J, Greer CW, Ampleman G, Thiboutot S, Renoux AY. **1999**. Ecotoxicological characterization of energetic substances using a soil extraction procedure. *Ecotoxicol. Environ. Safety* 43: 138-148.
- Sunahara GI, Robidoux P-Y, Gong P, Lachance B, Rocheleau S, Dodard SG, Sarrazin M, Hawari J, Thiboutot S, Ampleman G, Renoux AY **2001**. Laboratory and field approaches to characterize the ecotoxicology of polynitro explosives. In: *Environmental Toxicology and Risk Assessment: science, Policy, and Standardization – Implications for Environmental Decisions*, Greenberg BM, Hull RN, Roberts MH Jr, Gensemer RW (eds.), 10th Vol. STP 1403, ASTM, West Conshohocken, PA, p. 293-312.
- Suzuki K, Gomi T, Kaidoh T, Itagaki E. **1991**. Hydroxylation of o-halogenophenol and o-nitrophenol by salicylate hydroxylase. *J. Biochem. (Tokyo)*. 109: 348-353.
- Szecsody JE, Girvin DC, Devary BJ, Campbell JA. **2004**. Sorption and oxic degradation of the explosive CL-20 during transport in subsurface sediments. *Chemosphere* 56: 593-610.
- Talmage SS, Opresko DM, Maxwell CJ, Welsh CJE, Cretella FM, Reno PH, Daniel FB. **1999**. Nitroaromatic munition compounds: Environmental effects and screening values. *Rev. Environ. Contam. Toxicol.* 161: 1-156.

- Tedeschi G, Chen S, Massey V. **1995**. DT-diaphorase: redox potential, steady-state, and rapid reaction study. *J. Biol. Chem.* 270:1198-1204.
- The Merck Index*. **2001**. O'Neil MJ, Smith A, Heckelman PE (ed.), Merck & Co., Inc., Whitehouse Station, NJ.
- Tien M, Kirk TK. **1988**. Lignin peroxidase of *Phanerochaete chrysosporium*. *Methods Enzymol.* 161: 238-249.
- Trott S, Nishino SF, Hawari J, Spain JC. **2003**. Biodegradation of the nitramine explosive CL-20. *Appl. Environ. Microbiol.* 69: 1871-1874.
- US EPA **1979**. Methods for chemical analysis of water and wastes - Nitrogen, Nitrite. Method 354.1, United States Environmental Protection Agency, Washington, DC, USA.
- US EPA, Office of Toxic Substances. **1982**. Early seedling growth toxicity test. EG-13, United States Environmental Protection Agency, Washington, D.C, USA.
- US EPA. **1989**. Earthworm survival (*Eisenia foetida*). In *Protocols for Short Term Toxicity Screening for Hazardous Waste Sites*. EPA/600/3-88/029. Environmental Research Laboratory, Corvallis, OR, USA.
- US EPA **1996a**. Avian Dietary Toxicity Tests Ecological effects guidelines. EPA 712/C/96/140, United States Environmental Protection Agency, Washington, DC, USA.
- US EPA **1996b**. Avian Reproduction Test Ecological effects guidelines. EPA 712/C/96/141, United States Environmental Protection Agency, Washington, DC, USA.
- US EPA **1998**. Nitroaromatics and nitramines by high performance liquid chromatography. (HPLC). Method 8330A, United States Environmental Protection Agency, Washington, DC, USA.
- United States Department of Agriculture, National Resources Conservation Service. **1999**. *Soil Taxonomy* (Second Edition), Handbook No. 436, United States Government Printing Office, Washington, DC, USA.
- Uter W, Schwanitz HJ, Lessmann H, Schnuch A. **2001**. Glyoxal is an important allergen for (medical care) cleaning staff. *Int. J. Hyg. Environ. Health.* 204: 251-253.
- Wang LH, Tu SC, Lusk RC. **1984**. Apoenzyme of *Pseudomonas cepacia* salicylate hydroxylase. Preparation, fluorescence property, and nature of flavin binding. *J. Biol. Chem.* 259: 1136-1142.
- Wardle RB, Hinshaw JC, Braithwaite P, Rose M, Johnson G, Jones R, Poush K. **1996**. Synthesis of the caged nitramine HNIW (CL-20) 27.1-27.10; 27th Int. Annu. Conf. ICT, ADPA, Arlington, VI, USA. *Chem. Abstr.* 125: 172464v.
- Wardman P, Clark ED. **1976**. Oxygen inhibition of nitroreductase: electron transfer from nitro radical-anions to oxygen. *Biochem. Biophys. Res. Commun.* 69: 942-949.
- Weber WJ, DiGiano FA. **1996**. Energy Relationships: Applications to Heterogeneous Systems. p. 317-421. In *Process dynamics in environmental systems*. Wiley-Interscience, New-York, NY.
- Weber WJ, Huang W, Yu H. **1998**. Hysteresis in the sorption and desorption of hydrophobic organic contaminants by soils and sediments: 2. Effects of soil organic matter heterogeneity. *J. Contam. Hydrol.* 31:149-165.
- Westerhoff P, James J. **2003**. Nitrate removal in zero-valent iron packed columns. *Water Res.* 37:1818-1830.
- White-Stevens RH, Kamin H. **1972**. Studies of a flavoprotein, salicylate hydroxylase. I. Preparation, properties, and the uncoupling of oxygen reduction from hydroxylation. *J. Biol. Chem.* 247: 2358-2370.

- Whittaker MM, Kersten PJ, Nakamura N, Sanders-Loehr J, Schweizer ES, Whittaker JW. **1996**. Glyoxal oxidase from *Phanerochaete chrysosporium* is a new radical-copper oxidase. *J. Biol. Chem.* 271: 681-687.
- Winfield LE. **2001**. Development of a plant-based, short-term (<12 days) screening method for determination of 1,3,5-trinitro-1,3,5-triazine (RDX) bioavailability, bioconcentration, and phytotoxicity to selected terrestrial plants from soil matrices. Ph. D. thesis, University of Mississippi, MS, USA.
- Winfield LE, Rodgers JHJ, D'Surney SJ. **2004**. The responses of selected plants to short (<12 days) and long term (2, 4 and 6 weeks) hexahydro-1,3,5-trinitro-1,3,5-triazine (RDX) exposure. Part I: growth and developmental effects. *Ecotoxicology* 13: 335-347.
- Vyas PV, Shah BG, Trivedi GS, Gaur PM, Ray P, Adhikary SK. **2001**. Separation of inorganic and organic acids from glyoxal by electrodialysis. *Desalination* 140: 47-54.
- Xinqi Z, Nicheng S. **1996**. Crystal and molecular structures of ϵ -HNIW. *Chinese Sci. Bull.* 41: 574-576.
- Xue SK, Iskandar IK, Selim HM. **1995**. Adsorption-desorption of 2,4,6-trinitrotoluene and hexahydro-1,3,5-trinitro-1,3,5-triazine in soils. *Soil Sci.* 160: 317-327.
- Yadav GD, Gupta VR. **2000**. Synthesis of glyoxalic acid from glyoxal. *Process Biochem.* 36: 73-78.
- Yeung TC, Gidari, AS. **1980**. Purification and properties of a chicken liver glutathione S-transferase. *Arch. Biochem. Biophys.* 205: 404-411.
- Yinon J. **1990**. *Toxicity and metabolism of explosives*. CRC Press, Boca Raton, FL, USA, pp 145-170.
- Yoon JM, Oh BT, Just CL, Snooner JL. **2002**. Uptake and leaching of octahydro-1,3,5,7-tetranitro-1,3,5,7-tetrazocine by hybrid poplar trees. *Environ. Sci. Technol.* 36: 4649-4655.
- You KS. **1982**. Stereospecificities of the pyridine nucleotide-linked enzymes. *Meth. Enzymol.* 87: 101-126.
- Zhao X, Yinon J. **2002**. Identification of nitrate ester explosives by liquid chromatography-electrospray ionisation and atmospheric pressure chemical ionization mass spectrometry. *J. Chromatogr. A* 977:59-68.
- Zhao X, Shi N. **1996**. Crystal and molecular structures of ϵ -HNIW. *Chi. Sci. Bull.* 41: 574-576.
- Zuckermann H, Greenblatt GD, Haas Y. **1987**. OH Formation in the infrared multiphoton decomposition of jet-cooled cyclic nitramines. *J. Phys. Chem.* 91:5159-5161.

XXIII Appendix: Output

Publications

1. Bardai, G, Sunahara, G.I., Spear, P. A., Grosz, S., and Hawari, J. **(2006)** Purification of a cytosolic GST from Japanese quail(*Coturnix coturnix japonica*) capable of biotransforming CL-20 (submitted: *Environ. Toxicol. Chem.*)
2. Bhushan, B., A. Halasz, and J. Hawari **(2005)** Biotransformation of CL-20 by a dehydrogenase enzyme from *Clostridium* sp. EDB2. *Appl. Microbiol. Biotechnol.* 69: 448-455
3. Bhushan, B., Halasz, A., and Hawari, J. **(2005)** Stereo-specificity for pro-(R) hydrogen of NAD(P)H during enzyme-catalyzed hydride transfer to CL-20. *Biochem. Biophys. Research Communication* 337: 1080-1083.
4. Bhushan, B, Halasz, A., and Hawari, J. **(2006)** Effect of iron (III), humic acid, and anthraquinone-2,6-disulphonate on biodegradation of cyclic-nitramines by *Clostridium* sp. EBD2. *J. Appl. Microbiology* 100: 555-563.
5. Fournier, D., Monteil-Rivera, F., Halasz, A., Bhatt, M., and Hawari, J. **(2005)** Degradation of CL-20 by white-rot fungi. *Chemosphere* (**In press**).
6. Bardai, G., Sunahara, G. I., Spear, P. A., Martel, M., Gong, P., and Hawari, J. **(2005)** Effects of Dietary Administration of CL-20 on the Japanese Quail (*Coturnix coturnix japonica*), *Archives of Environmental Contamination and Toxicology* 49: 215-222.
7. Bonin, M.L., Bejan, D., Radovic-Hrapovic, Z., Halasz, A., Hawari, J., and Bunce, N.J. **(2005)** Indirect oxidation of RDX, HMX and CL-20 explosives in aqueous solution at boron-doped diamond electrodes. *Environmental Chemistry* 2(2): 125-129.
8. Dodard, S.G., Sunahara, G.I., Sarrazin, M., Gong, P., Kuperman, R.G., Ampleman, G., Thiboutot, S., and Hawari, J. **(2005)** Survival and reproduction of enchytraeid worms (Oligochaeta) in different soil types amended with cyclic nitramine explosives. *Environmental Toxicology and Chemistry*. 24(10): 2579-2587.
9. Groom, C., Halasz, A., Paquet, L., Thiboutot, S., Ampleman, G., and Hawari, J. **(2005)** Detection of nitroaromatic and cyclic nitramine compounds by cyclodextrin assisted electrophoresis quadrupole ion trap mass spectrometry. *J. Chromatogr. A* 1072: 73-82.
10. Balakrishnan, V.K., Monteil-Rivera, F., Halasz, A., Corbeanu, A., and Hawari, J. **(2004)** Decomposition of the polycyclic nitramine explosive, CL-20, by Fe⁰. *Environ. Sci. Technol.* 38: 6861-6866.
11. Balakrishnan, V.K., Monteil-Rivera, F., Gautier, M.A., and Hawari J. **(2004)** Sorption and stability of the polycyclic nitramine CL-20 in soil. *J. Environ. Qual.* 33:1362-1368.
12. Bhushan, B., Halasz, A., Spain, J.C., and Hawari J. **(2004)** Initial reaction(s) in biotransformation of CL-20 is catalyzed by salicylate 1-monooxygenase from *Pseudomonas* sp. strain ATCC 29352. *Appl. Environ. Microbiol.* 70:4040-4047.
13. Bhushan, B., Halasz, A., and Hawari, J. **(2004)** Nitroreductase catalyzed biotransformation of CL-20. *Biochem. Biophys. Res. Commun.* 322:271-276.
14. Bhushan, B., Halasz, A., Thiboutot, S., Ampleman, G., and Hawari J. **(2004)** Chemotaxis-mediated biodegradation of cyclic nitramine explosives RDX, HMX and CL-20 by

Clostridium sp. EDB2. *Biochem. Biophys. Res. Commun.* 316:816-821

15. Gong, P., Sunahara, G.I., Rocheleau, S., Dodard, S.G., Robidoux, P.Y., and Hawari J. (2004) Preliminary ecotoxicological characterization of a new energetic substance, CL-20. *Chemosphere* 56:653-658.
16. Hawari, J., Deschamps, S., Beaulieu, C., Paquet, L., Halasz, A. (2004) Photodegradation of CL-20: insights into the mechanisms of initial reactions and environmental fate. *Water Res.* 38: 4055-4064.
17. Monteil-Rivera, F., Paquet, L., Deschamps, S., Balakrishnan, V.K., Beaulieu, C., and Hawari, J. (2004) Physico-chemical measurements of CL-20 towards environmental applications: comparison with RDX and HMX. *J. Chromatogr. A* 1025:125-132.
18. Robidoux, P.Y., Sunahara, G.I., Savard, K., Berthelot, Y., Leduc, F., Dodard, S., Martel, M., Gong, P., and Hawari, J. (2004) Acute and chronic toxicity of the new explosive CL-20 to the earthworm (*Eisenia andrei*) exposed to amended natural soils. *Environ. Toxicol. Chem.* 23: 1026-1034.
19. Bhushan, B., Paquet, L., Spain, J.C., and Hawari, J. (2003) Biotransformation of 2,4,6,8,10,12-hexanitro-2,4,6,8,10,12-hexaazaisowurtzitane (CL-20) by denitrifying *Pseudomonas* sp. Strain FA1. *Appl. Environ. Microbiol.* 69:5216-5221.
20. Balakrishnan, V.K., Halasz, A., and Hawari, J. (2003) Alkaline hydrolysis of the cyclic nitramine explosives RDX, HMX and CL-20: New insights into degradation pathways obtained by the observation of novel intermediates. *Environ. Sci. Technol.*, 37:1838-1843.
21. Trott, S., Nishino, S.F., Hawari, J., and Spain, J.C. (2003) Biodegradation of the nitramine explosive CL-20. *Appl. Environ. Microbiol.* 69: 1871-1874.
22. Groom, C.A., Halasz, A., Paquet, L., D'Cruz, P., and Hawari, J. (2003) Cyclodextrin assisted capillary electrophoresis for determination of the cyclic nitramine explosives RDX, HMX and CL-20: a comparison with high performance liquid chromatography (HPLC). *J. Chromatogr. A*, 999:17-22.

Book Chapters & Critical Reviews:

1. Monteil-Rivera, F., A. Halasz, C. Groom, J.-S. Zhao, S. Thiboutot, G. Ampleman, and J. Hawari. (2005) "Fate and Transport of Explosives in the Environment: A Chemist's View" In "Ecotoxicology of Explosives and Unexploded Ordnance" EET Series Textbook, CRC, Ed Sunahara, Kuperman, Lutofo and Hawari (accepted).
2. Zhao, J. S., D. Fournier, S. Thiboutot, G. Ampleman and Hawari J. (2004) Biodegradation and Bioremediation of Explosives. In "Soil Biology", Bioremediation, Phytoremediation and Natural Attenuation, Springer-Verlag Berlin Heidelberg, Ed A. Singh and O. Ward. 55-80.
3. Hawari J.A., and A. Halasz (2002) Microbial Degradation of Explosives "In The Encyclopedia of Environmental Microbiology, (Ed) Gabriel Bitton, University of Florida," John Wiley & Sons Ltd, NY Amsterdam, The Netherlands 1979-1993.

Symposia & Proceedings

1. Hawari J. Biodegradation of Explosives: Environmental Fate, 18th Eastern Canadian Sym. of the Can. Assoc. on Water Quality (CAWQ), Ecole Polytechnique, Oct 18, **2002**, Montreal, Canada.
2. Groom C, Hawari J. **2002**. Cyclodextrin Assisted Capillary Electrophoresis for the Monitoring of Cyclic Nitramine Explosive Degradation. Proc. EnviroAnalysis, 2002, Toronto, Canada, ISBN 0-7709-0470-X, pp 453-458.
3. Hawari J, Zhao JS, Bhushan B, Hooper T, Halasz A, Spain J, Thiboutot S. Biodegradation of RDX, HMX and CL-20 by Isolates from Anaerobic Sludge and Soil. Partners in Environmental Technology, Tech. Symp. & Workshop (SERDP/ESTCP), Dec. 3-5, **2002**, Washington, DC, USA.
4. Groom C, Halasz A, Monteil-Rivera F, Hawari J. Extraction Technologies and Analytical Tools to Provide Insight into the Environmental Fate and Degradation Pathways of the New Explosive CL-20, 5th International Symposium on Advances in Extraction Technologies (ExTech), March 5-7, **2003**, Tampa, FL, USA.
5. Balakrishnan VK, Halasz A, Hawari, J. The Alkaline Hydrolysis of the Cyclic Nitramine Explosives RDX, HMX, and CL-20: New Insights into Degradation Pathways Obtained by the Observation of Novel Intermediates. 39th IUPAC Congress and the 86th Conference of the Canadian Society for Chemistry, Aug. 10-15, **2003**, Ottawa, Canada.
6. Dodard SG, Hawari J, Sarrazin M, Gong P, Paquet L, Ampleman G, Thiboutot S, Sunahara GI. Toxic effects of polynitro-organic compounds on enchytraeids (*Oligochaeta*) in freshly amended natural soils. The 30th Annual Aquatic Toxicity Workshop, Sept. 28 – Oct. 01, **2003**, Ottawa, Canada.
7. Robidoux PY, Sunahara GI, Savard K, Berthelot Y, Dodard S, Leduc F, Sarrazin M, Hawari J. Acute and chronic toxicity of the new explosive CL-20 in the earthworm (*Eisenia andrei*) exposed to amended natural soils. The 30th Annual Aquatic Toxicity Workshop, Sept. 28 – Oct. 01, **2003**, Ottawa, Canada.
8. Robidoux PY, Leduc F, Savard K, Berthelot Y, Dodard S, Martel M, Sarrazin M, Hawari J, Sunahara GI. Acute and chronic toxicity of the new explosive CL-20 in the earthworm (*Eisenia andrei*) exposed to amended natural soils. SETAC 24nd Annual Meeting Abstract Book, Nov. 8 –13, **2003**, Austin Convention Center, Austin, TX, USA.
9. Dodard SG, Gong P, Sarrazin M, Hawari J, Kuperman RG, Sunahara GI. Toxicity of CL-20 and other explosives to two species of enchytraeid worms. Partners in Environmental Technology Technical Symposium & Workshop (SERDP/ESTCP), Dec. 2-4, **2003**, Washington, DC, USA.
10. Rocheleau S, Gong P, Dodard SG, Martel M, Sarrazin M, Bush G, Hawari J, Sunahara GI. Effect of CL-20, a new explosive, on selected terrestrial plants, soil microbes, freshwater algae and marine bacteria. Partners in Environmental Technology, Technical Symposium & Workshop (SERDP/ESTCP), Dec. 2-4, **2003**, Washington, DC, USA.
11. Balakrishnan VK, Monteil-Rivera F, Gautier MA, Hawari J. Fate of the new explosive, CL-20, in soil. Partners in Environmental Technology, Technical Symposium & Workshop (SERDP/ESTCP), Dec. 2-4, **2003**, Washington, DC, USA.
12. Monteil-Rivera F, Manno D, Balakrishnan VK, Fournier D, Hawari J. Behavior of CL-20 in natural soil environments, Remediation of Chlorinated and Recalcitrant Compounds: The Fourth International Conference, May 24-27, **2004**, Monterey, CA, USA.

13. Fournier D, Bhatt M, Halasz A, Spain JC, Hawari J. Aerobic Degradation of the cyclic nitramines HMX and CL-20 by *Phanerochaete chrysosporium*. 104th General Meeting of the American Society for Microbiology (ASM), May 23-27, **2004**, New Orleans, LA, USA.
14. Halasz A, Groom C, Paquet L, Hawari J. Detection of nitroaromatics and cyclic nitramines by mass spectrometry (CE/MS and LC/MS). 6th International Symposium on Advances in Extraction Technologies (ExTech), Sept 6-8, **2004**, Leipzig, Germany.
15. Monteil-Rivera F, Halasz A, Bhushan B, Spain JC, Hawari J. Degradation routes of CL-20, Partners in Environmental Technology, Technical Symposium & Workshop (SERDP/ESTCP), Nov. 30-Dec. 2, **2004**, Washington, DC, USA.
16. Bardai G, Sunahara GI, Spear P, Martel M, Gong P, Hawari J. Effects of dietary administration of CL-20 to the Japanese quail (*Coturnix coturnix japonica*). Partners in Environmental Technology, Technical Symposium & Workshop (SERDP/ESTCP), Nov. 30-Dec. 2, **2004**, Washington, DC, USA.
17. Bardai G, Spear PA, Halasz A, Hawari J, Dodard S, Grosse S, Hoang J, Sunahara GI. Biotransformation of CL-20: New Toxicant Old Enzyme. TOXEN Conference Dec 9, **2005**. Montreal, Quebec
18. Bardai, G, Hawari J, Halasz A, Dodard S, Spear PA, Grosse S, Hoang J, Sunahara GI. Purification of a cytosolic GST from Japanese quail (*Coturnix coturnix japonica*) and the rabbit (*Oryctolagus cuniculus*) capable of biotransforming CL-20. Society of Environmental Toxicology and Chemistry. **2005**. 13 Nov- 17 Nov. Baltimore, MY.
19. Bardai G, Hawari J, Halasz A, Dodard S, Spear PA, Grosse S, Hoang J, Sunahara GI. Purification of Japanese quail and rabbit cytosolic glutathione S-transferases capable of biotransforming CL-20. 2005. Proceedings of the 32nd Annual Aquatic Toxicity Workshop: October 3 to 5 Waterloo, ONT.
20. Hawari et al. **2005** Laboratory Research Findings on the Environmental Behavior of the New Energetic Chemical, CL-20. SERDP 2005, 29Nov-2Dec), Washington, USA
21. Biotransformation of CL-20 by glutathione S-transferase. Proc of the 32nd Annual Aquatic Toxicity Workshop Oct 2-5, **2005**, Waterloo, Canada.
22. Environmental Biotechnology at BRI, NRCC, (Sep 9, 2004): UFZ: Center for Environmental Sciences, Leipzig, Germany

Award(s)

1. NRC-CANADA Outstanding achievement award-external recognition (**2004**)
2. UQAM-TOXEN Best Student Oral Presentation (**2005**)
3. Co-recipient of TTCP Frances Beaupre Award, UK: Fate and Impact of ECs (**2005**)

Students

1. Dominic Manno, **2003**, DEC Ecology, College Vannier, Montreal, Canada.
2. Mathieu Gautier, **2003**, MSc Chemistry, University of Poitiers, France.
3. Aurelian Corbeanu, **2004**, BSc Chemistry, University of Concordia, Montreal, Canada.
4. Mélissa Banville, **2004**, BSc Chemistry, University of Montreal, Canada.
5. Frédérique Matteau, **2004**, DEC Ecology, College Vannier, Montreal, Canada.
6. Ghalib Bardai, **2004**, MSc Environmental Toxicology, UQAM, Montreal, Canada.

Related Technical reports

1. Toxicity of Nitro-Heterocyclic and Nitroaromatic Energetic Chemicals to terrestrial Plants in a Natural Sandy Loam Soil, April 2005, US Army Research, Development and Engineering Command Edgewood Chemical Biological Center ECBC-TR-351, Aberdeen Proving Ground, MD 21010-5424.
2. *In ovo* Effects of Selected Energetic Substances on the Japanese Quail (*coturnix coturnix japonica*) Embryo (Report submitted to Sonia Thiboutot, DRDC Valcartier, DND Canada). NRCC # 45940
3. Characterization and Degradation of RDX, HMX and CL-20 in Soil, Sediments and Water. Final Report submitted to Sonia Thiboutot, DRDC, DND, Valcartier, Quebec, **June 10, 2005**, 175 pages + annexes. NRC # 47238
4. Characterization and Degradation of RDX, HMX and CL-20 in Soil Sediments and Waters, Submitted to Sonia Thiboutot, DRDC, DND, Valcartier, Quebec, **July 2004**, 118 pages + annexes.
5. Environmental Fate and Transport of a New Energetic Material, CL-20 (SERDP CP1256), Submitted to Bob Holst, 901 N Stuart St. #303, Arlington, Virginia 22203, **2003**, 98 pages.
6. Environmental Fate and Transport of a New Energetic Material, CL-20 (SERDP CP1256), Submitted to Bob Holst, 901 N Stuart St. #303, Arlington, Virginia 22203, **2002**, 80 pages

Collaborations

1. DRDC, DND, Canada, Guy Ampleman, Sonia Thiboutot: Provision of potential degradation products of CL-20 as reference standards to determine degradation/biotransformation pathways
2. Georgia Institute of Technology (formerly AFRL, FL), Jim Spain: Aerobic degradation of CL-20 using soil isolates
3. US Army Edgewood Chemical Biological Center (ECBC), MD, Roman Kuperman: Comparison of Toxicity data
4. Pacific Northwest National Laboratories (PNNL), Richland, WA, Jim Szecsody: Comparison of sorption/desorption data.
5. Guelph University, Guelph, Canada, Nigel Bunce and Pascale Bonnin: Electrochemical decomposition of CL-20

Cooperative Development

1. US Army Engineer Research and Development Center, Vicksburg, MS, H. Fredrickson: Knowledge exchange on CL-20 biodegradation.
2. Center for Environmental Engineering, Stevens Institute of Technology, Hoboken, NJ, C. Christodoulates: Meetings and knowledge exchange on CL-20 biodegradation.
3. Mitretek Systems, Atlanta, GA; Catherine Vogel: information provided to draft a report documenting and comparing all available data on the physiochemical parameters, fate and transport properties, and toxicities for CL-20 and RDX. The target audience for this report will be DOD acquisition program managers, their environmental support staffs, and DOD policy makers
4. Cranfield University, Shrivenham, Swindon, United Kingdom; Dr. Bellamy: we crossed checked intermediate reductive degradation products of CL-20 from our system using

Fe(0)/CL-20 and his system using metal powders (Pb) and SnCl₂. Results were harmonic with each other

Other Contributors

1. A.T.K. Thiokol Propulsion, Brigham City, UT, USA, Scott Hamilton, Scott Lusk and Karen Anderson.
2. NAWCWD, China Lake, CA, USA, Robin Nissan
3. SERDP, Dr. Andrea Leeson, Dr. Charles J. Pellerin and Dr. Robert W. Holst.

Program Manager: Dr. Andrea Leeson

XXIV Appendix: Publications

Alkaline Hydrolysis of the Cyclic Nitramine Explosives RDX, HMX, and CL-20: New Insights into Degradation Pathways Obtained by the Observation of Novel Intermediates

VIMAL K. BALAKRISHNAN,
ANNAMARIA HALASZ, AND
JALAL HAWARI*

Biotechnology Research Institute,
National Research Council of Canada,
6100 Royalmount Avenue,
Montréal, Quebec, Canada H4P 2R2

Hexahydro-1,3,5-trinitro-1,3,5-triazine (RDX, **I**) and octahydro-1,3,5,7-tetranitro-1,3,5,7-tetrazocine (HMX) hydrolyze at pH > 10 to form end products including NO_2^- , HCHO, HCOOH, NH_3 , and N_2O , but little information is available on intermediates, apart from the tentatively identified pentahydro-3,5-dinitro-1,3,5-triazacyclohex-1-ene (**II**). Despite suggestions that RDX and HMX contaminated groundwater could be economically treated via alkaline hydrolysis, the optimization of such a process requires more detailed knowledge of intermediates and degradation pathways. In this study, we hydrolyzed the monocyclic nitramines RDX, MNX (hexahydro-1-nitroso-3,5-dinitro-1,3,5-triazine), and HMX in aqueous solution (pH 10–12.3) and found that nitramine removal was accompanied by formation of 1 molar equiv of nitrite and the accumulation of the key ring cleavage product 4-nitro-2,4-diazabutanal (4-NDAB, $\text{O}_2\text{NNHCH}_2\text{NHCHO}$). Most of the remaining C and N content of RDX, MNX, and HMX was found in HCHO, N_2O , HCOOH, and NH_3 . Consequently, we selected RDX as a model compound and hydrolyzed it in aqueous acetonitrile solutions (pH 12.3) in the presence and absence of hydroxypropyl- β -cyclodextrin (HP- β -CD) to explore other early intermediates in more detail. We observed a transient LC-MS peak with a $[\text{M}-\text{H}]$ at 192 Da that was tentatively identified as 4,6-dinitro-2,4,6-triaza-hexanal ($\text{O}_2\text{NNHCH}_2\text{NNO}_2\text{CH}_2\text{NHCHO}$, **III**) considered as the hydrolyzed product of **II**. In addition, we detected another novel intermediate with a $[\text{M}-\text{H}]$ at 148 Da that was tentatively identified as a hydrolyzed product of **III**, namely, 5-hydroxy-4-nitro-2,4-diaza-pentanal ($\text{HOCH}_2\text{NNO}_2\text{CH}_2\text{NHCHO}$, **IV**). Both **III** and **IV** can act as precursors to 4-NDAB. In the case of the polycyclic nitramine 2,4,6,8,10,12-hexanitro-2,4,6,8,10,12-hexaazaisowurtzitane (CL-20), denitration (two NO_2^-) also led to the formation of HCOOH, NH_3 , and N_2O , but neither HCHO nor 4-NDAB were detected. The results provide strong evidence that initial denitration of cyclic nitramines in

water is sufficient to cause ring cleavage followed by spontaneous decomposition to form the final products.

Introduction

The cyclic nitramines hexahydro-1,3,5-trinitro-1,3,5-triazine (RDX) and octahydro-1,3,5,7-tetranitro-1,3,5,7-tetrazocine (HMX) are highly energetic compounds used in various propellants and conventional munitions (Figure 1). The manufacturing and usage of these toxic munitions (1–3) have resulted in severe contamination of both soils and groundwater (4, 5), thus necessitating their safe removal from the environment.

Numerous investigations have established that the typical decomposition (photochemical (6–8), thermal (9, 10), microbiological (11–15), or hydrolytic (16–18)) of RDX produces end products including nitrite (NO_2^-), nitrous oxide (N_2O), N_2 , ammonia (NH_3), formaldehyde (HCHO), formic acid (HCOOH), and CO_2 . Hoffsommer and co-workers (16) reported that RDX degradation in alkaline medium was initiated by a single denitration step to first form pentahydro-3,5-dinitro-1,3,5-triazacyclohex-1-ene (**II**), which then hydrolyzed further leading to rapid ring cleavage and decomposition. While only a few studies have been conducted with HMX, it has been shown that HMX undergoes alkaline hydrolysis at a slower rate than RDX (17, 18), to give a product distribution (NO_2^- , N_2O , NH_3 , N_2 , and HCOOH) similar to that obtained with RDX (19). The polycyclic nitramine 2,4,6,8,10,12-hexaazaisowurtzitane (CL-20) has only recently been synthesized (20, 21). Therefore, little information is currently available on its chemical and biological activity and fate.

Recently, we showed that both *Rhodococcus* sp. strain DN22 (11) and light (350 nm) (8) can successfully decompose RDX in water via initial denitration to produce 4-nitro-2,4-diazabutanal (4-NDAB, $\text{O}_2\text{NNHCH}_2\text{NHCHO}$) as a major ring cleavage product in both cases. In addition the end products that we found in the previous photochemical (8) and enzymatic (11) studies are basically similar and included NO_2^- , N_2O , NH_3 , HCHO, CO_2 , and H_2NCHO .

While many of the end products of RDX hydrolysis are known, intermediates and decomposition pathways are not well understood. Heilmann et al. (18) suggested that RDX and HMX contaminated waters could be economically treated using granular activated carbon (GAC) to first adsorb the explosive, followed by off-line regeneration of the laden GAC through alkaline hydrolysis. However, for this technology to be optimized, knowledge of intermediates and the degradation pathways of these two monocyclic nitramines is critical both to predict their behavior and enhance their removal from the environment.

Since the end products of RDX decomposition during enzymatic biodegradation with strain DN22 (11) were similar to those obtained via both alkaline hydrolysis (16–18) and photolysis (8), we hypothesize that following initial denitration of the cyclic nitramine, ring cleavage, and subsequent decomposition is largely dictated by the aqueous chemistry of the resulting intermediates. Therefore, if other cyclic nitramines such as MNX (hexahydro-1-nitroso-3,5-dinitro-1,3,5-triazine), HMX, and CL-20 produce end products similar to those of RDX, then their decomposition mechanisms should also be similar (18, 19). Hence, our objective in the present study was to provide additional insight into the degradation pathways of these cyclic nitramines by first determining whether RDX, HMX, MNX, and CL-20 hydrolyzed

* Corresponding author phone: (514)496-6267; fax: (514)496-6265; e-mail: jalal.hawari@nrc.gc.ca.

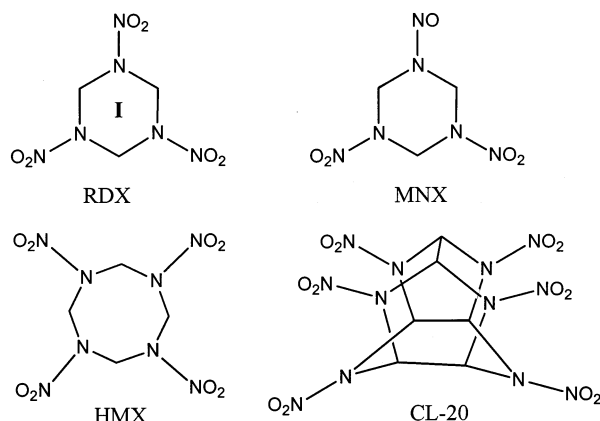


FIGURE 1. Representative structures of various cyclic nitramines.

in aqueous, alkaline (pH 10) conditions to produce similar end products. We then selected RDX as a model cyclic nitramine compound and hydrolyzed it in aqueous acetonitrile solutions (pH 12.3) in the presence and absence of hydroxypropyl- β -cyclodextrin (HP- β -CD) in an attempt to explore other early intermediates in more detail.

Experimental Section

Chemicals. Commercial grade RDX (purity > 99%), ring-labeled [^{15}N]-RDX (purity ca. 98%), HMX (purity > 99%), and hexahydro-1,3,5-trinitroso-1,3,5-triazine (TNX, 99% pure) were provided by the Defense Research and Development Canada (DRDC), Valcartier, Canada. 2,4,6,8,10,12-Hexanitro-2,4,6,8,10,12-hexaazaisowurtzitane (ϵ -CL-20) was provided by A.T.K. Thiokol Propulsion (Brigham City, UT). Hexahydro-1-nitroso-3,5-dinitro-1,3,5-triazine (MNX, 99% pure) was provided by R. Spanggord (SRI, Menlo Park, Ca). 4-Nitro-2,4-diazabutanol (4-NDAB) was obtained as described by Fournier et al. (11), and during revisions to this manuscript we confirmed its identity against an authentic sample of 4-NDAB synthesized by Dr. Jeffery Bottaro and Dr. Ron Spanggord (SRI, Menlo Park, CA). Methylene dinitramine was obtained from the rare chemical department, Aldrich, Canada. All other chemicals used in this work were reagent grade.

Hydrolyses of RDX, MNX, HMX, and CL-20 in Aqueous Solution at pH 10. To a series of dry 20 mL vials (each wrapped in aluminum foil) was added an aliquot of cyclic nitramine stock solution prepared in acetone. The acetone was evaporated in a fume hood, followed by the addition of 10 mL of a NaOH solution (pH 10) to give the following concentrations 215, 180, 110, and 100 mg L $^{-1}$ for RDX, MNX, HMX, and CL-20, respectively. The initial concentrations were kept well in excess of the maximum water solubility of each nitramine (ca. 50 mg L $^{-1}$ for RDX (22), 5 mg L $^{-1}$ for HMX (22), and 3.6 mg L $^{-1}$ for CL-20 (23)) in an attempt to generate sufficient amounts of intermediates to allow detection. The vials were sealed with Teflon coated serum caps and placed in a thermostated benchtop shaker at 30 °C and 200 rpm. Some vials were sparged with Argon for 2 h to allow analysis for N $_2$.

A second hydrolysis of HMX was also performed the same manner as described above, but at pH 12.3 instead of pH 10. The products formed at this elevated pH were identified after 60 h and after 120 h.

We used a gastight syringe to measure gaseous products (N $_2$ O and N $_2$) in the headspace, but for the analysis of the liquid medium we first quenched the reaction by adding an acidic MeCN solution (10 mL, pH 4.5). MeCN also solubilized undissolved starting material for subsequent analysis. The quenched vials were then stored in a refrigerator at 4 °C until analyzed.

Hydrolysis of RDX in 70% MeCN:30 H $_2$ O (v/v) Mixture.

RDX (0.1 g) or [^{15}N]-RDX was placed into a vial to which a 10 mL solution of NaOH (pH 12.3) in 70:30 (v/v) acetonitrile: water was added, giving an initial RDX concentration of 10 000 mg L $^{-1}$. MeCN was used to solubilize the high RDX concentration used, while a high pH was used to accelerate the reaction. The vial was sealed with a Teflon coated serum cap and placed in a thermostated benchtop shaker at 30 °C and 200 rpm. After 22 h, the reaction was quenched by the addition of HCl (1 M), and the mixture was then concentrated under reduced pressure (18 mmHg). The remaining mixture was passed through a column containing 3-aminopropyl-functionalized silica gel (Aldrich) using a 70% acetonitrile: 30% water (v/v) mixture to remove chloride and nitrite anions, preventing interference during LC-MS (ES $^{-}$) analysis (discussed below).

Hydrolysis of RDX in the Presence of Hydroxypropyl- β -cyclodextrin (HP- β -CD). HP- β -CD was used in an effort to stabilize putative early intermediates such as pentahydro-3,5-dinitro-1,3,5-triazacyclohex-1-ene (II) and its ring cleavage products (O $_2$ NNHCH $_2$ NNO $_2$ CH $_2$ NHCHO (III) and HOCH $_2$ -NNO $_2$ CH $_2$ NHCHO (IV)) by forming inclusion complexes. RDX (0.1 g) or [^{15}N]-RDX (0.1 g) was placed in a vial, followed by the addition of 10 mL of NaOH (pH 12.3) in 65:35 (v/v) acetonitrile:water containing 3% (wt/v) HP- β -CD. Hydrolysis and sample preparation for subsequent analysis was conducted as discussed above.

Analytical Procedures. The concentration of RDX, MNX, HMX, and CL-20 was determined using a reversed-phase HPLC connected to a photodiode array (PDA) detector, as described previously (11). Formaldehyde (HCHO) (24), [$^{15}\text{N}^{14}\text{NO}$] (45 Da), and [$^{14}\text{N}^{14}\text{NO}$] (44 Da) analyses were carried out as described by Sheremata and Hawari (25). Analyses of nitrite (NO $_2^{-}$), nitrate (NO $_3^{-}$), formate (HCOO $^{-}$), and ammonium (NH $_4^{+}$) were performed by capillary electrophoresis on a Hewlett-Packard 3D-CE equipped with a Model 1600 photodiode array detector and a HP capillary part number 1600-61232. The total capillary length was 64.5 cm, with an effective length of 56 cm and an internal diameter of 50 μm . For nitrite, nitrate, and formate, analyses were performed using sodium borate (25 mM) and hexamethonium bromide (25 mM) electrolytic solution at pH 9.2 (26). NH $_3$ (determined as NH $_4^{+}$) was analyzed using a formic acid (5 mM), imidazole (10 mM), and 18-crown-6 (50 mM) electrolytic solution at pH 5. In all cases, UV detection was performed at 215 nm (27).

A Micromass benchtop single quadrupole mass detector attached to a Hewlett-Packard 1100 Series HPLC system equipped with a DAD detector was used to analyze RDX ring cleavage intermediates. The samples were injected into a 4 μm -pore size Supelcosil CN column (4.6 mm i.d. \times 25 cm; Phenomenex, Torrance, Ca) at 35 °C. The solvent system was composed of 20% acetonitrile:80% water (v/v). For mass analysis, ionization was performed in a negative electrospray ionization mode, ES $^{-}$, producing mainly the deprotonated molecular mass ions [M - H]. The mass range was scanned from 30 to 400 Da with a cycle time of 1.6 s, and the resolution was set to 1 Da (width at half-height).

Results and Discussion

Alkaline Hydrolysis of Cyclic Nitramines: Product Distribution. Figure 2 shows that disappearance of RDX during hydrolysis in water (pH 10) is concomitant with the formation and accumulation of NO $_2^{-}$, N $_2$ O, and formaldehyde (HCHO). Although we were unable to detect formamide, we detected its hydrolyzed products HCOO $^{-}$ (0.18 μmol) and NH $_3$ (0.20 μmol , detected as NH $_4^{+}$). Amides are known to undergo spontaneous hydrolysis under alkaline conditions (28) to produce the corresponding amines and acids. Figure 2 also shows that the disappearance of RDX was accompanied by

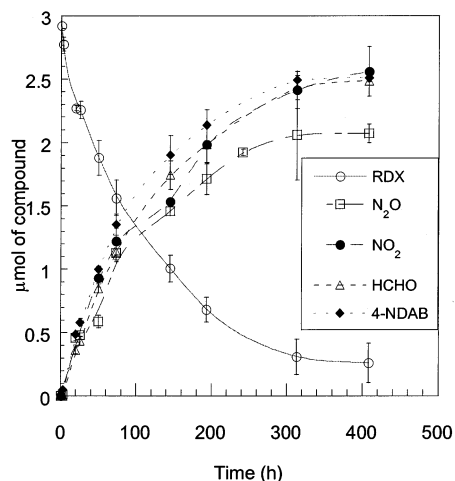


FIGURE 2. Time course of the alkaline hydrolysis of RDX at pH 10. Data points are the mean and error bars the standard deviation ($n = 3$).

the accumulation of the ring cleavage product 4-nitro-2,4-diazabutanal (4-NDAB, O_2NNHCH_2NHCHO), which was also a key product during photodenitration (8) and enzymatic degradation (11) of RDX. With the exception of our observation of 4-NDAB, the product distribution of the present RDX hydrolysis resembles that reported by Hoffsommer et al. (16), Croce and Okamoto (17), and Heilmann et al. (18).

Table 1 summarizes the normalized molar yields for the products obtained at the end of the hydrolysis experiments for RDX, MNX, HMX, and CL-20 at pH 10. From this table, it is apparent that the monocyclic nitramines (RDX, MNX, and HMX) lose 1 equiv of NO_2^- and form O_2NNHCH_2NHCHO (4-NDAB) as a major product. This is the first time that 4-NDAB formation has been conclusively demonstrated as a common feature in the alkaline hydrolyses of RDX, MNX, and HMX (Figure 3).

In addition to forming NO_2^- and 4-NDAB, MNX hydrolysis (see Supporting Information) produced N_2O (trace quantities), HCHO, and small amounts of $HCOO^-$ (0.35 μ mol) and NH_3 (0.33 μ mol) (Table 1), which presumably formed from the hydrolysis of formamide as discussed above. Likewise, HMX hydrolysis (Supporting Information) was accompanied by the release of 1 molar equiv of NO_2^- with the formation of the end products N_2O , HCHO, and 4-NDAB (Table 1). Since HMX hydrolyzes an order of magnitude more slowly than RDX (17), we followed only the first 5% of the reaction (i.e., 21 days) and were thus unable to unequivocally confirm the presence of NH_3 and $HCOO^-$. However, when we increased the pH to accelerate the reaction, we detected NH_3 and $HCOO^-$. After 60 h at pH 12.3, HMX decomposed to produce NO_2^- , N_2O , HCHO, 4-NDAB, NH_3 , and $HCOO^-$, just as we observed at pH 10 for RDX and MNX. Interestingly, after an additional 60 h at this elevated pH, 4-NDAB completely disappeared. This instability explains why 4-NDAB was not reported during earlier hydrolysis studies (16–19).

Finally, when we hydrolyzed CL-20 at pH 10 (Supporting Information), 2 molar equiv of NO_2^- were released instead of one and N_2O , NH_3 , and $HCOO^-$ formed, while HCHO and 4-NDAB did not (Table 1). The observation of NO_2^- emphasized once again the importance of initial denitration in the subsequent decomposition of CL-20. However, our inability to observe 4-NDAB is not surprising in view of the structural differences between the rigid caged polycyclic CL-20 which is characterized by the presence of C–C bonds (elongated) that are absent in the case of the monocyclic ones (Figure 1). CL-20 hydrolysis occurred at a faster rate ($1.09 \times 10^{-2} h^{-1}$) than was observed for either RDX ($7.21 \times$

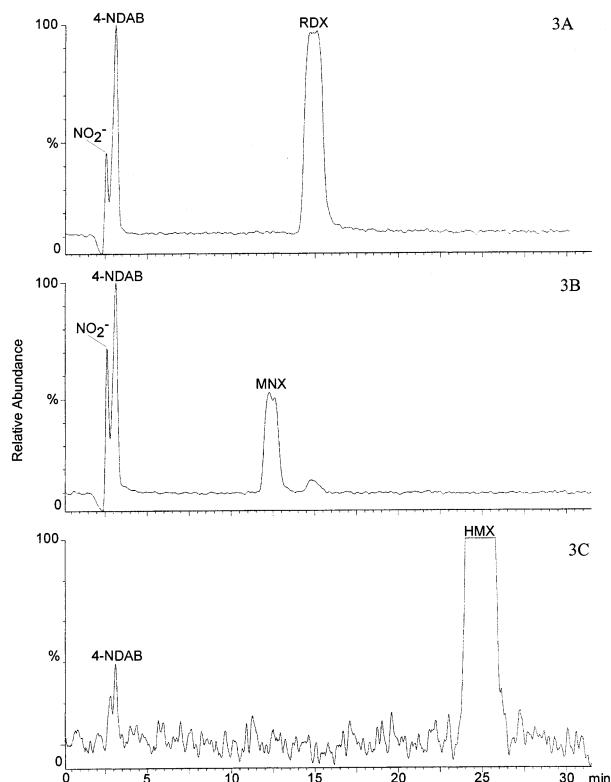


FIGURE 3. Typical LC/MS chromatograms of intermediates formed during hydrolysis of cyclic nitramines RDX, MNX and HMX in aqueous media at pH 10. (A) RDX after 8 days, (B) MNX after 1 day, (C) HMX after 15 days. Note that 4-nitro-2,4-diazabutanal (4-NDAB) appears as a key product in each case.

$10^{-3} h^{-1}$) or HMX ($\sim 1 \times 10^{-4} h^{-1}$) but slower than we found for MNX ($2.83 \times 10^{-2} h^{-1}$). The faster rate of hydrolysis observed with CL-20 compared to RDX and HMX decomposition most likely arises from the highly strained nature of the polycyclic nitramine cage (29), which renders CL-20 more susceptible to nucleophilic attack.

We were unable to observe any RDX nitroso products (hexahydro-1-nitroso-3,5-dinitro-1,3,5-triazine (MNX), hexahydro-1,3-dinitroso-5-nitro-1,3,5-triazine (DNX), and hexahydro-1,3,5-trinitroso-1,3,5-triazine (TNX)), which is also consistent with other reports on the alkaline hydrolysis of RDX (16–18). Indeed we found that hydrolysis on MNX under the same conditions failed to produce the dinitroso (DNX) or the trinitroso (TNX) compounds. Likewise, when we hydrolyzed HMX and CL-20 at pH 10, none of their corresponding nitroso products were observed. These results provide strong evidence that initial denitration is a key step responsible for the decomposition of cyclic nitramines in water.

For RDX, we found a C mass balance of 97% distributed as follows: HCHO (31.3%), HCOOH (2.3%), and O_2NNHCH_2NHCHO (63.4%) and a N mass balance of 90.7% distributed as follows: NO_2^- (16.2%), N_2O (25.6%), NH_3 measured as NH_4^+ (1.3%), and O_2NNHCH_2NHCHO (47.6%). For MNX, we found a C mass balance of 87.8% in HCHO (26.6%), HCOOH (5.05%), and O_2NNHCH_2NHCHO (56.1%) and a N mass balance of 60.45% distributed as follows: NO_2^- (15.6%), N_2O (0.14%), NH_3 measured as NH_4^+ (2.35%), and O_2NNHCH_2NHCHO (42.1%). Whereas for HMX, we found a C mass balance of 90% distributed as follows: HCHO (46.2%), O_2NNHCH_2NHCHO (43.8%) and a N mass balance of 86% distributed as follows: NO_2^- (14.7%), N_2O (38.5%), O_2NNHCH_2NHCHO (32.8%).

Identification of Early Intermediates in RDX Hydrolysis.

In none of the LC/MS chromatograms shown (Figures 3 and

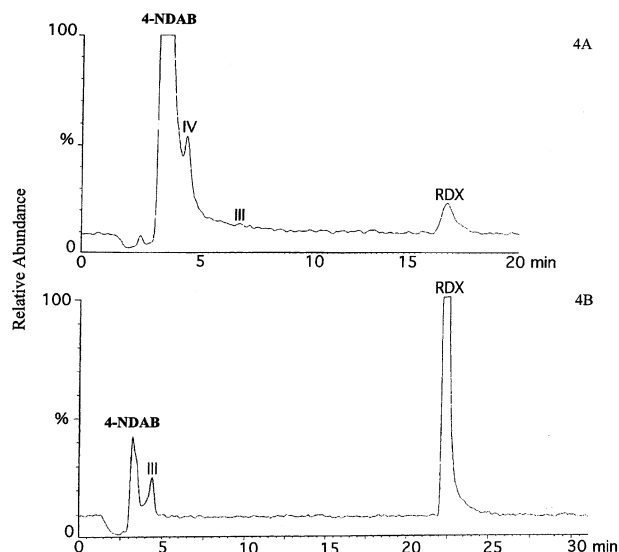


FIGURE 4. LC/MS chromatograms of RDX and the early intermediates formed during its degradation in acetonitrile:water (70:30% v/v) at pH 12.3. (A) In the absence of HP β CD and (B) in the presence of HP β CD (3% w/v). In the case of (B), the chromatogram was obtained using a SynergiPolar-RP column (4.6 mm id. \times 15 cm; Phenomenex, Torrance, CA) at 25 $^{\circ}$ C, and eluted using a methanol:water gradient. III: 4,6-dinitro-2,4,6-triaza-hexanal, IV: 5-hydroxy-4-nitro-2,4-diaza-pentanal.

4) were we able to directly detect pentahydro-3,5-dinitro-1,3,5-triaza-1-ene (**II**). Since **II** is an enamine, it should react quite readily with water through its reactive $\text{C}=\text{N}$ bond (30), and in fact, it is known that **II** hydrolyzes at a rate 5 orders of magnitude higher than RDX (**I**) (16, 17). Therefore, we hydrolyzed RDX in a MeCN:H₂O mixture in the presence and absence of HP- β -CD in an attempt to generate and stabilize sufficient amounts of **II** and other suspected key intermediates to allow their detection.

Figure 4A shows that RDX hydrolysis in a MeCN:H₂O mixture (70% v/v) produced 4-NDAB (r.t. 3.6 min) and two additional peaks marked **III** (r.t. 6.7 min) and **IV** (r.t. 4.4 min). **III** was detected only in trace amounts, but, as discussed below, the presence of HP- β -CD increased its yield (Figure 4B). Figure 5A shows **III** with a $[M - H]$ at 192 Da, matching a molecular mass formula of $\text{C}_3\text{H}_7\text{N}_3\text{O}_5$, and three other mass ion fragments at 46, 61, and 118 Da, representing $-\text{NO}_2$, $-\text{NHNO}_2$, and the deprotonated mass ion of $\text{O}_2\text{NNHCH}_2\text{NHCHO}$ (4-NDAB), respectively. When ring-labeled [^{15}N]-RDX was used, the $[M - H]$ ion appeared at 195 Da, confirming that this intermediate contained all three ^{15}N atoms originally present in the ring structure of RDX. In addition, the mass ion fragments appearing at 118 and 61 Da were shifted to 120 Da ($\text{O}_2^{14}\text{N}^{15}\text{NHCH}_2^{15}\text{NHCHO}$) and 62 Da ($^{15}\text{NH}^{14}\text{NO}_2$), respectively. We tentatively identified **III** as the ring cleavage intermediate 4,6-dinitro-2,4,6-triaza-hexanal ($\text{O}_2\text{NNHCH}_2\text{NNO}_2\text{CH}_2\text{NHCHO}$), considered as a hydrolyzed product of the presumably formed denitrated cyclohexene intermediate (**II**). Previously, we demonstrated that RDX photolysis in aqueous solution in a Rayonet photoreactor at 350 nm also produced intermediate $\text{O}_2\text{NNHCH}_2\text{NNO}_2\text{CH}_2\text{NHCHO}$, which was also attributed to the hydration of the initially formed denitrated intermediate **II** (8). This, however, is the first report of the formation of intermediate $\text{O}_2\text{NNHCH}_2\text{NNO}_2\text{CH}_2\text{NHCHO}$ via the alkaline hydrolysis of RDX.

Meanwhile, the peak labeled **IV** exhibited a $[M - H]$ at 148 Da, matching a molecular mass formula of $\text{C}_3\text{H}_7\text{N}_3\text{O}_4$. **IV** showed three other mass ion fragments at 46, 61, and 118 Da, representing $-\text{NO}_2$, $-\text{NHNO}_2$, and the $[M - H]$ of O_2 -

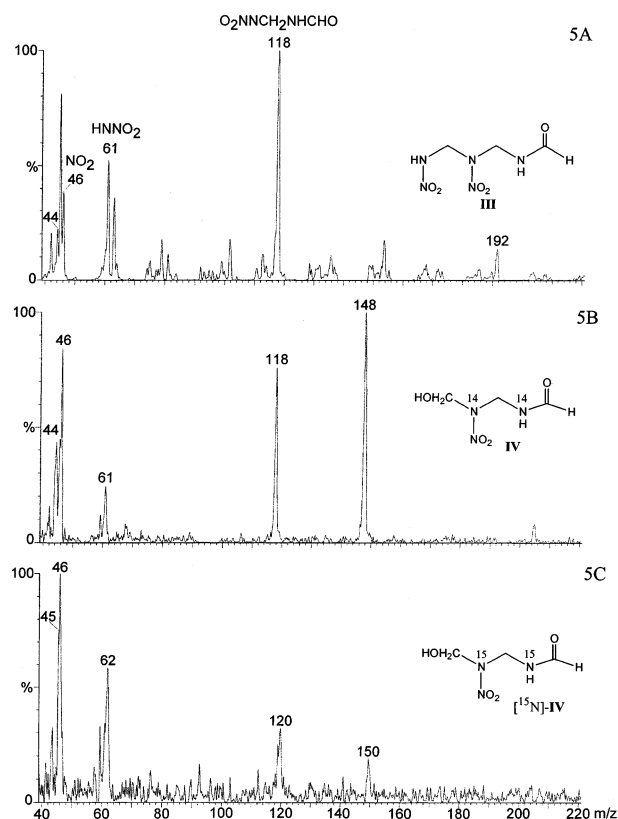


FIGURE 5. LC-MS (ES) mass spectra of 4,6-dinitro-4,6-diaza-hexanal (**III**) (A), 5-hydroxy-4-nitro-2,4-diaza-pentanal (**IV**) (B), and its ^{15}N labeled analogue ^{15}N -IV (C).

$\text{NNHCH}_2\text{NHCHO}$, respectively (Figure 5B). When ring-labeled [^{15}N]-RDX was used, the $[M - H]$ ion of **IV** shifted to 150 Da (Figure 5C), indicating that the intermediate contained only two of the three ring-labeled ^{15}N atoms in RDX. In addition, the $[M - H]$ peaks that were detected at 118 and 61 Da shifted to 120 ($\text{O}_2^{14}\text{N}^{15}\text{NHCH}_2^{15}\text{NHCHO}$) and 62 Da ($^{15}\text{NH}^{14}\text{NO}_2$) Da, respectively. Therefore, we suggested that the $[M - H]$ peak detected at 148 Da arose from the ring cleavage product 5-hydroxy-4-nitro-2,4-diaza-pentanal ($\text{HOCH}_2\text{NNO}_2\text{CH}_2\text{NHCHO}$, **IV**) that likely formed upon hydrolysis of $\text{O}_2\text{NNHCH}_2\text{NNO}_2\text{CH}_2\text{NHCHO}$ (**III**).

When we hydrolyzed RDX (1% w/v) in the presence of 3% HP- β -CD in a 65:35 (v/v) acetonitrile:water mixture at pH 12.3, we only observed **III** and 4-NDAB (Figure 4B). As indicated above, we had hoped that the use of HP- β -CD during the hydrolysis of **I** would stabilize its initial denitrated intermediate (**II**) through the formation of an inclusion complex and thus facilitate its detection. Instead, it appears that the addition of HP- β -CD stabilized **III** and allowed its unequivocal detection.

Decomposition Pathways of RDX. Based on product distribution and mass balance studies (Table 1) and the critical observation that denitration was a key step responsible for degradation of cyclic nitramines we proposed a degradation pathway for RDX as shown in Figure 6. The novel input in the present study is the discovery of several ring cleavage products including **III**, **IV**, and 4-NDAB (Figure 6). Although we were unable to detect the initially denitrated intermediate 3,5-dinitro-1,3,5-triazacyclohex-1-ene (**II**) due to its rapid hydrolysis in water (16), we were able to detect its hydrolyzed product **III**.

Figure 2 shows that for every mole of RDX that disappears, approximately 1 mol of 4-nitro-2,4-diaza-butanal (4-NDAB) is formed. However, we found that the disappearance of 0.14 μmol of RDX was accompanied by the formation of only 0.04

TABLE 1. Normalized Molar Yields of the Products Obtained upon Alkaline Hydrolysis (pH 10) of the Cyclic Nitramines RDX, MNX, HMX, and CL-20^d

cyclic nitramine	NO ₂ ⁻	N ₂ O	NH ₄ ⁺	4-NDAB	HCHO	HCOO ⁻
RDX ^a	0.972 ± 0.056	0.770 ± 0.130	0.075 ± 0.032	0.951 ± 0.005	0.939 ± 0.037	0.070 ± 0.005
MNX ^a	0.935 ± 0.005	0.008 ± 0.001	0.141 ± 0.035	0.842 ± 0.032	0.800 ± 0.027	0.152 ± 0.008
HMX ^b	1.15 ± 0.03	1.48 ± 0.06	nd ^c	0.859 ± 0.016	1.82 ± 0.04	nd ^c
CL-20 ^b	1.91 ± 0.09	0.910 ± 0.100	0.793 ± 0.049	not formed	not formed	0.493 ± 0.007

^a Values are the average of data from three replicate measurements; error values are the standard deviation. ^b Values are the average of data from duplicate measurements; error values are the standard deviation. ^c Due to its slow reaction rate, monitoring of HMX hydrolysis was stopped after 21 days. It is possible that NH₃ and HCOO⁻ formed but were at levels less than the detection limit of the capillary electrophoresis method. ^d Values were calculated from the product concentrations obtained at the end of each experiment, and the stoichiometries are calculated based on the number of moles of product observed for each mole of reactant consumed.

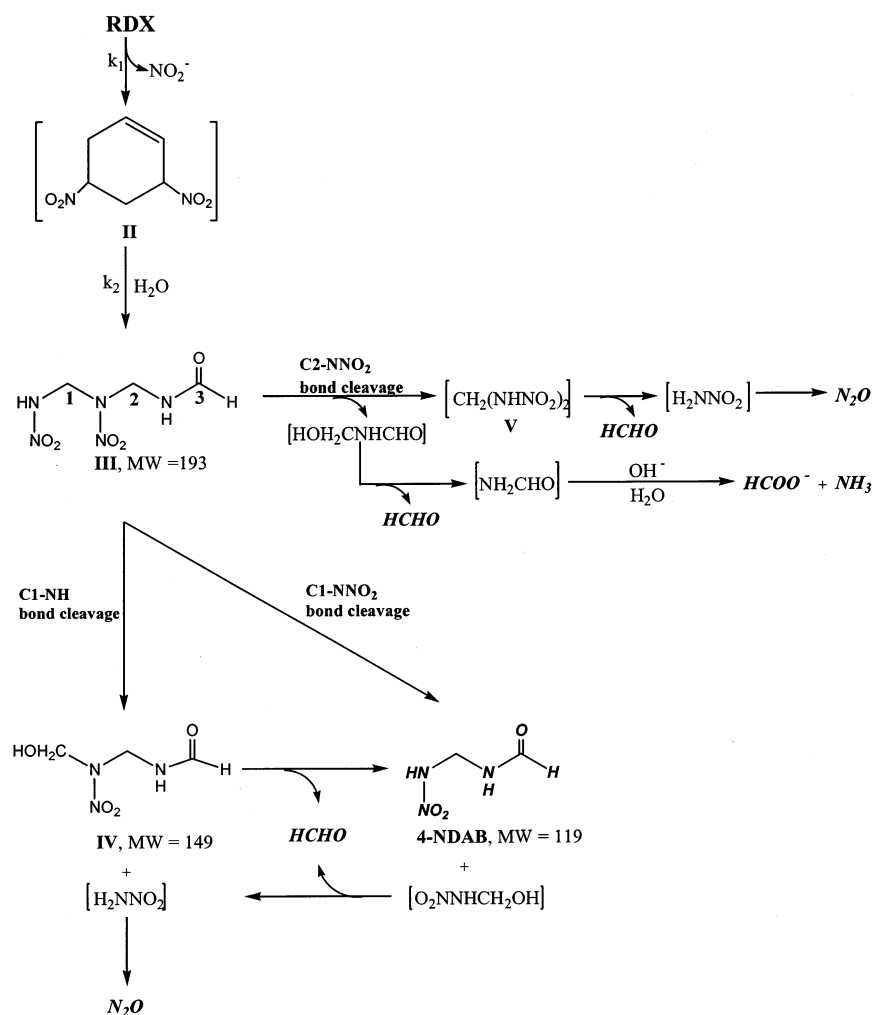


FIGURE 6. Major (attack at C1) and minor (attack at C2) pathways for the alkaline hydrolysis of RDX. Bracketed compounds were not observed.

μmol of 4-NDAB during the first 3 h, suggesting that there are intermediates en route to 4-NDAB. Also, both intermediates **III** and **IV** were found to contain a strong mass ion fragment at 118 Da (Figure 5) assigned to 4-NDAB, indicating that both **III** and **IV** act as precursors to the dead end product 4-NDAB.

Intermediates **III** and **IV** have different C–N bonds that are subject to hydrolytic cleavage. A plausible route for the formation of the novel intermediate observed with a $[\text{M} - \text{H}]$ at 148 Da (**IV**) could be via nucleophilic attack by OH^- at the C atom of the NH–C1 bond in **III**, accompanied by the loss of NH_2NO_2 (Figure 6). **IV** could then decompose to form 4-NDAB and HCHO. Alternatively, cleavage of the C1–NNO₂ bond in **III** would directly give rise to 4-NDAB and

hydroxymethyl nitramide, $\text{O}_2\text{NNHCH}_2\text{OH}$ (Figure 6). However $\text{O}_2\text{NNHCH}_2\text{OH}$, being an α -hydroxyalkyl nitramine, is expected to be unstable in water and should thus decompose to HCHO and N_2O (31). Finally, cleavage at the C2–NNO₂ bond in **III** would lead to the production of methylene dinitramine (**V**) and formamide, NH_2CHO (Figure 6). Although **V** was not detected, its presence cannot be excluded since it decomposes rapidly under alkaline conditions to produce HCHO and N_2O (32).

Clearly, nucleophilic attack at the C1 position in **III** is favored because C1, being surrounded on both sides by stronger electron-withdrawing nitramine groups, is more electrophilic than C2. Consequently, C1 is more susceptible to nucleophilic attack by OH^- than C2, explaining why attack

at C2 (producing HCOO^- and NH_4^+) is of only minor importance (Table 1). Interestingly, we observed **III** during both RDX photodenitration at 350 nm (8) and the present alkaline hydrolysis but were unable to observe **IV** prior to this work. However, the C1–NH bond cleavage that produces **IV** (Figure 6) is favored only when the solution pH exceeds the nitramine $\text{p}K_a$ of 6.55 (33), at which point nitramine can serve as a leaving group. Hence, we were able to observe intermediate **IV** during alkaline hydrolysis at pH 10 but not during photolysis at pH 5.5 (8).

The pathway proposed previously for photodenitration (8) is strikingly similar to the one proposed in the present study. However, in contrast to the single denitration event seen during either alkaline hydrolysis (present study) or photodenitration (8), Fournier et al. (11) reported the occurrence of two enzymatic denitration events en route to producing 4-NDAB. However, under extreme conditions ($[\text{NaOH}] > 19 \text{ M}$), the occurrence of two denitration events has been reported for RDX (16).

Both MNX and HMX also hydrolyze via initial denitration to produce NO_2^- , followed by a ring cleavage and spontaneous decomposition to N_2O , HCHO , and 4-NDAB. These findings indicate that the mechanism postulated for the alkaline hydrolysis of RDX applies more broadly to other monocyclic nitramine explosives. For MNX, the analogous intermediate to **III** is $\text{ONNHC}^*\text{H}_2\text{NNO}_2\text{C}^*\text{H}_2\text{NHCHO}$ (4-nitro-6-nitroso-2,4,6-triaza-hexanal). Since the C-2 position of this analogue is expected to be more electrophilic than the C-2 position in **III** itself, it becomes more amenable for nucleophilic substitution by OH^- . As a result, the minor pathway producing NH_3 and HCOO^- is of somewhat more importance with MNX than it is for RDX (see Table 1 for product distribution).

Finally, although the polycyclic nitramine CL-20 is structurally different from the monocyclic RDX, MNX, and HMX, its decomposition was also found to proceed via initial denitration (2 molar equiv of NO_2^-) to give end products including N_2O , NH_3 , and HCOO^- (Table 1). However, further studies are warranted to determine its intermediates and other ring cleavage products.

In conclusion, the present results confirm the hypothesis that a successful initial (primary) attack, denitration in this case, is the most critical step in the degradation of monocyclic and polycyclic nitramines. Once denitration occurs, ring cleavage becomes spontaneous and is dictated by the chemistry of the ensuing intermediates in water. The similarities observed in the decomposition patterns of cyclic nitramines under various chemical (present study), photochemical (8), and biochemical (11) conditions suggest that the employment of a more rapid chemical denitration process might serve as a useful probe into the early stages of the enzymatic and microbial mechanisms responsible for their decomposition.

Acknowledgments

The authors thank L. Paquet, C. Beaulieu, A. Corriveau, S. Deschamps, C. Groom, and P. D'Cruz for their technical assistance. V.K.B. thanks the Natural Sciences and Engineering Research Council and the National Research Council of Canada for a Fellowship. We also thank G. Ampleman and S. Thiboutot (DRDC, Valcartier, Canada) for providing RDX and HMX and Thiokol Propulsion (Brigham City, UT) for providing CL-20. Funding was provided by the U.S. DoD/DoE/EPA Strategic Environmental Research and Development Program (SERDP 1213 and SERDP 1256).

Supporting Information Available

Time course for the alkaline hydrolyses of MNX (Figure S1) and CL-20 (Figure S2) and product distribution for the alkaline

hydrolysis of HMX at pH 10 (Table S1). This material is available free of charge via the Internet at <http://pubs.acs.org>.

Literature Cited

- Robidoux, P. Y.; Hawari, J.; Thiboutot, S.; Ampleman, G.; Sunahara, G. *Environ. Pollut.* **2001**, *111*, 283.
- Talmage, S. S.; Opreko, D. M.; Maxwell, C. J.; Welsh, C. J. E.; Cretella, F. M.; Reno, P. H.; Daniel, F. B. *Rev. Environ. Contam. Toxicol.* **1999**, *161*, 1.
- McLellan, W.; Hartley, W. R.; Brower, M. *Health advisory for hexahydro-1,3,5-trinitro-1,3,5-triazine*; Technical Report PB90-273533; Office of Drinking Water, U.S. Environmental Protection Agency: Washington, DC, 1988.
- Myler, C. A.; Sisk, W. In *Environmental Biotechnology for Waste Treatment*; Saylor, G. S., Fox, R., Blackburn, J. W., Eds.; Plenum Press: New York, NY, 1991; p 137.
- Haas, R.; Schreiber, I.; von Low, E.; Stork, G. *Fresenius' J. Anal. Chem.* **1990**, *338*, 41.
- Bose, P.; Glaze, W. H.; Maddox, S. *Water Res.* **1998**, *32*, 1005.
- Peyton, G. R.; Lefavre, M. H.; Maloney, S. W. *CERL Technical Report 99/93*; (www.CECER.Army/TechReports); 1999.
- Hawari, J.; Halasz, A.; Groom, C.; Deschamps, S.; Paquet, L.; Beaulieu, C.; Corriveau, A. *Environ. Sci. Technol.* **2002**, *36*, 5117.
- Zhao, X.; Hints, E. J.; Lee, Y. T. *J. Chem. Phys.* **1988**, *88*, 801.
- Behrens, R., Jr.; Bulusu, S. *J. Phys. Chem.* **1991**, *95*, 5838.
- Fournier, D.; Halasz, A.; Spain, J.; Furesek, P.; Hawari, J. *Appl. Environ. Microbiol.* **2002**, *68*, 166.
- Oh, B. T.; Just, C. L.; Alvarez, P. J. *Environ. Sci. Technol.* **2001**, *35*, 4341.
- Coleman, N. V.; Nelson, D. R.; Duxbury, T. *Soil Biol. Biochem.* **1998**, *30*, 1159.
- Kitts, C. L.; Green, C. E.; Otley, R. A.; Alvarez, M. A.; Unkefer, P. J. *Can. J. Microbiol.* **2000**, *46*, 278.
- McCormick, N. G.; Cornell, J. H.; Caplan, A. M. *Appl. Environ. Microbiol.* **1981**, *42*, 817.
- Hoffsommer, J. C.; Kubose, D. A.; Glover, D. J. *J. Phys. Chem.* **1977**, *81*, 380.
- Croce, M.; Okamoto, Y. *J. Org. Chem.* **1979**, *44*, 2100.
- Heilmann, H. M.; Wiesmann, U.; Stenstrom, M. K. *Environ. Sci. Technol.* **1996**, *30*, 1485.
- Bishop, R. L.; Flesner, R. L.; Dell'Orco, P. C.; Spontarelli, T.; Larson, S. A.; Bell, D. A. *Ind. Eng. Chem. Res.* **1999**, *38*, 2254.
- Wardle, R. B.; Hinshaw, J. C.; Braithwaite, P.; Rose, M.; Johnson, G.; Jones, R.; Poush, K. Synthesis of the caged nitramine HNIW (CL-20) 27.1–27.10; 27th Int. Ann. Conf. ICT, ADPA, Arlington, VA, 1996.
- Nielsen, A. T.; Chafin, A. P.; Christian, S. L.; Moore, D. W.; Nadler, M. P.; Nissan, R. A.; Vanderah, D. J.; Gilardi, R. D.; George, C. F.; Flippin-Anderson, J. L. *Tetrahedron.* **1998**, *54*, 11793.
- Lynch, J. C.; Myers, K. F.; Brannon, J. M.; Delfino, J. J. *J. Chem. Eng. Data* **2001**, *46*, 1549.
- Groom, C. A.; Halasz, A.; Paquet, L.; D'Cruz, P.; Hawari, J. *J. Chromatogr. A* **2003**, in press.
- Summers, W. R. *Anal. Chem.* **1990**, *62*, 1397.
- Sheremata, T. W.; Hawari, J. *Environ. Sci. Technol.* **2000**, *34*, 3384.
- Okemgbo, A. A.; Hill, H. H.; Metcalf, S. G.; Bachelor, M. A. *J. Chromatogr. A* **1999**, *844*, 387.
- Beck, W. In *Applications of the HP 3D Capillary Electrophoresis System*; Heiger, D. N., Herold, M., Grimm, R., Eds.; Hewlett-Packard Company: Waldbronn, Germany, 1994; Vol. 1, p 53.
- Brown, R. S.; Bennet, A. J.; Slebocka-Tilk, H.; Jodhan, A. *J. Am. Chem. Soc.* **1992**, *114*, 3092.
- Zhao, X.; Shi, N. *Chinese Sci. Bull.* **1996**, *41*, 574.
- March, J. *Advanced Organic Chemistry*, 3rd ed.; Wiley-Interscience Publication, John Wiley & Sons: New York, U.S.A., 1985; pp 784–785.
- Halasz, A.; Spain, J.; Paquet, L.; Beaulieu, C.; Hawari, J. *Environ. Sci. Technol.* **2002**, *36*, 633.
- Lamberton, A. H.; Lindley, C.; Speakman, J. C. *J. Chem. Soc.* **1949**, 1650.
- Arrowsmith, C. H.; Awwal, A.; Euser, B. A.; Kresge, A. J.; Lau, P. P. T.; Onwood, D. P.; Tang, Y. C.; Young, E. C. *J. Am. Chem. Soc.* **1991**, *113*, 172.

Received for review September 30, 2002. Revised manuscript received February 18, 2003. Accepted February 28, 2003.

ES020959H

Biotransformation of 2,4,6,8,10,12-Hexanitro-2,4,6,8,10,12-Hexaazaisowurtzitane (CL-20) by Denitrifying *Pseudomonas* sp. Strain FA1

Bharat Bhushan,¹ Louise Paquet,¹ Jim C. Spain,² and Jalal Hawari^{1*}

Biotechnology Research Institute, National Research Council of Canada, Montreal, Quebec H4P 2R2, Canada,¹ and
U.S. Air Force Research Laboratory, Tyndall Air Force Base, Florida 32403²

Received 3 April 2003/Accepted 18 June 2003

The microbial and enzymatic degradation of a new energetic compound, 2,4,6,8,10,12-hexanitro-2,4,6,8,10,12-hexaazaisowurtzitane (CL-20), is not well understood. Fundamental knowledge about the mechanism of microbial degradation of CL-20 is essential to allow the prediction of its fate in the environment. In the present study, a CL-20-degrading denitrifying strain capable of utilizing CL-20 as the sole nitrogen source, *Pseudomonas* sp. strain FA1, was isolated from a garden soil. Studies with intact cells showed that aerobic conditions were required for bacterial growth and that anaerobic conditions enhanced CL-20 biotransformation. An enzyme(s) involved in the initial biotransformation of CL-20 was shown to be membrane associated and NADH dependent, and its expression was up-regulated about 2.2-fold in CL-20-induced cells. The rates of CL-20 biotransformation by the resting cells and the membrane-enzyme preparation were $3.2 \pm 0.1 \text{ nmol h}^{-1} \text{ mg}$ of cell biomass⁻¹ and $11.5 \pm 0.4 \text{ nmol h}^{-1} \text{ mg}$ of protein⁻¹, respectively, under anaerobic conditions. In the membrane-enzyme-catalyzed reactions, 2.3 nitrite ions (NO_2^-), 1.5 molecules of nitrous oxide (N_2O), and 1.7 molecules of formic acid (HCOOH) were produced per reacted CL-20 molecule. The membrane-enzyme preparation reduced nitrite to nitrous oxide under anaerobic conditions. A comparative study of native enzymes, dehaloenzymes, and a reconstituted enzyme(s) and their subsequent inhibition by diphenyliodonium revealed that biotransformation of CL-20 is catalyzed by a membrane-associated flavoenzyme. The latter catalyzed an oxygen-sensitive one-electron transfer reaction that caused initial N denitration of CL-20.

2,4,6,8,10,12-Hexanitro-2,4,6,8,10,12-hexaazaisowurtzitane (CL-20) is a high-energy polycyclic nitramine compound (17) with a rigid caged structure (Fig. 1). Due to its high energy content and superior explosive properties, it may replace conventionally used explosives such as hexahydro-1,3,5-trinitro-1,3,5-triazine (RDX) and octahydro-1,3,5,7-tetranitro-1,3,5,7-tetrazocine (HMX) in the future. The environmental, biological, and health impacts of this energetic chemical and its metabolic products are not known. The severe environmental contamination and biological toxicity of the widely used monocyclic nitramine explosives RDX and HMX are already well documented (11, 13, 16, 22). It is likely that due to its structural similarity with RDX and HMX, CL-20 may also pose a serious threat to the environment by contaminating soils, sediments, and groundwater. Therefore, the microbial degradation of CL-20 should be studied under in vitro and in vivo conditions in order to determine the reaction products and to gain insights into the mechanisms involved in its degradation.

Previous reports on the biodegradation and biotransformation of RDX and HMX by a variety of microorganisms (aerobic, anaerobic, and facultative anaerobes) and enzymes have shown that initial N denitration can lead to ring cleavage and decomposition (3, 5–6, 9, 12–15, 21, 26). In a recent study, Trott et al. (24) reported the aerobic biodegradation of CL-20 by the soil isolate *Agrobacterium* sp. strain JS71. The isolate

utilized CL-20 as the sole nitrogen source and assimilated 3 mol of nitrogen per mol of CL-20. However, no information was provided about the mechanism of CL-20 biodegradation.

In the present study, a denitrifying *Pseudomonas* sp. strain, FA1, that utilized CL-20 as a sole nitrogen source was isolated from a garden soil sample. The CL-20 biotransformation conditions were optimized in aqueous medium. The nature and function of the enzyme(s) responsible for the biotransformation of CL-20 by strain FA1 were studied. Stoichiometries of the products formed during the biotransformation of CL-20 by the membrane-associated enzyme(s) from *Pseudomonas* sp. strain FA1 were determined, and an initial enzymatic N denitration reaction mechanism is proposed.

MATERIALS AND METHODS

Chemicals. CL-20 in ϵ form and at 99.3% purity was provided by ATK Thiokol Propulsion, Brigham City, Utah. NADH, NADPH, diphenyliodonium chloride (DPI), flavin mononucleotide (FMN), flavin adenine dinucleotide (FAD), NaNO_2 , dicumarol, 2,2-dipyridyl, 2-methyl-1,2-di-3-pyridyl-1-propanone (metyrapone), and phenylmethanesulfonyl fluoride were purchased from Sigma Chemicals, Oakville, Ontario, Canada.

Nitrous oxide (N_2O) was purchased from Scott specialty gases, Sarnia, Ontario, Canada. Carbon monoxide (CO) was purchased from Aldrich Chemical Company, Milwaukee, Wis. All other chemicals were of the highest purity available.

Isolation and identification of the CL-20-degrading strain. One gram of garden soil was suspended in 20 ml of minimal medium (ingredients per liter of deionized water: K_2HPO_4 , 1.22 g; KH_2PO_4 , 0.61 g; NaCl, 0.20 g; MgSO_4 , 0.20 g; and succinate, 8.00 g [pH 7.0]) supplemented with CL-20 at a final concentration of $4.38 \text{ mg liter}^{-1}$ added from a $10,000\text{-mg liter}^{-1}$ stock solution made in acetone. The inoculated medium was incubated under aerobic conditions at 30°C on an orbital shaker (150 rpm) in the dark. The disappearance of CL-20 was monitored over several days. The enriched culture was plated periodically onto

* Corresponding author. Mailing address: Biotechnology Research Institute, National Research Council of Canada, 6100 Royalmount Ave., Montreal, Quebec H4P 2R2, Canada. Phone: (514) 496-6267. Fax: (514) 496-6265. E-mail: jalal.hawari@nrc.ca.

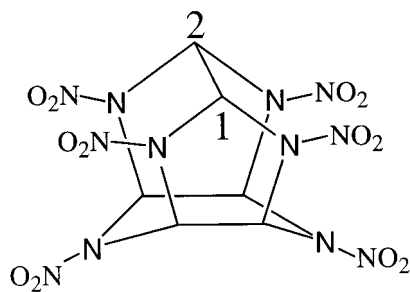


FIG. 1. Molecular structure of CL-20.

the same medium with 1.8% agar (Difco, Becton Dickinson and Co., Sparks, Md.), and surfaces of solidified agar plates were layered with $10 \mu\text{M}$ CL-20. The isolated colonies were subcultured three times with the same agar plates and were tested for their ability to biotransform CL-20 in liquid medium. Of the few isolated bacterial strains, a denitrifying strain capable of utilizing CL-20 as a sole nitrogen source, FA1, was selected for further study.

For identification and characterization of strain FA1, we used the standard biochemical techniques reported in *Bergey's Manual of Systematic Bacteriology* (19). Total cellular fatty acids (fatty acid methyl ester) analysis and 16S rRNA gene analysis were performed and analyzed by MIDI Laboratories (Newark, Del.).

Biotransformation studies with strain FA1. In biotransformation studies, CL-20 was added to the medium in concentrations above saturation levels (i.e., $\geq 10 \mu\text{M}$ or $4.38 \text{ mg liter}^{-1}$) from a $10,000\text{-mg liter}^{-1}$ stock solution made in acetone. The aqueous solubility of CL-20 has been reported as $3.6 \text{ mg liter}^{-1}$ at 25°C (10). Higher CL-20 concentrations were used in order to detect and quantify the metabolites which are otherwise produced in trace amounts during biotransformation. To determine the residual CL-20 during biotransformation studies, the media were inoculated in multiple identical batches of serum bottles. At each time point, the total CL-20 content in one serum bottle was solubilized in 50% aqueous acetonitrile and analyzed by a high-performance liquid chromatography (HPLC) (mentioned below).

A minimal medium (MM) was used for the CL-20 biotransformation studies and was composed of (per liter of deionized water) 1.22 g of K_2HPO_4 , 0.61 g of KH_2PO_4 , 0.20 g of NaCl, 0.20 g of MgSO_4 , 8.00 g of succinate, and 10 ml of trace elements (pH 7.0). Modified Wolfe's mineral solution was used as the trace element solution and was composed of (per liter of deionized water) 0.20 g of $\text{MnSO}_4 \cdot \text{H}_2\text{O}$, 0.10 g of $\text{CaCl}_2 \cdot 2\text{H}_2\text{O}$, 0.10 g of $\text{CoCl}_2 \cdot 6\text{H}_2\text{O}$, 0.15 g of ZnCl_2 , 0.01 g of $\text{CuSO}_4 \cdot 5\text{H}_2\text{O}$, 0.10 g of $\text{FeSO}_4 \cdot 7\text{H}_2\text{O}$, 0.05 g of Na_2MoO_4 , 0.05 g of $\text{NiCl}_2 \cdot 6\text{H}_2\text{O}$, and 0.05 g of $\text{Na}_2\text{WO}_4 \cdot 2\text{H}_2\text{O}$.

A comparative-growth experiment was performed with $(\text{NH}_4)_2\text{SO}_4$ and CL-20 as sole nitrogen sources to determine the number of nitrogen atoms from CL-20 that were incorporated into the biomass. Cells were grown in MM containing increasing concentrations of either $(\text{NH}_4)_2\text{SO}_4$ or CL-20 as a sole nitrogen source at 30°C under aerobic conditions on an orbital shaker (150 rpm) in the dark for 16 h. After the incubation period, the microbial growth yield in the form of total viable-cell counts were determined by a standard plate count method. In this method, the cultures were serially diluted in sterile phosphate-buffered saline (PBS) and spread plated onto Luria-Bertani agar plates (per liter of deionized water, 10 g of tryptone, 5 g of yeast extract, 10 g of NaCl, and 15 g of agar). All ingredients, except NaCl, were purchased from Becton Dickinson and Company. The plates were incubated at 30°C overnight. After incubation, the number of bacterial colonies grown in the plates was considered to determine the total viable-cell count per ml of the culture.

In order to determine the effect of alternate cycles of aerobic and anaerobic growth conditions on CL-20 biotransformation by the isolate FA1, cells were grown in MM containing 10 mM $(\text{NH}_4)_2\text{SO}_4$ and 25 μM CL-20 in two serum bottles under aerobic conditions up to a late log phase (optical density at 600 nm [OD_{600}], ~ 0.60), and then anaerobic conditions were created in one of the two growing cultures by flushing the headspace with argon for 30 min. The cultures were further grown to stationary phase. Growth and CL-20 disappearance in both serum bottles were monitored over the course of the experiment.

To determine whether the enzyme system responsible for CL-20 biotransformation was induced or constitutive, two batches of cells were grown in MM containing 10 mM $(\text{NH}_4)_2\text{SO}_4$ in the presence and absence of CL-20 (10 μM). At mid-log phase, the cells were harvested by centrifugation at 4°C and washed three times with PBS, pH 7.0. The washed cells (5 mg of wet biomass/ml) were

tested for their ability to biotransform CL-20 under aerobic and anaerobic conditions.

Preparation of cytosolic and membrane-associated enzymes. Bacterial cells were cultured in 2 liters of MM containing 10 mM $(\text{NH}_4)_2\text{SO}_4$ up to a mid-log phase (8 to 9 h; OD_{600} , 0.45) at 30°C and then induced with 10 μM CL-20. After induction, the cells were further incubated up to 12 to 16 h (OD_{600} , 0.95). Cells were harvested by centrifugation, washed three times with PBS (pH 7.0), and then suspended in 50 mM potassium phosphate buffer (pH 7.0) containing 1 mM phenylmethanesulfonyl acid and 100 mM NaCl. The washed cell biomass (0.2 g/ml) was subjected to disruption with a French press at $20,000 \text{ lb/in}^2$. The disrupted cell suspension was centrifuged at $9,000 \times g$ for 30 min at 4°C to remove cell debris and undisrupted cells. The supernatant was centrifuged at $165,000 \times g$ for 1 h at 4°C . The pellet (membrane protein fraction) and supernatant (soluble-protein fraction) thus obtained were separated and mixed with 10% glycerol, and aliquots were prepared and stored at -20°C until further use. The protein content was determined with a bicinchoninic acid protein assay kit from Pierce Chemical Company, Rockford, Ill.

Total flavin (FMN and FAD) contents in the crude extract, the membrane fraction, and the soluble-protein fractions were determined by a spectrophotometric method described by Aliverti et al. (1). Dehaloenzyme(s) and reconstituted dehaloenzyme(s) were prepared as described before (3).

Biotransformation assays. Enzyme-catalyzed biotransformation assays were performed under aerobic as well as anaerobic conditions in 6-ml glass vials. Anaerobic conditions were created by purging all the solutions with argon gas three times (10 min each time at 10-min intervals) and replacing the headspace air with argon in sealed vials. Each assay vial contained, in 1 ml of assay mixture, CL-20 (25 μM), NADH or NADPH (150 μM), a soluble-enzyme or membrane enzyme preparation (1.0 mg), and potassium phosphate buffer (50 mM, pH 7.0). Reactions were performed at 30°C . Different controls were prepared by omitting enzyme, CL-20, or NADH from the assay mixture. Boiled enzyme was also used as a negative control. Residual NADH or NADPH was measured as described before (3). Samples from the liquid and gas phases in the vials were analyzed for residual CL-20 and biotransformed products. The CL-20 biotransformation activity of the enzyme(s) was expressed as nanomoles per hour per milligram of protein unless otherwise stated.

The bioconversion of nitrite to nitrous oxide was determined by incubating 20 μM NaNO_2 with a membrane enzyme preparation using NADH as the electron donor. The disappearance of nitrite and the formation of nitrous oxide were measured periodically. Results were compared with those for a control without NaNO_2 .

Enzyme inhibition studies. Inhibition with DPI, an inhibitor of flavoenzymes that acts by forming a flavin-phenyl adduct (7), was assessed by incubating the enzyme preparation with DPI at different concentrations (0 to 2.0 mM) at room temperature for 30 min before CL-20 biotransformation activities were determined. Other enzyme inhibitors, such as dicumarol, carbon monoxide (60 s of bubbling through the enzyme solution), metyrapone, and 2,2-dipyridyl, were incubated with the enzyme preparation at different concentrations for 30 min at room temperature. Thereafter, the CL-20 biotransformation activity of the treated enzyme was determined.

Analytical procedures. CL-20 was analyzed with an HPLC connected to a photodiode array detector (λ , 230 nm). Samples (50 μl) were injected into a Supelcosil LC-CN column (4.6 mm [inside diameter] by 25 cm) (Supelco, Oakville, Ontario, Canada), and the analytes were eluted with an isocratic mobile phase of 70% methanol in water at a flow rate of 1.0 ml/min.

Nitrite (NO_2^-), nitrous oxide (N_2O), and formaldehyde (HCHO) were analyzed by previously reported methods (3–5).

Formic acid (HCOOH) was measured using an HPLC from Waters (pump model 600 and autosampler model 717 plus) equipped with a conductivity detector (model 430). The separation was made on a DIONEX IonPac AS15 column (2 by 250 mm). The mobile phase was 30 mM KOH, with a flow rate of 0.4 ml/min at 40°C . The detection of formic acid was enhanced by reducing the background with an autosuppressor from ALTECH (model DS-Plus), and the detection limit was 100 ppb.

Nucleotide sequence accession number. The 16S rRNA gene sequence of *Pseudomonas* sp. strain FA1 was deposited in GenBank under accession number AY312988.

RESULTS AND DISCUSSION

Isolation and identification of CL-20-degrading strain FA1.

The standard enrichment techniques were used to isolate CL-20-degrading strains from garden soil samples. The enrichment

experiments were carried out over a period of 3 weeks, and four CL-20-degrading strains designated FA1 to FA4 were isolated. Strain FA1 biotransformed CL-20 at a higher rate than those of the other isolates (data not shown) and was capable of utilizing CL-20 as a sole nitrogen source; therefore, it was selected for further study.

Strain FA2 was identified as a *Bacillus* species by 16S rRNA gene analysis, while strains FA3 and FA4 remained unidentified. FA1 was characterized by standard biochemical tests mentioned in *Bergey's Manual of Systematic Bacteriology* (19). Strain FA1 was a non-spore-forming, gram-negative, motile bacterium with a small rod structure (approximately 1.5 to 2.0 μm). Biochemically, it showed positive results for oxidase, catalase, and nitrite reductase and utilized succinate, fumarate, acetate, glycerol, and ethanol as sole carbon sources. It utilized CL-20, ammonium sulfate, ammonium chloride, and sodium nitrite as sole nitrogen sources. Total cellular fatty acid methyl ester analysis of strain FA1 showed a similarity index of 0.748 with *Pseudomonas putida* biotype A. On the other hand, 16S rRNA gene analysis showed that strain FA1 was 99% similar to *Pseudomonas* sp. strain C22B (GenBank accession number AF408939) isolated from a soil sample in a shipping container. No published data are available with regard to strain C22B. On the basis of the above data, we identified and named strain FA1 *Pseudomonas* sp. strain FA1.

Growth of strain FA1 on CL-20 as a nitrogen source. As mentioned above, strain FA1 was capable of utilizing CL-20, ammonium sulfate, ammonium chloride, and sodium nitrite as sole nitrogen sources. In order to determine the number of nitrogen atoms from CL-20 that were incorporated into biomass, cells were grown in MM containing different concentrations of either $(\text{NH}_4)_2\text{SO}_4$ or CL-20. After incubation, the growth yield in the form of total viable-cell counts was determined. The growth yield using CL-20 as the nitrogen source was about 1.83-fold higher than that observed with $(\text{NH}_4)_2\text{SO}_4$ (Fig. 2). No growth was observed in the control experiment without any nitrogen source. The ratio of growth yields in $(\text{NH}_4)_2\text{SO}_4$ to those in CL-20 (Fig. 2) indicated that of the 12 nitrogen atoms per CL-20 molecule, approximately 4 nitrogen atoms were assimilated into the biomass. In a previous report, a soil isolate, *Agrobacterium* sp. strain JS71, utilized CL-20 as a sole nitrogen source and assimilated 3 mol of nitrogen per mol of CL-20 (24).

Biotransformation of CL-20 by intact cells. In a study of the effect of an alternate cycle of aerobic and anaerobic growth conditions on CL-20 biotransformation, we observed that after anaerobic conditions were created in one of the two growing cultures at 9 h of growth, most of the CL-20 was biotransformed in the subsequent 2 h of incubation but that under aerobic conditions, it took more than 20 h to biotransform the same amount of CL-20 (Fig. 3). This experimental finding indicated that the growth of *Pseudomonas* sp. strain FA1 was faster under aerobic conditions and that CL-20 biotransformation by the mid-log-phase (8- to 9-h) culture was more rapid under anaerobic conditions.

An experiment with uninduced and CL-20 (10 μM)-induced cells showed CL-20 biotransformation activities of 1.4 ± 0.05 and $3.2 \pm 0.1 \text{ nmol h}^{-1} \text{ mg of protein}^{-1}$, respectively, indicating that CL-20 was biotransformed at a 2.2-fold-higher rate by the induced cells than by the uninduced cells. This experimen-

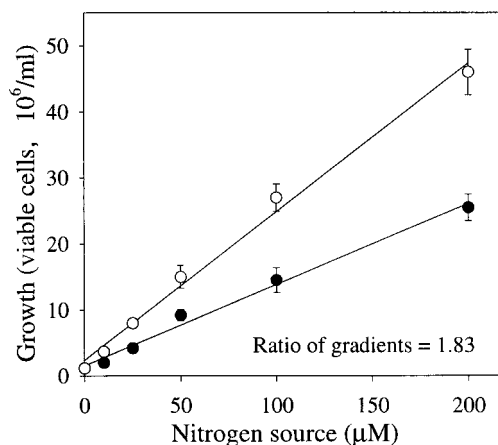


FIG. 2. Growth of *Pseudomonas* sp. strain FA1 at various concentrations of CL-20 (\circ) and $(\text{NH}_4)_2\text{SO}_4$ (\bullet). The viable-cell count in early-stationary-phase culture (16 h) was determined for each nitrogen concentration. The linear-regression curve for $(\text{NH}_4)_2\text{SO}_4$ has a gradient of 0.122 and an r^2 of 0.990. The linear-regression curve for CL-20 has a gradient of 0.224 and an r^2 of 0.992. Data are means of results from duplicate experiments, and error bars indicate standard errors. Some error bars are not visible due to their small size.

tal finding indicated that there may have been an up-regulation of an enzyme in the induced cells that might have been responsible for CL-20 biotransformation. In addition, the increase in activity may have been due to an improved uptake of CL-20 following induction of the cells with CL-20.

Localization of the enzyme(s) responsible for CL-20 biotransformation. The CL-20 biotransformation activities of cell crude extract, the cytosolic soluble enzyme(s), and the membrane enzyme(s) were determined under aerobic as well as anaerobic conditions. We found that all three enzyme fractions

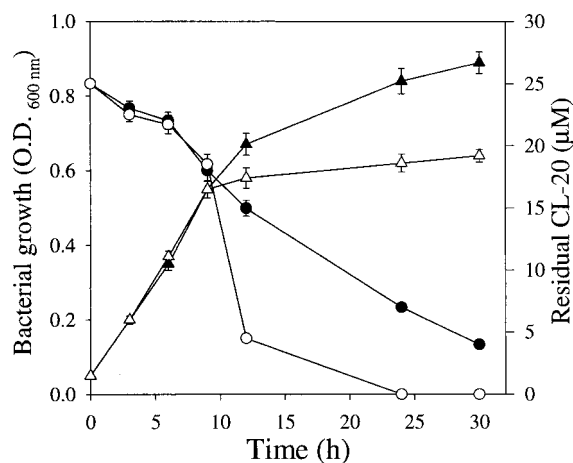


FIG. 3. Effects of an alternating cycle of aerobic and anaerobic growth conditions on the biotransformation of CL-20 by *Pseudomonas* sp. strain FA1. Shown are levels of growth (\blacktriangle) and CL-20 degradation (\bullet) under aerobic conditions. Open triangles and circles show the levels of growth and CL-20 biotransformation, respectively, under aerobic conditions (for the first 9 h) and then under anaerobic conditions. Data are means of results from triplicate experiments, and error bars indicate standard errors. Some error bars are not visible due to their small size.

TABLE 1. Effect of flavin contents in native- and deflavoenzyme preparations on the CL-20 biotransformation activities of various enzyme fractions from *Pseudomonas* sp. strain FA1 under anaerobic conditions^a

Enzyme(s)	Total flavin content in native enzyme(s) (nmol/mg of protein)	CL-20 biotransformation activity of native enzyme(s) (nmol h ⁻¹ mg of protein ⁻¹)	Total Flavin content in deflavoenzyme(s) (nmol/mg of protein)	CL-20 biotransformation activity of deflavoenzyme(s) (nmol h ⁻¹ mg of protein ⁻¹)
Cell crude extract	22.6 ± 1.3	15.6 ± 0.7	ND	ND
Cytosolic soluble enzyme(s)	5.5 ± 0.2	2.3 ± 0.05	1.2 ± 0.2	0.5 ± 0.05
Membrane-associated enzyme(s)	12.6 ± 0.6	11.5 ± 0.4	3.8 ± 0.3	2.7 ± 0.1

^a Data are means ± standard errors from triplicate experiments. ND, not determined.

exhibited higher activities under anaerobic conditions (Table 1) than those observed under aerobic conditions (data not shown). In the case of the membrane enzyme(s), CL-20 biotransformation was about fivefold higher under anaerobic conditions (11.5 ± 0.4 nmol h⁻¹ mg of protein⁻¹) than under aerobic conditions (2.5 ± 0.1 nmol h⁻¹ mg of protein⁻¹), indicating the involvement of an initial oxygen-sensitive step during the biotransformation of CL-20. As a result, the subsequent study was carried out under anaerobic conditions.

The CL-20 biotransformation activity of the membrane enzyme(s) using NADH or NADPH as an electron donor was 11.5 ± 0.4 or 2.1 ± 0.1 nmol h⁻¹ mg of protein⁻¹, respectively, indicating that the responsible enzyme was mainly NADH dependent.

The CL-20 biotransformation activities of membrane and soluble-enzyme fractions were 11.5 ± 0.4 and 2.3 ± 0.05 nmol h⁻¹ mg of protein⁻¹, respectively (Table 1), which clearly indicated that the enzyme(s) responsible for CL-20 biotransformation was membrane associated. The CL-20 biotransformation activities observed in the soluble-enzyme fraction presumably leached out from the membrane enzyme fraction during the cell disruption process.

Enzymatic biotransformation of CL-20 and product stoichiometry. The membrane enzyme(s) catalyzed the biotransformation of CL-20 optimally at pH 7.0. Activity remained unchanged between pHs 6.0 and 7.5, but higher or lower pHs caused reduction in activity (data not shown). A time course study carried out with the membrane enzyme(s) showed that CL-20 disappearance was accompanied by the formation of nitrite and nitrous oxide at the expense of the electron donor NADH (Fig. 4). After 2.5 h of reaction, each reacted CL-20 molecule produced about 2.3 nitrite ions, 1.5 molecules of nitrous oxide, and 1.7 molecules of formic acid (Table 2). Of the total 12 nitrogen atoms (N) and 6 carbon atoms (C) per reacted CL-20 molecule, we recovered approximately 5 N (as nitrite and nitrous oxide) and 2 C (as HCOOH) atoms, respectively. The remaining seven N and four C atoms may be present in an unidentified intermediate(s).

Pseudomonas sp. strain FA1 was a denitrifying bacterium; hence, nitrite was observed as a transient intermediate during CL-20 biotransformation and was partially converted to nitrous oxide. This observation was proved by incubating the membrane enzyme(s) with inorganic NaNO₂ under the same reaction conditions as those used for CL-20. The results showed an NADH-dependent reduction of nitrite (used as NaNO₂) to nitrous oxide (Fig. 5).

In biological systems, the enzymatic conversion of nitrite to

nitrous oxide occurs via a transient formation of nitric oxide (NO), and this process involves two enzymes, i.e., nitrite reductase (converts nitrite to nitric oxide) and nitric oxide reductase (converts nitric oxide to nitrous oxide). Since *Pseudomonas* species are known to produce these two reductase enzymes (2, 8), we assume that the membrane preparation from strain FA1 may contain these two enzymes.

Involvement of a flavoenzyme(s) in the biotransformation of CL-20. The total flavin contents were measured in crude extract, cytosolic soluble enzymes, and membrane enzymes. The membrane enzyme(s) contained about 56% of the total flavin content and retained about 74% of the total CL-20 biotransformation activity present in the crude extract (Table 1). In the deflavoenzyme preparation there was a corresponding decrease in flavin content as well as CL-20 biotransformation activity (Table 1), which indicated the involvement of a flavin moiety in CL-20 biotransformation. Furthermore, the CL-20 biotransformation activity of the deflavoenzyme was restored up to 75% after reconstitution with equimolar concentrations of FAD and FMN (100 μM each). The comparison of CL-20 biotransformation activities of the native enzyme (11.5 ± 0.4 nmol h⁻¹ mg of protein⁻¹), deflavoenzyme (2.7 ± 0.1 nmol h⁻¹ mg of protein⁻¹), and reconstituted enzyme(s) (8.90 ± 0.5 nmol h⁻¹ mg of protein⁻¹) clearly showed the involvement of a flavoenzyme(s) in the biotransformation of CL-20 by *Pseudo-*

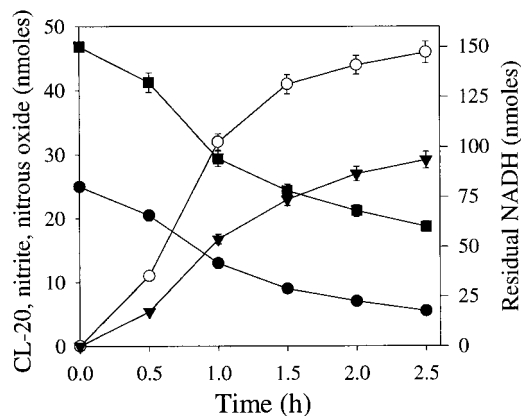


FIG. 4. Time course study of NADH-dependent biotransformation of CL-20 by a membrane-associated enzyme(s) from *Pseudomonas* sp. strain FA1 under anaerobic conditions. Symbols indicate the levels of CL-20 (●), NADH (■), nitrite (○), and nitrous oxide (▼). Data are means of results of triplicate experiments, and error bars indicate standard errors. Some error bars are not visible due to their small size.

TABLE 2. Stoichiometries of reactants and products during biotransformation of CL-20^a

Reactant or product	Amt (nmol)	Molar ratio of reactant to product per reacted CL-20 molecule
Reactants		
CL-20	20	1.0
NADH	90	4.5
Products		
Nitrite (NO ₂ ⁻)	46	2.3
Formate (HCOOH)	34	1.7
Nitrous oxide (N ₂ O)	29	1.5

^a CL-20 was biotransformed by a membrane-associated enzyme(s) (1 mg/ml) from *Pseudomonas* sp. strain FA1 at pH 7.0 and 30°C for 2.5 h under anaerobic conditions. The data are means of results of triplicate experiments.

monas sp. strain FA1. The free FAD and FMN also biotransformed CL-20 in the presence of NADH; however, the biotransformation rate was about fivefold lower than that of the native membrane enzyme(s). This finding additionally supported the involvement of a flavin-containing enzyme in CL-20 biotransformation and also indicated that the flavin moieties have to be in an enzyme-bound form in order to function efficiently.

Study with DPI showed a 62% inhibition of CL-20 biotransformation (Table 3). Analogously with previous reports which proved that DPI targets flavin-containing enzymes that catalyze one-electron transfer reactions (7, 18), the present study suggested the involvement of such an enzyme during the biotransformation of CL-20 by strain FA1. The involvement of a flavoenzyme in the biotransformation of RDX (3) and HMX (5) via one-electron transfer has already been established. In a previous study with diaphorase (a FMN-containing flavoenzyme from *Clostridium kluyveri*), an oxygen-sensitive one-electron transfer reaction that caused the N denitration of RDX, leading to its decomposition, was reported (3). However, a xanthine oxidase catalyzed an oxygen-sensitive, initial single N

TABLE 3. Effects of enzyme inhibitors on the CL-20 biotransformation activity of a membrane-associated enzyme(s)^c

Inhibitor (2 mM)	% CL-20 biotransformation activity ^a
None (control).....	100 ± 1.7
Diphenyliodonium.....	38 ± 2.3
Dicumarol.....	86 ± 3.5
Metyrapone.....	91 ± 2.8
Carbon monoxide ^b	87 ± 2.2
2,2-Dipyridyl.....	92 ± 3.4

^a One hundred percent CL-20 biotransformation activity was equivalent to 11.5 nmol h⁻¹ mg of protein⁻¹. Data are mean percentages of CL-20 biotransformation activity ± standard errors (*n* = 3).

^b Carbon monoxide was bubbled through the aqueous phase and headspace for 60 s in sealed vials.

^c The CL-20 biotransformation activity of the membrane-associated enzyme(s) (1 mg/ml) was determined at pH 7.0 and 30°C after 1 h under anaerobic conditions.

denitration of HMX at the FAD site, leading to the spontaneous decomposition of the molecule (5).

On the other hand, enzyme inhibitors such as dicumarol (a diphosphopyridine nucleotide-triphosphopyridine nucleotide-diaphorase inhibitor) (23), metyrapone, and CO (cytochrome P450 inhibitors) (6) and the metal chelator 2,2-dipyridyl did not show effective inhibition of the CL-20 biotransformation activity of the membrane enzyme(s) from strain FA1 (Table 3). The inhibition study ruled out the possibility of involvement of the above-mentioned enzymes or a similar type of enzyme during the biotransformation of CL-20 by *Pseudomonas* sp. strain FA1.

Proposed initial reaction of CL-20 biotransformation. According to the time course study described above, the disappearance of CL-20 was accompanied by the formation of nitrite (Fig. 4) and this reaction was oxygen sensitive. Additionally, the DPI-mediated inhibition of CL-20 degradation activity (Table 3) showed the involvement of a flavoenzyme catalyzing one-electron transfer. The evidence suggests that the CL-20 molecule undergoes enzyme-catalyzed one-electron reduction to form an anion radical of CL-20. This anion radical undergoes denitration to form a free radical, which eventually undergoes spontaneous ring cleavage and decomposition to produce nitrous oxide, nitrite, and formic acid. Previously, the one-electron transfer reaction catalyzed by a diaphorase, a flavoenzyme from *C. kluyveri*, which caused the N denitration of RDX, leading to its decomposition, was reported (3). The present study analogously with the results of initial biotransformations of other cyclic nitramine compounds, such as RDX (3) and HMX (5), supports an initial enzymatic N denitration of CL-20 prior to ring cleavage. On the other hand, thermolysis (20) and photolysis (J. Hawari, unpublished results) of CL-20 also suggested that an initial homolysis of a N—NO₂ bond in CL-20 leads to the formation of a N-centered free-radical that undergoes rapid ring cleavage and decomposition.

The source of nitrite ions in the present study is probably the four nitro groups bonded to the two cyclopentane rings in the CL-20 structure (Fig. 1). Nitrous oxide can be produced in two different ways: first, by enzymatic reduction of nitrite, and second, during secondary decomposition of the CL-20 free radical as it was previously suggested by Patil and Brill (20).

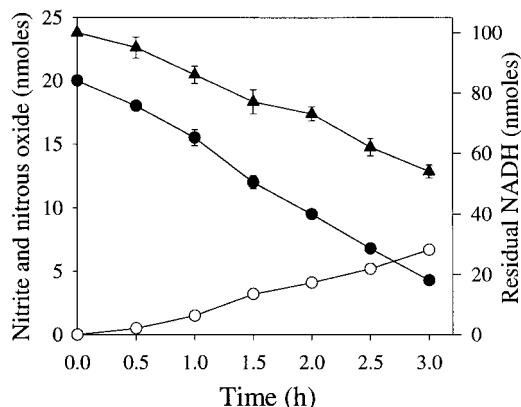


FIG. 5. Time course study of the NADH-dependent reduction of nitrite to nitrous oxide by a membrane-associated enzyme(s) from *Pseudomonas* sp. strain FA1 under anaerobic conditions. Symbols indicate the levels of nitrite (●), nitrous oxide (○), and NADH (▲). Data are means of results from triplicate experiments, and error bars indicate standard errors. Some error bars are not visible due to their small size.

Analogously, nitrous oxide was also produced during the secondary decomposition of RDX (3) and HMX (5, 14). Formic acid was presumably formed following denitration and the cleavage of the C—C bond (C₁—C₂ in Fig. 1). The C₁—C₂ bond bridging the two cyclopentanes in the CL-20 structure is relatively longer (25) and thus weaker than the other C—C bonds and would cleave more rapidly. Formaldehyde (HCHO), a major carbon compound produced during the biotransformation of RDX and HMX (3–5, 12–15), was not observed in the present study.

In conclusion, a *Pseudomonas* sp. strain capable of utilizing CL-20 as the sole nitrogen source, FA1, was isolated and identified from a soil sample. Strain FA1 grew well under aerobic conditions but biotransformed CL-20 under anaerobic conditions to produce nitrite, nitrous oxide, and formic acid. Studies with the deffavo form of the enzyme and its subsequent reconstitution and the inhibition of holoenzyme by DPI evidently support the involvement of a flavoenzyme in CL-20 biotransformation. Several lines of evidence in the present study have proved that the enzyme responsible for the biotransformation of CL-20 by strain FA1 is an NADH-dependent, membrane-associated flavoenzyme. The present study has provided the insights into the initial microbial and enzymatic biotransformation of CL-20 and some of its products that were not known before. However, further work is necessary to identify the intermediates and end products from CL-20 to supplement the mass balance study, which would help in determining the complete biodegradation pathway of CL-20. A vast literature available online (<http://www.ncbi.nlm.nih.gov>) revealed that *Pseudomonas* and the bacteria belonging to the family *Pseudomonadaceae* are prevalent in almost all types of environments, e.g., soils and marine and fresh water sediments. The present study therefore helps in understanding the environmental fate (biotransformation, biodegradation, and/or natural attenuation) of cyclic nitramine explosive compounds such as CL-20.

ACKNOWLEDGMENTS

We thank the Natural Sciences and Engineering Research Council and the National Research Council of Canada for a visiting fellowship to B. Bhushan and the Strategic Environmental Research and Development Program for funding the project (grant CU 1256). We also thank the Department of National Defense, Val Belair, Quebec, Canada, for its support.

Special thanks are due to Tara Hooper and Dominic Manno for their assistance. We sincerely acknowledge the analytical and technical support of A. Corriveau, C. Beaulieu, A. Halasz, S. Deschamps, and C. Groom. We also acknowledge the helpful discussions of V. Balakrishnan, D. Fournier, and J. S. Zhao and the critical suggestions of the editor and anonymous reviewers for improving the manuscript.

REFERENCES

- Aliverti, A., B. Curti, and M. A. Vanoni. 1999. Identifying and quantifying FAD and FMN in simple and in iron-sulfur-containing flavoproteins. *Methods Mol. Biol.* **131**:9–23.
- Arese, M., W. G. Zumft, and F. Cutruzzola. 2003. Expression of a fully functional *cd₁* nitrite reductase from *Pseudomonas aeruginosa* in *Pseudomonas stutzeri*. *Protein Expr. Purif.* **27**:42–48.
- Bhushan, B., A. Halasz, J. C. Spain, and J. Hawari. 2002. Diaphorase catalyzed biotransformation of RDX via N-denitration mechanism. *Biochem. Biophys. Res. Commun.* **296**:779–784.
- Bhushan, B., A. Halasz, J. Spain, S. Thiboutot, G. Ampleman, and J. Hawari. 2002. Biotransformation of hexahydro-1,3,5-trinitro-1,3,5-triazine (RDX) catalyzed by a NAD(P)H:nitrate oxidoreductase from *Aspergillus niger*. *Environ. Sci. Technol.* **36**:3104–3108.
- Bhushan, B., L. Paquet, A. Halasz, J. C. Spain, and J. Hawari. 2003. Mechanism of xanthine oxidase catalyzed biotransformation of HMX under anaerobic conditions. *Biochem. Biophys. Res. Commun.* **306**:509–515.
- Bhushan, B., S. Trott, J. C. Spain, A. Halasz, L. Paquet, and J. Hawari. 2003. Biotransformation of hexahydro-1,3,5-trinitro-1,3,5-triazine (RDX) by a rabbit liver cytochrome P450: insight into the mechanism of RDX biodegradation by *Rhodococcus* sp. strain DN22. *Appl. Environ. Microbiol.* **69**:1347–1351.
- Chakraborty, S., and V. Massey. 2002. Reaction of reduced flavins and flavoproteins with diphenyliodonium chloride. *J. Biol. Chem.* **277**:41507–41516.
- Forte, E., A. Urbani, M. Saraste, P. Sarti, M. Brunori, and A. Giuffrè. 2001. The cytochrome *cbb₃* from *Pseudomonas stutzeri* displays nitric oxide reductase activity. *Eur. J. Biochem.* **268**:6486–6490.
- Fournier, D., A. Halasz, J. C. Spain, P. Fiurasek, and J. Hawari. 2002. Determination of key metabolites during biodegradation of hexahydro-1,3,5-trinitro-1,3,5-triazine (RDX) with *Rhodococcus* sp. strain DN22. *Appl. Environ. Microbiol.* **68**:166–172.
- Groom, C. A., A. Halasz, L. Paquet, P. D'Cruz, and J. Hawari. 2003. Cyclo-dextrin-assisted capillary electrophoresis for determination of the cyclic nitramine explosives RDX, HMX and CL-20: comparison with high-performance liquid chromatography. *J. Chromatogr. A* **999**:17–22.
- Haas, R., E. von Löw Schreiber, and G. Stork. 1990. Conception for the investigation of contaminated munitions plants. 2. Investigation of former RDX-plants and filling stations. *Fresenius' J. Anal. Chem.* **338**:41–45.
- Halasz, A., J. Spain, L. Paquet, C. Beaulieu, and J. Hawari. 2002. Insights into the formation and degradation of methylenedinitramine during the incubation of RDX with anaerobic sludge. *Environ. Sci. Technol.* **36**:633–638.
- Hawari, J. 2000. Biodegradation of RDX and HMX: from basic research to field application, p. 277–310. In J. C. Spain, J. B. Hughes, and H.-J. Knackmuss (ed.), *Biodegradation of nitroaromatic compounds and explosives*. CRC Press, Boca Raton, Fla.
- Hawari, J., A. Halasz, S. Beaudet, L. Paquet, G. Ampleman, and S. Thiboutot. 2001. Biotransformation routes of octahydro-1,3,5,7-tetranitro-1,3,5,7-tetrazocine by municipal anaerobic sludge. *Environ. Sci. Technol.* **35**:70–75.
- Hawari, J., A. Halasz, T. Sheremata, S. Beaudet, C. Groom, L. Paquet, C. Rhofir, G. Ampleman, and S. Thiboutot. 2000. Characterization of metabolites during biodegradation of hexahydro-1,3,5-trinitro-1,3,5-triazine (RDX) with municipal sludge. *Appl. Environ. Microbiol.* **66**:2652–2657.
- Myler, C. A., and W. Sisk. 1991. Bioremediation of explosives contaminated soils (scientific questions/engineering realities), p. 137–146. In G. S. Saylor, R. Fox, and J. W. Blackburn (ed.), *Environmental bio/technology for waste treatment*. Plenum Press, New York, N.Y.
- Nielsen, A. T., A. P. Chafin, S. L. Christian, D. W. Moore, M. P. Nadler, R. A. Nissan, and D. J. Vanderah. 1998. Synthesis of polyazapocyclic caged polynitramines. *Tetrahedron* **54**:11793–11812.
- O'Donnell, V. B., G. C. Smith, and O. T. Jones. 1994. Involvement of phenyl radicals in iodonium inhibition of flavoenzymes. *Mol. Pharmacol.* **46**:778–785.
- Palleroni, N. J. 1984. Gram-negative aerobic rods and cocci: family I *Pseudomonadaceae*, p. 140–198. In N. R. Krieg and J. G. Holt (ed.), *Bergey's manual of systematic bacteriology*, vol. 1. Williams & Wilkins, Baltimore, Md.
- Patil, D. G., and T. B. Brill. 1991. Thermal decomposition of energetic materials. 53. Kinetics and mechanisms of thermolysis of hexanitrohexaazaisowurtzitane. *Combust. Flame* **87**:145–151.
- Seth-Smith, H. M. B., S. J. Rosser, A. Basran, E. R. Travis, E. R. Dabbs, S. Nicklin, and N. C. Bruce. 2002. Cloning, sequencing, and characterization of the hexahydro-1,3,5-trinitro-1,3,5-triazine degradation gene cluster from *Rhodococcus rhodochrous*. *Appl. Environ. Microbiol.* **68**:4764–4771.
- Talmage, S. S., D. M. Opreko, C. J. Maxwell, C. J. E. Welsh, F. M. Cretella, P. H. Reno, and F. B. Daniel. 1999. Nitroaromatic munition compounds: environment effects and screening values. *Rev. Environ. Contam. Toxicol.* **161**:1–156.
- Tedeschi, G., S. Chen, and V. Massey. 1995. DT-diaphorase: redox potential, steady-state, and rapid reaction study. *J. Biol. Chem.* **270**:1198–1204.
- Trott, S., S. F. Nishino, J. Hawari, and J. C. Spain. 2003. Biodegradation of the nitramine explosive CL-20. *Appl. Environ. Microbiol.* **69**:1871–1874.
- Xinqi, Z., and S. Nicheng. 1996. Crystal and molecular structures of e-HNIW. *Chin. Sci. Bull.* **41**:574–576.
- Zhao, J. S., A. Halasz, L. Paquet, C. Beaulieu, and J. Hawari. 2002. Biodegradation of RDX and its mononitroso derivative MNX by *Klebsiella* sp. strain SCZ-1 isolated from an anaerobic sludge. *Appl. Environ. Microbiol.* **68**:5336–5341.

Cyclodextrin-assisted capillary electrophoresis for determination of the cyclic nitramine explosives RDX, HMX and CL-20 Comparison with high-performance liquid chromatography[☆]

Carl A. Groom, Annamaria Halasz, Louise Paquet, Philomena D'Cruz, Jalal Hawari*

Biotechnology Research Institute, National Research Council Canada, 6100 Royalmount Avenue, Montreal, Quebec H4P 2R2, Canada

Abstract

A sulfobutyl ether- β -cyclodextrin-assisted electrokinetic chromatographic method was developed to rapidly resolve and detect the cyclic nitramine explosives 2,4,6,8,10,12-hexanitro-2,4,6,8,10,12-hexaaza-isowurtzitane (CL-20), octahydro-1,3,5,7-tetranitro-1,3,5,7-tetrazocine (HMX) and hexahydro-1,3,5-trinitro-1,3,5-triazine (RDX) and their related degradation intermediates in environmental samples. Development of the electrophoretic method required the measurement of the aqueous solubility of CL-20 which was determined to be 3.59 ± 0.74 mg/l at 25 °C (95% confidence interval, $n=3$). The performance of the method was then compared to results obtained from existing high-performance liquid chromatography methods including US Environmental Protection Agency method 8330.

Crown Copyright © 2003 Published by Elsevier Science B.V. All rights reserved.

Keywords: Explosives; RDX; HMX; CL-20; Nitramines

1. Introduction

The effort to produce lighter-mass munitions with greater explosive power has resulted in the addition of cyclic nitramines [e.g. 2,4,6,8,10,12-hexanitro-2,4,6,8,10,12-hexaaza-isowurtzitane (CL-20), octahydro-1,3,5,7-tetranitro-1,3,5,7-tetrazocine (HMX) and hexahydro-1,3,5-trinitro-1,3,5-triazine (RDX)] to supplement or replace aromatic energetic materials [*N*-2,4,6-tetranitro-*N*-methylaniline (Tetryl), 2,4,6-trinitrotoluene (TNT)] in rocket propellants and explosive formulations [1]. Structures for representative aromatic and cyclic nitramine explosives are shown in Fig. 1. With the exception of CL-20, which

is relatively new, the above compounds are identified as soil contaminants at explosive manufacturing or disposal sites and military training locations in Canada and the USA [2].

The environmental fate and toxicology of TNT and other aromatic explosives is fairly well established [3]. In contrast, the ecological fates of HMX and RDX and their degradation products are the subject of much current study [4,5], while almost no data are available for CL-20. Much information exists regarding the properties of these explosives as solid crystals, and defining their gaseous reaction products and energies of detonation. Controlled detonations of HMX and RDX exclusively produce low molecular mass products including nitrous oxide (N_2O), formaldehyde (HCHO), carbon dioxide (CO_2), and ammonia (NH_3) [6]. The detection of these compounds is a useful starting point for the identification of degradative pathways, and for fate

[☆]NRCC publication no. 45913.

*Corresponding author. Tel.: +1-514-496-6267; fax: +1-514-496-6265.

E-mail address: jalal.hawari@nrc.ca (J. Hawari).

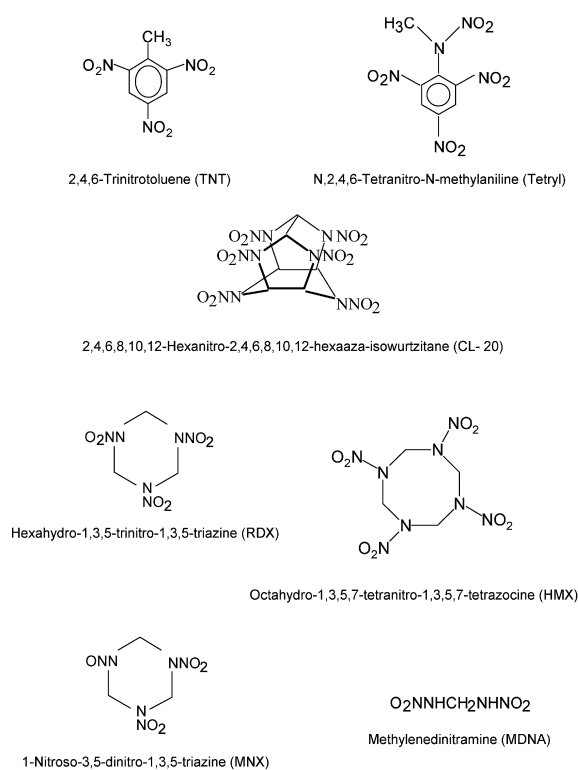


Fig. 1. Structural formulae of representative secondary aromatic and cyclic nitramine explosives.

and environmental impact assessment. To this end, much use is made of gas chromatography–mass spectrometry (GC–MS), solid-phase microextraction (SPME) and inorganic ion capillary electrophoresis (ICE) [7]. The degradation of explosives in soil and water, however, significantly differs from deflagration or detonation in at least four respects; (i) the reaction temperature is much lower, usually by 2–3 orders of magnitude, (ii) there is limited available reactant, usually in the mg/l range, (iii) the reactions occur in aqueous liquid environments, and (iv) relatively stable intermediates such as nitroso derivatives [8,9], methylenedinitramine [10] and 4-nitro-1,3-diaza-1-butanal [11] are observed. In the past, high-performance liquid chromatography, coupled to diode array UV detection (HPLC–UV) or electrospray mass spectrometric detection (LC–MS) have been used to analyze these explosives and their products in aqueous environmental samples [10]. Faster analytical methods are desirable, however, for the monitoring of chemical and enzymatic degra-

dations of this important family of energetic chemicals. Recently, sodium dodecylsulfate micellar electrokinetic chromatography (SDS-MEKC) [12] was employed in our laboratory for the rapid detection of TNT degradation intermediates, but this method does not adequately resolve nitramines which are much more polar in nature. Cyclodextrins may serve in the place of SDS micelles as pseudostationary ligands for the electrokinetic chromatographic (EKC) resolution of cyclic nitramines, as the polarity of the β -cyclodextrin inclusion cavity (approximately that of ethanol) is sufficiently matched with these analytes to allow complexation [13]. Charged cyclodextrins are routinely used for the resolution of enantiomeric pharmaceuticals [14], and have been applied for the CE-based analysis of aromatic explosives [15]. A sulfobutyl ether- β -cyclodextrin EKC method (CD-EKC) was developed for the detection of cyclic nitramines and some of their important degradation products in our laboratory.

2. Experimental

2.1. Materials

Epsilon CL-20 (purity 99.5%) was obtained from Thiokol Propulsion (Thiokol, UT, USA). RDX and HMX (with a purity >99%) were provided by Defense Research and Development Canada (DRDC) (Valcartier, Canada). Methylenedinitramine was obtained from Sigma–Aldrich (Oakville, Canada). Hexahydro-1-nitroso-3,5-dinitro-1,3,5-triazine (MNX) was obtained from SRI (Menlo Park, CA, USA). Advasep 4 sulfobutyl ether- β -cyclodextrin (tetrasodium salt, average degree of substitution 4), was purchased from CyDex (Overland Park, KS, USA). Tetryl, TNT, and all other nitroaromatic compounds were purchased from Supelco (Bellefonte, PA, USA). All other chemicals were obtained from Sigma as reagent grade.

2.2. Shaker flask determination of CL-20 aqueous solubility and stability

A 1 g/l stock solution of CL-20 in acetone was prepared and volumes ranging from 50 to 200 μ l were added to 500-ml serum bottles with PTFE-

coated caps. Following the evaporation of acetone the bottles were filled with 500 ml deionized water. The bottles were agitated for 24 h in a Lab-line Environ Shaker at 37 °C. Ten-ml aliquots were then removed and allowed to equilibrate and settle at 25 °C for 4 h before analysis using HPLC–UV as described below.

2.3. HPLC–UV analysis

The RDX, HMX, and CL-20 concentrations were determined by HPLC using a Waters chromatographic system composed of a Model 600 pump, a Model 717 Plus injector, a temperature control module, and Model 996 photodiode array detector connected to a Dell GX200 computer running Millennium³² (Waters) software. The column was a Supelcosil LC-CN (25 cm×4.6 mm, 5 µm; Supelco) maintained at 35 °C. The mobile phase (70% aqueous methanol) was run isocratically at 1 ml/min for the entire run time of 14 min. The detector was set to scan from 200 to 350 nm. Chromatograms were extracted at a wavelength of 230 nm with quantification taken from peak areas of external standards. Peaks were identified by comparison with elution times for external standards and by accompanying reference library diode array spectra as described earlier [10]. The injection volume was 50 µl. The limit of detection for this method was 0.02 mg/l (RSD=4.2%, *n*=5).

2.4. LC–MS analysis

The nitroso derivatives and ring cleavage products were analyzed by LC–MS with a Micromass Platform benchtop single quadrupole mass detector fronted by a Hewlett-Packard 1100 Series HPLC system equipped with a photodiode array detector. Samples (50 µl) were injected into a Supelcosil LC-CN column (25 cm×4.6 mm; 5 µm particle size; Supelco) thermostated at 35 °C. The solvent system consisted of a methanol–water gradient at a flow-rate of 1 ml/min. A first linear gradient was run from 10% to 20% methanol over 15 min followed by a second linear gradient from 20% to 60% over 5 min which was held for 3 min. This solvent ratio was returned to the initial conditions over 2 min and held for an extra 10 min. Analyte ionization was done in a negative electrospray ionization (ESI) mode produc-

ing mainly the deprotonated molecular mass ions $[M-H]^-$. The electrospray probe tip potential was set at 3.5 kV with a skimmer voltage of 30 V and an ion source temperature of 150 °C. The mass range was scanned from 40 to 400 u with a cycle time of 1.6 s and the resolution was set to 1 u (width at half-height). The detection limit was 0.004 mg/l (RSD=10%, *n*=3).

2.5. CE–UV analysis of nitramine explosives and their derivatives

MEKC separations with SDS were performed as described earlier [12]. Cyclodextrin-based EKC experiments (CD-EKC) were performed using a Hewlett-Packard (HP) ^{3D}CE instrument interfaced with a HP Vectra personal computer running HP Chemstation software. The HP ^{3D}CE system was fitted with a HP G-1600-31232 fused-silica bubble capillary with a total length of 64.5 cm, and an effective length (inlet to detection window) of 56 cm. The voltage was set at 30 kV and the temperature at 25 °C. Samples were injected by applying 50 mbar pressure to the capillary inlet for 5 s. The separation buffer was composed of 0.1 M sodium acetate buffer (pH 5.0) containing 10 mM sulfobutyl ether-β-cyclodextrin. Absorbances were monitored at wavelengths of 214, 230 and 280 nm. Unless otherwise indicated, the separation time was 18 min with 2 min separation buffer flushes of the capillary before each run. The total analysis time was therefore 20 min. The limit of detection for the method was 0.2 mg/l (RSD=5%, *n*=20).

3. Results and discussion

3.1. Polarity and aqueous solubility of RDX, HMX, and CL-20

CL-20 is a relatively new compound whose applications are currently under development, and many of its physicochemical properties are yet to be established. Epsilon CL-20, the most commonly used polymorph, is soluble in weakly polar organic solvents such as acetone (946 g/l) or ethyl acetate (450 g/l), but is insoluble in non-polar solvents such as toluene or benzene [16]. Its solubility in water was

not precisely determined and for this reason measurements were taken regarding CL-20 aqueous stability and solubility at ambient temperature. At 25 °C, the reported aqueous solubilities for RDX and HMX are 40.2 and 6.63 mg/l [2]. For CL-20, a maximum solubility of 3.59 ± 0.74 mg/l (95% confidence interval, $n=3$) at 25 °C (Fig. 2) was obtained from shake flask experiments. The hydrogen bonded lattice structure of the solvent (water) necessitates that solute polarity and molecular volume will have a strong effect on dissolution. The most common polymorphs of HMX, RDX, and CL-20 crystals have been examined using molecular dynamic simulations and X-ray diffraction to determine their molecular electronic structures and crystal packing densities [17–20]. For all three nitramines, polarized intramolecular electronic structures are observed, with partial charges of $-0.39e$ (e being the charge of a single electron) assigned to nitro group oxygens, and slight positive charges ($0.18e$) attributed to ring carbon nuclei. The three compounds are therefore weakly polar and dissolve readily in ketones such as acetone and to a lesser extent in alcohols such as methanol. They are not expected to dissolve extensively in non-polar solvents such as toluene, or in highly polar solvents such as *N*-methylformamide or water. The respective molecular volumes for RDX [17], HMX [18] and CL-20 [20] obtained from molecular dynamics estimates are 0.2118, 0.2607

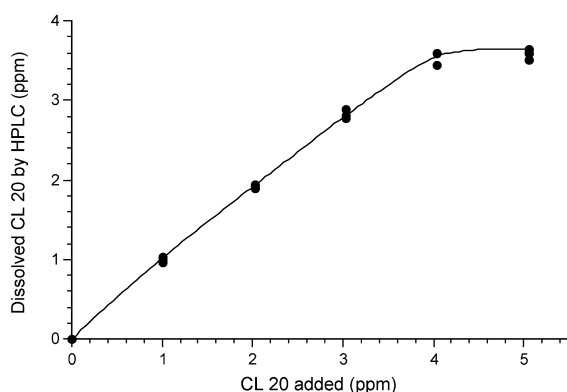


Fig. 2. Sub-saturation concentrations of 2,4,6,8,10,12-hexanitro-2,4,6,8,10,12-hexaaza-isowurtzitane (CL-20) in water at 25 °C as detected by HPLC vs. CL-20 concentration as calculated by stock solution addition. The aqueous saturation concentration appeared to be 3.59 mg/l.

and 0.3556 nl at 30 °C. The solubility of a solute in polar solvents decreases as molar volume increases, and this trend (i.e. solubility of RDX>HMX>CL-20) agrees with observed aqueous solubility measurements.

3.2. Resolution of cyclic nitramines using HPLC, SDS-MEKC and CD-EKC

The reversed-phase HPLC–UV method provides rapid, effective resolution for HMX, RDX and CL-20 (Fig. 3), with a quantitative detection limit of 0.02 mg/l. The use of 70% aqueous methanol mobile phase permitted the rapid detection of these analytes in 14 min, but under this condition methylenedinitramine was not retained by the column and for soil extracts the elution times of RDX nitroso-derivatives coincided with soil matrix peaks (data not shown). When the same liquid chromatographic system was used to front the electrospray ionization mass spectrometer, a gradient was applied which allowed for the observation of ring cleavage products. The increase in resolution and sensitivity was compromised, however, by the longer run time which increased to 35 min per sample.

SDS-MEKC is an effective method for the rapid resolution of aromatic explosives. Fig. 4 is an SDS-MEKC electropherogram demonstrating the separation of 14 explosives identified as priority pollutants by the US Environmental Protection Agency

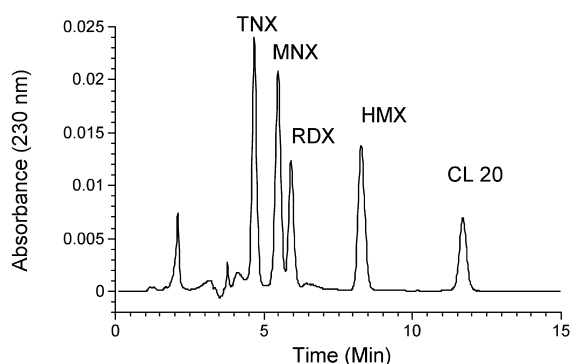


Fig. 3. Reverse phase HPLC–UV chromatogram of hexahydro-1,3,5-trinitroso-1,3,5-triazine (TNX), hexahydro-1-nitroso-3,5-dinitro-1,3,5-triazine (MNX), hexahydro-1,3,5-trinitro-1,3,5-triazine (RDX), octahydro-1,3,5,7-tetranitro-1,3,5,7-tetrazocine (HMX), and 2,4,6,8,10,12-hexanitro-2,4,6,8,10,12-hexaaza-isowurtzitane (CL-20).

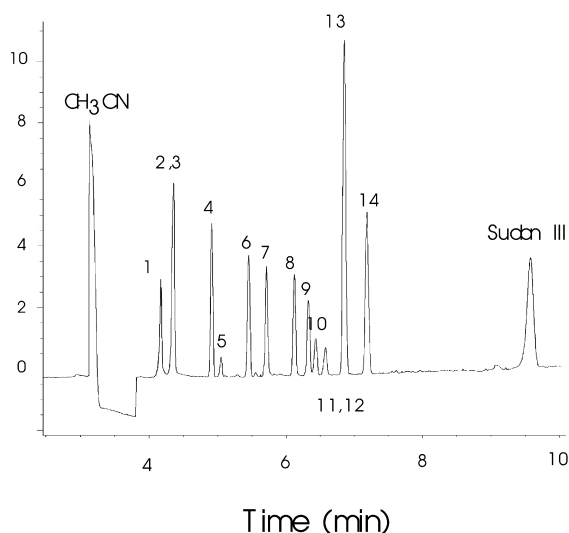


Fig. 4. MEKC separation of EPA method 8330 listed explosives in 12 mM sodium borate buffer pH 9.0, 50 mM sodium-dodecyl-sulfate, 25 °C. Peak identification: (1) octahydro-1,3,5,7-tetranitro-1,3,5,7-tetrazocine (HMX), (2) hexahydro-1,3,5-trinitro-1,3,5-triazine (RDX), (3) 1,3,5-trinitrobenzene, (4) 1,3-dinitrobenzene, (5) nitrobenzene, (6) 2,4,6-trinitrotoluene (TNT), (7) *N*-2,4,6-trinitro-*N*-methylaniline (Tetryl), (8) 2,4-dinitrotoluene, (9) 2,6-dinitrotoluene, (10) 2-nitrotoluene, (11) 3-nitrotoluene, (12) 4-nitrotoluene, (13) 2-amino-4,6-dinitrotoluene, (14) 4-amino-2,6-dinitrotoluene.

(EPA) method 8330 [21]. RDX and HMX partition poorly with SDS micelles and are observed to migrate close to the electroosmotic front. The polarity of the β -cyclodextrin cavity is estimated to be close to that of ethanol [13] and would therefore be more suitable for the solubilization of RDX, HMX, CL-20, and their degradation products. For cyclodextrins, however, the electrokinetic resolution of uncharged species is not solely based on polarity and hydrophobic interaction, but also on the geometry of the host–guest complexes. As previously stated, the molecular volumes for RDX [17], HMX [18] and CL-20 [20] are 0.2118, 0.2607 and 0.3556 nl at 30 °C. The volume for the β -cyclodextrin cavity is ~0.346 nl [13,22]; a value which allows for the complete inclusion of HMX and RDX, but restricts the complexation of CL-20. As indicated in Fig. 5, the three nitramines were observed to form complexes with sulfobutyl ether- β -cyclodextrin, and resolve electrophoretically.

Faster separations are possible using higher-pH

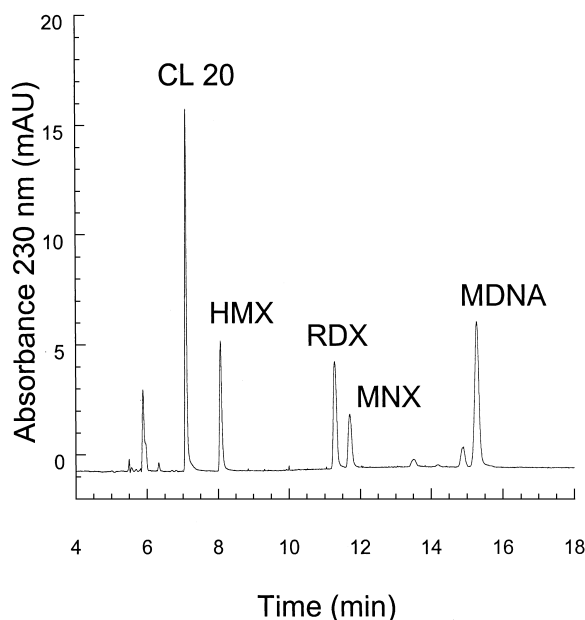


Fig. 5. Sulfobutyl ether- β -cyclodextrin-based CE separation of cyclic nitramines in 0.1 M sodium acetate, pH 5.0, containing 10 mM SB- β -cyclodextrin.

separation buffer, but cyclic nitramines and their degradation products are known to be stable in acid solution [6] and for this reason sodium acetate/acetic acid buffer (pH 5) was employed. The degradation products mononitroso-RDX (MNX) and methylenedinitramine (MDNA) also form complexes with sulfobutyl ether- β -cyclodextrin and their peaks are identified in Fig. 5. These compounds have been observed frequently in RDX degradation experiments using commercially obtained nitrate reductase enzyme [23], and domestic anaerobic sludge [10]. At present, the CD-EKC method is better applied to the rapid detection of cyclic nitramines and ring cleavage products in real time, while the HPLC (MS) method offers a 50-fold lower limit of detection in comparison with the CD-EKC or SDS-MEKC methods [0.004 mg/l (RSD=10%, $n=3$) vs. 0.2 mg/l (RSD=5%, $n=20$) and 0.5 mg/l (RSD=4%, $n=5$), respectively].

4. Conclusions

The solubility of the cyclic nitramine explosives

RDX, HMX, and CL-20 (40, 6.6 and 3.6 mg/l, respectively) in aqueous solution was observed to depend on analyte polarity and molecular volume. A comparison of reversed-phase HPLC, SDS-MEKC, and sulfobutyl ether- β -cyclodextrin EKC for the resolution of these compounds and their degradation products favoured the use of HPLC and CD-EKC. The HPLC method offers a lower detection limit (0.004 mg/l, RSD=10%, $n=3$), while the faster CD-EKC method facilitates real-time monitoring of experiments. The HPLC and the CD-EKC methods can be considered complimentary to each other in the determination of cyclic nitramines and their degradation products in environmental samples.

Acknowledgements

The authors would like to thank the Department of National Defence, Canada, for their technical support and for providing RDX and HMX. We also would like to thank Thiokol, USA for providing CL-20. The authors would also like to thank the US Department of Defence Strategic Environmental Research and Development Program (SERDP: CU 1213 and CP 1256) for funding the present work on RDX, HMX and CL-20.

References

- [1] J. Akhavan, in: *The Chemistry of Explosives*, Royal Society of Chemistry, Cambridge, UK, 1998, p. 1, Chapter 1.
- [2] J. Hawari, A. Halasz, in: G. Bitton (Ed.), *Encyclopedia of Environmental Microbiology*, Wiley, New York, 2000, p. 1.
- [3] J. Hawari, A. Halasz, L. Paquet, E. Zhou, B. Spencer, G. Ampleman, S. Thiboutot, *App. Environ. Microbiol.* 64 (2000) 2200.
- [4] P.-Y. Robidoux, J. Hawari, S. Thiboutot, S. Guiot, G. Ampleman, G.I. Sunahara, *Environ. Pollut.* 111 (2001) 283.
- [5] T.S. Sheremata, A. Halasz, L. Paquet, S. Thiboutot, G. Ampleman, J. Hawari, *Environ. Sci. Technol.* 35 (2001) 1037.
- [6] T. Urbanski, in: *Chemistry and Technology of Explosives*, Vol. 3, Pergamon Press, Oxford, 1983.
- [7] A.R. Timerbaev, *Analyst* 126 (2001) 964.
- [8] N.G. McCormick, J.H. Cornell, A.M. Kaplan, *Appl. Environ. Microbiol.* 42 (1981) 817.
- [9] J. Hawari, in: J.C. Spain, J.B. Hughes, H.-J. Knackmuss (Eds.), *Biodegradation of Nitroaromatic Compounds and Explosives*, Lewis, Boca Raton, FL, 2000, p. 277.
- [10] A. Halasz, J. Spain, L. Paquet, C. Beaulieu, J. Hawari, *Environ. Sci. Technol.* 36 (2002) 633.
- [11] D. Fournier, A. Halasz, J. Spain, P. Fiurasek, J. Hawari, *Appl. Environ. Microbiol.* 68 (2002) 166.
- [12] C.A. Groom, S. Beaudet, A. Halasz, L. Paquet, J. Hawari, *Environ. Sci. Technol.* 34 (2000) 2330.
- [13] K.A. Connors, *Chem. Rev.* 97 (1997) 1325.
- [14] R.J. Tait, D.O. Thompson, V.J. Stella, J.F. Stobaugh, *Anal. Chem.* 66 (1994) 4013.
- [15] J.H.T. Luong, G. Yong, *J. Chromatogr. A* 811 (1998) 225.
- [16] E. von Holtz, D. Ornellas, M.F. Foltz, J.E. Clarkson, *Prop. Explos. Pyrotech.* 19 (1994) 206.
- [17] D.C. Sorescu, B.M. Rice, D.L. Thompson, *J. Phys. Chem. B* 101 (1997) 798.
- [18] R. Pati, N. Sahoo, T.P. Das, S.N. Ray, *J. Phys. Chem. A* 101 (1997) 8302.
- [19] C. Sorescu, B.M. Rice, D.L. Thompson, *J. Phys. Chem. B* 102 (1998) 6692.
- [20] C. Sorescu, B.M. Rice, D.L. Thompson, *J. Phys. Chem. B* 102 (1998) 948.
- [21] US Environmental Protection Agency, Method 8330: Measurement of Explosive Contaminants in Soil, SW-846 update III, Part 4 1 (B), US EPA, Office of Solid Waste, US Government Printing Office, Washington, DC, 1997.
- [22] T.W. Sheremata, J. Hawari, *Environ. Sci. Technol.* 34 (2000) 3462.
- [23] B. Bhushan, A. Halasz, J. Spain, S. Thiboutot, G. Ampleman, J. Hawari, *Environ. Sci. Technol.* 36 (2002) 3104.

Biodegradation of the Nitramine Explosive CL-20

Sandra Trott,¹ Shirley F. Nishino,¹ Jalal Hawari,² and Jim C. Spain^{1*}

*Air Force Research Laboratory, Tyndall Air Force Base, Florida 32403,¹ and
Biotechnology Research Institute, National Research Council of Canada,
Montreal, Quebec H4P 2R2, Canada²*

Received 16 September 2002/Accepted 17 December 2002

The cyclic nitramine explosive CL-20 (2,4,6,8,10,12-hexanitro-2,4,6,8,10,12-hexaazaisowurtzitane) was examined in soil microcosms to determine whether it is biodegradable. CL-20 was incubated with a variety of soils. The explosive disappeared in all microcosms except the controls in which microbial activity had been inhibited. CL-20 was degraded most rapidly in garden soil. After 2 days of incubation, about 80% of the initial CL-20 had disappeared. A CL-20-degrading bacterial strain, *Agrobacterium* sp. strain JS71, was isolated from enrichment cultures containing garden soil as an inoculum, succinate as a carbon source, and CL-20 as a nitrogen source. Growth experiments revealed that strain JS71 used 3 mol of nitrogen per mol of CL-20.

CL-20 (2,4,6,8,10,12-hexanitro-2,4,6,8,10,12-hexaazaisowurtzitane) is a new, highly energetic explosive related to the explosives RDX (hexahydro-1,3,5-trinitro-1,3,5-triazine) and HMX (octahydro-1,3,5,7-tetranitro-1,3,5,7-tetrazocine) (Fig. 1). Due to its higher energy and its moderate sensitivity, CL-20 is expected to replace earlier explosives (19, 20, 22, 25). The production of CL-20 and its use in munitions and propellants can be expected to lead to environmental contamination. RDX and HMX, common contaminants in soil and groundwater at munition manufacturing sites and firing ranges, are toxic and possibly carcinogenic (7, 8, 11, 12, 16, 23, 27). Because of the structural similarity of CL-20 to RDX and HMX, it is likely that CL-20 has similar effects. So far, there is little information available about the properties of CL-20. In contrast to RDX and HMX, CL-20 is a caged molecule (Fig. 1). The water solubility of CL-20 is 4.8 mg/liter at 25°C (Stevens Institute of Technology [http://www.cee.stevens-tech.edu/ResProj.html]), which is lower than the solubility of the nitramines RDX and HMX (38.4 and 6.6 mg/liter at 20°C, respectively) (27).

The microbial degradation of RDX and HMX under aerobic and anaerobic conditions has been extensively investigated (1, 2, 4–6, 9, 13–15, 17, 21). Under anaerobic conditions, three degradation pathways have been proposed. The first includes the production of nitroso derivatives of RDX and HMX, which are subject to further degradation (15, 21). Hawari et al. suggested a second degradation pathway which includes the direct ring cleavage of RDX and HMX without the initial reduction of the nitro groups (14, 15). The third proposed degradation pathway is based on N denitration prior to ring cleavage (1).

Under aerobic conditions, RDX is degraded by a yet-unknown mechanism. The initial attack seems to be catalyzed by a cytochrome P450 (1a, 6, 24). RDX degradation by *Rhodococcus* sp. strain DN22 leads to the formation of nitrite, nitrous oxide, ammonia, formaldehyde, and a dead-end product with a molecular weight of 119 which was recently identified as 4-nitro-2,4-diazabutanal (1a, 5, 9). Fournier et al. proposed a deg-

radation pathway which includes an initial denitration of RDX followed by ring cleavage to formaldehyde and the dead-end product (9).

To the best of our knowledge, no biodegradation of CL-20 has been reported to date. It is, therefore, important to determine whether biodegradation might affect the fate and transport of CL-20 in terrestrial and aquatic ecosystems. To that end we evaluated the biodegradation of CL-20 in laboratory microcosms and isolated a bacterial strain that is able to grow on CL-20 as the sole nitrogen source.

CL-20 biodegradation in soil. Microcosms with dried and sieved garden and agricultural soils were incubated with CL-20 provided by the High Explosives Research and Development Facility at Eglin Air Force Base, Fla.

Microcosm experiments were conducted in 5-ml amber vials containing soil (2 g), sterile water (1.0 to 1.2 ml), and CL-20 (100 nmol). CL-20 was added from a 5 mM stock solution in methanol. The amounts of added water corresponded to the water absorptive capacity of the soils. For inhibiting microbial activity in soils, the added water contained glutaraldehyde (1%) and mercuric chloride (90 mg/liter). The microcosms were vigorously mixed by vortexing them and incubated in the dark at 30°C. For time course studies, one microcosm was sacrificed at each time point. The CL-20 concentrations in the microcosms in acetonitrile extracts were determined by high-pressure liquid chromatography (HPLC) analysis. The mobile phase (65% [vol/vol] acetonitrile, 0.1% [vol/vol] trifluoroacetic acid) was pumped at a flow rate of 1.0 ml/min over a Spherisorb C₈ column (250 by 4.6 mm; particle size, 5 µm; Alltech, Deerfield, Ill.) or a Synergi Polar-RP column (150 by 4.6 mm;

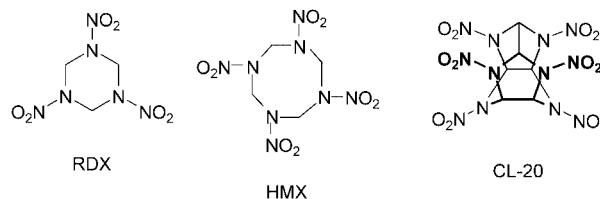


FIG. 1. Molecular structures of the cyclic nitramine explosives RDX, HMX, and CL-20.

* Corresponding author. Mailing address: Air Force Research Laboratory—MLQL, Building 1117, 139 Barnes Dr., Tyndall AFB, FL 32403. Phone: (850) 283-6058. Fax: (850) 283-6090. E-mail: Jim.Spain@Tyndall.af.mil.

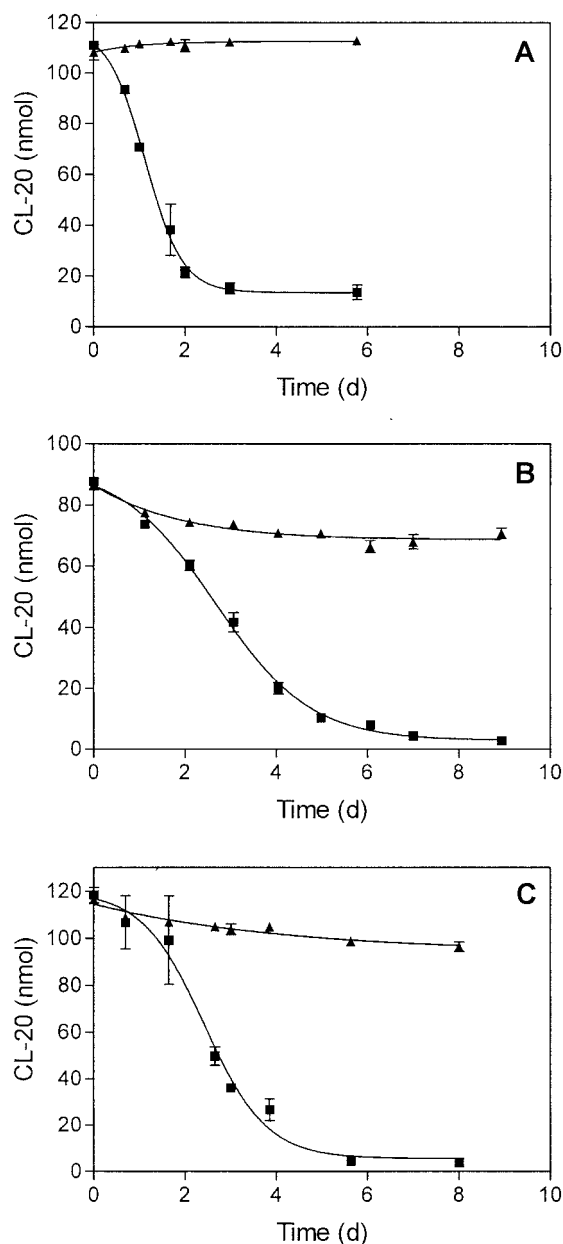


FIG. 2. CL-20 biodegradation in microcosms. Soils from Florida (A), Iowa (B), and Texas (C) were incubated with CL-20. CL-20 amounts are in nanomoles per microcosm. ■, active soil; ▲, soil with inhibited microbial activity. Degradation experiments were performed in triplicate. d, days.

particle size, 4 μm ; Phenomenex, Torrance, Calif.). Absorbance was measured at a wavelength of 230 nm.

CL-20 was degraded in all three soils (Fig. 2). The persistence of CL-20 in sterile controls indicated that the degradation process in active soil was biological. CL-20 degradation was fastest in the microcosms containing garden soil. CL-20 did not disappear completely in any of the soils. The incomplete degradation of CL-20 might be due to limited bioavailability. Residual amounts of CL-20 may be sorbed to the soil and therefore be unavailable for the microorganisms. In general, the availability of contaminants for microorganisms is

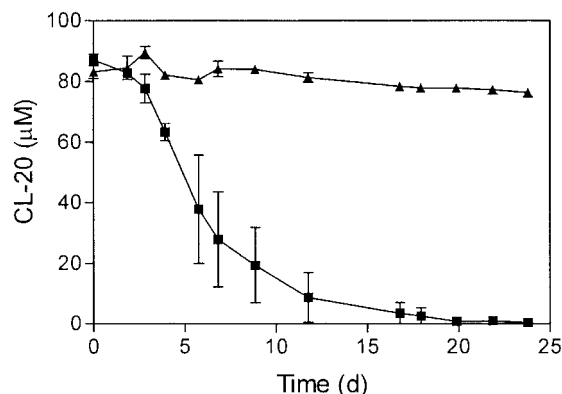


FIG. 3. CL-20 biodegradation in enrichments with Florida soil. ■, active soil; ▲, soil with inhibited microbial activity. Minimal medium was supplemented with succinate (20 mM) and CL-20 (100 μM). Enrichments were performed in triplicate. d, days.

dependent on the properties of the soil and the chemical compound, as well as on mass transport (3, 29).

During CL-20 degradation in the microcosms with garden soil, traces of a transient metabolite with a molecular weight of 247 could be detected by HPLC-mass spectrometry in the negative electrospray ionization mode. Further investigations are under way to identify the putative CL-20 degradation product.

It is not clear whether CL-20 degradation in the soil microcosms occurred aerobically or anaerobically. No precautions were taken to maintain aerobic conditions. Degradation started relatively quickly, so it can be assumed that CL-20 was degraded under aerobic conditions. On the other hand, it is possible that small anaerobic zones existed in the soil, where microbes could have degraded CL-20 anaerobically. In preliminary experiments CL-20 was also degraded under anaerobic conditions in sewage sludge (data not shown).

Enrichment and isolation of the *Agrobacterium* strain JS71. Enrichment cultures were carried out in 10 ml of M medium (pH 7.0) without sodium chloride (5). The medium was supplemented with CL-20 (100 μM) in methanol (5 mM stock solution) as the sole nitrogen source and succinate (20 mM) as the sole carbon source and inoculated with 1 g of Florida garden soil in 50-ml shake flasks. The cultures were incubated on a shaker at 30°C and 250 rpm. Microbial activity in the controls was inhibited by the addition of glutaraldehyde (1%) and mercuric chloride (90 mg/liter). The concentrations of CL-20 in the enrichments were determined by HPLC. Samples were mixed with 1.5 volumes of acetonitrile, and suspended material was removed by centrifugation prior to HPLC analysis.

CL-20 degradation in the first enrichment culture started after about 3 days (Fig. 3). The disappearance of CL-20 verified that CL-20 was degraded under aerobic conditions. CL-20 degradation in the enrichments was slower than its degradation in the soil microcosms, probably because of the smaller inoculum and the very low water solubility of CL-20. In contrast to the partial degradation of CL-20 in the soil microcosms, CL-20 was completely degraded in the enrichment cultures. The results support the hypothesis that some of the

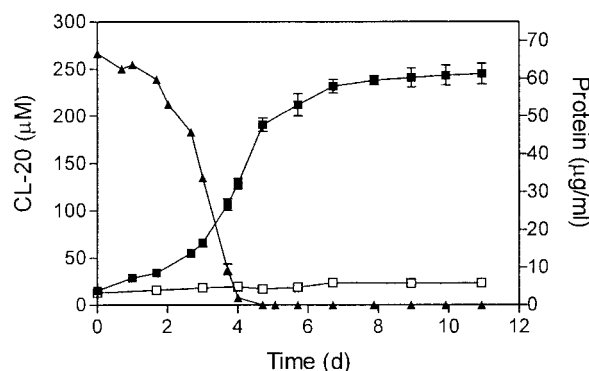


FIG. 4. Growth of *Agrobacterium* strain JS71. Aerobic cultures were grown in medium with 20 mM succinate–0.1% (vol/vol) Tween 80 with (■) and without (□) 250 μ M CL-20 as the sole nitrogen source. ▲, CL-20 concentration. The growth studies were performed in triplicate (■) or duplicate (□). d, days.

CL-20 in the microcosms (Fig. 2) was unavailable because of sorption to the soil.

After three subcultures of the enrichment, appropriate dilutions were plated on the above-named enrichment medium solidified with 1.5% (wt/vol) agarose (molecular biology grade). Single colonies were tested for the ability to grow on CL-20 as the sole nitrogen source. The selective enrichment yielded a bacterial strain that was able to grow with CL-20 as the sole nitrogen source. The 16S rRNA gene sequence from the isolate was determined and evaluated by Midi Labs (Newark, Del.). The 16S rRNA gene sequence indicated that the strain was most similar to *Agrobacterium rubi* (0.64% difference) and *Agrobacterium tumefaciens* (0.84% difference). The isolate was gram negative, motile, and rod shaped. These properties correspond to the characteristics of the genus *Agrobacterium* (18). The isolate was, therefore, named *Agrobacterium* sp. strain JS71.

The transformation of explosives by *Agrobacterium* strains has been described previously. *Agrobacterium* sp. strain 2PC was able to biotransform 2,4,6-trinitrotoluene to monoaminodinitrotoluenes (10). White et al. isolated an *Agrobacterium radiobacter* strain that transforms glycerol trinitrate to glycerol dinitrates and finally to glycerol mononitrates. The strain used two nitrogens from glycerol trinitrate as the nitrogen source for growth (28). An NADH-dependent reductase able to remove one nitro group from glycerol trinitrate in the form of nitrite was isolated from the strain (26). The enzyme also denitrated pentaerythrol tetranitrate, isosorbide dinitrate, and ethylene-glycol dinitrate but did not denitrate isopropyl nitrate, 2,4,6-trinitrotoluene, or RDX. Thus, the enzyme was able to reduce nitrate esters but not nitro groups connected to a carbon or nitrogen atom.

Growth studies with *Agrobacterium* strain JS71. The *Agrobacterium* strain JS71 was grown under the same nitrogen-limited conditions as those used for the enrichment cultures but with the addition of 250 μ M CL-20. CL-20 was added from a stock solution in methanol (20 mM). The optical densities of the cultures could not be determined because the undissolved CL-20 interfered with the absorption. Therefore, bacterial growth was estimated by determining the protein concentration. Cell suspensions were mixed 1:1 with acetone, and the

cells were collected by centrifugation and washed with 100 μ l of acetone. The pelleted cells were suspended in 0.1 M NaOH and incubated at 80°C for 5 min to lyse the cells. Protein concentrations were determined with a bicinchoninic acid protein assay kit (Pierce, Rockford, Ill.). CL-20 concentrations in the cultures were measured by HPLC after the addition of 4 volumes of acetonitrile to the samples and centrifugation as described above.

Strain JS71 grew in minimal medium containing succinate and CL-20 at a growth rate of 0.14 per day. The isolate did not grow with CL-20 as the sole nitrogen and carbon source. The slow growth of strain JS71 was probably due to the very low water solubility of CL-20. When the surfactant Tween 80 (0.1% [vol/vol]) was added to the cultures to increase the solubility and therefore the availability of CL-20, the growth rate was 0.59 per day (Fig. 4). Strain JS71 could not grow in media without a nitrogen source (Fig. 4) or in media containing RDX or HMX as the sole nitrogen source (data not shown).

The addition of Tween 80 to cultures containing CL-20 facilitated the determination of CL-20 concentrations in addition to increasing the growth rate. The disappearance of CL-20 and the growth of strain JS71 correlated directly, which suggested that initial metabolites of CL-20 were used as the nitrogen source.

To determine how many moles of nitrogen are assimilated from 1 mol of CL-20 by the *Agrobacterium* isolate, the strain was grown in various concentrations of CL-20 (25, 50, 100, and 250 μ M) or NaNO₂ (100, 200, 400, and 600 μ M) as the sole nitrogen source. The growth yield of strain JS71 in liquid medium was 213 \pm 13 g of protein per mol of CL-20 (Fig. 5). The growth yield in medium with NaNO₂ as the sole nitrogen source was 65 \pm 3 g of protein per mol of NaNO₂ (Fig. 5). Comparison of the growth yields suggests that the *Agrobacterium* strain JS71 uses 3 of the 12 nitrogen atoms from the CL-20 molecule.

Preliminary HPLC-mass spectrometry negative electrospray ionization mass analysis results indicated the formation of a metabolite with a molecular weight of 88 in cultures degrading CL-20 (data not shown). Further investigations are necessary to identify the structure of the intermediate.

The results indicate clearly that CL-20 is biodegraded

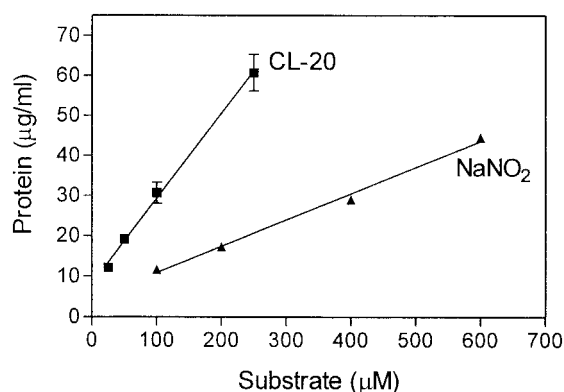


FIG. 5. Growth yield of *Agrobacterium* strain JS71 with 20 mM succinate and different concentrations of CL-20 (■) or NaNO₂ (▲). The CL-20 cultures were supplemented with 0.1% (vol/vol) Tween 80. All growth studies were performed in duplicate.

readily in soil. Therefore, CL-20 might be less persistent in the environment than RDX and HMX, which accumulate at contaminated sites. The lower water solubility of CL-20 will be a major determinant of its availability for biodegradation. Further investigation is required to elucidate the pathway and final products of CL-20 degradation.

Nucleotide sequence accession number. The 16S rRNA gene sequence of isolate JS71 was deposited at GenBank under accession number AY174112.

This work was funded by the U.S. Air Force Office of Research Science and the U.S. Strategic Environmental Research and Development Program and supported in part by the Oak Ridge Institute for Science and Education (U.S. Department of Energy).

We thank Joe Hughes, Bill Wallace, and Dan Lessner for providing soil samples.

REFERENCES

- Bhushan, B., A. Halasz, J. Spain, and J. Hawari. 2002. Diaphorase catalyzed biotransformation of RDX via N-denitration mechanism. *Biochem. Biophys. Res. Commun.* **296**:779–784.
- Bhushan, B., S. Trott, J. C. Spain, A. Halasz, L. Paquet, and J. Hawari. 2003. Biotransformation of hexahydro-1,3,5-trinitro-1,3,5-triazine (RDX) by a rabbit liver cytochrome P450: insight into the mechanism of RDX biodegradation by *Rhodococcus* sp. strain DN22. *Appl. Environ. Microbiol.* **69**:1347–1351.
- Binks, P. R., S. Nicklin, and N. C. Bruce. 1995. Degradation of hexahydro-1,3,5-trinitro-1,3,5-triazine (RDX) by *Stenotrophomonas maltophilia* PB1. *Appl. Environ. Microbiol.* **61**:1318–1322.
- Blackburn, J. W., and W. R. Hafker. 1993. The impact of biochemistry, bioavailability and bioactivity on the selection of bioremediation techniques. *Trends Biotechnol.* **11**:328–333.
- Boopathy, R. 2001. Enhanced biodegradation of cyclotetramethylenetetranitramine (HMX) under mixed electron-acceptor condition. *Bioresour. Technol.* **76**:241–244.
- Coleman, N. V., D. R. Nelson, and T. Duxbury. 1998. Aerobic biodegradation of the hexahydro-1,3,5-trinitro-1,3,5-triazine (RDX) as a nitrogen source by a *Rhodococcus* sp., strain DN22. *Soil Biol. Biochem.* **30**:1159–1166.
- Coleman, N. V., J. C. Spain, and T. Duxbury. 2002. Evidence that RDX biodegradation by *Rhodococcus* strain DN22 is plasmid-borne and involves a cytochrome P-450. *J. Appl. Microbiol.* **93**:463–472.
- Emery, D. D., and P. C. Faessler. 1997. First production-level bioremediation of explosives-contaminated soil in the United States. *Ann. N. Y. Acad. Sci.* **829**:326–340.
- Etnier, E. L. 1989. Water quality criteria for hexahydro-1,3,5-trinitro-1,3,5-triazine (RDX). *Regul. Toxicol. Pharmacol.* **9**:147–157.
- Fournier, D., A. Halasz, J. Spain, P. Fiurasek, and J. Hawari. 2002. Determination of key metabolites during biodegradation of hexahydro-1,3,5-trinitro-1,3,5-triazine with *Rhodococcus* sp. strain DN22. *Appl. Environ. Microbiol.* **68**:166–172.
- Fuller, M. E., and J. F. Manning, Jr. 1997. Aerobic gram-positive and gram-negative bacteria exhibit differential sensitivity to and transformation of 2,4,6-trinitrotoluene (TNT). *Curr. Microbiol.* **35**:77–83.
- Gong, P., J. Hawari, S. Thiboutot, G. Ampleman, and G. I. Sunahara. 2001. Ecotoxicological effects of hexahydro-1,3,5-trinitro-1,3,5-triazine on soil microbial activities. *Environ. Toxicol. Chem.* **20**:947–951.
- Haas, R., I. Schreiber, E. von Loew, and G. Stork. 1990. Conception for the investigation of contaminated munition plants. *Fresenius' J. Anal. Chem.* **338**:41–45.
- Hawari, J. 2000. Biodegradation of RDX and HMX: from basic research to field application. In J. C. Spain, J. B. Hughes, and H.-J. Knackmuss (ed.), *Biodegradation of nitroaromatic compounds and explosives*. CRC Press, Boca Raton, Fla.
- Hawari, J., A. Halasz, T. Sheremata, S. Beaudet, C. Groom, L. Paquet, C. Rhofir, G. Ampleman, and S. Thiboutot. 2000. Characterization of metabolites during biodegradation of hexahydro-1,3,5-trinitro-1,3,5-triazine (RDX) with municipal anaerobic sludge. *Appl. Environ. Microbiol.* **66**:2652–2657.
- Hawari, J., A. Halasz, S. Beaudet, L. Paquet, G. Ampleman, and S. Thiboutot. 2001. Biotransformation routes of octahydro-1,3,5,7-tetranitro-1,3,5,7-tetrazocine by municipal anaerobic sludge. *Environ. Sci. Technol.* **35**:70–75.
- Kaplan, A. S., C. F. Berghout, and A. Peczenik. 1965. Human intoxication from RDX. *Arch. Environ. Health* **10**:877–883.
- Kitts, C. L., D. P. Cunningham, and P. J. Unkefer. 1994. Isolation of three hexahydro-1,3,5-trinitro-1,3,5-triazine-degrading species of the family *Enterobacteriaceae* from nitramine explosive-contaminated soil. *Appl. Environ. Microbiol.* **60**:4608–4611.
- Krieg, N. R., and J. G. Holt (ed.). 1984. *Bergey's manual of systematic bacteriology*, vol. 1. Williams & Wilkins, Baltimore, Md.
- Larson, S. L., D. R. Felt, L. Escalon, J. D. Davis, and L. D. Hansen. 2001. Analysis of CL-20 in environmental matrices: water and soil. ERDC/EL TR-01-21. U.S. Army Engineer Research and Development Center, Vicksburg, Miss.
- Larson, S. L., D. R. Felt, J. L. Davis, and L. Escalon. 2002. Analysis of CL-20 in environmental matrices: water and soil. *J. Chromatogr. Sci.* **40**:201–206.
- McCormick, N. G., J. H. Cornell, and A. M. Kaplan. 1981. Biodegradation of hexahydro-1,3,5-trinitro-1,3,5-triazine. *Appl. Environ. Microbiol.* **42**:817–823.
- Nielsen, A. T., A. P. Chafin, S. L. Christian, D. W. Moore, M. P. Nadler, R. A. Nissan, and D. J. Vanderah. 1998. Synthesis of polyazapocyclic caged polynitramines. *Tetrahedron* **54**:11793–11812.
- Robidoux, P. Y., J. Hawari, S. Thiboutot, G. Ampleman, and G. I. Sunahara. 2001. Chronic toxicity of octahydro-1,3,5,7-tetranitro-1,3,5,7-tetrazocine (HMX) in soil determined using the earthworm (*Eisenia andrei*) reproduction test. *Environ. Pollut.* **111**:283–292.
- Seth-Smith, H. M. B., S. J. Rosser, A. Basran, E. R. Travis, E. R. Dabbs, S. Nicklin, and N. C. Bruce. 2002. Cloning, sequencing, and characterization of the hexahydro-1,3,5-trinitro-1,3,5-triazine degradation gene cluster from *Rhodococcus rhodochrous*. *Appl. Environ. Microbiol.* **68**:4764–4771.
- Simpson, R. L., P. A. Urtiew, D. L. Ornellas, G. L. Moody, K. J. Scribner, and D. M. Hoffman. 1997. CL-20 performance exceeds that of HMX and its sensitivity is moderate. *Propel. Explos. Pyrotech.* **22**:249–255.
- Snape, J. R., N. A. Walkley, A. P. Morby, S. Nicklin, and G. F. White. 1997. Purification, properties, and sequence of glycerol trinitrate reductase from *Agrobacterium radiobacter*. *J. Bacteriol.* **179**:7796–7802.
- Talmage, S. S., D. M. Opreko, C. J. Maxwell, C. J. E. Welsh, F. M. Cretella, P. H. Reno, and F. B. Daniel. 1999. Nitroaromatic munition compounds: environmental effects and screening values. *Rev. Environ. Contam. Toxicol.* **161**:1–156.
- White, G. F., J. R. Snape, and S. Nicklin. 1996. Biodegradation of glycerol trinitrate and pentaerythritol tetranitrate by *Agrobacterium radiobacter*. *Appl. Environ. Microbiol.* **62**:637–642.
- White, J. C., J. W. Kelsey, P. B. Hatzinger, and M. Alexander. 1997. Factors affecting sequestration and bioavailability of phenanthrene in soils. *Environ. Toxicol. Chem.* **16**:2040–2045.

Decomposition of the Polycyclic Nitramine Explosive, CL-20, by Fe⁰

VIMAL K. BALAKRISHNAN,
FANNY MONTEIL-RIVERA,
ANNAMARIA HALASZ,
AURELIAN CORBEANU, AND
JALAL HAWARI*

Biotechnology Research Institute,
National Research Council of Canada,
6100 Royalmount Avenue,
Montréal, Quebec, Canada H4P 2R2

CL-20 (2,4,6,8,10,12-hexanitro-2,4,6,8,10,12-hexaazaisowurtzitane), C₆H₆N₁₂O₁₂, is an emerging energetic chemical that may replace RDX, but its degradation pathways are not well-known. In the present study, zerovalent iron was used to degrade CL-20 with the aim of determining its products and degradation pathways. In the absence of O₂, CL-20 underwent a rapid decomposition with the concurrent formation of nitrite to ultimately produce nitrous oxide, ammonium, formate, glyoxal, and glycolate. LC/MS (ES-) showed the presence of several key products carrying important information on the initial reactions involved in the degradation of CL-20. For instance, a doubly denitrated intermediate of CL-20 was detected together with the mono- and dinitroso derivatives of the energetic chemical. Two other intermediates with [M - H]⁻ at 392 and 376 Da, matching empirical formulas of C₆H₇N₁₁O₁₀ and C₆H₇N₁₁O₉, respectively, were detected. Using ¹⁵N-labeled CL-20, the two intermediates were tentatively identified as the denitrohydrogenated products of CL-20 and its mononitroso derivative, respectively. The present experimental findings suggest that CL-20 degraded via at least two initial routes: one involving denitration and the second involving sequential reduction of the N-NO₂ to the corresponding nitroso (N-NO) derivatives prior to denitration and ring cleavage.

Introduction

The polycyclic nitramine 2,4,6,8,10,12-hexanitro-2,4,6,8,10,12-hexaazaisowurtzitane, CL-20 (Figure 1), is an emerging energetic chemical (1) that is currently under consideration for a wider military and industrial application. CL-20 has been found to be toxic (2, 3), thereby necessitating its removal from contaminated environments. Several abiotic or biotic reactions have recently been shown to degrade CL-20. For instance, CL-20 was found to be highly unstable in alkaline solutions (4) and to undergo microbial decomposition by *Clostridium* sp. EDB2 (5), salicylate 1-monooxygenase from *Pseudomonas* sp. ATCC 29352 (6), and *Pseudomonas* sp. FA1 (7). In their study with strain ATCC 29352, Bhushan and co-workers (6) applied LC/MS to detect various early intermediates in the degradation process. Imines were initially formed that were hydrated into α-hydroxy nitramines, which subsequently underwent ring cleavage and decomposition. The

same intermediates were observed during photolysis of CL-20 in aqueous solution (8). In all studied cases nitrite, nitrous oxide, ammonium, and formic acid were the main products detected, suggesting that initial denitration of CL-20 whether via chemical or biochemical means would lead to similar secondary decomposition in water (6).

Zerovalent iron has been widely used to degrade a variety of oxidized chemicals. For instance, Fe⁰ was found to degrade inorganic compounds such as nitrate ion (9–11), chlorinated solvents such as perchloroethylene (PCE) and carbon tetrachloride (CCl₄) (12–14), emerging contaminants in drinking water like *N*-nitrosodimethylamine (NDMA) (15, 16), and munitions wastes such as trinitrotoluene (TNT) (17). Recent studies showed that the monocyclic nitramine explosive, RDX (hexahydro-1,3,5-trinitro-1,3,5-triazine) (Figure 1), could be readily degraded by Fe⁰ (17–19) or Fe^{II} (20) and that permeable reactive barriers containing zerovalent iron may be effective for remediation of RDX-contaminated sites (17, 18, 21). With six N-NO₂ groups, CL-20 is also a good candidate for transformation via reductive processes, and zerovalent iron could be seen as a potential treatment technology applicable to the energetic chemical. In the present study, Fe⁰ was employed to degrade CL-20, and LC/MS was used to detect new degradation products and therefore gain new insight into its degradation routes. Understanding the degradation pathways of CL-20 will contribute to the development of effective remediation strategies.

Experimental Section

Chemicals. 2,4,6,8,10,12-Hexanitro-2,4,6,8,10,12-hexaazaisowurtzitane (ε-CL-20), ¹⁵N-amino-labeled CL-20, and ¹⁵N-nitro-labeled CL-20 were provided by A. T. K. Thiokol Propulsion (Brigham City, UT). Fe⁰ powder (100 mesh) having a surface area of 0.9821 m²/g (determined by BET analysis, Micromeritics, Norcross, GA) and oxygen and carbon contents of 0.54 and 0.28%, respectively, was obtained from Anachemia Chemicals (Montreal, QC, Canada), as was glycolic acid. Glyoxal (ethanedial), *O*-(2,3,4,5,6-pentafluorobenzyl)hydroxylamine hydrochloride (PFBHA), ferrozine (3-(2-pyridyl)-5,6-diphenyl-1,2,4-triazine-*p,p'*-disulfonic acid, monosodium salt), and iron(II) sulfate were obtained from Aldrich Chemicals. All other chemicals used in this study were of reagent grade, and used without further purification.

Degradation of CL-20 by Fe⁰. A series of 20-mL vials wrapped in aluminum foil and containing 10 mL of deionized water and 0.1 g of Fe⁰ powder were sealed with Teflon-coated serum caps and sparged with argon for 20 min. The redox potential of the solution was occasionally measured after sparging and found to be -225 mV, demonstrating the anaerobic atmosphere of the medium. An aliquot of CL-20 stock solution (1% w/v) prepared in acetonitrile was then added to the vials, giving an initial amount of CL-20 of 2.4 μmol. The initial CL-20 concentration (100 mg L⁻¹) was kept well in excess of its maximum water solubility (ca. 3.6 mg L⁻¹ at 25 °C; 22) in an attempt to generate sufficient amounts of reaction intermediates to allow detection. The vials were agitated at 50 rpm in a rotary shaker.

The following eight controls were prepared as described above: (1) Fe⁰, CL-20, water, in air; (2) Fe⁰, CL-20, dry acetonitrile, under argon; (3) Fe⁰, CL-20, dry acetonitrile, H₂ gas; (4) Fe(SO₄), CL-20, water, under argon; (5) Fe⁰, HCOO⁻, water, under argon; (6) Fe⁰, glyoxal, water, under argon; (7) Fe⁰, NO₂⁻, water, under argon; and (8) Fe⁰, N₂O, water, under argon.

Analytical Techniques. A gastight syringe was used to sample gaseous products from the headspace for subsequent

* Corresponding author phone: (514)496-6267; fax: (514)496-6265; e-mail: jalal.hawari@nrc-nrc.gc.ca.

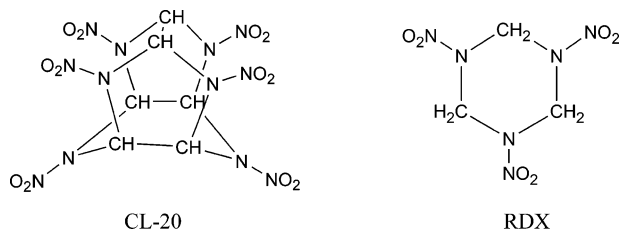


FIGURE 1. Structural formulas of RDX and CL-20.

analysis of nitrous oxide by GC-ECD as described by Sheremata and Hawari (23). Meanwhile, at the end of each reaction 10 mL of acetonitrile (CH_3CN) was added to the whole reaction mixture to solubilize any undissolved CL-20. The resulting solution was filtered through a $0.45\text{-}\mu\text{m}$ syringe filter, and CL-20 was analyzed by HPLC connected to a photodiode array (PDA) detector as described previously (24).

Analyses of nitrite (NO_2^-), nitrate (NO_3^-), formate (HCOO^-), and glycolate ($\text{HOCH}_2\text{COO}^-$) were performed by ion chromatography (IC) equipped with a conductivity detector after evaporating acetonitrile and removing the glyoxal by precipitation with PFBHA. The Waters IC system consisted of a model 600 pump, a model 717 autosampler plus, and a model 430 conductivity detector. Separation was performed on a Dionex IonPac AS15 column ($2\text{ mm} \times 250\text{ mm}$). The mobile phase was 30 mM KOH for nitrite and nitrate and 5 mM KOH for formate and glycolate, at a flow rate of 0.4 mL/min and 40°C . The detection of anions was enhanced by reducing the background with a model DS-Plus autosuppressor from Altech (Guelph, ON, Canada). Ammonia was determined by ion chromatography (IC). The IC system consisted of a resin-based Hamilton PRP-X200 cation chromatography column ($250\text{ mm} \times 2.1\text{ mm}$), a TSP model P4000 pump, an AS3000 autosampler, and a Waters Millipore model 431 conductivity detector. The mobile phase was 4 mM nitric acid with 30% methanol at a flow rate of 0.75 mL/min at 40°C .

To provide insight into the role of iron in catalyzing CL-20 degradation, the presence of Fe^{2+} and Fe^{3+} was determined using Stookey's Ferrozine method (25). Briefly, $100\text{ }\mu\text{L}$ of a 0.05 M solution of ferrozine was added to 2 mL of the filtered CL-20/ Fe^0 reaction mixture, and heated to ca. 80°C for 10 min. The solution was cooled to 21°C , and ammonium hydroxide/ammonium acetate buffer (pH 9) was added to achieve a solution pH of 6. The absorbance of the resulting magenta colored solution of Fe^{II} complex was measured at 562 nm , and the concentration of Fe^{II} in the sample was determined by comparison against a standard curve prepared using ferrous ammonium sulfate. To determine Fe^{III} , hydroxylamine hydrochloride (10% v/v) was added to the filtered CL-20/ Fe^0 reaction mixture in order to reduce Fe^{III} to Fe^{II} . The converted Fe^{II} was then determined by the same procedure, and $[\text{Fe}^{\text{III}}]$ was calculated by subtracting the amount of Fe^{II} found in the CL-20/ Fe^0 reaction mixture prior to the addition of hydroxylamine hydrochloride from the amount of Fe^{II} found after the addition of the amine.

Glyoxal ($\text{CHO}-\text{CHO}$) was determined as its derivatized product with *O*-(2,3,4,5,6-pentafluorobenzyl)hydroxylamine hydrochloride (PFBHA) (26). A solution of PFBHA (15 g L^{-1} ; $20\text{ }\mu\text{L}$) was added to 0.5 mL of aqueous sample, and the pH was adjusted to 3 with 5% HCl. After 1 h of reaction in the dark and at room temperature, 1 mL of acetonitrile was added to the mixture, and the resulting solution was analyzed by HPLC/UV-MS. The derivatized compound was analyzed in the positive electrospray mode (ES+) using a Micromass benchtop single quadrupole mass detector attached to a Hewlett-Packard 1100 series HPLC system equipped with a DAD detector. Separation was performed on a Supelcosil C8 column ($25\text{ cm} \times 4.6\text{ mm}$, $5\text{ }\mu\text{m}$) at 35°C using 1 mL/min

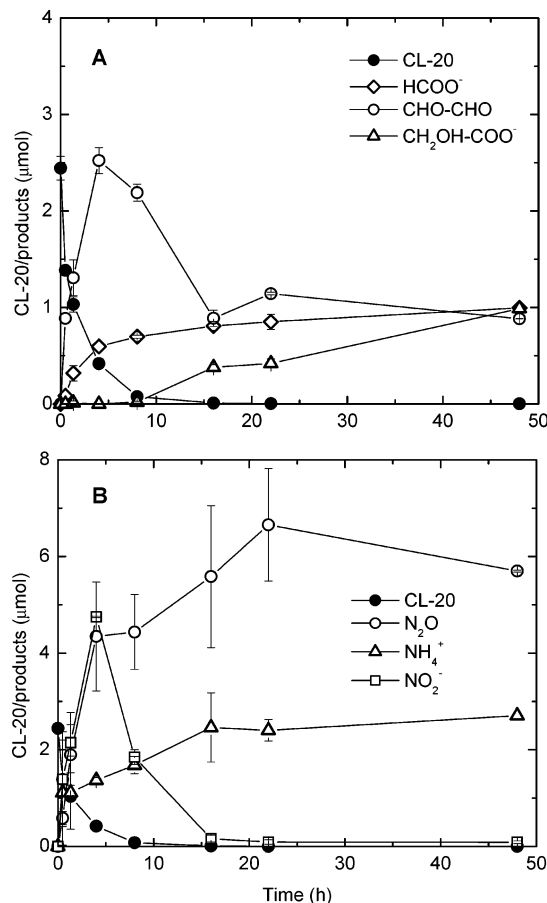


FIGURE 2. Time course of the Fe^0 -mediated anaerobic degradation of CL-20 in water. (A) Carbon-containing compounds. (B) Nitrogen-containing compounds. Data points are the mean and error bars the average deviation ($n = 2$).

of acetonitrile/water gradient (60% of acetonitrile to 90%, 10 min, 90% to 60%, 2 min, and 60% to 70%, 6 min). The identity of the derivatized compound was confirmed by comparing the mass spectrum obtained with that obtained with glyoxal and quantification was done by UV at 250 nm .

Intermediate products of CL-20 were analyzed by LC/MS using a Bruker benchtop ion trap mass detector attached to a Hewlett-Packard 1100 series HPLC system equipped with a DAD detector. The samples were injected into a $5\text{-}\mu\text{m}$ pore size Zorbax SB-C18 capillary column (0.5 mm i.d. by 150 mm ; Agilent, CA) at 25°C . The solvent system was composed of a $\text{CH}_3\text{CN}/\text{H}_2\text{O}$ gradient (30% v/v to 70% v/v) at a flow rate of $15\text{ }\mu\text{L/min}$. For mass analysis, negative electrospray ionization was used to produce deprotonated molecular ions $[\text{M} - \text{H}]^-$ or nitrate adduct ions $[\text{M} + \text{NO}_3]^-$. The mass range was scanned from 40 to 550 Da . The identity of the intermediates was confirmed using ^{15}N -amino- and ^{15}N -nitro-labeled CL-20. Nitrogen gas including $^{15}\text{N}^{14}\text{N}$ and $^{15}\text{N}^{15}\text{N}$ and nitrous oxide including $^{15}\text{N}^{14}\text{NO}$ and $^{15}\text{N}^{15}\text{NO}$ were analyzed using a GC/MS as described previously (23).

Results and Discussion

Degradation of CL-20 with Iron. Figure 2 shows that CL-20 ($2.4\text{ }\mu\text{mol}$) completely degraded within 10 h of reaction with Fe^0 (under anaerobic conditions) to form HCOO^- , NO_2^- , NH_4^+ , and N_2O . These products are the same as those reported in previous studies on the alkaline hydrolysis (4), photolysis (8), and microbial degradation (5–7) of CL-20. Formaldehyde, which is a common degradation product of RDX and HMX, was not detected here. However, while RDX and HMX are cyclic oligomers of methylene nitramine, CH_2-NNO_2 , CL-20

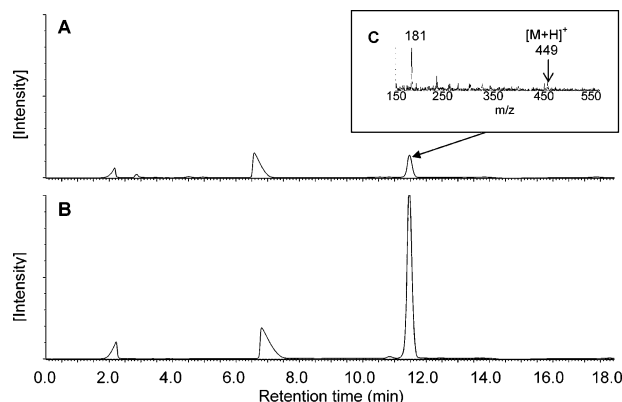


FIGURE 3. LC/UV chromatograms at 250 nm showing the detection of glyoxal. (A) CL-20/ Fe^0 reaction solution after derivatization. (B) Glyoxal standard solution after derivatization with pentafluorobenzylhydroxylamine. (C) MS (ES+) obtained for both the standard and the sample.

contains the repeating unit $\text{CH}-\text{NNO}_2$ where each carbon atom is bound to another carbon (Figure 1). Moreover, whereas RDX and HMX are both synthesized from formaldehyde, glyoxal ($\text{CHO}-\text{CHO}$) is used as the starting material in the synthesis of CL-20 (1, 27). We thus investigated the presence of glyoxal as a possible degradation product of CL-20.

Figure 3 shows the chromatograms obtained upon separately derivatizing the reaction mixture and a reference standard of glyoxal with PFBHA. The exact match between the sample and the standard conclusively proved that glyoxal was a product of CL-20 degradation, and to the best of our knowledge, this is the first such report. Glyoxal was analyzed throughout the reaction (Figure 2A) as the derivatized product of PFBHA. Since Figure 2A clearly shows that glyoxal was a transient species, we analyzed for its potential decomposition product(s). It has been reported that glyoxal in the presence of multivalent metal ions including Fe^{II} can be transformed into glycolic acid (28). A control containing glyoxal ($2.67 \mu\text{mol}$) and iron (0.1 g) led to the production of glycolic acid ($1.16 \mu\text{mol}$), demonstrating the transformation of glyoxal into glycolic acid under the present conditions. As a consequence, glycolic acid was also measured in the reaction medium (Figure 2A). Unlike glyoxal, formate did not react with iron under the current conditions.

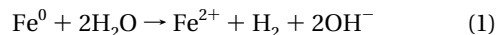
Figure 2B summarizes the nitrogen-containing products of CL-20. Of the nitrogen-containing product N_2O and ammonia (detected as NH_4^+) appeared to be stable, in agreement with what was observed when stirring Fe^0 (0.1 g) with $2 \mu\text{mol}$ of NH_4Cl or $0.11 \mu\text{mol}$ of N_2O . The transformation of nitrite after 16 h is consistent with the findings of other researchers who observed that Fe^0 could chemically reduce nitrite to ammonium (9, 12, 29). An experiment was specifically designed to evaluate the transformation of nitrite with iron under the present conditions. After contacting Fe^0 (0.1 g) with an aqueous solution of nitrite ($2.4 \mu\text{mol}$) for 16 h, NH_4^+ ($0.6 \mu\text{mol}$), N_2O ($0.12 \mu\text{mol}$), and N_2 (not quantified) were observed along with unreacted nitrite ($0.9 \mu\text{mol}$). A fraction of the ammonium and nitrous oxide detected at the end of the reaction likely resulted from the reduction of nitrite ions, as supported by the detection of $^{15}\text{N}^{15}\text{NO}$ (46 Da) when using ^{15}N -nitro-labeled CL-20.

After 4 h of reaction, 83% of CL-20 was transformed to give a carbon mass balance of 46.5% that was distributed between HCOO^- (formate, 4.9%) and $\text{CHO}-\text{CHO}$ (glyoxal, 41.6%). However, when the derivatization was performed at a higher temperature (65°C), some reaction intermediates decomposed further to give a greater yield of glyoxal (up to 60%). Analysis of the reaction medium by LC/MS at this time

confirmed the presence of several intermediates in the system (see next section). At the end of the reaction (48 h), the carbon mass balance decreased to 32.4% and was distributed as follows: HCOO^- (formate, 6.8%), $\text{CHO}-\text{CHO}$ (glyoxal, 12.1%), and $\text{CH}_2\text{OH}-\text{COO}^-$ (glycolate, 13.5%). The amount of glyoxal significantly decreased between 4 and 48 h to produce glycolate. However, the decrease in total C mass balance shows that glycolate was not the only product of glyoxal. The latter is a highly reactive dialdehyde (30) that can readily condense with alcohols and amines, which are suspected products in the system.

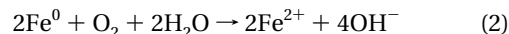
As for the nitrogen mass balance, it was 60.7% after 4 h, distributed among NO_2^- (19.6%), N_2O (35.5%), and NH_3 (5.6%). The use of ^{15}N -amino-labeled CL-20 led to the detection of a mass ion of 29 Da corresponding to $^{15}\text{N}-^{14}\text{N}$, confirming that N_2 was a product of CL-20, but we were unable to quantify it.

Insights into the Role of Fe^0 in Initiating the Decomposition of CL-20. Oxidation of Fe^0 to Fe^{II} in water is concomitant with a release of hydroxide ions in solution (eq 1), so that one might expect a pH increase as the reaction evolves. Since hydrolysis of CL-20 has been observed under alkaline conditions (4), a possible initiator for CL-20 decomposition was the OH^- resulting from oxidation of iron. The pH was thus measured at the end of each reaction and was found to remain constant at approximately 5.5, even after 120 h of reaction. The formation of formic and glycolic acids as products of CL-20 may be responsible for the pH stabilization. Hydrolysis of CL-20 was therefore excluded as a potential degradation route.



In the $\text{Fe}^0-\text{H}_2\text{O}$ system, there are three main reductants present upon the anaerobic corrosion of the metal (eq 1): Fe^0 , Fe^{II} , and H_2 (31). Neither iron powder in dry MeCN nor iron powder in dry MeCN in the presence of H_2 were able to degrade CL-20 (data not shown), suggesting that Fe^0 or H_2 would not be responsible for CL-20 decomposition. This observations added to the formation of Fe^{III} upon reduction of CL-20 led us to attribute the reductive process to Fe^{II} . For instance, we found that after 6 h of contact between CL-20 and Fe^0 approximately 5 ppm ($0.89 \mu\text{mol}$) of Fe^{III} was detected. By contrast, an oxygen-free control solution containing only Fe^0 and water (i.e., no CL-20) produced a negligible quantity of Fe^{III} ion in the same time span. When CL-20 ($2.3 \mu\text{mol}$) was mixed with FeSO_4 ($3.56 \mu\text{mol}$, 200 ppm in Fe^{II} as measured by Stookey's method) degradation did not occur, indicating that Fe^{2+} ions in solution were not responsible for the degradation of CL-20. Since dissolved Fe^{2+} ion had no impact on CL-20 degradation, the e-transfer to the energetic chemical that caused its degradation must have involved surface-bound Fe^{2+} . The involvement of surface bound Fe^{2+} was noted earlier for the destruction of a wide variety of environmental organic contaminants including CCl_4 (12, 14), trifluralin (32), nitrobenzenes (33, 34), and the nitramine, RDX (20).

Note that in the presence of oxygen, Fe^0 can still form Fe^{2+} (eq 2), but the electrons generated from Fe^{2+} oxidation are trapped by triplet oxygen, $^1\text{O}_2$ (a diradical in the ground state) instead of initiating CL-20 destruction. As a result, CL-20 degradation was not observed when the experiment was conducted in air.



Thus, in the absence of air, the oxidation of surface-bound Fe^{II} to Fe^{III} and the subsequent transfer of a single electron to CL-20 were likely responsible for the degradation of the energetic chemical. The resulting CL-20 anion radical is expected to rapidly denitrate to undergo spontaneous

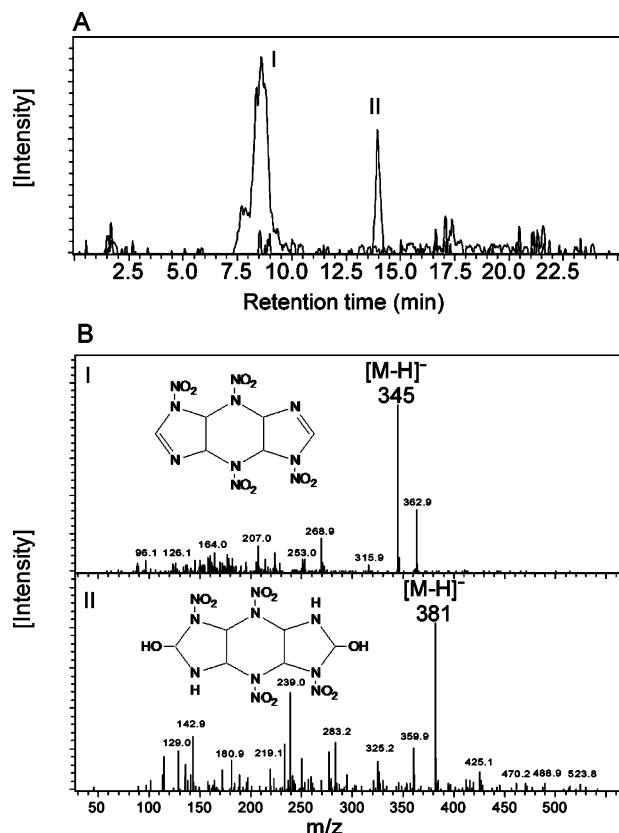


FIGURE 4. Typical LC/MS chromatograms of intermediates **I** and **II** formed upon the double denitration of CL-20 in the Fe^0 -mediated reaction. (A) Extracted ion chromatogram (EIC) of $m/z = 345$ (**I**) and 381 Da (**II**). (B) Mass spectra and structures of **I** and **II**.

decomposition as observed by Bhushan et al. (6). According to the crystal structure analysis of CL-20 (35), the elongated C–C bond at the top of the molecule is the weakest bond and should cleave first.

Potential Initial Decomposition Routes of CL-20. LC/MS analysis showed the presence of the imine (**I**) and its dicarbinol (**II**) intermediates with retention times of 8.6 and 14.0 min, respectively (Figure 4A). Intermediates **I** and **II**, which showed their $[M-H]^-$ ions at 345 and 381 Da (Figure 4B), respectively, were observed during biodegradation (6) and photodenitration (8) of the chemical. Imine **I** can be readily hydrated in water (36) and form the α -hydroxyalkyl-nitramine **II**. The resulting α -hydroxynitramines is unstable (36) and is expected to undergo a rapid ring cleavage (across the $O_2NN-COH$ bond) to ultimately produce formate from the elongated C–C bond and glyoxal from the remaining two C–C bonds in CL-20 (6).

In the present study, we were able to detect two new intermediates (**III** and **IV**) with retention times at 16.8 and 16.3 min, respectively (Figure 5A). The two intermediates had their $[M-H]^-$ at 421 and 405 Da each matching an empirical formula of $C_6H_6N_{12}O_{11}$ or $C_6H_6N_{12}O_{10}$, respectively (Figure 5B). The corresponding nitrate adduct ions $[M+NO_3]^-$ were detected at 484 and 468 Da, respectively. Using ^{15}N -ring-labeled and $^{15}NO_2$ -labeled CL-20, **III** and **IV** were detected at 427 and 411 Da, respectively, representing an increase of 6 amu in each case due to the presence of six ^{15}N atoms. In the case of ^{15}N -amino labeled CL-20 the adduct mass ions of the **III** and **IV** appeared at 490 and 474 Da, respectively, also showing an increase of 6 amu. However, in the case of $^{15}NO_2$ -labeled CL-20, the adduct mass ions of **III** and **IV** appeared at 491 and 475 Da, respectively, representing an increase of 7 amu. The extra 1 amu was attributed to the involvement of $^{15}NO_3^-$ originated from the

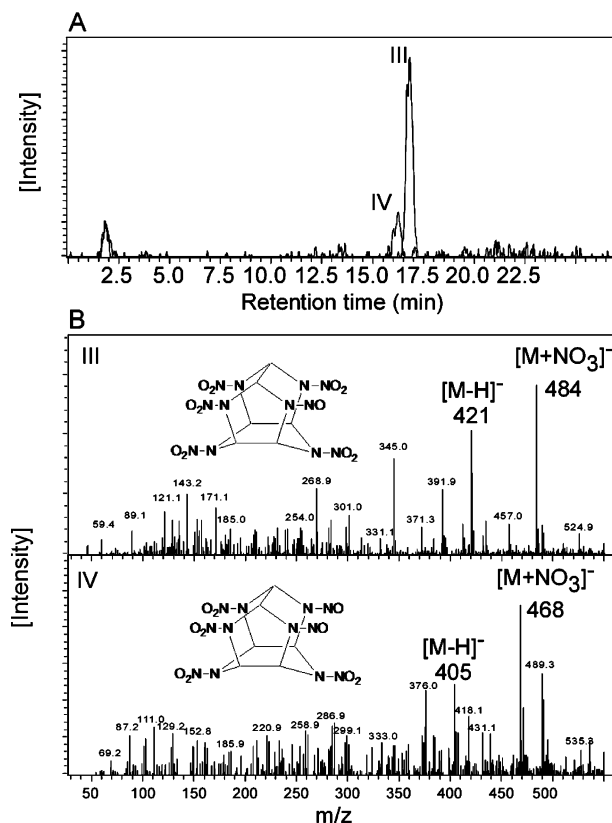


FIGURE 5. Typical LC/MS chromatograms of early intermediates **III** and **IV** in the Fe^0 -mediated decomposition of CL-20. (A) Extracted ion chromatogram (EIC) of $m/z = 484$ (**III**) and 468 Da (**IV**). (B) Mass spectra and structures of **III** and **IV**.

$^{15}NO_2$ -labeled CL-20. A similar nitrate adduct was detected during LC/MS analysis of CL-20 (500 Da) (8). We tentatively identified **III** and **IV** as the mononitroso and the dinitroso derivatives of CL-20 (Figure 5B). As far as we are aware, this is the first observation of nitroso products of CL-20. The transient observation of initially reduced nitroso products **III** and **IV** highlights the potential occurrence of second initial degradation route for CL-20, (i.e., the sequential reduction of N– NO_2 groups to the corresponding N–NO derivatives). Similar reduction has been reported for RDX with iron (19, 20), but no such reactions were known with CL-20.

Finally, Figure 6 shows the presence of two other key intermediates (**V** and **VI**) of CL-20 with their LC/MS peaks appearing at retention times of 13.9 and 13.4 min and their deprotonated molecular mass ions at 392 and 376 Da, respectively. The two intermediates showed their nitrate adduct ions $[M+NO_3]^-$ at 455 and 439 Da, respectively (Figure 6B). The use of $^{15}NO_2$ -labeled CL-20 led to the observation of **V** and **VI** at 397 and 381 Da, respectively, suggesting the loss of one NO_2 from CL-20. Intermediate **V** (Figure 6B) was tentatively identified as the denitrohydrogenated intermediate while intermediate **VI** (Figure 6B) was tentatively identified as its denitrohydrogenated mononitroso product of CL-20. The formation of the last two intermediates resembles the known pathway of the reductive dechlorination of polychlorinated compounds by zerovalent iron (dehalohydrogenation) (12, 14) where there is an apparent substitution of hydride for the leaving group (Cl^- or NO_2^-). While the finding that CL-20 can degrade via multiple pathways is important, the absence of reference standards for these newly detected intermediates prevented us from determining the quantitative contribution of each route in the decomposition of CL-20.

Environmental Significance. This study demonstrates that elevated concentrations of CL-20 (100 mg/L) can be

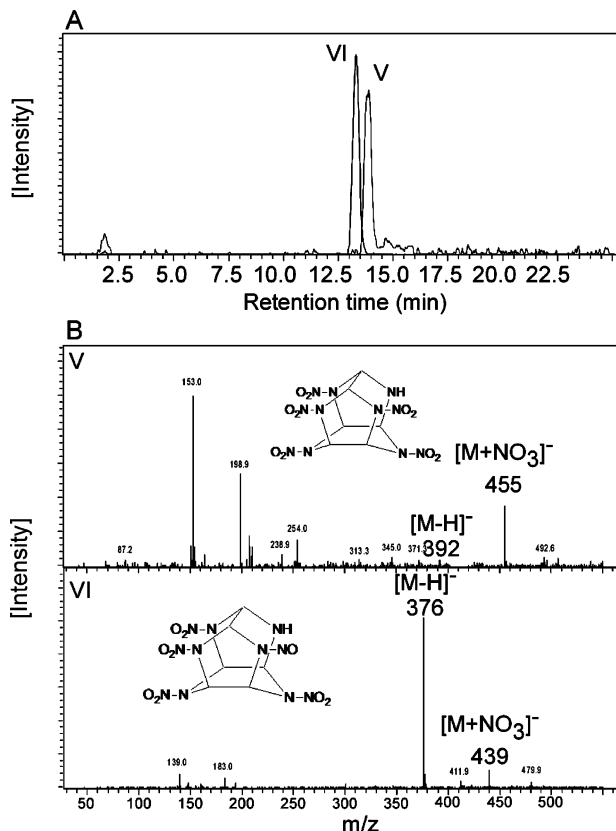


FIGURE 6. Typical LC/MS chromatograms of intermediates V and VI in the Fe^0 -mediated decomposition of CL-20. (A) Extracted ion chromatogram (EIC) of $m/z = 455$ (V) and 376 Da (VI). (B) Mass spectra and structures of V and VI.

efficiently decomposed within a few hours in the presence of zerovalent iron in water in the absence of oxygen. The technology of permeable reactive barriers composed of Fe^0 therefore holds great promise to rapidly remediate this potential emerging contaminant from anaerobic subsurface soils. While nitrous oxide and ammonium constitute the major nitrogen-containing products, formate, glyoxal, and glycolic acid were discovered as important products contributing to the carbon mass balance. Glyoxal is a known toxic chemical (37), and its formation as a product of CL-20 will require investigating its fate under natural conditions.

Acknowledgments

The authors are grateful to Alain Corriveau, Chantale Beaulieu, Stéphane Deschamps, and Zorana Radovich-Hrabovich for their excellent technical assistance. V.K.B. acknowledges the National Sciences and Engineering Research Council of Canada (N.S.E.R.C.) and the National Research Council of Canada (N.R.C.C.) for providing a Visiting Fellowship. We also thank Thiokol Propulsion (Brigham City, UT) for providing CL-20 and labeled [^{15}N]-CL-20. Funding was provided by the U.S. DoD/DoE/EPA Strategic Environmental Research and Development Program (SERDP CP1256).

Literature Cited

- Wardle, R. B.; Hinshaw, J. C.; Braithwaite, P.; Rose, M.; Johnson, G.; Jones, R.; Poush, K. Synthesis of the caged nitramine HNIW (CL-20) 27.1-27.10. Presented at the 27th International Annual Conference of ICT, ADPA, Arlington, VA, 1996.
- Robidoux, P. Y.; Sunahara, G. I.; Savard, K.; Berthelot, Y.; Dodard, S.; Martel, M.; Gong, P.; Hawari, J. Acute and chronic toxicity of new explosive CL-20 to the earthworm (*Eisenia andrei*) exposed to amended natural soils. *J. Environ. Toxicol. Chem.* **2004**, *23*, 1026–1034.

- Gong, P.; Sunahara, G. I.; Rocheleau, S.; Dodard, S. G.; Robidoux, P.-Y.; Hawari, J. Preliminary ecotoxicological characterization of a new energetic substance CL-20. *Chemosphere* **2004**, *56*, 653–658.
- Balakrishnan, V. K.; Halasz, A.; Hawari, J. The alkaline hydrolysis of the cyclic nitramine explosives RDX, HMX and CL-20: New insights into degradation pathways obtained by the observation of novel intermediates. *Environ. Sci. Technol.* **2003**, *37*, 1838–1843.
- Bhushan, B.; Halasz, A.; Thiboutot, S.; Ampleman, G.; Hawari, J. Chemotaxis-mediated biodegradation of cyclic nitramine explosives RDX, HMX, and CL-20 by *Clostridium* sp. EDB2. *Biochem. Biophys. Res. Commun.* **2004**, *316*, 816–821.
- Bhushan, B.; Halasz, A.; Spain, J. C.; Hawari, J. Initial reaction(s) in biotransformation of CL-20 is catalyzed by salicylate 1-monooxygenase from *Pseudomonas* sp. strain ATCC 29352. *Appl. Environ. Microbiol.* **2004**, *70*, 4040–4047.
- Bhushan, B.; Paquet, L.; Spain, J. C.; Hawari, J. Biotransformation of 2,4,6,8,10,12-hexanitro-2,4,6,8,10,12-hexaazaisowurtzitane (CL-20) by denitrifying *Pseudomonas* sp. strain FA 1. *Appl. Environ. Microbiol.* **2003**, *69*, 5216–5221.
- Hawari, J.; Deschamps, S.; Beaulieu, C.; Paquet, L.; Halasz, A. Photodegradation of CL-20: Insights into mechanisms of initial reactions and environmental fate. *Water Res.* **2004**, *38*, 4055–4064.
- Alowitz, M. J.; Scherer, M. M. Kinetics of nitrate, nitrite, and Cr(VI) reduction by iron metal. *Environ. Sci. Technol.* **2002**, *36*, 299–306.
- Westerhoff, P.; James, J. Nitrate removal in zero-valent iron packed columns. *Water Res.* **2003**, *37*, 1818–1830.
- Su, C.; Puls, R. W. Nitrate reduction by zerovalent iron: Effects of formate, oxalate, citrate, chloride, sulfate, borate, and phosphate. *Environ. Sci. Technol.* **2004**, *38*, 2715–2720.
- Scherer, M. M.; Richter, S.; Valentine, R. L.; Alvarez, P. J. J. Chemistry and microbiology of permeable reactive barriers for *in situ* groundwater clean up. *Crit. Rev. Environ. Sci. Technol.* **2000**, *26*, 221–264.
- Rosenthal, H.; Adrian, L.; Steiof, M. Dechlorination of PCE in the presence of Fe^0 enhanced by a mixed culture containing two *Dehalococcoides* strains. *Chemosphere* **2004**, *55*, 661–669.
- Helland, B.; Alvarez, P. J. J.; Schnoor, J. L. Reductive dechlorination of carbon tetrachloride with elemental iron. *J. Hazard. Mater.* **1995**, *41*, 205–216.
- Gui, L.; Gillham, R. W.; Odziemkowski, M. S. Reduction of *N*-nitrosodimethylamine with granular iron and nickel-enhanced iron. 1. Pathways and kinetics. *Environ. Sci. Technol.* **2000**, *34*, 3489–3494.
- Odziemkowski, M. S.; Gui, L.; Gillham, R. W. Reduction of *N*-nitrosodimethylamine with granular iron and nickel-enhanced iron. 2. Mechanistic studies. *Environ. Sci. Technol.* **2000**, *34*, 3495–3500.
- Hundal, L. S.; Singh, J.; Bier, E. L.; Shea, P. J.; Comfort, S. D.; Powers, W. L. Removal of TNT and RDX from water and soil using iron metal. *Environ. Pollut.* **1997**, *97*, 55–64.
- Singh, J.; Comfort, S. D.; Shea, P. J. Remediating RDX-contaminated water and soil using zero-valent iron. *J. Environ. Qual.* **1998**, *27*, 1240–1245.
- Oh, B.-T.; Just, C. L.; Alvarez, P. J. J. Hexahydro-1,3,5-trinitro-1,3,5-triazine mineralization by zerovalent iron and mixed anaerobic cultures. *Environ. Sci. Technol.* **2001**, *35*, 4341–4346.
- Gregory, K. B.; Larese-Casanova, P.; Parkin, G. F.; Scherer, M. M. Abiotic transformation of hexahydro-1,3,5-trinitro-1,3,5-triazine by Fe^{II} bound to magnetite. *Environ. Sci. Technol.* **2004**, *39*, 1408–1414.
- Comfort, S. D.; Shea, P. J.; Machacek, T. A.; Satapanajaru, T. Pilot-scale treatment of RDX-contaminated soil with zerovalent iron. *J. Environ. Qual.* **2003**, *32*, 1717–1725.
- Groom, C. A.; Halasz, A.; Paquet, L.; D'Cruz, P.; Hawari, J. Cyclodextrin-assisted capillary electrophoresis for determination of the cyclic nitramine explosives RDX, HMX and CL-20: Comparison with high-performance liquid chromatography. *J. Chromatogr. A* **2003**, *999*, 17–22.
- Sheremata, T. W.; Hawari, J. Mineralization of RDX by the white rot fungus *Phanerochaete chrysosporium* to carbon dioxide and nitrous oxide. *Environ. Sci. Technol.* **2000**, *34*, 3384–3388.
- Monteil-Rivera, F.; Paquet, L.; Deschamps, S.; Balakrishnan, V. K.; Beaulieu, C.; Hawari, J. Physico-chemical measurements of CL-20 for environmental applications. Comparison with RDX and HMX. *J. Chromatogr. A* **2004**, *1025*, 125–132.
- Stookey, L. L. Ferrozine—A new spectrophotometric reagent for iron. *Anal. Chem.* **1970**, *42*, 779–781.

- (26) Bao, M.; Pantani, F.; Griffini, O.; Burrini, D.; Santianni, D.; Barbieri, K. Determination of carbonyl compounds in water by derivatization-solid-phase microextraction and gas chromatographic analysis. *J. Chromatogr. A* **1998**, *809*, 75–87.
- (27) Sikder, A. K.; Sikder, N.; Gandhe, B. R.; Agrawal, J. P.; Singh, H. Hexanitrohexaazaisowurtzitane or CL-20 in India: Synthesis and characterization. *Def. Sci. J.* **2002**, *52*, 135–146.
- (28) Kiyoura, T.; Kogure, Y. Synthesis of hydroxyacetic acid and its esters from glyoxal catalyzed by multivalent metal ions. *Appl. Catal. A* **1997**, *156*, 97–104.
- (29) Kielemoes, J.; de Boever, P.; Verstraete, W. Influence of denitrification on the corrosion of iron and stainless steel powder. *Environ. Sci. Technol.* **2000**, *34*, 663–671.
- (30) Vyas, P. V.; Shah, B. G.; Trivedi, G. S.; Gaur, P. M.; Ray, P.; Adhikary, S. K. Separation of inorganic and organic acids from glyoxal by electrodialysis. *Desalination* **2001**, *140*, 47–54.
- (31) Matheson, L. J.; Tratnyek, P. G. Reductive dehalogenation of chlorinated methanes by iron metal. *Environ. Sci. Technol.* **1994**, *28*, 2045–2053.
- (32) Klupinski, T. P.; Chin, Y.-P. Abiotic degradation of trifluralin by Fe(II): Kinetics and transformation pathway. *Environ. Sci. Technol.* **2003**, *37*, 1311–1318.
- (33) Klausen, J.; Trober, S. P.; Haderlein, S. B.; Schwarzenbach, R. P. Reduction of substituted nitrobenzenes by Fe(II) in aqueous mineral suspensions. *Environ. Sci. Technol.* **1995**, *29*, 2396–2404.
- (34) Charlet, L.; Silvester, E.; Liger, E. N-compound reduction and actinide immobilization in surficial fluids by Fe(II): The surface $\equiv\text{Fe}^{\text{III}}\text{OFe}^{\text{II}}\text{OH}^{\circ}$ species, as major reductant. *Chem. Geol.* **1998**, *151*, 85–93.
- (35) Zhao, X.; Shi, N. Crystal and molecular structures of ϵ -HNIW. *Chin. Sci. Bull.* **1996**, *41*, 574–576.
- (36) March, J. *Advanced Organic Chemistry*, 3rd ed.; Wiley-Interscience: New York, 1985; pp 784–785.
- (37) Shangari, N.; Bruce, W. R.; Poon, R.; O'Brien, P. J. Toxicity of glyoxals—Role of oxidative stress, metabolic detoxification and thiamine deficiency. *Biochem. Soc. Trans.* **2003**, *31*, 1390–1393.

Received for review April 16, 2004. Revised manuscript received August 5, 2004. Accepted September 9, 2004.

ES049423H

Sorption and Stability of the Polycyclic Nitramine Explosive CL-20 in Soil

Vimal K. Balakrishnan, Fanny Monteil-Rivera, Mathieu A. Gautier, and Jalal Hawari*

ABSTRACT

The polycyclic nitramine CL-20 (2,4,6,8,10,12-hexanitro-2,4,6,8,10,12-hexaazaisowurtzitane) is being considered for use as a munition, but its environmental fate and impact are unknown. The present study consisted of two main elements. First, sorption–desorption data were measured with soils and minerals to evaluate the respective contributions of organic matter and minerals to CL-20 immobilization. Second, since CL-20 hydrolyzes at a pH of >7 , the effect of sorption on CL-20 degradation was examined in alkaline soils. Sorption–desorption isotherms measured using five slightly acidic soils ($5.1 < \text{pH} < 6.9$) containing various amounts of total organic carbon (TOC) revealed a nonlinear sorption that increased with TOC [K_d (0.33% TOC) = 2.4 L kg^{-1} ; K_d (20% TOC) = 311 L kg^{-1}]. Sorption to minerals (Fe_2O_3 , silica, kaolinite, montmorillonite, illite) was very low ($0 < K_d < 0.6 \text{ L kg}^{-1}$), suggesting that mineral phases do not contribute significantly to CL-20 sorption. Degradation of CL-20 in sterile soils having different pH values increased as follows: sandy agricultural topsoil from Varennes, QC, Canada (VT) ($\text{pH} = 5.6$; $K_d = 15 \text{ L kg}^{-1}$; 8% loss) $<$ clay soil from St. Sulpice, QC, Canada (CSS) ($\text{pH} = 8.1$; $K_d = 1 \text{ L kg}^{-1}$; 82% loss) $<$ sandy soil provided by Agriculture Canada (SAC) ($\text{pH} = 8.1$, $K_d = \text{approximately } 0 \text{ L kg}^{-1}$; 100% loss). The faster degradation in SAC soil compared with CSS soil was attributed to the absence of sorption in the former. In summary, CL-20 is highly immobilized by soils rich in organic matter. Although sorption retards abiotic degradation, CL-20 still decomposes in soils where pH is >7.5 , suggesting that it will not persist in even slightly alkaline soils.

THE POLYCYCLIC NITRAMINE CL-20 (Fig. 1) is a highly energetic explosive that is currently being considered for large-scale production and military applications. Presently, due to the relative novelty of CL-20, very little is known about its environmental fate. In general, the manufacturing and usage of munitions has resulted in severe contamination of both soils and ground water (Haas et al., 1990; Myler and Sisk, 1991). Like the monocyclic nitramines RDX (hexahydro-1,3,5-trinitro-1,3,5-triazine) and HMX (octahydro-1,3,5,7-tetra-nitro-1,3,5,7-tetrazocine) (Fig. 1) that have been reported to be toxic to a number of ecological receptors (Yinon, 1990; Talmage et al., 1999), CL-20 was recently found to be toxic to the earthworm (Robidoux et al., 2004). In contrast to currently used munitions, the adverse environmental consequences of widespread usage of CL-20 can be limited by investigating its transport, transformation, and impact in soil.

Recently, we showed that CL-20 readily underwent denitration under alkaline conditions in water ($\text{pH} = 10$) (Balakrishnan et al., 2003) at a faster rate than did the monocyclic nitramines RDX and HMX. From an

environmental perspective, an extension of this investigation to natural media that also encompasses the role of sorption–desorption on CL-20 hydrolysis in soil would be useful.

Sorption of organic chemicals to soil is a process that can affect mobility, degradation, and toxicity by reducing availability. A fundamental understanding of sorption and desorption mechanisms is therefore essential for accurate prediction of the fate and impact of organic contaminants in soils and ground water. Several soil properties, including organic carbon content, pH, cation exchange capacity (CEC), and the amount and type of clay may affect the sorption of organic compounds. Of these properties, organic carbon and clay minerals have been shown to have the highest influence on sorption of nonionic molecules (Huang et al., 1998; Weber et al., 1998; Karapanagioti et al., 2001). Previous studies performed with RDX (Leggett, 1985; Sheremata et al., 2001) and HMX (Brannon et al., 2002; Monteil-Rivera et al., 2003) revealed that both nitramines had a very low tendency to sorption and that this sorption was governed by the clay rather than the organic content of soil. To our knowledge, the sorption–desorption behavior of CL-20 in soils has not been reported in the literature.

In this study, we first measured sorption–desorption isotherms for CL-20 with five slightly acidic soils that varied in organic content. Then the extent of sorption on minerals was measured to evaluate the respective contribution of organic matter and minerals in immobilizing the explosive. Finally, we investigated the effect of sorption–desorption on the stability of CL-20 in sterile soils having different pH values.

MATERIALS AND METHODS

Chemicals

CL-20 (purity 99.3%, determined by reverse phase high performance liquid chromatography [HPLC]) was obtained from A.T.K. Thiokol Propulsion (Brigham City, UT), as an ϵ -form ($\geq 95\%$ as determined by IR). Silica (Grade 60, 60–200 mesh), Fe(III) oxide ($5 \mu\text{m}$, $>99\%$ pure), kaolinite, and montmorillonite K10 were obtained from Aldrich Chemicals (St. Louis, MO) and used as received. Monoclinic illite shale $\{(K,H_3O)(Al,Mg,Fe)_2(Si,Al)_4O_{10}[(OH)_2,H_2O]\}$ was obtained from Ward's Natural Science Establishment (Rochester, NY), ground, and passed through a 2-mm sieve. The pH of the powdered illite (initially = 8.60) was adjusted to 5.4 using

Abbreviations: CSS, clay soil from St. Sulpice; QC, Canada; FS, sandy forest soil provided by a local supplier; FSB, sandy forest soil from Boucherville, QC, Canada; GS, sandy garden soil obtained from a local supplier; HPLC, high performance liquid chromatography; K_d , distribution coefficient; K_F , Freundlich adsorption coefficient; K_{oc} , organic-carbon-normalized distribution coefficient; K_{ow} , n -octanol–water distribution coefficient; SAC, sandy soil provided by Agriculture Canada; SSL, Sassafra sandy loam; TOC, total organic carbon; VT, sandy agricultural topsoil from Varennes, QC, Canada.

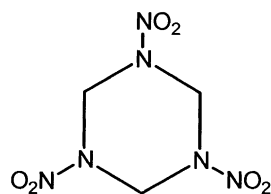
Biotechnology Research Institute, National Research Council of Canada, 6100 Royalmount Avenue, Montréal, QC, Canada H4P 2R2. Received 20 Oct. 2003. *Corresponding author (Jalal.Hawari@cnrc-nrc.gc.ca).

Published in J. Environ. Qual. 33:1362–1368 (2004).

© ASA, CSSA, SSSA

677 S. Segoe Rd., Madison, WI 53711 USA

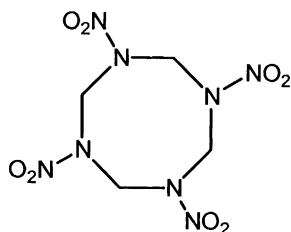
RDX



$$\text{Log } K_{ow} = 0.90$$

$$S_{aq.} (25^{\circ}\text{C}) = 56.4 \text{ mg L}^{-1}$$

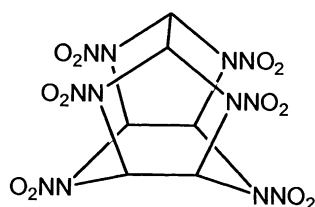
HMX



$$\text{Log } K_{ow} = 0.16$$

$$S_{aq.} (25^{\circ}\text{C}) = 4.5 \text{ mg L}^{-1}$$

CL-20



$$\text{Log } K_{ow} = 1.92$$

$$S_{aq.} (25^{\circ}\text{C}) = 3.6 \text{ mg L}^{-1}$$

Fig. 1. Structures and relevant physicochemical properties of selected nitramine explosives (data from Monteil-Rivera et al., 2004).

HCl in the sorption experiments. All other chemicals were of reagent grade and used without purification.

Soils

Seven soils were used in this study: (i) a Sassafras sandy loam (SSL) (fine-loamy, siliceous, semiactive, mesic Typic Hapludults) sampled in an uncontaminated open grassland on the property of U.S. Army Aberdeen Proving Ground, (Edgewood, MD); (ii) a sandy agricultural topsoil from Varennes, QC, Canada (VT); (iii) a sandy forest soil from Boucherville, QC, Canada (FSB); (iv) a sandy forest soil provided by a local supplier (FS); (v) a sandy garden soil obtained from a local supplier (GS); (vi) a clay soil from St. Sulpice, QC, Canada (CSS); and (vii) a sandy soil provided by Agriculture Canada (SAC). Soils were passed through a 2-mm sieve and air-dried before using. The soils differed with respect to total organic carbon, pH levels, and sand, silt, and clay content (Table 1). A portion of the VT, CSS, and SAC soils was sterilized, as described elsewhere (Sheremata et al., 2001), by gamma irradiation from a ^{60}Co source at the Canadian Irradiation Center (Laval, Quebec) with a dose of 50 kGy over 2 h.

General Sorption–Desorption Procedure

Batch sorption experiments were conducted at ambient temperature ($21 \pm 2^{\circ}\text{C}$) in 16-mL borosilicate centrifuge tubes fitted with Teflon-coated screw caps. For SSL and VT soils, 15 mL of CL-20 solution was added to 2 g of dried soil, while for all other soils and minerals, 10 mL of CL-20 solution and 1.34 g of dry sorbent were used. The tubes were wrapped in

Table 1. Characterization of soils used in this study.

Soil†	Granulometry			Total organic C (dry basis)	pH
	Sand	Silt	Clay		
	%				
VT	83	12	4	2.3	5.6
SSL	71	18	11	0.33	5.1
FSB	99.3		0.7‡	16	5.7
FS	89.8	9.1	1.2	20	6.9
GS	99.4		0.6‡	34	6.1
CSS	2.3	53.2	44.5	0.31	8.1
SAC	98.6	1.3	0.1	0.08	8.1

† VT, sandy agricultural topsoil from Varennes, QC, Canada; SSL, Sassafras sandy loam; FSB, sandy forest soil from Boucherville, QC, Canada; GS, sandy garden soil obtained from a local supplier; FS, sandy forest soil provided by a local supplier; CSS, clay soil from St. Sulpice, QC, Canada; SAC, sandy soil provided by Agriculture Canada.

‡ Value denotes silt + clay.

aluminum foil and agitated on a wrist-action shaker at 430 rpm for the desired contact time. They were then centrifuged for 30 min at $1170 \times g$, and the supernatant was filtered through a Millex-HV 0.45- μm filter (Millipore Corp., Billerica, MA). The filtrate collected after discarding the first 3 mL was analyzed by HPLC, as described below.

Desorption experiments were conducted by adding deionized water (15 mL for SSL and VT soils, 10 mL for other sorbents) to the pellet remaining in the tube after removing the supernatant, and agitating the suspensions for the required contact times. Samples were then centrifuged, filtered, and analyzed as described for sorption experiments. The solution volumes that remained in the soil at the end of the sorption and desorption phases were determined by weight and corrections were made to account for CL-20 present in these volumes.

To estimate CL-20 losses during the experiments, sorbed CL-20 was extracted with acetonitrile from the solid recovered after sorption or desorption as described in USEPA SW-846 Method 8330 (USEPA, 1997), modified to use an acidic calcium chloride solution (CaCl_2 : 5 g L^{-1} ; NaHSO_4 : 0.23 g L^{-1} ; pH = 3) in the sedimentation step.

Sorption and Desorption Kinetics

The time needed to establish sorption and desorption equilibria was determined by conducting kinetics experiments on the VT and GS soils. For sorption experiments, an aqueous solution of CL-20 (3 mg L^{-1}) was shaken with soil over a period ranging from 1 h to 14 d. For desorption kinetics experiments, the soils were first shaken with a 3 mg L^{-1} CL-20 solution for 72 h. After centrifugation, the supernatant was removed and the pellet was contacted with fresh deionized water over periods varying from 1 h to 6 d. Sorbed CL-20 was extracted from the recovered solid using acetonitrile as described above. The kinetics experiments were conducted in triplicate.

Sorption–Desorption Isotherms

Aqueous CL-20 solutions were prepared to give initial CL-20 concentrations ranging from 0.5 to 3.5 mg L^{-1} . Isotherms were measured using SSL, VT, FSB, FS, and GS soils. Sorption experiments were conducted over a period of 65 h for SSL, FS, and VT soils, and 72 h for FSB and GS soils, while desorption experiments were conducted over a period of 24 h (SSL and VT soils) and 48 h (FSB, FS, and GS soils). Following the general procedure described above, six replicates were used for each concentration. Three were extracted with acetonitrile immediately after sorption and the others were extracted after desorption. As a result, triplicate mea-

surements were obtained at each concentration for both the sorption and desorption steps. Blanks containing the same amount of soil and volume of water were subjected to the same test procedure for all soils. No interfering peaks were detected.

All sorption and desorption data were fitted to the linear (Eq. [1]) and Freundlich (Eq. [2]) equations:

$$x/m = K_d C \quad [1]$$

$$x/m = K_F C^{1/n} \quad [2]$$

where x/m is the mass of solute sorbed per unit mass at equilibrium (mg kg^{-1}), C is the aqueous phase concentration of solute at equilibrium (mg L^{-1}), K_d is the distribution coefficient (L kg^{-1}), K_F is the Freundlich constant that gives a measure of the adsorbent capacity ($\text{mg}^{1-1/n} \text{ kg}^{-1} \text{ L}^{1/n}$), and $1/n$ gives a measure of the intensity of sorption. Because the value of K_F depends on the value of $1/n$ for a given sample, K_F values could not be compared between different isotherms. The extent of sorption and desorption were compared using the K_d constants, denoted K_d^s and K_d^d for sorption and desorption, respectively. Although the K_d values varied with sorbate concentration for samples that exhibited a high level of nonlinearity, we treated the linear model as providing average K_d constants that were representative of the sorption processes for each soil. These average values were used to determine the K_{oc} values ($K_{oc} = K_d^s/f_{oc}$, where f_{oc} represents the fraction of organic carbon).

Behavior of CL-20 in Alkaline Soils

The effect of pH on the stability of CL-20 in soil was studied either by artificially adjusting the pH of VT soil suspensions or by using naturally alkaline soils. In the case of VT soil, the dried soil (1.34 g) was contacted for 2 h with 5 mL of water containing the amount of HCl or NaOH required to obtain a final pH ranging from 3 to 9. After adding 5 mL of an aqueous solution of CL-20 (3.5 mg L^{-1}), the slurries were agitated for 65 h. They were then centrifuged for 30 min at $1170 \times g$ and the pH was measured in the supernatant. The latter was then filtered through a Millex-HV 0.45- μm filter, diluted using acetonitrile acidified to a pH of 3 (with H_2SO_4), and analyzed by HPLC. Potential CL-20 products (nitrite, nitrate, and formate ions) were quantified in the most alkaline samples as described below. All the soil pellets were extracted with acetonitrile to calculate a total percent recovery of CL-20.

In the naturally alkaline soils, 10 mL of a CL-20 solution (3.5 mg L^{-1}) and 1.34 g of the sterile SAC (pH = 8.1) soil or sterile CSS (pH = 8.1) soil were agitated in borosilicate centrifuge tubes, using a wrist-action shaker at 430 rpm. At various time intervals, tubes were removed, and after centrifugation for 30 min at $1170 \times g$, the pH was measured in the supernatant and the latter was filtered. The filtrates collected after discarding the first 3 mL were diluted using acidified acetonitrile and analyzed by HPLC. The degradation products of CL-20, nitrite, nitrate, and formate ions were quantified as described below in the 14-d samples as well as in controls (sterile soil and water without CL-20) stirred for 14 d under similar conditions. The soils were extracted with acetonitrile and a total recovery was calculated for CL-20. For comparison, a similar experiment was conducted with sterile VT soil (pH = 5.6).

Analytical Methods

All CL-20 standards and samples were prepared in acidified (pH = 3) mixtures of 50:50 CH_3CN to H_2O since acidification prevented CL-20 degradation. Dissolved soil organic matter

or clay mineral that precipitated from solution at a pH of 3 were separated by centrifugation for 10 min at $16000 \times g$ with an Eppendorf (Hamburg, Germany) Centrifuge 5415D. The supernatant was subsequently analyzed by HPLC.

CL-20 analysis was performed by HPLC using a chromatographic system (ThermoFinnigan, San Jose, CA) composed of a Model P4000 pump, a Model AS3000 injector, including temperature control for the column, and a Model UV6000LP photodiode-array detector. The injection volume was 50 μL . The separation was completed on a Supelcosil LC-CN column (25 cm, 4.6 mm, 5 μm ; Supelco, Bellefonte, PA) maintained at 35°C. The mobile phase (70% aqueous methanol) was run isocratically at 1 mL min^{-1} for the entire run time of 14 min. Chromatograms were extracted at a wavelength of 230 nm and quantified using peak areas of external standards.

Nitrate (NO_3^-) and formate (HCOO^-) ions were quantified by ion chromatography (IC) equipped with a conductivity detector as described elsewhere (Monteil-Rivera et al., 2004). Analysis of nitrite (NO_2^-) ions was performed colorimetrically after producing the diazonium salt as described in USEPA Method 354.1 (USEPA, 1979).

RESULTS AND DISCUSSION

Sorption–Desorption Kinetics

Kinetics experiments were performed using VT (2.3% TOC) and GS (34% TOC) soils to determine the minimum time required to reach sorption and desorption equilibria. The sorption experiments revealed different behavior in both soils (Fig. 2). For GS soil, a rapid sorption occurred with maximal sorption (94%) reached within 1.5 h, while VT soil yielded a slower sorption, with approximately 200 h being required to attain sorption equilibrium (60% sorption). In the case of VT soil, a fast initial adsorption was followed by a slower migration and diffusion of the CL-20 into the soil matrix. These results show that the sorbing sites present in GS soil were more readily accessible than those present in VT soil, suggesting that different types of sites are involved in CL-20 immobilization by soils. No information is yet available on the sorption and desorption kinetics of CL-20 onto soils, but for the monocyclic nitramines RDX and HMX, a rapid sorption was reported to occur in less than 24 h for each compound in different soils, including VT soil (Xue et al., 1995; Myers et al., 1998; Sheremata et al., 2001; Monteil-Rivera et al., 2003). The slower sorption of CL-20 onto the VT soil is indicative of a different sorption mechanism for CL-20 than for RDX and HMX.

Desorption equilibria were achieved in less than 1 and 20 h for GS and VT soils, respectively (Fig. 2). As was the case for sorption, desorption of CL-20 from VT soil was probably delayed by the need for the chemical to diffuse through the soil structure.

CL-20 Sorption–Desorption Isotherms

Sorption and desorption isotherms of CL-20 in various soils are presented in Fig. 3 for the SSL, VT, FSB, FS, and GS soils. Since no microbial growth inhibitor was added to the media and nonsterile soils were used, some degradation of CL-20 was observed (2–16% depending on the soil used; Table 2) during the time frame

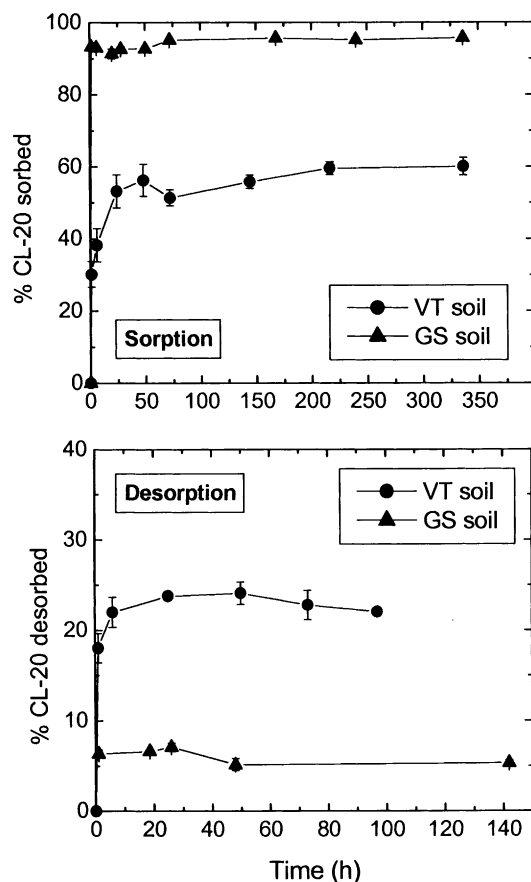


Fig. 2. Sorption and desorption kinetics for CL-20 with sandy agricultural topsoil from Varennes, QC, Canada (VT) and sandy garden soil obtained from a local supplier (GS). For desorption, y axis represents the amount of sorbed CL-20 that desorbs. Error bars represent the standard deviations of three replicates.

of the sorption-desorption isotherms (about one week). To account for CL-20 degradation, the amount of sorbed CL-20 was determined by extracting the soil with acetonitrile, rather than estimating it by difference from the aqueous concentration.

Non-linear regression procedures using Origin software (Microcal, 1999) were used for fitting Freundlich and linear ($1/n$ set equal to 1) isotherms to the sorption data. Values of the resulting parameters for the two models along with the r^2 values are presented in Table 2 and theoretical curves resulting from the Freundlich model are presented in Fig. 3. All sorbents exhibited nonlinear isotherms, with $1/n$ values ranging from 0.49 to 0.94. The r^2 values show that the Freundlich model fitted the equilibrium sorption data better than did the linear model. Moreover, the linear model was not appropriate for describing FSB and GS soils ($r^2 < 0.7$). The general nonlinearity of the isotherms observed in this study indicates that CL-20 sorption to soil occurs through interactions with different classes of sites having different sorption energies (Weber and DiGiano, 1996).

Table 2 clearly shows that sorption was significantly higher in the FS ($K_d = 311 \text{ L kg}^{-1}$), GS ($K_d = 187 \text{ L kg}^{-1}$), and FSB ($K_d = 37 \text{ L kg}^{-1}$) soils than in the VT ($K_d = 15.1 \text{ L kg}^{-1}$) and SSL ($K_d = 2.4 \text{ L kg}^{-1}$) soils.

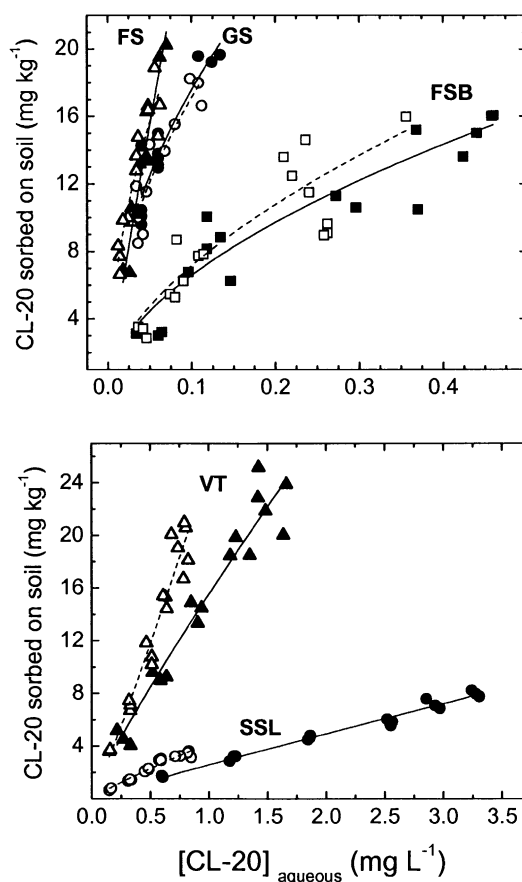


Fig. 3. Sorption-desorption isotherms for CL-20 in nonsterile Sassafras sandy loam (SSL); sandy agricultural topsoil from Varennes, QC, Canada (VT); sandy forest soil from Boucherville, QC, Canada (FSB); sandy garden soil obtained from a local supplier (GS); and sandy forest soil provided by a local supplier (FS) at ambient temperature. Sorption is denoted by filled symbols and solid lines; desorption by hollow symbols and dashed lines. For clarity, data obtained with soils having a high affinity for CL-20 (top) are presented separately from data obtained with soils having a low affinity for CL-20 (bottom).

The higher K_d (and K_F) values obtained in soils with higher organic content suggest that soil organic matter plays a determining role in CL-20 sorption. This result demonstrates a major difference in behavior between CL-20 and the two monocyclic nitramines, RDX and HMX, whose sorption onto soil was previously demonstrated to be independent of organic content (Leggett, 1985; Sheremata et al., 2001; Brannon et al., 2002; Monteil-Rivera et al., 2003). The higher $\log K_{ow}$ measured for CL-20, compared with that of RDX and HMX (Fig. 1; Monteil-Rivera et al., 2004), demonstrates a higher hydrophobicity of the former, which is probably responsible for its superior affinity toward soils with high organic content. Numerous relationships based on Eq. [3] have been developed between soil sorption coefficients (K_{oc}) and n -octanol-water coefficients (K_{ow}):

$$\log K_{oc} = m \log K_{ow} + b \quad [3]$$

where m and b are parameters extracted from linear regressions. To predict a K_{oc} value from a K_{ow} value, a reasonable similarity should be ensured between the

Table 2. Isotherm parameters, organic-carbon-normalized sorption coefficient (K_{oc}), and recoveries for CL-20 sorption and desorption by various soils.

Soil†	Experiment	Freundlich fitting			Linear fitting		K_{oc}	Recovery§
		$K_F‡$	$1/n‡$	r^2	$K_d‡$	r^2		
		$\text{mg}^{1-1/n} \text{ kg}^{-1} \text{ L}^{1/n}$			L kg^{-1}		L kg^{-1}	%
SSL	sorption	2.57 ± 0.11	0.94 ± 0.04	0.983	2.43 ± 0.04	0.981	736	97.0 ± 2.3
	desorption	4.22 ± 0.15	0.89 ± 0.07	0.956	4.43 ± 0.11	0.947		
VT	sorption	15.53 ± 0.50	0.87 ± 0.08	0.948	15.06 ± 0.42	0.928	655	97.3 ± 2.8
	desorption	25.09 ± 1.27	1.09 ± 0.11	0.932	24.14 ± 0.65	0.929		
FSB	sorption	23.76 ± 2.03	0.57 ± 0.06	0.884	36.86 ± 2.26	0.667	230	98.5 ± 8.2
	desorption	27.86 ± 5.27	0.59 ± 0.11	0.716	48.81 ± 3.38	0.569		
GS	sorption	54.83 ± 8.57	0.49 ± 0.06	0.867	187.43 ± 13.73	–0.027	551	92.6 ± 5.8
	desorption	54.31 ± 11.07	0.50 ± 0.08	0.834	190.59 ± 13.71	0.150		
FS	sorption	232.52 ± 71.31	0.90 ± 0.10	0.904	310.84 ± 9.37	0.895	1554	84.3 ± 11.0
	desorption	75.98 ± 16.47	0.53 ± 0.07	0.873	330.84 ± 21.95	0.402		

† SSL, Sassafras sandy loam; VT, sandy agricultural topsoil from Varennes, QC, Canada; FSB, sandy forest soil from Boucherville, QC, Canada; GS, sandy garden soil obtained from a local supplier; FS, sandy forest soil provided by a local supplier.

‡ For these columns, values following the \pm sign are standard errors. The term K_F is the Freundlich coefficient, while K_d is the distribution coefficient.

§ Average percent recovery of CL-20 for all sorption–desorption samples in one soil, as determined by adding the amount of sorbed CL-20 to the amount of CL-20 present in the aqueous phase. Error denotes standard deviation ($n = 36$ for SSL, VT, and FSB soils; $n = 24$ for GS soil; $n = 29$ for FS soil).

solute molecule of interest and the family of compounds used to establish the data set on which m and b are based (Sabljic et al., 1995). No correlation is currently available in the literature for nitramines, but by applying the general model given by Sabljic et al. (1995) for nonhydrophobic chemicals [defined as chemicals containing atoms other than C, H, and halogens ($m = 0.52$; $b = 1.02$)], a K_{oc} value of 104 L kg^{-1} was calculated for CL-20. The fact that this theoretical value is inferior to all those measured in the present study (see Table 2), coupled with the fact that the K_{oc} values measured varied by almost one order of magnitude, confirms that CL-20 adsorption onto organic matter is not limited to a pure physical distribution process, as suggested by the nonlinear isotherms. Therefore, the type, and not just the amount, of organic matter present in soils is a determining factor in the immobilization of CL-20.

A sorption–desorption hysteresis ($K_d^D > K_d^S$) was observed for the SSL and VT soils (Fig. 3, Table 2), while sorption to the FS and GS soils appeared to be fully reversible (K_d^D approximately equal to K_d^S). Meanwhile, the large divergence observed on the measurements performed with FSB soil made it hard to ascertain whether or not this soil gave rise to a sorption hysteresis. Hysteresis phenomena can be caused by organic matter or mineral constituents of soil. We assessed the sorption of CL-20 onto silica, ferric oxide, and three different clays (Table 3). Clays have been shown to play a determining role in the sorption of RDX and HMX (Brannon et al., 2002); when HMX was adsorbed on montmorillonite under similar conditions, a K_d^S value of 15.6 L kg^{-1} was

measured. The data presented in Table 3 demonstrate that CL-20 has a low tendency to adsorb on any of the mineral phases, and that it adsorbs much less on clay than do RDX and HMX. Based on FTIR measurements, Boyd et al. (2001) suggested that nitro-containing compounds are strongly retained by complexation between metals in clay minerals (e.g., K^+) and $-\text{NO}_2$ groups. With six $-\text{NO}_2$ groups, CL-20 contains more sites capable of interacting with such metals compared to RDX (three $-\text{NO}_2$) and HMX (four $-\text{NO}_2$). However, its polycyclic caged structure makes CL-20 a bulkier compound [approximately $6\text{--}7 \text{ \AA}$ in diameter, as estimated from crystallographic data (Zhao and Shi, 1996)] that is unable to migrate into the clay layers [$3\text{--}9 \text{ \AA}$ for a montmorillonite, approximately 5 \AA for a smectite (Brindley, 1981)]. Given the small contribution of mineral phases in CL-20 retention, the hystereses observed with VT and SSL soils were probably caused by the organic content of soil.

The full CL-20 recoveries we obtained on sonicating the sorbed soils in acetonitrile ruled out the formation of covalent bonds between CL-20 and organic matter as the reason for the hysteresis. Weber et al. (1998) previously suggested that the form of the soil organic matter played a critical role in the hystereses observed in the sorption–desorption behavior of hydrophobic organic compounds such as phenanthrene. Humic acids, with their large microporosities, allow for fast interaction with water, thus producing a reversible sorption. In contrast, condensed organic matter presents physically rigid zones that interact poorly with water and tend to trap any molecules sorbed within it, producing a sorption–desorption hysteresis (Weber et al., 1998). The hystereses observed in the present study could therefore have arisen from an entrapment of CL-20 in condensed organic matter. However, a matrix change that could occur from the sorption to the desorption step to give access to sites with higher sorbing capacity in the desorption batch should not be excluded.

Behavior of CL-20 in Alkaline Soils

The ability of CL-20 to be significantly sorbed to soils containing organic matter was demonstrated in

Table 3. Sorption and stability of CL-20 with minerals.

Mineral	pH	$K_d^S‡$	Recovery‡
		L kg^{-1}	%
Silica	6.0	0.35 ± 0.05	89.4 ± 0.9
Fe_2O_3	5.9	approximately 0	93.6 ± 1.0
Montmorillonite	2.4	0.62 ± 0.07	99.9 ± 1.6
Kaolinite	5.4	0.14 ± 0.04	95.7 ± 0.3
Illite	5.4§	0.30 ± 0.04	97.8 ± 0.5

† Distribution coefficient for sorption (mean \pm SD, $n = 3$).

‡ Average percent recovery of CL-20 determined after adding the amount of sorbed CL-20 to the amount of CL-20 present in the aqueous phase (mean \pm SD, $n = 3$).

§ After adjustment with HCl.

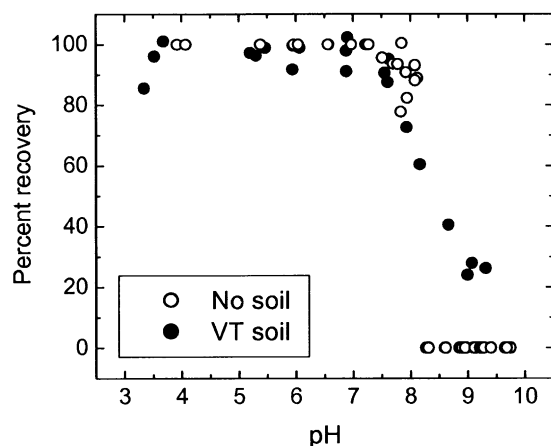


Fig. 4. Percent recovery of CL-20 after 65 h of agitation at different pH values and ambient temperature, in presence or absence of nonsterile sandy agricultural topsoil from Varennes, QC, Canada (VT).

the previous section. Given the previously established tendency of CL-20 to undergo rapid hydrolysis under alkaline conditions (pH = 10) (Balakrishnan et al., 2003), an investigation into the effect of soils on the hydrolysis process was deemed worthwhile. To generate a pH profile of CL-20 stability in soil, we adjusted the pH of VT soil and contacted it with CL-20 solution for 65 h. Below a pH of 7.5, percent recoveries remained approximately constant at approximately 100%, while above a pH of 7.5, CL-20 degraded (Fig. 4). Analyses of degradation products in the most alkaline soil samples showed that CL-20 disappearance was accompanied by the formation of NO_2^- and HCOO^- . The fact that degradation was observed in soils with a pH of >7.5 indicates that CL-20 will not persist in natural alkaline soil environments. In aqueous control samples of CL-20 (Fig. 4), degradation was observed at a pH of >7.5 and was complete at a pH of >8.1 . The greater extent of degradation observed in the control solutions than in the soils at a pH of >8 suggests that to a certain extent, the presence of soil protects CL-20 against decomposition.

Since CL-20 significantly degraded when we increased the pH of VT suspensions, the behavior of CL-20 was followed over time in two sterile, naturally alkaline soils. After 14 d of contact with sterile SAC and sterile CSS soils (pH = 8.1), 100 and 82% of the CL-20 degraded, respectively, compared with only 8% loss in sterile VT soil (pH = 5.6) (Fig. 5). Clearly, CL-20 is not stable in alkaline soils. Degradation in the naturally alkaline soils produced two equivalents of nitrite (NO_2^-) for each mole of CL-20 reacted, exactly as observed for the aqueous alkaline hydrolysis of CL-20 at a pH of 10 (Balakrishnan et al., 2003). Despite the equivalent pH values of both soils, CL-20 degraded faster in SAC soil than it did in CSS soil. The SAC soil contains very low amounts of the two most active sorbents in soils (0.1% clay and 0.08% TOC), whereas CSS soil contains clay (44.5%) and organic carbon (0.31%). As a result, CL-20 did not sorb onto SAC soil (K_d^s = approximately 0 L kg^{-1}) and was thus not protected from degradation. In contrast, the slight sorption to CSS soil ($K_d^s = 1.0 \pm 0.3 \text{ L kg}^{-1}$,

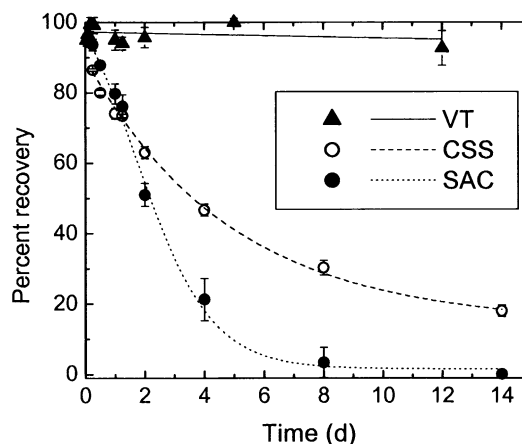


Fig. 5. Stability of CL-20 in sterile soils having various pH values (clay soil from St. Sulpice, QC, Canada [CSS] and sandy soil provided by Agriculture Canada [SAC], pH = 8.1; sandy agricultural topsoil from Varennes, QC, Canada [VT], pH = 5.6). Error bars represent the standard deviations of three replicates.

$n = 24$) retarded CL-20 hydrolysis. Therefore, sorption retarded the hydrolysis of the energetic chemical but did not prevent it.

CONCLUSIONS

This study reveals that CL-20 can be highly retained by soils. In contrast to the monocyclic nitramines, RDX and HMX, which are mainly adsorbed by the clay fraction of soil, CL-20 affinity for soil is governed by the organic content of soil, and only a small fraction of the energetic chemical is actually bound to the mineral phase. Even though sorption to soils retards abiotic degradation, CL-20 readily decomposes in natural soils where pH is >7.5 suggesting that, unlike RDX and HMX, CL-20 will not be a persistent organic pollutant in even slightly alkaline soils. As a result, the identification of intermediates and final products in the degradation of CL-20 is of paramount importance to fully define the environmental impact of this nitramine explosive. The identification of products resulting from CL-20 decomposition constitutes the focus of ongoing studies in our laboratory.

ACKNOWLEDGMENTS

The authors thank A. Corriveau and D. Manno for their technical assistance. V.K. Balakrishnan thanks the National Sciences and Engineering Research Council of Canada and the National Research Council of Canada for a Visiting Fellowship. We also thank Thiokol Propulsion (Brigham City, UT) for providing CL-20. Funding was provided by the U.S. DoD/DoE/EPA Strategic Environmental Research and Development Program (SERDP CP 1256).

REFERENCES

- Balakrishnan, V.K., A. Halasz, and J. Hawari. 2003. Alkaline hydrolysis of the cyclic nitramine explosives RDX, HMX, and CL-20: New insights into degradation pathways obtained by the observation of novel intermediates. *Environ. Sci. Technol.* 37:1838–1843.
- Boyd, S.A., G. Sheng, B.J. Teppen, and C.T. Johnston. 2001. Mechanisms for the adsorption of substituted nitrobenzenes by smectite clays. *Environ. Sci. Technol.* 35:4227–4234.

- Brannon, J.M., C.B. Price, C. Hayes, and S.L. Yost. 2002. Aquifer soil cation substitution and adsorption of TNT, RDX, and HMX. *Soil Sediment Contam.* 11:327–338.
- Brindley, G.W. 1981. Structures and chemical compositions of clay minerals. p. 1–21. *In* F.J. Longstaffe (ed.) *Short course in clays and the resource geologist*. Mineralogical Assoc. of Canada, Edmonton, AB.
- Haas, R., I. Schreiber, E. von Low, and G. Stork. 1990. Conception for the investigation of contaminated munition plants. 2. Investigation of former RDX plants and filling stations. *Fresenius' J. Anal. Chem.* 338:41–45.
- Huang, W., H. Yu, and W.J. Weber. 1998. Hysteresis in the sorption and desorption of hydrophobic organic contaminants by soils and sediments: 1. A comparative analysis of experimental protocols. *J. Contam. Hydrol.* 31:129–148.
- Karapanagioti, H.K., J. Childs, and D.A. Sabatini. 2001. Impacts of heterogeneous organic matter on phenanthrene sorption: Different soil and sediment samples. *Environ. Sci. Technol.* 35:4684–4690.
- Leggett, D.C. 1985. Sorption of military explosive contaminants on bentonite drilling muds. CRREL Rep. 85-18. U.S. Army Cold Regions Res. and Eng. Lab., Hanover, NH.
- Microcal. 1999. Origin Version 6.0. Microcal, Northampton, MA.
- Monteil-Rivera, F., C. Groom, and J. Hawari. 2003. Sorption and degradation of octahydro-1,3,5,7-tetranitro-1,3,5,7-tetrazocine in soil. *Environ. Sci. Technol.* 37:3878–3884.
- Monteil-Rivera, F., L. Paquet, S. Deschamps, V.K. Balakrishnan, C. Beaulieu, and J. Hawari. 2004. Physico-chemical measurements of CL-20 for environmental applications. Comparison with RDX and HMX. *J. Chromatogr. A* 1025:125–132.
- Myers, T.E., J.M. Brannon, J.C. Pennington, W.M. Davis, K.F. Myers, D.M. Townsend, M.K. Ochman, and C.A. Hayes. 1998. Laboratory studies of soil sorption/transformation of TNT, RDX, and HMX. Tech. Rep. IRRP-98-8. U.S. Army Corps of Eng., Waterways Exp. Stn., Vicksburg, MS.
- Myler, C.A., and W. Sisk. 1991. Bioremediation of explosives contaminated soil. p. 137–146. *In* G.S. Sayler, R. Fox, and J.W. Blackburn (ed.) *Environmental biotechnology for waste treatment*. Plenum Press, New York.
- Robidoux, P.Y., G.I. Sunahara, K. Savard, Y. Berthelot, S. Dodard, M. Martel, P. Gong, and J. Hawari. 2004. Acute and chronic toxicity of the new explosive CL-20 to the earthworm (*Eisenia andrei*) exposed to amended natural soils. *Environ. Toxicol. Chem.* 23: 1026–1034.
- Sabljić, A., H. Güsten, H. Verhaar, and J. Hermens. 1995. QSAR modelling of soil sorption. Improvements and systematics of log K_{oc} vs. log K_{ow} correlations. *Chemosphere* 31:4489–4514.
- Sheremata, T.W., A. Halasz, L. Paquet, S. Thiboutot, G. Ampleman, and J. Hawari. 2001. The fate of the cyclic nitramine explosive RDX in natural soil. *Environ. Sci. Technol.* 35:1037–1040.
- Talmage, S.S., D.M. Opresko, C.J. Maxwell, C.J.E. Welsh, F.M. Cretella, P.H. Reno, and F.B. Daniel. 1999. Nitroaromatic munition compounds: Environmental effects and screening values. *Rev. Environ. Contam. Toxicol.* 161:1–156.
- USEPA. 1979. Methods for chemical analysis of water and wastes—Nitrogen, nitrite. Method 354.1. USEPA, Washington, DC.
- USEPA. 1997. Nitroaromatics and nitramines by high performance liquid chromatography (HPLC). Method 8330 SW-846 Update III Part 4:1 (B). Office of Solid Waste, Washington, DC.
- Weber, W.J., and F.A. DiGiano. 1996. Energy relationships: Applications to heterogeneous systems. p. 317–421. *In* *Process dynamics in environmental systems*. Wiley-Interscience, New York.
- Weber, W.J., W. Huang, and H. Yu. 1998. Hysteresis in the sorption and desorption of hydrophobic organic contaminants by soils and sediments: 2. Effects of soil organic matter heterogeneity. *J. Contam. Hydrol.* 31:149–165.
- Xue, S.K., I.K. Iskandar, and H.M. Selim. 1995. Adsorption-desorption of 2,4,6-trinitrotoluene and hexahydro-1,3,5-trinitro-1,3,5-triazine in soils. *Soil Sci.* 160:317–327.
- Yinon, J. 1990. Cyclotrimethylenetrinitramine (RDX). Cyclotetramethylenetetranitramine (HMX). p. 145–170. *In* *Toxicity and metabolism of explosives*. CRC Press, Boca Raton, FL.
- Zhao, X., and N. Shi. 1996. Crystal and molecular structures of ϵ -HNIW. *Chin. Sci. Bull.* 41:574–576.

Initial Reaction(s) in Biotransformation of CL-20 Is Catalyzed by Salicylate 1-Monooxygenase from *Pseudomonas* sp. Strain ATCC 29352

Bharat Bhushan,¹ Annamaria Halasz,¹ Jim C. Spain,² and Jalal Hawari^{1*}

Biotechnology Research Institute, National Research Council of Canada, Montreal, Quebec H4P 2R2, Canada,¹
and U.S. Air Force Research Laboratory, Tyndall Air Force Base, Florida 32403²

Received 16 January 2004/Accepted 6 April 2004

CL-20 (2,4,6,8,10,12-hexanitro-2,4,6,8,10,12-hexaazaisowurtzitane) ($C_6H_6N_{12}O_{12}$), a future-generation high-energy explosive, is biodegradable by *Pseudomonas* sp. strain FA1 and *Agrobacterium* sp. strain JS71; however, the nature of the enzyme(s) involved in the process was not understood. In the present study, salicylate 1-monooxygenase, a flavin adenine dinucleotide (FAD)-containing purified enzyme from *Pseudomonas* sp. strain ATCC 29352, biotransformed CL-20 at rates of 0.256 ± 0.011 and 0.043 ± 0.003 nmol min⁻¹ mg of protein⁻¹ under anaerobic and aerobic conditions, respectively. The disappearance of CL-20 was accompanied by the release of nitrite ions. Using liquid chromatography/mass spectrometry in the negative electrospray ionization mode, we detected a metabolite with a deprotonated mass ion $[M - H]^-$ at 345 Da, corresponding to an empirical formula of $C_6H_6N_{10}O_8$, produced as a result of two sequential N denitration steps on the CL-20 molecule. We also detected two isomeric metabolites with $[M - H]^-$ at 381 Da corresponding to an empirical formula of $C_6H_{10}N_{10}O_{10}$. The latter was a hydrated product of the metabolite $C_6H_6N_{10}O_8$ with addition of two H₂O molecules, as confirmed by tests using ¹⁸O-labeled water. The product stoichiometry showed that each reacted CL-20 molecule produced about 1.7 nitrite ions, 3.2 molecules of nitrous oxide, 1.5 molecules of formic acid, and 0.6 ammonium ion. Diphenyliodonium-mediated inhibition of salicylate 1-monooxygenase and a comparative study between native, deflavo, and reconstituted enzyme(s) showed that FAD site of the enzyme was involved in the biotransformation of CL-20 catalyzed by salicylate 1-monooxygenase. The data suggested that salicylate 1-monooxygenase catalyzed two oxygen-sensitive single-electron transfer steps necessary to release two nitrite ions from CL-20 and that this was followed by the secondary decomposition of this energetic chemical.

CL-20 (2,4,6,8,10,12-hexanitro-2,4,6,8,10,12-hexaazaisowurtzitane) is a high-energy polycyclic nitramine compound with a rigid caged structure (25) (Fig. 1). Due to its superior explosive properties, it may replace the conventionally used explosives such as hexahydro-1,3,5-trinitro-1,3,5-triazine (RDX), octahydro-1,3,5,7-tetranitro-1,3,5,7-tetrazocine (HMX) and 2,4,6-trinitrotoluene (TNT) (Fig. 1) in the future. The environmental, biological, and health impacts of CL-20 and its metabolic products are not known. Severe environmental contamination (7, 12, 24) and biological toxicity (21, 30, 34, 36) as a result of the widespread use of monocyclic nitramine explosives such as RDX and HMX have been well documented. The U.S. Environmental Protection Agency has recommended a lifetime health advisory for RDX (9) and HMX (23). It is likely that due to its structural similarity to RDX and HMX, CL-20 (Fig. 1) may also cause similar environmental problems in soil, sediment, and groundwater. Therefore, the biodegradation of CL-20 must be understood in order to determine and predict its environmental fate and impact.

Previous reports of biotransformation and biodegradation of RDX and HMX by a variety of microorganisms and enzymes have shown that initial N denitration led to ring cleavage and decomposition (2, 3, 5, 10, 14, 28). Trott et al. (31) reported aerobic biodegradation of CL-20 by the soil isolate *Agrobacte-*

rium sp. strain JS71, which utilized CL-20 as a sole nitrogen source and assimilated 3 mol of nitrogen per mol of CL-20. However, no information was provided about the initial reactions involved in the biodegradation of CL-20. In a recent study, we reported that a flavoenzyme(s) from *Pseudomonas* sp. strain FA1 might have been responsible for the biotransformation of CL-20 via an initial N-denitration mechanism (4); however, we did not detect initial metabolite(s) to support our hypothesis. We also reported the presence of CL-20 biotransformation products such as nitrite, nitrous oxide, and formate (4).

Salicylate 1-monooxygenase (EC 1.14.13.1), a flavin adenine dinucleotide (FAD)-containing enzyme from *Pseudomonas* sp. strain ATCC 29352, is capable of catalyzing a variety of biochemical reactions (19). The physiological role of salicylate 1-monooxygenase is to biotransform salicylate to catechol (20). However, it demonstrates activity against many other substrates such as *o*-halogenophenol and *o*-nitrophenol (29), benzoates, and variety of other compounds (19). We hypothesized that CL-20, being an oxidized chemical, might act as a substrate of salicylate 1-monooxygenase by accepting an electron(s).

In the present study, we used salicylate 1-monooxygenase as a model flavoenzyme in experiments to determine the initial enzymatic reaction(s) involved in the biodegradation of CL-20 and to gain insights into how flavoenzyme-producing bacteria biotransform CL-20. In liquid chromatography/mass spectrometry (LC/MS) studies, uniformly ring-labeled [¹⁵N]CL-20 and H₂¹⁸O were used to identify the intermediate(s) produced

* Corresponding author. Mailing address: Biotechnology Research Institute, National Research Council of Canada, 6100 Royalmount Ave., Montreal, Quebec H4P 2R2, Canada. Phone: (514) 496-6267. Fax: (514) 496-6265. E-mail: jalal.hawari@nrc.ca.

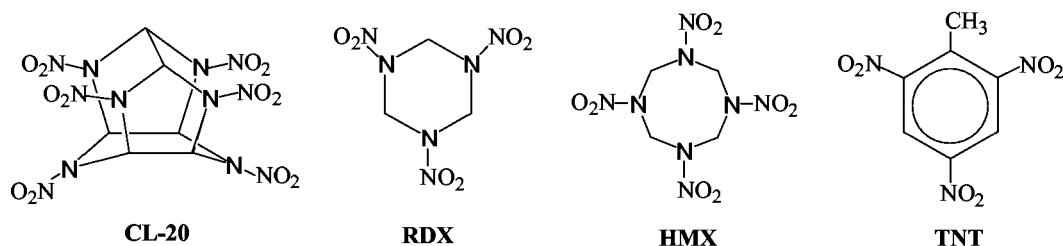


FIG. 1. Molecular structure of the explosives CL-20, RDX, HMX, and TNT.

during the course of reaction. Additionally, we studied the involvement of the FAD-site of salicylate 1-monooxygenase in CL-20 biotransformation.

MATERIALS AND METHODS

Chemicals. CL-20 (ϵ -form and 99.3% purity) and uniformly ring-labeled [^{15}N]CL-20 (ϵ -form and 90.0% purity) were provided by ATK Thiokol Propulsion, Brigham City, Utah. NADH, diphenyliodonium chloride (DPI), and flavin adenine dinucleotide (FAD) were purchased from Sigma Chemicals, Oakville, Ontario, Canada. Nitrous oxide (N_2O) was purchased from Scott Specialty Gases, Sarnia, Ontario, Canada. H_2^{18}O (95% normalized ^{18}O atoms) was purchased from Aldrich Chem. Co., Milwaukee, Wis. All other chemicals were of the highest purity grade.

Enzyme preparation and modification. Salicylate 1-monooxygenase from *Pseudomonas* sp. strain ATCC 29352 was purchased as a lyophilized powder (protein approximately 45% by the Biuret method) from Sigma Chemicals. Native enzyme activity against salicylate was determined as specified by the manufacturer. The enzyme was washed with phosphate buffer (pH 7.0) at 4°C using Biomax-5K membrane centrifuge filter units (Sigma Chemicals) to remove preservatives and then resuspended in the same buffer. The protein content was determined by using the bicinchoninic acid protein assay kit from Pierce Chemical Co., Rockford, Ill.

Apoenzyme (deffavo form) was prepared by removing FAD from salicylate 1-monooxygenase by using a previously reported method (32). Reconstitution was carried out by incubating the apoenzyme with $100\ \mu\text{M}$ FAD in 50 mM potassium phosphate buffer (pH 7.0) for 1 h at 4°C . The unbound FAD was removed by washing the enzyme with the same buffer, using Biomax-5K membrane centrifuge filter units.

Biotransformation assays. Enzyme-catalyzed biotransformation assays were performed under aerobic as well as anaerobic conditions by using 6-ml glass vials. Anaerobic conditions were created by purging the reaction mixture with argon gas for 20 min and by replacing the headspace air with argon in sealed vials. Each assay vial contained, in 1 ml of assay mixture, CL-20 or uniformly ring-labeled [^{15}N]CL-20 ($25\ \mu\text{M}$ or $11\ \text{mg liter}^{-1}$), NADH ($100\ \mu\text{M}$), enzyme preparation ($250\ \mu\text{g}$), and potassium phosphate buffer (50 mM; pH 7.0). Higher CL-20 concentrations than its aqueous solubility of $3.6\ \text{mg liter}^{-1}$ (11) were used to allow detection and quantification of the intermediate(s). Reactions were performed at 30°C . Three different controls were prepared by omitting enzyme, CL-20, or NADH from the assay mixture. Boiled enzyme was also used as a negative control. NADH oxidation was measured spectrophotometrically at 340 nm as described previously (2). Samples from the liquid and gas phases in the vials were analyzed for residual CL-20 and biotransformed products.

To determine the residual CL-20 concentrations during biotransformation studies, the reaction was performed with multiple identical vials. At each time point, the total CL-20 content in one reaction vial was solubilized in 50% aqueous acetonitrile and analyzed by high-pressure liquid chromatography (HPLC) (see below). The CL-20 biotransformation activity of salicylate 1-monooxygenase was expressed as nanomoles per minute per milligram of protein unless otherwise stated.

To demonstrate the effect of enzyme concentration on CL-20 biotransformation, a progress curve was generated for reactions under anaerobic conditions by incubating salicylate 1-monooxygenase at increasing concentrations (0.25 to 2.0 mg/ml) with $45\ \mu\text{M}$ CL-20 and $100\ \mu\text{M}$ NADH. The reactions conditions were the same as these described above.

To determine the incorporation of water into the CL-20 metabolite(s), H_2^{18}O was mixed with 100 mM potassium phosphate buffer (pH 7.0) at a ratio of 8:2. All other reaction ingredients and conditions were the same as those described above for the biotransformation of CL-20.

Enzyme inhibition studies. Inhibition with DPI, an inhibitor of flavoenzymes that acts by forming a flavin-phenyl adduct (6), was assessed by incubating salicylate 1-monooxygenase (1 mg) with DPI (0 to 0.5 mM) at room temperature for 15 to 20 min. After incubation, CL-20 biotransformation activities of the enzyme were determined by monitoring the residual CL-20 as described above.

Analytical procedures. CL-20 and its intermediates were detected and analyzed with a Bruker bench top ion trap mass detector attached to a Hewlett-Packard 1100 series HPLC system equipped with a photodiode array detector. The samples were injected into a $5\text{-}\mu\text{m}$ -pore-size Zorbax SB-C18 capillary column (0.5-mm internal diameter by 150 mm; Agilent) at 25°C . The solvent system was an acetonitrile/water gradient (30 to 70% [vol/vol]) at a flow rate of $15\ \mu\text{L min}^{-1}$. For mass analysis, ionization was performed in the negative electrospray ionization mode (ES $^-$), producing mainly deprotonated molecular mass ions $[\text{M} - \text{H}]^-$. The mass range was scanned from 40 to 550 Da.

The CL-20 concentration was quantified with an HPLC apparatus connected to a photodiode array detector (λ_{230}) as described previously (4). Nitrous oxide (N_2O) and formaldehyde (HCHO) were analyzed as previously reported (2, 3, 18). Ammonium cations were analyzed by an SP 8100 HPLC system equipped with a Waters 431 conductivity detector and a Hamilton PRP-X200 (250 mm by 4.6 mm by $10\ \mu\text{m}$) analytical column as described previously (17). Formic acid (HCOOH) and nitrite (NO_2^-) were quantified using a Waters HPLC system equipped with a conductivity detector as reported previously (4).

^{15}N -labeled N_2O (i.e., $^{15}\text{N}^{14}\text{NO}$) was analyzed by a 6890 gas chromatograph (Hewlett-Packard Mississauga, Ontario, Canada) coupled with a 5973 quadrupole mass spectrometer. A GS-Gas Pro capillary column (30 m by 0.32 mm) (J & W Scientific, Folsom, Calif.) was used under splitless conditions. The injector and mass spectrometer interface (MSD) were maintained at 150 and 250°C , respectively. The column was set at -25°C for 1.5 min and then raised to -10°C at a rate of $10^\circ\text{C min}^{-1}$, which was held for 5 min. The MSD was used in the scan mode (electron impact) between 10 and 50 Da. The total run time was 8 min, and $^{15}\text{N}^{14}\text{NO}$ was detected at a retention time of 5.5 min with a molecular mass of 45 Da.

RESULTS AND DISCUSSION

Salicylate 1-monooxygenase-catalyzed biotransformation of CL-20. Biotransformation of CL-20 with a purified salicylate 1-monooxygenase from *Pseudomonas* sp. strain ATCC 29352 was found to be NADH dependent and optimal at pH 7.0 and 30°C under dark conditions. A progress curve demonstrated a linear increase in CL-20 biotransformation as a function of enzyme concentration (Fig. 2). The rates of CL-20 biotransformation were 0.256 ± 0.011 and $0.043 \pm 0.003\ \text{nmol min}^{-1}\ \text{mg of protein}^{-1}$ under anaerobic and aerobic conditions, respectively, indicating the involvement of an initial oxygen-sensitive process. On the other hand, salicylate 1-monooxygenase activity against the physiological substrate salicylate was $580\ \text{nmol min}^{-1}\ \text{mg of protein}^{-1}$ under aerobic conditions. The low activity of enzyme against CL-20 might be due to three probable reasons. First, CL-20 is a hydrophobic compound with very little aqueous solubility ($3.6\ \text{mg liter}^{-1}$ at 25°C) (11), hence, its biotransformation rate is limited by the rate of mass transfer from solid to aqueous phase. In comparison, the aqueous solubility of salicylate is about $2,000\ \text{mg liter}^{-1}$ at 20°C .

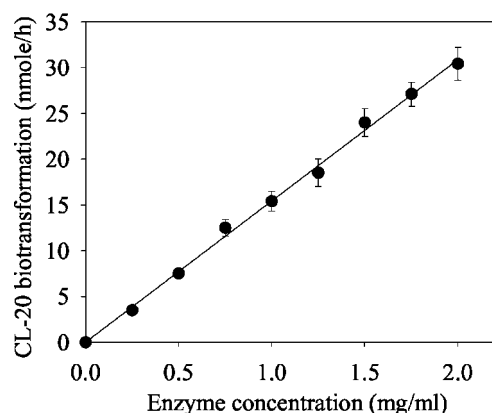


FIG. 2. Progress curve demonstrating CL-20 biotransformation as a function of salicylate 1-monooxygenase concentration. The linear-regression curve has a gradient of 15.42 and an r^2 of 0.99. Data are means of results from triplicate experiments, and error bars indicate standard errors. Some error bars are not visible due to their small size.

(*Merck Index*, 13th ed.) and would be higher at 30°C. Second, CL-20 is not a physiological substrate of salicylate 1-monooxygenase; hence, it is expected that its interaction with this enzyme would be rather slow. Third, CL-20 was biotransformed under anaerobic conditions, in contrast to the aerobic biotransformation of salicylate.

In a previous study, the rates of CL-20 biotransformation with a flavoenzyme(s) from *Pseudomonas* sp. strain FA1, under anaerobic and aerobic conditions, were 0.191 ± 0.006 and 0.041 ± 0.001 nmol min⁻¹ mg of protein⁻¹, respectively (4), which appear to be similar to those which we observed in the present study. The total flavin content in salicylate 1-monooxygenase and the flavoenzyme(s) from *Pseudomonas* sp. strain FA1 were 20.5 and 12.6 nmol mg of protein⁻¹, respectively. Hence, under anaerobic conditions, CL-20 biotransformation by the two enzymes in terms of their flavin contents were 0.012 and 0.015 nmol min⁻¹ nmol of flavin moiety⁻¹, respectively. We found that in all controls (see Materials and Methods), abiotic degradation of CL-20 was negligible after 1 h of reaction time. The maximum abiotic degradation of CL-20 (0.010 ± 0.001 nmol min⁻¹) was seen in a control with NADH under anaerobic conditions, which was only 4% of the CL-20 degradation catalyzed by salicylate 1-monooxygenase.

Molecular oxygen (O₂) inhibits CL-20 biotransformation in two possible ways: (i) by competing with CL-20 for accepting electrons at the FAD site, since O₂, in the absence of substrate, is known to accept electrons from the reduced salicylate 1-monooxygenase to produce H₂O₂ (19), and (ii) by quenching an electron from the CL-20 anion radical (described below), converting it back to the parent molecule (CL-20) and thus enforcing a futile redox cycling. Analogously, O₂-mediated inhibition of RDX anion radical formation was observed during biotransformation of RDX catalyzed by diaphorase (2). Due to the inhibitory effect of oxygen, the subsequent experiments were carried out under anaerobic conditions.

Time course studies showed a gradual disappearance of CL-20 at the expense of the electron donor NADH with concomitant release of nitrite (NO₂⁻) and nitrous oxide (N₂O) (Fig. 3). We found that N₂O, although produced during later steps of CL-20 biotransformation (described below), appeared

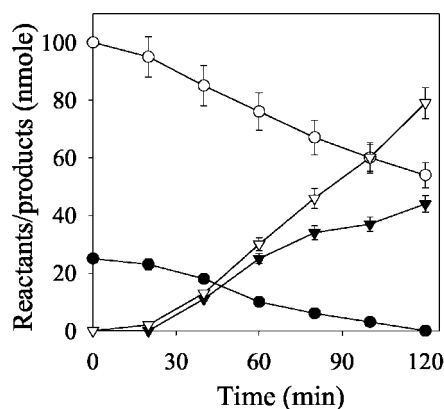


FIG. 3. Time course study of NADH-dependent biotransformation of CL-20 by salicylate 1-monooxygenase (1 mg) under anaerobic conditions. Data for residual CL-20 (●), NADH (○), nitrite (▼), and nitrous oxide (▽) are shown. The data are means of results from triplicate experiments, and error bars indicate standard errors. Some error bars are not visible due to their small size.

before NO₂⁻ in the assay medium, as shown in Fig. 3. This could be explained by two facts: (i) there was a large difference in the stoichiometries of nitrite (1.7) and nitrous oxide (3.2), and (ii) the nitrous oxide detection method (gas chromatography [GC] with electron capture detector) was much more sensitive (lowest-detection limit, 0.022 nmol) than the nitrite detection method (HPLC conductivity detector) (lowest detection limit, 5.434 nmol/ml). Hence, nitrous oxide was detected as early as 20 min into the reaction whereas nitrite was detected only after 30 min (Fig. 3). After 2 h of reaction, each reacted CL-20 molecule consumed about 1.9 NADH molecules and produced 1.7 nitrite ions, 3.2 molecules of nitrous oxide, 1.5 molecules of formic acid, and 0.6 molecule of ammonium (Table 1). Of the total 12 N atoms and 6 C atoms per

TABLE 1. Comparative stoichiometries of reactants and products during biotransformation of CL-20 by the salicylate 1-monooxygenase from *Pseudomonas* sp. strain ATCC 29352 and the membrane-associated enzyme(s) from *Pseudomonas* sp. strain FA1

Reactant or product	<i>Pseudomonas</i> sp. strain ATCC 29352 ^{a,c}		<i>Pseudomonas</i> sp. strain FA1 ^{b,c}	
	Amt (nmol)	Molar ratio of reactant to product per reacted CL-20 molecule	Amt (nmol)	Molar ratio of reactant to product per reacted CL-20 molecule
Reactants				
CL-20	25 ± 1.4	1.0 ± 0.05	20 ± 1.2	1.0 ± 0.06
NADH	48 ± 2.7	1.9 ± 0.10	90 ± 7.1	4.5 ± 0.35
Products				
Nitrite (NO ₂ ⁻)	43 ± 2.5	1.7 ± 0.09	46 ± 3.2	2.3 ± 0.16
Nitrous oxide (N ₂ O)	79 ± 5.3	3.2 ± 0.21	29 ± 1.6	1.5 ± 0.08
Formate (HCOOH)	37 ± 2.4	1.5 ± 0.09	34 ± 2.8	1.7 ± 0.13
Ammonium (NH ₄ ⁺)	15 ± 0.9	0.6 ± 0.04	ND ^d	ND

^a Reaction was performed at pH 7.0 and 30°C for 2 h under anaerobic conditions.

^b Data are from reference 4.

^c Data are mean ± standard error ($n = 3$).

^d ND, not determined.

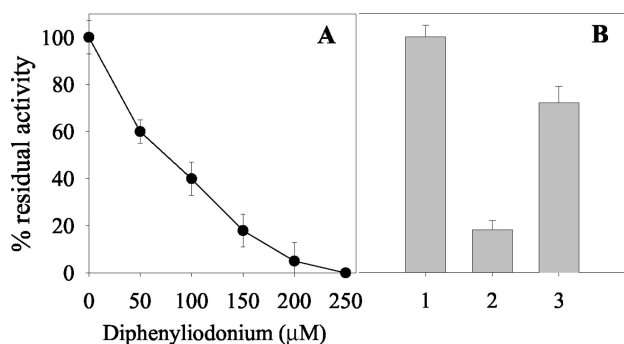


FIG. 4. (A) Concentration-dependent inhibition of salicylate 1-monooxygenase-catalyzed biotransformation of CL-20 by DPI. (B) Biotransformation of CL-20 by the native (bar 1), deflavo (bar 2), and reconstituted (bar 3) salicylate 1-monooxygenase (3). A 100% CL-20 biotransformation activity was equivalent to 0.256 ± 0.011 nmol min⁻¹ mg of protein⁻¹. Data are mean percentages of CL-20 biotransformation activity \pm standard errors ($n = 3$).

reacted CL-20 molecule, we recovered approximately 9 N (as NO₂⁻, N₂O, and NH₄⁺) and 2 C (as HCOOH) atoms, respectively. The remaining 3 N and 4 C atoms were probably present in an unidentified product(s). In comparison, a membrane-associated flavoenzyme(s) from *Pseudomonas* sp. strain FA1 produced 2.3 nitrite ions, 1.5 molecules of nitrous oxide, and 1.7 molecules of formic acid from each reacted CL-20 molecule (Table 1). Furthermore, during photodegradation of CL-20 at 300 nm in acetonitrile aqueous solution, which was also initiated by N denitration, the product distribution was similar to that in the present study but the stoichiometry was different; i.e., each reacted molecule of CL-20 produced 5.0, 5.3, 1.4, and 0.3 molecules of NO₂⁻, HCOOH, NH₃, and N₂O, respectively (15). The probable reason for the higher yields of NO₂⁻ and HCOOH in photolysis of CL-20 was attributed to the intense action of the high-energy wavelength λ₃₀₀ (energy, 400 kJ/mol), which caused rapid cleavage of N-NO₂ and -HC-NNO₂ bonds in CL-20 (15).

Involvement of the flavin-moiety (FAD) in CL-20 biotransformation. Salicylate 1-monooxygenase from *Pseudomonas* sp. strain ATCC 29352 is a dimeric protein with two identical subunits, each of which has an approximate molecular mass of 45.5 kDa and contains one molecule of FAD (33). DPI inhibited the biotransformation of CL-20 in a concentration-dependent manner (Fig. 4A). It is known that DPI inhibits flavoen-

zymes by the formation of flavin-phenyl adduct (6), which indicates the involvement of FAD in CL-20 biotransformation. Furthermore, DPI targets flavin-containing enzymes that catalyze one-electron transfer reactions (6, 26), which provided strong circumstantial evidence that a one-electron transfer process was involved in the initial reaction that might have caused N denitration of CL-20.

The involvement of FAD was additionally confirmed by assaying the deflavo and reconstituted forms of salicylate 1-monooxygenase against CL-20. The specific activities of the native, deflavo, and reconstituted forms of salicylate 1-monooxygenase against CL-20 were 0.256 ± 0.011 , 0.045 ± 0.003 , and 0.183 ± 0.008 nmol min⁻¹ mg of protein⁻¹, respectively, revealing that deflavo enzyme had lost about 82% of its activity compared to the native enzyme (Fig. 4B). The remaining 18% activity observed in the deflavo form was due to incomplete removal of FAD (data not shown), whereas the reconstituted enzyme, prepared by reconstitution of the deflavo enzyme with FAD, restored the CL-20 biotransformation activity up to 72% (Fig. 4B). The above results indicate the direct involvement of FAD in biotransformation of CL-20.

Free FAD (100 μM) also transformed CL-20 in the presence of NADH (100 μM) at a rate of 0.035 ± 0.003 nmol min⁻¹; however, the biotransformation rate was only 14% of that of the bound FAD present in native salicylate 1-monooxygenase. The above finding additionally supported the involvement of FAD in CL-20 biotransformation and suggested that the flavin moiety has to be enzyme bound in order to function efficiently. The involvement of a flavoenzyme(s) in biotransformation of RDX (2) and HMX (3) via a one-electron transfer process has previously been reported. In a study with flavin mononucleotide containing diaphorase from *Clostridium kluyveri*, we reported an oxygen-sensitive one-electron transfer reaction that caused an initial N denitration of RDX followed by spontaneous decomposition (2). On the other hand, a FAD-containing xanthine oxidase also catalyzed a similar reaction with HMX (3).

Detection and identification of metabolites. The metabolites, obtained by a reaction between salicylate 1-monooxygenase and CL-20 (metabolite I), were detected by their deprotonated molecular mass ion [M - H]⁻ in LC/MS (ES⁻) studies and are listed in Table 2. Intermediates III and IV appeared simultaneously, with retention times (*R_t*) of 8.2 and 7.5 min, respectively (Fig. 5A), but with the same [M - H]⁻ at 345 Da (Fig. 5C), corresponding to an empirical formula C₆H₆N₁₀O₈.

TABLE 2. Properties of metabolites detected and identified by LC/MS (ES⁻) during biotransformation of CL-20 catalyzed by salicylate 1-monooxygenase from *Pseudomonas* sp. strain ATCC 29352

Metabolite ^a	Retention time (<i>R_t</i>) (min)	Mass area in LC/MS (ES ⁻) extracted ion-chromatogram ^b	[M - H] ⁻ (Da) ^c	No. of nitrogen atoms from [¹⁵ N]CL-20 ring	No. of oxygen atoms from H ₂ ¹⁸ O	Proposed empirical formula
III	8.2	207,980	345	6	0	C ₆ H ₆ N ₁₀ O ₈
IV ^d	7.5	26,089	345	6	0	C ₆ H ₆ N ₁₀ O ₈
V	12.5	11,092	381	6	2	C ₆ H ₁₀ N ₁₀ O ₁₀
VI	1.9	71,672	381	6	2	C ₆ H ₁₀ N ₁₀ O ₁₀
VII	1.7	7,637	293	4	4	C ₆ H ₁₀ N ₆ O ₈

^a Tentative structures of these metabolites are shown in Fig. 6.

^b All mass areas of metabolites persisted for about 1.5 h and then gradually disappeared after 2.5 h of reaction.

^c Deprotonated mass ions.

^d IV, an isomer of III, was a minor intermediate, as shown in Fig. 5A.

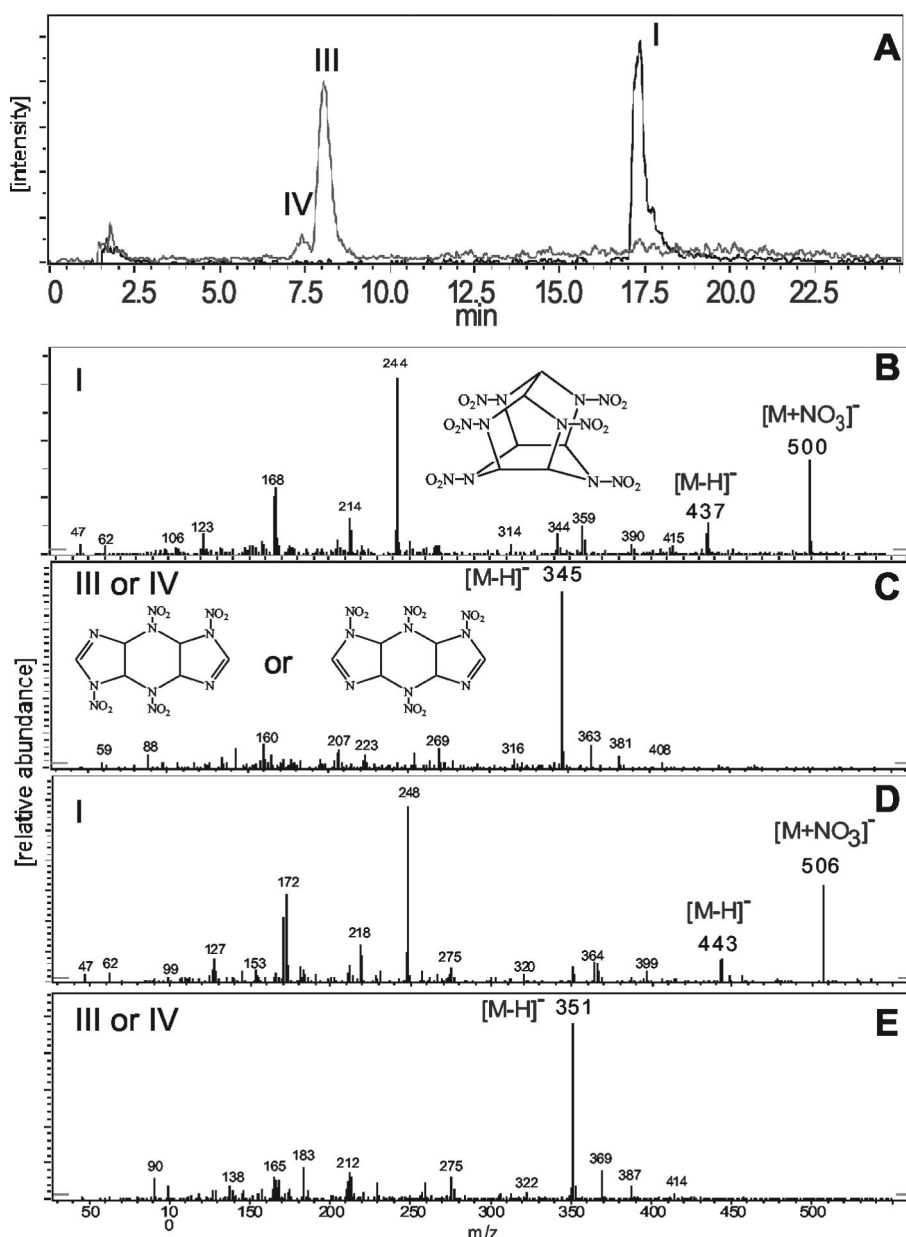


FIG. 5. (A) LC/MS (ES⁻) extracted ion chromatogram of CL-20 (I) and its metabolite (III or IV) produced by the reaction of CL-20 with salicylate 1-monooxygenase; the extracted mass ion of CL-20 was an adduct mass ion $[M + NO_3]^-$ at 500 Da, and the deprotonated mass ions $[M - H]^-$ of CL-20 (I) and its metabolite (III or IV) were 437 and 345 Da, respectively. (B to E) LC/MS (ES⁻) spectra of nonlabeled CL-20 (B), its metabolite III or IV (C), uniformly ring-labeled [¹⁵N]CL-20 (D), and its metabolite III or IV (E) showed deprotonated mass ions $[M - H]^-$ at 437, 345, 443, and 351 Da, respectively.

When ring-labeled [¹⁵N]CL-20 was used in the reaction, both intermediates III and IV showed a deprotonated molecular ion $[M - H]^-$ at 351 Da (Table 2; Fig. 5E), indicating that each intermediate included the six nitrogen atoms from the CL-20 ring. Moreover, the use of H₂¹⁸O did not affect the mass of intermediates III and IV. Intermediates III and IV, previously observed during photolysis of CL-20 (15), were tentatively identified as isomers resulting from the loss of two -NO₂ groups during the initial reaction(s) between CL-20 and salicylate 1-monooxygenase. In the present study, we described the secondary decomposition of intermediate III, (Fig. 6). Inter-

mediate IV, being an isomer of III, might also decompose like intermediate III.

Several other products, including V, VI, and VII, were also detected with *R*_t at 12.5, 1.9, and 1.7 min, respectively, and with $[M - H]^-$ at 381, 381, and 293 Da corresponding to empirical formulae of C₆H₁₀N₁₀O₁₀, C₆H₁₀N₁₀O₁₀, and C₆H₁₀N₆O₈, respectively (Table 2). Likewise, when uniformly ring-labeled [¹⁵N]CL-20 was used, the $[M - H]^-$ of products V, VI, and VII were observed at 387, 387, and 297 Da, respectively, indicating the incorporation of six ¹⁵N atoms into products V and VI and only four ¹⁵N atoms into product VII (Table 2). When

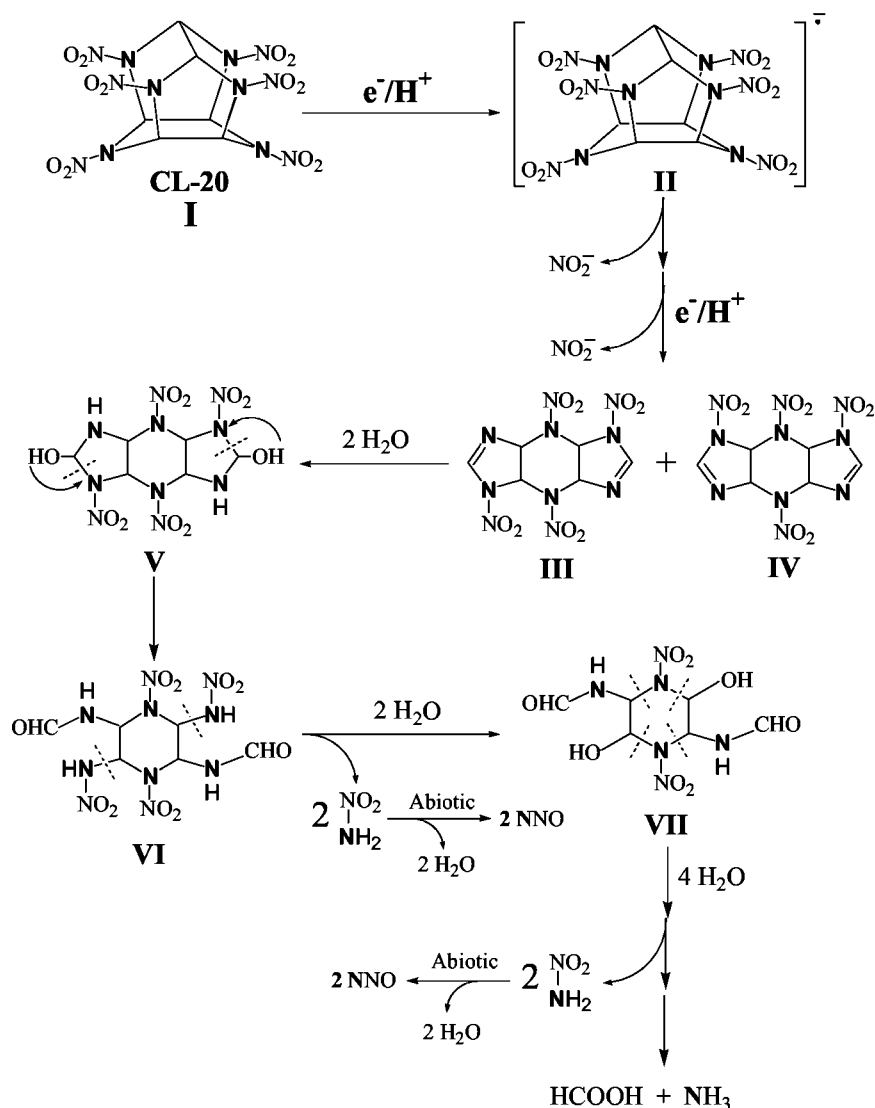


FIG. 6. Proposed pathway of the initial biotransformation of CL-20 catalyzed by salicylate 1-monooxygenase followed by secondary decomposition. Nitrogen atoms shown in bold were actually ring-nitrogens and were uniformly labeled in [^{15}N] CL-20. Secondary decomposition of intermediate III is shown; intermediate IV might also decompose like intermediate III. The intermediate shown in brackets was not detected.

the experiment was repeated with $H_2^{18}O$, the $[M - H]^-$ of products V, VI, and VII were observed at 385, 385, and 301 Da, respectively, indicating the incorporation of two ^{18}O atoms into products V and VI and four ^{18}O atoms into product VII (Table 2). Based on the above data, intermediate V was tentatively identified as a carbinol adduct ($C_6H_{10}N_{10}O_{10}$) whereas intermediates VI ($C_6H_{10}N_{10}O_{10}$) and VII ($C_6H_{10}N_6O_8$) were identified as sequential ring cleavage products (Table 2, Fig. 6). All the above metabolites were transient and completely disappeared after 2.5 h of reaction.

To determine the source of N_2O , experiments were performed with uniformly ring-labeled [^{15}N]CL-20. $^{15}N^{14}NO$ was detected with a molecular mass of 45 Da by GC-MS analysis, confirming that of the two nitrogen atoms in N_2O , one was from the labeled [^{15}N]CL-20 ring and the second was from the unlabeled peripheral nitro ($-NO_2$) group. We found that all of the N_2O in the present study was labeled and produced from

$N-NO_2$ groups released from the CL-20, as previously suggested by Patil and Brill (27). Analogously, N_2O generation from $N-NO_2$ has also been reported during biodegradation of RDX (13) and HMX (3). In a previous study, we reported that N_2O , besides being produced from $N-NO_2$, was also produced via nitrite reduction catalyzed by an enzyme preparation from *Pseudomonas* sp. strain FA1 (4). In contrast, the present study did not show N_2O production through nitrite reduction. For instance, when we incubated $NaNO_2$ (1 mM) with salicylate 1-monooxygenase and NADH under similar reaction conditions to those used for CL-20 biotransformation, we did not detect N_2O during 2 h of reaction, which additionally supported the idea that $N-NO_2$ was the only source of N_2O in the present study.

Proposed mechanism(s) of the initial reaction(s) followed by secondary decomposition of CL-20. Based on the gradual appearance of nitrite (Fig. 3), reaction inhibition by oxygen

and DPI, detection of an initial intermediate(s) (Fig. 5), and analogy to other systems (2, 3), we propose that salicylate 1-monooxygenase catalyzes a single-electron transfer to the CL-20 molecule (metabolite I) to produce an anion-radical (intermediate II) (Fig. 6). Spontaneous N denitration of intermediate II (i.e., release of the first NO_2^-) would produce a transient N-centered free radical, as previously proposed during biotransformation (4), thermolysis (27) and photodegradation (15) of CL-20. The N-centered free-radical, being unstable, must undergo rapid rearrangement by cleavage at the weaker C—C bond bridging the two cyclopentanes in CL-20 (35). The rearranged molecule would accept a second electron in order to release a second NO_2^- to produce two isomeric intermediates, III and IV (Table 2; Fig. 5 and 6). Stoichiometrically, two N- denitration steps would require an obligatory transfer of two electrons (equivalent to one NADH molecule); however, we found that 1.9 NADH molecules were consumed for each reacted CL-20 molecule (Table 1). The excess of NADH (i.e., the remaining 0.9 molecule) utilization could be due to two possible reasons: (i) some NADH could bind to the enzyme and go undetected, or (ii) it could be utilized by a yet unidentified CL-20 metabolite(s).

Intermediate III, produced as a result of two N denitration steps, underwent hydrolysis by the addition of two H_2O molecules across the two imine bonds ($-\text{C}=\text{N}-$) to produce an unstable carbinol derivative V, as confirmed by the experiment with H_2^{18}O (discussed above). Imine bonds are known to be unstable and to decompose rapidly in water (22). Hence, V might cleave at the $\text{O}_2\text{NN}-\text{CH}(\text{OH})$ bond following rearrangement to produce intermediate VI, which has a similar $[\text{M} - \text{H}]^-$ of 381 Da to that of intermediate V (Table 2; Fig. 6). Addition of a water molecule across an imine bond followed by ring opening has previously been detected during photolysis of CL-20 (15) and RDX (16) and during cytochrome P450-catalyzed biotransformation of RDX (5). Stoichiometric addition of two H_2O molecules to intermediate VI, confirmed by the experiment with H_2^{18}O , produced intermediate VII, with concomitant release of two nitramide molecules ($\text{NH}_2\text{-NO}_2$) (Table 2; Fig. 6). Intermediate VII, being an α -hydroxyalkyl nitramine, was unstable in water (8) and therefore decomposed to finally produce nitrous oxide, formic acid, and ammonia, as quantified in Table 1 and shown in Fig. 6.

In conclusion, we have provided the first biochemical evidence of the initial reaction(s) involved in the transformation of CL-20 catalyzed by salicylate 1-monooxygenase under anaerobic conditions. The mechanism described here is consistent with our previous enzymatic studies with RDX and HMX (2, 3), which also suggested that one-electron transfer is necessary and sufficient to cause N- denitration of RDX and HMX, leading to their spontaneous decomposition. Some of the CL-20 products observed in the present study are consistent with those reported previously with respect to alkaline hydrolysis (1), biotransformation (4), and photolysis (15). So far, very few reports are available with regard to microbial degradation of CL-20. For instance, *Agrobacterium* sp. strain JS71, a soil isolate, degraded CL-20 and assimilated 3 mol of nitrogen per mol of CL-20 (31). In a recent study, *Pseudomonas* sp. strain FA1 degraded CL-20 and assimilated about 4 mol of nitrogen per mol of CL-20 (4). However, the two previous studies (4, 31) detected no initial metabolite(s) and did

not describe the involvement of any specific enzyme(s). The present study thus advances our understanding of the initial steps involved in biotransformation of CL-20 by flavoenzyme(s)-producing bacteria. *Pseudomonas*, being the source of salicylate 1-monooxygenase and other flavoenzymes, seems to be a promising degrader of CL-20. The ubiquitous presence of *Pseudomonas* and similar bacteria in environments such as soil, marine and freshwater sediments, and estuaries would therefore help in understanding the fate of CL-20 in such environments.

ACKNOWLEDGMENTS

B. Bhushan thanks the Natural Sciences and Engineering Research Council (NSERC) and the National Research Council (NRC) of Canada for a visiting fellowship. We sincerely acknowledge the U.S. Strategic Environmental Research and Development Program (SERDP) for financial support (CP 1256). We also thank the Department of National Defense, Val Bélair, Canada, for their support.

We gratefully acknowledge the analytical and technical support of A. Corriveau and C. Beaulieu. Finally, the critical suggestions of reviewers helped in improving the manuscript.

REFERENCES

- Balakrishnan, V. K., A. Halasz, and J. Hawari. 2003. Alkaline hydrolysis of the cyclic nitramine explosives RDX, HMX, and CL-20: new insights into degradation pathways obtained by the observation of novel intermediates. *Environ. Sci. Technol.* **37**:1838–1843.
- Bhushan, B., A. Halasz, J. C. Spain, and J. Hawari. 2002. Diaphorase catalyzed biotransformation of RDX via N-denitration mechanism. *Biochem. Biophys. Res. Commun.* **296**:779–784.
- Bhushan, B., L. Paquet, A. Halasz, J. C. Spain, and J. Hawari. 2003. Mechanism of xanthine oxidase catalyzed biotransformation of HMX under anaerobic conditions. *Biochem. Biophys. Res. Commun.* **306**:509–515.
- Bhushan, B., L. Paquet, J. C. Spain, and J. Hawari. 2003. Biotransformation of 2,4,6,8,10,12-hexanitro-2,4,6,8,10,12-hexaazaisowurtzitane (CL-20) by denitrifying *Pseudomonas* sp. strain FA 1. *Appl. Environ. Microbiol.* **69**:5216–5221.
- Bhushan, B., S. Trott, J. C. Spain, A. Halasz, L. Paquet, and J. Hawari. 2003. Biotransformation of hexahydro-1,3,5-trinitro-1,3,5-triazine (RDX) by a rabbit liver cytochrome P450: insight into the mechanism of RDX biodegradation by *Rhodococcus* sp. strain DN22. *Appl. Environ. Microbiol.* **69**:1347–1351.
- Chakraborty, S., and V. Massey. 2002. Reaction of reduced flavins and flavoproteins with diphenyliodonium chloride. *J. Biol. Chem.* **277**:41507–41516.
- Clausen, J., J. Robb, D. Curry, and N. Korte. 2004. A case study of contaminants on military ranges: Camp Edwards, Massachusetts, USA. *Environ. Pollut.* **129**:13–21.
- Druckrey, H. 1973. Specific carcinogenic and teratogenic effects of 'indirect' alkylating methyl and ethyl compounds, and their dependency on stages of ontogenic development. *Xenobiotica* **3**:271–303.
- Etnier, E. L., and W. R. Hartley. 1990. Comparison of water quality criterion and lifetime health advisory for hexahydro-1,3,5-trinitro-1,3,5-triazine (RDX). *Regul. Toxicol. Pharmacol.* **11**:118–122.
- Fournier, D., A. Halasz, J. C. Spain, P. Fiurasek, and J. Hawari. 2002. Determination of key metabolites during biodegradation of hexahydro-1,3,5-trinitro-1,3,5-triazine (RDX) with *Rhodococcus* sp. strain DN22. *Appl. Environ. Microbiol.* **68**:166–172.
- Groom, C. A., A. Halasz, L. Paquet, P. D'Cruz, and J. Hawari. 2003. Cyclodextrin-assisted capillary electrophoresis for determination of the cyclic nitramine explosives RDX, HMX and CL-20: comparison with high-performance liquid chromatography. *J. Chromatogr. A* **999**:17–22.
- Haas, R., E. V. Löw, I. Schreiber, and G. Stork. 1990. Conception for the investigation of contaminated munitions plants. 2. Investigation of former RDX-plants and filling stations. *Fresenius J. Anal. Chem.* **338**:41–45.
- Halasz, A., J. Spain, L. Paquet, C. Beaulieu, and J. Hawari. 2002. Insights into the formation and degradation of methylenedinitramine during the incubation of RDX with anaerobic sludge. *Environ. Sci. Technol.* **36**:633–638.
- Hawari, J. 2000. Biodegradation of RDX and HMX: from basic research to field application, p. 277–310. In J. C. Spain, J. B. Hughes, and H.-J. Knackmuss (ed.), *Biodegradation of nitroaromatic compounds and explosives*. CRC Press, Inc., Boca Raton, Fla.
- Hawari, J. 2003. Environmental fate and transport of a new energetic material, CL-20. Annual Project Report, December 2003 (CP 1256). Strategic Environmental Research and Development Program, Arlington, Va.

16. Hawari, J., A. Halasz, C. Groom, S. Deschamps, L. Paquet, C. Beaulieu, and A. Corriveau. 2002. Photodegradation of RDX in aqueous solution: a mechanistic probe for biodegradation with *Rhodococcus* sp. *Environ. Sci. Technol.* **36**:5117–5123.
17. Hawari, J., A. Halasz, S. Beaudet, L. Paquet, G. Ampleman, and S. Thiboutot. 2001. Biotransformation routes of octahydro-1,3,5,7-tetranitro-1,3,5,7-tetrazocine by municipal anaerobic sludge. *Environ. Sci. Technol.* **35**:70–75.
18. Hawari, J., A. Halasz, T. Sheremata, S. Beaudet, C. Groom, L. Paquet, C. Rhofir, G. Ampleman, and S. Thiboutot. 2000. Characterization of metabolites during biodegradation of hexahydro-1,3,5-trinitro-1,3,5-triazine (RDX) with municipal sludge. *Appl. Environ. Microbiol.* **66**:2652–2657.
19. Kamin, H., R. H. White-Stevens, and R. P. Presswood. 1978. Salicylate hydroxylase. *Methods Enzymol.* **53**:527–543.
20. Katagiri, M., H. Maeno, S. Yamamoto, O. Hayaishi, T. Kitao, and S. Oae. 1965. Salicylate hydroxylase, a monooxygenase requiring flavin adenine dinucleotide. II. The mechanism of salicylate hydroxylation to catechol. *J. Biol. Chem.* **240**:3414–3417.
21. Levine, B. S., E. M. Furedi, D. E. Gordon, J. J. Barkley, and P. M. Lish. 1990. Toxic interactions of the munitions compounds TNT and RDX in F344 rats. *Fundam. Appl. Toxicol.* **15**:373–380.
22. March, J. 1985. *Advanced organic chemistry*, 3rd ed., p. 784–785. Wiley-Interscience, New York, N.Y.
23. McLellan, W., W. R. Hartley, and M. Brower. 1988. Health advisory for octahydro-1,3,5,7-tetranitro-1,3,5,7-tetrazocine. Technical report PB90–273533. Office of Drinking Water, U.S. Environmental Protection Agency, Washington, D.C.
24. Myler, C. A., and W. Sisk. 1991. Bioremediation of explosive-contaminated soils (scientific questions/engineering realities), p. 137–146. *In* G. S. Sayler, R. Fox, and J. W. Blackburn (ed.), *Environmental bio/technology for waste treatment*. Plenum Press, New York, N.Y.
25. Nielsen, A. T., A. P. Chafin, S. L. Christian, D. W. Moore, M. P. Nadler, R. A. Nissan, and D. J. Vanderah. 1998. Synthesis of polyazapolycyclic caged polynitramines. *Tetrahedron* **54**:11793–11812.
26. O'Donnell, V. B., G. C. Smith, and O. T. Jones. 1994. Involvement of phenyl radicals in iodonium inhibition of flavoenzymes. *Mol. Pharmacol.* **46**:778–785.
27. Patil, D. G., and T. B. Brill. 1991. Thermal decomposition of energetic materials. 53. Kinetics and mechanisms of thermolysis of hexanitrohexaazaisowurtzitane. *Combust. Flame* **87**:145–151.
28. Seth-Smith, H. M. B., S. J. Rosser, A. Basran, E. R. Travis, E. R. Dabbs, S. Nicklin, and N. C. Bruce. 2002. Cloning, sequencing and characterization of the hexahydro-1,3,5-trinitro-1,3,5-triazine degradation gene cluster from *Rhodococcus rhodochrous*. *Appl. Environ. Microbiol.* **68**:4764–4771.
29. Suzuki, K., T. Gomi, T. Kaidoh, and E. Itagaki. 1991. Hydroxylation of *o*-halogenophenol and *o*-nitrophenol by salicylate hydroxylase. *J. Biochem. (Tokyo)* **109**:348–353.
30. Talmage, S. S., D. M. Opresko, C. J. Maxwell, C. J. E. Welsh, F. M. Cretella, P. H. Reno, and F. B. Daniel. 1999. Nitroaromatic munition compounds: environment effects and screening values. *Rev. Environ. Contam. Toxicol.* **161**:1–156.
31. Trott, S., S. F. Nishino, J. Hawari, and J. C. Spain. 2003. Biodegradation of the nitramine explosive CL-20. *Appl. Environ. Microbiol.* **69**:1871–1874.
32. Wang, L. H., S. C. Tu, and R. C. Lusk. 1984. Apoenzyme of *Pseudomonas cepacia* salicylate hydroxylase. Preparation, fluorescence property, and nature of flavin binding. *J. Biol. Chem.* **259**:1136–1142.
33. White-Stevens, R. H., and H. Kamin. 1972. Studies of a flavoprotein, salicylate hydroxylase. I. Preparation, properties, and the uncoupling of oxygen reduction from hydroxylation. *J. Biol. Chem.* **247**:2358–2370.
34. Woody, R. C., G. L. Kearns, M. A. Brewster, C. P. Turley, G. B. Sharp, and R. S. Lake. 1986. The neurotoxicity of cyclotrimethylenetrinitramine (RDX) in a child: a clinical and pharmacokinetic evaluation. *J. Toxicol. Clin. Toxicol.* **24**:305–319.
35. Xinqi, Z., and S. Nicheng. 1996. Crystal and molecular structures of ϵ -HNIW. *Chin. Sci. Bull.* **41**:574–576.
36. Yinon, J. 1990. Toxicity and metabolism of explosives, p. 145–170. CRC Press, Inc., Boca Raton, Fla.

Nitroreductase catalyzed biotransformation of CL-20

Bharat Bhushan, Annamaria Halasz, Jalal Hawari*

Biotechnology Research Institute, National Research Council of Canada, 6100 Royalmount Avenue, Montreal, Que., Canada H4P 2R2

Received 2 July 2004

Abstract

Previously, we reported that a salicylate 1-monooxygenase from *Pseudomonas* sp. ATCC 29352 biotransformed CL-20 (2,4,6,8,10,12-hexanitro-2,4,6,8,10,12-hexaaza-isowurtzitane) ($C_6H_6N_{12}O_{12}$) and produced a key metabolite with mol. wt. 346 Da corresponding to an empirical formula of $C_6H_6N_{10}O_8$ which spontaneously decomposed in aqueous medium to produce N_2O , NH_4^+ , and $HCOOH$ [Appl. Environ. Microbiol. (2004)]. In the present study, we found that nitroreductase from *Escherichia coli* catalyzed a one-electron transfer to CL-20 to form a radical anion ($CL-20^{\cdot-}$) which upon initial N-denitration also produced metabolite $C_6H_6N_{10}O_8$. The latter was tentatively identified as 1,4,5,8-tetranitro-1,3a,4,4a,5,7a,8,8a-octahydro-diimidazo[4,5-b:4',5'-e]pyrazine [IUPAC] which decomposed spontaneously in water to produce glyoxal ($OHC-CHO$) and formic acid ($HCOOH$). The rates of CL-20 biotransformation under anaerobic and aerobic conditions were 3.4 ± 0.2 and 0.25 ± 0.01 nmol min⁻¹ mg of protein⁻¹, respectively. The product stoichiometry showed that each reacted CL-20 molecule produced about 1.8 nitrite ions, 3.3 molecules of nitrous oxide, 1.6 molecules of formic acid, 1.0 molecule of glyoxal, and 1.3 ammonium ions. Carbon and nitrogen products gave mass-balances of 60% and 81%, respectively. A comparative study between native-, deffavo-, and reconstituted-nitroreductase showed that FMN-site was possibly involved in the biotransformation of CL-20.

© 2004 Elsevier Inc. All rights reserved.

Keywords: Biotransformation; CL-20; Nitroreductase; *Escherichia coli*; Glyoxal

Anticipated military and commercial use of the newly synthesized energetic chemical, CL-20 (2,4,6,8,10,12-hexanitro-2,4,6,8,10,12-hexaazaisowurtzitane), in the near future [1] has opened the scope of research to study its environmental fate and impact. Biological and health impacts of CL-20 and its metabolic products are not known. There is one recent report which suggested an acute and chronic toxicity of CL-20 to earthworms exposed to amended natural soils [2]. It is likely that CL-20 may also raise similar environmental concerns as those experienced with RDX and HMX [3–6].

Several previous reports showed that biodegradation [7,8], photodegradation [9], and alkali-hydrolysis [10] of CL-20 produced $HCOOH$ as a carbon-product in addition

to several nitrogen-containing products such as nitrite, nitrous oxide, and ammonium. For instance, a membrane-associated flavoenzyme(s) from *Pseudomonas* sp. FA1 produced 2.3 nitrite ions, 1.5 molecules of nitrous oxide, and 1.7 molecules of formic acid from each reacted CL-20 molecule [7]. Whereas, salicylate 1-monooxygenase from *Pseudomonas* sp. ATCC 29352 produced 1.7 nitrite ions, 3.2 molecules of nitrous oxide, 0.6 ammonium ion, and 1.5 molecules of formic acid from each reacted CL-20 molecule [8]. In both previous studies [7,8], only formic acid (2 mol equivalents per mole of CL-20) was confirmed as a carbon product of CL-20. However, carbon mass-balance could not be determined due to the missing four mole equivalents of carbon in CL-20.

More recently, a new carbon-containing product, glyoxal, was detected and quantified (2 mol glyoxal/mol

* Corresponding author. Fax: +1 514 496 6265.

E-mail address: jalal.hawari@nrc.ca (J. Hawari).

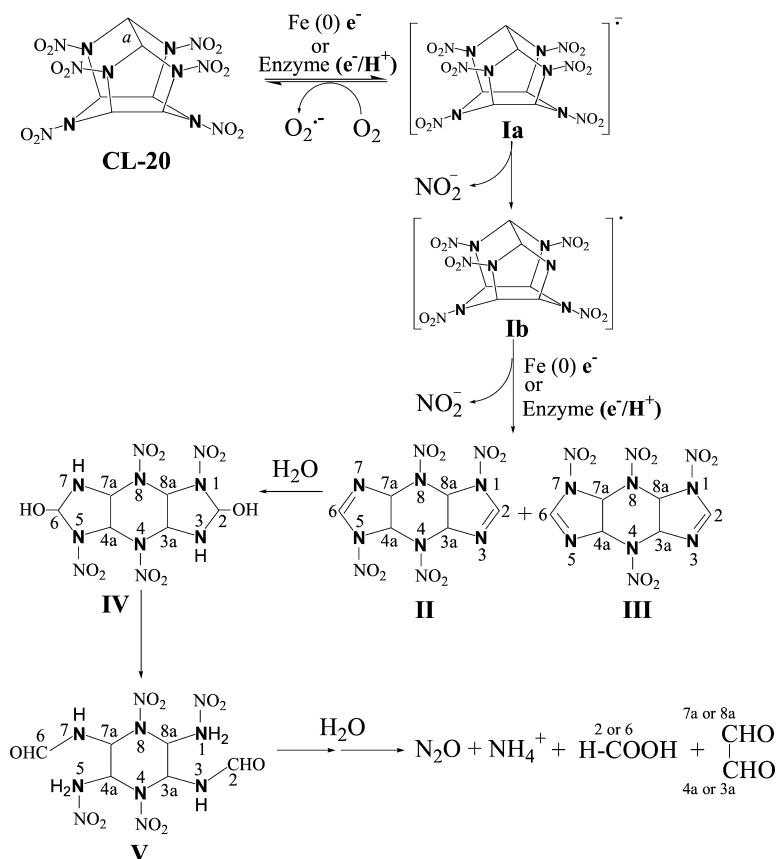


Fig. 1. Proposed pathway of CL-20 transformation (modified from [11]) by a nitroreductase from *Escherichia coli*. Intermediate shown inside bracket was not detected. Numbering on carbon products designates the source of carbon atoms from the CL-20 molecule.

CL-20) during CL-20 reaction with Fe(0) under anaerobic conditions and a pathway for glyoxal formation was proposed (Fig. 1) [11]. Balakrishnan et al. [11] proposed that CL-20 $^{\cdot-}$ radical-anion was produced via a one-electron transfer from Fe(0) to CL-20. The resulting CL-20 $^{\cdot-}$ upon denitration (loss of $2NO_2^{\cdot-}$) produced unstable intermediate II ($C_6H_6N_{10}O_8$) and its isomer III ($C_6H_6N_{10}O_8$). Both II and III undergo spontaneous hydrolysis in water to produce IV ($C_6H_{10}N_{10}O_{10}$) and its corresponding isomer (not shown in Fig. 1). The IV, being an α -hydroxyalkyl nitramine, was unstable in water [12] and therefore decomposed spontaneously in water to produce glyoxal and formic acid (Fig. 1).

In the present study, we hypothesized that an oxygen-sensitive nitroreductase from *Escherichia coli* should also biotransform CL-20 via an initial denitration to eventually give a similar product distribution as obtained with Fe(0). Nitroreductase catalyzed biotransformation of CL-20 allowed us to detect and quantify glyoxal in order to support the carbon mass-balance of the reaction. Superoxide dismutase (SOD)-sensitive cytochrome *c* reduction experiment was performed to determine the potential formation of an anion radical CL-20 $^{\cdot-}$ prior to N-denitration. Additionally, we deter-

mined the involvement of flavin-site of nitroreductase in CL-20 biotransformation.

Materials and methods

Chemicals. CL-20 (2,4,6,8,10,12-hexanitro-2,4,6,8,10,12-hexaazaisowurtzitane) in ϵ -form and 99.3% purity, and uniformly ring-labeled [^{15}N]CL-20 (ϵ -form and 90.0% purity) were provided by ATK Thiokol Propulsion, Brigham City, UT, USA.

NADH, flavin mononucleotide (FMN), glyoxal (40% solution), superoxide dismutase (SOD, EC 1.15.1.1, from *E. coli*), and cytochrome *c* (from horse heart, MW 12,384Da, purity 90%) were purchased from Sigma chemicals, Oakville, Ont., Canada. Nitrous oxide (N_2O) was purchased from Scott specialty gases, Sarnia, Ont., Canada. All other chemicals were of the highest purity grade.

Enzyme preparation and modification. Nitroreductase (purity of 90% by SDS-PAGE), from *E. coli*, was purchased from Sigma chemicals, Oakville, Ont., Canada. The enzyme was washed with phosphate buffer (pH 7.0) at 4°C using Biomax-5K membrane centrifuge filter units (Sigma chemicals, Oakville, Ont.) to remove preservatives and then re-suspended in the same buffer. Native enzyme activity was determined as per company guidelines. The protein content was determined by Pierce BCA (bicinchoninic acid) protein assay kit from Pierce chemicals company, Rockford, IL, USA.

Apoenzyme (deflavo-form) was prepared by removing FMN from the holoenzyme using a previously reported method [13]. Reconstitution was carried out by incubating the apoenzyme with 100 μ M FMN

in a potassium phosphate buffer (50 mM, pH 7.0) for 1 h at 4°C. The unbound FMN was removed by washing the enzyme with the same buffer using Biomax-5K membrane centrifuge filter units.

Biotransformation assays. Enzyme catalyzed biotransformation assays were performed under aerobic as well as anaerobic conditions in 6 ml glass vials. Anaerobic conditions were created by purging the reaction mixture with argon gas for 20 min and by replacing the headspace air with argon in sealed vials. Each assay vial contained, in 1 ml of assay mixture, CL-20 or uniformly ring-labeled [^{15}N]CL-20 (25 μM or 11 mg L^{-1}), NADH (100 μM), enzyme preparation (50 μg), and potassium phosphate buffer (50 mM, pH 7.0). Higher CL-20 concentrations, than its aqueous solubility of 3.6 mg L^{-1} [14], were used in order to allow detection and quantification of the intermediate(s). Reactions were performed at 30°C. Three different controls were prepared by omitting either enzyme, CL-20 or NADH from the assay mixture. Heat inactivated enzyme (90°C for 30 min) was also used as a negative control. NADH oxidation was measured spectrophotometrically at 340 nm as described before [8]. Samples from the liquid and gas phase in the vials were analyzed for residual CL-20 and biotransformed products.

To determine the residual CL-20 concentrations during biotransformation studies, the reaction was performed in multiple identical vials. At each time point, the total CL-20 content in one reaction vial was solubilized in 50% aqueous acetonitrile and analyzed by HPLC (see below). CL-20 biotransformation activity of nitroreductase was expressed as $\text{nmol min}^{-1} \text{mg of protein}^{-1}$ unless otherwise stated.

To demonstrate the effect of enzyme concentration on CL-20 biotransformation, a progress curve was made under anaerobic conditions by incubating nitroreductase at an increasing concentration (25–150 $\mu\text{g/ml}$) with CL-20 (45 μM) and NADH (200 μM). The reaction conditions were the same as described above.

The effect of molecular oxygen (O_2) on CL-20 biotransformation activity of nitroreductase was determined by performing the assays under aerobic conditions at pH 7.0 and 30°C. Formation of anion-radical $\text{CL-20}^{\cdot-}$ was determined by incubating CL-20 with nitroreductase in the presence of NADH, cytochrome *c* (75 μM), and SOD (150 $\mu\text{g ml}^{-1}$) as described previously [15,16]. Inhibition of cytochrome *c* reduction in the presence of SOD was monitored at 550 nm.

Analytical procedures. CL-20 and its intermediates, N_2O ($^{14}\text{N}^{14}\text{NO}$ and $^{15}\text{N}^{14}\text{NO}$), HCOOH , NO_2^- , and NH_4^+ , were analyzed as described previously [7,8].

Glyoxal was analyzed by a derivatization method as described by Bao et al. [17] with some modifications. A 20 μl solution (15 mg ml^{-1}) of *O*-2,3,4,5,6-pentafluorobenzyl-hydroxylamine hydrochloride (PFBHA) was added to 0.5 ml of an aqueous sample containing CL-20 products and 0.5 ml acetonitrile. pH was adjusted to 3.0 with 5% (v/v) of HCl. The reaction mixture was stirred in dark for 2 h at room temperature. The derivatized samples were analyzed with a LC/UV-MS (Platform LC, Micromass, Manchester, UK) at a wavelength of 250 nm by using positive electrospray (ES^+) ionization mode. Separation was performed on a Supelcosil C8 column (25 cm \times 4.6 mm ID, 5 μm) at 35°C using acetonitrile:water gradient (acetonitrile from 60% to 90% in 10 min, 90% to 60% in 2 min, and then 60% for 6 min) at a flow rate of 1 ml min^{-1} .

Results and discussion

Nitroreductase catalyzed biotransformation of CL-20

A purified nitroreductase, from *E. coli*, biotransformed CL-20 in a NADH-dependent manner at pH 7.0 and 30°C under anaerobic conditions. A progress curve demonstrated a linear increase in CL-20 biotransformation as a function of enzyme concentration (data

not shown). The rates of CL-20 biotransformation were 3.4 ± 0.2 and $0.25 \pm 0.01 \text{ nmol min}^{-1} \text{mg of protein}^{-1}$ (mean \pm SD; $n = 3$) under anaerobic and aerobic conditions, respectively, indicating the involvement of an oxygen-sensitive process. In all controls (see Materials and methods), we found a negligible abiotic removal of CL-20 during one hour of reaction time.

Oxygen-sensitivity of the reaction suggested that nitroreductase catalyzed a one-electron transfer to CL-20 to first produce an anion radical ($\text{CL-20}^{\cdot-}$) before N-denitration as previously reported during biotransformation of CL-20 with salicylate monooxygenase [8] or its reduction with Fe(0) [11]. Subsequently, we found that under aerobic conditions, superoxide dismutase (SOD) inhibited 30% of reduction of cytochrome *c* which suggested the formation of oxygen free-radical ($\text{O}^{\cdot-}$) during the reaction. Hence, molecular oxygen (O_2) inhibited CL-20 biotransformation by quenching an electron from the CL-20 anion-radical and converting it back to the parent molecule (CL-20), and thus enforcing a futile redox-cycling as shown in Fig. 1. Control experiments without nitroreductase showed that CL-20 was neither auto-oxidized nor it directly reduced cytochrome *c*. Analogously, O_2 -mediated inhibition of RDX anion-radical formation was previously reported during biotransformation of RDX with diaphorase [15]. Furthermore, the phenomenon of regeneration of parent nitro-compound during reaction of nitro anion-radical with molecular oxygen (O_2) in aerobic systems is well established [16,18–20]. Due to the inhibitory effect of oxygen, the subsequent experiments were carried out under anaerobic conditions.

Time-course of formation of initial metabolite II ($\text{C}_6\text{H}_6\text{N}_{10}\text{O}_8$)

In LC/MS (ES-) studies, we found two isomeric key intermediates II and III (Fig. 1) which appeared simultaneously as early as 5 min of the reaction with retention times (R_t) of 8.2 and 7.5 min, respectively (Fig. 2A). A time-course, considering the relative HPLC-UV areas, showed that both intermediates reached their maximum level after 30 min and then gradually declined during the course of reaction (Figs. 2A and B). As reported before [8,9], II and its isomer III were detected by LC/MS with similar deprotonated molecular mass ion $[\text{M-H}]^-$ at 345 Da corresponding to an empirical formula of $\text{C}_6\text{H}_6\text{N}_{10}\text{O}_8$ and were confirmed by using uniformly ring-labeled [^{15}N]CL-20. The product II was tentatively identified as 1,4,5,8-tetranitro-1,3a,4,4a,5,7a,8,8a-octa-hydro-diimidazo[4,5-*b*:4',5'-*e*]pyrazine which is a double-denitrated product of CL-20 (Fig. 1). Both II and III contain imine bonds ($-\text{C}=\text{N}-$) which are known to be unstable in water [21] and therefore decompose rapidly to produce ring-cleavage products (described below).

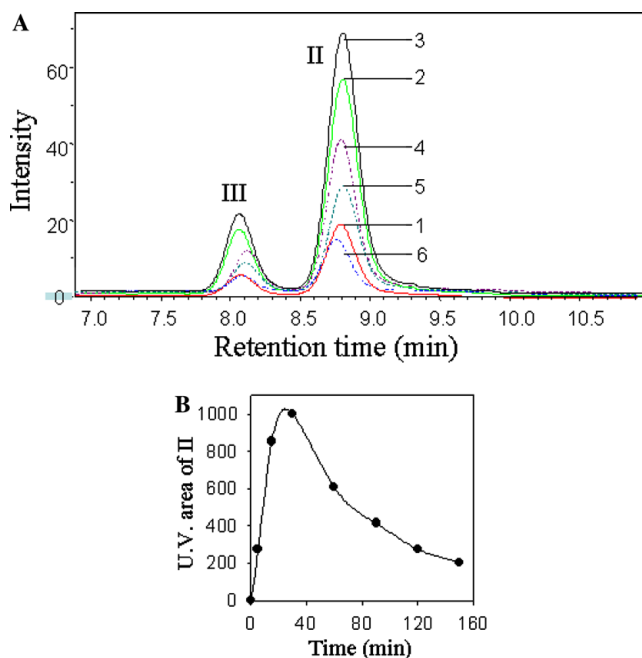


Fig. 2. (A) Time course of formation and disappearance of key metabolites II and III during biotransformation of CL-20 by nitroreductase. Chromatograms corresponding to numbers 1–3 indicate increasing formation of metabolite II at times 5, 15, and 30 min, respectively, whereas chromatograms 4–6 indicate disappearance of II at times 60, 90, and 150 min, respectively. Proposed molecular structures of II and III are shown in Fig. 1; (B) Formation and disappearance of II in terms of HPLC-UV-area as a function of time.

Detection and quantification of end-products including glyoxal (OHC-CHO)

Time-course studies showed a gradual disappearance of CL-20 at the expense of the electron-donor NADH with concomitant release of nitrite (NO_2^-), nitrous oxide (N_2O), and formate (Fig. 3). After 3 h of reaction, each reacted CL-20 molecule consumed about 1.3 NADH molecules and produced 1.8 nitrite ions, 3.3 molecules of nitrous oxide, 1.6 molecules of formic acid, 1.3

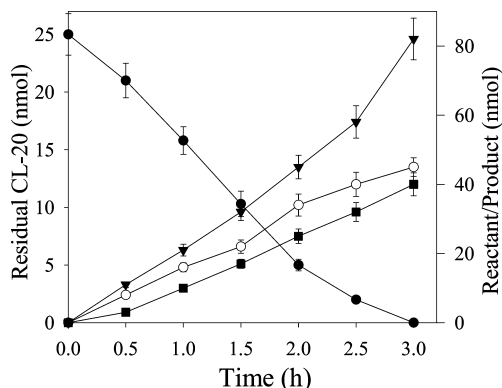


Fig. 3. Time-course study of NADH-dependent biotransformation of CL-20 by nitroreductase under anaerobic conditions. CL-20 (●), nitrite (○), nitrous oxide (▼), and formate (■). Data are means \pm SE ($n = 2$). Some error bars are not visible due to their small size.

ammonium ions, and 1.0 molecule of glyoxal (Table 1). With regard to glyoxal stoichiometry, we expected 2.0 mol of glyoxal per reacted mol of CL-20 as found previously during CL-20 reaction with $\text{Fe}(0)$ [11]. However, in the present study, we could recover only 1.0 mol equivalent of glyoxal due to the reason that glyoxal binds to the proteins via a non-enzymatic process called glycation [22] and therefore goes undetected. For instance, when we incubated glyoxal ($35 \mu\text{M}$) with enzyme ($50 \mu\text{g}$ nitroreductase) in one ml buffer for 2 days, about 44% of glyoxal disappeared and could not be recovered either by heating (80°C for 1 h) or by denaturing the enzyme with acetonitrile.

On the other hand, stoichiometry of NADH versus nitrite suggested that two single-electron transfer steps on CL-20 molecule released two nitrite ions. Of the total 12 nitrogen atoms (N) and 6 carbons (C) per reacted CL-20 molecule, we recovered approximately 10 N (as NO_2^- , N_2O , and NH_4^+) and 4 C (as HCOOH and glyoxal), respectively. The product distribution gave carbon and nitrogen mass-balance of 60% and 81%, respectively (Table 1). The product distribution in the present study was very similar, though with different relative yields, to those observed previously during photolysis of CL-20 [9] and the CL-20 reaction with $\text{Fe}(0)$ [11]. A close similarity in product distributions among the above-investigated biotic and abiotic reactions suggested that once CL-20 undergoes initial N-denitration, the subsequent spontaneous reactions in water are basically similar.

We found that N_2O , even though produced at later steps of CL-20 biotransformation (described below), appeared before NO_2^- in the assay medium as shown in Fig. 3. This could be explained by two facts, first, there was a large difference in stoichiometries of nitrite (1.8) and nitrous oxide (3.3); second, nitrous oxide detection method (GC-electron capture detector) was much more sensitive (lowest detection limit of 0.022 nmol) than the nitrite detection method (HPLC-conductivity detector) (lowest detection limit of $5.434 \text{ nmol ml}^{-1}$). A comparative study between ^{14}N -CL-20 and uniformly-ring-labeled- ^{15}N -CL-20 using GC-MS analysis showed that N- NO_2 groups in CL-20 were the source of N_2O , detected as $^{14}\text{N}^{14}\text{NO}$ (44 Da) and $^{15}\text{N}^{14}\text{NO}$ (45 Da), respectively, which is in accordance with our previous study [8].

On the other hand, we observed that formate appeared earlier in the assay medium compared to glyoxal (data not shown) which indicated that formate might have been originated as the ring-cleavage product as a result of initial denitration followed by rapid cleavage of the weakest C–C bond designated as *a* in CL-20 structure [23] (Fig. 1). Whereas, the source of glyoxal was most probably the other two C–C bonds ($\text{C}_{4a}\text{--C}_{7a}$ or $\text{C}_{3a}\text{--C}_{8a}$) in CL-20 (Fig. 1).

Formation of glyoxal during CL-20 degradation appears to be thermodynamically favorable since it is used

Table 1

Stoichiometry and mass-balance of reactants and products after 3 h of reaction between CL-20 and nitroreductase under anaerobic conditions at pH 7.0 and 30°C

Reactant/product	Amount (nmol)	Molar ratio per mole of reacted CL-20	% Carbon recovery	% Nitrogen recovery
<i>Reactants</i>				
CL-20	25 ± 1.8	1.0 ± 0.07	100	100
NADH	34 ± 2.3	1.3 ± 0.08	NA	NA
<i>Products</i>				
Nitrite	45 ± 2.7	1.8 ± 0.10	NA	15.0
Nitrous oxide	82 ± 6.4	3.3 ± 0.25	NA	55.0
Ammonium	33 ± 2.5	1.3 ± 0.05	NA	10.8
Formic acid	40 ± 3.3	1.6 ± 0.13	26.6	NA
Glyoxal	25 ± 1.3	1.0 ± 0.05	33.3	NA
Total mass-balance			59.9	80.8

Data are means ± SE ($n = 2$).

to synthesize CL-20 [24]. Under alkaline conditions or in the presence of Fe(0), glyoxal further converts to glycolic acid [11,25]. However, in the present study at neutral conditions (pH 7.0), glyoxal was accumulated as an end-product. Under biological conditions, further conversion of either glyoxal (OHC—CHO) or glycolic acid (HOH₂C—COOH) to glyoxylic acid (HOOC—CHO) requires involvement of glyoxal oxidase or glycolate oxidase, respectively [25,26]. The formation of glyoxal as a CL-20 product is environmentally significant since glyoxal is a reactive α -oxoaldehyde and its biological toxicity is well known [22]. Glyoxal is also produced in biological systems as a result of glucose auto-oxidation, DNA oxidation by oxygen free-radicals, and lipid oxidation [22,27]. It reacts with proteins and nucleic acids by forming covalent bonds via a non-enzymatic process called glycation thus leading to a variety of clinical manifestations [22]. It is a known mutagen [22] and an important allergen [28]. Thus, glyoxal produced from CL-20 may significantly contribute to the biological toxicity of CL-20.

Involvement of flavin-moiety in CL-20 biotransformation

Nitroreductase, from *E. coli*, is a monomeric protein with a mol. wt. of 24 kDa and contains one molecule of flavin-moiety (FMN) per enzyme monomer [29]. The involvement of FMN in CL-20 biotransformation was determined by assaying deflavo- and reconstituted-form of nitroreductase against CL-20. The specific activities of the native-, deflavo-, and reconstituted-form of nitroreductase against CL-20 were 3.4 ± 0.2 , 0.4 ± 0.03 , and $2.75 \pm 0.2 \text{ nmol min}^{-1} \text{ mg}$ of protein⁻¹, respectively, revealing that deflavo-enzyme lost about 88% of its activity compared to the native-enzyme (Fig. 4). The remaining 12% activity observed in deflavo-enzyme was due to incomplete removal of FMN (data not shown). Whereas, the reconstituted enzyme, prepared by reconstitution of deflavo-enzyme with FMN, restored the CL-20 biotransformation activity up to 81%

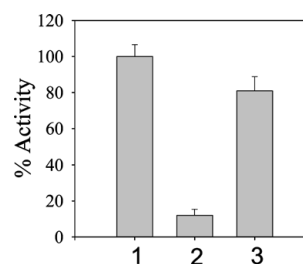


Fig. 4. Biotransformation of CL-20 by the native- (1), deflavo- (2), and reconstituted-nitroreductase (3). One hundred percent CL-20 biotransformation activity was equivalent to $3.4 \pm 0.2 \text{ nmol min}^{-1} \text{ mg}$ of protein⁻¹. Data are mean percentages of CL-20 biotransformation activity ± SE ($n = 3$).

(Fig. 4). The above results suggested the involvement of FMN in biotransformation of CL-20. Furthermore, the free FMN (100 μM) also transformed CL-20 in the presence of NADH (200 μM) at a rate of $0.17 \pm 0.02 \text{ nmol min}^{-1}$, however, the biotransformation rate was only 5% of the enzyme-bound-FMN present in native nitroreductase. This finding additionally supported the involvement of FMN in CL-20 biotransformation and also suggested that flavin-moiety functions more efficiently in enzyme-bound form.

In conclusion, the present study provided the first biochemical evidence for the quantitative formation of glyoxal and HCOOH during enzymatic biotransformation of CL-20. This study supported the previous finding of glyoxal production during chemical degradation of CL-20 with Fe(0). In the latter case, however, glyoxal was further converted to glycolic acid [11]. Detection and quantification of glyoxal supported the carbon mass-balance. Literature reported so far revealed that very few reports are available with regard to microbial and enzymatic degradation of CL-20. The present study thus provides a better understanding of the products and mass-balance of CL-20 reaction with nitroreductase(s)- or similar enzyme(s)-producing bacteria. Further work, however, is required to determine the fate

and impact of glyoxal, a known toxic compound, in the environment.

Acknowledgments

B. Bhushan thanks the Natural Sciences and Engineering Research Council (NSERC) and the National Research Council (NRC) of Canada for a visiting fellowship. We sincerely acknowledge the Strategic Environmental Research and Development Program (SERDP), USA, for financial support (CP 1256). We also thank the Department of National Defense, Val Bélair, Canada, for their support. We gratefully acknowledge Mr. A. Corriveau and Ms. C. Beaulieu for analytical and technical support, and Drs. Fanny-Monteil Rivera and V. Balakrishnan for helpful discussions.

References

- [1] J. Giles, Green explosives: collateral damage, *Nature* 427 (2004) 580–581.
- [2] P.Y. Robidoux, G.I. Sunahara, K. Savard, Y. Berthelot, S. Dodard, M. Martel, P. Gong, J. Hawari, Acute and chronic toxicity of new explosive CL-20 to the earthworm (*Eisenia andrei*) exposed to amended natural soils, *Environ. Toxicol. Chem.* 23 (2004) 1026–1034.
- [3] R. Haas, E.v.L. Schreiber, G. Stork, Conception for the investigation of contaminated munitions plants. 2. Investigation of former RDX-plants and filling stations, *Fresenius J. Anal. Chem.* 338 (1990) 41–45.
- [4] J. Clausen, J. Robb, D. Curry, N. Korte, A case study of contaminants on military ranges: Camp Edwards, Massachusetts, USA, *Environ. Pollut.* 129 (2004) 13–21.
- [5] S.S. Talmage, D.M. Opresko, C.J. Maxwell, C.J.E. Welsh, F.M. Cretella, P.H. Reno, F.B. Daniel, Nitroaromatic munition compounds: environmental effects and screening values, *Rev. Environ. Contam. Toxicol.* 161 (1999) 1–156.
- [6] Y. Kucukardali, H.V. Acar, S. Ozkan, S. Nalbant, Y. Yazgan, E.M. Atasoyu, O. Keskin, A. Naz, N. Akyatan, M. Gokben, M. Danaci, Accidental oral poisoning caused by RDX (Cyclonite): a report of 5 cases, *J. Intensive Care Med.* 18 (2003) 42–46.
- [7] B. Bhushan, L. Paquet, J.C. Spain, J. Hawari, Biotransformation of 2,4,6,8,10,12-hexanitro-2,4,6,8,10,12-hexaazaisowurtzitane (CL-20) by denitrifying *Pseudomonas* sp. strain FA1, *Appl. Environ. Microbiol.* 69 (2003) 5216–5221.
- [8] B. Bhushan, A. Halasz, J.C. Spain, J. Hawari, Initial reaction(s) in biotransformation of CL-20 catalyzed by salicylate 1-monooxygenase from *Pseudomonas* sp. ATCC 29352, *Appl. Environ. Microbiol.* 70 (2004) 4040–4047.
- [9] J. Hawari, S. Deschamps, C. Beaulieu, L. Paquet, A. Halasz, Photodegradation of CL-20: insights into the mechanisms of initial reactions and environmental fate, *Water Res.* (in press).
- [10] V.K. Balakrishnan, A. Halasz, J. Hawari, Alkaline hydrolysis of the cyclic nitramine explosives RDX, HMX, and CL-20: new insights into degradation pathways obtained by the observation of novel intermediates, *Environ. Sci. Technol.* 37 (2003) 1838–1843.
- [11] V. Balakrishnan, F. Monteil-Rivera, A. Halasz, J. Hawari, Decomposition of the polycyclic nitramine explosive, CL-20, by Fe(0), *Environ. Sci. Technol.* (2004), in press.
- [12] H. Druckrey, Specific carcinogenic and teratogenic effects of 'indirect' alkylating methyl and ethyl compounds, and their dependency on stages of ontogenic development, *Xenobiotica* 3 (1973) 271–303.
- [13] R.L. Koder, C.A. Haynes, M.E. Rodgers, D.W. Rodgers, A.F. Miller, Flavin thermodynamics explain the oxygen insensitivity of enteric nitroreductases, *Biochemistry* 41 (2002) 14197–14205.
- [14] C.A. Groom, A. Halasz, L. Paquet, P. D'Cruz, J. Hawari, Cyclodextrin-assisted capillary electrophoresis for determination of the cyclic nitramine explosives RDX, HMX, and CL-20: comparison with high-performance liquid chromatography, *J. Chromatogr. A* 999 (2003) 17–22.
- [15] B. Bhushan, A. Halasz, J.C. Spain, J. Hawari, Diaphorase catalyzed biotransformation of RDX via N-denitration mechanism, *Biochem. Biophys. Res. Commun.* 296 (2002) 779–784.
- [16] Z. Anusevicius, J. Sarlauskas, H. Nivinskas, J. Segura-Aguilar, N. Cenas, DT-diaphorase catalyzes N-denitration and redox cycling of tetryl, *FEBS Lett.* 436 (1998) 144–148.
- [17] M. Bao, F. Pantani, O. Griffini, D. Burrini, D. Santianni, K. Barbieri, Determination of carbonyl compounds in water by derivatization-solid-phase microextraction and gas chromatographic analysis, *J. Chromatogr. A* 809 (1998) 75–87.
- [18] R.L. Koder, O. Oyedele, A.F. Miller, Retro-nitroreductase, a putative evolutionary precursor to *Enterobacter cloacae* strain 96-3 nitroreductase, *Antioxid. Redox Signal.* 3 (2001) 747–755.
- [19] M.V. Orna, R.P. Mason, Correlation of kinetic parameters of nitroreductase enzymes with redox properties of nitroaromatic compounds, *J. Biol. Chem.* 264 (1989) 12379–12384.
- [20] P. Wardman, E.D. Clarke, Oxygen inhibition of nitroreductase: electron transfer from nitro radical-anions to oxygen, *Biochem. Biophys. Res. Commun.* 69 (1976) 942–949.
- [21] M.B. Smith, J. March, in: A. And (Ed.), *Advanced Organic Chemistry: Reactions, Mechanisms, and Structure*, fifth ed., Wiley-Interscience, Wiley, New York, 2001, pp. 532–533.
- [22] N. Shangari, W.R. Bruce, R. Poon, P.J. O'Brien, Toxicity of glyoxals—role of oxidative stress, metabolic detoxification and thiamine deficiency, *Biochem. Soc. Trans.* 31 (2003) 1390–1393.
- [23] Z. Xinqi, S. Nicheng, Crystal and molecular structures of ϵ -HNIW, *Chinese Sci. Bull.* 41 (1996) 574–576.
- [24] A.T. Nielsen, A.P. Chafin, S.L. Christian, D.W. Moore, M.P. Nadler, R.A. Nissan, D.J. Vanderah, Synthesis of polyazapolycyclic caged polynitramines, *Tetrahedron* 54 (1998) 11793–11812.
- [25] G.D. Yadav, V.R. Gupta, Synthesis of glyoxalic acid from glyoxal, *Process Biochem.* 36 (2000) 73–78.
- [26] M.M. Whittaker, P.J. Kersten, N. Nakamura, J. Sanders-Loehr, E.S. Schweizer, J.W. Whittaker, Glyoxal oxidase from *Phanerochaete chrysosporium* is a new radical-copper oxidase, *J. Biol. Chem.* 271 (1996) 681–687.
- [27] N. Murata-Kamiya, H. Kamiya, H. Kaji, H. Kasai, Mutational specificity of glyoxal, a product of DNA oxidation, in the lacI gene of wild-type *Escherichia coli* W3110, *Mutat. Res.* 377 (1997) 255–262.
- [28] W. Uter, H.J. Schwanitz, H. Lessmann, A. Schnuch, Glyoxal is an important allergen for (medical care) cleaning staff, *Int. J. Hyg. Environ. Health* 204 (2001) 251–253.
- [29] G.N. Parkinson, J.V. Skelly, S. Neidle, Crystal structure of FMN-dependent nitroreductase from *Escherichia coli* B: a prodrug-activating enzyme, *J. Med. Chem.* 43 (2000) 3624–3631.

Chemotaxis-mediated biodegradation of cyclic nitramine explosives RDX, HMX, and CL-20 by *Clostridium* sp. EDB2

Bharat Bhushan,^a Annamaria Halasz,^a Sonia Thiboutot,^b Guy Ampleman,^b and Jalal Hawari^{a,*}

^a Biotechnology Research Institute, National Research Council of Canada, 6100 Royalmount Avenue, Montreal, Que., Canada H4P 2R2

^b Defence Research Establishment, Valcartier, DND, Que., Canada G3J 1X5

Received 3 February 2004

Abstract

Cyclic nitramine explosives, RDX, HMX, and CL-20 are hydrophobic pollutants with very little aqueous solubility. In sediment and soil environments, they are often attached to solid surfaces and/or trapped in pores and distribute heterogeneously in aqueous environments. For efficient bioremediation of these explosives, the microorganism(s) must access them by chemotaxis ability. In the present study, we isolated an obligate anaerobic bacterium *Clostridium* sp. strain EDB2 from a marine sediment. Strain EDB2, motile with numerous peritrichous flagella, demonstrated chemotactic response towards RDX, HMX, CL-20, and NO_2^- . The three explosives were biotransformed by strain EDB2 via N-denitration with concomitant release of NO_2^- . Biotransformation rates of RDX, HMX, and CL-20 by the resting cells of strain EDB2 were 1.8 ± 0.2 , 1.1 ± 0.1 , and $2.6 \pm 0.2 \text{ nmol h}^{-1} \text{ mg wet biomass}^{-1}$ (mean \pm SD; $n = 3$), respectively. We found that commonly seen RDX metabolites such as TNX, methylenedinitramine, and 4-nitro-2,4-diazabutanol neither produced NO_2^- during reaction with strain EDB2 nor they elicited chemotaxis response in strain EDB2. The above data suggested that NO_2^- released from explosives during their biotransformation might have elicited chemotaxis response in the bacterium. Biodegradation and chemotactic ability of strain EDB2 renders it useful in accelerating the bioremediation of explosives under in situ conditions.

© 2004 Elsevier Inc. All rights reserved.

Keywords: Biodegradation; Chemotaxis; *Clostridium*; Cyclic nitramines; RDX; HMX; CL-20

Increasing use of RDX (hexahydro-1,3,5-trinitro-1,3,5-triazine) and HMX (octahydro-1,3,5,7-tetranitro-1,3,5,7-tetrazocine) has severely contaminated both marine and terrestrial environments around the world. The main sources of contamination are, dumping of huge amounts of unexploded ordnance (UXO), effluents from explosive manufacturing plants, military training, ordnance waste disposal by open burning/open detonation (OB/OD), land mines, and commercial use of explosives in propellants and mining [1–4]. Department of defense (DoD) and energy (DoE), USA, alone has over 21,000 contaminated sites and most of them are contaminated with explosives [5]. DoD of Canada has estimated 103 training sites and 3 OB/OD sites which are contaminated with RDX, HMX, and 2,4,6-trinitrotol-

uene (TNT) [6]. Cyclic nitramine explosives such as RDX and HMX cause adverse effects on biological systems, environment, and human health [7–11]. US environmental protection agency (USEPA) has recommended a lifetime health advisory for RDX [12] and HMX [13]. It is likely that due to its structural similarity with RDX and HMX, CL-20 (2,4,6,8,10,12-hexanitro-2,4,6,8,10,12-hexaazaisowurtzitane) (Fig. 1), a future generation high performance explosive, may also cause similar environmental problem. The cleanup of explosive(s) contaminated sites is a matter of growing concern among environmental protection groups.

Cyclic nitramines lack the electronic stability of aromatic compounds such as TNT and therefore an initial attack, whether biological or chemical, on the molecule(s) leads to their rapid spontaneous decomposition [3,14–18]. Bioremediation of contaminants, with little aqueous solubility, has always been a challenging task.

* Corresponding author. Fax: +1-514-496-6265.

E-mail address: jalal.hawari@nrc.ca (J. Hawari).

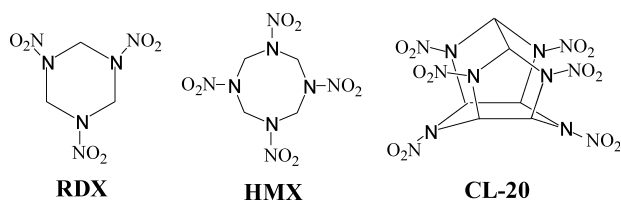


Fig. 1. Molecular structures of RDX, HMX, and CL-20.

Rates of biodegradation of such chemicals are limited by the rates of their mass-transfer from non-aqueous phase. In sediments and soil environments, hydrophobic pollutants are often attached to solid surfaces and/or trapped in pores. Cyclic nitramine explosives such as RDX, HMX, and CL-20 (Fig. 1) constitute one such class of chemicals with very little water solubilities of 40.0, 6.6, and 3.6 mg L⁻¹, respectively [19], and therefore distribute heterogeneously in marine and terrestrial environments. In order to degrade the explosive, the potential microorganism(s) must come in contact with the molecule. Bacterial chemotaxis is one such process that brings microbes closer to the contaminated sites and thus enhances the rate of biodegradation [20,21]. Motile and chemotactic microorganisms have advantage over non-motile and non-chemotactic ones by having the ability of sensing the explosive and thus move to form high-population densities around the chemical [22]. The dense microbial population can tolerate higher concentration of toxic chemicals [23] and reproduce more rapidly thus stimulating a rapid cleanup. Bacterial chemotaxis to a variety of organic pollutants and their subsequent degradation has been studied extensively [20,21,24–28] however no report is available so far with regard to cyclic nitramine explosives.

In the present study, we isolated an obligate anaerobic bacterium *Clostridium* sp. strain EDB2 from a marine sediment collected from a shipwreck site near Halifax Harbor in Canada. The strain demonstrated chemotaxis response towards the three cyclic nitramine explosives, RDX, HMX, and CL-20, and successfully degraded them. The present study is thus a model system to understand the environmental significance of chemotactic bacteria in accelerating the biodegradation of cyclic nitramine explosives under in situ conditions.

Materials and methods

Chemicals

Commercial grade RDX, HMX (chemical purity >99% for both explosives), [UL-¹⁴C]RDX (chemical purity >98%, radiochemical purity 97%, and specific radioactivity 28.7 μCi mmol⁻¹), and [UL-¹⁴C]HMX (chemical purity >94%, radiochemical purity 91%, and specific radioactivity 101.0 μCi mmol⁻¹) were provided by the Defense Research and Development Canada (DRDC), Valcartier, Quebec. Hexahydro-1-nitroso-3,5-dinitro-1,3,5-triazine (MNX) and 4-nitro-2,4-diazabutanol were obtained from SRI International (Menlo Park,

CA). Hexahydro-1,3,5-trinitroso-1,3,5-triazine (TNX) was synthesized according to the method described by Brockman et al. [29]. Methylenedinitramine (MDNA) was obtained from the rare chemical department of Aldrich, Oakville, ON, Canada. ε-CL-20 (99.3% purity) was provided by ATK Thiokol Propulsion, Brigham City, UT, USA. Microcapillaries (1 and 5 μl), low-melting-point agarose, and NADH were purchased from Sigma chemicals, Canada. Nitrous oxide (N₂O) was purchased from Scott specialty gases, Sarnia, ON, Canada. All other chemicals were of highest purity grade.

Marine sediment samples were collected from a shipwreck site (200 m deep-sea bed) at 50 nautical miles east of the Halifax harbor, Canada. Chemical analysis showed that sediment was composed of silt, clay, sand, and total organic matter at a concentration of 90.45%, 8.25%, 1.30%, and 1.90%, w/w, respectively. Major metals were Fe, Ca, Al, and Na at a concentration of 40, 24, 15, and 10 g kg⁻¹, respectively. pH of sediment was 7.7.

Media composition

Medium M1 was composed of (per liter): NaCl, 10.0 g; NaHCO₃, 2.5 g; NaH₂PO₄, 0.6 g; KCl, 0.2 g; NH₄Cl, 0.5 g; and Fe(III)-citrate, 12.25 g. Ingredients were mixed in hot water. pH was adjusted to 7.0 with 10 N NaOH. One liter medium was bubbled with N₂:CO₂ (80:20) for 45 min. After autoclaving at 121 °C for 20 min, we added filter-sterilized anaerobic solutions of lactate and glucose, 25 mM each; peptone, 1.0 g; trace elements, 10 ml; and vitamin mixture, 10 ml. Trace elements and vitamin mixture were same as reported [30]. Medium M2 was composed of (per liter): peptone, 8 g; yeast extract, 2 g; NaCl, 10 g; and glucose and lactate, 25 mM each. For making solid agar slants or plates, 1.8% agar powder (Difco) was added to the medium.

Isolation of chemotactic bacteria

Enrichments were carried out by adding RDX, HMX, and CL-20 together (30 μM each) and sediment (1% w/v) to medium M1 followed by incubation at room temperature for about 2 weeks under strict anaerobic conditions (N₂:CO₂, 80:20). The enriched culture (2.0 ml) was suspended in 3.0 ml phosphate-buffered saline (PBS) (100 mM, pH 7.0) supplemented with glucose (5 mM) as carbon and energy source. The cell-suspension was sealed in 10 ml vials under strict anaerobic conditions. Microcapillaries, sealed at one end, were then charged with 5 μM solution of either RDX, HMX or CL-20, inserted into the above sealed vials by piercing through the butyl rubber septum, and partly dipped into the enriched culture as shown in Fig. 2. After every 24 h of incubation, one capillary was taken out, plated onto the agar slants of both media M1 and M2, and incubated at room temperature under anaerobic conditions. This exercise was repeated every 24 h for about two weeks to allow isolation of a motile and chemotactic bacterial strain. The isolated strain formed small, black colonies (≤1 mm diameter) on solidified medium M1, and small, white, shining colonies (≤1 mm diameter) on solidified medium M2.

Bacterial identification

Morphological, physiological, and biochemical characterization of the isolated strain was performed by standard methods described for gram-staining, spore-staining, catalase, oxidase, and H₂S production, and nitrate- and nitrite-reduction, in the manual of methods for general bacteriology [31]. 16S rRNA gene analysis (1200 bases) and mol% G+C content of the strain were performed by laboratory services division, University of Guelph, ON, Canada. The strain was named EDB2 (EDB stands for explosive degrading bacterium).

Following microscopy techniques were performed to determine morphology, motility, flagella, and cell count: (1) phase contrast microscopy was used to observe cell-motility by hanging drop method [31] using standard microscope glass slides with cavity. It was also used for bacterial cell count with Petroff–Hausser counter (Hausser

Sealed microcapillary

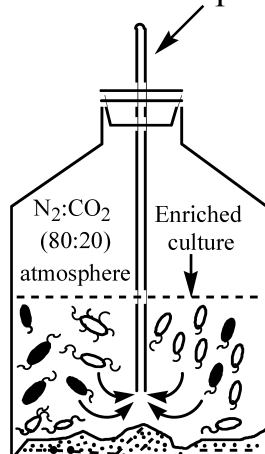


Fig. 2. Schematic representation of the technique used to isolate chemotactic bacteria. An air-tight 10 ml glass vial containing 5 ml enriched culture under anaerobic conditions. A 5 μ l microcapillary containing an explosive solution and sealed at outer end inserted into glass vial.

Scientific, Horsham, PA, USA); (2) transmission electron microscopy (TEM) was used to observe bacterial morphology and type of flagella. For TEM, bacterial cells were negatively stained as follows: a 20 μ l of mid-log-phase culture was placed onto a formvar (polyvinyl formaldehyde) coated grid of mesh size 400. After 4 min of incubation at room temperature the excess fluid was drained off with Whatman filter paper. The culture sticking to the grid was stained with 2% ammonium molybdate for about 30 s. Excess stain was drained and grid was washed with double-distilled water. The grid was air-dried and observed under a transmission electron microscope (Hitachi H7500).

Chemotaxis assays

Qualitative agarose-plug assay. This assay was conducted as described by Childers et al. [32] with some modifications using low-melting-point agarose (1.6% w/v, Sigma Chemicals, Canada). Briefly, a chemotaxis chamber of dimensions 20 \times 20 \times 1.5 mm was made with two plastic strips glued to a glass slide. A drop of low-melting-point agarose containing an explosive compound was placed on a glass coverslip and inverted onto the plastic strips. Bacterial cells, grown anaerobically in 100 ml of medium M2 supplemented with RDX, HMX, and CL-20 together (15 μ M each), were washed once with PBS buffer and resuspended in 8 ml PBS buffer containing 1 mM glucose as energy source before transferring to the chemotaxis chamber. The latter was then transferred to a plastic tube sealed with a rubber stopper followed by flushing with N₂:CO₂ (80:20) to create anaerobic conditions and then incubated at 30 °C. Bacterial ring formation around the agarose-drop was observed for 60 min. Two separate controls were used for comparison; the first contained agarose-drop with buffer alone, and the second contained autoclaved killed cells against a test chemical(s).

Quantitative microcapillary assay. A modified version of previously described method [24] was used. The cyclic nitramines, at a defined concentration, were charged into 1 μ l microcapillaries (Drummond Scientific Company, Broomall, PA, USA). The latter were inserted into a U-shaped chamber (similar to the chemotaxis chamber as mentioned above but without agarose-drop) already flooded with cell suspension of strain EDB2. The U-shaped chamber was then incubated under anaerobic conditions for 30 min. Microcapillaries were removed from the chamber and the cells sticking outside the capillaries were washed away with PBS buffer. Cells accumulated inside the capillaries were counted by Petroff–Hausser counter following serial dilutions. Controls were same as mentioned above.

Biotransformation assays for RDX, HMX, and CL-20

Biotransformation assays were performed in 6 ml air-tight glass vials under strict anaerobic conditions by purging the reaction mixture with argon for 20 min. Each assay vial contained (1 ml of assay mixture) either RDX (20 μ M), HMX (20 μ M) or CL-20 (20 μ M) and resting-cell preparation (5 mg wet biomass ml⁻¹) in a potassium phosphate buffer (50 mM, pH 7.0). To determine the effect of NADH on rate of biotransformation of explosive(s), NADH (200 μ M) was added to the reaction vial(s) and incubated at 30 °C. Three different controls were prepared by omitting either resting-cells, NADH or both from the assay mixture. Residual NADH was measured as described before [18]. The energetic chemicals and their biotransformed products were analyzed as previously described [15–18]. Explosive degradation activity of the cells was expressed as nmol h⁻¹ mg cell biomass⁻¹ unless otherwise stated.

Biomining of RDX and HMX in sediment microcosms

Sediment microcosms were prepared in four different combinations under anaerobic conditions (N₂) as follows: (1) 2 g native-sediment and 2 ml of 50 mM PBS (100 mM, pH 7.0); (2) 2 g sterile-sediment (gamma-irradiated) and 2 ml PBS; (3) 2 g native-sediment, 1 ml PBS, and 1 ml bacterial culture (2×10^8 cells ml⁻¹); and (4) 2 g sterile-sediment, 1 ml PBS, and 1 ml bacterial culture (2×10^8 cells ml⁻¹). Radiolabeled [UL-¹⁴C]RDX (33 μ g g⁻¹ sediment equivalent to 50,118 dpm) and [UL-¹⁴C]HMX (16 μ g g⁻¹ sediment equivalent to 54,310 dpm) were added to the microcosms through rubber septum using a syringe and needle. A small glass tube, placed inside microcosm, containing 0.5 ml of 0.5 M KOH was used as ¹⁴CO₂ trap. Evolution of ¹⁴CO₂ was determined in terms of dpm counts in KOH solution by using a liquid scintillation counter (Packard, Tri-Carb 4530, model 2100 TR, Packard Instruments Company, Meriden, CT). Experiments were performed in duplicate. *Note.* CL-20 was not included in this experiment because of unavailability of radiolabeled [UL-¹⁴C]CL-20.

Results and discussion

Isolation and identification of strain EDB2

We isolated an obligate anaerobic bacterial strain EDB2, from a marine sediment, by using a new technique devised to isolate chemotactic bacteria (see Materials and methods, and Fig. 2). Strain EDB2 was small rods of length 1.8–3.5 μ m and diameter 0.7–1.0 μ m, and exhibited gram-variable character. Spores were not seen in a stationary-growth-phase culture. The temperature and pH optima for the growth were 30 °C and 7.0, respectively. Strain EDB2 was motile with the help of numerous peritrichous flagella (Fig. 3). It was catalase and oxidase negative, and produced H₂S from S₂O₃²⁻. Also, it reduced nitrate and nitrite to N₂O using NADH as electron-donor. 16S rRNA gene analysis of 1200 bases (GenBank Accession No. AY510270) showed that strain EDB2 was 97% similar to *Clostridium xylanolyticum* (GenBank Accession No. X76739) and *Clostridium* strain DR7 (GenBank Accession No. Y10030). Strain EDB2 differed from *C. xylanolyticum* for having higher mol% G + C content of 53.6 compared to 40%, and for its potential to reduce nitrite and nitrate. No published description was available for *Clostridium* strain DR7.

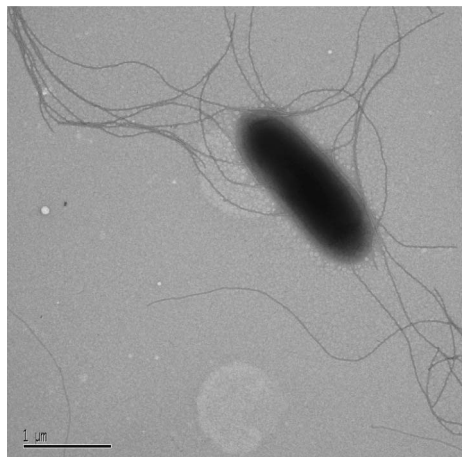


Fig. 3. Transmission electron micrograph of negatively stained cell of strain EDB2. Bar indicates 1 μ m.

The results showed that strain EDB2 belonged to genus *Clostridium* however it did not match with any closely related species.

Chemotaxis response of strain EDB2 towards explosives

Agarose-plug assays showed qualitative chemotaxis of strain EDB2 in the form of visible bright rings around the agarose-plug(s) containing RDX, HMX, CL-20 or nitrite. Control agarose-plug containing only buffer did not show chemotaxis response (Fig. 4). Whereas, microcapillary assays showed quantitative chemotaxis response of strain EDB2 towards the three explosives and the nitrite ion (Table 1). Since we found that biotransformation of RDX, HMX, and CL-20 occurred via an initial N-denitration (discussed below), we presumed that nitrite released from the explosive molecules was

Table 1
Quantitative chemotaxis assay with strain EDB2 by microcapillary method

Compound	Concentration (μ M)	Chemotaxis index ^a
Buffer ^b	—	1.0 \pm 0.1
RDX	10	5.0 \pm 0.4
HMX	10	2.4 \pm 0.2
CL-20	8	7.2 \pm 0.5
MNX	10	5.9 \pm 0.4
TNX	10	1.3 \pm 0.1
Nitrite	10	7.9 \pm 0.6
	100	18.5 \pm 1.3

^a Ratio of the number of cells accumulated inside the capillary containing test compound to the number of cells accumulated inside the capillary containing only buffer (i.e., 850 \pm 90 cells); data are means \pm SD (n = 3).

^b Negative control without compound.

responsible for eliciting a chemotaxis response in strain EDB2. Hexahydro-1-nitroso-3,5-dinitro-1,3,5-triazine (MNX), a RDX metabolite that also released nitrite on reaction with strain EDB2, elicited a chemotaxis response in strain EDB2 (Fig. 4 and Table 1). On the other hand, HMX, being the most recalcitrant (discussed below), elicited the least chemotaxis response (Table 1). Our hypothesis was strengthened when hexahydro-1,3,5-trinitroso-1,3,5-triazine (TNX), a RDX metabolite without a nitro group [33], did not elicit chemotaxis response (Table 1). Additionally, methylenedinitramine and 4-nitro-2,4-diazabutanal, both ring-cleavage metabolites from RDX and/or HMX [15–18], neither released nitrite during their reaction with resting cells of strain EDB2 nor they elicited chemotaxis response in strain EDB2. Other known carbon products of cyclic nitramines, i.e., HCHO and HCOOH which lack NO₂[−] elicited a poor chemotaxis response in bacterium (data

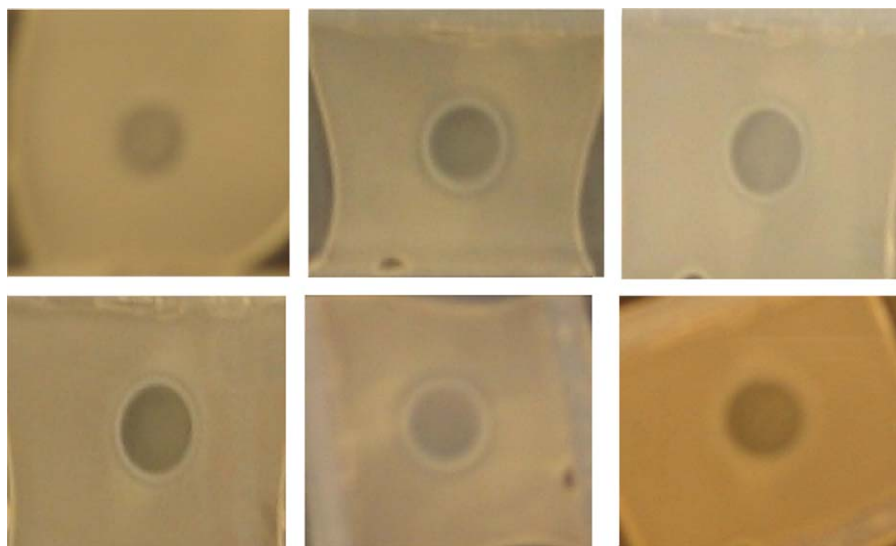


Fig. 4. Qualitative chemotaxis assay with strain EDB2 by agarose-plug method. Bright ring of bacterial cells around the plug indicated chemotaxis. Top line (left to right): buffer alone, nitrite, and RDX; bottom line (left to right): MNX, CL-20, and HMX.

not shown). The above data confirmed that nitrite released from the explosives was primarily responsible for inducing chemotaxis response in strain EDB2. Once gathered around the contaminated site, strain EDB2 may form high population density and reproduce more rapidly as demonstrated by other bacteria [22,23]. As a result, a higher degradation rate of energetic chemicals can be achieved by strain EDB2 as previously reported with regard to bacterial degradation of naphthalene [20,21].

Biodegradation of cyclic nitramine explosives

Growing-culture of strain EDB2 biotransformed the three explosives, in medium M2, as a function of its growth with the following order, i.e., CL-20 > RDX > HMX (Fig. 5). In the resting-cell study, biotransformation rates of RDX, HMX, and CL-20 by strain EDB2 were 1.8 ± 0.2 , 1.1 ± 0.1 , and 2.6 ± 0.2 $\text{nmol h}^{-1} \text{mg biomass}^{-1}$ (mean \pm SD; $n = 3$), respectively, whereas, in the presence of $100 \mu\text{M}$ NADH, the biotransformation rates of the three explosives enhanced to 4.5 ± 0.3 , 2.5 ± 0.3 , and 7.2 ± 0.6 $\text{nmol h}^{-1} \text{mg biomass}^{-1}$ (mean \pm SD; $n = 3$), respectively. In contrast, a negligible response was observed upon addition of $100 \mu\text{M}$ NADPH indicating the involvement of an unidentified NADH-dependent enzyme(s). No degradation was observed in control experiments without resting cells within 1 h of assay time. We found that biotransformation of RDX or HMX was accompanied by the formation of NO_2^- , N_2O , HCHO , and HCOOH . Whereas, biotransformation of CL-20 produced NO_2^- , N_2O , and HCOOH . The products obtained from each explosive were similar to those observed previously [15–18].

Resting-cells of strain EDB2 also catalyzed NADH-dependent biotransformation of HCHO to HCOOH which did not accumulate (data not shown). In a subsequent experiment, strain EDB2 mineralized 40% of

H^{14}CHO (of the total $340 \mu\text{g H}^{14}\text{CHO/L}$ medium) with evolution of $^{14}\text{CO}_2$ after 4 days of incubation in medium M1 suggesting an intermediary formation of HCOOH .

To mimic the in situ conditions, mineralization experiments were performed in sediment-microcosms. When strain EDB2 (2×10^8 cells ml^{-1}) was incubated with native-sediment in the presence of either $[\text{UL-}^{14}\text{C}] \text{RDX}$ or $[\text{UL-}^{14}\text{C}] \text{HMX}$, we obtained 70% (of the total 33 mg RDX/kg sediment) and 46% (of the total 16 mg HMX/kg sediment) mineralization, respectively, after 18 days. In contrast, in native-sediment alone, only 17% and 8% mineralization was obtained for RDX and HMX, respectively. On the other hand, when strain EDB2 was inoculated in sterile-sediment, mineralization of RDX and HMX was only 11% and 2%, respectively. We found that compared to the sterile-sediment, the mineralization of $[\text{UL-}^{14}\text{C}] \text{RDX}$ and $[\text{UL-}^{14}\text{C}] \text{HMX}$ by strain EDB2 in the liquid medium M1 was 30% and 13%, respectively, after 18 days. The reason for rapid mineralization of RDX and HMX in liquid medium attributed to a better accessibility of explosive molecules to the bacterial cells. Taken together, the above data suggested that strain EDB2 seems to be a promising degrader of cyclic nitramine explosives under native-sediment (or in situ) conditions.

In conclusion, the present study demonstrated a chemotaxis-mediated biodegradation of cyclic nitramine explosives where local population of strain EDB2 first initiates biotransformation of cyclic nitramines with release of NO_2^- . The NO_2^- thus produced attracts other distantly located bacterial cells to help accelerate the biodegradation process. In comparison to the conventional microbial degradation where microorganism(s) fortuitously come in contact with the energetic chemicals, the present study emphasizes the use of chemotactic bacteria for efficient removal of explosives in contaminated sites. This is the first report which showed that a pure bacterial culture (strain EDB2) accessed the three hydrophobic cyclic nitramine explosives by chemotaxis and degraded them to innocuous products. The properties demonstrated by strain EDB2 renders it useful for the cleanup of sites contaminated with cyclic nitramines.

Acknowledgments

Special thanks are due to Cindy Leggiadro of Institute of Marine Biosciences, Halifax, for electron microscopy work. We thank Dominic Faucher for collecting sediment samples and Fanny Monteil-Rivera for reviewing the manuscript. We gratefully acknowledge the Office of Naval Research (ONR) (Grant N000140310269) and the Strategic Environmental Research and Development Program (SERDP), USA (CP 1256), for funding. B. Bhushan thanks Natural Sciences and Engineering Research Council (NSERC) and National Research Council (NRC) of Canada for a visiting fellowship. We also thank the Department of National Defense, Val Bélair, Canada, for their support. We sincerely acknowledge the analytical and technical support of L. Paquet, A. Corriveau, and C. Beaulieu.

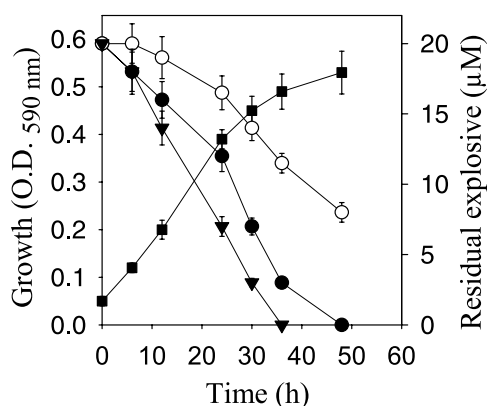


Fig. 5. Biotransformation of RDX (●), HMX (○), and CL-20 (▼) by strain EDB2 as a function of its growth (■). Data are means \pm SD ($n = 3$). Some error bars are not visible due to their small size.

References

- [1] R. Haas, E.v.L. Schreiber, G. Stork, Conception for the investigation of contaminated munitions plants. 2. Investigation of former RDX-plants and filling stations, *Fresenius J. Anal. Chem.* 338 (1990) 41–45.
- [2] C.A. Myler, W. Sisk, in: G.S. Sayler, R. Fox, J.W. Blackburn (Eds.), *Environmental Biotechnology for Waste Treatment: Bioremediation of Explosives Contaminated Soils (Scientific Questions/Engineering Realities)*, Plenum Press, New York, 1991, pp. 137–146.
- [3] J. Hawari, in: J.C. Spain, J.B. Hughes, H.J. Knackmuss (Eds.), *Biodegradation of Nitroaromatic Compounds and Explosives: Biodegradation of RDX and HMX: From Basic Research to Field Application*, CRC Press, Boca Raton, FL, 2000, pp. 277–310.
- [4] J. Clausen, J. Robb, D. Curry, N. Korte, A case study of contaminants on military ranges: Camp Edwards, Massachusetts, USA, *Environ. Pollut.* 129 (2004) 13–21.
- [5] J.W. Talley, P.M. Sleeper, Roadblocks to the implementation of biotreatment strategies, *Ann. N. Y. Acad. Sci.* 829 (1997) 16–29.
- [6] S. Thiboutot, G. Ampleman, A. Gagnon, A. Marois, T.F. Jenkins, M.E. Walsh, P.G. Thorne, T.A. Ranney, Characterization of anti-tank firing ranges at CFB Valcartier. Report DREV-R-9809. WATC Wainwright and CFAD Dundurn, Quebec, 1998.
- [7] J. Yinon, *Toxicity and Metabolism of Explosives*, CRC Press, Boca Raton, FL, 1990.
- [8] S.S. Talmage, D.M. Opresko, C.J. Maxwell, C.J.E. Welsh, F.M. Cretella, P.H. Reno, F.B. Daniel, Nitroaromatic munition compounds: environmental effects and screening values, *Rev. Environ. Contam. Toxicol.* 161 (1999) 1–156.
- [9] R.C. Woody, G.L. Kearns, M.A. Brewster, C.P. Turley, G.B. Sharp, R.S. Lake, The neurotoxicity of cyclotrimethylenetrinitramine (RDX) in a child: a clinical and pharmacokinetic evaluation, *J. Toxicol. Clin. Toxicol.* 24 (1986) 305–319.
- [10] B.S. Levine, E.M. Furedi, D.E. Gordon, J.J. Barkley, P.M. Lish, Toxic interactions of the munitions compounds TNT and RDX in F344 rats, *Fundam. Appl. Toxicol.* 15 (1990) 373–380.
- [11] P. Gong, J. Hawari, S. Thiboutot, G. Ampleman, G.I. Sunahara, Toxicity of octahydro-1,3,5,7-tetranitro-1,3,5,7-tetrazocine (HMX) to soil microbes, *Bull. Environ. Contam. Toxicol.* 69 (2002) 97–103.
- [12] E.L. Etnier, W.R. Hartley, Comparison of water quality criterion and lifetime health advisory for hexahydro-1,3,5-trinitro-1,3,5-triazine (RDX), *Regul. Toxicol. Pharmacol.* 11 (1990) 118–122.
- [13] W. McLellan, W.R. Hartley, M. Brower, Health advisory for octahydro-1,3,5,7-tetranitro-1,3,5,7-tetrazocine, Technical Report PB90-273533, Office of Drinking Water, US Environmental Protection Agency, Washington, DC, 1988.
- [14] J. Hawari, S. Beaudet, A. Halasz, S. Thiboutot, G. Ampleman, Microbial degradation of explosives: biotransformation versus mineralization, *Appl. Microbiol. Biotechnol.* 54 (2000) 605–618.
- [15] B. Bhushan, A. Halasz, J.C. Spain, J. Hawari, Diaphorase catalyzed biotransformation of RDX via N-denitration mechanism, *Biochem. Biophys. Res. Commun.* 296 (2002) 779–784.
- [16] B. Bhushan, S. Trott, J.C. Spain, A. Halasz, L. Paquet, J. Hawari, Biotransformation of hexahydro-1,3,5-trinitro-1,3,5-triazine (RDX) by a rabbit liver cytochrome P450: insight into the mechanism of RDX biodegradation by *Rhodococcus* sp. DN22, *Appl. Environ. Microbiol.* 69 (2003) 1347–1351.
- [17] B. Bhushan, L. Paquet, A. Halasz, J.C. Spain, J. Hawari, Mechanism of xanthine oxidase catalyzed biotransformation of HMX under anaerobic conditions, *Biochem. Biophys. Res. Commun.* 306 (2003) 509–515.
- [18] B. Bhushan, L. Paquet, J.C. Spain, J. Hawari, Biotransformation of 2,4,6,8,10,12-hexanitro-2,4,6,8,10,12-hexaazaisowurtzitane (CL-20) by denitrifying *Pseudomonas* sp. strain FA1, *Appl. Environ. Microbiol.* 69 (2003) 5216–5221.
- [19] C.A. Groom, A. Halasz, L. Paquet, P. D'Cruz, J. Hawari, Cyclodextrin-assisted capillary electrophoresis for determination of the cyclic nitramine explosives RDX, HMX and CL-20: comparison with high-performance liquid chromatography, *J. Chromatogr. A* 999 (2003) 17–22.
- [20] A.M.J. Law, M.D. Aitken, Bacterial chemotaxis to naphthalene desorbing from a nonaqueous liquid, *Appl. Environ. Microbiol.* 69 (2003) 5968–5973.
- [21] R.B. Marx, M.D. Aitken, Bacterial chemotaxis enhances naphthalene degradation in a heterogeneous aqueous system, *Environ. Sci. Technol.* 34 (2000) 3379–3383.
- [22] S. Park, P.M. Wolanin, E.A. Yuzbashyan, P. Silberzan, J.B. Stock, R.H. Austin, Motion to form a quorum, *Science* 301 (5630) (2003) 188.
- [23] E.P. Greenberg, Tiny teamwork, *Nature* 424 (2003) 134.
- [24] S.K. Samanta, B. Bhushan, A. Chauhan, R.K. Jain, Chemotaxis of a *Ralstonia* sp. SJ98 toward different nitroaromatic compounds and their degradation, *Biochem. Biophys. Res. Commun.* 296 (2000) 117–123.
- [25] B. Bhushan, S.K. Samanta, A. Chauhan, A.K. Chakraborti, R.K. Jain, Chemotaxis and biodegradation of 3-methyl-4-nitrophenol by *Ralstonia* sp. SJ98, *Biochem. Biophys. Res. Commun.* 275 (2000) 129–133.
- [26] R.E. Parales, J.L. Ditty, C.S. Harwood, Toluene-degrading bacteria are chemotactic towards the environmental pollutants benzene, toluene, and trichloroethylene, *Appl. Environ. Microbiol.* 66 (2000) 4098–4104.
- [27] R.E. Parales, C.S. Harwood, Bacterial chemotaxis to pollutants and plant-derived aromatic molecules, *Curr. Opin. Microbiol.* 5 (2002) 266–273.
- [28] G. Pandey, R.K. Jain, Bacterial chemotaxis toward environmental pollutants: role in bioremediation, *Appl. Environ. Microbiol.* 68 (2002) 5789–5795.
- [29] F.J. Brockman, D.C. Downing, G.F. Wright, Nitrolysis of hexamethylenetetramine, *Can. J. Res. B* 27 (1949) 469–474.
- [30] D.R. Lovley, R.C. Greening, J.G. Ferry, Rapidly growing rumen methanogenic organism that synthesizes coenzyme M and has a high affinity for formate, *Appl. Environ. Microbiol.* 48 (1984) 81–87.
- [31] P. Gerhardt, *Manual of Methods for General Bacteriology*, American Society for Microbiology, Washington, DC, 1981.
- [32] S.E. Childers, S. Ciufo, D.R. Lovley, *Geobacter metallireducens* accesses insoluble Fe(III) oxide by chemotaxis, *Nature* 416 (2002) 767–769.
- [33] N.G. McCormick, J.H. Cornell, A.M. Kaplan, Biodegradation of hexahydro-1,3,5-trinitro-1,3,5-triazine, *Appl. Environ. Microbiol.* 42 (1981) 817–823.

Preliminary ecotoxicological characterization of a new energetic substance, CL-20 [☆]

Ping Gong ¹, Geoffrey I. Sunahara ^{*}, Sylvie Rocheleau, Sabine G. Dodard, Pierre Yves Robidoux, Jalal Hawari

Biotechnology Research Institute, National Research Council of Canada, 6100 Royalmount Avenue, Montreal, Que., Canada H4P 2R2

Received 28 August 2003; received in revised form 20 February 2004; accepted 21 April 2004

Abstract

A new energetic substance hexanitrohexaazaisowurtzitane (or CL-20) was tested for its toxicities to various ecological receptors. CL-20 (ϵ -polymorph) was amended to soil or deionized water to construct concentration gradients. Results of Microtox (15-min contact) and 96-h algae growth inhibition tests indicate that CL-20 showed no adverse effects on the bioluminescence of marine bacteria *Vibrio fischeri* and the cell density of freshwater green algae *Selenastrum capricornutum* respectively, up to its water solubility (ca. 3.6 mg l⁻¹). CL-20 and its possible biotransformation products did not inhibit seed germination and early seedling (16–19 d) growth of alfalfa (*Medicago sativa*) and perennial ryegrass (*Lolium perenne*) up to 10 000 mg kg⁻¹ in a Sassafras sandy loam soil (SSL). Indigenous soil microorganisms in SSL and a garden soil were exposed to CL-20 for one or two weeks before dehydrogenase activity (DHA) or potential nitrification activity (PNA) were assayed. Results indicate that up to 10 000 mg kg⁻¹ soil of CL-20 had no statistically significant effects on microbial communities measured as DHA or on the ammonium oxidizing bacteria determined as PNA in both soils. Data indicates that CL-20 was not acutely toxic to the species or microbial communities tested and that further studies are required to address the potential long-term environmental impact of CL-20 and its possible degradation products.

Crown Copyright © 2004 Published by Elsevier Ltd. All rights reserved.

Keywords: CL-20; Higher plants; Green algae *Selenastrum capricornutum*; Microtox; Dehydrogenase; Potential nitrification

1. Introduction

Hexanitrohexaazaisowurtzitane (HNIW), commonly known as CL-20, is a recently developed energetic

compound (Nielsen, 1991). It is predicted that CL-20 significantly enhances performance in the areas of specific impulse and/or density in propellants, and in detonation velocity and pressure in explosives (Wardle et al., 1996). These advantages have made CL-20 a possible alternative for the currently used polynitramines RDX (hexahydro-1,3,5-trinitro-1,3,5-triazine) and HMX (octahydro-1,3,5,7-tetranitro-1,3,5,7-tetrazocine) (Fig. 1). However, it is also recognized that the environmental fate and impact of this new compound must be understood and the potential environmental risks be fully assessed prior to its adoption as a commonly used energetic material. It was based on these considerations

[☆] Assigned NRC publication no. 45969.

^{*} Corresponding author. Tel.: +1-514-496-8030; fax: +1-514-496-6265.

E-mail address: geoffrey.sunahara@cnrc-nrc.gc.ca (G.I. Sunahara).

¹ Present address: Environmental Laboratory, USACE Engineer, Research and Development Center, CEERD-EP-P, 3909 Halls Ferry Road, Vicksburg, MS 39180, USA.

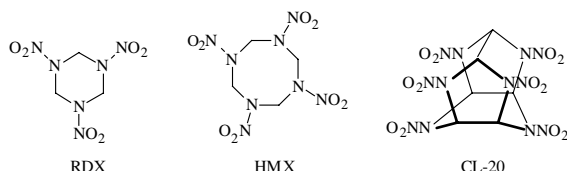


Fig. 1. Chemical structures of RDX, HMX and CL-20.

that the US Strategic Environmental Research and Development Program (SERDP) launched a multi-year, multi-disciplinary research program to collect data on the environmental behavior and impact of CL-20. As part of this effort, we carried out a battery of ecotoxicological tests including terrestrial, aquatic, and avian toxicity studies. This article describes some of the ecotoxicological results obtained in our laboratory.

As far as we know, there is no documented study on the toxicity of CL-20 to ecological receptors such as birds, higher plants, fish, algae, microorganisms, and soil invertebrates. Previous studies have shown that monocyclic RDX and HMX are potent reproductive toxicants to earthworms (Robidoux et al., 2000, 2001) and can be accumulated in earthworm tissues (Lachance et al., 2002). Higher plants and soil microorganisms are not sensitive to RDX and HMX, but plant uptake and translocation were reported by several investigators, suggesting potential food chain biomagnification (Harvey et al., 1991; Best et al., 1999; Thompson et al., 1999; Gong et al., 2001, 2002a; Winfield, 2001; Groom et al., 2002; Rocheleau et al., 2002; Yoon et al., 2002). It was hypothesized that CL-20, being a polycyclic polynitramine and possessing the characteristic N–NO₂ bonds, would show similar behavior to RDX and HMX due to their structural similarity. In the present study, toxicity tests were performed using freshly amended materials because CL-20 has not been released to the environment and no contaminated matrices (soil and water) are available.

2. Material and methods

2.1. Chemicals and reagents

CL-20 (CAS# 135285-90-4, ϵ -polymorph) was obtained from Thiokol Propulsion (Thiokol, Utah, USA). HPLC analysis indicated that the purity of the product was 99.3%. For the purpose of comparison, the structures of CL-20, RDX, and HMX are shown in Fig. 1. TNT was obtained from ICI Explosives Canada (McMasterville, PQ). All the other chemicals were purchased from Sigma-Aldrich Canada.

2.2. Higher plant toxicity test

Plants were exposed to freshly amended CL-20 in Sassafra sandy loam soil (SSL). The SSL (obtained

from R.G. Kuperman) was collected from an uncontaminated open grassland on the property of Aberdeen Proving Ground (Edgewood, MD). Vegetation and surface organic matter were removed and the top 15 cm of the A horizon was collected. The soil was then sieved (5 mm) and air-dried. The physicochemical characteristics of SSL such as low organic C content and low pH (Table 1), rendered it a low adsorptive capacity and a high level of bioavailability. The two chosen plant species were perennial ryegrass (*Lolium perenne*) and alfalfa (*Medicago sativa*) representing monocotyledon and dicotyledon plants, respectively. CL-20 was dissolved in acetone and amended to the soil in order to obtain gradients of artificial contamination. The amended soil was left overnight (ca. 18 h) in a chemical hood to allow the evaporation of acetone. In the range-finding tests, five nominal concentrations (1, 10, 100, 1000, and 10 000 mg kg⁻¹) as well as a solvent control (acetone) and a blank control (deionized water) were tested in triplicate. Boric acid was used as the reference toxicant. Definitive or limit tests were conducted using the two controls and the highest concentration (10 000 mg kg⁻¹) with eight replicates.

The plant toxicity test was performed in accordance with standardized test guidelines (USEPA, 1989; ASTM, 1998). Briefly, 20 seeds of each plant species were sown in a 4-in. pot containing 200 g of soil (dry weight). Alfalfa seeds were inoculated with nitrogen-fixing bacteria prior to the test. Deionized water was added to the soil to achieve 75% of water holding capacity. The pot was then placed in a 1-l polyethylene bag closed with an elastic band to prevent water loss. A growth chamber was used for all phytotoxicity tests. Conditions of the growth chamber were set as follows: 25 °C (16 h)/20 °C (8 h) day/night cycle, light intensity 5000 ± 500 lux, and lights off in the first two days of each test. Measurement endpoints were seedling emergence (germination) and

Table 1
Physicochemical properties of the soils used for terrestrial toxicity tests

Soil	SSL	GS-3
USDA classification	Sandy loam	Silty clay loam
Origin	Grassland	Garden
Organic C (%) ^a	0.3	3.5
Kjeldahl N (%)	0.04	0.28
CEC (cmol kg ⁻¹)	4.3	ND ^b
pH	5.0	6.5
Texture (%)		
Sand	71	11
Silt	18	59
Clay	11	30
Water holding capacity (%)	21	83

^a Determined after dry combustion (ISO, 1995).

^b Not determined.

shoot fresh or dry biomass. Germinated seeds were counted after five (alfalfa) and seven (ryegrass) days. The emerged seedlings were allowed to grow for another two weeks before the test was terminated. At termination, germinated seeds were counted and the above ground shoots were harvested. Shoot dry biomass was obtained after drying at 70 °C for 24 h.

2.3. Microbial toxicity tests

Due to the low microbial activities in SSL, an uncontaminated garden soil GS-3 was also used for the tests. The GS-3 soil was kept moist (with field moisture) and frozen at –20 °C. Soil was thawed overnight at 4 °C and pre-incubated at 24 ± 2 °C for one week before the tests. CL-20 (powder) was directly amended to both soils without using any organic solvent. After amendment, the air-dried SSL and GS-3 soils were brought to 40% of their respective water holding capacity. Treated and control soils were incubated at 24 ± 2 °C in darkness for one (range-finding test) or two (limit test) weeks before microbial bioassays. Two microbial bioassays, i.e., dehydrogenase activity (DHA) and potential nitrification activity (PNA), were carried out following the procedures described elsewhere (Gong et al., 1999, 2002b). The range-finding tests were conducted using four replicates for every treatment whereas the limit test used ten replicates. The concentrations tested were 0, 1, 10, 100, 1000, and 10 000 mg kg^{–1} in the range-finding tests. In the limit tests, only the control and the highest concentration (10 000 mg kg^{–1}) were tested.

2.4. Aquatic toxicity tests

CL-20 was dissolved in acetone and then diluted in water to have 1% (v v^{–1}) of acetone in water for each CL-20 concentration. This carrier concentration was not toxic to *Selenastrum capricornutum* and *Vibrio fischeri* (Sunahara et al., 1998). A saturated solution of CL-20 in acetone was used as the stock solution for serial dilution. Two aquatic bioassays, the 15-min Microtox (*V. fischeri*) and the freshwater green algae (*S. capricornutum*) 96-h growth inhibition tests, were performed as described earlier (Sunahara et al., 1998). Each concentration or treatment was repeated three times in range-finding tests. In the definitive (limit) tests, eight replicates were used for the control and the highest concentration. For QA/QC purposes, TNT (2,4,6-trinitrotoluene) was used as the positive control, whereas phenol and zinc sulphate as reference toxicants for Microtox and the algae tests, respectively.

2.5. Chemical and statistical analysis

The nominal concentrations of CL-20 in amended soil or water were confirmed by chemical analysis using

US-EPA Method 8330A SW-846 (USEPA, 1998; Larson et al., 2002; Groom et al., 2003). Preliminary studies revealed that aqueous samples should be diluted in acetonitrile (1:1, v v^{–1}) and acidified to pH 3. To extract CL-20 from soil samples, 2 g of soil (dry weight) was combined with 10 ml of acetonitrile in a 16-ml glass tube, vortexed for one min, and sonicated at 20 °C for 18 ± 2 h. The sample was then centrifuged at 2700 rpm for 30 min. The supernatant (5 ml) was combined with 5 ml of CaCl₂/NaHSO₄ aqueous solution (5 and 0.2 g l^{–1}, respectively) in a 20-ml vial. After precipitation (30 min), the supernatant was filtered using 0.45 µm-Millipore PTFE filters. The filtrate was analyzed using an HPLC with UV detection at 230 nm. The limit of detection was 0.02 mg l^{–1}. Experimental results were subjected to analysis of variance (ANOVA), the Fisher's least significant differences, or two-tailed Student's *t*-tests. Treatment effects were considered statistically significant at *p* < 0.05.

3. Results and discussion

3.1. Aquatic toxicity tests

Preliminary tests show that up to its water solubility (3.59 ± 0.74 mg l^{–1} at 25 °C; Groom et al., 2003), CL-20 did not cause significant toxic effects on both the marine bacteria *V. fischeri* and the freshwater green algae *S. capricornutum* (data not shown). Results from definitive (limit) tests (Table 2) confirmed those from range-finding tests. In contrast, the positive control TNT inhibited the bioluminescence of *V. fischeri* by 22–65% at 0.2–5 mg l^{–1} (IC₅₀ = 1.0 ± 0.3 mg l^{–1}), and the growth of *S. capricornutum* by 10–96% at 0.2–1.25 mg l^{–1}

Table 2
Toxicological effects of CL-20 on the bioluminescence (15-min light reduction) of *Vibrio fischeri* and the 96-h growth (cell density) of *Selenastrum capricornutum*

CL-20 concentration ^a (mg l ^{–1})	Inhibition of (% of control) ^b	
	Light reduction (<i>V. fischeri</i>)	Cell density (<i>S. capricornutum</i>)
Control	0.0 ± 3.4	0.0 ± 13.4
D-1	1.0 ± 2.3	–20.2 ± 18.6
D-2	0.7 ± 3.2	–2.1 ± 22.7
D-3	–1.9 ± 2.6	1.5 ± 16.6
D-4	–4.5 ± 2.6	4.3 ± 12.7
D-5	–4.9 ± 2.0	5.4 ± 9.1
D-6	–3.2 ± 3.8	1.3 ± 9.2

^a For the Microtox and algal growth inhibition tests, the starting concentrations (D-6) were 2.76 and 3.64 mg l^{–1}, respectively. Serial dilutions (1:1, v v^{–1}) were then prepared (i.e., D-5 to D-1).

^b Expressed as mean ± standard deviation, *n* = 8 (control and D-6 groups); otherwise *n* = 3.

($IC_{50} = 0.8 \pm 0.2 \text{ mg l}^{-1}$) in a dose-dependent manner (data not shown). The results of TNT are consistent with our previous reported values (Microtox, 15-min IC_{50} : 0.95 mg l^{-1} ; Freshwater green algae, 96-h IC_{50} : 0.73 mg l^{-1}) (Sunahara et al., 1998). These results indicate that, compared with TNT, CL-20 is not toxic to the two aquatic species.

3.2. Higher plant tests

Up to the highest test concentration ($10\,000 \text{ mg kg}^{-1}$), CL-20 did not show any major and significant adverse effects on both plant species in SSL for both range-finding and limit tests (Table 3). In fact, ryegrass shoot biomass in CL-20 treated soils was significantly higher than that in the controls, but this effect was not concentration-dependent. Up to $200 \mu\text{g CL-20 g}^{-1}$ dry plant was found in the ryegrass shoots (data not shown). Chemical analyses of freshly amended soil samples indicate very good recoveries ($98 \pm 3\%$) of CL-20 in the limit test. However, nearly 20% of the amended CL-20 was not recovered from the soil after the test, and the exact fate of CL-20 loss was unknown. Possible pathways include biodegradation (e.g., nitrate reductase activity) (Bhushan et al., 2003) or hydrolysis (Balakrishnan et al., 2003; Trott et al., 2003), plant uptake,

and binding to soil particles ($K_d = 2.43 \text{ l kg}^{-1}$ in the SSL soil; Montel-Rivera, F., personal communication).

3.3. Microbial toxicity tests

Preliminary results show that SSL had very low microbial activities measured as DHA ($2.2 \pm 0.2 \text{ nmol INF g}^{-1} \text{ soil h}^{-1}$) and PNA ($8.5 \pm 1.4 \text{ ng nitrite-N g}^{-1} \text{ soil h}^{-1}$). Therefore, a garden soil (GS-3) was also used and exposed to CL-20. No significant adverse effects were observed on indigenous microorganisms in the one-week exposure range-finding test. Both DHA and PNA were not affected up to the highest amendment level of $10\,000 \text{ mg kg}^{-1}$ in the GS-3 soil (Table 4). Limit tests (two-week exposure) confirmed these results except that PNA was significantly enhanced in the GS-3 soil treated with $10\,000 \text{ mg kg}^{-1}$ of CL-20 as compared with that in the control soil. Further studies indicate that CL-20 might be used as a nitrogen source by soil microorganisms (Bhushan et al., 2003; Trott et al., 2003). For instance, we found that CL-20 in the limit tests is biodegradable with the release of nitrite that can be further oxidized to nitrate (unpublished data). Recently, it has been shown that CL-20 can undergo abiotic (Balakrishnan et al., 2003) and enzymatic (Bhushan et al., 2003) decomposition via initial denitration. In addition,

Table 3

Toxicological effects of CL-20 on higher plants (alfalfa and ryegrass) in a Sassafras sandy loam soil

CL-20 concentration (mg kg^{-1} dry soil)		Alfalfa			Ryegrass		
Nominal	Measured	Germination (%) ^a	Fresh biomass (%) ^b	Dry biomass (%) ^b	Germination (%) ^a	Fresh biomass (%) ^b	Dry biomass (%) ^b
<i>Range-finding test^c</i>							
Carrier control	0.0 ± 0.0	83 ± 2			93 ± 3		
1	0.6 ± 0.0	85 ± 0	-7 ± 6	-1 ± 9	97 ± 3	$-8 \pm 2^*$	-7 ± 2
10	8.8 ± 0.4	82 ± 4	3 ± 16	-1 ± 6	93 ± 3	$-14 \pm 3^*$	$-14 \pm 5^*$
100	96 ± 3	77 ± 6	10 ± 13	6 ± 11	$83 \pm 2^*$	$12 \pm 2^*$	6 ± 2
1000	960 ± 22	87 ± 4	-12 ± 6	-1 ± 3	95 ± 3	5 ± 2	1 ± 2
10 000	9832 ± 341	85 ± 5	-15 ± 13	-9 ± 12	93 ± 3	$-10 \pm 3^*$	5 ± 1
ANOVA		$p > 0.05$	$p > 0.05$	$p > 0.05$	$p < 0.05$	$p < 0.05$	$p < 0.05$
<i>Limit test^d</i>							
Carrier control	0.0 ± 0.0	ND	ND	ND	87 ± 4		
10 000	9832 ± 341^e	ND	ND	ND	91 ± 2	-26 ± 5	-14 ± 5
	7964 ± 158^f						
<i>t</i> -Test (two-tailed)					$p > 0.05$	$p < 0.05$	$p > 0.05$

* Significantly different from the control using the Fisher's least significant differences test.

^a Expressed as mean \pm standard error and using the numbers of emerged seedlings after 5 and 7 d exposure for alfalfa and ryegrass, respectively.

^b Expressed as mean \pm standard error and calculated as percentage change compared to the carrier (acetone) control after 16 and 19 d exposure for alfalfa and ryegrass, respectively. There was no significant difference between the carrier (acetone) and the blank (water) control. Negative values indicate stimulatory effects, whereas positive values denote inhibition.

^c Three replicates per treatment.

^d Eight replicates per treatment. ND: not done.

^e Measured CL-20 concentration in soil at the start of the test.

^f Measured CL-20 concentration in soil at the end of the test.

Table 4

Toxicological effects of CL-20 on indigenous soil microorganisms in a Sassafras sandy loam soil (SSL) and a garden soil (GS-3)

Nominal conc. (mg kg ⁻¹ soil)	GS-3		SSL	
	DHA ^a	PNA ^a	DHA ^a	PNA ^a
<i>Range-finding test^b</i>				
Control (water)	0.0 ± 2.5	0.0 ± 2.7	0.0 ± 6.4	0.0 ± 8.2
1	-8.9 ± 3.5	2.3 ± 2.4	0.2 ± 4.9	-9.5 ± 3.6
10	9.9 ± 8.6	-0.4 ± 1.8	-10.2 ± 5.0	-4.8 ± 1.4
100	7.0 ± 4.5	4.0 ± 1.9	-8.2 ± 3.9	7.0 ± 0.8
1000	-8.4 ± 3.1	-0.5 ± 3.0	1.6 ± 5.3	-4.1 ± 6.7
10 000	-2.1 ± 3.3	0.0 ± 3.0	-3.2 ± 4.7	-5.9 ± 8.3
ANOVA	$p > 0.05$	$p > 0.05$	$p > 0.05$	$p > 0.05$
<i>Limit test^c</i>				
Control (water)	0.0 ± 4.3	0.0 ± 0.8	0.0 ± 3.2	0.0 ± 5.2
10 000	-2.2 ± 4.0	-13.9 ± 1.4	5.0 ± 0.9	-10.8 ± 4.8
<i>t</i> -Test (two-tailed)	$p > 0.05$	$p < 0.05$	$p > 0.05$	$p > 0.05$

^a DHA: dehydrogenase activity; PNA: potential nitrification activity. Expressed as mean ± standard error and calculated as percentage change from the control (the mean of control = 100%). Negative values indicate stimulatory effects whereas positive values denote inhibition.

^b Four replicates per treatment (one-week exposure).

^c Ten replicates per treatment (two-week exposure). HPLC analysis of soil extracts indicated that recovery of CL-20 was 121 ± 12% in SSL ($n = 5$) or 88 ± 5% in GS-3 soil ($n = 5$) ($p < 0.05$, two-tailed Student's *t*-test).

an independent study has reported that CL-20 (2000 mg kg⁻¹) can enhance the microbial respiration activity in a forest soil (Stevens Institute of Technology, 2003).

4. Conclusions

Data presented in this article indicate that CL-20 is not toxic to marine bacteria *V. fischeri*, freshwater green algae *S. capricornutum*, terrestrial higher plants and indigenous soil microorganisms. However, other results obtained from our and other laboratories indicate that CL-20 is highly toxic to soil invertebrates such as the earthworm *Eisenia andrei* and enchytraeids (Robidoux et al., 2004; Kuperman, R.G., personal communication). This implies the importance of using a battery of ecotoxicological assays to assess potential environmental impacts of new chemical compounds. Further studies are also required to address the potential long-term environmental impact of CL-20 and its possible degradation products.

Evidence from the present and other studies (e.g., Robidoux et al., 2004; Kuperman, R.G., personal communication) also indicates that CL-20 has a similar ecotoxicological potency to RDX and HMX because both RDX and HMX exhibited no or low toxicity to *V. fischeri*, *S. capricornutum* (Sunahara et al., 1998), soil microbial communities (Gong et al., 2001, 2002a) and higher plants (Harvey et al., 1991; Best et al., 1999; Thompson et al., 1999; Winfield, 2001; Rocheleau et al., 2002), and they also showed high reproductive toxicity to earthworms (Robidoux et al., 2000, 2001) as well as a

high lethality to enchytraeids (S. Dodard, unpublished data).

Acknowledgements

We thank Ghalib Bardai, Manon Sarrazin, Majorie Martel, Genevieve Bush and Alain Corriveau for their technical assistance, the US Strategic Environmental Research and Development Program (SERDP Project CP1256) for financial support, and the Thiokol Propulsion Inc. for providing the ϵ -CL-20.

References

- American Society for Testing and Materials (ASTM), 1998. Standard Guide for Conducting Terrestrial Plant Toxicity Tests. West Conshohocken, PA, USA. ASTM E 1963–1998.
- Balakrishnan, V.K., Halasz, A., Hawari, J., 2003. Alkaline hydrolysis of the cyclic nitramine explosives RDX, HMX and CL-20: new insights into degradation pathways obtained by the observation of novel intermediates. Environ. Sci. Technol. 37, 1838–1843.
- Best, E.P.H., Sprecher, S.L., Larson, S.L., Fredrickson, H.L., Bader, D.F., 1999. Environmental behavior of explosives in groundwater from the Milan Army Ammunition Plant in aquatic and wetland plant treatments: uptake and fate of TNT and RDX in plants. Chemosphere 39, 2057–2072.
- Bhushan, B., Paquet, L., Spain, J.C., Hawari, J., 2003. Biotransformation of 2,4,6,8,10,12-hexanitro-2,4,6,8,10,12-hexaazaisowurtzitane (CL-20) by a denitrifying *Pseudomonas* sp. FA 1. Appl. Environ. Microbiol. 69, 5216–5221.

- Gong, P., Siciliano, S.D., Greer, C.W., Paquet, L., Hawari, J., Sunahara, G.I., 1999. Effects and bioavailability of 2,4,6-trinitrotoluene in spiked and field-contaminated soils to indigenous microorganisms. *Environ. Toxicol. Chem.* 18, 2681–2688.
- Gong, P., Hawari, J., Thiboutot, S., Ampleman, G., Sunahara, G.I., 2001. Ecotoxicological effects of hexahydro-1,3,5-trinitro-1,3,5-triazine (RDX) on soil microbial activities. *Environ. Toxicol. Chem.* 20, 947–951.
- Gong, P., Hawari, J., Thiboutot, S., Ampleman, G., Sunahara, G.I., 2002a. Toxicity of octahydro-1,3,5,7-tetranitro-1,3,5,7-tetrazocine (HMX) to soil microbes. *Bull. Environ. Contam. Toxicol.* 69, 97–103.
- Gong, P., Siciliano, S.D., Srivastava, S., Greer, C.W., Sunahara, G.I., 2002b. Assessment of pollution-induced microbial community tolerance to heavy metals in soil using ammonia-oxidizing bacteria and Biolog assay. *Hum. Ecol. Risk Assess.* 8, 1067–1081.
- Groom, C.A., Halasz, A., Paquet, L., Morris, N., Olivier, L., Dubois, C., Hawari, J., 2002. Accumulation of HMX (octahydro-1,3,5,7-tetranitro-1,3,5,7-tetrazocine) in indigenous and agricultural plants grown in HMX-contaminated anti-tank firing-range soil. *Environ. Sci. Technol.* 36, 112–118.
- Groom, C.A., Halasz, A., Paquet, L., D'Cruz, P., Hawari, J., 2003. Cyclodextrin-assisted capillary electrophoresis for determination of the cyclic nitramine explosives RDX, HMX and CL-20 comparison with high-performance liquid chromatography. *J. Chromatogr. A* 999, 17–22.
- Harvey, S.D., Fellows, R.J., Cataldo, D.A., Bean, R.M., 1991. Fate of the explosive hexahydro-1,3,5-trinitro-1,3,5-triazine (RDX) in soil and bioaccumulation in bush bean hydroponic plants. *Environ. Toxicol. Chem.* 10, 845–855.
- ISO (International Organization for Standardization), 1995. ISO 10694: Soil quality—Determination of organic and total carbon after dry combustion (elementary analysis). Geneva, Switzerland.
- Lachance, B., Leduc, F., Rocheleau, S., Apte, J., Sarrazin, M., Martel, M., Dodard, S., Bardai, G., Kuperman, R.G., Checkai, R.T., Hawari, J., Sunahara, G.I., 2002. Bioaccumulation of five energetic materials in Sassafras sandy loam soil. In: *Proceedings of Partners in Environmental Technology*, Washington, DC, December 3–5, 2002, p. 46.
- Larson, S.L., Felt, D.R., Davis, J.L., Escalon, L., 2002. Analysis of CL-20 in environmental matrices: water and soil. *J. Chromatogr. Sci.* 40, 201–206.
- Nielsen, A.T., 1991. Polycyclic amine chemistry. In: Olah, G.A., Squire, D.R. (Eds.), *Chemistry of Energetic Materials*. Academic Press, San Diego, CA, pp. 95–124.
- Robidoux, P.Y., Svendsen, C., Caumartin, J., Hawari, J., Ampleman, G., Thiboutot, S., Weeks, J.M., Sunahara, G.I., 2000. Chronic toxicity of energetic compounds in soil using the earthworm (*Eisenia andrei*) reproduction test. *Environ. Toxicol. Chem.* 19, 1764–1773.
- Robidoux, P.Y., Hawari, J., Bardai, G., Paquet, L., Ampleman, G., Thiboutot, S., Sunahara, G.I., 2001. TNT, RDX, and HMX decrease earthworm (*Eisenia andrei*) life-cycle responses in a spiked natural forest soil. *Arch. Environ. Contam. Toxicol.* 43, 379–388.
- Robidoux, P.Y., Sunahara, G.I., Savard, K., Berthelot, Y., Leduc, F., Dodard, S., Martel, M., Gong, P., Hawari, J., 2004. Acute and chronic toxicity of the new explosive CL-20 to the earthworm (*Eisenia andrei*) exposed to amended natural soils. *Environ. Toxicol. Chem.* 23, 1026–1034.
- Rocheleau, S., Martel, M., Bardai, G., Wong, S., Sarrazin, M., Dodard, S., Kuperman, R.G., Checkai, T.R., Hawari, J., Sunahara, G.I., 2002. Toxicity of five energetic materials to plants exposed in Sassafras sandy loam soil. In: *Proceedings of SETAC 23rd Annual Meeting in North America*, Salt Lake City, UT, November 16–20, 2002, p. 189.
- Stevens Institute of Technology, 2003. Available from <www.cce.stevens-tech.edu/ResProj.html>.
- Sunahara, G.I., Dodard, S., Sarrazin, M., Paquet, L., Ampleman, G., Thiboutot, S., Hawari, J., Renoux, A.Y., 1998. Development of a soil extraction procedure for ecotoxicity characterization of energetic compounds. *Ecotoxicol. Environ. Safety* 39, 185–194.
- Thompson, P.L., Ramer, L.A., Schnoor, J.L., 1999. Hexahydro-1,3,5-trinitro-1,3,5-triazine translocation in poplar trees. *Environ. Toxicol. Chem.* 18, 279–284.
- Trott, S., Nishino, S.F., Hawari, J., Spain, J.C., 2003. Biodegradation of the nitramine explosive CL-20. *Appl. Environ. Microbiol.* 69, 1871–1874.
- United States Environmental Protection Agency (USEPA), 1989. Seed germination and root elongation toxicity tests in hazardous waste site evaluation: methods development and applications. Corvallis, OR. USEPA Corvallis Environmental Research Laboratory Report PB90-113184.
- United States Environmental Protection Agency (USEPA), 1998. Nitroaromatics and nitramines by high performance liquid chromatography (HPLC)—Method 8330A. Available from <<http://www.epa.gov/epaoswer/hazwaste/test/pdfs/8330a.pdf>>.
- Wardle, R.B., Hinshaw, J.C., Braithwaite, P., Rose, M., 1996. Synthesis of the caged nitramine HNIW (CL 20). In: *27th International Annual Conference on ICT (Proceedings)*, Jahrestagung, Karlsruhe, 27, pp. 1–10.
- Winfield, L.E., 2001. Development of a short-term (<12 days), plant-based, screening “tool” for determination of hexahydro-1,3,5-trinitro-1,3,5-triazine (RDX) bioavailability, phytotoxicity, and bioconcentration in selected terrestrial plants. Ph.D. Dissertation, University of Mississippi, MS, USA.
- Yoon, J.M., Oh, B.-T., Just, C.L., Schnoor, J.L., 2002. Uptake and leaching of octahydro-1,3,5,7-tetranitro-1,3,5,7-tetrazocine by hybrid poplar trees. *Environ. Sci. Technol.* 36, 4649–4655.

Photodegradation of CL-20: insights into the mechanisms of initial reactions and environmental fate

Jalal Hawari*, Stephane Deschamps, Chantale Beaulieu, Louise Paquet,
Annamaria Halasz

Biotechnology Research Institute, National Research Council of Canada, 6100 Royalmount Ave., Montreal, Quebec, Canada H4P 2R2

Received 6 November 2003; received in revised form 28 May 2004; accepted 30 June 2004

Abstract

Hexanitrohexaazaisowurtzitane (HNIW) or CL-20 is a caged structure polycyclic nitramine that may replace RDX and HMX as a common use energetic chemical. To provide insight into the environmental fate of CL-20 we photolyzed the chemical in a Rayonet photoreactor (254–350 nm) and with sunlight in aqueous solutions. Previously, we found that initial photodenitration of the monocyclic nitramine RDX leads to ring cleavage and decomposition. Presently, we found that photolysis of the rigid molecule CL-20 produced NO_2^- , NO_3^- , NH_3 , HCOOH , N_2 and N_2O . Using LC/MS (ES-) we detected several key intermediates carrying important information on the initial steps involved in the degradation of CL-20. The identities of the intermediates were confirmed using a uniformly ring labeled ^{15}N -[CL-20]. When CL-20 was photolyzed in the presence of H_2^{18}O , D_2O or $^{18}\text{O}_2$ we obtained a product distribution suggesting that the energetic chemical degraded via at least two initial routes; one involved sequential homolysis of $\text{N}-\text{NO}_2$ bond(s) and another involved photorearrangement prior to hydrolytic ring cleavage and decomposition in water.

© 2004 Elsevier Ltd. All rights reserved.

Keywords: CL-20; Degradation; Photolysis; Denitration; Photorearrangement

1. Introduction

High-density polynitropolyaza-caged compounds are new emerging chemicals that contain high energy and has the potential to be used in several industrial and military applications. A typical energetic chemical of this family is 2,4,6,8,10,12-hexanitro-2,4,6,8,10,12-hexaazatetracyclo [5.5.0.0^{5,9}.0^{3,11}] dodecane (CL-20) or hexanitrohexaazaisowurtzitane (HNIW), which was recently synthesized by Nielsen et al. (1987, 1990) and

later adopted by Thiokol for large-scale production (Wardle et al., 1996).

Previous practices involving the less strained monocyclic nitramines such as hexahydro-1,3,5-trinitro-1,3,5-triazine (RDX) and octahydro-1,3,5,7-tetranitro-1,3,5,7-tetrazocine (HMX) including manufacturing, testing and training, demilitarization and open burning/open detonation (OB/OD) have resulted in severe soil and groundwater contamination (Haas et al., 1990; Myler and Sisk, 1991). It has been shown that both monocyclic nitramines RDX and HMX are modestly toxic to aquatic organisms (Yinon, 1990; Sunahara et al., 2001; Talmage et al., 1999), earthworms (Robidoux et al., 2000, 2001) and indigenous soil microorganisms (Sunahara et al., 2001; Gong et al., 2001). Future wide military

*Corresponding author. Tel: +1-514-496-6267; fax: +1-514-496-6265.

E-mail addresses: jalal.hawari@nrc.ca,
jalal.hawari@cnrc-nrc.gc.ca (J. Hawari).

practices with CL-20 may also result in environmental contamination of soil and groundwater.

CL-20 is a heterocyclic nitramine, which, like RDX and HMX, contains the characteristic N–NO₂ functional groups (Fig. 1). Therefore, the three energetic chemicals RDX, HMX and CL-20 are expected to show some sort of similarities in their chemical (and even enzymatic) reactions. However, CL-20 is a polycyclic nitramine characterized by having a strained three-dimensional cage structure, whereas RDX and HMX are two-dimensional monocyclic nitramines (Fig. 1). For instance, both RDX and HMX are cyclic oligomers of methylenenitramine, CH₂–N–NO₂, ([CH₂NNO₂]₃ for RDX and [CH₂NNO₂]₄ for HMX). Whereas CL-20 contains the repeating unit CH–N–NO₂ (Wardle et al., 1996; Nielsen et al., 1998), with characteristic C–C linkages. Therefore, we predict that the above structural differences can also cause significant variations in the degradation pathway(s) of CL-20 from those reported for RDX and HMX in the environment (Hawari et al., 2002; Bhushan et al., 2003a).

Recently, we discovered that denitration of RDX by photolysis (Hawari et al., 2002), hydrolysis (Balakrishnan et al., 2003) or incubation with *Rhodococcus* sp. strain DN22 (Fournier et al., 2002) or a Cytochrome P450 enzyme (Bhushan et al., 2003b) lead to effective decomposition. The product distribution in all previous cases was basically similar and included HCHO, HCOOH, NH₂CHO, NH₃, NO₂[–], NO₃[–], and N₂O. We concluded that once denitration takes place, RDX undergoes ring cleavage and spontaneous decomposition in water. As far as we are aware little information is available on the photodegradation of CL-20 in solution. Pace and Kalyanaraman (1993) reported the cleavage of an N–NO₂ bond during CL-20 photolysis by trapping the generated NO₂ radical in dimethyl sulfoxide (DMSO) followed by detection of the spin adduct using ESR spectroscopy. No other information on the identity of the degradation products was provided. On the other hand, solid state photochemistry of the energetic chemical has been reported by Pace (1991) and Ryzhkov and McBride (1996) and was suggested to proceed via the primary cleavage of an N–NO₂ bond.

As discussed above with RDX decomposition following its photodenitration, we predict that CL-20, being

also a cyclic nitramine with C–N–NO₂ linkages, can undergo decomposition following initial denitration in water. Our objective in the present study is thus to test the above hypothesis and photolyze CL-20 in aqueous and MeCN/H₂O solutions using a Rayonet photoreactor (254–350 nm) and sunlight. We hope that the discovery of early intermediate products during photolysis of CL-20 can provide insight into the degradation pathway(s) of the energetic chemical and thus its environmental fate and behavior.

2. Materials and methods

2.1. Chemicals

CL-20 as an ϵ -form (purity 99.3% determined by HPLC) and ring labeled ¹⁵N-[CL-20] (purity 90% determined by HPLC) were obtained from Thiokol Propulsion (Thiokol Utah 84302 USA). Elemental composition of CL-20 was determined on a Carlo Erba EA 1108 analyzer (University of Montreal, QC, Canada) and was found to be C 16.84%, N 37.52%, H 1.06% (calculated values for C₆H₆N₁₂O₁₂: C 16.45%, N 38.36%, H 1.38%). Upon analysis by LC-MS(ES-) we detected an impurity (0.5%) with a [M–H] at 434 Da corresponding to a monoacetylated CL-20. Acetonitrile, formic acid, formaldehyde, D₂O, H₂¹⁸O and ¹⁸O₂ were from Aldrich, Canada.

2.2. Irradiation experiments

A Rayonet RPR-100 photoreactor fitted with a merry-go-round apparatus (Southern New England Co, Hamden, CT) equipped with either 16 254 nm (35 W), 300 nm (21 W) or 350 nm (24 W) fluorescent lamps were used as light sources. In some experiments photolysis was conducted using sunlight. Photolysis was conducted in 20 mL quartz tubes each charged with a 10 mL of aqueous or aqueous acetonitrile solutions (50%v/v) of CL-20 (3.5 and 50 mg/L, respectively). Acetonitrile was added to water to increase solubility of CL-20 (3.5 mg/L at 20 °C) (Groom et al., 2003) in an attempt to generate sufficient amounts of intermediates to allow detection.

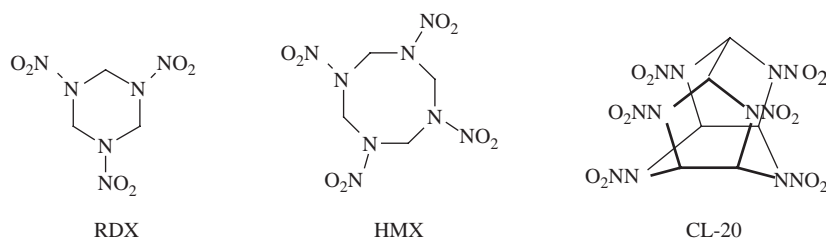


Fig. 1. Typical structures of RDX, HMX and CL-20.

Photolysis was carried out in either degassed (Ar bubbling) or non-degassed (with O₂ or ¹⁸O₂ bubbling) tubes sealed with Teflon-coated mininert valves. Controls containing CL-20 were kept in the dark during the course of the experiment. To determine the role of water in the photolysis process we photolyzed CL-20 (3.5 mg/L) in the presence of D₂O and H₂¹⁸O. The temperature of the reactor was maintained at 25 °C.

2.3. Analytical methods

A Bruker bench-top ion trap mass detector attached to a Hewlett-Packard 1100 Series HPLC system equipped with a PDA detector was used to analyze for CL-20 and its intermediates. The samples were injected into a 5 µm-pore size Zorbax SB-C18 capillary column (0.5 mm ID by 150 mm; Agilent, CA) at 25 °C. The solvent system was composed of a MeCN/water gradient (30% v/v to 70% v/v) at a flow rate of 15 µL/min. For mass analysis, ionization was performed in a negative electrospray ionization mode, ES(–), producing mainly the deprotonated molecular mass ions [M–H]. The mass range was scanned from 40 to 550 Da.

The concentration of CL-20 was followed using an HPLC (Thermo Separation Products) composed of a pump (model P4000), an auto injector (model AS1000) and a photodiode-array detector (model UV6000LP). The sample was injected on a Supelcosil LC-CN column (25 cm, 4.6 mm, 5 µm) maintained at 35 °C. The solvent system consisted of isocratic methanol/water mixture (70% v/v) at a flow rate of 1 mL/min. The detector was set to scan from 200 to 350 nm then the chromatograms were extracted at a wavelength of 230 nm.

Formic acid (HCOOH), nitrite (NO₂[–]) and nitrate (NO₃[–]) were measured using an HPLC from Waters (pump model 600 and auto-sampler model 717 plus) equipped with a conductivity detector (model 430). The acetonitrile content of the sample was removed under a high flow of helium before injection. The separation was made on a Dionex IonPac AS15 column (2 × 250 mm). The mobile phase was 30 mM KOH at a flow rate of 0.4 mL/min and 40 °C. The detection of anions was enhanced by reducing the background with an auto suppressor from Altech (model DS-Plus). Detection limits were 100 ppb for formate and nitrate, and 250 ppb for nitrite. Ammonium cation was analyzed using a SP 8100 HPLC system equipped with a Waters 431 conductivity detector and a Hamilton PRP-X200 (250 mm × 4.6 mm × 10 µm) analytical cation exchange column as described earlier (Hawari et al., 2001). Analysis of N₂ and N₂O was performed as previously described (Fournier et al., 2002). Formaldehyde (HCHO) was analyzed as described by Summers (1990) and Hawari et al. (2002).

3. Results and discussion

3.1. Photodegradation of CL-20 in aqueous solutions

We found that photolysis of CL-20 in aqueous (3.5 mg/L) or MeCN/water (50 mg/L) solutions (50% v/v) at either 254, 300 or 350 nm led to the disappearance of the energetic chemical, but the presence of MeCN increased solubility of the energetic chemical and consequently led to the accumulation of sufficient amounts of products that facilitated detection. The removal of CL-20 at 300 nm was accompanied with the concurrent formation and accumulation of nitrite (NO₂[–]), nitrate (NO₃[–]), ammonia (NH₃) and formic acid (HCOOH) (Fig. 2) and trace amount of glyoxal (HCOHCO) was detected (data not shown). Nitrogen (N₂) and nitrous oxide (N₂O) were detected in trace amounts. Apparently NO₃[–] was produced from photo-oxidation of NO₂[–]. Bose et al. (1998) reported that photo-oxidation of the cyclic nitramine RDX with ozone at 230 nm also produced nitrate.

When photolysis was carried out at 254 nm CL-20 disappeared rapidly. For instance it took approximately 1 h to photodegrade CL-20 (50 mg/L) at 300 nm (Fig. 2) whereas it took less than 1 min to remove the same amount of CL-20 at 254 nm in MeCN/water solution. On the other hand, photolysis of CL-20 at either 350 nm or with sunlight gave closely related product distribution but at rates much lower than those observed using the Rayonet photoreactor at shorter wavelengths (Fig. 2). In dark controls containing CL-20 in either water or MeCN/water solutions no appreciable reduction in the concentration of the energetic chemical was observed within the time course of the experiment.

In general, we found that the present photodegradation of the caged structure polycyclic nitramine CL-20 was much more rapid than RDX (Hawari et al., 2002). The extreme reactivity of CL-20 as compared to monocyclic nitramines has also been noted during their thermal decomposition (Oxley et al., 1994; Korsounskii et al., 2000). Korsounskii et al. (2000) found that the thermal decomposition of HMX and CL-20 in solution proceeded via N–NO₂ cleavage with first-order rate constants (*k*) of 1.6×10^{-5} and $4.4 \times 10^{-3} \text{ s}^{-1}$, respectively. The increased ring strain in CL-20 was suggested to accelerate the decomposition of the energetic chemical as compared to the less strained monocyclic nitramines (Oxley et al., 1994).

3.2. Intermediates and insight into the mechanisms of initial reactions

Fig. 3A–C represents the UV chromatogram of CL-20 (I) after photolysis at 254, 300 and 350 nm, respectively. As Fig. 3 show we were able to detect several suspected intermediates (II–VI) of the energetic chemical. The

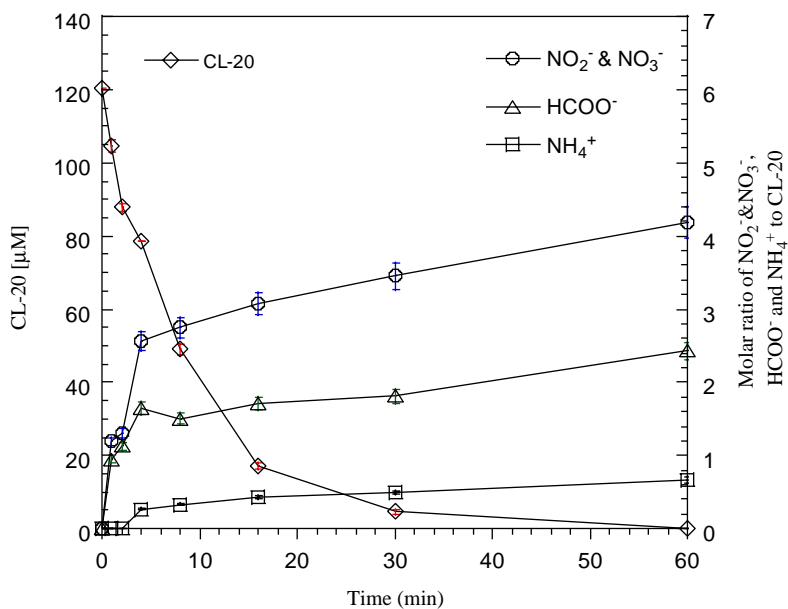


Fig. 2. A time course study for the photolysis of CL-20 (1.20 μmol) at 300 nm and 25 °C in MeCN/water solutions (50% v/v) showing formation of nitrite (NO_2^-), nitrate (NO_3^-), ammonium (NH_4^+) and formic acid (HCOOH).

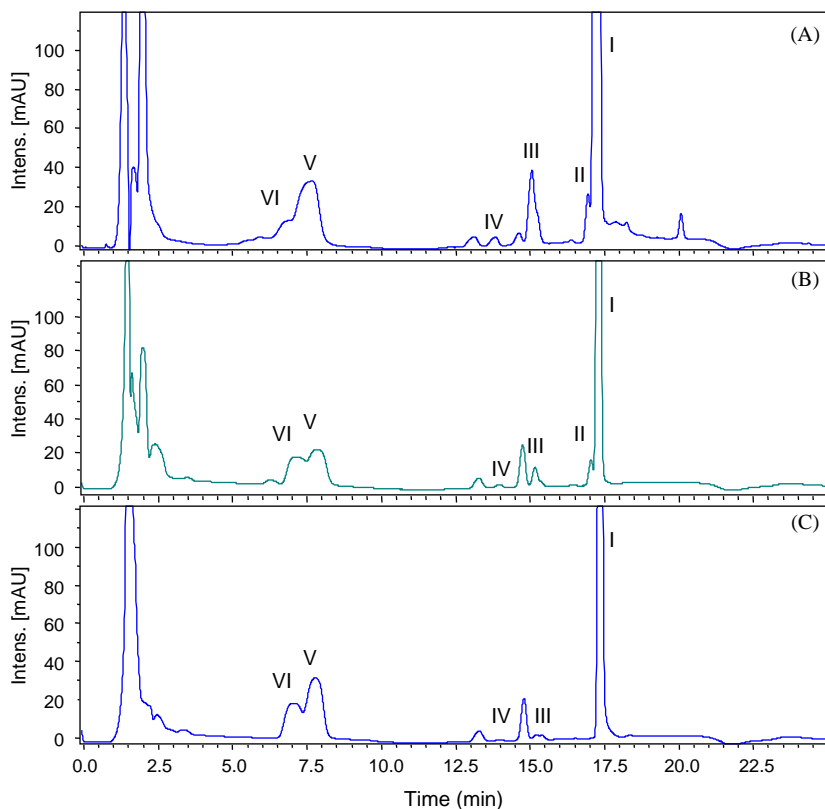


Fig. 3. LC/UV (230 nm) chromatogram of CL-20 after photolysis at 254 nm for 20 s (A), 300 nm for 15 min (B) and 350 nm for 6 h (C) in acetonitrile-water (50% v/v).

suspected intermediates were tentatively identified using LC/MS(ES[−]) as their adduct mass ($[M + NO_3]^-$) or deprotonated molecular ($[M - H]^-$) mass ions (Fig. 4A–D, Fig. 5A and B).

3.2.1. Photorearranged products

Peak I with a retention time (r.t.) of 17.5 min was that of CL-20 which appeared as a nitrate adduct $[M + NO_3]^-$ at 500 Da (Fig. 4A and Fig. 5–1a). Such adducts have been detected during the LC/MS(ES[−]) analysis of RDX (Zhao and Yinon, 2002). Whereas peaks II–VI represented the intermediate products of I. Peak II, appearing at 17.2 min, was only detected in trace amounts and showed a $[M - H]^-$ molecular mass ion at 421 Da, matching a molecular formula of $C_6H_6N_{11}O_{11}$. The mass spectrum of II showed another characteristic mass ion at 484 Da representing the nitrated mass ion adduct $[M + NO_3]^-$. Using the ring labeled ^{15}N -CL-20 the previously detected mass ions (421 and 484 Da) for II were observed at 427 and 490 Da (an increase of 6 amu), respectively, suggesting the involvement of the six ^{15}N -ring atoms of the intermediate (Fig. 5b). We tentatively identified II as the

mononitroso derivative of CL-20 (Fig. 4B and Fig. 5IIa and b). This peak was observed when photolysis was carried out at both 254 and 300 nm, although at higher concentration in the former case (Fig. 3). It has been reported that thermolysis (Shu et al., 2002) and photolysis (Peyton et al., 1999) of RDX can lead to the formation of the nitroso product via homolysis of an N–NO₂ bond followed by a secondary reaction that involved the generated N centered species and nitric oxide (NO). Also RDX (Zukermann et al., 1987; Capellos et al., 1989) and HMX (Zukermann et al., 1987) have been reported to photodissociate to produce ·OH radical via a five membered ring intermediate formed by a transfer of H from a α -CH to one of the two oxygens in a N–NO₂ (1,5-H shift) bond in the molecule. The subsequent loss of OH from the five membered ring would yield a product with a nitroso functionality. We presumed that both rearrangements described above for monocyclic nitramines RDX and HMX might also be applicable to polycyclic nitramines such as CL-20.

The other two small peaks III and IV which appeared at a r.t. of 15.2 and 14.1 min, respectively, each showed a

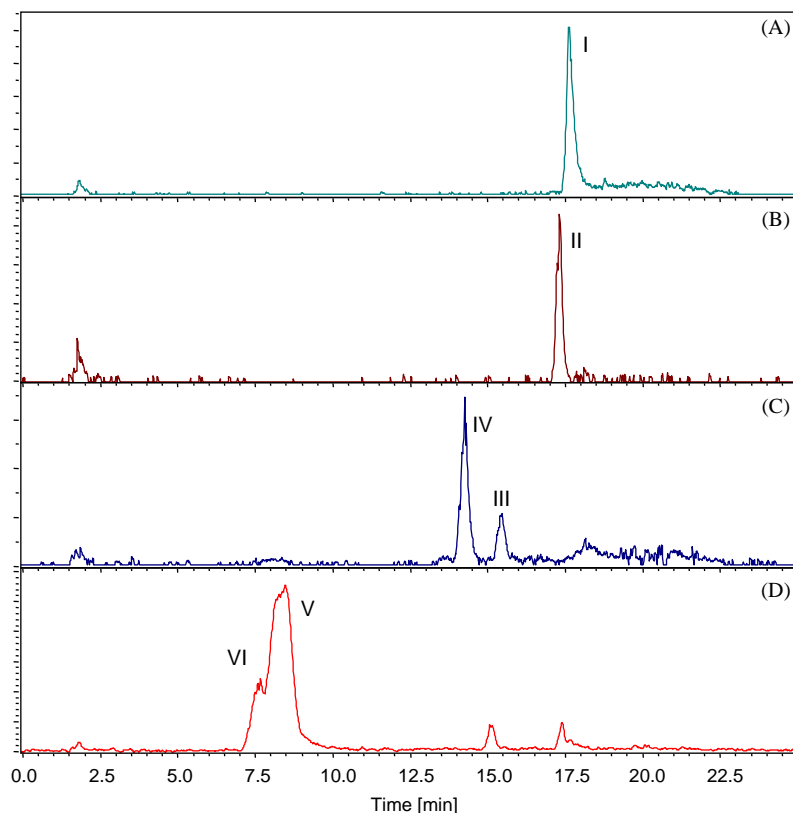


Fig. 4. LC/MS (ES[−]) extracted ion chromatograms of CL-20 and its products after photolysis at 300 nm. Extracted mass ion adducts $[M + NO_3]^-$ were 500 Da (A, I), 484 Da (B, II) and deprotonated mass ion $[M - H]^-$ were 408 Da (C, III and IV) and 345 Da (D, V and VI).

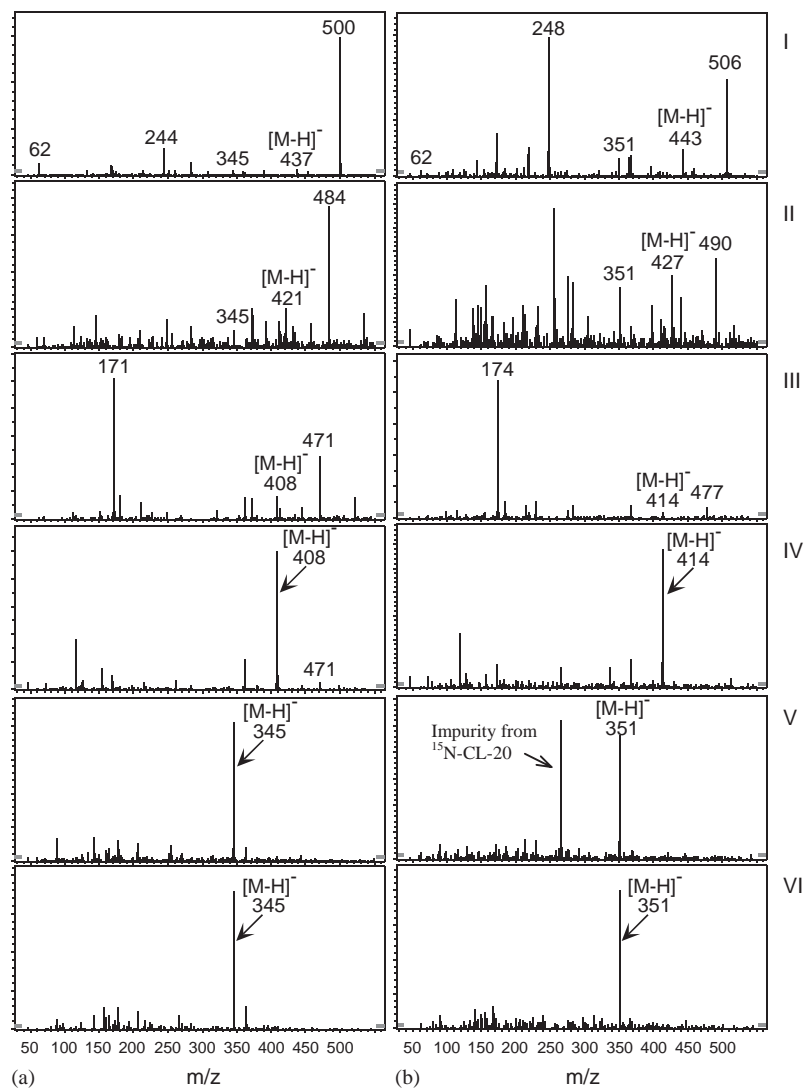


Fig. 5. LC/MS (ES-) spectra of CL-20 (I) and its initial intermediates (II to VI) observed during photolysis at 300 nm in MeCN/H₂O (50% v/v), (a) from non-labeled and (b) from uniformly ring labeled ¹⁵N-[CL-20].

[M-H]⁻ at 408 Da matching a molecular formula of C₆H₇N₁₁O₁₁ (Fig. 4C and Fig 5IIIa and IVa). Also a characteristic mass ion at 471 Da appeared for each of the two products (III and IV), representing a nitrate molecular mass ion adduct [M+NO₃]⁻. When we photolyzed the ring labeled ¹⁵N-[CL-20] the previously detected mass ions for III and IV were observed at 414 Da (an increase of 6 amu), suggesting once again the presence of the 6 ¹⁵N ring atoms in each of the two intermediates (Fig. 5b). We tentatively identified the intermediates as either a photorearranged carbinol (III) or a rearranged ketone (IV) formed via initial loss of 1NO from CL-20 and the gain of 1H from water (Fig. 6). Bulusu et al. (1970) reported similar rearrange-

ments during electron impact—spectrometric analysis of cyclic nitramines.

When photolysis was conducted in either H₂¹⁸O or D₂O the 408 Da intermediate was observed at 408 and 409 Da, respectively, suggesting that water acted as H (or D) donor during its reaction with CL-20 (Fig. 6). Whereas the presence of ¹⁸O₂ during photolysis did not affect the detected mass ions, but we detected the labeled ¹⁸O in nitrate (N¹⁸O¹⁶O₂⁻) only.

3.2.2. Cleavage of N-NO₂

The two LC/MS peaks V and VI, with retention times at 6.9 and 7.9 min, respectively, showed the same [M-H]⁻ at 345 Da each matching a molecular formula

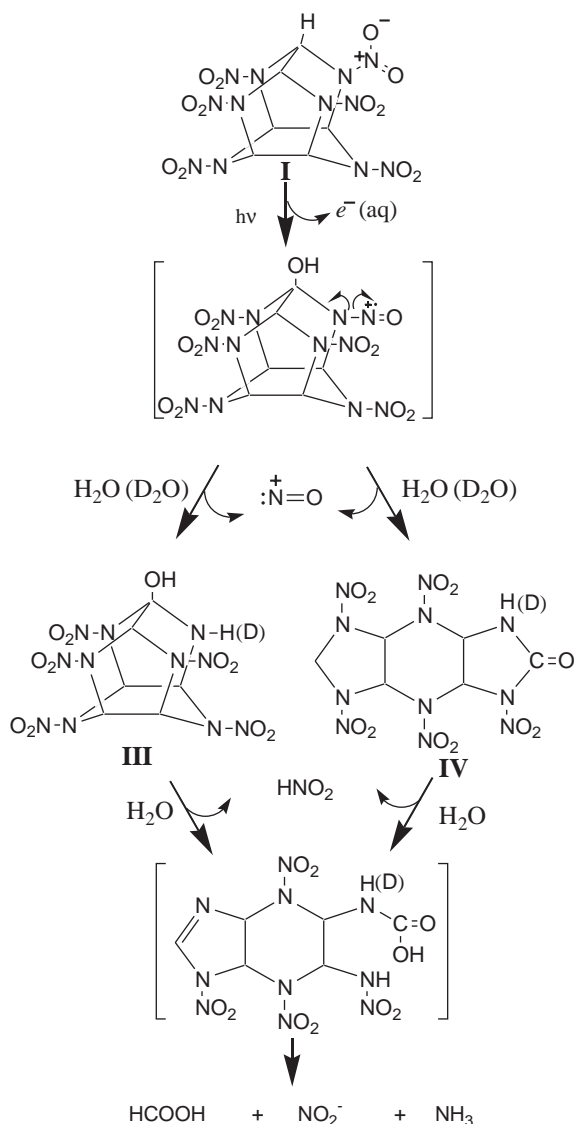


Fig. 6. Postulated photorearrangement routes of CL-20 at 300 nm in MeCN/water (50% v/v).

of $C_6H_6N_{10}O_8$ (Fig. 4D and Fig. 5Va and VIa). Once again when we photolyzed the ring labeled ^{15}N -[CL-20] the two intermediates V and VI showed their $[M-H]$ at 351 Da (an increase of 6 amu), suggesting the involvement of 6 ^{15}N atoms in the formation of each product (Fig. 5b). We tentatively identified V and VI as a pair of isomers of the diene products formed after the successive loss of two nitro groups from CL-20 (Fig. 7).

We also detected an intermediate with a r.t. at 2.0 min and a $[M-H]^-$ at 381 Da with a characteristic mass ion fragment at 190 Da, matching a molecular formula of $C_6H_{10}N_{10}O_{10}$. Photolysis of CL-20 in either $H_2^{18}O$ or D_2O the 381 Da product appeared at 385 Da and its

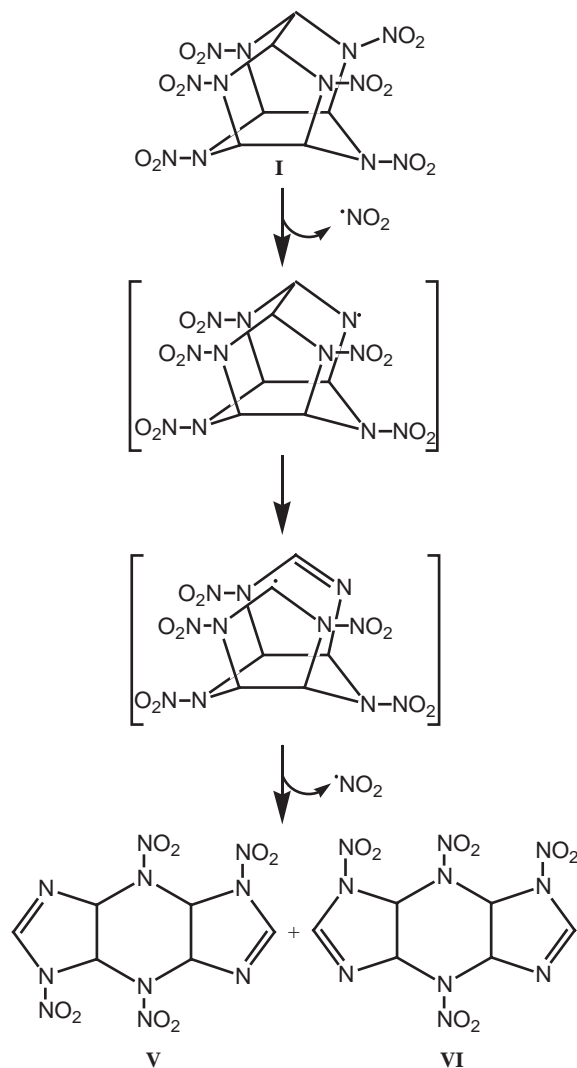


Fig. 7. Postulated photodenitration routes of CL-20 at 300 nm in an aqueous acetonitrile solution.

mass ion fragment at 192 Da, suggesting that $2H_2O$ molecules reacted with the former product (V) (Fig. 8). When photolysis was repeated in the presence of $^{18}O_2$ no ^{18}O was detected in either intermediate. The intermediate was tentatively identified as the hydrolytic ring cleavage product (VII) of the diene V (or VI) (Fig. 8). Previously we found that the above intermediates, particularly V and VI were detected following initial denitration of I during incubation with the one electron transfer enzyme salicylate monooxygenase (Bhushan et al., 2004). In addition we found that following photodenitration of the cyclic nitramine RDX, H_2O reacts with the generated enamine bond ($-C=N-$) to

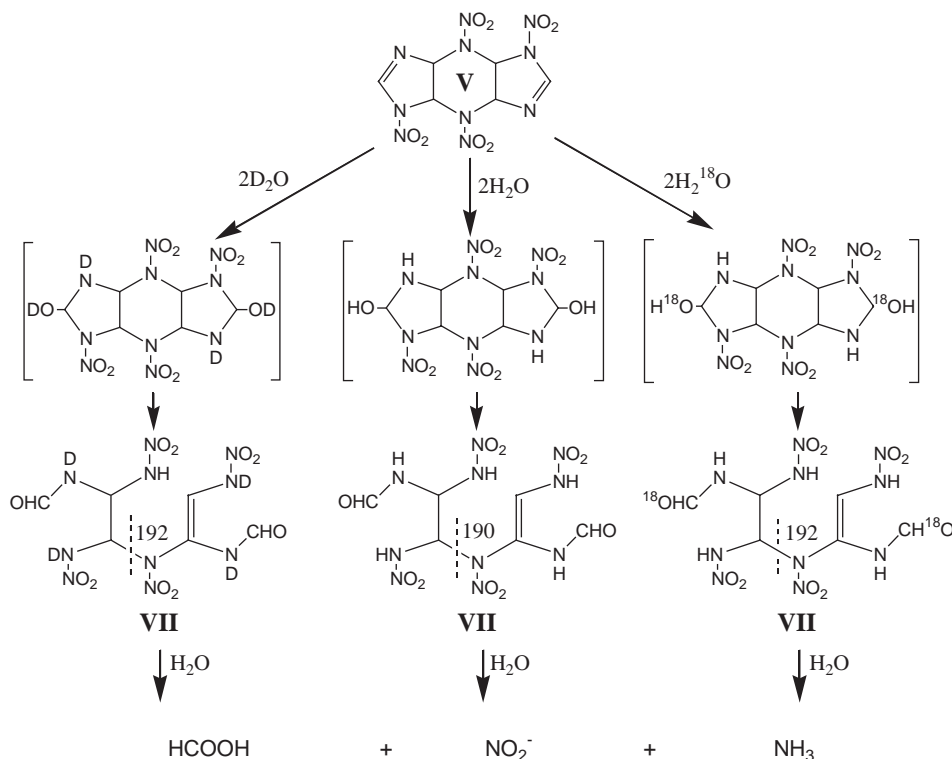


Fig. 8. Postulated secondary decomposition routes following initial denitration of CL-20.

produce an unstable carbinol that dissociates rapidly in water to HCHO, N_2O and 4-nitro-2,4-diazabutanal (Hawari et al., 2002). We thus suggested that a similar pathway might have been responsible for the formation of VII during the photolysis of the polycyclic nitramine CL-20 (Fig. 8).

3.3. Reaction stoichiometry and regioselectivity of denitration

Fig. 2 shows that the initial disappearance of the energetic chemical at 300 nm ($0.168 \mu\text{mol min}^{-1}$) was accompanied with the formation of NO_2^- ($0.237 \mu\text{mol min}^{-1}$), HCOOH ($0.219 \mu\text{mol min}^{-1}$) and NH_3 ($0.011 \mu\text{mol min}^{-1}$). The formation of NO_2^- and HCOOH was concurrent with the disappearance of CL-20, but NH_3 seemed to appear only after 5 min of photolysis. The delay in the detection of NH_3 as shown in Fig. 2 was best explained as due to the involvement of the inner aza N in its formation which first necessitated ring cleavage following denitration.

After 16 h, the reaction stoichiometry for the reacted CL-20 ($1.2 \mu\text{mol}$) was $6.11 \mu\text{mol}$ for NO_2^- and NO_3^- , $1.65 \mu\text{mol}$ for NH_3 and $6.34 \mu\text{mol}$ for HCOOH, suggesting that approximately five of six peripheral NO_2 and

5.3 of Cs in CL-20 were detected in the form of NO_2^- and HCOOH, respectively. The remaining N (mainly ring aza) were apparently involved in the production of N_2O ($0.267 \mu\text{mol}$), N_2 (trace) and unidentified products.

The rapid initial formation of nitrite and most importantly HCOOH was more likely attributed to an initial denitration step followed by a rapid ring cleavage possibly at the elongated C–C bond bridging the two cyclopentane rings (Fig. 7). We suggested that following homolysis of an N– NO_2 bond, the resulting N-centered free radical would undergo a rapid rearrangement to get rid of the strained rigid structure with the loss of another NO_2 radical to give the diene V (or its isomer VI) (Fig. 7). Patil and Brill (1991) reported that following N– NO_2 homolytic cleavage of CL-20 the molecule could undergo rapid ring opening to rid itself from the strained rigid structure. The diene V (Fig. 7) has two reactive allylic N– NO_2 bonds that might also undergo rapid homolytic cleavage with light, supporting the rapid release of 4NO_2^- as nitrite ion during the first 10 min of photolysis (Fig. 2). Several researchers studied the regioselectivity of cleaving the N– NO_2 bond during photolysis of CL-20 in the solid phase (Pace, 1991; Ryzhkov and McBride, 1996) and concluded that one of

the N–NO₂ bonds located at one of the two cyclopentane rings in CL-20 are preferentially cleaved. The formation of NO₂[−] during photolysis of CL-20 can be achieved by either concerted elimination of HONO or direct homolysis of an N–NO₂ bond. Such reactions have been frequently reported to occur during photolysis of RDX and HMX (Hawari et al., 2002; Peyton et al., 1999; Zukermann et al., 1987; Capellos et al., 1989). The energy associated with 254 and 300 nm is 472 and 400 kJ mol^{−1}, respectively, and therefore either wavelength should be sufficient to cleave the N–NO₂ bond(s) (BDE 204.9 kJ mol^{−1}) in CL-20 (Behrens and Bulusu, 1991).

The secondary reactions responsible for the formation of products such as HCOOH, NH₃ and N₂ are not clear yet. However, we presumed that the decomposition of the unstable diols (VII) (Fig. 8) of the diene V (or its isomer VI) would lead to their formation. Likewise the hydrolytic decomposition of either intermediate III or IV (Fig. 6) could lead to HCOOH, NH₃ and NO₂[−]. Interestingly, when we hydrolyzed CL-20 at pH 10 we found that the removal of the nitramine was accompanied by the formation of two molar equivalents of NO₂[−], NH₃ and HCOOH, respectively (Balakrishnan et al., 2003). More recently Bhushan et al. (2003c) showed that a denitrifying bacteria (*Pseudomonas* strain FA1) can also degrade the energetic chemical via initial enzymatic denitration to produce nitrite, nitrous oxide and HCOOH. The striking similarity in the product distribution of the present photolysis study and those of the alkaline hydrolysis (Balakrishnan et al., 2003) and biodegradation of CL-20 (Bhushan et al., 2003c, 2004) suggested that initial denitration whether chemical, photochemical or enzymatic is sufficient to decompose the energetic chemical to produce almost similar products.

4. Conclusions

In conclusion, photolysis of CL-20 at 300 nm led to rapid decomposition and the formation of nitrite and HCOOH in almost stoichiometric amounts after 16 h. Reaction at shorter wavelengths (λ₂₅₄ nm) was much more rapid, but reaction at longer wavelengths (λ₃₅₀ nm or sunlight) was much slower. Following the detection of several transient intermediates we suggested that initial photorearrangement and homolysis of one of the N–NO₂ bond(s) might have been responsible for the decomposition of CL-20. However, we were unable to quantify the relative importance of each route in the decomposition process. The discovery of several CL-20 intermediates and the knowledge gained on their reactions should provide insight into the mechanism of CL-20 photodecomposition and thus help predict the environmental fate and impact of the energetic chemical.

Acknowledgements

We would like to thank Mr. A. Corriveau for his technical assistance. We would also like to thank ATK Thiokol for providing CL-20 and Dr. K. Anderson from ATK Thiokol for helpful discussions. Funding was provided by the US DoD/DoE/EPA Strategic Environmental Research and Development Program (SERDP # CP 1256).

References

- Balakrishnan, V., Halasz, A., Hawari, J., 2003. Alkaline hydrolysis of the cyclic nitramine explosives RDX, HMX, and CL-20: new insights into degradation pathways obtained by the observation of novel intermediates. *Environ. Sci. Technol.* 37, 1838–1843.
- Behrens Jr., R., Bulusu, S., 1991. Thermal decomposition of energetic materials. 2. Deuterium isotopic effects and isotopic scrambling in condensed-phase decomposition of octahydro-1,3,5,7-tetranitro-1,3,5,7-tetrazocine. *J. Phys. Chem.* 95, 5838–5845.
- Bhushan, B., Paquet, L., Halasz, A., Spain, J.C., Hawari, J., 2003a. Mechanism of xanthine oxidase catalyzed biotransformation of HMX under anaerobic conditions. *Biochem. Biophys. Res. Com.* 306, 509–515.
- Bhushan, B., Trott, S., Spain, J.C., Halasz, A., Paquet, L., Hawari, J., 2003b. Biotransformation of hexahydro-1,3,5-trinitro-1,3,5-triazine (RDX) by a rabbit liver cytochrome P450: insight into the mechanism of RDX biodegradation by *Rhodococcus* sp. strain DN22. *Appl. Environ. Microbiol.* 69, 1347–1351.
- Bhushan, B., Paquet, L., Spain, J.C., Hawari, J., 2003c. Biotransformation of 2,4,6,8,10,12-hexanitro-2,4,6,8,10,12-hexaazaisowurtzitane (CL-20) by a denitrifying *Pseudomonas* sp. FA 1. *Appl. Environ. Microbiol.* 69 (9), 5216–5221.
- Bhushan, B., Halasz, A., Spain, J.C., Hawari, J., 2004. Initial reaction(s) in biotransformation of CL-20 catalyzed by salicylate 1-monooxygenase from *Pseudomonas* sp. *Appl. Environ. Microbiol.* 70 (7), 4040–4047.
- Bose, P., Glaze, W.H., Maddox, S., 1998. Degradation of RDX by various advanced oxidation processes: II. Organic by-products. *Water Res.* 32, 1005–1018.
- Bulusu, S., Axenrod, T., Milne, G.W.A., 1970. Electron-impact fragmentation of some secondary aliphatic nitramines. Migration of the nitro group in heterocyclic nitramines. *Org. Mass Spectrometry* 3, 13–21.
- Capellos, C., Papagiannakopoulos, P., Liang, Y.-L., 1989. The 248 nm photodecomposition of hexahydro-1,3,5-trinitro-1,3,5-triazine. *Chem. Lett.* 164, 533–538.
- Fournier, D., Halasz, A., Spain, J.C., Fiurasek, P., Hawari, J., 2002. Determination of key metabolites during biodegradation of hexahydro-1,3,5-trinitro-1,3,5-triazine (RDX) with *Rhodococcus* sp. strain DN22. *Appl. Environ. Microbiol.* 68, 166–172.
- Gong, P., Hawari, J., Thiboutot, S., Ampleman, G., Sunahara, G.I., 2001. Ecotoxicological effects of hexahydro-1,3,5-trinitro-1,3,5-triazine (RDX) on soil microbial activities. *Environ. Toxicol. Chem.* 20, 947–951.

- Groom, C.A., Halasz, A., Paquet, L., D'Cruz, P., Hawari, J., 2003. Cyclodextrin assisted CE of cyclic nitramine explosives and their degradation products: a comparison with HPLC. *J. Chromatogr. A* 999, 17–22.
- Haas, R., Schreiber, I., Low, E.V., Stork, G., 1990. Conception for the investigation of contaminated munitions plants. 2. Investigation of former RDX-plants and filling stations. *Fresenius J. Anal. Chem.* 338, 41–45.
- Hawari, J., Halasz, A., Beaudet, S., Paquet, L., Ampleman, G., Thiboutot, S., 2001. Biotransformation routes of octahydro-1,3,5,7-tetranitro-1,3,5,7-tetrazocine by municipal anaerobic sludge. *Environ. Sci. Technol.* 35, 70–75.
- Hawari, J., Halasz, A., Groom, C., Descamps, S., Paquet, L., Beaulieu, C., Corriveau, A., 2002. Photodegradation of RDX in aqueous solution: a mechanistic probe for biodegradation with *Rhodococcus* sp. *Environ. Sci. Technol.* 36, 5117–5123.
- Korsounskii, B.L., Nedel'ko, V.V., Chukanov, N.V., Larikova, T.S., Volk, F., 2000. Kinetics of thermal decomposition of hexanitrohexaazaisowurtzitane. *Russ. Chem. Bull.* 49, 812–818.
- Myler, C.A., Sisk, W., 1991. Bioremediation of explosives contaminated soils. In: Saylor, G.S., Fox, R., Blackburn, J.W. (Eds.), *Environmental Biotechnology for Waste Treatment*. Plenum Press, New York pp. 137–146.
- Nielsen, A.T., Christian, S.L., Moore, D.W., Gilardi, R.D., George, C.F., 1987. Synthesis of 3,5,12-triazawurtzitane (3,5,12-triazatetracyclo[5.3.1.1^{2,6}.0^{4,9}]dodecanes). *J. Org. Chem.* 52, 1656–1662.
- Nielsen, A.T., Nissan, R.A., Vanderah, D.J., Coon, C.L., Gilardi, R.D., George, C.F., Flippen-Anderson, J., 1990. Polyazapolycyclics by condensation of aldehydes with amines. 2. Formation of 2,4,6,10,12-hexabenzyl-2,4,6,8,10,12-hexaazatetracyclo [5.5.0.0^{5,9}.0^{3,11}] dodecanes from glyoxal and benzylamines. *J. Org. Chem.* 55, 1459–1466.
- Nielsen, A.T., Chafin, A.P., Christian, S.L., Moore, D.W., Nadler, M.P., Nissan, R.A., Vanderah, D.J., Gilardi, R.D., George, C.F., Flippen-Anderson, J.L., 1998. Synthesis of polyazapolycyclic caged polynitramines. *Tetrahedron* 54, 11793–11812.
- Oxley, J.C., Kooh, A.B., Szekeres, R., Zheng, W., 1994. Mechanisms of nitramine thermolysis. *J. Phys. Chem.* 98, 7004–7008.
- Pace, M.D., 1991. EPR spectra of photochemical NO₂ formation in monocyclic nitramines and hexanitrohexaazaisowurtzitane. *J. Phys. Chem.* 95, 5858–5864.
- Pace, M.D., Kalyanaraman, B., 1993. Spin trapping of nitrogen dioxide radical from photolytic decomposition of nitramines. *Free Rad. Biol. Med.* 15, 337–342.
- Patil, D.G., Brill, T.B., 1991. Thermal decomposition of energetic materials. 53. Kinetics and mechanism of thermolysis of hexanitrohexaazaisowurtzitane. *Combust Flame* 87, 145–151.
- Peyton, G.R., LeFaivre, M.H., Maloney, S.W., 1999. CERL Technical Report 99/93, (www.CECER.Army/TechReports).
- Robidoux, P.-Y., Svendsen, C., Caumartin, J., Hawari, J., Ampleman, G., Thiboutot, S., Weeks, J.M., Sunahara, G.I., 2000. Chronic toxicity of energetic compounds in soil determined using the earthworm (*Eisenia andrei*) reproduction test. *Environ. Toxicol. Chem.* 19, 1764–1773.
- Robidoux, P.-Y., Hawari, J., Thiboutot, S., Ampleman, G., Sunahara, G.I., 2001. Chronic toxicity of octahydro-1,3,5,7-tetranitro-1,3,5,7-tetrazocine (HMX) in soil using the earthworm (*Eisenia andrei*) reproduction test. *Environ. Pollut.* 11, 283–292.
- Ryzhkov, L.R., McBride, J.M., 1996. Low-temperature reactions in single crystals of two polymorphs of the polycyclic nitramine 15N-HNIW. *J. Phys. Chem.* 100, 163–169.
- Shu, Y., Dubikhim, V.V., Nazin, G.M., Manelis, G.B., 2002. Chain and monomolecular decomposition of hexogen in solutions. *Russ. Chem. Bull. Int. Ed.* 51, 1433–1440.
- Summers, W.R., 1990. Characterization of formaldehyde and formaldehyde-releasing preservatives by combined reversed phase cation-exchange high performance liquid chromatography with postcolumn derivatization using Nash's reagent. *Anal. Chem.* 62, 1397–1402.
- Sunahara, G.I., Robidoux, P.-Y., Gong, P., Lachance, B., Rocheleau, S., Dodard, S.G., Sarrazin, M., Hawari, J., Thiboutot, S., Ampleman, G., Renoux, A.Y., 2001. Laboratory and field approaches to characterize the ecotoxicology of polynitro explosives. In: Greenberg, B.M., Hull, R.N., Roberts Jr., M.H., Gensemer, R.W. (Eds.), *Environmental Toxicology and Risk Assessment, Science, Policy, and Standardization—Implications for Environmental Decisions*, STP 1403, ASTM, Vol. 10, West Conshohocken, PA, pp. 293–312.
- Talmage, S.S., Opresko, D.M., Maxwell, C.J., 1999. Nitroaromatic munition compounds: environmental effects and screening values. *Rev. Environ. Contam. Toxicol.* 16, 1–156.
- Wardle, R.B., Hinshaw, J.C., Braithwaite, P., Rose, M., Johnson, G., Jones, R., Poush, K., 1996. Synthesis of the caged nitramine HNIW (CL-20) 27.1–27.10, 27th International Annual Conference ICT, ADPA, Arlington, VI, USA. *Chem Abstr* 125, 172464v.
- Yinon, J., 1990. *Toxicity and Metabolism of Explosives*. CRC Press, Boca Raton, FL, pp. 145–170.
- Zhao, X., Yinon, J., 2002. Identification of nitrate ester explosives by liquid chromatography-electrospray ionisation and atmospheric pressure chemical ionization mass spectrometry. *J. Chromatogr. A* 977, 59–68.
- Zukermann, H., Greenblatt, G.D., Haas, Y., 1987. OH Formation in the infrared multiphoton decomposition of jet-cooled cyclic nitramines. *J. Phys. Chem.* 91, 5159–5161.

Physico-chemical measurements of CL-20 for environmental applications Comparison with RDX and HMX

Fanny Monteil-Rivera, Louise Paquet, Stéphane Deschamps,
Vimal K. Balakrishnan, Chantale Beaulieu, Jalal Hawari*

Biotechnology Research Institute, National Research Council of Canada, 6100 Royalmount Avenue, Montreal, Que., H4P 2R2 Canada

Abstract

CL-20 is a polycyclic energetic nitramine, which may soon replace the monocyclic nitramines RDX and HMX, because of its superior explosive performance. Therefore, to predict its environmental fate, analytical and physico-chemical data must be made available. An HPLC technique was thus developed to measure CL-20 in soil samples based on the US Environmental Protection Agency method 8330. We found that the soil water content and aging (21 days) had no effect on the recoveries (>92%) of CL-20, provided that the extracts were kept acidic (pH 3). The aqueous solubility of CL-20 was poor (3.6 mg l^{-1} at 25°C) and increased with temperature to reach 18.5 mg l^{-1} at 60°C . The octanol–water partition coefficient of CL-20 ($\log K_{\text{OW}} = 1.92$) was higher than that of RDX ($\log K_{\text{OW}} = 0.90$) and HMX ($\log K_{\text{OW}} = 0.16$), indicating its higher affinity to organic matter. Finally, CL-20 was found to decompose in non-acidified water upon contact with glass containers to give NO_2^- (2 equiv.), N_2O (2 equiv.), and HCOO^- (2 equiv.). The experimental findings suggest that CL-20 should be less persistent in the environment than RDX and HMX.

© 2003 Elsevier B.V. All rights reserved.

Keywords: Octanol–water partition coefficients; Solubility; Soil; CL-20; RDX; HMX; Nitramines; Explosives

1. Introduction

Past and present high-scale manufacturing, use, and disposal of explosives have resulted in severe environmental contamination [1]. Explosives such as the cyclic nitramines, RDX (hexahydro-1,3,5-trinitro-1,3,5-triazine) and HMX (octahydro-1,3,5,7-tetranitro-1,3,5,7-tetrazocine) (Fig. 1), are toxic to various terrestrial and aquatic receptors [2,3], and the provision of chemical and analytical data on their transport and transformation mechanisms in soil has been the subject of extensive study. Due to their high energy content, polynitropolyaza-caged compounds seem more attractive than the presently used RDX and HMX. A typical energetic chemical of this family is 2,4,6,8,10,12-hexanitro-2,4,6,8,10,12-hexaazatetracyclo[5.5.0.0^{5,9}.0^{3,11}]dodecane or hexanitrohexaazaisowurtzitane (HNIW), commonly known as CL-20 (Fig. 1), which was synthesized by Nielsen [4] and later adopted by Thiokol for pilot scale production [5]. Because of its superior ballistic, detonation and explosive performance, CL-20 may soon replace RDX and HMX.

However, to limit the consequences of its use, the environmental fate, transport and impact of CL-20 should first be thoroughly understood.

Prediction of the environmental fate (transport and transformation) of a new chemical such as CL-20 requires accurate analysis of the compound and its degradation products in both water and soil samples. The stability of the compound while being manipulated and analyzed should be well characterized. Moreover, physico-chemical parameters such as the octanol–water partition coefficient (K_{OW}), the aqueous solubilities and the soil sorption coefficients (K_d) must become known in order to foresee both bioaccumulation in terrestrial and aquatic biota and migration through subsurface soil that causes groundwater contamination [6]. CL-20 is a relatively new compound and most of its physico-chemical parameters have yet to be determined. The objectives of the present study were threefold: first, to provide the reader with an optimized analytical method to quantify CL-20 in aqueous and soil matrices; second, to make data available on its aqueous solubility at different temperatures (5 – 60°C) as well as its octanol/water partition and soil sorption coefficients; and finally, to provide insight into the stability of CL-20 in water.

* Corresponding author. Tel.: +1-514-4966267; fax: +1-514-4966265.
E-mail address: jalal.hawari@nrc-nrc.gc.ca (J. Hawari).

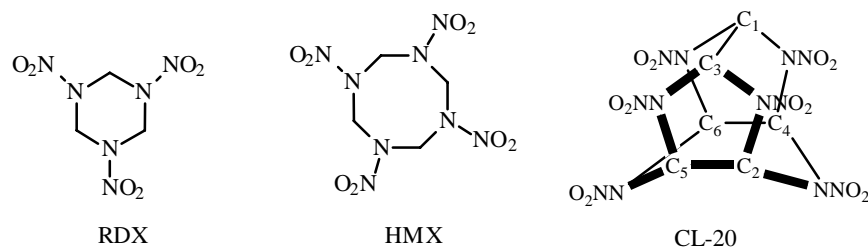


Fig. 1. Structural formulae of nitramine explosives (for clarity protons are omitted).

2. Experimental

2.1. Materials

CL-20 (purity 99.3%, determined by HPLC) was obtained from A.T.K. Thiokol Propulsion (Brigham City, UT, USA), as an ϵ -form ($\geq 95\%$ as determined by IR). Elemental composition was determined on a Carlo Erba EA 1108 analyzer and was found to be C (16.84%), N (37.52%), H (1.06%) (calculated values for $C_6H_6N_{12}O_{12}$: C (16.45%), N (38.36%), H (1.38%)). RDX and HMX (with a purity $>99\%$) were provided by Defense Research and Development Canada (DRDC), Valcartier, Que., Canada.

Hydroxypropyl- β -cyclodextrin (HP- β -CD) and heptakis-2,6-di-*O*-methyl- β -cyclodextrin (DM- β -CD) were obtained from Aldrich. Reagent grade inorganic chemicals ($CaCl_2$, $NaHSO_4$, H_2SO_4) were used as well as deionized Milli-Q^{UV} plus (Millipore) water. The solvents used were acetonitrile (CH_3CN , HPLC grade) and methanol (CH_3OH , HPLC grade) from J.T. Baker, acetone (CH_3COCH_3 , HPLC grade) from Fisher and octan-1-ol from Aldrich.

The soil (Sassafras Sandy Loam, referenced as SSL) was sampled in an uncontaminated open grassland on the property of US Army Aberdeen Proving Ground (Edgewood, MD, USA). It has a particle size distribution of 11% clay ($<2\ \mu m$), 18% silt ($2\text{--}53\ \mu m$), and 71% sand ($>53\ \mu m$), a pH of 5.1, a cation exchange capacity of 5.0 meq./100 g and a total organic carbon content of 0.33%.

2.2. HPLC analysis of CL-20

CL-20 stock standard solutions ($10\ g\ l^{-1}$) and intermediate standard solutions (100, 10, 1, $0.1\ mg\ l^{-1}$) were prepared in acetonitrile and stored at $4^\circ C$ in 16 ml glass tubes equipped with PTFE-coated screw caps and wrapped with aluminum. Calibration standards at a minimum of five concentrations ($0.05\text{--}25\ mg\ l^{-1}$) were prepared by diluting the intermediate standard solutions to yield solutions containing acidified water ($0.2\ g\ l^{-1}$ sodium bisulfate) and acetonitrile in a 50:50 (v/v) ratio.

Aqueous samples were diluted with acidified ($250\ \mu l$ concentrated $H_2SO_4\ l^{-1}$) CH_3CN to give a CH_3CN –water (50:50 (v/v)) mixture. If analysis could not be performed

on the day of preparation, samples were stored at $4^\circ C$ away from light.

For soil samples, US Environmental Protection Agency (EPA) SW-846 method 8330 [7] was used with slight modification. Dried soil (2.0 g) was weighed into 16 ml glass tubes with PTFE-lined caps. Samples and associated quality-control samples were spiked with surrogate (RDX) and CL-20 solutions in acetone to get concentrations of CL-20 in soil ranging from 1 to $10\ 000\ mg\ kg^{-1}$. Solvent was allowed to evaporate overnight in the fume-hood before subsequent extraction by CH_3CN (10 ml/each tube) using sonication at $20^\circ C$ for 18 h. After centrifugation at $1170 \times g$ for 30 min, a volume of supernatant (5 ml) was combined with 5 ml of a $CaCl_2$ – $NaHSO_4$ aqueous solution (5 and $0.2\ g\ l^{-1}$, respectively) instead of the usual solution of calcium chloride. The resulting sample was shaken, allowed to stand for 30 min and filtered through a $0.45\ \mu m$ Millipore PTFE filter, discarding the first 3 ml. The filtrate was analyzed by HPLC.

In order to assess the effect of water on the extraction efficiency, some samples were supplemented with water ($0.353\ ml$ (15% (w/w)) or $2\ ml$ (50% (w/w))) following acetone evaporation. One third of the samples were extracted immediately, a second third after being stored at $10^\circ C$ and in the dark for 7 days, and the final third after being stored for 21 days under similar conditions.

The CL-20 concentration was analysed by HPLC using a chromatographic system (ThermoFinnigan, San Jose, CA, USA) composed of a Model P4000 pump, a Model AS3000 injector, including temperature control for the column, and a Model UV6000LP Photodiode-Array Detector. The separation was completed on a Supelcosil LC-CN column ($25\ cm \times 4.6\ mm$, $5\ \mu m$; Supelco, Oakville, Canada) maintained at $35^\circ C$. The mobile phase (70% aqueous methanol) was run isocratically at $1\ ml/min$ for the entire run time of 14 min. The detector was set to scan from 200 to 350 nm. Chromatograms were extracted at a wavelength of 230 nm with quantification taken from peak areas of external standards. Peaks were identified by comparison with elution times for external standards and UV spectra. The injection volume was $50\ \mu l$.

The concentrations of RDX and HMX were determined using a reversed-phase HPLC connected to a photodiode array detection (DAD) system, as described previously for RDX [8].

2.3. Determination of aqueous solubility as a function of temperature

The solubilities (S) of CL-20, RDX and HMX were determined in water at temperatures (T) of 5, 10, 15, 20, 25, 30, 40, 50 and 60 °C according to the procedure described by Lynch et al. [9]. An excess amount of explosive (0.015 g) was added to 100 ml of deionized water (pH 5.5) in a glass bottle. The samples were stirred at 200 rpm and at the required temperature in a thermostated bath (Innova 3000 (New Brunswick Sci.)), away from light. After a 48 h stirring period, the suspension was filtered and diluted 1:1 in acidified acetonitrile (pH 3). The resulting solution was analyzed by HPLC. All experiments were performed in triplicate.

The solubility of CL-20 was also measured in the presence of two cyclodextrins (CDs): hydroxypropyl- β -cyclodextrin (HP- β -CD) and heptakis-2,6-di-*O*-methyl- β -cyclodextrin (DM- β -CD). An excess of CL-20 (300 mg l⁻¹) was combined with increasing concentrations of cyclodextrin (0–5% (w/v)) and solubility was measured after 18 h of equilibration at room temperature (21 ± 2 °C).

2.4. Determination of *n*-octanol/water partition coefficient

Partition coefficients were measured at 21 ± 2 °C as described in the OECD Guideline 107 [10]. A preliminary K_{OW} measurement was done with RDX to check the need to saturate octanol with water and water with octanol before doing the actual measurement. Similar results were obtained with saturated (log K_{OW} = 0.90) and non-saturated (log K_{OW} = 0.90) solvents. Thus, the measurements were performed with non-saturated solvents. Various volumes (3 or 4 ml) of an aqueous solution of explosive (CL-20: 3.48 mg l⁻¹; HMX: 4.01 mg l⁻¹; RDX: 11.20 mg l⁻¹) were added to octan-1-ol (2 or 3 ml) in a 16 ml PTFE-lined capped glass tube. The mixtures were equilibrated for four 10 min shaking periods spaced 10 min apart. The tubes were centrifuged for 10 min at 1170 × *g*. The concentration of the substrate in water was determined by HPLC as described above. The octanol fraction was diluted (1:3) with a solution containing 70% methanol in water and the concentration of CL-20 was determined by HPLC. Experiments were run in triplicate.

2.5. Determination of RDX, HMX and CL-20 K_d values with SSL soil

Batch sorption experiments were conducted at ambient temperature (21 ± 2 °C) for 72 h. A solution (15 ml) of RDX, HMX or CL-20 (0.5–40 mg l⁻¹ for RDX; 0.5–4 mg l⁻¹ for HMX and CL-20) was agitated with 2 g dried SSL soil in a 16 ml borosilicate centrifuge tubes fitted with PTFE-coated screw caps, away from light and at 430 rpm (Model 75 Wrist Action shaker; Burrell, Pittsburgh, PA, USA). After centrifugation at 1170 × *g* for 30 min, the supernatant was filtered through a Millex-HV 0.45 µm filter (Millipore, Bedford, MA, USA), and analyzed by HPLC after discarding the first

3 ml. The remaining pellet was extracted with acetonitrile to measure the amount of sorbed explosive. The respective isotherms (i.e. sorbed amount in µg g⁻¹ as a function of the equilibrium concentration in mg l⁻¹) were plotted and the K_d values were obtained from the slopes of linear isotherms.

2.6. Stability of CL-20 in solution

The stability of CL-20 was determined in aqueous and aqueous acetonitrile solutions as a function of temperature. In aqueous acetonitrile media, the solutions (2.5 mg l⁻¹) were allowed to sit at either 10 °C or ambient temperature (21 ± 2 °C) for 7 days and samples were periodically analyzed for CL-20 by HPLC. In water, the solutions (3.5 mg l⁻¹) were agitated in PTFE-capped glass headspace vials at 150 rpm at either 30 °C or ambient temperatures (21 ± 2 °C). Vials were sampled periodically over 14 days to measure the suspected CL-20 degradation product N₂O in the headspace and other products such as nitrite (NO₂⁻), nitrate (NO₃⁻) and formate (HCOO⁻) in the liquid. N₂O analyses were carried out as described by Sheremata and Hawari [11]. Analyses of nitrite, nitrate and formate were performed by ion chromatography (IC) equipped with a conductivity detector. The Waters IC system consisted of a Model 600 Pump, a Model 717 Autosampler Plus, and a Model 430 conductivity detector. Separation was performed on a Dionex IonPac AS15 column (250 mm × 2 mm). The mobile phase was 30 mM KOH (aq.) at a flow rate of 0.4 ml min⁻¹ at 40 °C. The detection of anions was enhanced by reducing the background with a Model DS-Plus autosuppressor from Altech. Detection limits were 150 ppb.

In another experiment, the stability of CL-20 in water was measured at ambient temperature (21 ± 2 °C) using two types of frequently encountered container materials (glass or polypropylene), under static or agitated conditions. The aqueous CL-20 solution was added to either 16 ml borosilicate centrifuge tubes fitted with PTFE-coated screw caps, or 15 ml polypropylene centrifuge tubes. All tubes were wrapped in aluminum foil. Half the tubes were then agitated on a Wrist Action shaker at 430 rpm (Burrell), while the other half were allowed to remain static. Tubes were sampled periodically over 28 days for analysis by HPLC. These experiments were conducted in triplicate.

3. Results and discussion

3.1. Quantification of CL-20 in aqueous and soil samples

Because explosives are often applied as mixtures, it is important to establish conditions that permit a good separation amongst CL-20 and other energetic chemicals. Analysis by HPLC of a mixture containing RDX, HMX and CL-20 using the previously mentioned conditions gave a well resolved chromatogram with retention times of 4.8, 5.9 and 8.3 min, respectively (Fig. 2). Peak areas were used

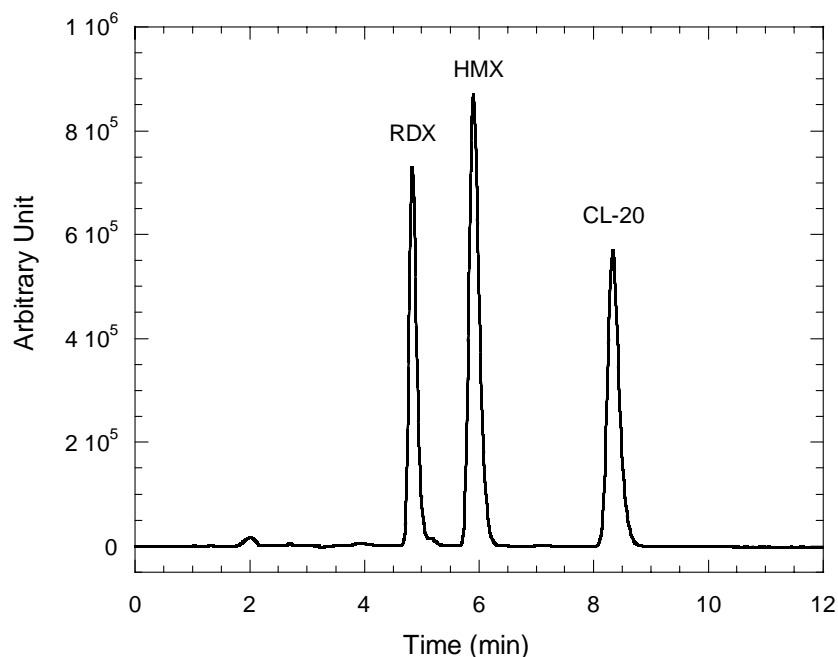


Fig. 2. A typical HPLC chromatogram showing separation of CL-20 from RDX and HMX. Column: LC-CN; mobile phase: water–methanol (30:70); flow rate: 1 ml min⁻¹; detection: DAD (λ = 230 nm).

to quantify chromatographic signals and excellent linearity was obtained over the entire range of CL-20 concentrations used (0.05–25 mg l⁻¹) ($y = 6.4864 \times 10^5 x$; $R^2 = 0.99996$). The instrumental detection limit (IDL) and the instrumental quantification limit (IQL) were found to be 3 and 9 $\mu\text{g l}^{-1}$, respectively (R.S.D. = 3.8%, $n = 10$).

Larson et al. [12] recently published an HPLC method for analyses of CL-20 in water and soil samples but the susceptibility of CL-20 to decomposition has not been reported. For instance, we found that CL-20 degrades significantly in aqueous acetonitrile media (Fig. 3), and that degradation is more rapid at 21 °C (65% after 7 days) than at 10 °C (8% after 7 days). We also found that decomposi-

tion can be significantly reduced by acidifying the medium to pH 3 (Fig. 3). Therefore, in order to avoid a possible degradation of CL-20, all aqueous samples should be analyzed after a 50:50 (v/v) dilution with acidified CH₃CN. CL-20 is a weak acid that, upon losing one of its labile protons, can undergo successive degradation steps. It hydrolyses in water under rather mild alkaline conditions. Since acetonitrile is known to be a more powerful proton acceptor than water [13], it may favor the initial deprotonation of CL-20 and hence cause decomposition even in neutral media. Acidification of the media prevents the removal of the labile proton from CL-20, thereby stabilizing the chemical.

In the case of soil samples, extraction was performed as described in US EPA SW-846 method 8330 [7]. As a consequence of the instability of CL-20 observed in aqueous acetonitrile media, the extract was added to a solution of CaCl₂ containing 0.2 g l⁻¹ of sodium bisulfate to bring the solution pH to 3. The method detection limit (MDL) and the method quantification limit (MQL) were determined and found to be 0.06 and 0.20 mg kg⁻¹, respectively ($n = 10$; R.S.D. = 10.7%). CL-20 recoveries were found to stand within the interval 83% < R < 113% ($n = 20$, S.D. = 4.9%, average = 97.9%).

Single laboratory precision method and recovery data are gathered in Table 1 for soil samples spiked with different concentrations of CL-20. Precision was good for replicate analyses and excellent recoveries (96–106%) were obtained over a wide range of concentrations. The addition of water (0, 0.353, or 2 ml of water, corresponding to soils containing 0, 15, or 50% moisture) did not affect the extracted amounts

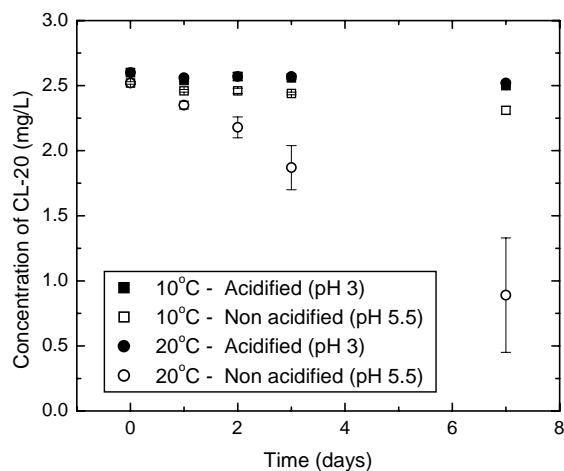


Fig. 3. Effect of acidification and temperature on the stability of CL-20 in water/acetonitrile (50/50) media.

Table 1
Recovery data for soil samples spiked with different concentrations of CL-20

Nominal concentration (mg kg ⁻¹)	Water (%)	Measured concentration (mg kg ⁻¹)	S.D. (<i>n</i> = 3)	R.S.D. (%)	Mean recovery (%)
1.00	0	1.040	0.156	14.990	104.0
	15	1.015	0.021	2.041	101.5
	50	1.000	0.028	2.771	100.0
5.00	0	5.107	0.535	10.477	102.1
	15	5.166	0.062	1.202	103.3
	50	5.300	0.080	1.508	106.0
10.00	0	10.373	0.211	2.037	103.7
	15	10.156	0.188	1.855	101.6
	50	10.400	0.126	1.212	104.0
100.00	0	99.247	1.385	1.396	99.2
	15	99.354	1.078	1.085	104.0
	50	101.656	0.321	0.315	101.7
1000.00	0	978.733	6.481	0.662	97.9
	15	994.578	11.404	1.147	99.5
	50	1001.720	15.574	1.555	100.2
10000.00	0	10261.667	137.114	1.336	102.6
	15	9669.702	394.638	4.081	96.7
	50	9978.400	334.422	3.351	99.8

of CL-20. No degradation of CL-20 occurred when adding 2 ml of water to the 10 ml of acetonitrile and sonicating the mixture for 18 h at 20 °C, thus demonstrating the applicability of the method to both dry and wet samples. Aging (21 days) of spiked samples with 0 or 15% water showed that CL-20 extractability was not affected and that irreversible binding did not occur within this period of time.

3.2. Solubility of CL-20 in water

The aqueous solubility (*S*) of RDX and HMX has been shown to vary significantly with temperature [9,14]. Since the temperatures to which explosives are exposed in the environment may vary from below 0 to greater than 50 °C, the solubility of CL-20 was measured in water over a temperature range of 5–60 °C. For comparison, aqueous solubilities of RDX and HMX were also measured under similar conditions. The solubility data collected are gathered in Table 2. As with RDX and HMX, the aqueous solubility of CL-20 increases with the temperature, but to a lesser extent. The solubility of CL-20 is much lower than that of RDX, whereas the comparison with HMX is more complex: CL-20 is more soluble than HMX at lower temperatures but the trend is reversed at temperatures above 20 °C.

For ideal solutions, the amount of a compound, *B*, present in solution at saturation can be estimated using Eq. (1).

$$\ln x_B = - \left(\frac{\Delta H_{\text{fus}}}{R} \right) \left(\frac{1}{T} - \frac{1}{T^*} \right), \quad (1)$$

where x_B is the mole fraction of solute *B*, ΔH_{fus} the enthalpy of fusion of solute *B*, *R* the ideal gas constant, *T* the temperature at which equilibrium is considered and T^* the melting temperature of solute *B*. While aqueous solutions

of explosives are not ideal, the relationship between *S* and *T* follows Eq. (2) as described by Lynch et al. [9]:

$$\ln S = A - \frac{B}{T}, \quad (2)$$

where *S* is the solubility and *A* and *B* are arbitrary constants.

Data were thus plotted as $\ln S$ versus $1/T$ (with *T* in K)) and linear regressions were performed for the three explosives as shown in Fig. 4. The lower slope observed for CL-20 suggests that this compound has a smaller enthalpy of melting than either RDX or HMX. The linearization allowed comparison of the data from the present study to those reported previously for temperatures other than those investigated here. Solubilities for RDX are in good agreement with data reported by Townsend and Myers [14], but are slightly higher than the solubilities recently measured by Lynch et al.

Table 2
Aqueous solubilities (*S*) of RDX, HMX and CL-20 as a function of temperature and log *K*_{OW} values measured at ambient temperature

<i>T</i> (°C)	RDX	HMX	CL-20
<i>S</i> (mg l ⁻¹) (<i>n</i> = 3)			
5	16.01 (±0.16)	1.32 (±0.16)	1.97 (±0.08)
10	22.19 (±0.12)	1.67 (±0.14)	2.12 (±0.04)
15	29.67 (±0.57)	2.27 (±0.09)	2.48 (±0.02)
20	42.58 (±1.32)	3.34 (±0.12)	3.16 (±0.04)
25	56.35 (±1.79)	4.46 (±0.03)	3.65 (±0.04)
30	n.d.	n.d.	4.89 (±0.03)
40	122.94 (±0.94)	11.83 (±0.09)	7.39 (±0.06)
50	n.d.	n.d.	11.62 (±0.01)
60	342.71 (±3.25)	39.69 (±2.24)	18.48 (±0.80)
Log <i>K</i> _{OW} (<i>n</i> = 9)			
21	0.90 (±0.03)	0.165 (±0.006)	1.92 (±0.02)

Values within parentheses are S.D.; n.d.: non determined.

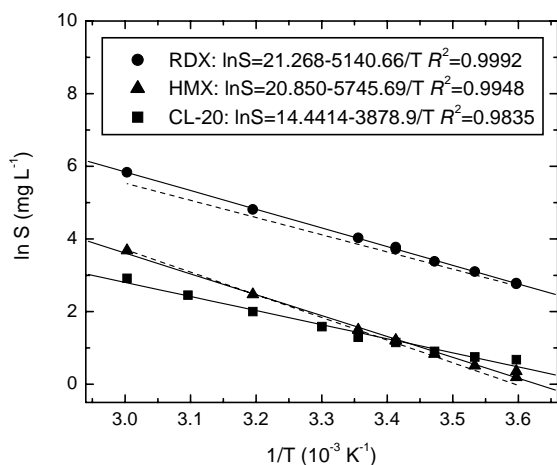


Fig. 4. Solubilities of RDX, HMX and CL-20 in water as a function of temperature (solid lines: linear regressions from the present study; dashed lines: linear regressions from [9] for RDX and HMX).

[9] represented in dashed lines in Fig. 4. As for HMX, solubility data are consistent with those reported by Lynch et al. [9] and significantly higher than those reported by Spangord et al. [15]. Overall, the values measured for RDX and HMX agree reasonably well with literature data.

While thinking of a soil washing technology that could be used to remediate a CL-20-contaminated soil, we looked for an environmentally friendly chemical able to increase the solubility of CL-20 in water. Cyclodextrins fit these requirements as they are nontoxic [16] and they were shown to be capable of enhancing the solubility of a number of common organic compounds [17]. The effect of two cyclodextrins (HP- β -CD and DM- β -CD) on the solubility of CL-20 in water was thus studied (Fig. 5). While the presence of both cyclodextrins significantly increased the aqueous solubility of CL-20, the most remarkable effect was induced by DM- β -CD with a 25-fold increase observed when the

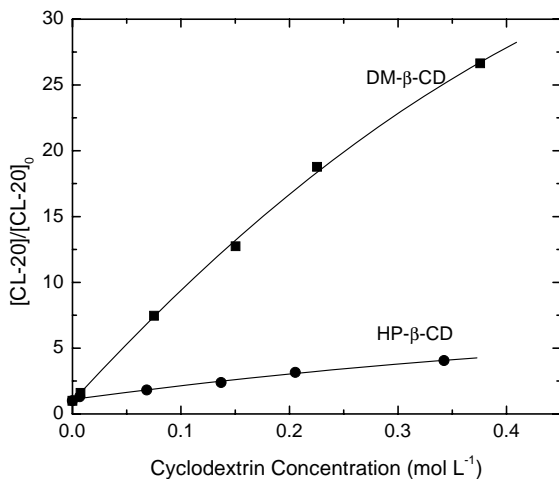


Fig. 5. Solubility of CL-20 in water in presence of β -cyclodextrins, relative to the solubility of CL-20 in water ($[\text{CL-20}]_0$).

cyclodextrin was present at a concentration of 0.38 mol l^{-1} . In addition to the large solubility enhancement however, we found that DM- β -CD favors the decomposition of the energetic compound as determined by the disappearance of CL-20 in the filtered supernatant (80% loss after 14 days) and the detection of nitrite ions. Therefore, aqueous solutions of cyclodextrins would be more efficient than water to extract CL-20 from a contaminated soil.

3.3. Octan-1-ol/water partition coefficient (K_{OW}) of nitramines

The determination of the octan-1-ol–water partition coefficient (K_{OW}) is of environmental importance because this parameter can be used to predict soil adsorption, migration through subsurface soil and bioaccumulation in terrestrial and aquatic biota. Several log K_{OW} values have been reported for RDX, in relatively good agreement with each other (0.81, 0.86 and 0.87 ([18] and references cited therein)), whereas more disparate values were measured for HMX (0.06 and 0.26 ([18] and references cited therein)). Values of log K_{OW} were measured for RDX, HMX and CL-20 using different combinations of water/octan-1-ol mixtures and different amounts of nitramine. Three different sets of conditions were used for each explosive and each set was run in triplicate. The average of the nine measurements is reported in Table 2. Regardless of the octanol/water ratios used, K_{OW} values remained basically constant and a value of 82.6 ± 0.9 ($\log K_{OW} = 1.92 \pm 0.02$) was obtained for CL-20, significantly higher than the partition coefficients for RDX (8.0 ± 0.6) and HMX (1.46 ± 0.02). This finding suggests that CL-20 will sorb onto soils more strongly than RDX and HMX and that this hydrophobic interaction will be particularly important in soils containing high amounts of organic matter. K_d values obtained for RDX, HMX and CL-20 onto SSL soil (0.3, 0.7, and 2.41 kg^{-1} for RDX, HMX and CL-20, respectively) confirmed the higher affinity of the latter for soils.

3.4. Stability of CL-20 in water

From the stability results presented in Fig. 6, it appears that agitation in borosilicate glass vials causes greater loss of CL-20 (38% after 17 days) than in agitated polypropylene vials (15% after 17 days). In addition, when the vials remained static at ambient temperature, decomposition decreased (15 and 8% in glass and polypropylene, respectively). We detected nitrite (NO_2^-) and formate (HCOO^-) ions in the agitated vials, which we previously detected during the alkaline hydrolysis (pH 10) [19] of CL-20. No CL-20 was recovered from the tubes walls after washing them with CH_3CN , suggesting that no CL-20 sorption took place.

The effect of temperature on CL-20 stability was investigated by agitating sealed head-space glass vials at 150 rpm and either 30°C or ambient temperature ($21 \pm 2^\circ\text{C}$). Interestingly, 90% of the original CL-20 degraded at 30°C after

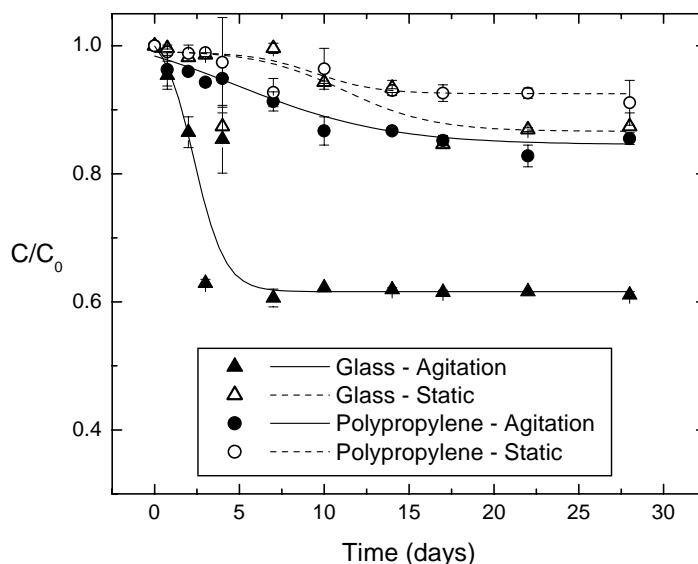


Fig. 6. Stability of aqueous solutions of CL-20 at ambient temperature ($21 \pm 2^\circ\text{C}$) in glass and polypropylene containers (static = 0 rpm; agitation: 430 rpm).

2 weeks, as compared to 33% at ambient temperature (Fig. 7). Once again, the losses were accompanied by the formation of end products such as nitrite (NO_2^- , ca. 2 equiv.), nitrous oxide (N_2O , ca. 2 equiv.), and formate (HCOO^- , ca. 2 equiv.).

The present experimental findings show that CL-20 is unstable and the extent of decomposition depends on the rate of agitation and temperature. The release of 2 mol of NO_2^- ions per mole of reacted CL-20 indicates a partial denitration of the molecule. The detection of 2 mol of HCOO^- ions and 2 mol of N_2O per reacted CL-20 indicates the occurrence of ring cleavage, with a probable initial cleavage at the longer and weaker $\text{C}_1\text{--C}_3$ bond between the two cyclopentane rings of CL-20 (1.590 Å compared to 1.575 Å for

$\text{C}_6\text{--C}_4$ and $\text{C}_2\text{--C}_5$ bonds (Fig. 1)) [20]. These observations are very similar to what was observed in hydrolysis at pH 10 [19], indicating that an initial denitration step is responsible for the lack of stability of CL-20 and its decomposition.

In contrast, neither RDX nor HMX was found to degrade during agitation under the same conditions. However, the polycyclic CL-20 is a more highly strained and thus less stable molecule than are the monocyclic nitramines. Given that nitramine explosives such as RDX are sensitive to friction [21], we suggest that friction obtained during agitation might generate enough energy to cause decomposition of the most sensitive CL-20. With a wetting contact angle of 100.6° in water [22], polypropylene surfaces exhibit a much lower flow friction than borosilicate surfaces (contact angle

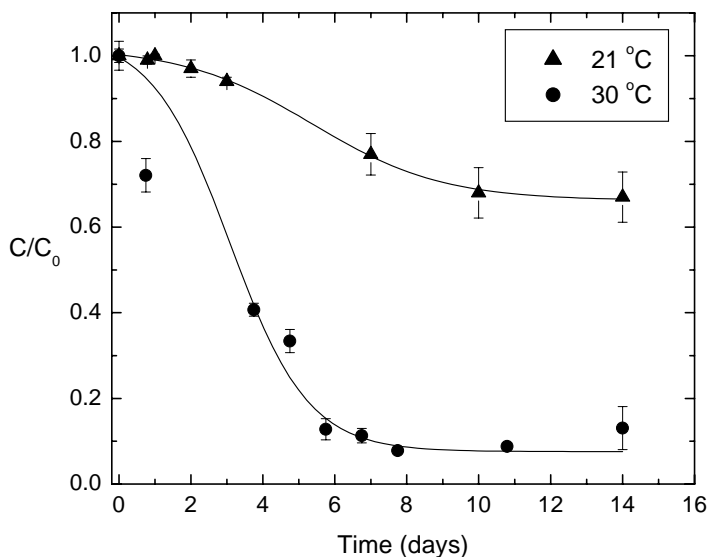


Fig. 7. Effect of temperature on stability of aqueous solutions of CL-20 in glass vials agitated at 150 rpm.

in water: 38.5° [23]). Therefore, the higher stability of CL-20 in polypropylene as compared to borosilicate may result from the lower flow friction, and as a consequence, lower shear force induced in the former. Similarly, heating a solution to 30 °C provides a thermal energy that could enhance the degradation process, explaining why CL-20 degrades faster at 30 °C than it does at ambient temperatures.

4. Conclusion

The present study demonstrates that CL-20 can be extracted from soil samples with high recoveries, regardless of the water content or short-term aging of soil. The poor solubility of CL-20 in water (2.0 mg l⁻¹ at 5 °C and 18.5 mg l⁻¹ at 60 °C) and its higher log *K*_{OW} value compared to those of RDX and HMX (1.92, 0.90, and 0.16, respectively) suggest that CL-20 will migrate less in soil than RDX and HMX. Also, aqueous solutions of CL-20 exhibit significant abiotic losses when agitated in glass containers or when exposed to temperatures above 30 °C. The present experimental findings can be used to provide understanding of the environmental fate of CL-20 that awaits wide scale production and field applications.

Acknowledgements

The authors thank the Department of National Defence, Canada, for providing RDX and HMX. We would also like to thank Thiokol, USA for providing CL-20. V.K.B. thanks the Natural Sciences and Engineering Research Council of Canada and the National Research Council of Canada for a Fellowship. The authors would also like to thank the US DoD Strategic Environmental Research and Development Program (SERDP: CU 1213 and CP 1256) for financial funding of the present work on RDX, HMX and CL-20.

References

- [1] J. Hawari, A. Halasz, in: G. Bitton (Ed.), *The Encyclopedia of Environmental Microbiology*, Wiley, Amsterdam, 2002, p. 1979.
- [2] J. Yinon, *Toxicity and Metabolism of Explosives*, CRC Press, Boca Raton, FL, 1990, pp. 145–170.
- [3] S.S. Talmage, D.M. Opresko, C.J. Maxwell, C.J.E. Welsh, F.M. Cretella, P.H. Reno, F.B. Daniel, *Environ. Contam. Toxicol.* 161 (1999) 1.
- [4] A.T. Nielsen, US Department of Navy, US Patent Office Application Case No. 70631, 24 June 1987.
- [5] R.B. Wardle, J.C. Hinshaw, P. Braithwaite, M. Rose, G. Johnston, R. Jones, K. Poush, in: *Proceedings of the 27th International Annual Conference on ICT, ADPA, Arlington, VA, 25–28 June 1996*, pp. 27–31.
- [6] C.T. Chiou, D.W. Schmedding, *Environ. Sci. Technol.* 16 (1982) 4.
- [7] US Environmental Protection Agency Method 8330 SW-846 update III Part 4: 1 (B), Nitroaromatics and nitramines by high performance liquid chromatography (HPLC), Office of Solid Waste, Washington, DC, 1997.
- [8] D. Fournier, A. Halasz, J. Spain, P. Fiurasek, J. Hawari, *Appl. Environ. Microbiol.* 68 (2002) 166.
- [9] J.C. Lynch, K.F. Myers, J.M. Brannon, J.J. Delfino, *J. Chem. Eng. Data* 46 (2001) 1549.
- [10] OECD Guideline for Testing of Chemicals 107: Partition Coefficient (*n*-octanol/water) (flask-shaking method), adopted on 12 May 1981.
- [11] T.W. Sheremata, J. Hawari, *Environ. Sci. Technol.* 34 (2000) 3384.
- [12] S.L. Larson, D.R. Felt, J.L. Davis, L. Escalon, *J. Chromatogr. Sci.* 40 (2002) 201.
- [13] E. Buncl, J.M. Dust, *Carbanion Chemistry—Structures and Mechanisms*, Oxford University Press, New York, 2003, p. 8.
- [14] D.M. Townsend, T.E. Myers, Technical Report IRRP-96-1, US Army Engineer Waterways Experiment Station, Vicksburg, MS, 1996.
- [15] R.J. Spanggord, W.R. Mabey, T.W. Chou, D.L. Haynes, P.L. Alferness, D.S. Tse, T. Mill, *Environmental Fate Studies of HMX Screening Studies*, Final Report, Phase I, LSU-4412, SRI International, Menlo Park, CA, 1982.
- [16] J. Szejtli, in: D. Duchêne (Ed.), *Cyclodextrins and Their Industrial Uses*, Edition de Santé, Paris, France, 1987 (Chapter 5).
- [17] X. Wang, M.L. Brusseau, *Environ. Sci. Technol.* 27 (1993) 2821.
- [18] D.H. Rosenblatt, E.P. Burrows, W.R. Mitchell, D.L. Parmer, in: O. Hutzinger (Ed.), *The Handbook of Environmental Chemistry*, Springer, Berlin, Heidelberg, 1991, p. 195.
- [19] V.K. Balakrishnan, A. Halasz, J. Hawari, *Environ. Sci. Technol.* 37 (2003) 1838.
- [20] X. Zhao, N. Shi, *Chinese Sci. Bull.* 41 (1996) 574.
- [21] M. Williams, M. Wingrave, *Propell. Explos. Pyrotech.* 27 (2002) 241.
- [22] B. Glasmacher-Seiler, S. Voigt, H. Reul, in: W. Lemm (Ed.), *The Reference Materials of the European Communities*, Kluwer, Dordrecht, 1992, p. 85.
- [23] L. Crenshaw, D.W. DeVoe, J.R. Fleming, J.F. Imbalzano, D. Kemkes, *Pharm. Eng.* 21 (2001) 34.

ACUTE AND CHRONIC TOXICITY OF THE NEW EXPLOSIVE CL-20 TO THE EARTHWORM (*EISENIA ANDREI*) EXPOSED TO AMENDED NATURAL SOILS

PIERRE YVES ROBIDOUX,* GEOFFREY I. SUNAHARA, KATHLEEN SAVARD, YANN BERTHELOT, SABINE DODARD, MAJORIE MARTEL, PING GONG, and JALAL HAWARI

Applied Ecotoxicology Group, Biotechnology Research Institute, National Research Council of Canada, 6100 Royalmount Avenue, Montreal, Quebec H4P 2R2, Canada

(Received 5 June 2003; Accepted 8 September 2003)

Abstract—Monocyclic nitramine explosives such as 1,3,5-trinitro-1,3,5-triazacyclohexane (RDX) and octahydro-1,3,5,7-tetranitro-1,3,5,7-tetrazocine (HMX) are toxic to a number of ecological receptors, including earthworms. The polycyclic nitramine CL-20 (2,4,6,8,10,12-hexanitro-2,4,6,8,10,12-hexaazaisowurtzitane) is a powerful explosive that may replace RDX and HMX, but its toxicity is not known. In the present study, the lethal and sublethal toxicities of CL-20 to the earthworm (*Eisenia andrei*) are evaluated. Two natural soils, a natural sandy forest soil (designated RacFor2002) taken in the Montreal area (QC, Canada; 20% organic carbon, pH 7.2) and a Sassafras sandy loam soil (SSL) taken on the property of U.S. Army Aberdeen Proving Ground (Edgewood, MD, USA; 0.33% organic carbon, pH 5.1), were used. Results showed that CL-20 was not lethal at concentrations of 125 mg/kg or less in the RacFor2002 soil but was lethal at concentrations of 90.7 mg/kg or greater in the SSL soil. Effects on the reproduction parameters such as a decrease in the number of juveniles after 56 d of exposure were observed at the initial CL-20 concentration of 1.6 mg/kg or greater in the RacFor2002 soil, compared to 0.2 mg/kg or greater in the SSL soil. Moreover, low concentrations of CL-20 in SSL soil (~0.1 mg/kg; nominal concentration) were found to reduce the fertility of earthworms. Taken together, the present results show that CL-20 is a reproductive toxicant to the earthworm, with lethal effects at higher concentrations. Its toxicity can be decreased in soils favoring CL-20 adsorption (high organic carbon content).

Keywords—Hexanitrohexaazaisowurtzitane Soil Toxicity Reproduction Earthworm

INTRODUCTION

Toxicities of energetic materials such as TNT, 1,3,5-trinitro-1,3,5-triazacyclohexane (RDX), and octahydro-1,3,5,7-tetranitro-1,3,5,7-tetrazocine (HMX) have been assessed in many different laboratory and field studies [1–10]. Presently, TNT, RDX, and HMX are the most prevalent sources of contamination at thousands of military sites around the world [10]. Energetic materials such as TNT, RDX, and HMX are toxic at relatively low concentrations to a number of organisms, including the earthworm *Eisenia andrei* [1–5].

The recently synthesized energetic compound CL-20 (2,4,6,8,10,12-hexanitro-2,4,6,8,10,12-hexaazaisowurtzitane) is a powerful polycyclic nitramine explosive that may replace RDX and HMX [11] (Fig. 1). Propellants and explosive formulations using CL-20 are expected to have better performance in terms of specific impulse, burn rate, ballistics, and detonation velocity compared to those of RDX and HMX [11]. However, considering that the monocyclic nitramines RDX and HMX reduce the fertility of earthworms [5], one may hypothesize that the polycyclic nitramine CL-20 is also toxic.

Few studies regarding the environmental impacts of CL-20 are available. Thus, before large-scale production of CL-20 and its use by the military, more information concerning the environmental fate and effects of this energetic chemical is needed. The toxicological data presented here may help future managers of sites contaminated with CL-20 to make more informed decisions before the release of this new explosive in the environment. In addition, the toxicological data derived

using a standard toxicity test method and quality-control procedures may be used to determine preliminary soil-quality criteria.

In the present study, the toxicological effects of CL-20 on survival and life-cycle parameters such as growth (wet wt change) and productivity of cocoons and juveniles of *E. andrei* were assessed in a freshly amended, natural sandy forest soil (designated RacFor2002) and a Sassafras sandy loam (SSL) soil. The two soils, SSL and RacFor2002, were selected with different organic content and pH so that the effect of bio-availability (sorption) could be evaluated.

MATERIALS AND METHODS

Chemicals and reagents

The ϵ -CL-20 (chemical abstract service registry number 135285-90-4; purity, >99%) was obtained from ATK Thiokol Propulsion (Brigham, UT, USA). The pesticide carbendazim (Chemical Abstract Service registry number 10605-21-7) and potassium chloride (KCl; Chemical Abstract Service registry number 7447-40-7) were used as reference toxicants and were obtained from Aldrich (Milwaukee, WI, USA) and EM Science (Darmstadt, Germany), respectively. Deionized water (American Society for Testing and Materials, type II) was obtained using a Millipore® Super-Q water purification system (Millipore, Bedford, MA, USA) or a Zenopure® Mega-90 laboratory water system (Zenon Environmental, Système d'eau O.B.L.X., St-Bruno, QC, Canada). Glassware was washed with phosphate-free detergent followed by rinses with acetone, nitric acid (10%, vol/vol), and deionized water.

* To whom correspondence may be addressed
(pierre-yves.robidou@nrc-nrc.gc.ca).
National Research Council Canada Publication 45922.

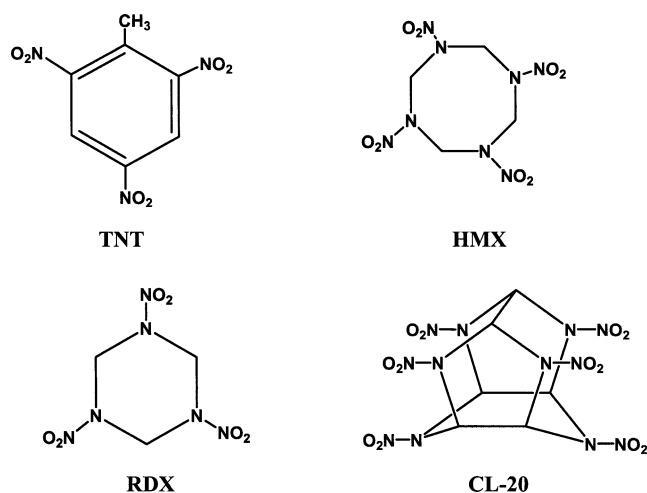


Fig. 1. Typical structures of the nitroaromatic 2,4,6-trinitrotoluene (TNT), monocyclic nitramine explosives 1,3,5-trinitro-1,3,5-triazacyclohexane (RDX), and octahydro-1,3,5,7-tetranitro-1,3,5,7-tetrazocine (HMX), and the polycyclic nitramine 2,4,6,8,10,12-hexaazaisowurtzitane (CL-20).

Soil characteristics and handling

A sandy-type natural forest soil sample taken in the Montreal area (designated as RacFor2002) was obtained from a local supplier (Racicot, Boucherville, QC, Canada) and had the following physical characteristics: Proportion of soil fractions were 89.8% sand (50–2,000 μm), 9.1% silt (2–50 μm), and 1.2% clay (<2 μm); soil sample had 36% moisture, 20% total organic carbon, a cation-exchange capacity of 48.2 cmol/kg, and pH 7.2. Chemical characterization of this RacFor2002 soil showed that organic contaminants (e.g., polycyclic aromatic hydrocarbon, polychlorinated biphenyl, and pesticides) were not detected, except for di(2-ethylhexyl) phthalate (2.8 mg/kg). Using standard soil extraction analytical methods, the total concentrations of toxic metals in the forest soil were low (5.8 mg/kg of Ag, 73 mg/kg of Ba, 2.0 mg/kg of Co, 12 mg/kg of Cr, 67 mg/kg of Cu, 310 mg/kg of Mn, 8.9 mg/kg of Ni, 11 mg/kg of Pb, and 180 mg/kg of Zn) or were not detected (As, Be, Li, Cd, Mo, Sb, Se, and Sn). Total concentrations of other metals were 5,600 mg/kg of Al, 9.0 mg/kg of B, 16,000 mg/kg of Ca, 4,800 mg/kg of Fe, 2,000 mg/kg of Mg, 410 mg/kg of Na, 77 mg/kg of Sr, 120 mg/kg of Ti, and 6.2 mg/kg of V. In addition, total concentrations of nutrients were 11,000 mg/kg of P, 10,000 mg/kg of Kjeldhal N (i.e., Kjeldhal nitrogen), and 1 400 mg/kg of K.

The Sassafra sandy loam (designated as SSL) soil sample was provided by Roman Kuperman (U.S. Army Edgewood Chemical Biological Center, Aberdeen Proving Ground, Edgewood, MD). A soil sample was collected from an uncontaminated, open grassland on the property of the U.S. Army Aberdeen Proving Ground. Vegetation and surface organic matter were removed, and the top 15 cm of the A horizon was collected and sieved through a 2-mm screen and air-dried. The SSL soil had the following physical characteristics: 71% sand; 18% silt, 11% clay, 0.33 % organic carbon, a cation-exchange capacity of 5.0 cmol/kg, and pH 5.1. The total concentrations of toxic metals in the SSL soil were low (33 mg/kg of Ba, 4.3 mg/kg of Co, 7.9 mg/kg of Cr, 14 mg/kg of Cu, 77 mg/kg of Mn, 6.1 mg/kg of Ni, and 30 mg/kg of Zn) or were not detected (Ag, As, B, Be, Li, Cd, Mo, Pb, Sb, Se, Sr, and Sn). Total concentrations of other metals were 7,900 mg/kg of Al, 870

mg/kg of Ca, 13,000 mg/kg of Fe, 900 mg/kg of Mg, 24 mg/kg of Na, 150 mg/kg of Ti, and 14 mg/kg of V. In addition, total concentrations of nutrients were 100 mg/kg of P, 420 mg/kg of Kjeldhal N, and 640 mg/kg of K.

Artificial soil (used as a substrate for the reference toxicants) consisted of 70% (wt/wt) grade 4010 silica sand (Unimin Canada, St. Canut, QC, Canada), 20% colloidal kaolinite clay (CAS 1332-56-7), and 10% 2-mm sieved Canadian sphagnum peat according to the Organisation for Economic Cooperation and Development Guideline [12]. Peat, sand, and clay were obtained from local suppliers. Calcium carbonate (1%, wt/wt) was used to adjust the pH of the wetted substrate to 6.0 ± 0.5 (mean \pm SD).

The RacFor2002 and SSL soils were spiked using different concentrations of CL-20 in acetone solution. The forest soil RacFor2002 samples were first placed into 1.5-L glass jars, whereas the SSL soil (500 g dry wt) was placed into 1-L glass jars. The CL-20 was dissolved in acetone to obtain a stock solution (~5,000 mg/L), which was dissolved at a defined concentration before being spiked into the soil. An aliquot (12.8 ml/kg of RacFor2002 soil and 20 ml/kg of SSL soil) of each solution was added to a soil layer (thickness, 2.5 cm). Acetone was then evaporated in the dark in a chemical hood to reach a low and nontoxic level (<0.1 $\mu\text{l/g}$ dry soil). Spiked soils were then mixed for 18 h in a rotary mixer. The above procedure was repeated with different defined concentrations (range, 0.5–5,000 mg/L) to obtain the selected nominal soil CL-20 concentrations (~0.01, 0.1, 1.0, 10, and 100 mg/kg dry soil) for the earthworm reproduction assays.

A solvent control (i.e., soil amended with acetone only) and a negative control (i.e., soil with water added only) were included in the experimental design. In the present study, 24 h (SSL soil) and 48 h (forest soil) of evaporation led to 0.04 μl acetone/g dry soil or less and 0.003 μl acetone/g soil or less, respectively. For the quality-control assays, reference toxicants (carbendazim and KCl) were first dissolved in water before being added to 500 g of dry artificial soil placed into 1-L glass jars.

At the beginning of each experiment, three replicates of 200 g of dry soil (earthworm lethality test) or four replicates of 500 g (earthworm reproduction test) per concentration were rehydrated to 75% of the water-holding capacity with deionized water or with separate solutions of the pure reference toxicants (KCl and carbendazim for earthworm lethality and reproduction assays, respectively). The water-holding capacity (21.2 and 123.4 ml/100 g for SSL and RacFor2002 soil, respectively) was determined by saturating the soil with deionized water and measuring the water content [13].

Earthworms

The oligochaetes *E. andrei* were obtained from Carolina Biological Supply (Burlington, NC, USA) and were initially used to establish the laboratory cultures. Animals were maintained in earthworm bedding (Magic Products, Amherst, WI, USA) supplemented with dry cereal (Magic Worm Food; Magic Products) at $20 \pm 1^\circ\text{C}$, 70–80% humidity, and a 16:8-h light:dark cycle. In the following toxicity tests, only adult earthworms (wet wt, 300–600 mg) having a well-developed clitellum were used.

Earthworm lethality test

The lethal effects of CL-20 on *E. andrei* in SSL were assessed using the U.S. Environmental Protection Agency Meth-

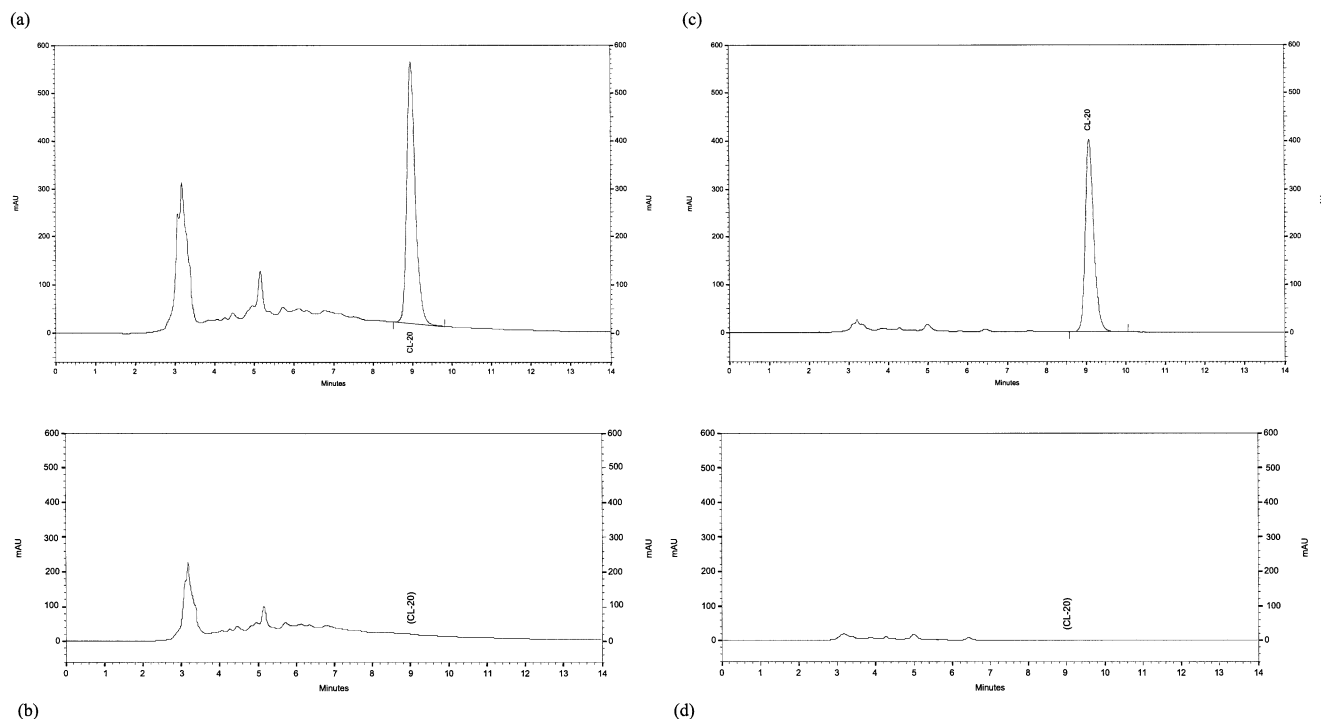


Fig. 2. Representative high-performance liquid chromatograms of acetonitrile extracts of a sandy-type forest (RacFor2002) soil spiked with acetone solution containing (a) or not containing (b) the polycyclic nitramine hexanitrohexaazaisowurtzitane (CL-20; 134 mg/kg) as well as extracts of Sassafras sandy loam soil containing (c) or not containing (d) CL-20 (89 mg/kg).

od EPA/600/3-88/029 [14]. After acclimation for 1 to 4 d in clean soil, 10 *E. andrei* were individually washed, weighed, and added to each replicate glass jar containing the test soil sample. The glass jars were closed using a geotextile and perforated lids with 1.6-mm air holes. The number of surviving *E. andrei* (determined in triplicate) was recorded after 7 and 14 d of exposure, as were their individual wet body weights (14 d).

Earthworm reproduction test

The effects of explosives-spiked soils (RacFor2002 and SSL) on growth and reproduction of *E. andrei* were assessed using the International Organization for Standardization Method 103390 [15]. Following acclimation in clean soil, 10 *E. andrei* were individually rinsed, weighed, and added to each replicate jar containing the toxicant-amended soil. Glass jars were closed using a geotextile and lids with 1.6-mm air holes. Food (2 g of dry cereal) was added to the surface of the test matrix at the beginning of the experiment and then once weekly. The earthworms were hand-sorted from the soil, and the number of surviving *E. andrei* (per replicate) as well as the individual weight (wet biomass) were recorded at 28 d. The remaining soil (containing cocoons) was then returned to its respective jar and incubated for another 28 d to continue the exposure of cocoons and juveniles to the test soil. At the end of the experiment (test day 56), the soils were wet sieved, and the number of hatched and nonhatched cocoons as well as the number of juveniles and their biomass were recorded. The pH was measured before and after each test using a 1:5 (vol/vol) suspension of soil in water [16]. Water content was also measured by loss of soil weight on drying both before and after each test.

Chemical analyses

The residual acetone at the beginning of toxicity assays was determined using headspace gas chromatographic analyses as described earlier [13]. The limit of detection of the instrument was 100 $\mu\text{g/L}$ acetone.

Concentrations of CL-20 in acetone solutions and soil were determined by high-performance liquid chromatography (HPLC) using a modified version of U.S. Environmental Protection Agency Method 8330 [17]. Solutions of CL-20 (~5,000 mg/L) were prepared in acetone for the assays. An aliquot of the solution was first mixed with acetonitrile (1:9, vol/vol) and then with deionized water acidified with NaHSO_4 (1:1, vol/vol) before the analyses. Soil samples were extracted at the beginning ($t = 0$), after 28 d, and at the end ($t = 56$ d) of the experiments. Briefly, acetonitrile (10 ml) was added to a portion of a weighed soil sample (2 g) and then vortexed for 1 min. The sample was then sonicated (60 Hz) for 18 ± 2 h at 20°C . Next, 5 ml of supernatant were combined with 5 ml of $\text{CaCl}_2/\text{NaHSO}_4$ aqueous solution (5 and 0.2 g/L, respectively) and then filtered through a 0.45- μm Millipore polytetrafluoroethylene membrane. The first 3 ml of filtrate were discarded, and the remainder was analyzed using a Thermo Finnigan (San Jose, CA, USA) chromatographic system composed of a model P4000 pump; a model AS1000 autosampler, including temperature control for the column; and a model ultraviolet 6000LP photodiode-array detector. The column used was a CN reverse-phase HPLC column (25 cm \times 4.6 mm, 5 μm ; Supelcosil LC-CN; Supelco, Oakville, ON, Canada). Temperature of the autosampler was held at 10°C . The initial solvent composition was 30% water and 70% methanol. Retention time (RT) of CL-20 ranged from 8 to 10 min. The detector was set to 230 nm.

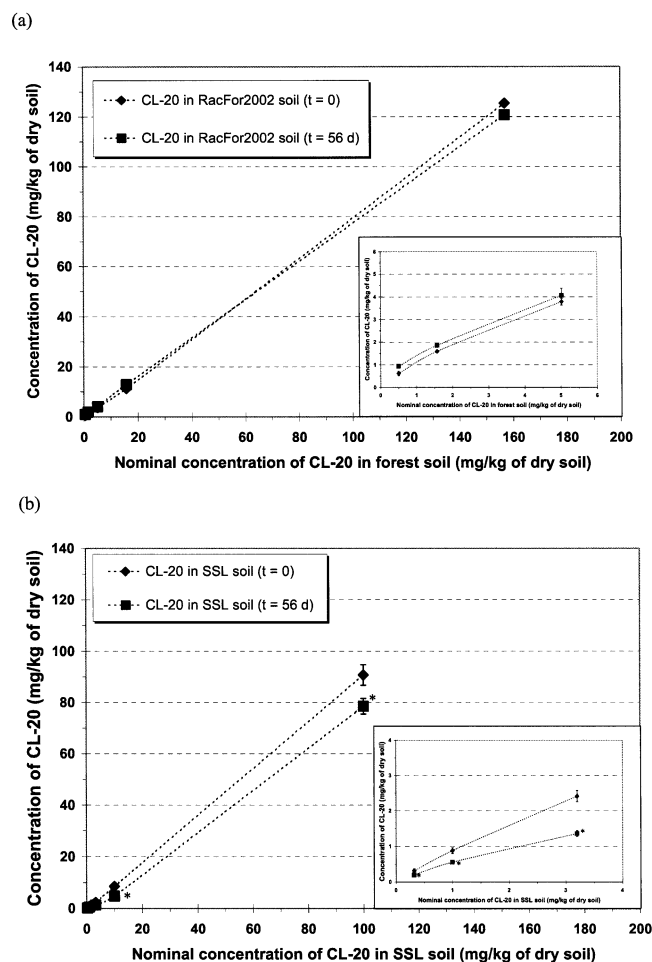


Fig. 3. Mean polycyclic nitramine hexanitrohexaazaisowurtzitane (CL-20) concentrations measured in the sandy-type forest (RacFor2002; a) and Sassafras sandy loam (SSL; b) soil ($n = 4$) at days 0 (\diamond) and 56 (\blacksquare) compared to CL-20 nominal concentrations. Error bars indicate standard deviations. An asterisk indicates a significant difference ($p \leq 0.05$) compared to the corresponding initial concentrations ($t = 0$). Figure inset shows the same data at low concentrations.

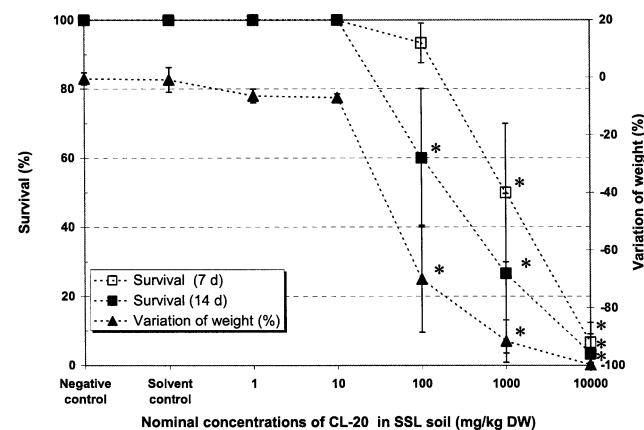


Fig. 4. Lethal and sublethal (wt) effects of the polycyclic nitramine hexanitrohexaazaisowurtzitane (CL-20) to *Eisenia andrei* using a standard toxicity test method. Survival after 7 d (\square) and 14 d (\blacksquare) of exposure ($n = 10$ earthworms \times 3 replicates/concentration at start of experiment) and variation of weight (i.e., wt loss; \blacktriangle) after 14 d of exposure. Error bars indicate standard deviation. An asterisk indicates a significant difference ($p \leq 0.05$) compared to negative and solvent controls. SSL = Sassafras sandy loam; DW = dry weight.

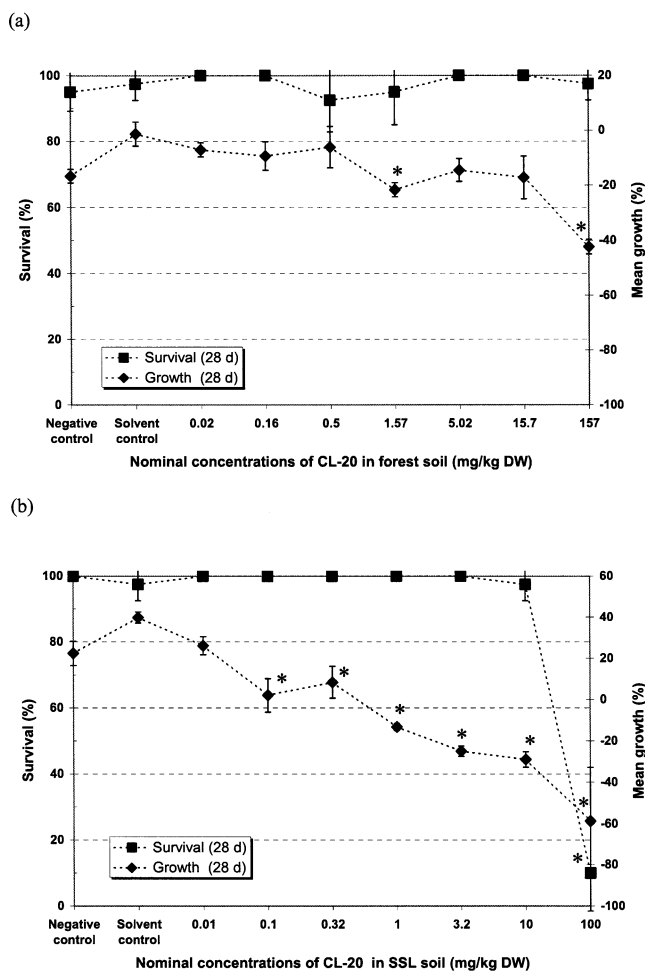


Fig. 5. Lethal (\blacksquare) and sublethal (\diamond ; growth) effects of the polycyclic nitramine hexanitrohexaazaisowurtzitane (CL-20) to *Eisenia andrei* in the sandy-type forest (RacFor2002; a) and Sassafras sandy loam (SSL; b) soil after 28 d of exposure ($n = 10$ earthworms \times 4 replicates/concentration at start of experiment). Error bars indicate standard deviation. An asterisk indicates a significant difference ($p \leq 0.05$) compared to negative and solvent controls. DW = dry weight.

Quality control

All experiments were done in triplicate (for the lethality test) or quadruplicate (for the reproduction test) and included negative controls (soil with water added only; no toxic substances added) and solvent controls (soil amended with acetone only). Mortality, growth, and reproduction endpoints for the reference toxicants as well as other established criteria (e.g., response in the negative control, temperature) were verified against laboratory in-house control data to validate the toxicological analyses. The positive-control results using the reference toxicants carbendazim (median effect concentration [EC₅₀] for the number of juveniles after 56 d was 0.88 mg/kg dry artificial soil) and KCl (median lethal concentration [LC₅₀] of adult earthworms after 14 d was 7,000 mg/kg dry artificial soil) were consistent with in-house data and those of previous studies [4].

Data analysis

Toxicity endpoints such as the lethal concentration causing a percentage mortality, the estimated effect concentration causing a percentage (EC_p) inhibition of a measurement endpoint compared to solvent control groups, the no-observed-effect

concentration (NOEC), and the lowest-observed-effect concentration (LOEC) were determined using the ToxCalc program (Ver 5.0; Tidepool Scientific Software, McKinleyville, CA, USA). The 10% effective concentration, 20% effective concentration (EC20), and EC50 were chosen as representative point estimates of three toxicity levels. Linear interpolation with bootstrapping was used for point-estimates. Dunnett's multiple-comparison test was used to determine the LOEC and NOEC ($p \leq 0.05$). Data are expressed as the average \pm standard deviation (survival and reproductive parameters) or standard error (growth parameters). The differences between initial and final concentrations were analyzed with a heteroscedastic t test (unequal variance) and with a nonparametric test (Mann-Whitney U test or Wilcoxon matched-pairs test) to observe differences ($p \leq 0.05$) among the treatment concentrations.

RESULTS

CL-20 soil concentrations during the 56-d toxicity experiments

The initial measured concentration of CL-20 in soil ranged from 0.45 to 125.4 mg/kg dry soil in the RacFor2002 forest soil and from 0.31 to 90.7 mg/kg in SSL soil. Examples of HPLC chromatograms of solvent extracts for noncontaminated and CL-20 spiked soil samples are shown in Figure 2. The RacFor2002 soil extracts (Fig. 2a and b) had a higher background signal (RT = 4–8 min) than SSL soil extracts (Fig. 2c and d), presumably because RacFor2002 soil has a higher organic matter content compared to SSL soil. For SSL soil, the method detection limit and method quantification limit were 0.06 and 0.2 mg CL-20/kg dry soil, respectively; for the RacFor2002 soil, the limit of quantification was estimated to 0.5 mg CL-20/kg. The method detection limit was not determined for RacFor2002 soil, but CL-20 was measured in all spiked soil samples, the results of which suggest that the detection limit would be similar (i.e., 0.06 mg CL-20/kg dry soil) to that of SSL soil. However, the measured concentrations of CL-20 in two samples of the RacFor2002 soil were higher (0.45 ± 0.02 and 0.46 ± 0.10 mg/kg) than their nominal concentrations (0.016 and 0.157 mg/kg, respectively). At CL-20 concentrations less than 0.5 mg/kg of RacFor2002 soil, differences between nominal and initial measured concentrations may be caused by a possible interference with organic matter. For CL-20 concentrations less than 0.2 mg/kg of SSL soil or less than 0.5 mg/kg of RacFor2002 soil, nominal concentrations were used for the toxicity endpoint calculations.

The concentration of CL-20 remained constant in the RacFor2002 soil ($\leq 3.8\%$ of initial values) over the 56-d exposure period (Fig. 3a) but decreased significantly ($\leq 43.9\%$ of initial exposure concentrations) at all SSL soil concentrations (Fig. 3b). At nominal concentrations less than 0.5 mg/kg, the measured concentrations of CL-20 decreased at 28 d (in the RacFor2002) and reached below the detection limit after 56 d in both SSL and RacFor2002 soil samples.

Effects of CL-20 on adult earthworm survival in amended SSL and RacFor2002 forest soil

Exposure to CL-20-spiked SSL soil caused significant effects on *E. andrei*, as evidenced by concentration-dependent decreases in survival and body weight (Figs. 4 and 5). A preliminary acute test using the SSL soil showed that the survival of adult earthworms significantly decreased at nominal concentrations of 100 mg/kg or greater after 14 d of exposure

(Fig. 4). After 7 d of exposure, survival decreased using nominal CL-20 concentrations of 1,000 mg/kg or greater. The wet weight of earthworms exposed for 14 d was also significantly decreased at 100 mg/kg.

Exposure to CL-20 for 28 d showed that survival of adult earthworms was not affected at 157 mg CL-20/kg dry soil (nominal concentration) in the forest soil (Fig. 5a and Table 1). In the SSL soil, survival was decreased by 90% at 100 mg/kg dry soil (Fig. 5b), and the LC50 was 53.4 mg/kg. Survival was not significantly decreased at 10 mg/kg dry SSL soil (Fig. 5b and Table 2). Growth was significantly reduced at 1.57 mg/kg of CL-20 or greater in RacFor2002 soil only, whereas growth was decreased at 0.1 mg/kg or greater in SSL soil (Tables 1 and 2).

Effects of CL-20 on earthworm fertility in amended SSL and RacFor2002 forest soil

Results of the earthworm reproduction studies show that fertility was decreased at 1.57 mg CL-20/kg dry soil or greater (nominal concentration) using the RacFor2002 soil (Table 1) or at 0.1 mg CL-20/kg or greater using the SSL soil (Table 2). These effects occurred at nonlethal concentrations.

Table 3 summarizes the toxicity endpoints (LOEC, NOEC, lethal concentration causing a percentage, and ECp) for CL-20 in both RacFor2002 and SSL soils compared to controls. The CL-20 in the RacFor2002 soil decreased the number of juveniles (one of the most sensitive reproduction endpoints). The EC20 of this effect was 0.57 mg CL-20/kg dry soil and corresponded to other reproduction responses within the same concentration range. These responses include decreases in the total (e.g., EC20 = 0.62 mg/kg) and hatched (e.g., EC20 = 0.67 mg/kg) number of cocoons. The CL-20 was more toxic in the SSL soil than in RacFor2002 soil, as determined using the number of juveniles as the endpoint as well as the total and hatched numbers of cocoons (EC20 < 0.01 mg/kg).

DISCUSSION

The present study shows that CL-20 decreases the survival and reproductive capacity of the earthworm *E. andrei*. Sublethal effects were observed in two different sandy soils. The RacFor2002 forest soil had 20% organic carbon content and pH 7.2, whereas the SSL soil had a lower organic content (0.33%) and lower pH (5.1). Lethal and sublethal effects of CL-20 were more dramatic in the SSL soil compared to the RacFor2002 soil. For example, CL-20 was lethal in the SSL soil at initial concentrations of 90.7 mg/kg or greater but was not lethal at 125 mg/kg in the RacFor2002 soil. Also, growth of adults was diminished at nominal concentrations of 0.01 mg CL-20/kg or greater in the SSL soil and at initial concentrations of 1.57 mg CL-20/kg or greater in the RacFor2002 soil. Fertility was significantly reduced at a nominal concentration of 0.1 mg CL-20/kg (LOEC) in the SSL soil, whereas a significant effect on fertility was seen at initial concentrations of 1.57 mg/kg (LOEC) or greater using the RacFor2002 soil.

It is not known why CL-20 in freshly amended SSL soil was more toxic to earthworms than it was in the RacFor2002 soil. A number of factors should be considered. Chemical analysis indicated that the SSL soil had a lower water-holding capacity and cation-exchange capacity as well as a higher silt and clay content compared to the forest RacFor2002 soil. Also, the SSL soil had a lower organic carbon and pH compared to the RacFor2002 soil.

Decreased toxicity and bioavailability of CL-20 may be

Table 1. Responses of the earthworm (*Eisenia andrei*) to hexanitrohexaazaisowurtzane (CL-20) spiked forest RacFor2002 soil^a

Parameter	CL-20 nominal concentrations (mg/kg dry soil)							
	Control	0.02	0.16	0.50	1.57	5.02	15.7	157
CL-20 initial measured concentrations (mean \pm SD, mg/kg dry soil)								
Adult survival/replicate (% \pm SD; 28 d)	ND	0.45 \pm 0.10 ^b	0.46 \pm 0.02 ^b	0.62 \pm 0.15	1.59 \pm 0.11	3.79 \pm 0.15	11.3 \pm 1.1	125 \pm 8
Adult growth/worm (mg \pm SE [% \pm SE]; 28 d)	97.5 \pm 5.0 -5.8 \pm 19.9 [-1.3 \pm 4.4]	100 -35.6 \pm 14.3 [-7.0 \pm 2.6]	100 -44.4 \pm 24.4 [-9.3 \pm 5.2]	92.5 \pm 9.6 -30.2 \pm 37.0 [-6.1 \pm 7.6]	95.0 \pm 5.0 -101.5 \pm 10.0 [-21.6 \pm 2.5] ^c	100 -70.7 \pm 20.9 [-14.5 \pm 4.2] ^c	100 -81.0 \pm 39.0 [-17.2 \pm 7.8] ^c	97.5 \pm 5.0 -205.6 \pm 14.0 [-42.3 \pm 2.7] ^c
No. cocoons/replicate (\pm SD; 56 d)	90.0 \pm 9.5	82.3 \pm 16.3	82.0 \pm 21.5	62.0 \pm 17.2	36.3 \pm 15.9	16.8 \pm 3.4 ^d	1.5 \pm 1.9 ^d	0 ^d
No. hatched cocoons/replicate (\pm SD; 56 d)	76.0 \pm 11.5	66.3 \pm 19.3	76.0 \pm 21.2	54.5 \pm 17.4	29.8 \pm 15.0	12.0 \pm 4.3 ^d	1.0 \pm 1.4 ^d	0 ^d
Hatchability (hatched cocoons/total no. cocoons [% \pm SD]; 56 d)	84.2 \pm 4.0	79.4 \pm 12.0	92.2 \pm 8.1	87.7 \pm 11.9	80.8 \pm 6.9	70.2 \pm 11.9	62.5 \pm 17.7	NA
No. juveniles/replicate (\pm SD; 56 d)	249.3 \pm 36.8	173.8 \pm 48.2	192.3 \pm 70.7	146.3 \pm 42.5	71.3 \pm 30.4 ^d	29.5 \pm 7.3 ^d	0.5 \pm 0.6 ^d	0 ^d
Biomass of juveniles/replicate (mg \pm SD; 56 d)	3,186 \pm 1,059	1,921 \pm 428	2,296 \pm 673	1,712 \pm 646	901.9 \pm 384.5 ^d	937.3 \pm 656.2 ^d	13.0 \pm 21.0 ^d	0 ^d
Biomass/juvenile (mg \pm SD; 56 d)	13.0 \pm 4.6	11.6 \pm 3.7	12.3 \pm 4.7	11.8 \pm 4.1	12.8 \pm 1.4	29.4 \pm 17.2	25.9 \pm 25.6	0 ^d
No. juveniles/hatched cocoon (\pm SD; 56 d)	3.3 \pm 0.2	2.6 \pm 0.2	2.6 \pm 1.8	2.9 \pm 0.9	2.5 \pm 0.6	2.7 \pm 1.2	0.5 \pm 0.7	0 ^d

^a n = 4 replicates; Control = 12.8 ml/kg dry soil of acetone added and evaporated before the rehydration (75% water-holding capacity) of the soil; Adult growth = mean change in body weight during the experiment (average of final minus initial body wt); RacFor2002 = sandy-type forest soil taken in the Montreal area (QC, Canada); SE = standard error; SD = standard deviation; ND = not detected (method detection limit, 0.06 mg/kg dry soil); method quantification limit, 0.5 mg/kg dry soil; NA = not determined.

^b Interference with soil matrix suspected.

^c Significant effect on growth compared to negative and solvent controls ($p \leq 0.05$).

^d Significant effect on reproduction parameter compared to negative and solvent controls ($p \leq 0.05$).

Table 2. Responses of earthworm (*Eisenia andrei*) to hexanitrohexaazaisowurtzitane (CL-20) spiked SSL soil^a

Parameter	CL-20 nominal concentrations (mg/kg dry soil)						
	Control	0.01	0.1	0.32	1.0	3.2	10
CL-20 initial measured concentrations (mean \pm SD, mg/kg dry soil)							
Adult survival/replicate (% \pm SD; 28 d)	ND	ND	ND	0.31 \pm 0.06	0.89 \pm 0.08	2.41 \pm 0.16	8.58 \pm 0.73
Adult growth/worm (mg \pm SE [% \pm SE]; 28 d)	97.5 \pm 5.0 165.6 \pm 9.4 [39.8 \pm 2.6]	100 113.3 \pm 20.0 [26.2 \pm 4.4] 42.0 \pm 8.6	100 7.0 \pm 33.6 [2.1 \pm 8.2] ^b 27.8 \pm 15.4 ^c	100 32.6 \pm 29.1 [8.4 \pm 7.7] ^b 7.3 \pm 6.2 ^c	100 -53.9 \pm 5.7 [-13.3 \pm 1.7] ^b 0 ^c	100 -104.3 \pm 10.7 [-25.0 \pm 2.5] ^b 0 ^c	97.5 \pm 5.0 -128.4 \pm 15.4 [-29.0 \pm 3.8] ^b 0 ^c
No. cocoons/replicate (\pm SD; 56 d)	57.8 \pm 9.5						
No. hatched cocoons/replicate (\pm SD; 56 d)	49.8 \pm 9.2	34.5 \pm 6.2	19.8 \pm 15.8 ^c	4.8 \pm 4.6 ^c	0 ^c	0 ^c	0 ^c
Hatchability (hatched cocoons/total no. cocoons [% \pm SD]; 56 d)	86.3 \pm 8.2	82.6 \pm 6.0	72.3 \pm 12.7	53.1 \pm 41.3	NA	NA	NA
No. juveniles/replicate (\pm SD; 56 d)	117.5 \pm 25.0	83.3 \pm 25.4	33.5 \pm 7.8 ^c	1.0 \pm 1.4 ^c	0 ^c	0 ^c	0 ^c
Biomass of juveniles/replicate (mg \pm SD; 56 d)	784.9 \pm 209.0	480.3 \pm 124.2	308.7 \pm 40.7	5.8 \pm 8.5 ^c	0 ^c	0 ^c	0 ^c
Biomass/juvenile (mg \pm SD; 56 d)	6.8 \pm 1.8	6.0 \pm 1.8	9.9 \pm 2.9	5.5 \pm 0.7	0 ^c	0 ^c	0 ^c
No. juveniles/hatched cocoon (\pm SD; 56 d)	1.7 \pm 1.0	2.4 \pm 0.5	2.4 \pm 0.6	1.7 \pm 0.7	0.1 \pm 0.2 ^c	0 ^c	0 ^c

^a n = 4 replicates; Control = 20 ml/kg dry soil of acetone added and evaporated before the rehydration (75% water-holding capacity) of the soil; Adult growth = mean change in body weight during the experiment (average of final minus initial body wt); SSL = Sassafras sandy loam soil taken on the property of U.S. Army Aberdeen Proving Ground (Edgewood, MD); SE = standard error; SD = standard deviation; ND = not detected (method detection limit, 0.06 mg/kg dry soil; method quantification limit, 0.2 mg/kg dry soil); NA = not determined.

^b Significant effect on growth compared to negative and solvent controls ($p \leq 0.05$).

^c Significant effect on reproduction parameter compared to negative and solvent controls ($p \leq 0.05$).

Table 3. Lethal and sublethal effects of hexanitrohexaazaisowurtzitane (CL-20) on earthworm (*Eisenia andrei*) using freshly amended natural soils^a

Parameter	NOEC (mg/kg)	LOEC (mg/kg)	LC10 or EC10 (mg/kg [95% CI])	LC20 or EC20 (mg/kg [95% CI])	LC50 or EC50 (mg/kg [95% CI])
RacFor2002 soil					
Survival of adults (28 d)	125	>125	>125	>125	>125
Growth of adults (28 d)	125	>125	<0.01 ^b	<0.01 ^b	<0.01 ^b
No. total cocoons (56 d)	1.59	3.79	0.36 (<0.01–1.15)	0.62 (<0.01–1.38)	1.50 (0.65–3.10)
No. hatched cocoons (56 d)	1.59	3.79	0.39 (<0.01–1.19)	0.67 (<0.01–1.45)	1.45 (0.29–3.13)
No. juveniles (56 d)	0.62	1.59	0.31 (<0.01–1.10)	0.57 (<0.01–1.24)	1.30 (0.09–2.87)
SSL soil					
Survival of adults (28 d)	8.57	90.7	16.0 (8.1–19.7)	25.3 (17.8–29.5)	53.4 (46.3–63.0)
Growth of adults (28 d)	<0.01 ^b	0.01 ^b	<0.01 ^b	0.01 (<0.01–0.02) ^b	0.04 (0.03–0.08) ^b
No. total cocoons (56 d)	<0.01 ^b	0.01 ^b	<0.01 ^b	0.01 (<0.01–0.04) ^b	0.09 (0.03–0.16) ^c
No. hatched cocoons (56 d)	<0.01 ^b	0.01 ^b	<0.01 ^b	0.01 (<0.01–0.03) ^b	0.07 (0.02–0.12) ^b
No. juveniles (56 d)	<0.01 ^b	0.01 ^b	<0.01 ^b	0.01 (<0.01–0.04) ^b	0.05 (<0.01–0.08) ^c

^a 95% CI = 95% confidence intervals; NOEC = no-observed-effect concentration; LOEC = lowest-observed-effect concentration; LC10 = estimated lethal concentration for 10% of the organisms tested; LC20 = estimated lethal concentration for 20% of the organisms tested; LC50 = estimated lethal concentration for 50% of the organisms tested (median); EC10 = estimated concentration causing 10% inhibition of measured response; EC20 = estimated concentration causing 20% inhibition of measured response; EC50 = estimated concentration causing 50% inhibition of measured response (median); RacFor2002 = sandy-type forest soil; SSL = Sassafras sandy loam. Data are expressed on a dry soil basis.

^b Less than the method detection limit of 0.06 mg/kg dry soil.

^c Less than the method quantification limit of 0.2 mg/kg dry soil.

explained by differences in organic carbon content between the RacFor2002 and SSL soils. Also, preliminary studies were carried out to determine CL-20 K_d (sorption constant) values. For this, batch sorption experiments were conducted at ambient temperature ($21 \pm 2^\circ\text{C}$) for 72 h. Solutions of CL-20 were agitated with soil in the dark. After centrifugation (1,170 g for 30 min), the supernatant was filtered (pore size, 0.45 μm) and analyzed by HPLC. The remaining pellet was extracted with acetonitrile to measure the amount of sorbed explosive. The respective isotherms (i.e., sorbed amount in $\mu\text{g/g}$ as a function of the equilibrium concentration in mg/L) were plotted, and the K_d values were obtained from the slopes of linear isotherms. These preliminary studies confirmed that CL-20 sorption in RacFor2002 soil ($K_d > 300 \text{ L/kg}$) is higher than in SSL soil ($K_d = 2.4 \text{ L/kg}$; F. Montiel-Rivera, National Research Council of Canada, Montreal, QC, unpublished data).

On the other hand, it is unlikely that the slightly alkaline pH in the RacFor2002 soil (pH 7.2) compared to the SSL soil (pH 5.0) contributed to the observed differences in CL-20 toxicity. Balakrishnan et al. [18] reported that CL-20 can be hydrolyzed relatively easily at greater than pH 7 to produce nitrite and formic acid. However, the HPLC results presented in this article indicate that CL-20 concentrations were unchanged in the RacFor2002 soil, indicating that pH was not a major factor in determining the bioavailability and toxicity of CL-20 in the present study. Closer examination of the effect of pH and organic carbon content on the bioavailability and toxicity of CL-20 will be carried out in future studies.

For reproduction effects, LOEC values of 58.8, 46.7, and 15.6 mg/kg observed earlier for TNT, RDX, and HMX, respectively [5], were at least one order of magnitude higher than that for CL-20 (Table 3), indicating that lethal and sublethal effects of CL-20 to earthworms occurred at relatively low concentrations [3–5]. Lethal effects of CL-20 occurred at concentrations as low as 90.7 mg/kg (LOEC) in the SSL soil. These differences in toxic responses suggest that the hazardous effects of energetic contaminants, including CL-20, cannot be explained by a common mechanism of toxicity. This may not be surprising in view of the marked differences in their phys-

ico-chemical properties caused by differences in their chemical structures (Fig. 1). For instance, TNT is polynitroaromatic, RDX and HMX are monocyclic nitramines, but CL-20 is a rigid polycyclic nitramine.

Environmental agencies and future managers of explosive-contaminated sites should be cognizant that CL-20 is relatively more toxic to earthworms than other explosives. Based on laboratory toxicological data, CL-20 may have hazardous effects on soil organisms and pose a significant risk to other ecosystem components.

CONCLUSION

The CL-20 has significant lethal and sublethal effects on the earthworm *E. andrei*. Fertility of earthworms was reduced at CL-20 concentrations as low as 0.1 mg/kg dry soil using SSL soil. These effects were observed at higher concentrations in the RacFor2002 forest soil than in the SSL soil. The exact reason for this difference in effects between SSL and RacFor2002 soil is not known, but it is probably caused by the presence of high organic carbon content in the latter case, which decreased the bioavailability of CL-20 because of high sorption to the soil matrix.

Acknowledgement—We thank Frédéric Leduc, Manon Sarrazin, Aurélie Auroy, and Louise Paquet from Biotechnology Research Institute of the National Research Council of Canada for their assistance. We also thank Roman Kuperman for providing the SSL soil. Gratitude is also expressed to Sonia Thiboutot and Guy Ampleman from Defense Research and Development Canada—Valcartier for their interest in the study. These studies were partially funded by the U.S. Department of Defense/Department of Energy/Environmental Protection Agency Strategic Environmental Research and Development Program (CP1256).

REFERENCES

1. Dodard S, Renoux AY, Powlowski J, Sunahara GI. 2003. Lethal and subchronic effects of 2,4,6-trinitrotoluene on *Enchytraeus albidus* in spiked artificial soil. *Ecotoxicol Environ Saf* 54:131–138.
2. Jarvis AS, McFarland VA, Honeycutt ME. 1998. Assessment of the effectiveness of composting for the reduction of toxicity and

- mutagenicity of explosives soil. *Ecotoxicol Environ Saf* 39:131–135.
3. Phillips CT, Checkai RT, Wentsel RS. 1993. *Toxicity of Selected Munitions and Munition-Contaminated Soil on the Earthworm (Eisenia foetida)*. U.S. Army Chemical and Biological Defense Agency, Edgewood Research, Development and Engineering Center, Research and Technology Directorate, Aberdeen Proving Ground, MD.
 4. Robidoux PY, Hawari J, Thiboutot S, Ampleman G, Sunahara GI. 1999. Acute toxicity of 2,4,6-trinitrotoluene (TNT) in the earthworm (*Eisenia andrei*). *Ecotoxicol Environ Saf* 44:311–321.
 5. Robidoux PY, Hawari J, Bardai G, Paquet L, Ampleman G, Thiboutot S, Sunahara GI. 2002. TNT, RDX, and HMX decrease earthworm (*Eisenia andrei*) life-cycle responses in a spiked natural forest soil. *Arch Environ Contam Toxicol* 43:379–388.
 6. Robidoux PY, Hawari J, Thiboutot S, Sunahara GI. 2002. Ecotoxicological risk assessment of an explosives contaminated site. In Sunahara GI, Renoux AY, Gaudet CL, Thellen C, Pilon A, eds, *Environmental Analysis of Contaminated Sites*. John Wiley, New York, NY, USA, pp 335–359.
 7. Robidoux PY, Svendsen C, Sarrazin M, Hawari J, Thiboutot S, Ampleman G, Week JM, Sunahara GI. 2002. Evaluation of tissue and cellular biomarkers to assess 2,4,6-trinitrotoluene (TNT) exposure in earthworm: Effect-based assessment in laboratory studies using *Eisenia andrei*. *Biomarkers* 7:306–321.
 8. Simini M, Wentsel RS, Checkai R, Phillips C, Chester NA, Major MA, Amos JC. 1995. Evaluation of soil toxicity at Joliet Army Ammunition Plant. *Environ Toxicol Chem* 14:623–630.
 9. Sunahara GI, Robidoux PY, Gong P, Lachance B, Rocheleau S, Dodard S, Hawari J, Thiboutot S, Ampleman G, Renoux AY. 2001. Laboratory and field approaches to characterize the ecotoxicology of energetic substances. In Greenberg BM, Hull RN, Roberts MH Jr, Gensemer RW, eds, *Environmental Toxicology and Risk Assessment: Science, Policy and Standardization—Implications for Environmental Decisions*, Vol 10. STP 1403. American Society for Testing and Materials, Philadelphia, PA, pp 293–312.
 10. Talmage SS, Opresko DM, Maxwell CJ, Welsh CJE, Cretella FM, Reno PH, Daniel FB. 1999. Nitroaromatic munition compounds: Environmental effects and screening values. *Rev Environ Contam Toxicol* 161:1–156.
 11. Larson SL, Felt DR, Escalon L, Davis JD, Hansen LD. 2001. *Analysis of CL-20 in Environmental Matrices: Water and Soil*. ERDC/EL TR-01-21. U.S. Army Engineer Research and Development Center, Vicksburg, MS.
 12. Organization for Economic Cooperation and Development. 1984. Earthworm, acute toxicity tests. In *Guideline of the OECD for Testing Chemical Products*. Paris, France.
 13. Robidoux PY, Svendsen C, Caumartin J, Hawari J, Ampleman G, Thiboutot S, Weeks JM, Sunahara GI. 2000. Chronic toxicity of energetic compounds in soil determined using the earthworm (*Eisenia andrei*) reproduction test. *Environ Toxicol Chem* 19:1764–1773.
 14. U.S. Environmental Protection Agency. 1989. Earthworm survival (*Eisenia foetida*). Protocols for short term toxicity screening for hazardous waste sites. EPA/600/3-88/029. Environmental Research Laboratory, Corvallis, OR.
 15. International Organization for Standardization. 1994. Soil quality—Determination of pH. ISO 103390. International Standard. Geneva, Switzerland.
 16. International Organization for Standardization. 1998. Soil quality—Effects of soil pollutants on earthworms (*Eisenia fetida*). Part 2: Determination of effects on reproduction. ISO 11268-2.2. International Standard. Geneva, Switzerland.
 17. U.S. Environmental Protection Agency. 1997. Method 8330: Nitroaromatics and nitramines by high performance liquid chromatography (HPLC). In *Test Methods for Evaluating Solid Waste*. SW-846. Update III, Part 4:1 (B). Office of Solid Waste, Washington, DC.
 18. Balakrishnan VK, Halasz A, Hawari J. 2003. Alkaline hydrolysis of the cyclic nitramine explosives RDX, HMX and CL-20: New insights into degradation pathways obtained by observation of novel intermediates. *Environ Sci Technol* 37:1838–1843.

Effects of Dietary Administration of CL-20 on Japanese Quail *Coturnix coturnix japonica*

G. Bardai,^{1,2} G. I. Sunahara,¹ P. A. Spear,² M. Martel,¹ P. Gong,¹ J. Hawari¹

¹ Biotechnology Research Institute, National Research Council of Canada, 6100 Royalmount Avenue, Montreal Quebec, Canada H4P 2R2

² Centre de Recherche TOXEN, Département des Sciences Biologiques, Université du Québec à Montréal, CP 8888, Succursale Centre-ville, Montréal Québec, Canada H3C 3P8

Received: 12 November 2004 / Accepted: 5 February 2005

Abstract. Hexanitrohexaazaisowurtzitane, or CL-20, is an emerging highly energetic compound currently under consideration for military applications. With the anticipated wide use of CL-20, there is the potential for soil and groundwater contamination resulting in adverse toxicologic effects on environmental receptors. Presently, there is a lack of data describing the toxic effects of CL-20 on avian species. The present study describes the effect of CL-20 on Japanese quail (*Coturnix coturnix japonica*) modified from standard toxicity test guidelines. First, a 14-day subacute assay was adopted using repeated gavage doses (0, 307, 964, 2439, 3475, or 5304 mg CL-20/kg body weight (BW)/d for 5 days followed by no CL-20 exposure (vehicle only) for 10 days. Second, a subchronic feeding assay (0, 11, 114, or 1085 mg CL-20/kg feed) was done for 42 days. During both studies, no overt toxicity was observed in the CL-20-treated birds. During the first 5 days of the subacute study, CL-20-exposed birds showed a dose-dependent decrease in BW gain, whereas increased liver weight, plasma sodium, and creatinine levels were observed in birds receiving the highest dose tested. For the subchronic study, embryo weights were significantly decreased in a dose-dependent manner. Embryos from CL-20-exposed birds were observed to have multiple cranial and facial deformities, beak curvatures, possible mid-brain enlargement, and classic one-sided development with microphthalmia (nonstatistical comparisons with control embryos). A trend toward decreased number of eggs laid per female bird was also observed. We conclude that CL-20 (or its degradation products) elicits few effects in adults but may affect avian development, although these preliminary findings should be confirmed.

Hexanitrohexaazaisowurtzitane, or CL-20 (Fig. 1), is a high-density polynitro compound currently under consideration for military application. CL-20 is envisaged to deliver 10% to 20% higher performance than octahydro-1,3,5,7-tetranitro-1,3,5,7-tetrazocine (HMX) and better performance than hexahydro-1,3,5-trinitro-1,3,5-triazine (RDX) (Nielsen *et al.* 1998; Geetha *et al.* 2003). RDX and HMX are common contaminants found in soil at military-related sites, and the toxicity of these nitramines to terrestrial vertebrate species such as mammals, amphibians, and birds is becoming better known (Schneider *et al.* 1976; Levine *et al.* 1981; Talmage *et al.* 1999; Gogal *et al.* 2003; Johnson *et al.* 2004). Gogal *et al.* (2003) found the approximate lethal dose of acute oral RDX exposure in northern bobwhite (*Colinus virginianus*) to be 280 mg/kg body weight (BW) for male and 187 mg/kg BW for female birds. The dose-dependent effects of RDX also included a decrease in food intake, BW, and spleen and liver mass for 14 days but not for 90 days of exposure. Although the effects of CL-20 in plant and soil invertebrate species have been recently reported (Gong *et al.* 2004; Robidoux *et al.* 2004), no data are available on the toxicity of CL-20 in birds.

CL-20 is a polycyclic nitramine characterized by having N-NO₂ bonds, similar to the two monocyclic nitramines RDX and HMX. Based on these structural similarities, we hypothesized that the effects of CL-20 to birds will be similar to those of RDX. In the present study, we investigated the toxic effects of CL-20 on the gallinaceous test species Japanese quail (*Coturnix coturnix japonica*) exposed to repeated daily doses of CL-20. We selected this species because it is amenable to laboratory toxicity testing, and species of this order can have significant dietary exposure to soil based on their foraging and behavioral habits. This species has been used in many standard toxicity testing regimes for standard avian toxicity testing (American Society for Testing and Materials [ASTM] 1997; United States Environmental Protection Agency [USEPA] 1996a, 1996b; Organization for Economic Cooperation and Development [OECD] 1984a, 1984b). Data generated using these standardized toxicity test methods will be useful for the ecotoxicologic risk assessment of birds exposed to CL-20.

Correspondence to: G. I. Sunahara; email: geoffrey.sunahara@nrc-nrc.gc.ca

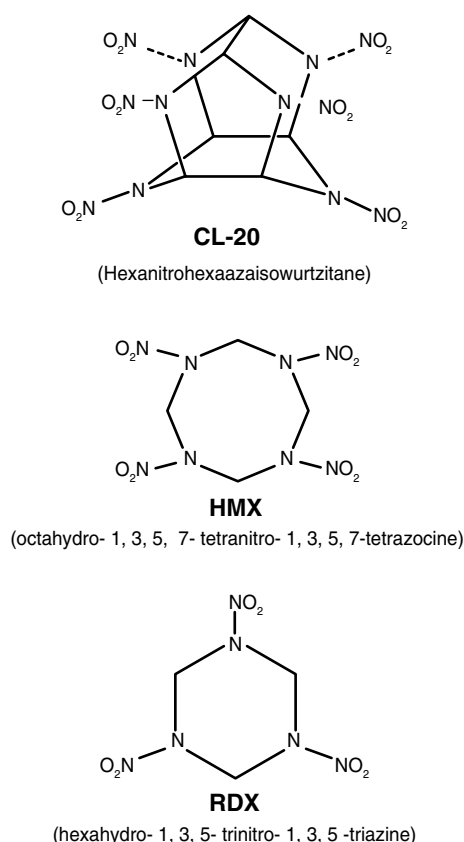


Fig. 1. Molecular structures of the cyclic nitramine explosives CL-20, HMX, and RDX. CL-20 = hexanitrohexaazaisowurtzitane; HMX = octahydro-1,3,5,7-tetranitro-1,3,5,7-tetrazocine; RDX = hexahydro-1,3,5-trinitro-1,3,5-triazine

Materials and Methods

Chemicals and Reagents

CL-20 (Chemical Abstracts Service [CAS] no. 135285-90-4) in the ϵ form (purity >95%) was obtained from ATK Thiokol Propulsion (Brigham City, UT). Acetonitrile and acetone (high-performance liquid chromatography [HPLC]-grade) were obtained from EM Science (Darmstadt, Germany). All other chemicals and reagents were of the highest grades of purity available and were obtained from Anachemia (Milwaukee, WI). Deionized water was obtained using a Zenopure Mega-90 water purification system (Zenon Environmental Inc, Burlington, Ontario). All glassware was washed with phosphate-free detergent, rinsed with acetone, and acid washed before a final rinse with deionized water.

Raising of Test Species

Fertilized Japanese quail (*C. coturnix japonica*) eggs ($n = 70$ for subacute study and $n = 120$ for subchronic study) obtained from a local breeder (Couvoir Simetin, Mirabel, PQ, Canada) were placed in an environment-controlled incubator at $37^{\circ}\text{C} \pm 1^{\circ}\text{C}$ (SD), with $65\% \pm 5\%$ relative humidity, and turned 180° every fourth hour. Three days before hatching, rotation of eggs was stopped and the

relative humidity increased to 70%. Eggs were grouped at the center of the incubator on a 5-mm mesh until they hatched. When dry, quail chicks were transferred to a heated brooder (35°C achieved using an electric resistance element) under constant illumination with red incandescent light to prevent eye damage. Birds were fed a diet of powdered Turkey Starter (Purina Mills, St Louis, MO) and tap water *ad libitum* until 14 days of age. Quail were then maintained under controlled conditions of temperature ($22.0^{\circ}\text{C} \pm 3.0^{\circ}\text{C}$), relative humidity ($50.0\% \pm 6.0\%$), and lighting (14 hours light to 10 hours dark).

Experimental Design

The subacute study (Fig. 2A) described in this article was modified from the USEPA (1996a) and OECD (1984a) guidelines. Forty-four 2-week-old quail were weighed, banded, and observed for any abnormalities. A blood sample (1 ml) was taken from the jugular vein (described later), and each bird was then randomly assigned to one of six groups ($n = 7$ to 8/group for $n = 44$ total). Animals were housed together in stainless steel cages (61 cm wide x 76 cm long x 41 cm high; 10-mm mesh floor) (2 to 3 individuals/cage) and were uniquely identified by a leg band. Two days later, birds were gavaged daily for 5 days with pulverized commercial feed (Ralston Purina Turkey Grower) containing CL-20. Briefly, the feed was pulverized using a hand-held blender until a granular consistency was formed, then CL-20 was added. The CL-20-contaminated feed was prepared daily, and the doses were adjusted to the BW that was taken daily during the dosing period (1% of BW). To deliver the contaminated feed, the desired quantity was transferred into a 5-ml syringe, and 1 ml water was added to the syringe to form a slurry. A 10-gauge stainless steel curved feeding tube equipped with a Luer Lock fitting (Becton Dickinson, Canada) onto the syringe was inserted down the esophagus to the crop. The slurry was administered gently to ensure minimal regurgitation. The calculated doses delivered (mg CL-20/kg BW) were 307 ± 1 , 964 ± 8 , 2439 ± 12 , 3475 ± 5 , and 5304 ± 53 . A second blood sample (from 1 to 1.5 ml) was collected 5 days after completion of the dosing. At the end of the experiment (day 14 of study), birds were anesthetized and a third blood sample (5 ml) was procured. While under deep anaesthesia, birds were killed (as desired later), and the organs (heart, brain, liver, and spleen) were weighed and frozen at -80°C for residual CL-20 analysis. The somatic index (%) was calculated as the wet organ weight (g) per 100 g BW.

The subchronic study described in this article was modified from the USEPA (1996b) and OECD (1984b) guidelines. The lighting period was changed (16 hours light to 8 hours dark) to provide optimal reproductive conditions when the quail were 2 weeks old. The birds ($n = 48$) were then randomly assigned to one of each of the four dose groups (described below) in triplicate. Each exposure was conducted in triplicate, each group (three female and one male bird) was housed in stainless steel cages (described above). Quail were uniquely identified by a leg band. During this period, close surveillance was required to monitor any signs of increased aggression. Individuals injured or demonstrating incompatible behavior relative to the group were replaced. Eggs were collected and incubated during the pre-exposure period to verify fertility and thus ensure that only proven breeders were included in this study. Two days before the start of feeding CL-20 diets when quail were 54 days old, a blood sample (2 ml) was taken from each bird. The diets were prepared by mixing CL-20 (previously dissolved in acetone) with commercial feed (Ralston Purina Turkey Grower) to achieve nominal concentrations described later. Acetone was allowed to evaporate, and the CL-20 feed mixture was then placed in glass jars and stored at $4.0^{\circ}\text{C} \pm 2.0^{\circ}\text{C}$ in the absence of light. Measured concentrations of

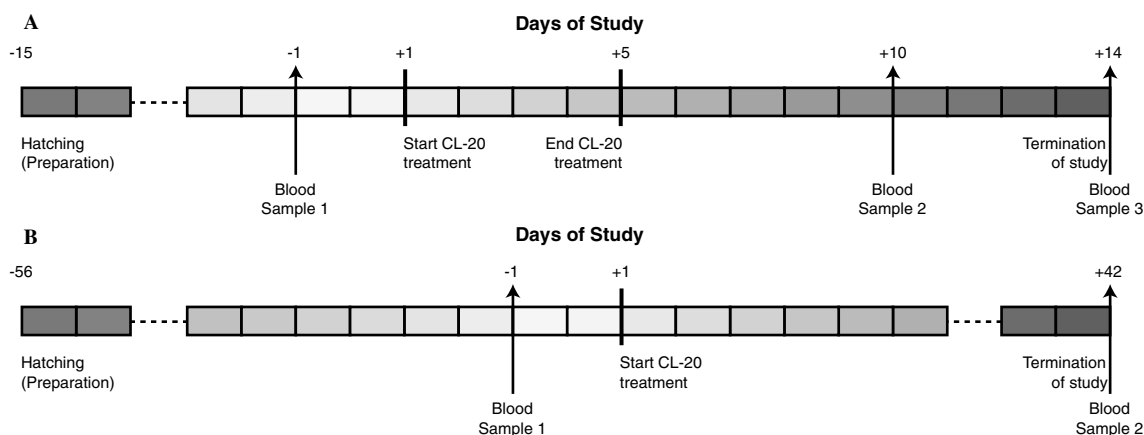


Fig. 2. Schedule for the two CL-20 exposure studies. (A) Subacute study. (B) Subchronic study

CL-20 in the feed were analyzed using HPLC (11 ± 1 , 114 ± 26 , and 1085 ± 52 mg CL-20/kg feed corresponding to the nominal exposure groups of 10, 100, and 1000 mg/kg BW, respectively), and were found to be consistent throughout the study. All feed was provided daily *ad libitum*. Daily feed consumption was estimated as the difference between initial and final feed weight plus the quantity of unconsumed pellets recovered from the litter pans, which was determined daily for the first 2 weeks of the study and then on every alternate day.

A subsample of eggs (based on total eggs collected, $n = 15$ to 20/d) were collected and frozen at -80°C ; the remaining eggs ($n = 10$ to 12 collected/d) were stored in a refrigerator ($16^{\circ}\text{C} \pm 1^{\circ}\text{C}$ and 60% to 70% humidity) for 5 days. Eggs of the latter group were then incubated at 37.8°C and 60% relative humidity. After 8 days of incubation, the eggs were cooled to 4°C , and embryos were removed and weighed. Embryos were then preserved in capped vials containing 10% formalin, and they were stored at room temperature in the dark until further evaluation of developmental effects. Embryos were evaluated according to the Hamburger-Hamilton system (1951) for normal stages of chick embryo development. At the end of the 6-week exposure period, the adult birds were killed and examined for gross lesions. Liver, spleen, heart, and brain were excised, weighed, frozen in liquid nitrogen, and stored at -80°C before residual CL-20 analyses.

For both studies, birds were monitored daily for changes in health or disposition (*i.e.*, alertness, appearance). For the subacute study, BW gain was measured daily for the duration of the gavage phase and then on study days 10 and 14. Body weight and feed consumption for the subchronic study were measured daily for a 2-week period and then on every alternate day. At the end of the experiments, birds were anesthetized (2% to 5% isoflurane), and killed (90% CO_2 and 10% O_2). Moribund animals were treated in the same fashion. Manipulation and handling were in accordance with the Canadian Council on Animal Care guidelines (1984).

Blood Collection and Analysis

For clinical chemistry and hematological analyses, female quail blood was collected from the jugular vein with a 27-gauge needle and 3-ml syringe containing 100 μl 1% ethylenediaminetetraacetic acid solution in saline. Male birds were not considered for this study because of the low number of male birds per exposure group (1 male bird/3 female

birds/replicate, 3 replicates/exposure group). Blood was thoroughly mixed, and 250 μl was removed for whole-blood analysis. Plasma was prepared in 1.5-ml Eppendorf tubes centrifuged at $13,000 \times g$ for 5 minutes and was used either fresh for clinical chemistry analysis to screen for biochemical and pathologic abnormalities or was stored at -80°C for plasma residual CL-20 analysis. Quail plasma was analyzed to determine its clinical chemistry profile (Beckman LX20 Pro, Rochester, NY); the tests measured Na, K, Cl, glucose, creatinine, total protein, PO_4 , total bilirubin, direct bilirubin, uric acid, Mg, cholesterol, alanine aminotransferase, aspartate aminotransferase (AST), alkaline phosphatase, amylase, lactate dehydrogenase, and triglycerides. For hematologic analysis, one drop of anticoagulated blood was placed on a microscope slide, and a smear was made. The blood smear was fixed in methanol, stained with modified Wright-Giemsa, and the leukocyte differential performed when 100 leukocytes (lymphocytes, heterophils, monocytes, basophils, and eosinophils) were enumerated. Heterophil-to-lymphocyte ratios were calculated to investigate stress. For hematocrit (HCT) determination, a nonheparinized hematocrit capillary tube was filled with anticoagulated blood. The bottom of the capillary tube was sealed with a clay plug and centrifuged for 5 minutes at 3000 rpm, and the HCT was determined as the ratio between total capillary volume and the packed cell volume (PCV).

CL-20 Extraction from Quail Tissue

CL-20 extractions were performed according to USEPA Method No. 8330A (USEPA 1998) with the following modifications. For CL-20 exposure studies, whole organs taken from test animals were immediately homogenized on ice in 7 ml cold acetonitrile using a Polytron tissue homogenizer (30 seconds for brain and spleen or 1 minute for heart and liver) in Teflon tubes. After overnight sonication in the dark at 8°C (60 Hz; Branson 3200, Danbury, CT), samples were centrifuged at 4°C for 10 minutes at $10,000 \times g$. To 5 ml of the decanted supernatant was added an equal volume of a CaCl_2 (90 mM)- NaHSO_4 (1.6 mM) solution, and the resulting mixture was vortexed for 30 seconds and stored at 4°C for 2 hours to precipitate proteins. The resulting solution was filtered through a $0.45\text{-}\mu\text{m}$ membrane before HPLC analysis (described later). To increase the sensitivity of the previously described method, the supernatants of different tissue samples (liver, heart, brain, and kidney) were also concentrated. Each supernatant (5 ml) was evaporated to dryness in a Speed Vac (Savant, Hicksville, NY). To the precipitate was added 500 μl acetonitrile, and the mixture was vortexed for 1 minute, after which the CaCl_2 - NaHSO_4 solution

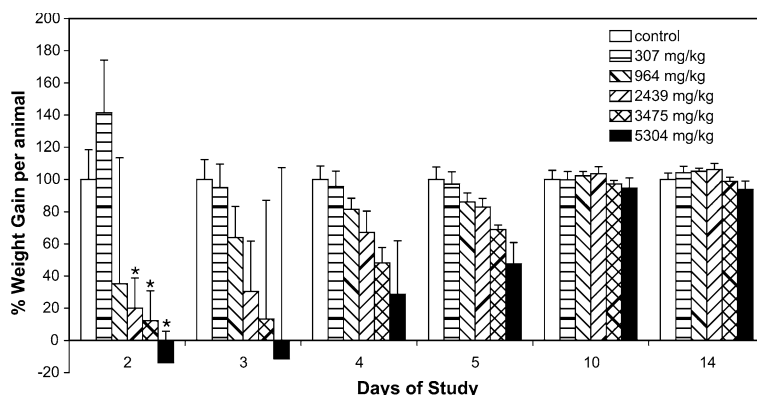


Fig. 3. Changes in BW of juvenile Japanese quail gavaged with CL-20 for 5 days (subacute study). Exposure schedule is shown in Figure 2. Each value (expressed as percent of control, which was set at 100%) is the average \pm SEM ($n = 6$ to 10 birds). *Value is statistically different from the control ($p \leq 0.05$). The average BWs of the control group ($g \pm$ SEM) ($n = 6$ birds) for study days 2, 3, 4, 5, 10, and 14 were 98 ± 8 , 106 ± 6 , 116 ± 7 , 126 ± 8 , 172 ± 8 , and 202 ± 9 , respectively

was added as described previously. For the control recovery studies, whole organs (liver, brain, spleen, or heart) were taken from non-treated quail and spiked with varying concentrations of CL-20 before being immediately frozen at -80°C for 24 hours. The organs were then thawed in cold acetonitrile, and CL-20 was extracted as previously described.

Extraction of CL-20 from the Test Diet

Acetonitrile extractions of test diet were also performed using the USEPA Method No. 8330A (USEPA 1998). One ml 1.6 mM NaHSO_4 prepared in water was added to 2 g feed and vortexed for 10 seconds. To this was added 10 ml (for feed containing 10 mg CL-20/kg feed) or 20 ml acetonitrile (for feed containing 100 to 1000 mg CL-20/kg feed), before vortexing for 1 minute.

HPLC Analysis

In brief, a ThermoFinnigan chromatographic system composed of a model P4000 pump, a model AS1000 injector, and a model UV6000LP photodiode-array detector ($\lambda = 230$ nm) was used. A Supelcosil LC-CN column (250 \times 4.6 mm, 5- μm particles; Supelco, Bellefonte, PA) was used for separation with a column heater set at 35°C . The isocratic mobile phase consisted of methanol and water (70/30 v/v) delivered at 1.0 ml/min. The sample volume injected was 50 μl with a 14-minute run time. The limit of quantification was 0.05 mg/L. Relative SD for the instrument precision was $<1.3\%$ for concentrations ≥ 0.5 mg CL-20/L and 7.5% for a concentration of 0.05 mg CL-20/L.

Statistical Analysis

The data were evaluated by two-way and repeated measures analysis of variance (ANOVA). Differences between exposure groups and their respective controls were considered significant when $p \leq 0.05$ using the Dunnett's test. Statistical analysis was performed using JMPIN software (version 4; SAS Institute, Cary, NC).

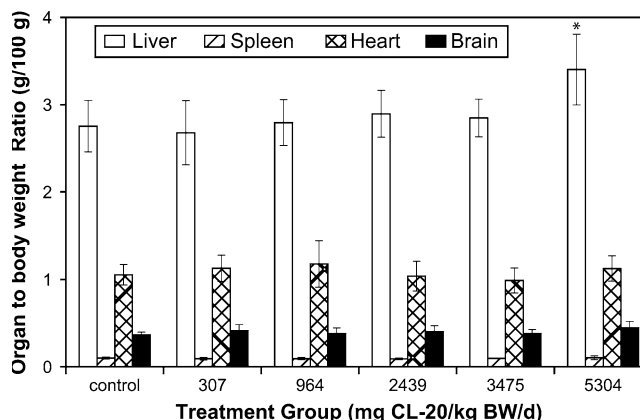


Fig. 4. Somatic index of selected organs of juvenile Japanese quail gavaged with CL-20 for 5 days followed by 10 days of vehicle only (no CL-20). Data are expressed as mean \pm SD ($n = 44$ birds). Study design is shown in Figure 2. *Value is statistically different from the control ($p \leq 0.05$)

Results

Subacute Study

No clinical or overt toxic symptoms were observed during the 5-day exposure period to CL-20. The change in average weight gain (expressed as the percent of respective control) for each exposure group is shown in Figure 3. Data indicate that a dose-dependent decrease in BW gain occurred during the first 5 days of the study ($p \leq 0.05$). On the second study day, the CL-20 quail exposure groups ≥ 964 mg/kg BW/d gained less weight than the control group ($p \leq 0.05$); however, this effect was not detected by the end of the study (day 14 or 10 d of no CL-20 exposure). Initial BWs before exposure were not significantly different between groups (data not shown).

Liver weights were significantly increased in the highest dose group (5304 mg/kg BW/d), whereas other organ weights (brain and spleen) were not significantly different between CL-

Table 1. Selected plasma biochemical parameters of adult Japanese quail exposed to CL-20 by gavage for 5 days followed by 10 days of exposure with no CL-20

Parameters	CL-20 exposure groups (mg CL-20 kg BW/d) ^a					
	0	307	964	2439	3475	5304
PO ₄ (mmol/L)	3.22 ± 0.21 ^b	2.89 ± 0.26	2.91 ± 0.26	2.53 ± 0.21	2.73 ± 0.24	2.96 ± 0.39
TP (g/L)	19.2 ± 3.6	22.0 ± 2.6	22.3 ± 2.9	18.4 ± 2.9	20.8 ± 2.8	21.63 ± 3.25
Glu (mmol/L)	16.3 ± 1.0	17.0 ± 0.7	16.7 ± 1.0	16.4 ± 1.2	17.1 ± 1.3	16.36 ± 1.45
Cre (μmol/L)	20.0 ± 2.6	18.6 ± 3.2	20.3 ± 4.0	18.2 ± 5.4	21.8 ± 4.4	25.00 ± 3.16*
Na (mmol/L)	143.9 ± 0.8	145.5 ± 1.0	144.0 ± 0.8	144.6 ± 2.7	149.5 ± 1.6	151.7 ± 2.70*
ALP (IU/L)	592 ± 327	711 ± 253	1056 ± 301	485 ± 396	328 ± 275	509 ± 230
ALT (IU/L)	4.25 ± 1.50	4.20 ± 1.30	5.00 ± 0.82	4.80 ± 0.84	4.50 ± 1.05	4.50 ± 0.76
Uric (μmol/L)	201.3 ± 53.3	239.2 ± 78.1	269.0 ± 134.8	195.0 ± 37.6	216.0 ± 101.8	300.6 ± 68.5
AMY (IU/L)	336 ± 71	460 ± 190	377 ± 197	178 ± 60	436 ± 136	377 ± 193
AST (IU/L)	101.3 ± 11.7	87.3 ± 10.0	94.0 ± 10.1	107.2 ± 21.9	95.5 ± 13.5	101.9 ± 11.8
Chol (mmol/L)	5.32 ± 0.74	4.06 ± 0.91	5.17 ± 1.52	5.63 ± 2.50	4.67 ± 0.98	5.38 ± 1.44
Dbili (μmol/L)	1.25 ± 0.24	0.95 ± 0.21	0.78 ± 0.31	1.40 ± 0.50	0.83 ± 0.27	1.16 ± 0.49
Tbili- (μmol/L)	2.8 ± 0.5	2.6 ± 1.6	4.0 ± 1.2	2.2 ± 1.3	2.3 ± 1.1	3.5 ± 0.9
GGT (IU/L)	6.5 ± 4.5	8.8 ± 2.3	8.0 ± 1.4	8.4 ± 0.9	7.5 ± 2.2	10.0 ± 2.2
LDH (IU/L)	59.8 ± 13.0	48.8 ± 8.4	47.0 ± 9.5	49.2 ± 12.8	41.0 ± 12.7	56.4 ± 28.8
TG (mmol/L)	1.84 ± 0.20	1.42 ± 0.32	2.05 ± 0.91	2.04 ± 0.52	1.49 ± 0.36	2.06 ± 0.78
Mg (mmol/L)	0.15 ± 0.50	0.20 ± 0.01	0.28 ± 0.05	0.11 ± 0.14	0.10 ± 0.04	0.13 ± 0.7

ALP = Alkaline phosphatase.

ALT = Alanine aminotransferase.

AMY = Amylase.

AST = Aspartate aminotransferase.

Chol = Cholesterol.

CL-20 = Hexanitrohexaazaisowurtziane.

Cre = Creatinine.

Dbili = Billirubin.

GGT = γ glutamyltransferase.

Glu = Glucose.

LDH = Lactate dehydrogenase.

Tbili = Total Billirubin.

TG = Triglycerides.

TP = Total proteins.

^a Measured concentrations of CL-20 intake by gavaged quails.^b Data are expressed as mean ± SD ($n = 4$ to 8 birds/exposure group).* Exposure group is significantly different from control using Dunnett's test ($p \leq 0.05$).

20-treated and control groups (Fig. 4). Increases in plasma sodium and creatinine levels were found in birds treated with 5304 mg CL-20/kg BW/d compared with controls (Table 1). Hematologic parameters (heterophil-to-lymphocyte ratios and hematocrit) in the subacute study were not statistically different between exposure groups compared with controls (data not shown).

Subchronic Study

No clinical or overt toxic symptoms were observed during the 42-day exposure period in this study. Aggressive behavior was noted in one individual who was subsequently isolated from the control group. Another bird from a different control group had to be killed because of injuries inflicted by an aggressive control bird that was subsequently removed from the triplicate. These observations were not related to exposure. Based on feed consumption (feed consumed per number of individuals in each dose group) and mean BW, the calculated daily doses

to quail consuming the CL-20 diet were 0, 0.96, 10, and 94 mg CL-20/kg BW for the measured 0, 11, 114, and 1085 mg CL-20/kg feed exposure groups, respectively. Throughout this study, no differences in feed consumption or BW were observed between exposure groups (data not shown). Clinical chemistry analysis of quail blood taken from the subchronic study (Table 2) revealed that the AST level was increased by 1.25 times in the birds of the highest measured feed dose level (1085 mg CL-20/kg) relative to controls ($p \leq 0.05$).

Embryo weight was found to decrease significantly and in a dose-dependent manner (Fig. 5). Based on the measured exposure concentration, the unbounded lowest observed adverse effect level for this effect was 11 mg/kg feed. The unintentional evaporation of the preserving medium from some of the storage vials caused a dehydration of the embryos, thus making these samples unsuitable for further analysis. Embryos in vials that still contained formalin were analyzed. In the 114 mg/kg feed exposure group, two of the six embryos had multiple (cranial and facial) deformities, whereas in the highest dose group (1085 mg/kg feed), three of the nine embryos experienced beak curvatures, possible mid-brain

Table 2. Selected plasma biochemical parameters of adult Japanese quail fed CL-20 for 42 days

Parameters	CL-20 exposure groups (mg CL-20/kg feed) ^a			
	0	11	114	1085
PO ₄ (mmol/L)	2.87 ± 0.63 ^b	2.56 ± 0.39	3.03 ± 0.84	2.11 ± 0.71
TP (g/L)	31.6 ± 4.0	30.1 ± 2.3	33.5 ± 1.7	28.3 ± 3.2
Glu (mmol/L)	15.1 ± 0.99	15.4 ± 1.29	14.5 ± 0.8	14.4 ± 0.9
Cre (μmol/L)	30.3 ± 9.6	32.4 ± 4.7	24.4 ± 6.1	27.0 ± 9.6
Na (mmol/L)	144.4 ± 3.6	142.3 ± 1.3	139.8 ± 3.5	142.3 ± 1.3
ALT (IU/L)	5.16 ± 1.60	4.83 ± 2.22	6.00 ± 1.63	6.50 ± 1.51
Uric (μmol/L)	213.4 ± 58.7	303.0 ± 147.0	136.8 ± 71.2	232.3 ± 131.5
AMY (IU/L)	507 ± 179	368 ± 222	643 ± 304	472 ± 154
AST (IU/L)	133.3 ± 11.6	144.8 ± 23.5	154.6 ± 27.4	167.2 ± 23.2 *
Chol (mmol/L)	6.27 ± 2.06	4.84 ± 1.76	7.39 ± 3.85	4.63 ± 1.34
Tbili (μmol/L)	7.65 ± 1.97	6.94 ± 1.45	8.12 ± 1.39	6.98 ± 0.96
GGT (IU/L)	5.88 ± 1.64	6.57 ± 1.13	6.13 ± 2.41	6.43 ± 1.90
LDH (IU/L)	54.8 ± 59.0	31.3 ± 27.0	34.8 ± 51.0	74.2 ± 39.0
TG (mmol/L)	11.7 ± 2.4	9.8 ± 2.7	10.8 ± 2.2	9.2 ± 2.7
Mg (mmol/L)	1.63 ± 0.33	1.36 ± 0.23	1.48 ± 0.29	1.34 ± 0.25
K (mmol/L)	2.9 ± 0.5	3.2 ± 0.3	2.7 ± 0.3	2.9 ± 0.4
Cl (mmol/L)	110.1 ± 4.2	107.8 ± 3.9	107.1 ± 3.5	110.3 ± 3.2

ALT = Alanine aminotransferase.

AMY = Amylase.

AST = Aspartate aminotransferase.

Chol = Cholesterol.

CL-20 = Hexanitrohexaazaisowurtzitane.

Cre = Creatinine.

GGT = γ -glutamyltransferase.

Glu = Glucose.

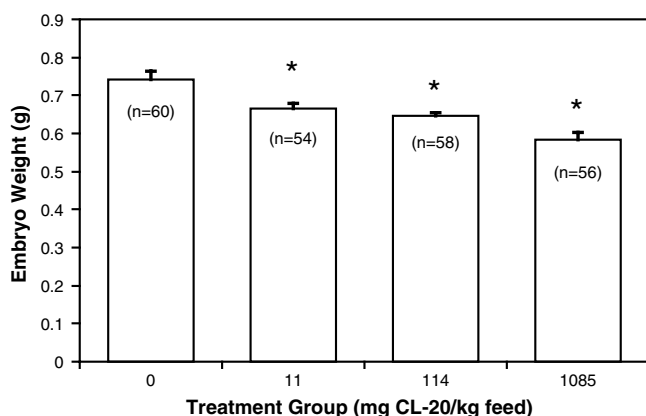
LDH = Lactate dehydrogenase.

Tbili = Total bilirubin.

TG = Triglycerides.

TP = Total proteins

Uric = Uric acid.

^a Measured concentration in feed using USEPA Method 8330A.^b Data are expressed as mean ± SD ($n = 7$ to 9 birds group).* Exposure group is significantly different from control using Dunnett's test ($p \leq 0.05$).**Fig. 5.** Effects of 42 days of dietary exposure to CL-20 on Japanese quail embryo weights. Data are mean embryo weight ± SD (n = number of embryos evaluated). *Value is statistically different from the control ($p \leq 0.05$)

enlargement, and classic one-sided development with microphthalmia. These CL-20 exposure-related deformities were not observed in the control group; however, two of the nine

control embryos showed very slight ocular asymmetric deviations. No decrease in the rate of development was detected; all embryos were at stages 30 to 31 (Hamburger and Hamilton 1951). In addition, CL-20 exposure tended to decrease the number of eggs laid per female bird ($0.48 < p < 0.99$ for the different treatment groups using the Dunnett's two-sided t test for multiple comparisons) compared with controls (Fig. 6).

CL-20 Recovery from Tissue

CL-20 was not detected in the plasma or selected organs (brain, spleen, heart, and liver) of quail treated with CL-20 (data not shown), despite the excellent recovery of the chemical (99% to 105%) using different spiked tissues (Figs. 7 and 8). This method was specific for CL-20 detection only.

Discussion

Few acute and subchronic effects were found from oral CL-20 exposure to quail in this study. However, our 42-day subchronic study indicated that CL-20 exposure led to significant

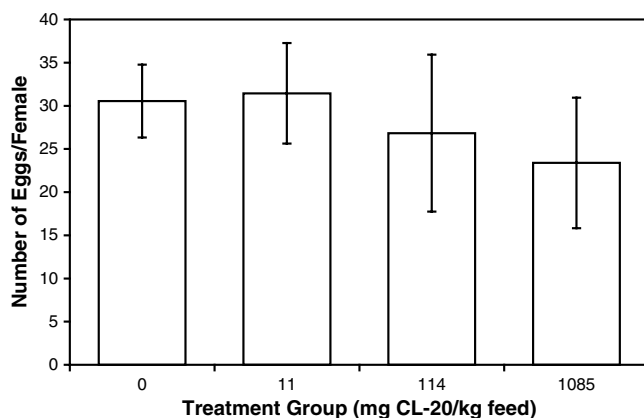


Fig. 6. Effects of 42 days of dietary exposure to CL-20 on the mean number of eggs produced per hen. These exposure effects were not significant compared with controls ($p > 0.05$)

decreases in embryo weight without a corresponding effect on developmental stage. This would suggest an effect on energy metabolism rather than a decrease in the rate of embryonic development *per se*. Although we have evidence that CL-20 exposure caused abnormal developmental effects, these results should be considered preliminary until a more rigorous teratologic evaluation is done using increased number of replicates. Bhushan *et al.* (2004a, 2004b) reported the formation of nitrite NO_2^- , nitrous oxide N_2O , ammonia, formic acid, ammonium, or glyoxal from the enzymatic biodegradation of CL-20 by the flavin containing enzymes, nitroreductase, and salicylate 1-monooxygenase. Quail have been found to possess both phase I and II biotransformation enzymes (Gregus *et al.* 1983). It is possible that quail may possess similar enzymes capable of degrading CL-20 and that the presence of the resulting degradation products may be related to the observed CL-20 toxicity in our present studies. A preliminary survey of the avian toxicity literature failed to identify studies characterizing the toxic effects of the latter CL-20 degradation products to quail. To further characterize the reported effect of embryo malformation by CL-20 and gain more information about the mechanism of CL-20 toxicity (direct and indirect effects of CL-20 on the embryo), *in ovo* approaches are suggested.

Earlier studies have shown that exposure to the monocyclic nitramine explosive RDX causes central nervous system disturbances in birds (northern bobwhite), terrestrial salamanders, and mammals (rats and miniature swine) (Schneider *et al.* 1976; Levine *et al.* 1981; Gogal *et al.* 2003; Johnson *et al.* 2004). Rats injected intraperitoneally with 500 mg RDX/kg BW had seizures before death. Miniature swine treated intravenously with RDX showed convulsions from 12 to 24 hours after exposure. A recent study reported that red-backed salamanders (*Plethodon cinereus*) exposed to 5,000 mg RDX/kg soil in laboratory microcosms for 28 days showed signs of neuromuscular effects including lethargy, convulsions, rolling and gaping motions, and hyperactivity as well as marked weight loss (Johnson *et al.* 2004). In contrast to these earlier studies using RDX, none of the CL-20 treated birds in our present studies exhibited signs of neurotoxicity.

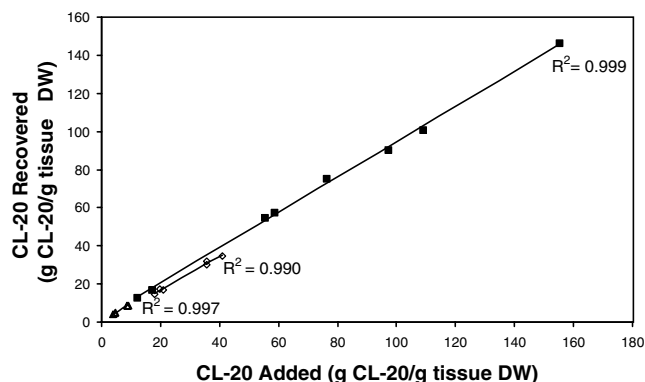


Fig. 7. Recovery of CL-20 using spiked tissue samples (\triangle = brain; \diamond = spleen; \blacksquare = heart) and modified USEPA Method No. 8330A. R^2 value was determined by linear regression using least-squares method

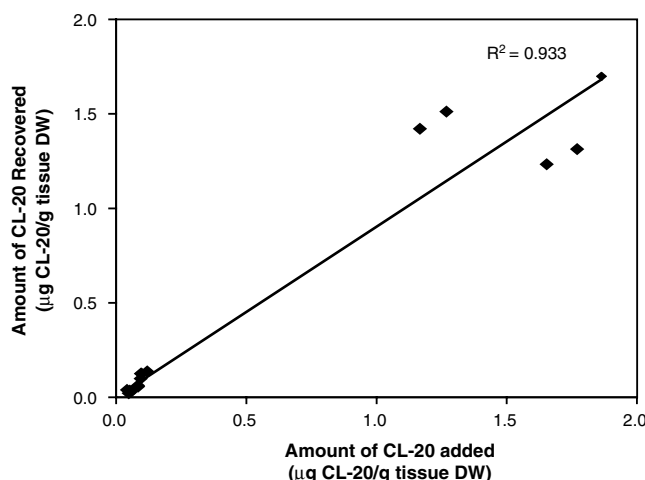


Fig. 8. Recovery of CL-20 from spiked liver tissue using modified USEPA Method No. 8330A.

Earlier studies by Gogal *et al.* (2003) showed that RDX in a water vehicle was lethal to the northern bobwhite at a single dose (≥ 187 mg RDX/kg BW) after 72 hours exposure. In our subacute study, CL-20 caused no mortality in adult Japanese quail gavaged with up to 5304 mg CL-20/kg BW. These data suggest that CL-20 is not as lethal to galliform species as RDX. Physicochemical differences between RDX (aqueous solubility at 20°C = 42.58 mg/L, $\log K_{ow}$ = 0.90) and CL-20 (aqueous solubility at 20°C = 3.16 mg/L, $\log K_{ow}$ = 1.92) (Monteil-Rivera *et al.* 2004) may favor the absorption or bioavailability of RDX relative to CL-20 and may help to explain the differences in acute toxicity.

Increased liver-to-BW ratios were observed in the highest dose group (5304 mg CL-20/kg BW/d) at 10 days post-CL-20 exposure, whereas the spleen- and heart-to-BW ratios were not significantly altered compared with controls. This effect contrasts with the earlier results showing decreased liver-to-BW ratios observed for northern bobwhite exposed to RDX in feed (Gogal *et al.* 2003). Birds exposed to RDX for 14 days caused

significant increases in hematologic parameters such as heterophil counts and the heterophil-to-lymphocyte ratio as well as an increase in PCV (Gogal *et al.* 2003). In contrast, our study using CL-20 did not show an effect of exposure on the heterophil-to-lymphocyte ratio or PCV, suggesting that CL-20 is not an immunotoxicant or a mitogen, at least not during this period of exposure. It is possible that immunologic effects may have occurred but were reversed during our exposure schedule that allowed 10 days of no exposure to CL-20.

In conclusion, although CL-20 has certain structural similarities to the monocyclic nitramine RDX (Fig. 1), this polycyclic nitramine does not appear to demonstrate the same profile of toxicities as RDX in quail. Our present study has provided basic toxicity data and suggests that further research should be carried out to study the developmental effects of CL-20 in birds.

Acknowledgments. We thank Fanny Monteil-Rivera and Mark S. Johnson for their review of an earlier version of the manuscript. In addition, we thank Manon Sarrazin, Sabine Dodard, and Louise Paquet from Biotechnology Research Institute (National Research Council of Canada) for their technical assistance; the United States Strategic Environmental Research and Development Program (SERDP Project No. CP1256) for financial support; and Thiokol Propulsion Inc. for providing the ϵ -CL-20. This article was assigned NRC publication 47222.

References

- ASTM (1997) Standard practice for conducting subacute dietary toxicity tests with avian species. American Society for Testing and Materials, West Conshohocken, PA
- Bhushan B, Halasz A, Hawari J (2004a) Nitroreductase catalyzed biotransformation of CL-20. *Biochem Biophys Res Commun* 322:271–276
- Bhushan B, Halasz A, Spain JC, Hawari J (2004b) Initial reaction(s) in biotransformation of CL-20 is catalyzed by salicylate 1-monooxygenase from *Pseudomonas* sp. Strain ATCC 29352. *Appl Environ Microbiol* 70:4040–4047
- Canadian Council on Animal Care (1984) Japanese quail. In: Guide to the care and use of experimental animals. Available at: http://www.ccac.ca/en/CCAC_programs/Guidelines_Policies/GUIDES/ENGLISH/TOC_V2.htm. Accessed: 11 April 2005
- Geetha M, Nair UR, Sarwade DB, Gore GM, Asthana SN, Singh H (2003) Studies on CL-20: The most powerful high energy material. *J Therm Anal Cal* 73:913–922
- Gogal RM, Johnson MS, Larsen CT, Prater MR, Duncan RB, Ward DL *et al.* (2003) Dietary oral exposure to 1,3,5-trinitro-1,3,5-triazine in the northern bobwhite (*Colinus virginianus*). *Environ Toxicol Chem* 22:381–387
- Gong P, Sunahara GI, Rocheleau S, Dodard SG, Robidoux PY, Hawari J (2004) Preliminary ecotoxicological characterization of a new energetic substance, CL-20. *Chemosphere* 56:653–658
- Gregus Z, Watkins JB, Thompson TN, Harvey MJ, Rozman K, Klaassen CD (1983) Hepatic phase I and phase II biotransformations in quail and trout: Comparison to other species commonly used in toxicity testing. *Toxicol Appl Pharmacol* 67:430–441
- Hamburger V, Hamilton HL (1951) A series of normal stages in the development of the chick embryo. *J Morphol* 88:49–92
- Johnson MS, Paulus HI, Salice CJ, Checkai RT, Simini M (2004) Toxicologic and histopathologic response of the terrestrial salamander *Phethodon cinereus* to soil exposure of 1,3,5-trinitrohexahydro-1,3,5-triazine. *Arch Environ Contam Toxicol* 47:496–501
- Levine BS, Furedi EM, Gordon DE, Burns JM, Lish PM (1981) Thirteen-week toxicity study of hexahydro-1,3,5-trinitro-1,3,5-triazine (RDX) in Fischer 344 rats. *Toxicol Lett* 8:241–245
- Monteil-Rivera F, Paquet L, Deschamps S, Balakrishnan VK, Beaulieu C, Hawari J (2004) Physico-chemical measurements of CL-20 for environmental applications: Comparison with RDX and HMX. *J Chromatogr A* 1025:125–132
- Nielsen AT, Chafin AP, Christian SL, Moore DW, Nadler MP, Nissan RA *et al.* (1998) Synthesis of polyazapolycyclic caged polynitramines. *Tetrahedron* 54:11793–11812
- OECD (1984a) OECD guidelines for testing of chemicals. Avian dietary toxicity test. Organization for Economic Cooperation and Development, Paris, France
- OECD (1984b) OECD guidelines for testing of chemicals. Avian reproduction test. Organization for Economic Cooperation and Development, Paris, France
- Robidoux PY, Sunahara GI, Savard K, Berthelot Y, Dodard S, Martel M, *et al.* (2004) Acute and chronic toxicity of the new explosive CL-20 to the earthworm (*Eisenia andrei*) exposed to amended natural soils. *Environ Toxicol Chem* 23:1026–1034
- Schneider NR, Bradley SL, Andersen ME (1976) Toxicology of cyclotrimethylene-trinitramine (RDX): Distribution and metabolism in the rat and miniature swine AFRR1 SR76-34. Armed Forces Radiobiology Research Institute, Bethesda, MD
- Talmage SS, Opresko DM, Maxwell CJE, Welsh JE, Cretella FM, Reno PH, *et al.* (1999) Nitroaromatic munition compounds: Environmental effects and screening values. *Rev Environ Contam Toxicol* 161:1–156
- USEPA (1996a) Avian dietary toxicity tests ecological effects guidelines. EPA 712/C/96/140. United States Environmental Protection Agency
- USEPA (1996b) Avian reproduction test ecological effects guidelines. EPA 712/C/96/141. United States Environmental Protection Agency
- USEPA (1998) Nitroaromatics and nitramines by high performance liquid chromatography (HPLC)-Method 8330A. In: Test methods for evaluating solid waste, physical/chemical methods. SW-846 update III, part 4:1 (B). United States Environmental Protection Agency Office of Solid Waste

Stereo-specificity for pro-(*R*) hydrogen of NAD(P)H during enzyme-catalyzed hydride transfer to CL-20

Bharat Bhushan, Annamaria Halasz, Jalal Hawari *

Biotechnology Research Institute, National Research Council of Canada, 6100 Royalmount Avenue, Montreal, Que., Canada H4P 2R2

Received 20 September 2005

Available online 5 October 2005

Abstract

A dehydrogenase from *Clostridium* sp. EDB2 and a diaphorase from *Clostridium kluyveri* were reacted with CL-20 to gain insights into the enzyme-catalyzed hydride transfer to CL-20, and the enzyme's stereo-specificity for either pro-*R* or pro-*S* hydrogens of NAD(P)H. Both enzymes biotransformed CL-20 at rates of 18.5 and 24 nmol/h/mg protein, using NADH and NADPH as hydride-source, respectively, to produce a N-denitrohydrogenated product with a molecular weight of 393 Da. In enzyme kinetics studies using reduced deuterated pyridine nucleotides, we found a kinetic deuterium isotopic effect of 2-fold on CL-20 biotransformation rate using dehydrogenase enzyme against (*R*)NADD as a hydride-source compared to either (*S*)NADD or NADH. Whereas, in case of diaphorase, the kinetic deuterium isotopic effect of about 1.5-fold was observed on CL-20 biotransformation rate using (*R*)NADPD as hydride-source. In a comparative study with LC–MS, using deuterated and non-deuterated NAD(P)H, we found a positive mass-shift of 1 Da in the N-denitrohydrogenated product suggesting the involvement of a deuteride (D^-) transfer from NAD(P)D. The present study thus revealed that both dehydrogenase and diaphorase enzymes from the two *Clostridium* species catalyzed a hydride transfer to CL-20 and showed stereo-specificity for pro-*R* hydrogen of NAD(P)H.

© 2005 Elsevier Inc. All rights reserved.

Keywords: CL-20; *Clostridium* sp.; Dehydrogenase; Diaphorase; Hydride transfer

CL-20 (2,4,6,8,10,12-hexanitro-2,4,6,8,10,12-hexaazaisowurtzitane) is a newly synthesized future-generation energetic chemical [1] which may replace the conventionally used explosives such as hexahydro-1,3,5-trinitro-1,3,5-triazine (RDX), octahydro-1,3,5,7-tetranitro-1,3,5,7-tetrazocine (HMX), and 2,4,6-trinitrotoluene (TNT) [2]. It is likely that extensive use of CL-20 in the near future may also raise similar environmental, biological, and health concerns as those previously experienced with other cyclic nitramines such as RDX and HMX [3–5]. Recent toxicological studies have shown the adverse effects of CL-20 in various biological receptors [6–8].

Several previous studies have shown that CL-20 can be degraded by microorganisms such as *Pseudomonas* sp. FA1, *Clostridium* sp. EDB2, *Agrobacterium* sp. strain

JS71, and white-rot fungi [9–12], by enzymes e.g., monooxygenase, nitroreductase, and dehydrogenase [10,13,14], and by indigenous degraders present in soils and sediments [15,16]. However, none of these reports has emphasized on the mechanism of hydride-transfer to CL-20.

Previously, a DT-diaphorase from rat liver catalyzed a hydride transfer from NADPH to a nitramine compound, 2,4,6-trinitrophenyl-*N*-methylnitramine (Tetryl), to produce a corresponding N-denitrohydrogenated product [17]. In another report, a diaphorase from *Clostridium kluyveri* catalyzed a hydride transfer to a cyclic nitramine compound, RDX, followed by N-denitration [18]. Based on the stoichiometry of NADH consumed per reacted RDX molecule, Bhushan et al. [18] proposed the formation of a corresponding N-denitrohydrogenated product. The latter, however, could not be detected probably due to its very short half-life. More recently, a dehydrogenase enzyme from *Clostridium* sp. EDB2 degraded CL-20 via the formation of

* Corresponding author. Fax: +1 514 496 6265.

E-mail address: jalal.hawari@nrc.ca (J. Hawari).

the N-denitrohydrogenated product [10]. None of the above studies elaborated on the enzyme's stereo-specificity for either pro-*R* or pro-*S* hydrogens of NADH.

In the present study, we employed two enzymes, a dehydrogenase from *Clostridium* sp. EDB2, and a diaphorase from *C. kluyveri*, to study the enzyme-catalyzed hydride transfer to CL-20, and to gain insights into the enzyme's stereo-specificity for either pro-*R* or pro-*S* hydrogens of NAD(P)H. We used LC–MS (ES[−]) to detect a mass-shift in the N-denitrohydrogenated product following CL-20 reactions with NAD(P)H and NAD(P)D as a hydride-source. Hydrogen–deuterium exchange between the ND-group of N-denitrohydrogenated product and the water was also examined during the reaction.

Materials and methods

Chemicals. CL-20 (2,4,6,8,10,12-hexanitro-2,4,6,8,10,12-hexaazaisowurtzitane) in ϵ -form and 99.3% purity was provided by ATK Thiokol Propulsion, Brigham City, UT, USA. NAD⁺, NADP⁺, ATP, 2-propanol-*d*₈, ethanol-*d*₅, alcohol dehydrogenase, D-glucose-*d*₁, glucose-6-phosphate dehydrogenase, and hexokinase were purchased from Sigma–Aldrich chemicals, Oakville, Ont., Canada. All other chemicals were of the highest purity grade.

Enzymes preparation. A dehydrogenase enzyme was isolated and purified from *Clostridium* sp. EDB2 as described before [10]. A diaphorase (EC 1.8.1.4) from *C. kluyveri* was obtained as a lyophilized powder from Sigma chemicals, Oakville, Ont., Canada. The enzyme was suspended in 50 mM potassium phosphate buffer (pH 7.0) and filtered through a Biomax-5K membrane filter (Sigma chemicals) before resuspending into the same buffer. The native enzyme activity of diaphorase was estimated spectrophotometrically at 340 nm (as per company guidelines) as the rate of oxidation of NADH using 2,6-dichlorophenol-indophenol as an electron acceptor.

Synthesis of deuterated and non-deuterated pyridine nucleotides. (R)NADD was synthesized by the method described by Ganzhorn and Plapp [19] with some modifications. A total of 25 mM NAD⁺, 200 mM ethanol-*d*₅, and 75 U alcohol dehydrogenase were dissolved in 5 mL of 50 mM Tris-buffer, pH 9.0. The reaction was allowed to proceed at 37 °C, and the formation of (R)NADD was monitored by following the increase in absorbance at 340 nm. When no further increase in the OD₃₄₀ was observed, the enzyme was separated from the reaction mixture using 10 kDa molecular weight cutoff filter (Centriprep YM10, Amicon Bio-separations, Bedford, MA).

(S)NADD was synthesized by the modified method described by Sucharitakul et al. [20]. The reaction mixture was composed of: 25 mM NAD⁺, 35 mM D-glucose-*d*₁, 80 mM ATP, and 75 U each of hexokinase and glucose-6-phosphate dehydrogenase in 4 mL of 100 mM phosphate-buffer at pH 8.0. The reaction was allowed to proceed at room temperature until a maximum absorbance was achieved at 340 nm. Enzymes were removed with 5 kDa molecular weight cutoff filter. For proper controls, non-deuterated (S)NADH and (R)NADH were also synthesized by utilizing the non-deuterated components and by using the identical procedures that were used for (S)NADD and (R)NADD, respectively.

Furthermore, (R)NADPD and (S)NADPD were synthesized by the methods described by Pollock and Barber [21]. Non-deuterated (S)NADPH and (R)NADPH were also synthesized by utilizing the non-deuterated components and by using the identical procedures that were used for (S)NADPD and (R)NADPD, respectively.

Biotransformation assays. Enzyme catalyzed biotransformation assays were performed under anaerobic conditions in 6 ml glass vials. Anaerobic conditions were created by purging the reaction mixture with argon gas for 20 min in sealed vials. Each assay vial contained, in 1 mL assay mixture, CL-20 (25 μ M or 11 mg/L), NADH(D) or NADPH(D) (200 μ M), enzyme preparation (250 μ g), and potassium phosphate buffer (50 mM, pH 7.0).

Reactions were performed at 30 °C. Three different controls were prepared by omitting either enzyme, CL-20 or NAD(P)H(D) from the assay mixture. Heat-inactivated enzyme was also used as a negative control. NAD(P)H(D) oxidation was measured spectrophotometrically at 340 nm as described before [18]. Samples from the liquid phase in the reaction vials were analyzed periodically for the residual CL-20, and the N-denitrohydrogenated product.

For enzyme kinetics, enzyme and CL-20 reactions were performed at increasing CL-20 concentrations in the presence of NADH(D) in case of dehydrogenase and NADPH(D) in case of diaphorase. The data thus obtained were used to generate standard Lineweaver–Burk plots (double reciprocal plots).

Analytical techniques. CL-20 was analyzed with a LC–MS using a negative electro-spray ionization mode (ES[−]) to produce deprotonated molecular mass ion as described previously [10,22,23]. Whereas, N-denitrohydrogenated product was detected, with a LC–MS, as an [M+TFA][−] adduct at *m/z* 506 Da following addition of trifluoroacetic acid (TFA) in the mobile phase. Protein concentrations were estimated by bicinchoninic acid (BCA) kit (Pierce Chemicals, Rockford, IL) using bovine serum albumin as standard.

Results and discussion

Two purified enzymes, a dehydrogenase from *Clostridium* sp. EDB2 and a diaphorase from *C. kluyveri*, biotransformed CL-20 (I) at rates of 18.5 and 24 nmol/h/mg protein, using NADH and NADPH as a hydride-source, respectively, to produce a denitrohydrogenated product (II) (Fig. 1). The latter had a HPLC-retention time and a molecular mass of 11.8 min and 393 Da (detected as

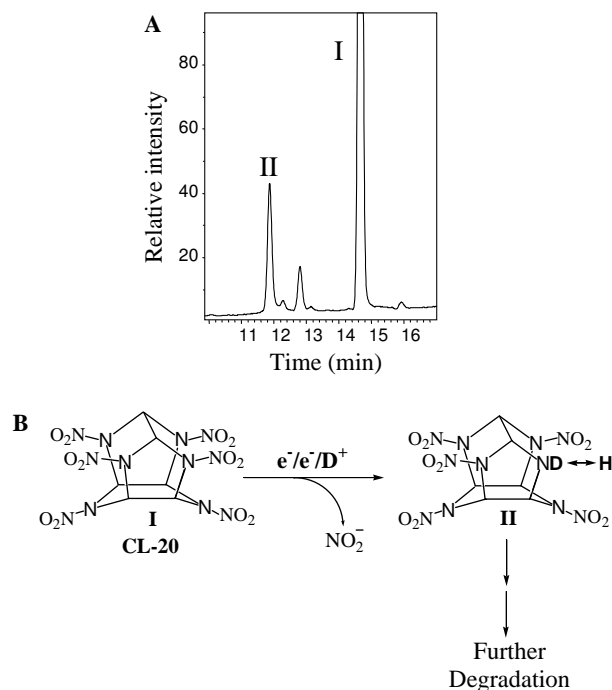


Fig. 1. (A) HPLC–UV chromatogram of CL-20 (I) and N-denitrohydrogenated product (II) obtained during CL-20 reaction with diaphorase from *C. kluyveri* at pH 7.0 and 30 °C. HPLC–UV chromatogram of N-denitrohydrogenated product obtained with dehydrogenase was published elsewhere [10]. (B) Proposed hydride transfer reaction of CL-20 and possible hydrogen–deuterium exchange between ND-group of product II and water.

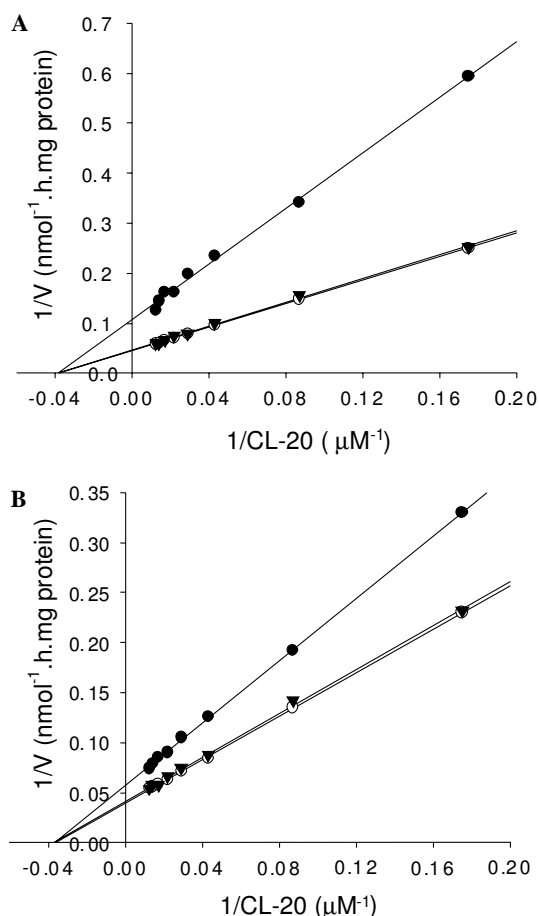


Fig. 2. Standard Lineweaver–Burk plots of CL-20 concentration versus its enzymatic biotransformation rate. (A) Plots using dehydrogenase enzyme from *Clostridium* sp. EDB2 in the presence of either NADH (○), (S)NADD (▼), or (R)NADD (●). (B) Plots using diaphorase enzyme from *C. kluyveri* in the presence of either NADPH (○), (S)NADPD (▼) or (R)NADPD (●). Data are means of the triplicate experiments, and the standard deviations were within 8% of the mean values.

[M+TFA][−] adduct mass at *m/z* 506 Da), respectively. Product II was produced as a result of an obligate transfer of a hydride ion at the N-NO₂ group of CL-20 with the concomitant release of a nitro-group (Fig. 1). The product II, as reported in our previous study, was unstable in water, and therefore readily decomposed to finally produce NO₂[−], N₂O, and HCOOH [10]. Product II was previously detected during photolysis and Fe(0)-mediated degradation of CL-20; however in these reactions, NAD(P)H was not used as reducing agent [22,23]. On the contrary, in enzyme catalyzed reduction reactions, the reduced pyridine nucleotides such as NADH or NADPH mainly serve as the source of hydride [19–21,24].

To understand the stereo-specific effect of pro-*R* and pro-*S* hydrogens on hydride transfer reactions, both enzymes, dehydrogenase and diaphorase, were reacted with CL-20 in the presence of either deuterated or non-deuterated reduced pyridine nucleotides. In case of dehydrogenase enzyme, when Lineweaver–Burk plots of (S)NADD and (R)NADD were compared with that of NADH, we found a 2-fold deuterium isotopic effect with (R)NADD (i.e.,

*V*_{max} was 2-fold less with (R)NADD) compared to NADH, whereas results with (S)NADD were similar to those of NADH (Fig. 2A). This study revealed that dehydrogenase stereo-specifically utilized pro-(*R*)-hydride of NADH for CL-20 reduction and that the isotope effect is due to the cleavage of (4*R*)-deuterium-carbon bond in NADH.

Furthermore, in case of diaphorase, when Lineweaver–Burk plots of (S)NADPD and (R)NADPD were compared with that of NADPH, we found a 1.5-fold deuterium isotopic effect with (R)NADPD compared to NADPH, whereas results with (S)NADPD were closely identical to those obtained with NADPH (Fig. 2B). This study showed that diaphorase stereo-specifically transferred a pro-(*R*)-hydride of NADPH to CL-20 in order to produce denitrohydrogenated product II, and that the isotope effect is due to the cleavage of (4*R*)-deuterium-carbon bond in NADPH.

In order to confirm the presence of hydride, from NAD(P)H, in product II (MW 393 Da), we performed enzymatic reactions with CL-20 in the presence of either NADD or NADPD containing deuterated pro-*R* or deuterated pro-*S* hydrogens. In a comparative study with LC–MS, using dehydrogenase, we found a positive mass-shift of 1 Da in product II using (R)NADD compared to either NADH or (S)NADD, suggesting the involvement of a deuteride (D[−]) transfer from (R)NADD. Surprisingly, the mass signal, corresponding to mono-deuterated product II with MW 394 Da (detected as [M+TFA][−] adduct mass at *m/z* 507 Da), rapidly decreased with time with a concomitant increase in the non-deuterated mass signal corresponding to MW 393 Da (detected as [M+TFA][−] adduct mass at *m/z* 506 Da) (Table 1). Similar results were obtained when diaphorase was reacted with CL-20 in the presence of (R)NADPD (data not shown). The above experimental evidence suggested that the deuterium at ND-group of the product II might be labile, and therefore we detected a rapid exchange of D ↔ H between ND-group and water (Fig. 1B) as marked by the rapidly decreased mass signal of mono-deuterated product II during the course of reaction (Table 1).

Table 1

Time-course of H ↔ D exchange between ND-group of N-denitrohydrogenated product and water as followed with a LC–MS during dehydrogenase catalyzed hydride transfer from (R)NADD to CL-20

Reaction time (min)	Mass signal intensity of N-denitrohydrogenated product	
	Non-deuterated [M _{h7} +TFA] ^a m/z 506 Da	Deuterated [M _{h6,d1} +TFA] ^a m/z 507 Da
Control ^b	216,211	0
0	0	0
5	74,759	2440
10	104,799	578
20	120,673	342

^a Molecular mass of N-denitrohydrogenated product of CL-20 as an adduct with TFA (trifluoroacetic acid).

^b CL-20 was reacted with dehydrogenase in the presence of NADH for 20 min.

Several enzymes have previously been reported to be stereo-specific towards either (*R*)- or (*S*)-hydrogens of NAD(P)H for a hydride transfer to a variety of substrates [19–21,24]. However, the present study is the first one that showed stereo-specificity of two enzymes, dehydrogenase and diaphorase from *Clostridium* species, toward (*R*)-hydrogens of NAD(P)H for a hydride transfer to an environmentally significant cyclic nitramine compound, CL-20. Taken together, the data presented here extend our fundamental knowledge about the role of enzyme-catalyzed hydride transfer reactions in CL-20 biotransformation.

Acknowledgments

We sincerely acknowledge the DoD/DoE/EPA, Strategic Environmental Research and Development Program (SERDP), USA, for financial support (CP 1256). We thank the Department of National Defense (DND), Val Bélair, Canada, for their support. We gratefully acknowledge Mr. Alain Corriveau for analytical and technical support.

References

- [1] A.T. Nielsen, A.P. Chafin, S.L. Christian, D.W. Moore, M.P. Nadler, R.A. Nissan, D.J. Vanderah, Synthesis of polyazapolycyclic caged polynitramines, *Tetrahedron* 54 (1998) 11793–11812.
- [2] J. Giles, Green explosives: collateral damage, *Nature* 427 (2004) 580–581.
- [3] J. Yinon (Ed.), *Toxicity and Metabolism of Explosives*, CRC Press, Boca Raton, Florida, 1990, pp. 145–170.
- [4] S.S. Talmage, D.M. Opresko, C.J. Maxwell, C.J.E. Welsh, F.M. Cretella, P.H. Reno, F.B. Daniel, Nitroaromatic munition compounds: environment effects and screening values, *Rev. Environ. Contam. Toxicol.* 161 (1999) 1–156.
- [5] B. Hoek, Military explosives and health: organic energetic compound syndrome, *Med. Confl. Surviv.* 20 (2004) 326–333.
- [6] P. Gong, G.I. Sunahara, S. Rocheleau, S. Dodard, P.Y. Robidoux, J. Hawari, Preliminary ecotoxicological characterization of a new energetic substance, CL-20, *Chemosphere* 56 (2004) 653–658.
- [7] P.Y. Robidoux, G.I. Sunahara, K. Savard, Y. Berthelot, S. Dodard, M. Martel, P. Gong, J. Hawari, Acute and chronic toxicity of the new explosive CL-20 to the earthworm (*Eisenia andrei*) exposed to amended natural soils, *Environ. Toxicol. Chem.* 23 (2004) 1026–1034.
- [8] G. Bardai, G.I. Sunahara, P.A. Spear, M. Martel, P. Gong, J. Hawari, Effects of dietary administration of CL-20 on Japanese quail *Coturnix japonica*, *Arch. Environ. Contam. Toxicol.* (2005) [published online on July 6].
- [9] B. Bhushan, L. Paquet, J.C. Spain, J. Hawari, Biotransformation of 2,4,6,8,10,12-hexanitro-2,4,6,8,10,12-hexaazaisowurtzitane (CL-20) by a denitrifying *Pseudomonas* sp. FA1, *Appl. Environ. Microbiol.* 69 (2003) 5216–5221.
- [10] B. Bhushan, A. Halasz, J. Hawari, Biotransformation of CL-20 by a dehydrogenase enzyme from *Clostridium* sp. EDB2, *Appl. Microbiol. Biotechnol.* (2005) [published online on April 20].
- [11] S. Trott, S.F. Nishino, J. Hawari, J.C. Spain, Biodegradation of the nitramine explosive CL-20, *Appl. Environ. Microbiol.* 69 (2003) 1871–1874.
- [12] D. Fournier, F. Monteil-Rivera, A. Halasz, M. Bhatt, J. Hawari, Degradation of CL-20 by white-rot fungi, *Chemosphere* (2005) [published online on Aug. 18].
- [13] B. Bhushan, A. Halasz, J.C. Spain, J. Hawari, Initial reaction(s) in biotransformation of CL-20 is catalyzed by salicylate 1-monooxygenase from *Pseudomonas* sp. strain ATCC 29352, *Appl. Environ. Microbiol.* 70 (2004) 4040–4047.
- [14] B. Bhushan, A. Halasz, J. Hawari, Nitroreductase catalyzed biotransformation of CL-20, *Biochem. Biophys. Res. Commun.* 322 (2004) 271–276.
- [15] J.E. Szecsody, D.C. Girvin, B.J. Devary, J.A. Campbell, Sorption and oxic degradation of the explosive CL-20 during transport in subsurface sediments, *Chemosphere* 56 (2004) 593–610.
- [16] N. Strigul, W. Braid, C. Christodoulatos, W. Balas, S. Nicolich, The assessment of the energetic compound 2,4,6,8,10,12-hexanitro-2,4,6,8,10,12-hexaazaisowurtzitane (CL-20) degradability in soil, *Environ. Pollut.* (2005) [published online on July 14].
- [17] Z. Anusevicius, J. Sarlauskas, H. Nivinskas, J. Segura-Aguilar, N. Cenas, DT-diaphorase catalyzes N-denitration and redox cycling of tetryl, *FEBS Lett.* 436 (1998) 144–148.
- [18] B. Bhushan, A. Halasz, J.C. Spain, J. Hawari, Diaphorase catalyzed biotransformation of RDX via N-denitration mechanism, *Biochem. Biophys. Res. Commun.* 296 (2002) 779–784.
- [19] A.J. Ganzhorn, B.V. Plapp, Carboxyl groups near the active site zinc contribute to catalysis in yeast alcohol dehydrogenase, *J. Biol. Chem.* 263 (1988) 5446–5454.
- [20] J. Sucharitakul, P. Chaiyen, B. Entsch, D.P. Ballou, The reductase of *p*-hydroxyphenylacetate 3-hydroxylase from *Acinetobacter baumannii* requires *p*-hydroxyphenylacetate for effective catalysis, *Biochemistry* 44 (2005) 10434–10442.
- [21] V.V. Pollock, M.J. Barber, Kinetic and mechanistic properties of biotin sulfoxide reductase, *Biochemistry* 40 (2001) 1430–1440.
- [22] J. Hawari, S. Deschamps, C. Beaulieu, L. Paquet, A. Halasz, Photodegradation of CL-20: insights into the mechanisms of initial reactions and environmental fate, *Water Res.* 38 (2004) 4055–4064.
- [23] V.K. Balakrishnan, F. Monteil-Rivera, A. Halasz, A. Corbeanu, J. Hawari, Decomposition of polycyclic nitramine explosive, CL-20, by Fe⁰, *Environ. Sci. Technol.* 38 (2004) 6861–6866.
- [24] K.-S. You, Stereospecificities of the pyridine nucleotide-linked enzymes, *Methods Enzymol.* 87 (1982) 101–126.

Bharat Bhushan · Annamaria Halasz · Jalal Hawari

Biotransformation of CL-20 by a dehydrogenase enzyme from *Clostridium* sp. EDB2

Received: 7 March 2005 / Revised: 1 April 2005 / Accepted: 4 April 2005 / Published online: 20 April 2005
© Springer-Verlag 2005

Abstract In a previous study, a marine isolate *Clostridium* sp. EDB2 degraded 2,4,6,8,10,12-hexanitro-2,4,6,8,10,12-hexaazaisowurtzitane (CL-20) under anaerobic conditions (Bhushan B, Halasz A, Thiboutot S, Ampleman G, Hawari J (2004c) Chemotaxis-mediated biodegradation of cyclic nitramine explosives RDX, HMX, and CL-20 by *Clostridium* sp. EDB2. Biochem Biophys Res Commun 316:816–821); however, the enzyme responsible for CL-20 degradation was not known. In the present study, we isolated and purified an enzyme, from strain EDB2, responsible for CL-20 degradation. The enzyme was membrane-associated and NADH-dependent and had a molecular weight of 56 kDa (with SDS-PAGE). N-terminal amino acid sequence of enzyme revealed that it belonged to dehydrogenase class of enzymes. The purified enzyme degraded CL-20 at a rate of 18.5 nmol/h mg protein under anaerobic conditions. Carbon and nitrogen mass balance of the products were 100 and 64%, respectively. In LC–MS–MS studies, we detected three different initial metabolites from CL-20, i.e., mono-nitroso derivative, denitrohydrogenated product, and double-denitrated isomers with molecular weight of 422, 393, and 346 Da, corresponding to presumed empirical formulas of $C_6H_6N_{12}O_{11}$, $C_6H_7N_{11}O_{10}$, and $C_6H_6N_{10}O_8$, respectively. Identity of all the three metabolites were confirmed by using ring-labeled [^{15}N]CL-20 and the nitro-group-labeled [$^{15}NO_2$]CL-20. Taken together, the above data suggested that the enzyme degraded CL-20 via three different routes: *Route A*, via two single electron transfers necessary to release two nitro-groups from CL-20 to produce two double-denitrated isomers; *Route B*, via a hydride transfer necessary to produce a denitrohydrogenated product; and *Route C*, via transfer of two redox equivalents to CL-20 necessary to

produce a mono-nitroso derivative of CL-20. This is the first biochemical study which showed that CL-20 degradation can be initiated via more than one pathway.

Introduction

2,4,6,8,10,12-Hexanitro-2,4,6,8,10,12-hexaazaisowurtzitane (CL-20) is a newly synthesized future-generation energetic chemical (Nielsen et al. 1998), which is likely to replace the conventionally used explosives such as hexahydro-1,3,5-trinitro-1,3,5-triazine (RDX), octahydro-1,3,5,7-tetranitro-1,3,5,7-tetrazocine (HMX), and 2,4,6-trinitrotoluene (TNT) in the future. Initial reports on biological toxicity of CL-20 (Gong et al. 2004; Robidoux et al. 2004) have prompted the research in the area of determining its environmental fate and impacts. It is quite likely that extensive use of CL-20 in the near future (Giles 2004) may also raise similar environmental, biological, and health concerns as those previously experienced with structurally similar cyclic nitramines such as RDX and HMX (Etnier and Hartley 1990; Hoek 2004; McLellan et al. 1988; Talmage et al. 1999; Woody et al. 1986; Yinon 1990).

Several previous reports on microbial (*Pseudomonas* sp. FA1) (Bhushan et al. 2003), enzymatic (salicylate 1-mono-oxygenase and nitroreductase) (Bhushan et al. 2004a,b), and chemical (alkali hydrolysis) (Balakrishnan et al. 2003) degradation of CL-20 have shown that this compound can be degraded via an initial N-denitration route. Recently, it was found that photodegradation and Fe(0)-mediated degradation of CL-20 occurred via three different routes as shown in Fig. 1, i.e., N-denitration (route A), N-denitrohydrogenation (route B), and formation of mono-nitroso derivative of CL-20 (route C) (Balakrishnan et al. 2004; Hawari et al. 2004). However, no biological reaction has been reported so far, which showed that CL-20 biotransformation can proceed through a route other than initial N-denitration.

In our previous study, we showed that *Clostridium* sp. EDB2 degraded CL-20 under anaerobic conditions (Bhushan et al. 2004c); however, the enzyme responsible for CL-20

B. Bhushan · A. Halasz · J. Hawari (✉)
Biotechnology Research Institute,
National Research Council of Canada,
6100 Royalmount Avenue,
Montreal, Quebec, H4P 2R2, Canada
e-mail: jalal.hawari@nrc.ca
Tel.: +1-514-4966267
Fax: +1-514-4966265

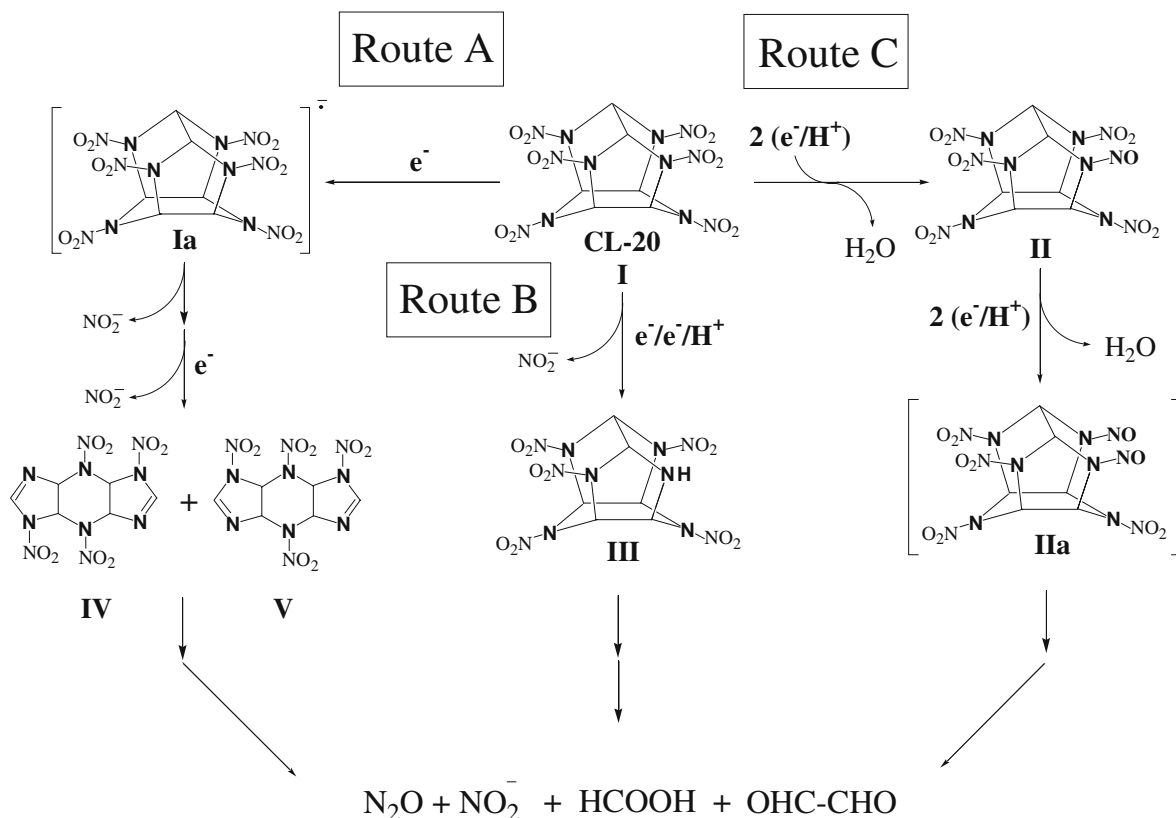


Fig. 1 Proposed pathway of biotransformation of CL-20 catalyzed by a dehydrogenase enzyme from *Clostridium* sp. EDB2. Intermediates shown inside bracket were not detected

degradation was not known. Therefore, the objective of the present study was to isolate and purify the enzyme(s), responsible for CL-20 degradation, from strain EDB2. LC-MS (ES⁻) was used to determine the initial products and other intermediates produced during CL-20 degradation. We used uniformly ring-labeled [¹⁵N]CL-20 and uniformly nitro-group-labeled [¹⁵NO₂]CL-20 to identify the intermediate(s). Radiolabeled [¹⁴C]CL-20 was used, due to the unavailability of authentic standards, to quantify the initial metabolites (in terms of radioactivity distribution) in order to supplement the product mass balance.

Materials and methods

Chemicals

2,4,6,8,10,12-Hexanitro-2,4,6,8,10,12-hexaazaisowurtzitane (CL-20) in ϵ -form and 99.3% purity, uniformly ring-labeled [¹⁵N]CL-20 (87.6% purity), uniformly nitro-group-labeled [¹⁵NO₂]CL-20 (99.4% purity), and [UL-¹⁴C]CL-20 (96.7% chemical purity, 95.7% radiochemical purity, and specific activity of 294.5 μ Ci/mmol) were provided by ATK Thiokol Propulsion (Brigham City, UT, USA). Nitrous oxide (N₂O) was purchased from Scott Specialty Gases (Sarnia, ON, Canada). All other chemicals were of the highest purity grade.

Enzyme purification and characterization

Cells of *Clostridium* sp. EDB2 were grown as described before (Bhushan et al. 2004c). The cell biomass was washed two times with normal saline and one time with suspension buffer (Tris-HCl 25 mM, sucrose 25 mM, PMSF 1 mM, EDTA 5 mM, DTT 0.5 mM). The washed cell biomass (0.2 g/ml) was subjected to disruption with a French press at 20,000 lb/in². The disrupted cell suspension was centrifuged at 9,000 $\times g$ for 30 min at 4°C to remove cell debris and undrupted cells. The supernatant thus obtained was ultracentrifuged at 165,000 $\times g$ for 1 h at 4°C. The pellet (membrane protein fraction) and supernatant (soluble protein fraction) were separated. The membrane-associated protein fraction was dissociated from the membrane preparation by stirring with 0.2% Triton-X-100 for 1 h in an ice bath. The soluble and insoluble fractions of the membrane preparation were separated by ultracentrifugation, and the soluble membrane fraction, thus obtained, was retained. The low molecular weight proteins and peptides were removed from the soluble membrane fraction using 30 kDa cut off membrane, Centriprep YM30 (Amicon Bioseparations). The partially purified protein fraction was concentrated which showed activity against CL-20 in the presence of NADH under anaerobic conditions. Therefore, this protein fraction was subjected to further purification with ion-exchange chromatography with Q-sepharose column (HiTrap Q XL, Amersham Biosciences) using AKTA protein purification system

(Amersham Pharmacia). Column bed volume and flow rate were 5.0 ml and 1.5 ml/min, respectively. The proteins bound to the column were eluted with step-gradient method using a 20 mM Tris-HCl (pH 8.0) buffer supplemented with an increasing NaCl concentration (i.e., an increment of 50 mM of NaCl after every 7 min).

Enzyme purity and molecular weight were determined with standard SDS-PAGE procedure using 10% polyacrylamide gel (Laemmli 1970). The protein content was determined with a Bicinchoninic acid protein assay kit from Pierce Chemical Company (Rockford, IL). Enzyme specificity for electron donor was determined by assaying the enzyme against CL-20 in the presence of either NADH or NADPH. K_m and V_{max} values against CL-20 were determined with standard Lineweaver-Burk's plots.

N-terminal amino acid sequencing

The purified enzyme was blotted onto a polyvinylidene fluoride (PVDF) membrane (Problott membrane AB #400994) using the method as follows: protein sample (about 250 pmol) was subjected to electrophoresis using a mini gel (Mini Protean II, Electrophoresis Cell, Bio-Rad). Thereafter, the gel was soaked in a transfer buffer [10 mM of cyclohexylamino-1-propanesulfonic acid (CAPS) and 10% v/v methanol, pH 11.0] for 5 min. The gel was sandwiched between two sheets of PVDF and assembled into a blotting apparatus (Mini Protean II, Bio-Rad). Electroelution of proteins was carried out at room temperature for 15 min at 250 mA in transfer buffer. After blotting, the PVDF membranes were stained with Coomassie blue R-250. N-terminus sequence of the isolated protein, on PVDF membrane, was obtained by automated Edman degradation performed on a model Procise cLC 494 cLC protein sequencer from Applied Biosystems employing the general protocol of Hewick et al. (1981). About 1 pmol of the protein (on Problott membrane AB #400994) was loaded onto the sequencer. A standard program using liquid-phase TFA was employed for sequencing. The phenylthiohydantoin amino acid (PTH-aa) derivatives were determined by comparison with standards (PTH standards, AB) analyzed on-line on a capillary separation system (ABI 140D).

Biotransformation assays

Enzyme catalyzed biotransformation assays were performed under anaerobic conditions in 6-ml glass vials. Anaerobic conditions were created by purging the reaction mixture with argon gas for 20 min in sealed vials. Each assay vial contained, in 1 ml of assay mixture, CL-20 (25 μ M or 11 mg l^{-1}), NADH (150 μ M), enzyme preparation (250 μ g), and potassium phosphate buffer (50 mM, pH 7.0). Higher CL-20 concentrations, as compared to its aqueous solubility of 3.6 mg l^{-1} , were used in order to allow detection and quantification of the intermediate(s). Reactions were performed at 30°C. Three different controls were prepared by omitting either enzyme, CL-20, or NADH from the assay

mixture. Heat-inactivated enzyme was also used as a negative control. NADH oxidation was measured spectrophotometrically at 340 nm as described before (Bhushan et al. 2002). Samples from the liquid and gas phases in the vials were analyzed for residual CL-20 and biotransformed products.

To determine the residual CL-20 concentrations during biotransformation studies, at each time point, the total CL-20 content in one reaction vial was solubilized in 50% aqueous acetonitrile and analyzed by HPLC (see below). Enzyme activity against CL-20 was expressed as nanomoles per hour per milligrams of protein unless otherwise stated.

CL-20 and its intermediates, glyoxal (OHC-CHO), HCOOH, N_2O , and NO_2 , were analyzed as described previously (Balakrishnan et al. 2004; Bhushan et al. 2003, 2004a,b,c; Hawari et al. 2004). Nitrous oxide detection method (gas chromatograph with electron capture detector) was much more sensitive (lowest detection limit 0.022 nmol/ml) compared to the nitrite detection method (HPLC ion conductivity detector) (lowest detection limit 5.434 nmol/ml).

Due to unavailability of the authentic reference samples of CL-20 intermediates, we quantified the initial metabolites in terms of dpm (radioactivity) counts using radiolabeled [^{14}C]CL-20. A reacted CL-20 sample was injected into HPLC-UV, the fractions corresponding to each metabolite were collected, and the radioactivity (in terms of dpm) associated with them were measured with a liquid scintillation counter (Packard, Tri-Carb 4530, model 2100 TR, Packard Instruments Company, Meriden, CT).

Attempted isolation and purification of metabolite IV, 1,4,5,8-tetranitro-1,3a,4,4a,5,7a,8,8a-octahydro-diimidazo[4,5-b:4',5'-e]pyrazine ($\text{C}_6\text{H}_6\text{N}_{10}\text{O}_8$)

Previously, we hypothesized that metabolite, IV (and its isomer V) (Fig. 1), was unstable in water and decomposes spontaneously to eventually produce N_2O , glyoxal, and HCOOH (Balakrishnan et al. 2004; Bhushan et al. 2004a,b; Hawari et al. 2004). In order to determine the fate of metabolite IV in the degradation pathway, we produced and purified this compound by degrading CL-20 with resting cells of *Clostridium* sp. EDB2. The bacterial cells were grown in anaerobic batch culture containing 1 l of Luria-Bertani broth supplemented with 15 mg l^{-1} of CL-20. The cells were separated by centrifugation, washed three times with normal saline, and suspended in 100 ml of 50 mM phosphate buffer pH 7.0. CL-20 (10 mg) was added to the cell suspension from a stock solution made in acetone. Reaction was performed under anaerobic conditions (under argon atmosphere) for 1 h, and thereafter, cells were removed by centrifugation. The supernatant containing the metabolite(s) was passed through Sep-Pak RDX column (Supelco Co.). Metabolite IV and residual CL-20 were retained on the column. The loaded column was first washed with 10 ml of water followed by 10 ml of 10% aqueous acetonitrile solution. The bound metabolite fractions were

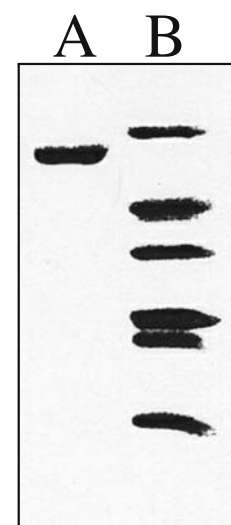
then eluted with 50% aqueous acetonitrile solution. One-milliliter-size fractions were collected and subjected to LC–MS (ES⁺) to follow the elution profile of metabolite IV. The latter was eluted and collected in acetonitrile–water (1:1) mixture. Acetonitrile was evaporated under argon gas, and water phase, containing the metabolite, was lyophilized at -50°C . The dried material, thus obtained, was stored at -20°C . A part of purified metabolite IV was suspended in deionized water and its disappearance was followed over time using LC–MS (ES⁺).

Results and discussion

Enzyme isolation and properties

Previously, we reported that resting cells of strain EDB2 biotransformed CL-20 under anaerobic conditions in the presence of NADH. We detected some end-products including NO_2^- , N_2O , and HCOOH ; however, no other intermediates were detected (Bhushan et al. 2004c). In the present study, we isolated and purified an enzyme, responsible for CL-20 biotransformation, from strain EDB2. Various protein fractions were made from strain EDB2, and their activities against CL-20 were determined under both aerobic and anaerobic conditions. We found that enzyme activity towards CL-20 was largely associated with membrane protein fraction (Table 1). Subsequent ion-exchange chromatography using Q-sepharose gave a purified enzyme fraction at 300 mM NaCl step-elution gradient. The molecular weight of purified enzyme was found to be 56 kDa as determined with standard SDS-PAGE (Fig. 2). The N-terminal amino acid sequence (20 amino acids) of the enzyme was “AVKVAINGFGRIGRLAFRQM.” A comparison with BLAST database revealed that N-terminal amino acid sequence of purified enzyme matched with a variety of de-

Fig. 2 SDS-PAGE picture showing band of purified dehydrogenase enzyme from *Clostridium* sp. EDB2 in lane A, and the standard molecular weight protein markers in lane B (from top to bottom 66, 45, 36, 29, 24, and 14.2 kDa)



hydrogenases from several *Clostridium* spp., e.g., glyceraldehyde-3-phosphate dehydrogenases from *Clostridium pasteurianum* and *Clostridium acetobutylicum*, 20 α -hydroxysteroid dehydrogenase from *Clostridium scindens*, myo-inositol 2-dehydrogenase from *Clostridium tetani*, and Fe–S oxidoreductase from *Clostridium thermocellum* with *E*-values of 8×10^{-9} , 3×10^{-8} , 2×10^{-5} , 0.018, and 0.19, respectively. Therefore, we classified the enzyme, isolated from strain EDB2, in dehydrogenase class.

The enzyme activity against CL-20 under anaerobic and aerobic conditions were 18.5 and 1.6 nmol/h mg protein, respectively, in the presence of NADH, suggesting that anaerobic conditions favored the reaction. As reported in our previous study (Bhushan et al. 2004b), molecular oxygen (O_2) quenches electron from the CL-20 free-radical anion, converting it back to the parent CL-20 molecule and thus enforcing a futile redox cycling. Analogously, in the present study, route A (Fig. 1), being the major pathway of CL-20 biotransformation that occurs via formation of CL-20 free-radical anion (discussed below), was inhibited under aerobic conditions. Therefore, subsequent experiments were carried out under anaerobic conditions. In enzyme-kinetic studies, we found that the purified enzyme degraded CL-20 at a rate of 18.5 and 2.7 nmol/h mg protein (Table 1) in the presence of NADH and NADPH, respectively, indicating that the enzyme was mainly NADH-dependent. The apparent K_m and V_{\max} values against CL-20, determined with standard Lineweaver–Burks plots, were found to be 26.8 μM and 25 nmol/h mg protein, respectively.

Biotransformation of CL-20 with purified enzyme

In a time course study, the biotransformation of CL-20 was accompanied by gradual release of nitrite and nitrous oxide (Fig. 3). The concomitant formation of nitrite with the removal of CL-20 indicated that degradation of the energetic chemical proceeded via initial N-denitration route (Fig. 1a); however, we were not sure whether this was the only degradation route. Contrariwise, the release of nitrous

Table 1 Purification of CL-20 degrading dehydrogenase enzyme from *Clostridium* sp. EDB2

Protein fraction	Total protein (mg)	Total enzyme activity ^a	Specific activity ^b	Yield (%)	Purification-fold
(1) Crude extract	280.0	1,568	5.6	100	1.0
(2) Soluble fraction	202.0	465	2.3	29.6	0.4
(3) Membrane-associated fraction	56.4	547	9.7	34.9	1.7
(4) Membrane fraction washed and concentrated with Centriprep YM30	23.2	283	12.2	18.0	2.1
(5) Ion exchange (Q-sepharose)	5.7	106	18.5	6.7	3.3

^aEnzyme activity was determined against CL-20

^bSpecific activity was determined in terms of nanomoles of CL-20 degraded per hour per milligrams of protein

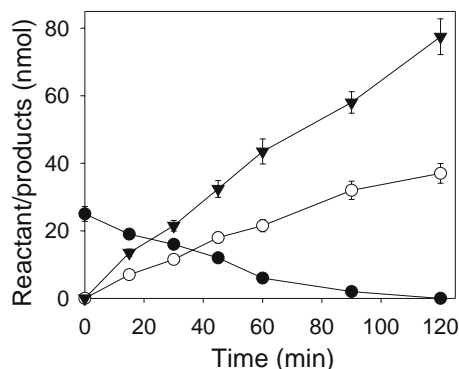


Fig. 3 Time course of biotransformation of CL-20 by the purified enzyme (1 mg) from *Clostridium* sp. EDB2 under anaerobic conditions. Residual CL-20 (●), nitrite (○), and nitrous oxide (▼). Data are means of results from triplicate experiments, and error bars indicate standard errors. Some error bars are not visible due to their small size

oxide from CL-20 was indicative of ring opening and decomposition of the molecule. This is to be noted that CL-20 is unstable in water if kept for longer hours (Monteil-Rivera et al. 2004); however, in the present study, we performed enzymatic reactions for short time period (up to 2 h) and found negligible CL-20 degradation in control experiments without enzyme.

Furthermore, during a time-course reaction using HPLC-UV, we detected three different initial metabolites, II, III, IV (and isomer V), that appeared simultaneously as early as 15 min of the reaction (Fig. 4a). The deprotonated molecular mass ion $[M-H]^-$ of the metabolites, II, IV, and V, as determined with LC-MS (ES⁻) were 421, 345, and 345 Da, corresponding to presumed empirical formulas of $C_6H_6N_{12}O_{11}$, $C_6H_6N_{10}O_8$, and $C_6H_6N_{10}O_8$, respectively (Fig. 4c, e–f). Metabolites IV and V had identical masses and therefore were identified as isomers. However, IV and V were differed in their retention times of 8.65 and 8.10 min, respectively (Fig. 4 and Table 2), most probably due to difference in their polarities. On the other hand, metabolite III was detected as a mass of nitrate adduct $[M+NO_3]^-$ at 455 Da corresponding to a presumed empirical formula of $C_6H_7N_{11}O_{10}$ (Fig. 4d). The retention times and $[M-H]^-$ of all the detected metabolites were closely similar with those detected earlier during Fe(0)-mediated reduction and photodegradation of CL-20 (Balakrishnan et al. 2004; Hawari et al. 2004).

Further confirmation of the above metabolites was carried out by using uniformly ring-labeled $[^{15}N]$ CL-20. The $[M-H]^-$ of products II, IV and V were observed at 427, 351, and 351 Da, respectively, whereas product III was observed as a nitrate adduct $[M+NO_3]^-$ at 461 Da, indicating an increase in mass by 6 Da in each case representing the incorporation of the six $[^{15}N]$ -ring atoms in all the metabolites. Subsequently, when experiment was performed with nitro-group-labeled $[^{15}NO_2]$ CL-20, the $[M-H]^-$ of products II, IV, and V were observed at 427, 349, and 349 Da, respectively. Contrariwise, product III was observed as a nitrate adduct $[M+NO_3]^-$ at 460 Da, indicating the incorporation of six $[^{15}N]$ atoms in II, five $[^{15}N]$ atoms in III, and

only four $[^{15}N]$ atoms in IV and V. Experiments with uniformly ring-labeled $[^{15}N]$ CL-20 and nitro-group-labeled $[^{15}NO_2]$ CL-20 did confirm the identities of II, III, and IV and V as mono-nitroso derivative, denitrohydrogenated product, and double-denitrated product of CL-20, respectively (Fig. 1). All of the above metabolites were transient and disappeared with time to eventually produce nitrite, nitrous oxide, glyoxal, and formate (Figs. 1 and 3). The properties of the above metabolites are described in Table 2.

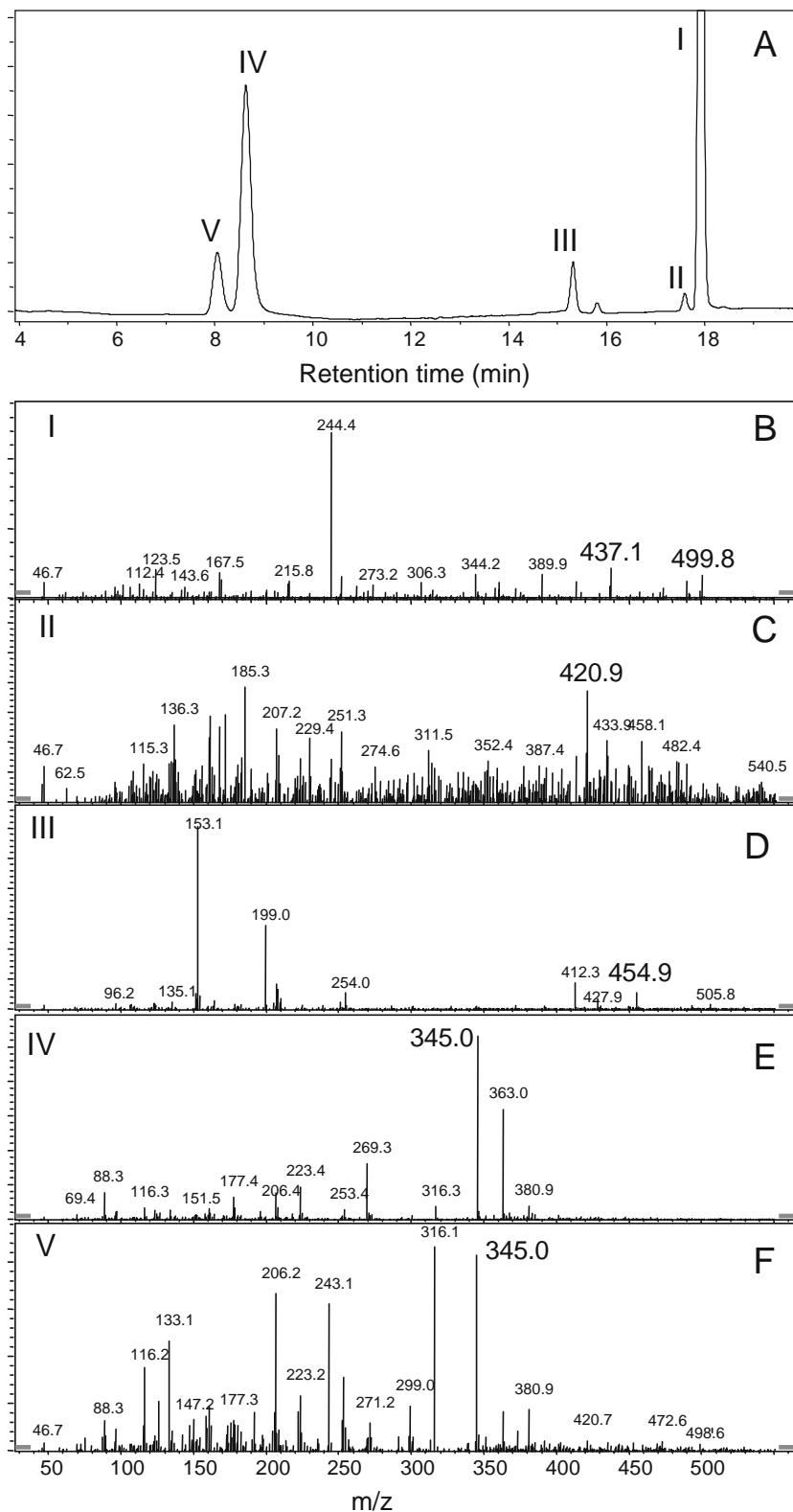
Due to unavailability of authentic standards of CL-20 metabolites, we quantified each metabolite by using ^{14}C -radiolabeled CL-20. Since each of II, III, IV, and V inherited six carbons from the parent CL-20 molecule, the radioactivity associated with each of them and their molar quantities should be comparable with that of CL-20. Therefore, relative quantification of radiolabeled metabolites was carried out by determining the amount of radioactivity (in terms of dpm) associated with each metabolite following their separation and fractionation with HPLC and by comparing them with that of CL-20. Radioactivity distribution associated with metabolites, in terms of percentage of CL-20, has been shown in detail in Table 3. We were able to recover almost 100% of the carbon mass at 15 and 45 min of the time course.

The nitrogen mass balance was determined from a parallel time-course experiment as shown in Fig. 3. At 2-h experiment, we recovered 1.5 mol NO_2^- and 3.1 mol N_2O per reacted mole of CL-20, which accounted for a total of 64% nitrogen. The remaining nitrogen would most probably be present in metabolites III, IV, V, and other unidentified polar products as shown in Table 3.

Insight into the secondary degradation pathway

In our previous studies, we hypothesized that metabolite IV should be unstable in aqueous medium due to the presence of two imine ($-C=N-$) bonds, which are very prone to attack by water molecules (March 1985). We also verified, with LC-MS-MS, the addition of two water molecules to IV using ^{18}O -labeled water ($H_2^{18}O$) and D_2O (Bhushan et al. 2004a; Hawari et al. 2004). In the present study, we isolated and purified IV using resting cells of strain EDB2 (see “Materials and methods”). A part of purified IV was suspended in deionized water and its disappearance was followed over time using LC-MS (Fig. 5a). We found that metabolite IV was unstable in water and was gradually converted to another metabolite IVa (with a $[M-H]^-$ at 381 Da) by the addition of two water molecules across $-C=N-$ bonds. The apparent half-life of IV in deionized water at 10°C was determined as 150 min (Fig. 5a). Furthermore, IVa underwent rearrangement accompanied by ring cleavage to produce metabolite IVb, which also have a $[M-H]^-$ at 381 Da (Fig. 5b). The latter disappeared with time, suggesting that IVb was also unstable in water. Intermediates IV, IVa, and IVb were also detected during enzymatic and photodegradation of CL-20 in aqueous solution (Bhushan et al. 2004a; Hawari et al. 2004), suggesting that initial denitration whether chemical, physical, or biological leads

Fig. 4 (a) LC-UV chromatogram of CL-20 (I) and its metabolites (II–V) produced during the reaction of CL-20 with enzyme from *Clostridium* sp. EDB2. LC/MS (ES[−]) spectra of the deprotonated mass ions $[M-H]^{-}$ of CL-20 (I) and its metabolites II, IV, and V were at 437 Da (b), 421 Da (c), 345 Da (e), and 345 Da (f), respectively, whereas metabolite III was detected as an adduct mass ion $[M+NO_3]^{-}$ at 455 Da (d)



to spontaneous decomposition of the molecule. However, intermediates II and III, as described above, were produced in small amounts and did not persist in the aqueous medium; hence, their fates were not determined.

Taken together, the above data suggested that the enzyme degraded CL-20 via three different routes (Fig. 1): *Route A*, via two single electron transfers necessary to release two nitro-groups from CL-20 to produce two double-denitrated isomers, IV and V; *Route B*, via a hydride transfer necessary

Table 2 Properties of CL-20 and the intermediates detected and identified by LC/MS (ES^-) during biotransformation of CL-20 catalyzed by dehydrogenase from *Clostridium* sp. EDB2

CL-20 and intermediates ^a	Retention time (min)	$[\text{M}-\text{H}]^-$ (Da) ^b	Nitrogen atoms from labeled ring [^{15}N]CL-20	Nitrogen atoms from labeled nitro-groups [$^{15}\text{NO}_2$]CL-20	Proposed empirical formula
(CL-20) I	17.90	437	6	6	$\text{C}_6\text{H}_6\text{N}_{12}\text{O}_{12}$
II	17.60	421	6	6	$\text{C}_6\text{H}_6\text{N}_{12}\text{O}_{11}$
III	15.25	392	6	5	$\text{C}_6\text{H}_7\text{N}_{11}\text{O}_{10}$
IV ^c	8.65	345	6	4	$\text{C}_6\text{H}_6\text{N}_{10}\text{O}_8$
V ^c	8.10	345	6	4	$\text{C}_6\text{H}_6\text{N}_{10}\text{O}_8$

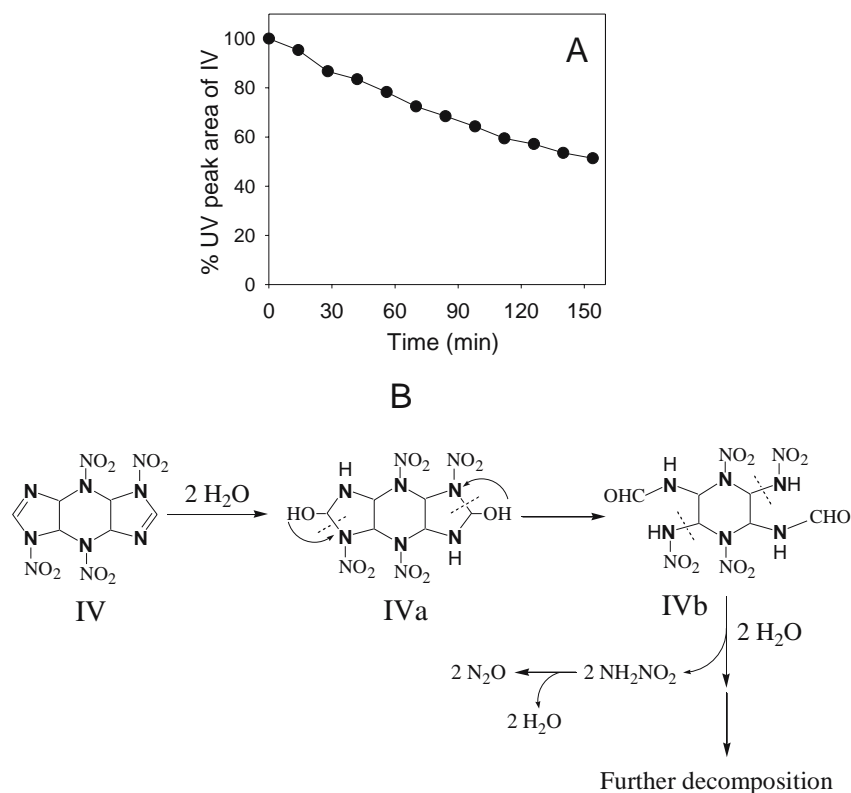
^aTentative structures of these intermediates are shown in Fig. 1^bDeprotonated molecular mass ions are shown in Fig. 4^cIsomeric intermediates differ in their retention time**Table 3** Radioactivity distribution among [^{14}C]CL-20 and its degradation products recovered after 15- and 45-min incubation with dehydrogenase enzyme from strain EDB2

CL-20 and products	Percent of ^{14}C radioactivity counts	
	15 min	45 min
(1) Residual CL-20 (I)	58.2	28.4
(2) Intermediate II ^a	<1.0	Trace amount
(3) Intermediate III ^a	3.3	<1.0
(4) Intermediates (IV and V) ^a	7.0	10.1
(5) Other polar products ^b	33.0	63.2
(6) Total recovery of radioactivity	101.5	101.7

^aThese metabolites are shown in Figs. 1 and 4a^bPolar products contained glyoxal, formate, and unidentified product(s)

to produce a denitrohydrogenated product, III; and *Route C*, via transfer of two redox equivalents necessary to produce a mono-nitroso derivative (II) of CL-20.

In conclusion, we demonstrated for the first time that a dehydrogenase class of enzyme from anaerobic bacterial strain EDB2 biotransformed CL-20 via three different pathways which were previously not known in biological systems. The present data suggested that route A may be a major pathway in CL-20 biodegradation followed by routes B and C (Table 3 and Fig. 1). The present study has further strengthened our previous findings (Balakrishnan et al. 2004; Bhushan et al. 2003, 2004a,b; Hawari et al. 2004) that an initial reaction(s) either via denitration, denitrohydrogenation, and/or nitrosation is necessary and sufficient to destabilize CL-20 molecule leading to its ring opening and decomposition. The data presented here improved our basic

Fig. 5 **a** Abiotic decomposition of metabolite IV in deionized water at 10°C. **b** Proposed decomposition pathway of metabolite IV

understanding of microbial/enzyme-mediated degradation of CL-20 and revealed the possible fate of this energetic chemical in the environment.

Acknowledgements We sincerely acknowledge the DoD/DoE/EPA, Strategic Environmental Research and Development Program (SERDP), USA, for financial support (CP 1256). We also thank the Department of National Defense (DND), Val Bélair, Canada, for their support. We gratefully acknowledge Mr. A. Corriveau and Ms. C. Beaulieu for analytical and technical support. We thank two anonymous reviewers for their helpful suggestions.

References

- Balakrishnan VK, Halasz A, Hawari J (2003) Alkaline hydrolysis of the cyclic nitramine explosives RDX, HMX, and CL-20: new insights into degradation pathways obtained by the observation of novel intermediates. *Environ Sci Technol* 37:1838–1843
- Balakrishnan VK, Monteil-Rivera F, Halasz A, Corbeau A, Hawari J (2004) Decomposition of polycyclic nitramine explosive, CL-20, by Fe^0 . *Environ Sci Technol* 38:6861–6866
- Bhushan B, Halasz A, Spain JC, Hawari J (2002) Diaphorase catalyzed biotransformation of RDX via N-denitration mechanism. *Biochem Biophys Res Commun* 296:779–784
- Bhushan B, Paquet L, Spain JC, Hawari J (2003) Biotransformation of 2,4,6,8,10,12-hexanitro-2,4,6,8,10,12-hexaazaisowurtzitane (CL-20) by a denitrifying *Pseudomonas* sp. FA1. *Appl Environ Microbiol* 69:5216–5221
- Bhushan B, Halasz A, Spain JC, Hawari J (2004a) Initial reaction(s) in biotransformation of CL-20 is catalyzed by salicylate 1-monoxygenase from *Pseudomonas* sp. strain ATCC 29352. *Appl Environ Microbiol* 70:4040–4047
- Bhushan B, Halasz A, Hawari J (2004b) Nitroreductase catalyzed biotransformation of CL-20. *Biochem Biophys Res Commun* 322:271–276
- Bhushan B, Halasz A, Thiboutot S, Ampleman G, Hawari J (2004c) Chemotaxis-mediated biodegradation of cyclic nitramine explosives RDX, HMX, and CL-20 by *Clostridium* sp. EDB2. *Biochem Biophys Res Commun* 316:816–821
- Etnier EL, Hartley WR (1990) Comparison of water quality criterion and lifetime health advisory for hexahydro-1,3,5-trinitro-1,3,5-triazine (RDX). *Regul Toxicol Pharmacol* 11:118–122
- Giles J (2004) Green explosives: collateral damage. *Nature* 427:580–581
- Gong P, Sunahara GI, Rocheleau S, Dodard S, Robidoux PY, Hawari J (2004) Preliminary ecotoxicological characterization of a new energetic substance, CL-20. *Chemosphere* 56:653–658
- Hawari J, Deschamps S, Beaulieu C, Paquet L, Halasz A (2004) Photodegradation of CL-20: insights into the mechanisms of initial reactions and environmental fate. *Water Res* 38:4055–4064
- Hewick RM, Hunkapiller MW, Hood LE, Dreyer WJ (1981) A gas-liquid solid phase peptide and protein sequenator. *J Biol Chem* 256:7990–7997
- Hoek B (2004) Military explosives and health: organic energetic compound syndrome? *Med Confl Surviv* 20:326–333
- Laemmli UK (1970) Cleavage of structural proteins during the assembly of the head of bacteriophage T4. *Nature* 227:680–685
- March J (1985) *Advanced organic chemistry*, 3rd edn. Wiley-Interscience Publication, New York, pp 784–785
- McLellan W, Hartley WR, Brower M (1988) In: Health advisory for octahydro-1,3,5,7-tetranitro-1,3,5,7-tetrazocine. Technical report PB90-273533, Office of Drinking Water, U.S. Environmental Protection Agency, Washington, DC
- Monteil-Rivera F, Paquet L, Deschamps S, Balakrishnan VK, Beaulieu C, Hawari J (2004) Physico-chemical measurements of CL-20 for environmental applications: comparison with RDX and HMX. *J Chromatogr A* 1025:125–132
- Nielsen AT, Chafin AP, Christian SL, Moore DW, Nadler MP, Nissan RA, Vanderah DJ (1998) Synthesis of polyazapolycyclic caged polynitramines. *Tetrahedron* 54:11793–11812
- Robidoux PY, Sunahara GI, Savard K, Berthelot Y, Dodard S, Martel M, Gong P, Hawari J (2004) Acute and chronic toxicity of the new explosive CL-20 to the earthworm (*Eisenia andrei*) exposed to amended natural soils. *Environ Toxicol Chem* 23:1026–1034
- Talmage SS, Opresko DM, Maxwell CJ, Welsh CJE, Cretella FM, Reno PH, Daniel FB (1999) Nitroaromatic munition compounds: environment effects and screening values. *Rev Environ Contam Toxicol* 161:1–156
- Woody RC, Kearns GL, Brewster MA, Turley CP, Sharp GB, Lake RS (1986) The neurotoxicity of cyclotrimethylenetrinitramine (RDX) in a child: a clinical and pharmacokinetic evaluation. *J Toxicol Clin Toxicol* 24:305–319
- Yinon J (1990) In: Toxicity and metabolism of explosives. CRC Press, Boca Raton, FL, pp. 145–170

Indirect Oxidation of RDX, HMX, and CL-20 Cyclic Nitramines in Aqueous Solution at Boron-Doped Diamond Electrodes

Pascale M. L. Bonin,^A Dorin Bejan,^A Zorana Radovic-Hrapovic,^A Annamaria Halasz,^B Jalal Hawari,^B and Nigel J. Bunce^{A,C}

^A Department of Chemistry, University of Guelph, Guelph, Ontario N1G 2W1, Canada.

^B Biotechnology Research Institute, National Research Council of Canada, Montréal, Québec H4P 2R2, Canada.

^C Corresponding author. Email: bunce@chembio.uoguelph.ca

Environmental Context. Nitramine explosives, including RDX, HMX, and the more newly developed CL-20, are the source of groundwater contamination ('pinkwater') especially around military installations. These materials all possess an abundance of nitro (NO_2) groups, which, like synthetic organohalogens, render them resistant to biodegradation and thereby allows them to persist in the soil and waters. In this study it was shown that these substances can be indirectly oxidized at a boron-doped diamond electrode to small molecules (carboxylic acids and mineralized nitrogen-containing compounds).

Abstract. Electrochemical oxidation at boron-doped diamond (BDD) electrodes was examined as a possible technique for the remediation of water contaminated with nitramine explosives. The advantage of BDD is that it promotes indirect oxidation by electrogenerated active intermediates, such as hydroxyl radicals. For the three explosives RDX, HMX, and CL-20, degradation in both acetonitrile/water mixtures and in water alone was suggested to involve an initial denitration, followed by spontaneous decomposition of the molecules, the net result being the complete transformation of the nitramines to small molecules. Although the rate of degradation increased with current density, the current efficiency was highest at low current densities.

Keywords. electrochemistry — electrodes (boron-doped diamond) — explosives — water treatment

Manuscript received: 20 January 2005.

Final version: 3 March 2005.

Introduction

Hexahydro-1,3,5-trinitro-1,3,5-triazine and octahydro-1,3,5,7-tetranitro-1,3,5,7-tetrazocine (RDX and HMX, Fig. 1) are widely used commercial and military explosives.^[1] Their production, usage, and toxicity^[2–5] have resulted in both soil and groundwater contamination,^[6,7] leading to a need for remediation of both process wastewater and contaminated groundwater. Methods proposed include alkaline hydrolysis of RDX and HMX,^[8,9] Fenton oxidation ($\text{H}_2\text{O}_2/\text{Fe}^{2+}$),^[10] enhanced Fenton oxidation through pretreatment with zero-valent iron,^[11] and transformation by iron(II) bound to magnetite.^[12] RDX and HMX have also been found to decompose photochemically,^[13–17] biologically,^[18–24] and, in the case of RDX, electrochemically, both oxidatively and reductively.^[25–27]

CL-20 (2,4,6,8,10,12-hexanitro-2,4,6,8,10,12-hexaazaisowurtzitane, Fig. 1) is a more recently developed polycyclic nitramine explosive with superior explosive properties to RDX and HMX.^[28,29] Relatively little is yet known about its environmental behaviour and fate. Under strongly alkaline conditions, CL-20 spontaneously decomposes to formic acid, nitrous oxide, and ammonium ion.^[9] Similar products, formic

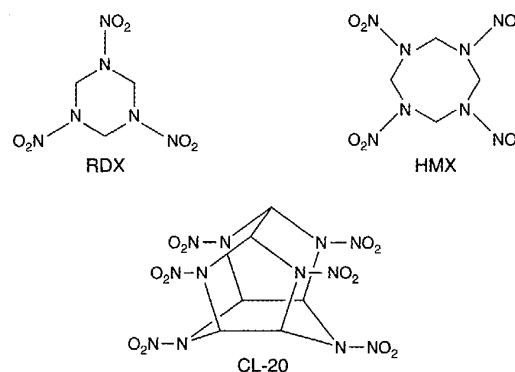


Fig. 1.

acid, nitrous oxide, and nitrite, were observed when CL-20 was degraded by the denitrifying *Pseudomonas* sp. strain FA1.^[30,31] This process involved catalysis by the enzyme salicylate 1-monooxygenase; it involves CL-20 as an electron acceptor that competes with O_2 at the flavin site of the enzyme. In both cases, the degradation proceeded via initial denitration, with the release of nitrite ion, followed by spontaneous ring cleavage.

Electrochemical oxidation of recalcitrant wastes offers an inherently clean technology because oxidation involves removal of electrons rather than addition of chemical oxidants.^[32–34] Moreover, electrons are less costly than chemical reagents.^[35] Advances in oxidative electrochemistry include the development of corrosion-resistant anodes including 'dimensionally stable anodes' (DSAs) such as Ti/IrO₂ and Ti/SnO₂, that consist of a micron-thickness layer of oxide deposited on the base metal, and the newly developed material boron-doped diamond (BDD), which offers an exceptionally wide potential window.^[36] BDD promotes indirect oxidation by electrogenerated active intermediates, such as hydroxyl radicals.^[37] Diamond electrodes are also very stable mechanically^[36] and are resistant to chemical change during electrolysis;^[38] this is why BDD is being recognized as a promising material for the electrochemical oxidation of organics for wastewater treatment.^[32,34,37–40] In the present study, we used BDD electrodes to investigate the oxidative electrochemistry of RDX, HMX, and CL-20, in the context of the remediation of nitramine-contaminated water.

Experimental

Chemicals

RDX (purity >98% by HPLC) was synthesized following a procedure derived from Hale.^[41] Its identity was confirmed by chromatographic comparison to an analytical standard ($\geq 98\%$ pure) from Chem Service Inc. (mp 205.5°C and mmp 208°C). Commercial grade RDX (purity >99%) was provided by Defense Research and Development Canada (DRDC; Valcartier, PQ), as were ring-labelled [¹⁵N]-RDX (purity >98%) and HMX (purity >99%). CL-20 (99.3% purity) and [¹⁵N]-CL-20 were provided by ATK Thiokol (Brigham City, UT). Under normal laboratory illumination, non-degassed solutions of RDX and HMX in acetonitrile (ACN)/H₂O (50/50 v/v) were stable over time, but those of CL-20 had to be freshly prepared before each experiment. Methylenedinitramine (MDNA) was obtained from the Rare Chemical Library of Aldrich, Canada. 4-Nitro-2,4-diazabutanol (4-NDAB) was synthesized by Dr Jeffrey Botaro and Dr Ron Spangord (SRI, Menlo Park, CA). All other chemicals used in this work were reagent grade.

Analysis

Disappearance of RDX, HMX, and CL-20 was monitored using an HPLC system comprising pump (Waters model 600, flow rate 1.0 mL min⁻¹), injector (Rheodyne, 20 μ L sample loop), and tunable absorbance detector (Waters model 486, operated at 240 nm). The data were processed using *Millennium* ver. 3.2 software (Waters). Separations involving RDX, HMX, and CL-20 were achieved on a stainless steel column (Genesis C18, 250 mm \times 4.6 mm). The mobile phase was ACN/H₂O (65/35 v/v) at a flow rate of 1 mL min⁻¹ and 23°C. Under these conditions, retention times for the starting materials were RDX 4.3 \pm 0.1 min, HMX 4.0 \pm 0.1 min, and CL-20 6.5 \pm 0.1 min. Triplicate electrolyses were performed for each condition studied; the reproducibility in any run at each time point was within $\pm 2\%$; apparent first-order rate constants are reported $\pm 1\sigma$. Analyses for RDX, HMX, and CL-20 were also performed using reversed-phase HPLC connected to a photodiode array (PDA) detector, as described previously.^[23,30,31]

Formic acid was measured using an HPLC system comprising pump (Waters model 600 and model 717), autosampler, conductivity detector (Waters model 4300), and column (Dionex Ion Pac AS15, 250 mm \times 2 mm). The mobile phase was 30 mM KOH with a flow rate of 0.4 mL min⁻¹ at 40°C. The detection of formic acid was enhanced by reducing the background with an autosuppressor (Alltech model DS-Plus).

Nitrite and nitrate ions were monitored using an HPLC system comprising pump (Spectra Physics model SP8800/8880), conductivity

detector (Waters model 431), and ion chromatography column (Hamilton PRP-X100, 250 mm \times 4.1 mm). The mobile phase was 2.5% methanol in 4 mM *p*-hydroxybenzoic acid solution adjusted to pH 8.5 with NaOH. Analyses were carried out at 40°C at a flow rate of 2 mL min⁻¹.

Ammonium was analyzed using an HPLC system (Waters 8100 system), conductivity detector (Waters model 431), and analytical cation exchange column (Hamilton PRP-X2009, 250 mm \times 4.6 mm) as described earlier.^[19] The search for gaseous products N₂O, H₂, O₂, N₂, and CH₄ was carried out as described previously.^[19]

Ring-cleavage products of RDX, MDNA, and 4-NDAB, were analyzed using an HPLC system equipped with a diode array detector, as specified in ref. [9]. Glyoxal, a product of CL-20, was analyzed after derivatization^[42] with 20 μ L of a 15 mg mL⁻¹ solution of *O*-2,3,4,5,6-pentafluorobenzylhydroxylamine hydrochloride (PFBHA), which was added to a mixture of aqueous sample (0.5 mL) and acetonitrile (0.5 mL), adjusted to pH 3 with 5% HCl. The reaction mixture was stirred in the dark for 2 h at room temperature then analyzed by LC/UV-MS (Platform LC, Micromass) at a wavelength of 250 nm, and using positive electrospray (ES+) ionization mode. Separation was performed on a Supelcosil C8 column (250 mm \times 4.6 mm) at 35°C using an ACN/H₂O gradient at a flow rate of 1 mL min⁻¹ (from 60% to 90% ACN over 10 min, from 90% to 60% over 2 min, and at 60% for 6 min).

Total organic carbon (TOC) and total nitrogen (TN) measurements were performed using a TOC-VCSN (Shimadzu) analyzer.

Voltammetry

The potentiostat (EG&G model 273A) was fitted with a conventional three-electrode glass cell. Data were processed with *Electrochemistry Power Suite* ver. 2.12.1 software (Princeton Applied Research). The working electrode was a 3-mm diameter boron-doped diamond (BDD) electrode (Windsor Scientific), the counter electrode was a Pt wire, and the reference electrode was a Pt foil (2.5 \times 2.5 cm). The solvent was ACN/H₂O (50/50 v/v), using 0.1 M KCl as supporting electrolyte. Potassium ferricyanide (5 mM) was also present as a reference; the ferri/ferrocyanide couple is a standard redox system to provide benchmark data for diamond electrodes.^[36]

Electrolysis

Electrolyses were carried out under galvanostatic conditions using a potentiostat/galvanostat (model 363, Princeton Applied Research). The plug flow reactor was a flow-through, sandwich type Teflon cell constructed in-house with two inner compartments of 58 mm \times 15 mm \times 4.5 mm each; these were divided for some experiments by a cation-exchange membrane (Nafion 424, DuPont). Teflon tubing was used for all connections. Solutions were delivered using a peristaltic pump (C/L, Masterflex) at a flow rate of 2 mL min⁻¹.

The working electrode was a rectangular (50 mm \times 15 mm \times 1 mm) plaque of BDD on polySi (CSEM, Neuchâtel) with a Ti/Au backside which was connected to a platinum feeder. Trials were also made using a Ti/IrO₂ DSA (Eltech) as working electrode. In all the experiments, the counter electrode was a piece of stainless steel (50 mm \times 15 mm \times 1 mm) with a silver feeder. Solutions of RDX, HMX, or CL-20 (2.0 mM) were electrooxidized in ACN/H₂O (50/50 v/v) at pH 6.0, with 10 mM Na₂SO₄ as supporting electrolyte. For the divided cell experiments, the anolyte was as just described while the catholyte comprised ACN/H₂O (50/50 v/v) with 10 mM Na₂SO₄. In order to mimic contaminated-water scenarios, other experiments employed fully aqueous solutions of 0.24 mM (54.0 mg L⁻¹) RDX, 0.017 mM (4.9 mg L⁻¹) HMX, or 0.0084 mM (3.7 mg L⁻¹) CL-20 (solubility reported in ref. [43]).

In most experiments the reactor was operated in recirculation mode, with the solution exiting the electrolytic cell returned to the storage reservoir. In the experiments using a divided cell, the catholyte was not recirculated. Samples were taken at time intervals (30 min) equivalent to integral numbers of passes through the cell, based on the flow rate (2 mL min⁻¹) and the volume in the reservoir (60 mL). Other experiments were designed to replicate a cascade of reactors. A given volume of solution was passed through the reactor, collected, and then reintroduced

into the reactor, after removing a sample for analysis. The volume of solution was corrected for the aliquot(s) withdrawn.

Results and Discussion

Voltammetry

Cyclic voltammograms of 2.0 mM solutions of RDX, HMX, and CL-20 at a BDD working electrode were recorded from 0 to -2.3 to 0 V at a scan rate of 50 mV s^{-1} in deaerated ACN/ H_2O (50/50 v/v) containing 0.1 M KCl and $5 \text{ mM K}_3\text{Fe}(\text{CN})_6$. During the negative sweep, ferricyanide gave a reduction peak at -0.41 V , with reoxidation of ferrocyanide at -0.15 V . RDX, HMX, and CL-20 showed irreversible reduction peaks at -1.55 , -1.61 , and -1.63 V versus Pt/ PtO_2 , respectively. By comparison with the currents of the ferri/ferrocyanide couple, the reductions of RDX, HMX, and CL-20 all involved 4 ± 0.4 electron transfers. By analogy with our previous work,^[27] we conclude that for all three nitramine explosives, the four-electron change represents reduction of a single *N*-nitro group to the corresponding *N*-hydroxylamine. Cyclic voltammetry of RDX, HMX, and CL-20 in the oxidative direction from 0 to $+2.4$ to 0 V gave no indication of direct oxidation, indicating that electrolytic oxidation of the nitramine explosives must occur indirectly, involving oxidation products from water such as hydroxyl radicals.^[37-40] Consistent with this view, RDX could also be degraded by hydroxyl radicals generated from Fenton chemistry.

Electrolyses

A solution of 2.0 mM RDX in ACN/ H_2O (50/50 v/v) was electrolyzed in a divided cell at a current density of 53 mA cm^{-2} and a flow rate of 1 mL min^{-1} . At a BDD anode, 95% of the RDX had degraded after 180 min; in a divided cell, this shows that the course of the reaction must be oxidative. Essentially no degradation was observed at Ti/ IrO_2 during this time (Fig. 2). We attribute the difference in behaviour between Ti/ IrO_2 and BDD to their different mechanisms of action. At Ti/ IrO_2 , the substrate is oxidized at the electrode itself where a transient 'higher oxide' is formed on the IrO_2 surface. BDD functions chiefly to produce reactive oxidation products from water, such as hydroxyl radicals; these have been detected by 'spin trapping' with a nitron spin trap.^[44]

Removal of the membrane and adjustment of the flow rate to 2 mL min^{-1} , to give similar hydraulic conditions and an equal detention time in the cell, led to slightly faster degradation of RDX ($k_{\text{undiv}} = 0.021 \pm 0.001 \text{ min}^{-1}$ versus $k_{\text{div}} = 0.017 \pm 0.001 \text{ min}^{-1}$). The similarity of these rate constants suggests that the mechanism of degradation must again be principally oxidative, with faster degradation in the undivided cell due to competing reduction of RDX at the stainless steel cathode. Because any hydroxylamine formed by reduction would itself be highly susceptible to attack by hydroxyl radicals, the combination of oxidation at BDD and reduction at stainless steel acted synergistically.

RDX, HMX, and CL-20 degraded readily in the undivided cell under all the electrolysis conditions investigated. At a current density of 53 mA cm^{-2} and flow rate

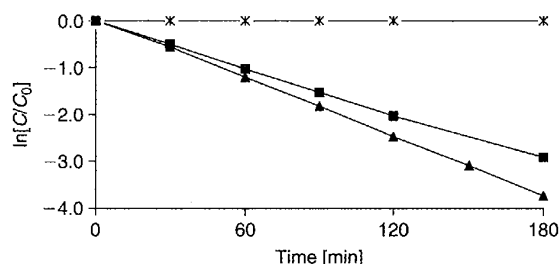


Fig. 2. Electrochemical oxidation of a solution of 2.0 mM RDX in ACN/ H_2O (50/50 v/v) at a current density of 53 mA cm^{-2} . Natural logarithm of the ratio of the concentration to the initial concentration versus time using a Ti/ IrO_2 anode in a divided cell (*), a BDD anode in a divided cell (■), and a BDD anode in an undivided cell (▲).

Table 1. Amounts of starting material, total nitrogen (TN), and total organic carbon (TOC) after each pass through the reactor
Conditions: current density 53 mA cm^{-2} , flow rate of 2 mL min^{-1}

Pass number	Recirculation experiments [%] ^A			Multiple reactor experiments [%] ^B		
	RDX	HMX	CL-20	RDX	TN	TOC
0	100	100	100	100	100	100
1	56	53	49	52	95	84
2	30	28	23	28	95	75
3	16	13	10	17	95	62
4	9	7	5	9	95	58
5	4	4	2	—	—	—
6	2	2	1	—	—	—

^A 2.0 mM nitramine in 50/50 v/v ACN/ H_2O .

^B 54 mg L^{-1} RDX in 100% H_2O .

2 mL min^{-1} , solutions of RDX, HMX, and CL-20 (each 60 mL of 2.0 mM in ACN/ H_2O (50/50 v/v)) electrolyzed at similar rates—apparent first-order rate constants were $k_{\text{RDX}} = 0.021 \pm 0.001 \text{ min}^{-1}$, $k_{\text{HMX}} = 0.022 \pm 0.0004 \text{ min}^{-1}$, and $k_{\text{CL-20}} = 0.026 \pm 0.001 \text{ min}^{-1}$. Again, this suggests similar chemistry for all three nitramines. After six passes through the reactor under recirculation conditions, greater than 98% of all three starting materials had disappeared (Table 1); further electrolysis yielded undetectable concentrations of the starting materials (data not shown). Experiments at lower (1 mM) and higher (4 mM) initial RDX concentrations showed the rate of reaction to be directly proportional to concentration, that is, the apparent first-order rate constant for degradation was independent of substrate concentration (Fig. 3). This is consistent with a bimolecular reaction between substrate and hydroxyl radicals in the bulk solution.

The rate of oxidative degradation of the model compound RDX (2.0 mM) in ACN/ H_2O (50/50 v/v), using a BDD electrode and a flow rate of 2 mL min^{-1} , increased with current density but not linearly—at 40 , 53 , and 80 mA cm^{-2} , $k = 0.018 \pm 0.001$, 0.021 ± 0.001 , and $0.026 \pm 0.0004 \text{ min}^{-1}$. This is also consistent with the hydroxyl radical mechanism: a higher current favours faster water oxidation, but the higher rate of formation of reactive species such as hydroxyl radicals is offset by their faster bimolecular oxidation to molecular O_2 .

Rate constants for the degradation of 2.0 mM RDX in ACN/ H_2O (50/50 v/v) at a BDD anode and current density

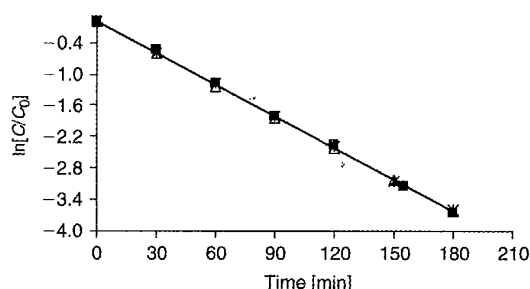


Fig. 3. Electrochemical oxidation of solutions of RDX in ACN/H₂O (50/50 v/v) at a current density of 53 mA cm⁻² and a flow rate of 2 mL min⁻¹. Natural logarithm of the ratio of the concentration to the initial concentration versus time for an initial concentration of 1 mM RDX (■), 2 mM RDX (△), and 4 mM RDX (*).

53 mA cm⁻² were studied as a function of flow rate—at 1, 2, and 3 mL min⁻¹, $k = 0.015 \pm 0.0004$, 0.021 ± 0.001 , and 0.026 ± 0.0001 min⁻¹. This counterintuitive increase in the observed rate constant arises because the experiments were performed in recirculation mode. A faster flow rate means that in each pass, the concentration of substrate is depleted less but more moles of substrate are oxidized per unit time due to recirculation. In parallel single-pass experiments, the degradation rate, based on concentration, fell with increasing flow rate because the residence time of the substrate in the cell was shorter.

Experiments in recirculation mode at a current density of 53 mA cm⁻² and a flow rate of 2 mL min⁻¹ on solutions of RDX, HMX, and CL-20 (each 60 mL of 2.0 mM in ACN/H₂O (50/50 v/v)) showed that 30%, 28%, and 23% respectively of the original material remained unreacted after two passes (60 min, Table 1). In previous work with RDX under reductive conditions,^[27] we detected MDNA and 4-NDAB as intermediates. These were not found in the present study, where smaller molecules, such as formic acid, accounted for only 7% of the carbon mass from RDX. A similar situation was observed for CL-20, where 0.54 mol of formic acid was formed per mol of CL-20 degraded, and glyoxal OHC-CHO, a product specific to CL-20, was detected in trace amounts. Finally, from HMX, no carbon-containing products were detected at significant concentration.

With respect to nitrogenous products, RDX and HMX behaved similarly, each affording one mole of NH₄⁺ and one mole of {NO₃⁻ + NO₂⁻} per mole of nitramine consumed. CL-20 behaved differently, yielding five moles of {NO₃⁻ + NO₂⁻} and one-half mole of NH₄⁺ for each mole degraded. Nitrate ion was always in considerable excess over nitrite—from RDX and CL-20, the ratio NO₃⁻ : NO₂⁻ was ~9 : 1 and from HMX only NO₃⁻ was detected. The stoichiometry suggests that nitrate ion is formed by attack of OH[•] at a nitro group of the nitramine, initially forming HNO₃ and an amino radical, consistent with the well known propensity of OH radicals to add faster to unsaturated centres than to abstract hydrogen from C—H groups, Eqn (1):^[45]

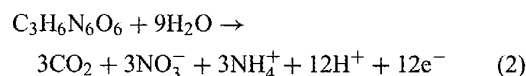


In the undivided cell, some of the nitrate ion can be reduced to NO₂⁻,^[46] and subsequently to N₂O, which was also detected

in trace amounts. The stoichiometry suggests that while the nitro groups are converted principally to nitrate, the ring nitrogen atoms are ultimately released in equivalent molar yield as ammonia, at least from RDX and HMX. The more complex structure of CL-20 makes ammonia extrusion less facile.

Further work was carried out on solutions of RDX (54.0 mg L⁻¹) in 100% H₂O at a current density of 53 mA cm⁻² and a flow rate of 2 mL min⁻¹ (Table 1). Consistent with the results in ACN/H₂O, 28% of the RDX was still present after two passes, while 9% was left after four passes. There was excellent agreement between the rates of degradation in ACN/H₂O (50/50 v/v) and pure water for all three nitramine explosives. TN and TOC analyses were performed with electrolyzed solutions of RDX, but not with HMX and CL-20 due to their low solubility (<5 mg L⁻¹). TN analysis showed that essentially none of the nitrogen of RDX was lost from solution, even when the original substrate had been almost completely mineralized, consistent with conversion into simple inorganic ions. TOC analyses indicated that soluble organic species persisted in solution longer than the starting material RDX. After two passes, 28% of the original RDX still remained, but 75% of the carbon mass was still present in solution; after four passes, with only 9% of the RDX remaining, 58% of the carbon mass was still present (Table 1). This lag time between the degradation of the RDX molecules and complete mineralization is consistent with the presence of small-molecule, non-UV-absorbing species in solution, such as small carboxylic acids.

Current efficiencies (CE) were calculated assuming a one electron transfer, as described previously.^[27] After one pass at a current density of 53 mA cm⁻² and a flow rate of 2 mL min⁻¹, the concentration of RDX in water had decreased from 0.24 to 0.12 mM (apparent CE 0.1%); while for a current density of 1.3 mA cm⁻², the concentration decreased from 0.24 to 0.21 mM (apparent CE 1%). However, this simple calculation ignores the influence of complete mineralization on the current efficiency.



At the early stages of reaction, about half the lost RDX was mineralized, suggesting overall current efficiencies in the range 0.6–6% for the range of current studied (400–10 mA). These low current efficiencies are consistent with the hydroxyl radical mechanism, in that a significant amount of the current goes unproductively into release of O₂. The bimolecular combination of water oxidation intermediates, such as hydroxyl radicals, is inevitably promoted at higher current. From the practical perspective, there is a tension between raising the rate of reaction by increasing the current and increasing the current efficiency, which requires low currents.

Conclusions

This study confirms that indirect oxidation at BDD electrodes can be successfully employed to electrochemically

oxidize nitramine-contaminated water, which is an important environmental issue in the context of pollutant plumes from military sites. For the three explosives studied, RDX, HMX, and CL-20, degradation was found to occur at comparable rates. TOC and TN analyses showed that the ultimate fate of the substrate is oxidation to small molecules and ions, though this process lagged behind the disappearance of substrate. The rate of degradation increased with current density, but the current efficiency was highest at low current densities.

Acknowledgements

Financial support was provided by the Natural Sciences and Engineering Research Council of Canada through a Post-doctoral Fellowship to P.M.L.B. and a research grant to N.J.B., and by the USA Strategic Environmental Research and Development Program (DOE, DOD, and EPA).

References

- [1] J. Hawari, A. Halasz, *The Encyclopedia of Environmental Microbiology* **2002**, pp. 1979–1993 (John Wiley & Sons: New York, NY).
- [2] W. McLellan, W. R. Hartley, M. Brower, *Health Advisory for Hexahydro-1,3,5-trinitro-1,3,5-triazine. Technical Report PB90-273533* **1988** (US EPA: Washington, DC).
- [3] J. Yinon, *Toxicity and Metabolism of Explosives* **1990** (CRC Press: Boca Raton, FL).
- [4] S. S. Talmage, D. M. Opreko, C. J. Maxwell, C. J. E. Welsh, F. M. Cretella, P. H. Reno, F. B. Daniel, *Rev. Environ. Contam. Toxicol.* **1999**, *161*, 1.
- [5] P. Y. Robidoux, J. Hawari, S. Thiboutot, G. Ampleman, G. Sunahara, *Environ. Pollut.* **2001**, *111*, 283. doi:10.1016/S0269-7491(00)00070-1
- [6] T. C. Schmidt, K. Steinbach, E. von Low, G. Stork, *Chemosphere* **1998**, *37*, 1079. doi:10.1016/S0045-6535(98)00106-4
- [7] C. A. Myler, W. Sisk, *Environmental Biotechnology for Waste Treatment* (Eds G. S. Sayler, R. Fox, J. W. Blackburn) **1991**, pp. 137–146 (Plenum Press: New York, NY).
- [8] J. C. Hoffsommer, D. A. Kubose, D. J. Glover, *J. Phys. Chem.* **1977**, *81*, 380.
- [9] V. K. Balakrishnan, A. Halasz, J. Hawari, *Environ. Sci. Technol.* **2003**, *37*, 1838. doi:10.1021/ES020959H
- [10] K.-D. Zoh, M. K. Strenstrom, *Water Res.* **2002**, *36*, 1331. doi:10.1016/S0043-1354(01)00285-8
- [11] S.-Y. Oh, P. C. Chiu, B. J. Kim, D. K. Cha, *Water Res.* **2003**, *37*, 4275. doi:10.1016/S0043-1354(03)00343-9
- [12] K. B. Gregory, P. Larese-Casanova, G. F. Parkin, M. M. Scherer, *Environ. Sci. Technol.* **2004**, *38*, 1408. doi:10.1021/ES034588W
- [13] D. J. Glover, J. C. Hoffsommer, *Photolysis of RDX. Identification and Reaction of Products. Technical Report NSWC TR-79-349* **1979** (Naval Surface Weapons Center: Silver Spring, MD).
- [14] P. Bose, W. H. Glaze, D. S. Maddox, *Water Res.* **1998**, *32*, 1005. doi:10.1016/S0043-1354(97)00308-4
- [15] R. Alnaizy, A. Akgerman, *Water Res.* **1999**, *33*, 2021. doi:10.1016/S0043-1354(98)00424-2
- [16] J. Hawari, A. Halasz, C. Groom, S. Deschamps, L. Paquet, C. Beaulieu, A. Corriveau, *Environ. Sci. Technol.* **2002**, *36*, 5117. doi:10.1021/ES0207753
- [17] M.-J. Liou, M.-C. Lu, J.-N. Chen, *Water Res.* **2003**, *37*, 3172. doi:10.1016/S0043-1354(03)00158-1
- [18] N. G. McCormick, J. H. Cornell, A. M. Kaplan, *Appl. Environ. Microbiol.* **1981**, *42*, 817.
- [19] J. Hawari, A. Halasz, T. Sheremata, S. Beaudet, C. Groom, L. Paquet, C. Rhofir, G. Ampleman, S. Thiboutot, *Appl. Environ. Microbiol.* **2000**, *66*, 2652. doi:10.1128/AEM.66.6.2652-2657.2000
- [20] C. Groom, S. Beaudet, A. Halasz, L. Paquet, J. Hawari, *J. Chromatogr. A* **2001**, *909*, 53. doi:10.1016/S0021-9673(00)01043-8
- [21] C. Groom, A. Halasz, L. Paquet, N. Morris, L. Olivier, C. Dubois, J. Hawari, *Environ. Sci. Technol.* **2002**, *36*, 112. doi:10.1021/ES0110729
- [22] B. Bhushan, A. Halasz, J. Spain, S. Thiboutot, G. Ampleman, J. Hawari, *Environ. Sci. Technol.* **2002**, *36*, 3104. doi:10.1021/ES011460A
- [23] D. Fournier, A. Halasz, J. Spain, P. Fiurasek, J. Hawari, *Appl. Environ. Microbiol.* **2002**, *68*, 166. doi:10.1128/AEM.68.1.166-172.2002
- [24] S. Campbell, R. Ogoshi, G. Uehara, Q. X. Li, *Paper ENVR-097 in 227th ACS National Meeting 2004* (ACS: Washington, DC).
- [25] A. M. Martins, M. Ferreira, G. Tremiliosi-Filho, *Abstract 789 in Proc. 200th Electrochemical Society Meeting 2001* (The Electrochemical Society: Pennington, NJ).
- [26] R. B. Doppalapudi, G. A. Sorial, S. W. Maloney, *Environ. Eng. Sci.* **2002**, *19*, 115. doi:10.1089/10928750252953741
- [27] P. M. L. Bonin, D. Bejan, L. Schutt, J. Hawari, N. J. Bunce, *Environ. Sci. Technol.* **2004**, *38*, 1595. doi:10.1021/ES0305611
- [28] R. B. Wardle, J. C. Hinshaw, P. Braithwaite, M. Rose, G. Johnson, R. Jones, K. Pousch, in *27th Int. Annu. Conf. Energetic Materials 1996* (Fraunhofer ICT: Karlsruhe).
- [29] A. T. Nielsen, A. P. Chafin, S. L. Christian, D. W. Moore, M. P. Nadler, R. A. Nissan, D. J. Vanderah, R. D. Gilardi, C. F. George, J. L. Gilardi, *Tetrahedron* **1998**, *54*, 11793.
- [30] B. Bhushan, L. Paquet, J. C. Spain, J. Hawari, *Appl. Environ. Microbiol.* **2003**, *69*, 5216. doi:10.1128/AEM.69.9.5216-5221.2003
- [31] B. Bhushan, A. Halasz, J. C. Spain, J. Hawari, *Appl. Environ. Microbiol.* **2004**, *70*, 4040. doi:10.1128/AEM.70.7.4040-4047.2004
- [32] A. M. Polcaro, M. Mascia, S. Palmas, A. Vacca, *Electrochim. Acta* **2004**, *49*, 649. doi:10.1016/J.ELECTACTA.2003.09.021
- [33] E. Brillas, J. Casado, *Chemosphere* **2002**, *47*, 241. doi:10.1016/S0045-6535(01)00221-1
- [34] D. Gandini, E. Mahé, P. A. Michaud, W. Haenni, A. Perret, Ch. Comninellis, *J. Appl. Electrochem.* **2000**, *30*, 1345. doi:10.1023/A:1026526729357
- [35] F. C. Walsh, *Pure Appl. Chem.* **2001**, *73*, 1819.
- [36] R. G. Compton, J. S. Foord, F. Marken, *Electroanal.* **2003**, *15*, 1349. doi:10.1002/ELAN.200302830
- [37] J. Iniesta, P. A. Michaud, M. Panizza, Ch. Comninellis, *Electrochem. Comm.* **2001**, *3*, 346. doi:10.1016/S1388-2481(01)00174-6
- [38] P. Cañizares, F. Martínez, M. Díaz, J. García-Gómez, M. A. Rodrigo, *J. Electrochem. Soc.* **2002**, *149*, D118. doi:10.1149/1.1490359
- [39] M. Panizza, P. A. Michaud, G. Cerisola, Ch. Comninellis, *J. Electroanal. Chem.* **2001**, *507*, 206. doi:10.1016/S0022-0728(01)00398-9
- [40] M. A. Rodrigo, P. A. Michaud, I. Duo, M. Panizza, G. Cerisola, Ch. Comninellis, *J. Electrochem. Soc.* **2001**, *148*, D60. doi:10.1149/1.1362545
- [41] G. C. Hale, *J. Chem. Soc.* **1925**, *47*, 2754.
- [42] M. Bao, F. Pantini, O. Griffini, D. Burrini, D. Santianni, K. Barbieri, *J. Chromatogr. A* **1998**, *809*, 75. doi:10.1016/S0021-9673(98)00188-5
- [43] F. Monteil-Rivera, L. Paquet, S. Deschamps, V. K. Balakrishnan, C. Beaulieu, J. Hawari, *J. Chromatogr. A* **2004**, *1025*, 125. doi:10.1016/J.CHROMA.2003.08.060
- [44] B. Marselli, J. Garcia-Gomez, P.-A. Michaud, M. A. Rodrigo, Ch. Comninellis, *J. Electrochem. Soc.* **2003**, *150*, D79. doi:10.1149/1.1553790
- [45] A compilation of second-order OH reaction rate constants in solution is available through NRDL Radiation Chemistry Data Center. <http://www.rcdc.nd.edu/compilations/hydroxyl/OH.htm>
- [46] J. O'M. Bockris, B. Kim, *J. Appl. Electrochem.* **1997**, *27*, 623. doi:10.1023/A:1018419316870

SURVIVAL AND REPRODUCTION OF ENCHYTRAEID WORMS, OLIGOCHAETA, IN DIFFERENT SOIL TYPES AMENDED WITH ENERGETIC CYCLIC NITRAMINES

SABINE G. DODARD,[†] GEOFFREY I. SUNAHARA,*[†] ROMAN G. KUPERMAN,[‡] MANON SARRAZIN,[†] PING GONG,[†] GUY AMPLEMAN,[§] SONIA THIBOUTOT,[§] and JALAL HAWARI[†]

[†]Biotechnology Research Institute, National Research Council of Canada, 6100 Royalmount Avenue, Montreal, Quebec H4P 2R2, Canada

[‡]U.S. Army Edgewood Chemical Biological Center, 5183 Blackhawk Road, Aberdeen Proving Ground, Maryland 21010-5424

[§]Defense Research and Development Canada, 2459 Pie IX Boulevard, Val Bélair, Quebec G3J 1X5, Canada

(Received 14 March 2005; Accepted 7 April 2005)

Abstract—Hexanitrohexaazaisowurtzitane (CL-20), a new polycyclic polynitramine, has the same functional nitramine groups (N-NO₂) as the widely used energetic chemicals hexahydro-1,3,5-trinitro-1,3,5-triazacyclohexane (royal demolition explosive [RDX]) and octahydro-1,3,5,7-tetranitro-1,3,5,7-tetrazocine (high-melting explosive [HMX]). Potential impacts of CL-20 as an emerging contaminant must be assessed before its use. The effects of CL-20, RDX, or HMX on adult survival and juvenile production by potworms *Enchytraeus albidus* and *Enchytraeus crypticus* were studied in three soil types, including Sassafras sandy loam (1.2% organic matter [OM], 11% clay, pH 5.5), an agricultural soil (42% OM, 1% clay, pH 8.2), and a composite agricultural–forest soil (23% OM, 2% clay, pH 7.9) by using ISO method 16387 (International Standard Organization, Geneva, Switzerland). Results showed that CL-20 was toxic to *E. crypticus* with median lethal concentration values for adult survival ranging from 0.1 to 0.7 mg/kg dry mass (DM) when using the three tested soils. In addition, CL-20 adversely affected juvenile production by both species in all soils tested, with median effective concentration (EC50) values ranging from 0.08 to 0.62 mg/kg DM. *Enchytraeus crypticus* and *E. albidus* were similarly sensitive to CL-20 exposure in the composite agricultural–forest soil, which supported reproduction by both species and enabled comparisons. Correlation analysis showed weak or no relationship overall among the soil properties and reproduction toxicity endpoints. Neither RDX nor HMX affected ($p > 0.05$) adult survival of either species below 658 and 918 mg/kg DM, respectively, indicating that CL-20 is more toxic to enchytraeids than RDX or HMX. Examination of data shows that CL-20 should be considered as a potential reproductive toxicant to soil invertebrates, and that safeguards should be considered to minimize the potential for release of CL-20 into the environment.

Keywords—Hexanitrohexaazaisowurtzitane 1,3,5-Trinitro-1,3,5-triazacyclohexane Octahydro-1,3,5,7-tetranitro-1,3,5,7-tetrazocine Enchytraeid worms Natural soils

INTRODUCTION

Soil contamination with energetic chemicals is commonly associated with military operations that involve munitions manufacturing, disposal, testing, and training. Concentrations of heterocyclic nitramines hexahydro-1,3,5-trinitro-1,3,5-triazacyclohexane (royal demolition explosive [RDX]) and octahydro-1,3,5,7-tetranitro-1,3,5,7-tetrazocine (high-melting explosive [HMX]) in soil have been reported to exceed 3,000 mg/kg in military training impact ranges [1,2]. In addition to these energetic chemicals, a new polycyclic nitramine, hexanitrohexaazaisowurtzitane (2,4,6,8,10,12-hexanitro-2,4,6,8,10,12-hexaazaisowurtzitane) or CL-20, is being considered for large-scale production as an alternative to RDX and HMX [3,4]. The relative toxicity of CL-20 (in comparison to the other nitramines) is not known, so it is not clear whether ecotoxicological risk management action must be taken in case of accidental release in the environment.

Limited information is available on the effects of CL-20 on soil microorganisms, terrestrial plants, and aquatic biota [5,6]. Recently, Robidoux et al. [6] found that CL-20 significantly decreased survival of adult earthworms (*Eisenia andrei*) at 90.7 mg/kg and production of juveniles at 0.01 mg/kg (nominal concentration), but no published information is available on the effects of CL-20 for other soil invertebrates

including enchytraeids. More information is necessary to assess the potential ecotoxicological effects of CL-20 in the terrestrial environment.

The development of ecotoxicological benchmarks for energetic materials (EMs) in soil has become a critical need in recent years [7–9] (<http://www.epa.gov/superfund/programs/risk/ecorisk/ecossl.pdf>). Enchytraeid worms have been increasingly used in ecotoxicological studies with EMs to develop such benchmarks for use in ecological risk assessment of contaminated sites associated with military operations that commonly produce elevated levels of EMs in soil [10–15]. The present study was conducted to determine the toxicity of the nitramine EMs CL-20, RDX, and HMX in freshly amended soils, to the two enchytraeid species *Enchytraeus crypticus* and *Enchytraeus albidus*. Three soil types were selected to determine the effects of contrasting soil properties (pH, organic matter [OM], and clay contents) on the toxicity of the three nitramines to enchytraeid worms. Similar to the two monocyclic nitramines RDX and HMX, CL-20 contains the characteristic N-NO₂ functional groups (Fig. 1) but has a strained cage polycyclic nitramine structure with higher energy and lower aqueous solubility [16]. To determine the relative toxicities of these nitramines on enchytraeids, we designed our studies to test the null hypothesis that the effects of CL-20, RDX, or HMX are similar, because of apparent similarity in their molecular structures. Alternatively, any ecotoxicological differences among the three nitramines could be established

* To whom correspondence may be addressed
(geoffrey.sunahara@nrc-nrc.gc.ca).

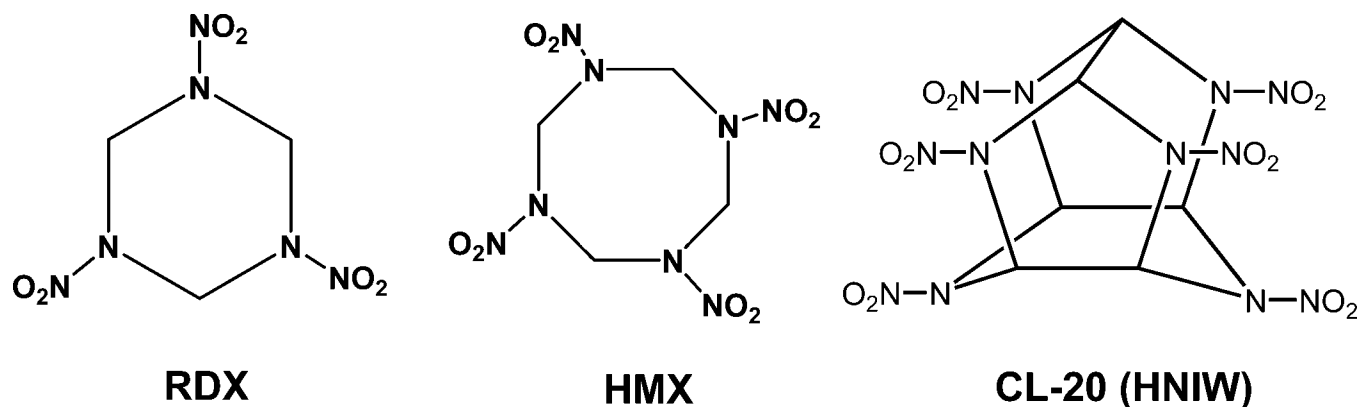


Fig. 1. Chemical structures of the three cyclic nitramines used in this study: hexahydro-1,3,5-trinitro-1,3,5-triazacyclohexane (RDX), octahydro-1,3,5,7-tetranitro-1,3,5,7-tetrazocine (HMX), and hexanitrohexaazaisowurtzitane (CL-20).

by assessing toxicities of RDX or HMX for the same enchytraeid species in parallel with the CL-20 studies. This approach enables direct comparisons of ecotoxicological data determined under similar experimental conditions and addresses the following objectives: to assess the toxicity of CL-20 in soil to enchytraeid worms and develop toxicological benchmarks that can be used for ecological risk assessment at contaminated sites; to compare the toxicity of CL-20 with that of currently used cyclic nitramines RDX and HMX; and to determine the effect of soil type as the exposure substrate on the polynitramine toxicity to enchytraeids.

MATERIALS AND METHODS

Chemicals and reagents

We obtained CL-20 (CAS 135285-90-4) from ATK Thiokol Propulsion (Brigham City, UT, USA) and RDX (CAS 121-82-4) and HMX (CAS 2691-41-0) from Produits Chimiques Expro (Valleyfield, QC, Canada). All EMs used were $\geq 99\%$ pure. All other chemicals, including carbendazim (methyl benzimidazol-2-yl carbamate; CAS 10605-21-7; $\geq 97\%$ pure), were American Chemical Society (ACS) reagent grade or higher and were obtained from either BDH (Toronto, ON, Canada) or Aldrich Chemical (Milwaukee, WI, USA). Deionized water (American Society for Testing and Materials Type I) was obtained by using a Millipore® Super-Q water purification system (Nepean, ON, Canada) and was used throughout this study. All glassware was washed with phosphate-free detergent, rinsed with acetone, and acid-washed before a final and thorough rinse with deionized water.

Preparation of test soils

The soils used for this study were Sassafra sandy loam (designated SSL; fine-loamy, siliceous, mesic Typic Hapludult), an agricultural soil (designated RacAg2002; fine-sandy, composite), and a 50:50 mixture of forest and agricultural soils (designated Rac50-50; fine-sandy, composite). Sassafra sandy loam soil was selected because it has physical and chemical properties supporting relatively high bioavailability of EMs [9] (www.epa.gov/superfund/programs/risk/ecorisk/ecossl.htm), including low OM and clay contents, which is necessary for developing ecotoxicological values protective of soil biota. The RacAg2002 and Rac50-50 soils with high OM contents were selected to maximize the reproduction potential for *E. albidus*, which favors organic soils. Furthermore, we expected that greater microbial activity, which is usually associated with

greater soil OM content, would facilitate more rapid biotic degradation and transformation of CL-20 in these soils compared with SSL soil, thus providing additional information for data interpretation. The RacAg2002 and Rac50-50 soils also are representative of several northern forest ecosystems and may become relevant for future risk assessment needs. The SSL soil was collected from uncontaminated open grassland on the property of Aberdeen Proving Ground (Maryland, USA). Vegetation and the organic horizon were removed to just below the root zone and the top 15 cm of the A-horizon was collected. The RacAg2002 and Rac50-50 soils were obtained from a local supplier (Transport Maurice Racicot & Fils, Boucherville, QC, Canada). All soil samples were sieved through a 5-mm mesh screen, air dried for at least 72 h, and mixed periodically to ensure uniform drying. The soil was then passed through a 2-mm sieve, and was stored at room temperature before use. The pH of the soils was measured before each test, by using the CaCl_2 method [17]. The soil moisture content and water-holding capacity were measured according to the enchytraeid reproduction test guidelines [18]. Selected soil properties are summarized in Table 1.

Individual 400-g batches of air-dried soils were amended with CL-20, RDX, or HMX in acetone to obtain nominal target concentrations (mg/kg, dry mass [DM]) of 0.001, 0.05, 0.10, 0.5, 1, and 10 for CL-20; 175, 200, 300, and 700 for RDX; or 200, 500, and 1,000 for HMX. Selection of RDX and HMX concentrations in soil used in the present experiments were based on earlier studies [19–22]. Solvent controls for soil treatments were amended with acetone only. Soil samples were

Table 1. Physical and chemical characteristics of test soils^a

Parameters	SSL	RacAg2002	Rac50-50
pH	5.5	8.2	7.9
Water-holding capacity (% v/w)	21	320	93
CEC ^b (cmol/kg)	5.5	69.6	20.3
Organic matter (% w/w)	1.2	42	23
Texture ^c			
Sand, 50–2,000 μm	71	90	87
Silt, 2–50 μm	18	9	11
Clay, <2 μm	11	1	2

^a Soils used: SSL = Sassafra sandy loam; RacAg2002 = agricultural soil; Rac50-50 = composite mixture of forest and agricultural soils.

^b CEC = cation exchange capacity.

^c Values are expressed as % (w/w), and include organic matter contents.

left for at least 16 h in a darkened chemical hood to allow the evaporation of the solvent. Each amended soil sample was mixed for 18 h on a three-dimensional rotary mixer, as described earlier by Kuperman et al. [14]. The soils were then hydrated with ASTM Type I water to a soil-specific percent of the water-holding capacity (WHC) for toxicity testing. Hydrated soils were allowed to moisture equilibrate for 24 h before use for toxicity testing or chemical analyses. Triplicate soil samples collected from each soil batch for chemical analyses were stored at 4°C and were analyzed within one week.

To prepare CL-20 concentrations as low as 0.001 mg/kg DM for subsequent toxicity testing, a different procedure was used. Solutions of CL-20 ranging from 0.002 to 2.0 mg/L were first prepared in acetone and then diluted with ASTM Type I water 24 h before toxicity testing. The final concentration of acetone in water was 1% (v/v), a concentration that did not affect survival or reproduction of enchytraeids. Depending on the soil type and WHC, 5 to 10 ml of each solution was added to 20 g of dry soil. Final CL-20 concentrations (mg/kg DM) in SSL soil were nominal 0, 0.001, 0.05, 0.1, and 0.5, and analytically determined 2.98 and 9.79. The nominal concentrations in either RacAg2002 or Rac50-50 soils were 0, 0.001, 0.01, 0.05, 0.1, 0.5, and 1.0 mg/kg DM.

Culturing and handling of test species

Laboratory cultures of *E. albidus* Henle 1837 (white potworm), and *E. crypticus* were originally provided by J. Römbke (Frankfurt, Germany) and the U.S. Army Edgewood Chemical Biological Center (Aberdeen Proving Grounds), respectively. Enchytraeids were cultured separately in a mixture (1:1, w/w) of garden soil (designated GS1) and Organization for Economic Cooperation and Development standard artificial soil [23] adjusted to 60% of the WHC, according to Römbke and Moser [24]. The GS1 was a sandy loam soil with the following properties: 70% sand, 23% silt, 7% clay, pH 6.9, 76% WHC, 11.2% total organic carbon, and 0.38% Kjeldahl N (K-N). The artificial soil had the following properties: 70% sand, 20% kaolin clay, and 10% grounded peat. Soil pH was adjusted to 6.0 ± 0.5 with CaCO_3 . The potworms were fed once a week with commercially available oats (Pablum® Oat cereal, H.J. Heinz Company of Canada, North York, ON, Canada). Mature *E. albidus* with visible eggs in the clitellum region were acclimated in RacAg2002, SSL, or Rac50-50 soils for 24 h before testing. Cultures of *E. crypticus* were maintained in the test soils for two to three months before testing; therefore, no acclimatization was required.

Enchytraeid reproduction and survival test

The enchytraeid reproduction and survival test used in the present study was adapted from the ISO 16387 bioassay [18]. Briefly, a 20-g DM sample of each soil type was placed into separate 200-ml glass jars, and was hydrated to 85 to 100% of their respective WHC. After the 24-h equilibration period, 40 or 50 mg of lyophilized oats for *E. albidus* or *E. crypticus*, respectively, were mixed into the soil in each jar. Ten acclimated enchytraeids were then added to each test container. Each toxicity test was replicated ($n = 3$) and included negative (no chemicals added), carrier (acetone-treated soil after acetone evaporation), and positive (reference toxicant, carbendazim) controls. Each jar was covered with a glass petri dish to prevent moisture loss during the incubation period. All containers were placed in an environment-controlled incubator at 20°C and 16:8 h light:dark cycle. The containers were weighed

once a week and the water loss was replenished with the appropriate amount of ASTM type I water. Lyophilized oats (20 mg for *E. albidus* and 50 mg for *E. crypticus*) were added weekly to each test container.

Adult survival was assessed on day 21 of the tests for *E. albidus*, and on day 14 for *E. crypticus*. All surviving adults were removed from the soil and were counted. The soil (containing cocoons and juveniles) was then returned to the same test container, adjusted to the initial moisture level, and was incubated for an additional 21 d for tests with *E. albidus* and 14 d for *E. crypticus*. Juvenile production by each species was assessed by counting the number of hatched juveniles on day 42 (*E. albidus*) or day 28 (*E. crypticus*) of the test. For this, 5 ml of 95% ethanol was added to each soil sample as a tissue preservative, and approximately 250 μl of Bengal Rose biological stain (1% solution in ethanol) was added to each container. Water was added into each container at the soil level followed by 30% AM-30 Ludox colloidal silica (Sigma-Aldrich Canada, Oakville, ON, Canada) in order to have a depth of 1 to 2 cm of liquid above the soil surface. Ludox allowed soil particles to stay at the bottom, whereas pink-stained enchytraeids floated. This method of harvesting and enumerating enchytraeids from soil is rapid and highly efficient [25].

Quality control

The fungicide carbendazim was used as the reference toxicant in SSL soil for *E. crypticus*, and in artificial soil for either *E. crypticus* or *E. albidus*. Carbendazim ($\geq 97\%$ purity) was applied in the following concentrations (mg/kg DM) in artificial soil: 10, 25, 50, 75, and 100 for tests with *E. crypticus*, and 1.0, 2.5, 5.0, 10, and 50 for tests with *E. albidus*. Validity criteria for the positive controls were based on in-house control data and published reports [12]. The test validity criteria for negative controls included more than 80% survival of adult potworms, an average of 25 or higher for number of juveniles produced, and a coefficient of variation of 50% or less [18]. All definitive tests for CL-20 toxicity with *E. crypticus* and *E. albidus* in Rac50-50 soil complied with the validity criteria of the ISO 16387 guideline [18]. In addition, the median effective concentration (EC50) value for juvenile production by *E. albidus* in the positive control with artificial soil was 1.6 mg carbendazim/kg DM, and was consistent with the work of Römbke and Moser [24]. The EC50 values for juvenile production by *E. crypticus* were 44 mg/kg in artificial soil and 8.5 mg/kg in SSL soil, and were within the baseline values established for our laboratory culture of *E. crypticus*. Mean adult survival in negative controls ranged from 84 to 97% in tests with *E. crypticus*, and was 99% in test with *E. albidus*. Mean number of juveniles produced by *E. crypticus* in negative controls ranged from 117 to 856, and was 45 for *E. albidus* in Rac50-50 soil. The coefficient of variation values for the negative control of each individual test ranged from 10.1 to 29%. Reproduction of *E. albidus* was not supported in SSL soil that had properties (pH and OM content; Table 1) outside the optimal requirements (near neutral pH, and high OM content) for this species [24]. The reasons for poor reproduction of *E. albidus* in RacAg2002 are not clear, but could be related to a relatively high soil pH, cation exchange capacity, or other properties that were not determined in this soil.

Chemical analysis of energetic nitramines

Acetonitrile extractions of CL-20, RDX, or HMX from amended soils were performed according to U.S. Environ-

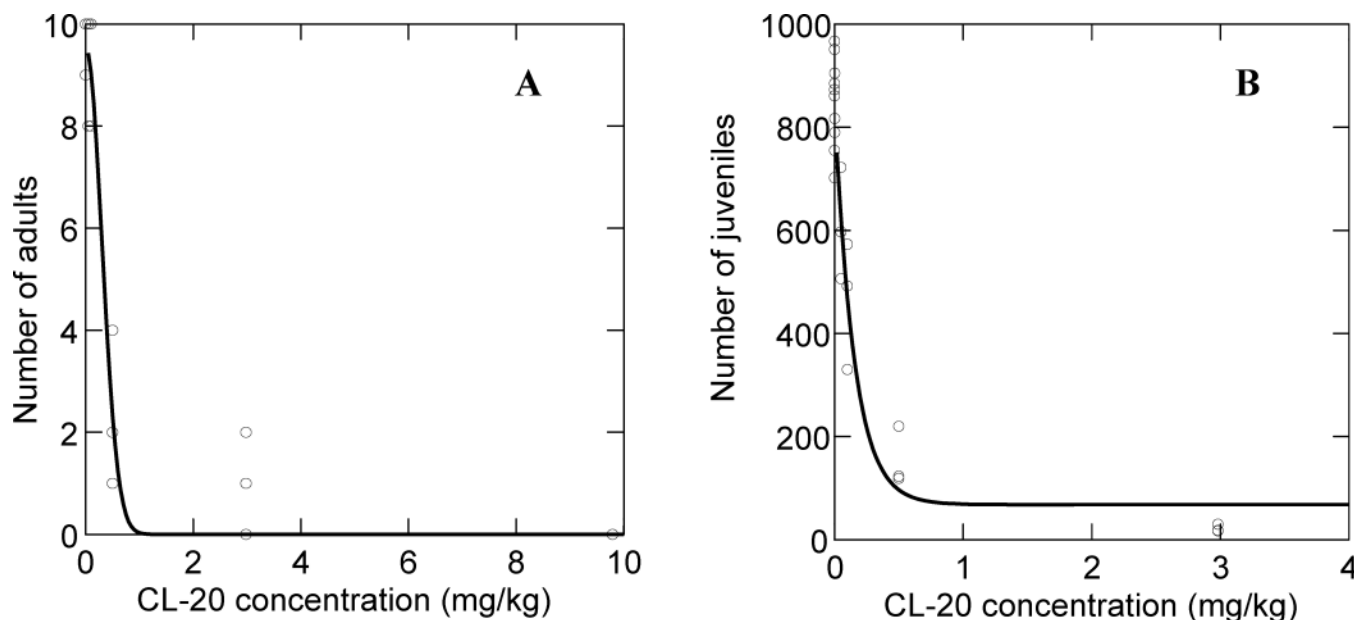


Fig. 2. Adult survival (A) and juvenile production (B) by *Enchytraeus crypticus* exposed to hexanitrohexaazaisowurtzitane (CL-20) in freshly amended Sassafras sandy loam soil (SSL).

mental Protection Agency Method 8330A [26]. Soil extracts were analyzed and quantified by using a high-performance liquid chromatography–ultraviolet detection system as described elsewhere [6,21]. The limit of detection of liquid samples ($\mu\text{g/L}$) was approximately 50 for CL-20, 50 for RDX, and 100 for HMX. Precision was $\geq 95\%$ (standard deviation $< 2\%$, signal to noise ratio = 10). The limit of quantification in SSL soil was 0.25 mg/kg for both CL-20 and RDX, and 0.5 mg/kg for HMX. Both RacAg2002 and Rac50-50 soils showed background signals changing the quantification limit for CL-20 to 2.0 and 0.5 mg/kg, respectively. Therefore, only nominal values are reported for all CL-20 concentrations below 2 mg/kg.

Statistical analyses

Definitive tests data were statistically analyzed to determine toxicological benchmarks based on acute (adult survival) and chronic (juvenile production) measurement endpoints. The primary focus of these analyses was to determine toxicological benchmarks that are based on concentration–response relationships for the chronic measurement endpoints. Several regression models described in Stephenson et al. [27] were evaluated to identify the best fit for the individual data sets generated in each toxicity test. This selection was based on several parameters, including examination of histograms of the residuals for the best appearance (i.e., most random scattering) and stem-and-leaf graphs to ensure that normality assumptions were met; examination of the regression line generated by each model to select one with the closest fit to the data points; and comparison of the variances, asymptotic standard errors, coefficients of determination, and the range of 95% confidence intervals (CIs) associated with the point estimates to identify a model that generated the smallest values or range for each parameter. Based on these criteria, two models were chosen that gave the best fit for the toxicity data. These models included an exponential model (for CL-20 effect on reproduction of *E. crypticus* in SSL)

$$Y = a \times e^{\{[\log(1 - p)]/ECp\} \times C) + b}$$

and logistic (Gompertz) model (for all remaining pairings)

$$Y = a \times e^{\{[\log(1 - p)] \times (C/ECp)^b\}}$$

where Y is the number for a measurement endpoint (e.g., number of juveniles); a is the control response; e is the base of the natural logarithm; p is the targeted endpoint inhibition/100 (e.g., 0.50 for EC50); ECp is the estimate of effect concentration for a specified percent effect; C is the exposure concentration in test soil; and b is a scale parameter.

The ECp parameters used in this study included the concentrations of CL-20, RDX, or HMX that produce a 20% (EC20) or 50% (EC50) reduction in the measurement endpoint. The EC20 parameter based on a reproduction endpoint is the preferred parameter for deriving soil invertebrate ecological soil screening level (Eco-SSL) values according to the U.S. Environmental Protection Agency approach [9]. The EC50, a commonly reported value, and survival data also were included to enable comparisons of the results produced in this study with results reported by other researchers.

Analysis of variance was used to determine the bounded (where possible) no-observed-effect concentration (NOEC) and lowest-observed-effect concentration (LOEC) values for adult survival or juvenile production data. Means separations were performed by using Fisher's least significant difference pairwise comparison tests. A significance level of $p \leq 0.05$ was accepted for determining the NOEC and LOEC values. Pearson correlation analysis was used to test for relationships among the soil properties and reproduction toxicity endpoints for CL-20. Statistical analyses were performed by using SYSTAT® 7.0.1 [28].

RESULTS AND DISCUSSION

Toxicity of CL-20 to enchytraeids

Both adult survival and juvenile production by *E. crypticus* were affected by exposure to soils initially amended with CL-20, within the concentration ranges tested in the definitive tests (Figs. 2 to 4). The present studies indicate that CL-20 exposure was toxic to the enchytraeids based on its lethal and sublethal

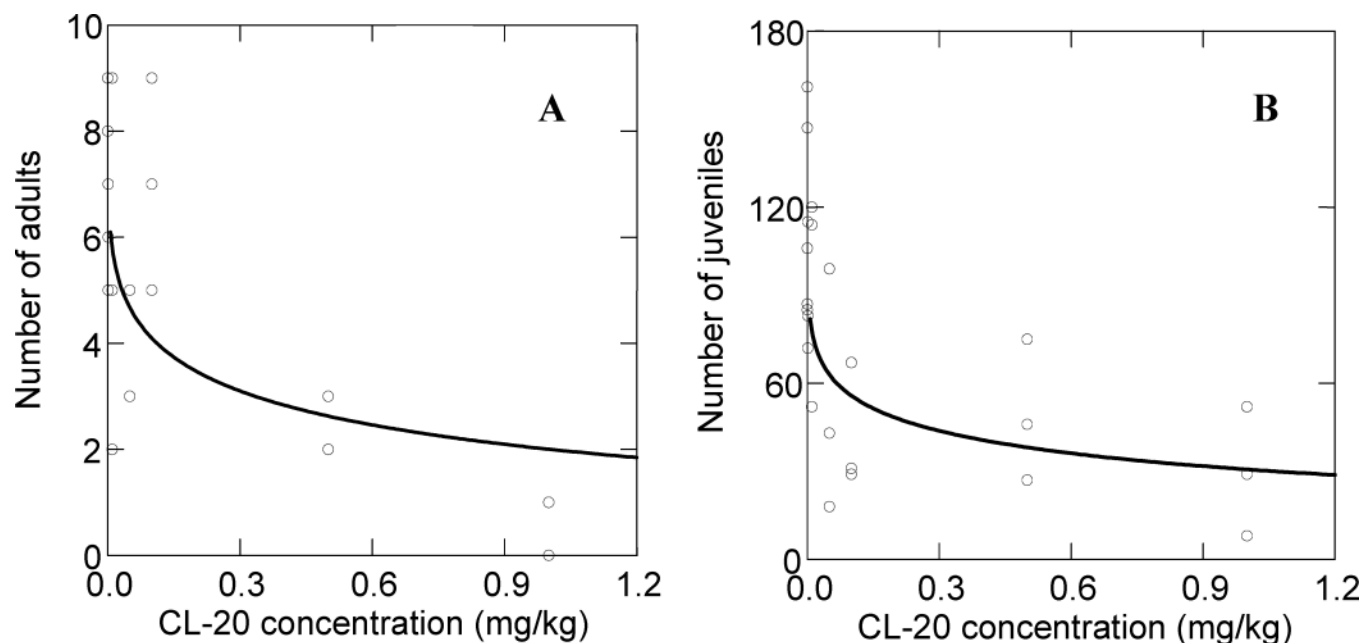


Fig. 3. Adult survival (A) and juvenile production (B) by *Enchytraeus crypticus* exposed to hexanitrohexaazaisowurtzitane (CL-20) in freshly amended RacAg2002 soil.

effects. Ecotoxicological benchmarks summarized in Table 2 show that CL-20 in soil was highly toxic to *E. crypticus* in the three soil types tested, with median lethal concentration (LC50) and EC50 values ranging from 0.1 to 0.7, and from 0.08 to 0.62 mg/kg, respectively. Reproduction was a more sensitive assessment endpoint compared with adult survival in all soil types tested (Table 2). The order of CL-20 toxicity in soils (from greatest to least) for *E. crypticus* was RacAg2002 > SSL > Rac50-50 soils based on EC50 values for juvenile production.

Exposure to CL-20 did not adversely affect survival of adult *E. albidus* in RacAg2002 soil up to and including 1 mg/kg, but caused a concentration-dependent decrease in juvenile production in the Rac50-50 soil (Fig. 5A and Table 2). No con-

centration-response relationships could be determined for juvenile production by *E. albidus* in SSL or RacAg2002 soils, which did not support reproduction of this species. Accordingly, data for CL-20 toxicity for *E. albidus* in EMs-amended SSL or RacAg2002 should be interpreted with caution. To our knowledge, there are no published studies describing the toxicity of CL-20 to enchytraeids.

Earlier studies by Dodard et al. [12] have shown that exposure to EMs such as 2,4,6-trinitrotoluene (TNT) in amended soil causes decreased production of juvenile *E. albidus*. This exposure is also associated with the degradation of TNT in both the soil as well as in the enchytraeids [13]. Dodard et al. [12] also showed that TNT amended in soil was 5 to 10 times more lethal to juveniles than to adult potworms. Therefore,

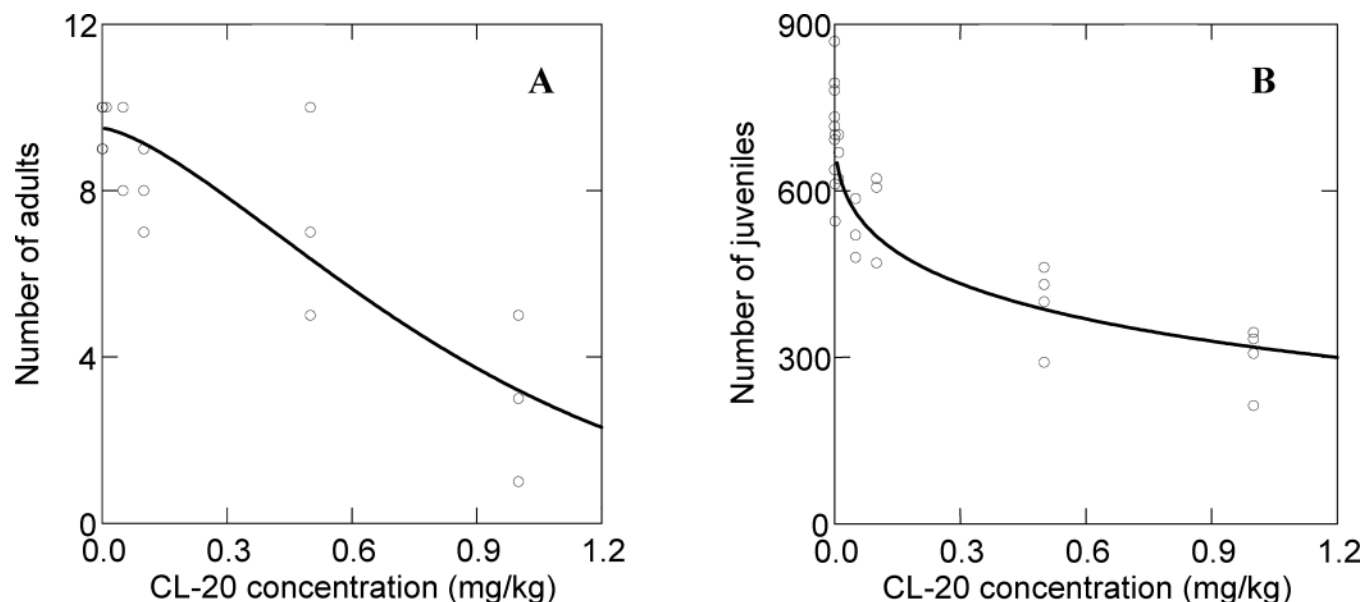


Fig. 4. Adult survival (A) and juvenile production (B) by *Enchytraeus crypticus* exposed to hexanitrohexaazaisowurtzitane (CL-20) in freshly amended Rac50-50 soil (composite mixture of forest and agricultural soil).

Table 2. Toxicological benchmarks (mg/kg) for hexanitrohexaazaisowurtzitane (CL-20) determined in freshly amended soils by using the enchytraeid survival and reproduction test with *Enchytraeus crypticus* and *Enchytraeus albidus*^a

Species and soil ^b	Adult survival ^c				Juvenile production ^d			
	LC20 (95% CI)	LC50 (95% CI)	LOEC	NOEC	EC20 (95% CI)	EC50 (95% CI)	LOEC	NOEC
<i>E. crypticus</i>								
SSL	0.2 (0.1–0.4)	0.4 (0.2–0.5)	0.5	0.1	0.04 (0.02–0.05)	0.12 (0.07–0.16)	0.05	0.001
RacAg2002	0.003 (0–0.02)	0.1 (0–0.3)	0.05 ^e	0.01 ^e	0.001 (0–0.01)	0.08 (0–0.24)	0.05	0.01
Rac50-50	0.3 (0.1–0.5)	0.7 (0.6–0.9)	0.5	0.1	0.03 (0–0.08)	0.62 (0.26–0.98)	0.05 ^e	0.01 ^e
<i>E. albidus</i>								
SSL	0.006 (0–0.02)	0.2 (0–0.4)	0.05	0.001	ND ^f	ND	ND	ND
RacAg2002	>1.0	>1.0	>1.0	1.0	ND	ND	ND	ND
Rac50-50	>0.5	>0.5	0.5	0.1	0.05 (0–0.13)	0.19 (0.04–0.34)	0.5 ^e	0.1 ^e

^a Mortality was assessed on day 14 for *E. crypticus*, and on day 21 for *E. albidus*, by counting the number of surviving adult enchytraeids. Reproduction was assessed on day 28 for *E. crypticus*, and on day 42 for *E. albidus*, by counting the number of juvenile enchytraeids.

^b SSL = Sassafras sandy loam soil; RacAg2002 = agricultural soil; Rac50-50 = composite mixture of forest and agricultural soil.

^c LC = lethal concentration; CI = confidence interval; LOEC = lowest-observed-effect concentration; NOEC = no-observed-effect concentration.

^d EC = effective concentrations.

^e Based on Bonferroni adjusted comparison probabilities.

^f ND = not determined because SSL and RacAg2002 soils did not support reproduction of *E. albidus*.

the decreased enchytraeid juvenile production resulting from exposure to TNT or its degradation products may have been due, at least in part, to lower numbers of surviving adults as well as juveniles. This explanation is not likely for *E. albidus* exposed to CL-20 in Rac50-50 soil in the present study, because CL-20 decreased juvenile production without any evidence of adult mortality (no significant change in the number of surviving adults).

Toxicity benchmarks for CL-20 determined in the present study with enchytraeids are generally consistent with data from the only published study on *E. andrei* [6]. Toxicity of CL-20 for adult enchytraeids was greater compared with LC50 values (53.4 and >125 mg/kg in SSL and RacFor2002, respectively) for *E. andrei* [6]. The EC50 values for reproduction endpoints for *E. andrei* (cocoon production and viability, and juvenile production) ranged from 0.05 to 0.09 mg/kg in the same SSL soil type, and from 1.3 to 1.5 mg/kg in RacFor2002 soil that had properties similar to RacAg2002 soil of the present study

[6]. Our studies showed that *E. crypticus* and *E. albidus* were similarly sensitive to CL-20 exposure in Rac50-50 soil, based on NOEC or LOEC values for adult survival, and on EC50 or EC20 values (95% CI basis) for juvenile production (Table 2). In contrast, SSL sustained greater CL-20 toxicity to adult *E. albidus* compared to *E. crypticus*, although suboptimal properties of this soil for *E. albidus* could contribute to increased sensitivity of this species in SSL.

Recent studies by Lachance et al. [29] showed that TNT and its (bio)transformed products (2-aminodinitrotoluene and 4-aminodinitrotoluene) were responsible for causing toxic effects to earthworms *E. andrei* exposed to TNT-amended soils. It is not yet determined whether the toxicity of CL-20 to enchytraeids, like TNT to earthworms, was caused by the parent energetic chemical, or by its degradation products formed by biotic and abiotic processes in soil. It is known that CL-20 can be degraded in nonsterile soils [30], under alkaline conditions [31,32], or in the presence of zero-valent metals such

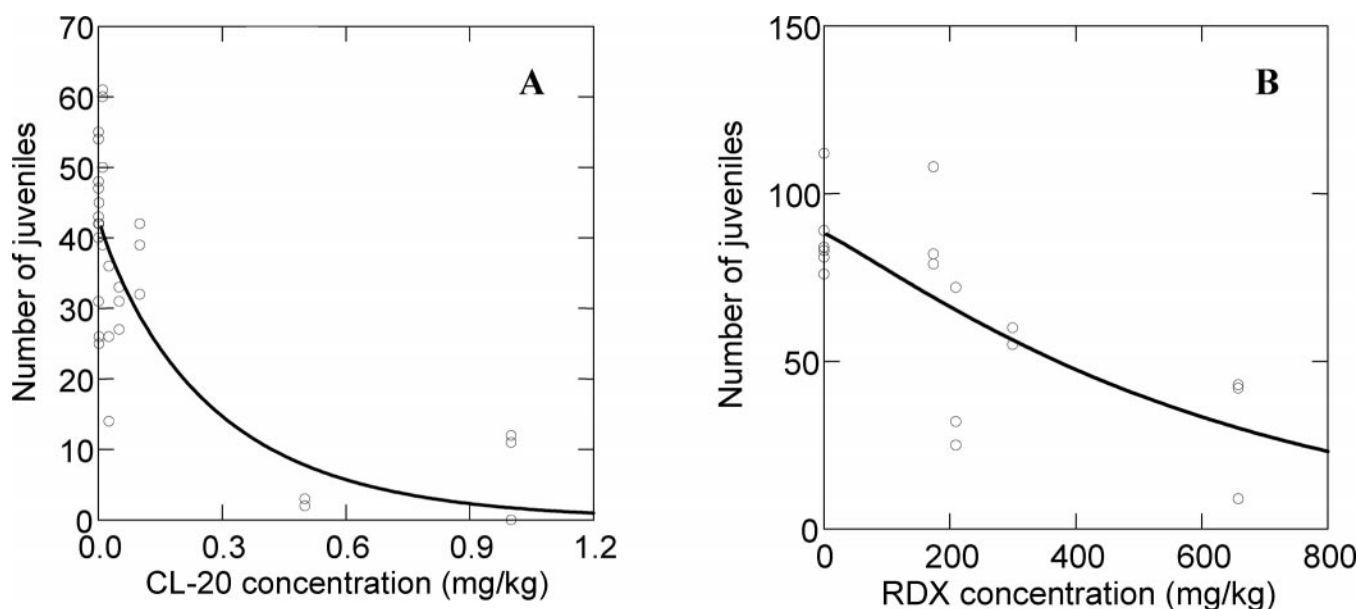


Fig. 5. Effects of hexanitrohexaazaisowurtzitane (CL-20) (A, nominal concentrations) or hexahydro-1,3,5-trinitro-1,3,5-triazacyclohexane (RDX) (B, measured concentrations) on juvenile production by *Enchytraeus albidus* in freshly amended Rac50-50 soil.

Table 3. Effects of RDX and HMX on adult survival and juvenile production (means \pm standard deviation) by two enchytraeid species in a freshly amended composite soil Rac50-50^a

Test groups	Concentrations (mg/kg) ^b	Adult survival		Number of juveniles produced	
		<i>Enchytraeus albidus</i>	<i>Enchytraeus crypticus</i>	<i>E. albidus</i>	<i>E. crypticus</i>
Negative control	0	9.3 \pm 0.6	9.7 \pm 0.6	83 \pm 7	622 \pm 50
Solvent control	0	10.0 \pm 0.0	10.0 \pm 0.0	92 \pm 17	569 \pm 85
RDX	174	9.0 \pm 1.0	9.3 \pm 0.6	90 \pm 16	512 \pm 81
	209	10.0 \pm 0.0	9.3 \pm 0.6	43* \pm 25	515 \pm 168
	299	9.7 \pm 0.6	9.3 \pm 0.6	58* \pm 3	460 \pm 103
	658	9.7 \pm 0.6	10.0 \pm 0.0	31* \pm 19	474 \pm 34
HMX	205	10.0 \pm 0.0	9.7 \pm 0.6	98 \pm 21	522 \pm 61
	484	9.0 \pm 1.0	9.7 \pm 0.6	88 \pm 8	476 \pm 40
	918	9.7 \pm 0.6	10.0 \pm 0.0	75 \pm 0.6	572 \pm 115

^a RDX = hexahydro-1,3,5-trinitro-1,3,5-triazacyclohexane; HMX = octahydro-1,3,5,7-tetranitro-1,3,5,7-tetrazocine.

^b Concentrations are based on acetonitrile extraction and high-performance liquid chromatography–ultraviolet detection using U.S. Environmental Protection Agency Method 8330A [26].

* Significant difference from the respective solvent control ($p \leq 0.05$).

as iron [33] to produce nitrite (NO_2^-), nitrous oxide (N_2O), ammonia (NH_3), formic acid (HCOOH), and glyoxal (HCOCHO). The higher pH value of RacAg2002 compared with SSL and Rac50-50 soils could accelerate the hydrolysis of CL-20 and the concomitant formation of greater quantities of potentially more toxic chemicals to enchytraeids such as glyoxal or formic acid [34]. However, preliminary studies by our research team have indicated that when glyoxal or formic acid was separately amended in SSL soil at concentrations ranging from 1 to 100 mg/kg DM, no lethal effects on the earthworms were observed. Therefore, formation of CL-20 degradation products other than glyoxal or formic acid can be important for understanding the mechanisms of CL-20 toxicity in soil and requires further investigations. These products may include the early reactive intermediates such as free radicals and imines [32,35,36] that can lead to cell organelle injury, and the subsequent toxicity to soil invertebrates.

Comparison of the effects of energetic nitramines on enchytraeids

Comparison of the effects of CL-20, RDX, and HMX on the two enchytraeid species was possible only in Rac50-50 soil because neither SSL nor RacAg2002 could support reproduction of *E. albidus*. Exposure of *E. crypticus* or *E. albidus* to RDX or HMX in Rac50-50 soil did not affect ($p > 0.05$) adult survival up to their respective highest concentrations of 658 and 918 mg/kg (Table 3). Juvenile production by either species was unaffected by HMX in all exposure concentrations tested in this soil. In contrast to HMX, exposure of *E. albidus* to RDX significantly ($p \leq 0.05$) decreased juvenile production at 209 mg/kg (bounded LOEC) and elicited a concentration-dependent response (Fig. 5B) producing the EC20 and EC50 values of 161 and 444 mg/kg, respectively. Exposure of *E. crypticus* to RDX did not significantly affect ($p > 0.05$) juvenile production up to the highest tested concentration of 658 mg/kg (Table 3).

Experimentally determined toxicological benchmark data for the enchytraeid worm *E. albidus* in Rac50-50 soil showed that the toxicity of CL-20 was three orders of magnitude greater compared with RDX, based on EC50 values for reproduction. The difference in toxicity between CL-20 and HMX was even greater for *E. crypticus*, which was not affected by exposure to RDX up to the highest concentration of 658 mg/kg tested in Rac50-50 soil. The greatest contrast in the effects of

nitramines on either enchytraeid species was observed between CL-20 and HMX, which did not adversely affect either adult survival or reproduction up to 918 mg/kg DM. These results do not support our initial hypothesis that cyclic nitramines CL-20, RDX, and HMX sustain similar toxicities to the enchytraeid worms because of apparent similarities in their molecular structures and functional groups. Toxicity data for RDX determined in our studies agree with the results of Schäfer and Achazi [10], who reported that RDX did not affect *E. crypticus* up to 1,000 mg/kg in standard LUFA 2.2 soil aged for one month before the exposure. More recent studies by Kuperman et al. [14] that used higher RDX concentrations for *E. crypticus* exposures in SSL soil, produced an EC50 value of 51,413 mg/kg, five orders of magnitude difference compared with CL-20 effects on this species determined in our study (EC50 of 0.12 mg/kg). Results of our present studies with HMX are consistent with findings by Kuperman et al. [14], who reported no adverse effects of HMX on *E. crypticus* in freshly amended SSL soil up to 21,750 mg/kg. Based on the results of the present studies and those reported by others [14], the order of toxicity of cyclic nitramines to enchytraeids in freshly amended soils is (from greatest to least) CL-20 > RDX > HMX.

Both CL-20 and RDX can degrade in soil more easily than does HMX. Analyses of soil samples from sites associated with past and present practices involving extensive use of Octol (containing 70% [w/w] HMX, 30% TNT, and <1% RDX) showed that only HMX was detected as the principal contaminant in soil [37,38] or in plant tissue [39]. Furthermore, Robidoux et al. [40] detected HMX in earthworm tissue after a 28-d exposure to soils collected from an antitank firing range containing a number of contaminants including HMX. The polycyclic nitramine CL-20 was found to biotransform faster than the monocyclic nitramines RDX or HMX under similar conditions [35]. The order of toxicity of the three EMs parallels their order of chemical and biochemical reactivity, suggesting that these chemicals can exert their toxic effects, at least in part, through their degradation products. However, it should be noted that the above toxicity order also follows the order of respective log octanol–water partition coefficient (K_{ow}) values for the studied EMs (CL-20: 1.92 > RDX: 0.90 > HMX: 0.16) [41], and that the toxicity could be favored by a higher log K_{ow} and a higher tissue uptake of the EM into the soil organisms.

Toxicity of CL-20 in different soil types

Soil types used in assessments of CL-20 toxicity varied predominantly in percent WHC, OM and clay contents, pH, and cation exchange capacity (Table 1). The soil WHC is dependent on OM content and texture, and was not included in the correlation analysis. The relationships among the remaining soil properties and CL-20 toxicity for reproduction of *E. crypticus* (EC20 level) were analyzed by using pairwise Pearson correlations. Analysis showed weak or no relationships overall ($p > 0.3$) among the soil properties (pH, OM, clay, or cation exchange capacity) and CL-20 toxicity (data not shown). The strongest correlations were determined for cation exchange capacity ($r = -0.843$, $p = 0.362$), and percent OM ($r = -0.614$, $p = 0.579$), and the weakest for percent clay ($r = 0.231$, $p = 0.852$), and pH ($r = -0.275$, $p = 0.822$). The effects of soil properties on the bioavailability and toxicity of the cyclic nitramines to soil invertebrates have not been adequately investigated [6,14,22]. However, CL-20 is highly immobilized by soils rich in OM, and its bioavailability, affected by sorption to soil constituents, could vary depending on the pH, and the amount and quality of OM [32]. The SSL soil used in the present study had low OM content and was hypothesized to support relatively higher bioavailability and resulting toxicity of CL-20, compared with the composite RacAg 2002 or Rac50-50 soils. Results of definitive tests showed that this was not the case; RacAg2002 soil sustained the greatest CL-20 toxicity to survival of adult *E. crypticus* and reproduction based on LC50 or EC50 values (Table 2). These results show that more soil types with contrasting soil properties should be included in future toxicity assessments to determine the effect of specific soil constituents on the bioavailability and toxicity of nitramine energetic chemicals.

CONCLUSION

The present study showed clearly that exposure to CL-20 is highly toxic to *E. crypticus* and *E. albidus*. Toxicity of CL-20 was orders of magnitude greater compared to the currently used energetic compounds RDX and HMX. Although CL-20 undergoes hydrolysis in alkaline soils, it can be a persistent soil contaminant in the vadose zone of neutral and acidic soils. The present uncertainties regarding soil constituents affecting CL-20 degradation require further investigations of the fate of CL-20 in soil. Identification of all intermediate and final products of CL-20 degradation, rates of formation, and their effects on soil biota are necessary before the ecological risks and impacts of this new cyclic nitramine in the soil vadose zone can be more clearly understood.

Acknowledgement—This research was supported, in part, by the U.S. Department of Defense, through the Strategic Environmental Research and Development Program (projects CP-1256 and CP-1254). We thank Fanny Monteil-Rivera (National Research Council of Canada) for her helpful comments of an earlier version of this paper. We also thank McGill Environmental Laboratory (Montreal, QC, Canada), and COR-EM (Quebec City, QC, Canada) for providing their analytical services for some of the soil samples. National Research Council Canada publication 45938.

REFERENCES

- Simini M, Wentsel RS, Checkai RT, Phillips CT, Chester NA, Major MA, Amos JC. 1995. Evaluation of soil toxicity at Joliet Army Ammunition Plant. *Environ Toxicol Chem* 14:623–630.
- Jenkins TF, Grant CL, Walsh ME, Thorne PG, Thiboutot S, Ampleman G, Ranney TA. 1999. Coping with spatial heterogeneity effects on sampling and analysis at an HMX contaminated antitank firing range. *Field Anal Chem Technol* 3:19–28.
- Nielsen AT, Christian SL, Moore DW, Gilardi RD, George CF. 1987. Synthesis of 3,5,12-triazawurtzitanes (3,5,12-triazatetracyclo[5.3.1.1^{2,6}.0^{4,9}] dodecanes). *J Org Chem* 52:1656–1662.
- Wardle RB, Hinshaw JC, Braithwaite P, Rose M, Johnson G, Jones R, Poush K. 1996. Synthesis of the caged nitramine HNIW (CL-20). *Proceedings*, 27th International Annual Conference, Fraunhofer Institute for Chemical Technology (ICT), Karlsruhe, Germany, June 25–28, pp 27.1–27.10.
- Gong P, Sunahara GI, Rocheleau S, Dodard SG, Robidoux PY, Hawari J. 2004. Preliminary ecotoxicological characterization of a new energetic substance, CL-20. *Chemosphere* 56:653–658.
- Robidoux PY, Sunahara GI, Savard K, Berthelot Y, Dodard S, Martel M, Gong P, Hawari J. 2004. Acute and chronic toxicity of the new explosive CL-20 to the earthworm (*Eisenia andrei*) exposed to amended natural soils. *Environ Toxicol Chem* 23:1026–1034.
- Talmage SS, Opresko DM, Maxwell CJ, Welsh CJE, Cretella FM, Reno PH, Daniel FB. 1999. Nitroaromatic munition compounds: Environmental effects and screening values. *Rev Environ Contam Toxicol* 161:1–156.
- Sunahara GI, Robidoux PY, Gong P, Lachance B, Rocheleau S, Dodard SG, Sarrazin M, Hawari J, Thiboutot S, Ampleman G, Renoux AY. 2001. Laboratory and field approaches to characterize the soil ecotoxicology of polynitro explosives. In Greenberg BM, Hull RN, Roberts MH Jr, Gensmer RW, eds, *Environmental Toxicology and Risk Assessment: Science, Policy and Standardization—Implications for Environmental Decisions*, Vol 10. STP 1403. American Society for Testing and Materials, Philadelphia, PA, pp 293–312.
- U.S. Environmental Protection Agency. 2003. Ecological soil screening level guidance. OSWER Directive 9285.7-55. Washington, DC.
- Schäfer R, Achazi RK. 1999. The toxicity of soil samples containing TNT and other ammunition derived compounds in the enchytraeid and collembola-biotest. *Environ Sci Pollut Res* 6:213–219.
- Schäfer RK. 2002. Evaluation of the ecotoxicological threat of ammunition derived compounds to the habitat function of soil. PhD thesis. Freien Universität, Berlin, Germany.
- Dodard SG, Renoux AY, Powlowski J, Sunahara GI. 2003. Lethal and subchronic effects of 2,4,6-trinitrotoluene (TNT) on *Enchytraeus albidus* in spiked artificial soil. *Ecotoxicol Environ Saf* 54:131–138.
- Dodard SG, Powlowski J, Sunahara GI. 2004. Biotransformation of 2,4,6-trinitrotoluene (TNT) by enchytraeids (*Enchytraeus albidus*) in vivo and in vitro. *Environ Pollut* 131:263–273.
- Kuperman RG, Simini M, Phillips CT, Checkai RT, Kolakowski JE, Kurnas CW, Sunahara GI. 2003. Survival and reproduction of *Enchytraeus crypticus* (Oligochaeta, Enchytraeidae) in a natural sandy loam soil amended with the nitro-heterocyclic explosives RDX and HMX. *Pedobiologia* 47:651–656.
- Kuperman RG, Checkai RT, Simini M, Phillips CT, Kolakowski JE, Kurnas CW. 2005. Weathering and aging of TNT in soil increases toxicity to potworm *Enchytraeus crypticus*. *Environ Toxicol Chem* 24:2509–2518.
- Larson SL, Felt DR, Escalon L, Davis JD, Hansen LD. 2001. Analysis of CL-20 in environmental matrices: water and soil. Technical Report ERDC/EL TR-01-21. U.S. Army Corps of Engineers, Vicksburg, MS.
- International Organization for Standardization. 1994. Soil quality—Determination of pH. ISO 10390: 1994 (E). Geneva, Switzerland.
- International Organization for Standardization. 2003. Soil quality: Effects of pollutants on Enchytraeidae (*Enchytraeus* sp)—Determination of effects on reproduction and survival. ISO DIS 16387: 2003. Geneva, Switzerland.
- Phillips CT, Checkai RT, Wentsel RS. 1993. Toxicity of selected munitions and munition-contaminated soil on the earthworm (*Eisenia foetida*). Technical Report ERDEC-TR-037. U.S. Army Chemical and Biological Defense Agency, Aberdeen Proving Ground, MD.
- Robidoux PY, Svendsen C, Coumartin J, Hawari J, Ampleman G, Thiboutot S, Weeks JM, Sunahara GI. 2000. Chronic toxicity of energetic compounds in soil determined using the earthworm

- (*Eisenia andrei*) reproduction test. *Environ Toxicol Chem* 19: 1764–1773.
21. Robidoux PY, Hawari J, Bardai G, Paquet L, Ampleman G, Thiboutot S, Sunahara GI. 2002. TNT, RDX, and HMX decrease earthworm (*Eisenia andrei*) life-cycle responses in a spiked natural forest soil. *Arch Environ Contam Toxicol* 43:379–388.
 22. Simini M, Kuperman RG, Phillips CT, Checkai RT, Kolakowski JE, Kurnas CW, Sunahara GI. 2003. Reproduction and survival of *Eisenia andrei* in a sandy loam soil amended with the nitroheterocyclic explosives RDX and HMX. *Pedobiologia* 47:657–662.
 23. Organization for Economic Cooperation and Development. 1984. Guidelines for testing of chemicals: Earthworm acute toxicity test. Guideline 207. Paris, France.
 24. Römbke J, Moser T. 1999. Organization and performance of an international ringtest for the validation of the enchytraeid reproduction test. Research Report 296 64 906 (UBA-FB 98-104). Environmental Research of the Federal Ministry of the Environment, Nature Conservation and Nuclear Safety, German Federal Environment Agency, Berlin.
 25. Phillips C, Kuperman R. 1999. A rapid and highly-efficient method for extracting enchytraeids from soil. *Pedobiologia* 43:523–527.
 26. U.S. Environmental Protection Agency. 1998. Nitroaromatics and nitramines by high performance liquid chromatography—Method 8330A. In *Test Methods for Evaluating Solid Waste, Physical/Chemical Methods*. SW-846 update III, part 4:1 (B). National Technical Information Service, Springfield, VA.
 27. Stephenson GL, Koper N, Atkinson GF, Solomon KR, Scroggins RP. 2000. Use of nonlinear regression techniques for describing concentration–response relationships of plant species exposed to contaminated site soils. *Environ Toxicol Chem* 19:2968–2981.
 28. Statistical Package for the Social Sciences. 1997. *SYSTAT® 7.01 for Windows*. Chicago, IL, USA.
 29. Lachance B, Renoux AY, Sarrazin M, Hawari J, Sunahara GI. 2004. Toxicity and bioaccumulation of reduced TNT metabolites in the earthworm *Eisenia andrei* exposed to amended forest soil. *Chemosphere* 55:1339–1348.
 30. Trott S, Nishino SF, Hawari J, Spain JC. 2003. Biodegradation of the nitramine explosive CL-20. *Appl Environ Microbiol* 69: 1871–1874.
 31. Balakrishnan VK, Halasz A, Hawari J. 2003. Alkaline hydrolysis of the cyclic nitramine explosives RDX, HMX, and CL-20: New insights into degradation pathways obtained by the observation of novel intermediates. *Environ Sci Technol* 37:1838–1843.
 32. Balakrishnan VK, Monteil-Rivera F, Gauthier MA, Hawari J. 2004. Sorption and stability of the polycyclic nitramine explosive CL-20 in soil. *J Environ Qual* 33:1362–1368.
 33. Balakrishnan VK, Monteil-Rivera F, Halasz A, Corbeanu A, Hawari J. 2004. Decomposition of the polycyclic nitramine explosive, CL-20 by Fe⁰. *Environ Sci Technol* 38:6861–6866.
 34. Shangari N, Bruce WR, Poon R, O'Brien PJ. 2003. Toxicity of glyoxals—Role of oxidative stress, metabolic detoxification and thiamine deficiency. *Biochem Soc Trans* 31:1390–1393.
 35. Bhushan B, Halasz A, Thiboutot S, Ampleman G, Hawari J. 2004. Chemotaxis-mediated biodegradation of cyclic nitramine explosives RDX, HMX, and CL-20 by *Clostridium* sp. EDB2. *Biochem Biophys Res Commun* 316:816–821.
 36. Hawari J, Deschamps S, Beaulieu C, Paquet L, Halasz A. 2004. Initial reactions in the photodegradation of CL-20 in aqueous solution: Insights into the mechanisms of initial reactions. *Water Res* 38:4055–4064.
 37. Jenkins TF, Walsh ME, Thorne PT, Miyares PH, Ranney TA, Grant CL, Esparza JR. 1998. Site characterization for explosives contamination at a military firing range impact area. CRREL Special Report 98-9. Cold Regions Research and Engineering Laboratory, U.S. Army Corps of Engineers, Hanover, NH.
 38. Dubé P, Ampleman G, Thiboutot S, Gagnon A, Marois A. 1999. Characterization of potentially explosives-contaminated sites at CFB Gagetown. Report DREV-TR-1999-13. Defense Research Establishment Valcartier, Department of National Defense Canada, Valcartier, QC.
 39. Groom CA, Halasz A, Paquet L, Morris N, Olivier L, Dubois C, Hawari J. 2002. Accumulation of HMX (octahydro-1,3,5,7-tetranitro-1,3,5,7-tetrazocine) in indigenous and agricultural plants grown in HMX-contaminated anti-tank firing-range soil. *Environ Sci Technol* 36:112–118.
 40. Robidoux PY, Dubois C, Hawari J, Sunahara GI. 2004. Assessment of soil toxicity from an antitank firing range using *Lumbricus terrestris* and *Eisenia andrei* in mesocosms and laboratory studies. *Ecotoxicology* 13:603–614.
 41. Monteil-Rivera F, Paquet L, Deschamps S, Balakrishnan VK, Beaulieu C, Hawari J. 2004. Physico-chemical measurements of CL-20 for environmental applications. Comparison with RDX and HMX. *J Chromatogr A* 1025:125–132.

Detection of nitroaromatic and cyclic nitramine compounds by cyclodextrin assisted capillary electrophoresis quadrupole ion trap mass spectrometry

Carl A. Groom^a, Annamaria Halasz^a, Louise Paquet^a,
Sonia Thiboutot^b, Guy Ampleman^b, Jalal Hawari^{a,*}

^a Biotechnology Research Institute, National Research Council of Canada, 6100 Royalmount Avenue, Montreal, Canada PQ H4P 2R2

^b Defence Research and Development Canada, Val-Belair, Canada PQ G3J 1X5

Available online 8 January 2005

Abstract

An Agilent ^{3D}CE capillary electrophoresis system using sulfobutylether- β -cyclodextrin (SB- β -CD)–ammonium acetate separation buffer pH 6.9 was coupled to a Bruker Esquire 3000+ quadrupole ion trap mass detector via a commercially available electrospray ionization interface with acetonitrile sheath flow. The CE–MS system was applied in negative ionization mode for the resolution and detection of nitroaromatic and polar cyclic or caged nitramine energetic materials including TNT [2,4,6-trinitrotoluene, formula mass (FW) 227.13], TNB (1,3,5-trinitrobenzene, FW 213.12), RDX (hexahydro-1,3,5-trinitro-1,3,5-triazine, FW 222.26) HMX (octahydro-1,3,5,7-tetranitro-1,3,5,7-tetrazocine, FW 296.16), and CL-20 (2,4,6,8,10,12-hexanitro-2,4,6,8,10,12-hexaazaisowurtzitane, FW 438.19). The CE–MS system conformed to the high-performance liquid chromatography with ultraviolet absorbance detection (HPLC–UV) and HPLC–MS reference methods for the identification of energetic contaminants and their degradation products in soil and marine sediment samples.

© 2004 Elsevier B.V. All rights reserved.

Keywords: Electrokinetic chromatography; Nitroaromatic compounds; Cyclic nitramines; Explosives; Environmental analysis

1. Introduction

The overproduction of military explosives and propellants has resulted in their inadvertent release to soil and aquatic environments [1], and the potential toxicity of these materials and their degradation products has prompted governments to initiate programs for the identification and characterization of contaminated sites [2,3]. The most frequently occurring soil contaminants (TNT: 2,4,6-trinitrotoluene, HMX: octahydro-1,3,5,7-tetranitro-1,3,5,7-tetrazocine, and RDX: hexahydro-1,3,5-trinitro-1,3,5-triazine) are analyzed by C₁₈ reverse phase high-performance liquid chromatography with ultraviolet absorbance detection (HPLC–UV) [US Environmental Protection Agency (EPA) Method EPA 8330, Nitroaromatics and explosives in soil][4]. This method uses equipment readily available to analytical laboratories, and offers $\mu\text{g/l}$ detec-

tion limits, but requires known reference analytical standards for unequivocal peak identification. The method is therefore somewhat problematic for the discovery of novel degradation products. The use of atmospheric electrospray ionization-mass spectrometry (ESI-MS) [5–10] or atmospheric pressure chemical ionization mass spectrometry (APCI-MS) [11–14] with HPLC has greatly assisted in the identification of new intermediates and the definition of environmental degradation pathways for energetic materials [15–20]. Frequently, however, the C₁₈ reversed-phase HPLC system does not resolve polar metabolites, and analyte identification is heavily dependent on mass spectra. Alternative separation methods, including gas chromatography [21–23], CN- or C₈-reversed-phase HPLC [24], ion exclusion HPLC [25,26], and micellar electrokinetic chromatography [27] are consequently of interest for use with mass spectrometry for the improved resolution and identification of energetic contaminants. Cyclic nitramine explosives of moderate polarity are resolved using sulfobutylether- β -cyclodextrin (SB- β -CD) assisted capillary

* Corresponding author. Tel.: +1 514 496 6267; fax: +1 514 496 6265.
E-mail address: jalal.hawari@cnrc-nrc.gc.ca (J. Hawari).

electrophoresis [28] and here we report on the coupling of this separation method to a quadrupole ion trap mass spectrometer for the identification of frequently encountered explosives and their degradation products in environmental samples.

2. Experimental

2.1. Materials

CL-20 (2,4,6,8,10,12-hexanitro-2,4,6,8,10,12-hexaazaisowurtzitane, purity 99.3% as determined by HPLC, 95% epsilon form as determined by IR) was provided by Thiokol Propulsion (Brigham City, UT, USA). HMX, RDX, and TNX (hexahydro-1,3,5-trinitroso-1,3,5-triazine, purity of all chemicals >99%) were provided by Defense Research and Development Canada (DRDC), Valcartier, Canada. MNX (hexahydro-1-nitroso-3,5-dinitro-1,3,5-triazine, purity 98%) was obtained from SRI International (Menlo Park, CA, USA). TNT and TNB (1,3,5-trinitrobenzene) analytical standards were purchased from Supelco (Oakville, Canada). Contaminated soil from an explosive manufacturing site (Produits Chimiques Expro, Valleyfield, Canada) was obtained from the BRI applied ecotoxicology group (Montreal, Canada). Contaminated marine sediment core samples (Ordinance range UXO, Oahu Island, HW, USA) were provided by the US Naval Research Laboratory (Arlington, VA, USA). Advasep 4 (sulfobutylether- β -cyclodextrin, sodium salt) [29], was purchased from Cydex (Overland Park, KS, USA). CE grade ammonium acetate was purchased from Agilent Technologies (New Castle, DE, USA). Formic acid was purchased from Fluka (Munich, Germany). HPLC grade acetone and 2-propanol were purchased from Fisher Scientific (Montreal, Canada). Acetonitrile and methanol were obtained from Mallinckrodt Baker (Phillipsburg, NJ, USA). Ethyl acetate was provided by BDH (Poole, UK). Aqueous solutions were prepared using deionized Milli-Q plus (Millipore) water. All other chemicals (HCHO, HCl, NaOH, H₃PO₄) used were obtained from Aldrich (Oakville, Canada). Standard analytical solutions (1000 mg/l) were prepared by adding crystals of analyte to acetonitrile with verification of concentration by HPLC as described earlier [16]. Samples were prepared by diluting analytical standards or soil extracts in 10 mM ammonium acetate buffer pH 6.9.

2.2. CE system

CE separations were carried out using an Agilent ^{3D}CE instrument (Agilent, Waldbronn, Germany). Fused silica capillaries (total length (L) 90 cm, effective length to UV detection window (l) 21.5 cm, internal diameter 50 μ m) were purchased from Agilent. Unless otherwise indicated, separations were carried out at 30 kV and 25 °C. Sample injections were performed hydrodynamically (50 mbar, 1–10 s). The separation buffer was 10 mM sulfobutylether- β -cyclodextrin,

10 mM ammonium acetate pH 6.9. New capillaries were conditioned by flushing with water (5 min), 1 M HCl (5 min), water (5 min), 1 M NaOH (5 min) and separation buffer (15 min). Following this the capillaries were conditioned electrophoretically by applying 30 kV for 15 min with subsequent replenishment of anodic and cathodic buffer vials. In between runs the capillaries were rinsed for 30 s in 10 mM ammonium acetate, and then flushed with separation buffer for 3 min.

2.3. MS system

A Bruker Esquire 3000 plus ion trap spectrometer (Bruker-Daltonics, Boston, MA, USA) equipped with an Agilent atmospheric electrospray ionization source (Agilent, Waldbronn, Germany) was employed for mass detection. The electrospray was operated in negative ion mode to produce mainly deprotonated molecular mass ions $[M - H]^{-1}$. Nitrogen was used as drying gas at 150 °C, with a pressure of 816 mbar (12 psi) and at a flow rate of 7 l/min. Sheath liquid was pumped to the atmospheric pressure interface using an Agilent model 1100 isocratic pump with a 100:1 flow splitter to deliver 6 μ l/min. The capillary voltage was set at 6000 V with an end plate offset of –500 V. Observed electrospray currents ranged from 5 to 17 nA. The scanning mass to charge range was 40 to 600 m/z with a scanning speed of 13000 m/z per second. The resulting baseline peak width resolution was 0.6 U. The maximum accumulation time was 50 ms.

2.4. Soil and sediment analysis

Soil and sediment samples were extracted by sonication in acetonitrile in accordance with EPA Method 8330 [4]. The HPLC–UV analyses were performed as described by Fournier et al. [30]. Sediment samples were also analyzed as follows using a Hewlett-Packard 6890 gas chromatograph equipped with electron-capture detection (GC-ECD). Acetonitrile extracts (2 μ l) were injected onto a Restek (Bellefonte, PA, USA) Rtx-TNT capillary column (6 m \times 0.530 mm, 1.50 μ m) with helium as carrier gas at a flow rate of 60 ml/min and 680 mbar (10 psi). The column was initially held at 100 °C for 2 min, then raised to 200 °C at a rate of 10 °C/min. The temperature was then ramped at a rate of 20 °C/min to 230 °C and maintained there for 13.5 min. The injector and detector temperatures were 250 and 300 °C, respectively. A Restek 8095 calibration mix A was employed for reference calibration. The instrumental quantification limits (μ g/l) for this method were as follows: TNT, 0.6; RDX, 8.9; HMX, 10.9; 1,3,5-TNB, 1.9; 2,6-DNT, 0.3; 2,4-DNT, 1.6.

3. Results and discussion

3.1. Mass spectra of analytes in the presence of cyclodextrin

Beta cyclodextrins are widely known to be cyclic oligosaccharides containing seven glucopyranose units

linked exclusively through alpha (1–4) saccharide bonds to form a single ring. The cyclic orientation provides a truncated cone structure that is hydrophilic on the exterior and lipophilic at the interior cavity. Native cyclodextrins are of limited aqueous solubility or inclusion capacity, so the parent macrocycles are frequently modified by electrophilic persubstitution at the available hydroxyl groups of carbons 2, 3, or 6 of each glucopyranose subunit to produce charged or alkylated derivatives [31–33]. Selective modification at the specified hydroxyl groups is difficult, and a range of isomers is usually obtained using the above methods. It is theoretically possible to achieve a degree of substitution of 21 in the case of beta cyclodextrin, with numerous possibilities for the synthesis of positional or regioisomers. Commercially available modified cyclodextrins are therefore obtained as a mixture of isomers with varied degrees of substitution, and this has an effect on both pseudostationary phase electrophoretic mobilities, and on the observed mass spectrum.

The cyclodextrin applied in this study was Advasep 4 (Cydex, Overland Park, KS, USA) [29], a mixture of sulfobutyl ether derivatives of beta cyclodextrin (SB- β -CD) that vary in the degree of substitution from one to nine with a claimed overall effective average degree of substitution (d.s.) of 4. The low pK_a of the acid groups at the end of the carbon butyl chains causes the side chains to be charged at all pH values >2 ($pK_a < 1$). The presence of such diverse highly charged species in the CE separation buffer results in complex, but well defined CE–MS background spectra. The spectrum observed for an infusion of 10 mM ammonium acetate, 10 mM SB- β -CD (pH 6.9) separation buffer and acetonitrile sheath fluid is presented in Fig. 1A. The tentative identities of the observed molecular mass ions are listed in Table 1. Mass-to-charge values (m/z) were found for cyclodextrin derivatives with degrees of substitution of 4, 5, 6, and 7 (m/z values 418.7, 362.1, 324.4 and 297.4, respectively). Spectral lines are also observed for the monosodium adducts of cyclodextrin derivatives with degrees of substitution 5–7 (m/z values

458.3, 393.4 and 350.6, respectively). Similar mass spectra for preparations of SB- β -CD were presented by Grard et al. [34].

Various forms of ion spray mass spectrometry have been applied to the analysis of explosives by many workers. Using electrospray ionization triple-quadrupole MS on acetonitrile solutions of a wide range of explosives, Casetta and Garofolo [6] noted that TNT and other resonance stabilized nitroaromatic compounds formed deprotonated anionic $[M - H]^{-1}$ molecular mass ions, while explosives lacking in acidic protons tended to form acetate $[M + 59]^{-1}$ or formate $[M + 46]^{-1}$ mass ion adducts. The presence of acetate or formate was attributed to impurity of the acetonitrile infusion solvent. Fig. 1B provides the mass spectrum for an infusion of separation buffer containing TNT (FW 227.13), TNB (FW 213.12), RDX (FW 222.26), HMX (FW 296.16), and CL-20 (FW 438.19) at 10 mg/l concentration. The dominant mass ion signals observed in the spectrum are those of the substituted cyclodextrin derivatives (i.e. m/z 362.1, etc.). The aromatic explosives TNT and TNB produced signals at 226 and 212 m/z corresponding to their deprotonated parent ions $[TNT - H]^{-1}$ and $[TNB - H]^{-1}$, and signals at m/z 244 and 230 representing their deprotonated ion water adducts $[TNT - H + H_2O]^{-1}$ and $[TNB - H + H_2O]^{-1}$, respectively. Acetate adducts for RDX and HMX were indicated by the observation of signals at m/z values of 281 ($[RDX + CH_3CO_2]^{-1}$) and 355 ($[HMX + CH_3CO_2]^{-1}$), respectively. A weak signal observed for CL-20 at m/z 500 was tentatively assigned to the composition $[CL-20 + NO_3]^{-1}$, as the signal for NO_3^- (m/z 62) is observed in the mass spectra for CL-20 and other analytes (Figs. 1B and 2). CL-20 was reported to undergo denitration in aqueous or water–acetonitrile solutions at neutral [35] or alkaline [18] pH, to yield nitrite anion (NO_2^- , m/z 46), but not nitrate [18,35–37], and this reaction is accelerated in the presence of dimethyl- β -cyclodextrin [18,35]. The SB- β -CD CE separation buffer at pH 6.9 is therefore not well suited to the detection of CL-20. It is interesting to note that nitrate for-

Table 1

Identities of potential and observed ion fragments using negative mode electrospray ionization with 10 mM sulfobutylether- β -cyclodextrin (SB- β -CD) in 10 mM ammonium acetate pH 6.9 as capillary electrophoretic buffer and 100% acetonitrile as sheath fluid

Tentative mass ion	Degree of substitution (d.s.)	Charge (z)	Molecular mass (m)	m/z calculated	m/z observed
$[CH_3CO_2]^{-1}$	–	1	59	59	59
$[2CH_3CO_2 + Na]^{-1}$	–	1	141	141	141
$[SB_1 - H]^{-1}$	1	1	1269	1269	
$[SB_2 - 2H]^{-2}$	2	2	1404	702	
$[SB_3 - 3H]^{-3}$	3	3	1539	513	513
$[SB_4 - 4H]^{-4}$	4	4	1674	418.5	419.3
$[SB_5 - 5H]^{-5}$	5	5	1809	361.8	362.1
$[SB_6 - 6H]^{-6}$	6	6	1944	324	324.4
$[SB_7 - 7H]^{-7}$	7	7	2079	297	297.4
$[SB_8 - 8H]^{-8}$	8	8	2214	276.75	277
$[SB_9 - 9H]^{-9}$	9	9	2349	261	
$[SB_5 - 5H + Na]^{-4}$	5	4	1832	458	458.5
$[SB_6 - 6H + Na]^{-5}$	6	5	1961	392.5	393.1
$[SB_7 - 7H + Na]^{-6}$	7	6	2102	350.3	350.6

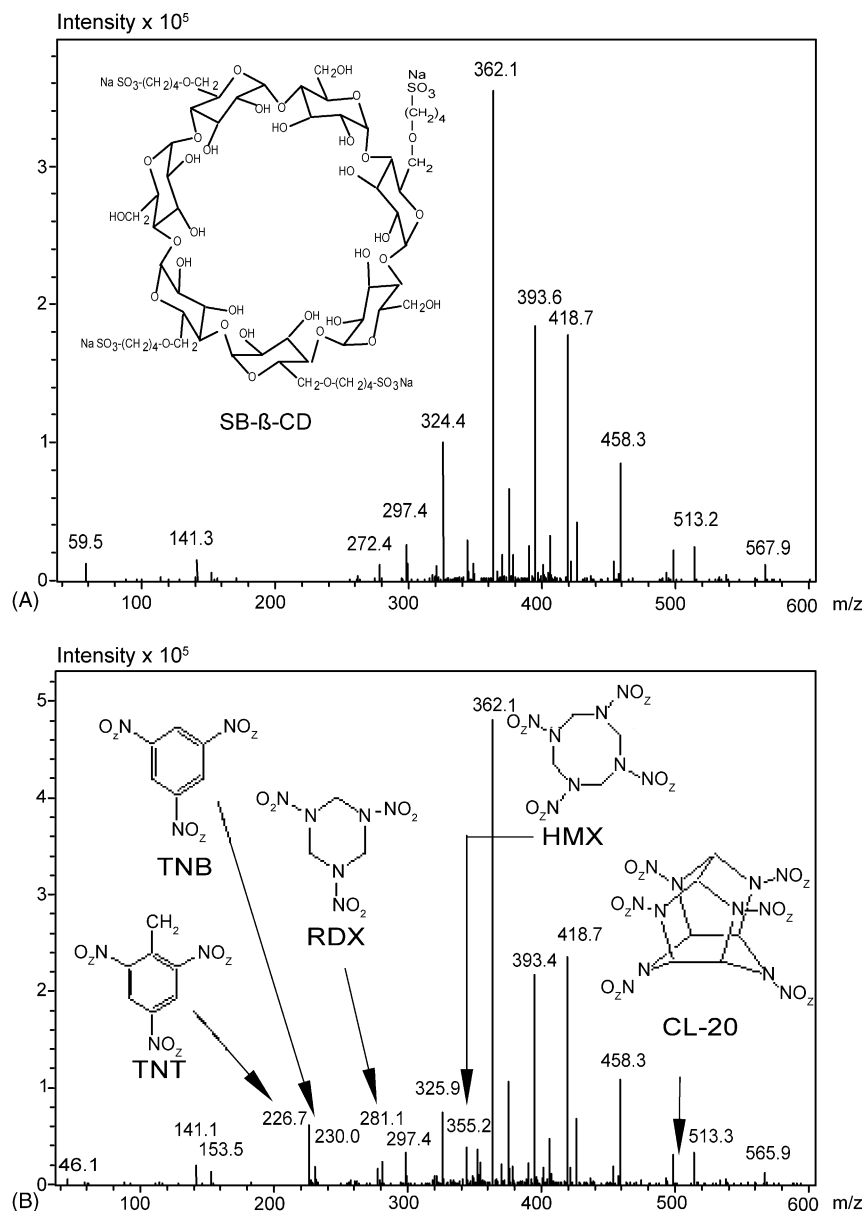


Fig. 1. (A) Mass spectrum for a 10 mM infusion of Advasep 4 sulfobutylether- β -cyclodextrin SB- β -CD (structure shown as inset, d.s. 4) in 10 mM ammonium acetate pH 6.9, with acetonitrile sheath fluid. (B) Mass spectrum for the above infusion containing 10 mg/l TNT, TNB, RDX, HMX and CL-20 (structures shown as inset) with mass ion intensities indicated respectively for m/z values of 226, 230, 281, 355, and 500.

mation from nitrite was reported for the photodegradation of RDX [17] and that a dominant mass signal of m/z 500 is observed in the LC-MS spectra reported for the photodegradation of CL-20 [38].

The presence of highly charged cyclodextrins in the electrospray aerosol may affect the identification of target explosive analytes in at least two respects: (1) The presence of high molecular weight, non-volatile ions in high concentration will inhibit the passage of target analytes to the vapour phase, and (2) If the analyte in question forms a highly stable inclusion complex with the cyclodextrin, then the observed mass signal will be that of the non-covalent inclusion complex and not the parent molecular ion. Bakhtiar and Bulusu [39] examined

the complexation of HMX, RDX, and 1,3,3-trinitroazetidine (TNAZ) with neutral cyclodextrins using positive ionization electrospray triple quadrupole MS and observed complexes for the cationic (Na^+ , NH_4^+ , K^+) adducts of RDX and neutral β - and γ -cyclodextrins in infusions containing 250 ppm RDX and cyclodextrin. The tentative β -CD complexes and mass to charge ratios were $[\beta\text{-CD} + \text{RDX} + 2\text{NH}_4 + \text{K}]^{2+}$ (m/z 1283), $[\beta\text{-CD} + \text{RDX} + \text{NH}_4]^+$ (m/z 1375), $[\beta\text{-CD} + \text{RDX} + \text{Na}]^+$ (m/z 1380), and $[\beta\text{-CD} + \text{RDX} + \text{K}]^+$ (m/z 1396). Similar phenomena were reported by Srinivasan and Bartlett [40] for the CE-MS analysis of neutral β -cyclodextrins complexed with barbiturate ion.

Table 2

Average peak height intensities of extracted ions (cps) observed for 10 mg/l injections (10 s 50 mbar) of selected energetic compounds using different sheath fluids (standard deviation provided in brackets, $n = 5$)

Sheath fluid	Isopropanol	Ethanol	Methanol	Ethyl acetate	Acetone	Acetonitrile	Water
Compound							
CL-20 (m/z 500)	N.D.	N.D.	N.D.	N.D.	87 (79)	370 (85)	N.D.
TNT (m/z 226)	1880 (228)	342 (112)	623 (287)	3912 (351)	17165 (1030)	36903 (559)	N.D.
TNB (m/z 230)	1670 (170)	187 (320)	498 (172)	23439 (1523)	22473 (1143)	42178 (1898)	N.D.
HMX (m/z 355)	8387 (528)	237 (281)	10169 (543)	137 (162)	24724 (506)	23690 (1092)	N.D.
RDX (m/z 281)	9664 (473)	871 (138)	12853 (753)	518 (751)	18872 (430)	21635 (1073)	N.D.
MXN (m/z 265)	9444 (483)	181 (243)	5069 (101)	4178 (376)	28592 (202)	35178 (372)	N.D.
TNX (m/z 233)	1543 (338)	9664 (453)	18887 (491)	851 (383)	61764 (982)	54970 (1923)	N.D.

A previous CE–UV study [28] indicated that nitroaromatic and cyclic nitramine explosives associated weakly with SB- β -CD, and it is unlikely that analyte–cyclodextrin complexes would be stable in the presence of acetonitrile sheath fluid. Nevertheless, the scan ranges were extended with limits of 40–1000 m/z to detect possible noncovalent complexes with the distribution of substituted cyclodextrins observed in the separation buffer mass spectrum. In this case the expected m/z values for inclusion complexes [i.e. m/z values of 492.5 and 474 for HMX and RDX complexes respectively, with SB- β -CD (d.s. = 4)] were not observed. Attempts to observe the negative ions for TNT ($[M]^{-1}$; m/z 227), RDX ($[M + NO_2 - H]^{-1}$; m/z 267) and HMX ($[M + NO_2 - H]^{-1}$; m/z 341) as reported by Yinon et al. [7] were also unsuccessful.

A separation of CL-20, TNB, TNT, HMX, and RDX analytical standards (10 mg/l, hydrodynamic injection volume 96 nl, actual analyte mass amount 96 pg) in 10 mM ammonium acetate is shown as Fig. 2. The overall capillary length (L) was 90 cm and the effective length to the UV window (l) was 21.5 cm. The UV trace (230 nm) revealed the electroosmotic front (EOF) to arrive at the UV detection window after 2.5 min, and at 10.3 min a corresponding dip in capillary current from a steady state value of 23 μ A signified the passage of the EOF to the electrospray ionization (ESI) interface. Peaks for the EOF and analytes arrived at the interface earlier than predicted using total length/effective length ratios. This slight increase in the bulk fluid velocity was due to the entrainment of all fluids exiting the electrospray needle by the nitrogen drying gas which flowed at 7 l/min (816 mbar and 150 °C). The capillary internal diameter was 50 μ m and

the corresponding average flow rate from the capillary was 0.17 μ l/min. The sheath fluid flow rate was set at 6 μ l/min, which resulted in a 1/35 dilution of the CE flow in acetonitrile at the ESI interface. Under these conditions the total ion current decreased from 5×10^5 counts per second (cps) to a steady state value of 2.6×10^5 cps after 2 min. Extracted adduct or molecular ion traces with corresponding peak mass spectra (baseline mass spectra subtracted) for CL-20, TNB, TNT, HMX, and RDX are respectively indicated for m/z values of 500, 230, 226, 355 and 281.

3.2. Sheath flow liquid selection

The effect of sheath fluid choice on the negative electrospray ionization of cyclic nitramines resolved in 30 kV electrophoretic separations (10 mM SB- β -CD/10 mM ammonium acetate pH 6.9) was examined using the polar organic solvents acetone, acetonitrile, 2-propanol, ethyl acetate, ethanol, methanol, and water. The analytes in question (CL-20, TNT, TNB, HMX, RDX, MXN, TNX) were observed to ionize best in acetonitrile and acetone (Table 2) which possessed the highest volatilities and lowest viscosities of the selected solvents (Table 3). Ethyl acetate, which also has a high volatility and relatively low viscosity, apparently was not sufficiently polar to maintain analyte solubility. Generally, when applying negative ionization electrospray, ionization increases with sheath liquid volatility, and decreases with respect to solvent surface tension and viscosity. The dielectric constant (polarity) of the sheath liquid must also be sufficient to maintain the solubilization of analytes following droplet separation from the Taylor cone and desolvation

Table 3

Physical properties of selected sheath fluids (20 °C) [44]

Sheath fluid	Vapour pressure (Torr)	Viscosity (cP)	Surface tension (dyn/cm)	Density (g/mL)	Polarity index	Dipole moment (Debye)	Dielectric constant
Isopropanol	33	2.3	18.3	0.785	3.9	1.66	19.9
Ethanol	43.9	1.2	23.75	0.9	5.2	1.69	24.55
Methanol	97.7	0.59	22.55	0.791	5.1	2.87	32.7
Ethyl acetate	73	0.45	23.75	0.9	4.4	1.88	6.02
Acetone	184.5	0.32	23.32	0.79	5.1	2.69	20.7 ^a
Acetonitrile	88.8	0.37	19.1	0.782	5.8	3.44	37.5
Water	23.78	1	72.8	0.997	9	1.84	80.1

^a 25 °C.

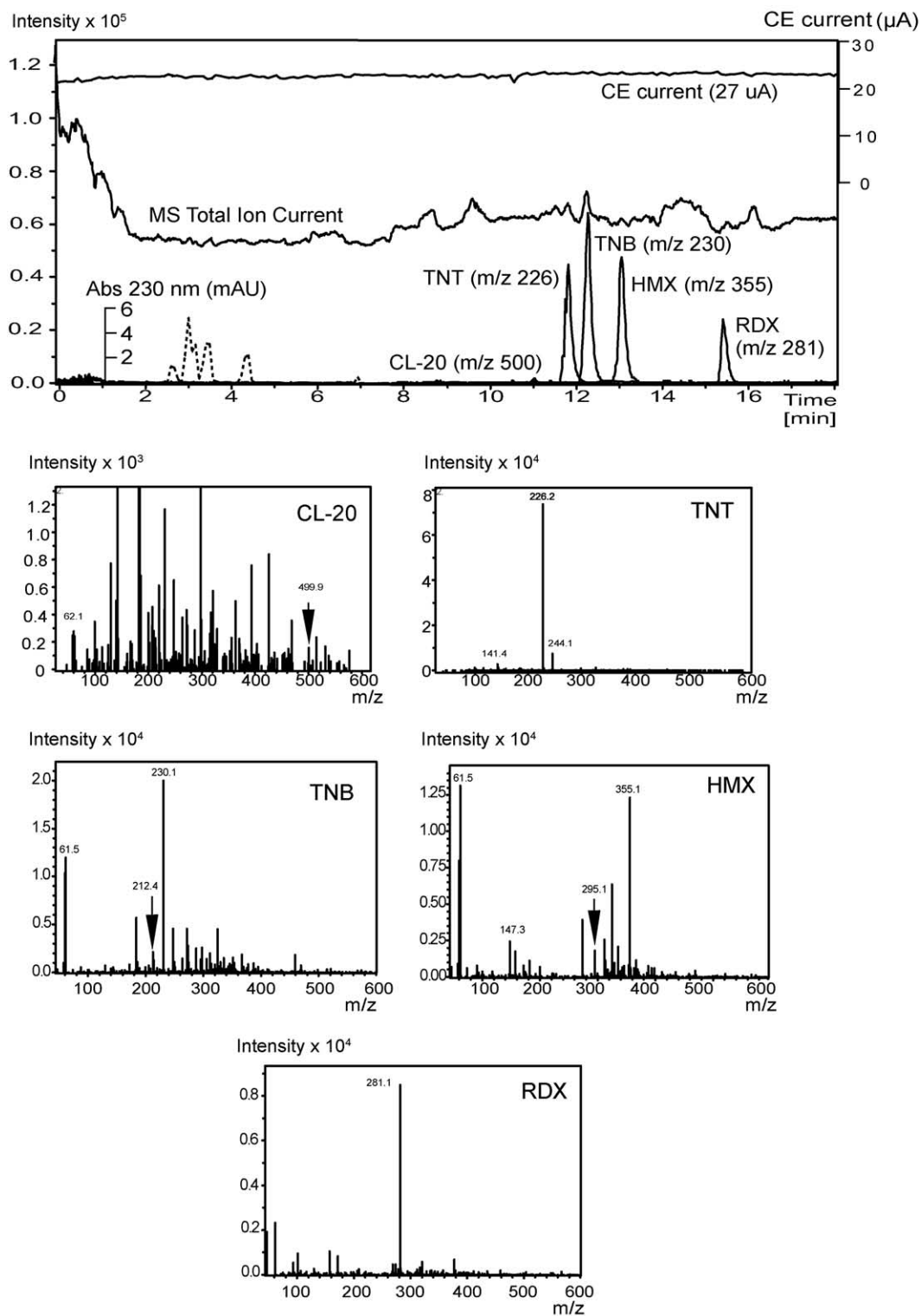


Fig. 2. CE-MS separation (30 kV, 10 mM acetate, 10 mM Advasep 4) with mass spectra for a 10 mg/l injection (10 s, 50 mbar, injection volume 56 nl) of TNT, TNB, RDX, HMX and CL-20 (actual mass amount: 96 pg) in 10 mM acetate pH 6.9. CE-UV trace (230 nm) as indicated by broken line. Extract ion traces (m/z values 226, 230, 281, 355, and 500, respectively) indicated by solid lines.

[41]. The aprotic nature of acetone and acetonitrile may act to enhance acetate adduct formation and ionization of the cyclic nitramines. The solubility of SB- β -CD in the sheath fluid appears to have little effect on analyte ionization, as evidenced by the poor performance of sheath fluids (methanol, ethanol, and water) in which SB- β -CD is known to be soluble [42]. The various sulfobutylether- β -cyclodextrin derivatives present in Advasep-4 are sufficiently soluble in acetonitrile to permit the passage of intact deprotonated parent ions $[\text{SB}_n\text{-nH}]^{-n}$ to the mass detector (Fig. 1, Table 1).

3.3. Effect of buffer components on signal intensity

Figs. 3 and 4 respectively represent the effects of ammonium acetate and cyclodextrin concentration in the separation buffer on analyte ionization. Fig. 3 indicated that increases in separation buffer acetate concentration decreased the ionization of nitroaromatic explosives, primarily due to competition with acetate ions at the electrospray droplet interface as indicated by the increased acetate extracted ion intensities (m/z 59) observed. Ion pairing of ammonium with $[\text{M} - \text{H}]^{-1}$ nitroaromatic parent anions may also decrease their abundance in the electrospray. The signal intensities for the nitramine explosives increased with acetate concentrations up to 20 mM, and indicated that increased acetate concentration served to enhance the formation of acetate adducts with these non-aromatic compounds at the electrospray interface. At acetate concentrations higher than 20 mM the ionization of cyclic nitramines gradually decreased in the same manner as for the aromatic analytes. This trend is an indication that once adduct ion formation is maximized, the passage of adduct ions to the gas phase will vary as a function of their mole fraction at the electrospray droplet surface.

As indicated in Fig. 4, three-fold increases in signal intensity were observed for the nitroaromatic compounds TNT

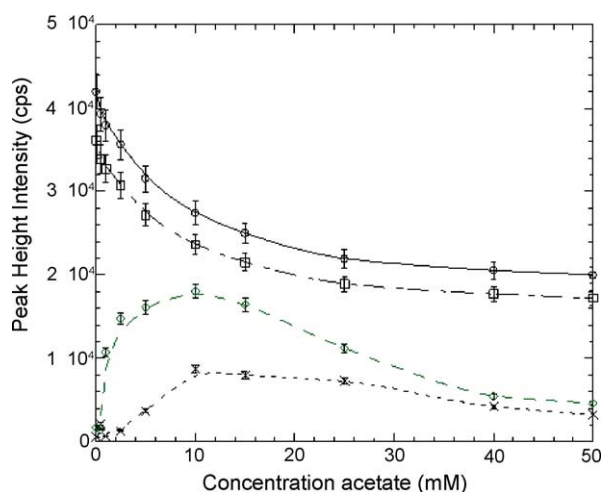


Fig. 3. Peak height intensities of selected analytes as a function of ammonium acetate concentration. All other conditions as in Fig. 2. Symbols: (○) TNB, (□) TNT, (◇) HMX, (×) RDX. (Error bar = 1 standard deviation, $n = 5$.)

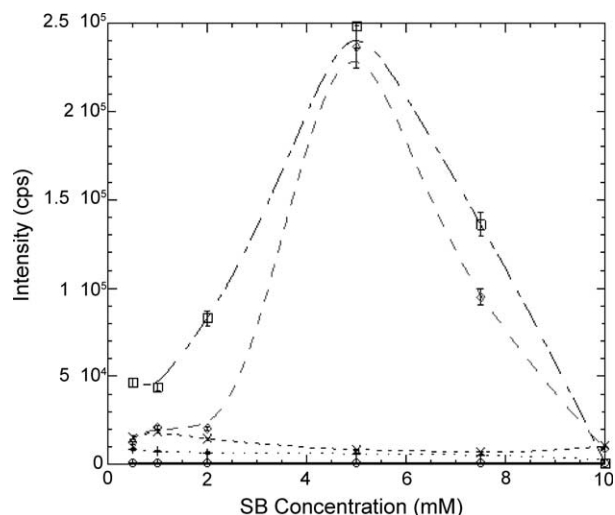


Fig. 4. Peak height intensities of selected analytes with variation in cyclodextrin concentration. All other conditions as in Fig. 2. Symbols: (○) EOF, (□) TNT, (◇) TNB, (×) HMX, (+) RDX. (Error bar = 1 standard deviation, $n = 5$.)

and TNB when the cyclodextrin concentration was increased from 2 to 5 mM. Signal intensities for HMX and RDX were relatively insensitive to increased cyclodextrin concentration in the range of 0.5–10 mM. The increase in signal observed for the aromatic compounds may be attributed to their 1000-fold greater volatility in comparison with HMX and RDX, as any improvement in the resolution of nitroaromatic compounds will be amplified by greater ionization efficiency which is a function of analyte volatility.

3.4. Application to environmental samples

The practicality of the CE method for the analysis of real samples was examined using samples analyzed by other available methods (HPLC–UV, HPLC–MS, GC–ECD). Generally, the extracted molecular ion response curves for quadrupole ion trap spectrometers increase hyperbolically with ion concentration and saturate to a constant value at the upper analyte concentration limit. Consequently, the quantitative linear dynamic range for selected quantification standards using the CE–MS method was narrow; varying between 10 mg/l and the instrumental quantification limit (0.05 mg/l). The observed instrumental limits of detection and quantification for the CE–MS method and for the validated HPLC–UV reference method (EPA 8330) are compared in Table 4. Triple quadrupole and time of flight mass detectors are recognized to have greater dynamic ranges in comparison with ion traps, and to be more suitable for quantification, but the multiple MS (MS^n) capability of the latter instruments facilitates degradative product identification [43]. However, the dominant factor in MS detector selection is often availability.

A CE–MS electropherogram for the extract (acetonitrile sonication) of explosive contaminated marine sediment is shown as Fig. 5. An extracted ion trace at m/z 181 revealed peaks observed at 15.2 and 16.3 min, and were respectively attributed to the deprotonated parent ions ($[\text{M} - \text{H}]^{-1}$) of 2,6-

Table 4

Instrumental detection limits (IDL)^a and instrumental quantification limits (IQL)^b for selected reference standards with cyclodextrin assisted CE–MS and with C₁₈ HPLC–UV (Method 8330)

Method	CL-20	TNT	TNB	HMX	RDX	TNX	MNX
IDL (mg/l)							
CE–MS	0.50	0.025	0.025	0.025	0.025	0.025	0.025
HPLC–UV	0.005	0.003	0.002	0.011	0.008	0.005	0.005
IQL (mg/l)							
CE–MS	5	0.05	0.05	0.05	0.05	0.05	0.05
HPLC–UV	0.010	0.013	0.007	0.006	0.028	0.050	0.050

^a The minimum concentration applied at which peak height was distinguished as greater than three times the baseline variation ($n > 5$).

^b The minimum concentration applied at which the standard error of the mean was less than 5% ($n > 5$).

dinitrotoluene (2,6-DNT) and 2,4-dinitrotoluene (2,4-DNT). The C₁₈ HPLC–UV analysis of this extract also indicated the presence of 2,6-DNT and 2,4-DNT, but with incomplete resolution of the two compounds, possibly due to matrix components. Analysis of the extract using GC–ECD identified 2,4-DNT and 2,6-DNT at concentrations of 0.716 and 0.095 mg/kg. The CE–MS method therefore conformed to the other available methods for the identification of explosives and their degradation products.

Fig. 6 shows the electropherogram for an extract of contaminated soil obtained from an ammunition manufacturing site. HPLC–UV analysis revealed that this extract contained 34 mg/l of TNX (hexahydro-1,3,5-trinitroso-1,3,5-triazine) as confirmed using a reference standard, and quantities of tetranitroso-HMX (4NO-HMX; octahydro-1,3,5,7-tetranitroso-1,3,5,7-tetrazacene), and trinitroso-HMX (3NO-HMX; octahydro-1-nitro-3,5,7-trinitroso-1,3,5,7-tetrazacene), compounds for which no

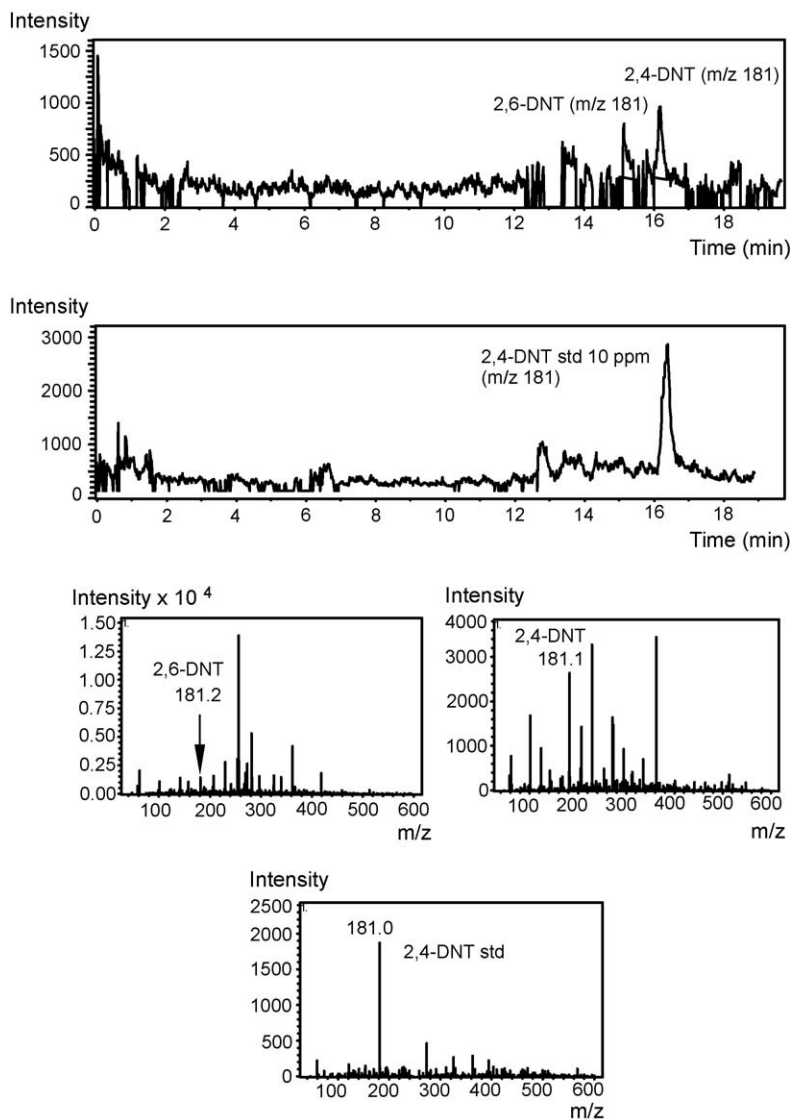


Fig. 5. Extracted ion electropherograms and mass spectra for 2,6-dinitrotoluene and 2,4-dinitrotoluene obtained from acetonitrile extract injections (10 s, 50 mbar) of contaminated marine sediment.

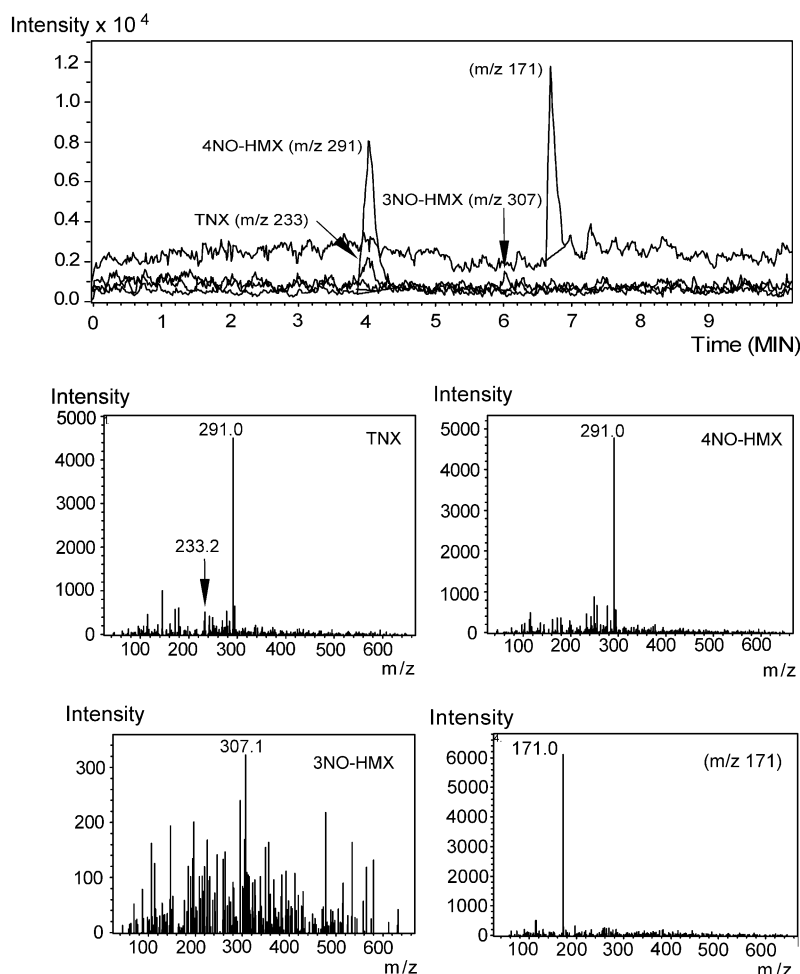


Fig. 6. Extracted ion electropherograms for hexahydro-1,3,5-trinitroso-1,3,5-triazine (TNX), octahydro-1,3,5-trinitroso-7-nitro-1,3,5,7-tetrazocine (3NO-HMX), octahydro-1,3,5,7-tetranitroso-1,3,5,7-tetrazocine (4NO-HMX) obtained from acetonitrile extracts of soil from an explosive manufacturing site.

commercial analytical standards were available. The electropherogram for this sample has peaks for extracted ions with mass to charge ratios of 233 (TNX, acetate adduct), 291 (4NO-HMX, acetate adduct), 307 (3NO-HMX, acetate adduct). A peak observed at 6.7 min (m/z 171) was initially hypothesized to be a diacetyl sodium adduct ion of formaldehyde $[\text{HCHO} + 2(\text{CH}_3\text{CO}_2) + \text{Na}]^{-1}$. Diacetyl sodium adduct ions $[2(\text{CH}_3\text{CO}_2) + \text{Na}]^{-1}$ (m/z 141.1) are uniformly observed in the electrospray background spectrum (Fig. 1, Table 1) and formaldehyde is a recognized degradation product of cyclic nitramines, including RDX and HMX [18]. However, no mass signals at m/z 171 were observed for injections of formaldehyde analytical standards. Further study using ^{15}N -labeled HMX, purified 4NO-HMX, and the quadrupole's MS-MS capability will better serve to define the identity of this degradation product.

4. Conclusion

A sulfobutylether- β -cyclodextrin assisted capillary electrophoresis system was applied in conjunction with

a quadrupole ion-trap mass spectrometer for the identification of contaminant nitroaromatic and cyclic nitramine explosives and their degradation products. The work demonstrates the use of cyclodextrin dependent CE-MS for the analysis of explosives in environmental samples, and offers potential for the identification of highly polar or charged degradation products.

Acknowledgements

The authors wish to thank Thiokol Propulsion (Brigham City UT USA) for the provision of CL-20. We gratefully acknowledge the provision of funding by the US DoD Strategic Environmental Research and Development Program (SERDP CU 1213 and CP1256) and by the US Office of Naval Research (Award N000140310269).

References

- [1] J.C. Spain, in: J.C. Spain, J.B. Hughes, H.-J. Knackmuss (Eds.), *Biodegradation of Nitroaromatic Compounds and Explosives*, CRC Press, Boca Raton FL, 2002, p. 1, Chapter 1.

- [2] United States General Accounting Office, Report GAO-04-147 Military Munitions: DOD Needs to Develop a Comprehensive Approach for Cleaning Up Contaminated Sites, December 2003.
- [3] Report of the Auditor General, National Defence, Office of the Auditor General of Canada, April 2003 (Chapter 7).
- [4] Method 8330, Nitroaromatics and nitramines by high performance liquid chromatography (HPLC); test methods evaluating solid waste, SW-846 update III. Part 4 (B), EPA, Office of Solid Waste, Washington, DC, 1997.
- [5] R.C. Willoughby, R.F. Browner, *Anal. Chem.* 56 (1984) 2626.
- [6] B. Cassetta, F. Garofolo, *Org. Mass Spectrom.* 29 (1994) 517.
- [7] J. Yinon, J.E. McClellan, R.A. Yost, *Rapid Comm. Mass Spectrom.* 11 (1997) 1961.
- [8] A. Gapeev, M. Sigman, J. Yinon, *Mass Spectrom.* 17 (2003) 943.
- [9] J. Yinon, D.-G. Hwang, *J. Chromatogr.* 268 (1983) 45.
- [10] Z. Wu, C.L. Hendrickson, R.P. Rodgers, A.G. Marshall, *Anal. Chem.* 74 (2002) 1879.
- [11] R.D. Voyksner, J. Yinon, *J. Chromatogr.* 354 (1986) 393.
- [12] C.S. Evans, R. Sleeman, J. Luke, B.J. Keely, *Rapid Commun. Mass Spectrom.* 16 (2002) 1883.
- [13] Y. Takada, H. Nagano, S. Masao, Y. Hashimoto, M. Sakairi, K. Kusumoto, T. Ota, J. Nakamura, *Prop. Expl. Pyrotech.* 27 (2002) 224.
- [14] X. Zhao, J. Yinon, *J. Chromatogr. A* 977 (2002) 59.
- [15] J. Hawari, A. Halasz, L. Paquet, E. Zhou, B. Spencer, G. Ampleman, S. Thiboutot, *Appl. Environ. Microbiol.* 64 (1998) 2200.
- [16] A. Halasz, J. Spain, C. Beaulieu, J. Hawari, *Environ. Sci. Technol.* 36 (2002) 633.
- [17] J. Hawari, A. Halasz, C.A. Groom, S. Deschamps, L. Paquet, C. Beaulieu, A. Corriveau, *Environ. Sci. Technol.* 36 (2002) 5117.
- [18] V.K. Balakrishnan, A. Halasz, J. Hawari, *Environ. Sci. Technol.* 37 (2003) 1838.
- [19] T.W. Sheremata, J. Hawari, *Environ. Sci. Technol.* 34 (2000) 3384.
- [20] D. Fournier, A. Halasz, J. Spain, R.J. Spanggord, J.C. Bottaro, J. Hawari, *Appl. Environ. Microbiol.* 70 (2004) 1123.
- [21] D.T. Burns, R.J. Lewis, *Anal. Chim. Acta* 307 (1995) 89.
- [22] S. Campbell, R. Ogoshi, G. Uehara, Q.X. Li, *J. Chromatogr. Sci.* 41 (2003) 284.
- [23] M. Bader, T. Göen, J. Müller, J. Angerer, *J. Chromatogr. B* 710 (1998) 91.
- [24] S. Waite, *LC GC* 12 (2003) 34.
- [25] J.B.F. Lloyd, *Anal. Chem.* 56 (1984) 1907.
- [26] B.K. Glod, M. Baumann, *J. Sep. Sci.* 26 (2003) 1547.
- [27] D.M. Northrop, D.E. Martire, W.A. MacCrehan, *Anal. Chem.* 63 (1991) 1038.
- [28] C.A. Groom, A. Halasz, L. Paquet, P. D'Cruz, J. Hawari, *J. Chromatogr. A* 999 (2003) 17.
- [29] Advasep 4 Material safety data sheet MSDS Number ADV4-001, Cydex, Overland Park, KS, 1999.
- [30] D. Fournier, A. Halasz, J. Spain, P. Fiurasek, J. Hawari, *Appl. Environ. Microbiol.* 68 (2002) 166.
- [31] A.R. Khan, P. Forgo, K.J. Stine, V.T. D'Souza, *Chem. Rev.* 98 (1998) 1977.
- [32] T. Kraus, M. Budesinsky, J. Zavada, *J. Org. Chem.* 66 (2001) 4595.
- [33] T. De Boer, R.A. de Zeeuw, G.J. de Jong, K. Ensing, *Electrophoresis* 21 (2000) 3220.
- [34] S. Grard, C. Elfakir, M. Dreux, *J. Chromatogr. A* 925 (2001) 79.
- [35] F. Monteil-Rivera, L. Paquet, S. Deschamps, V.K. Balakrishnan, C. Beaulieu, J. Hawari, *J. Chromatogr. A* 1025 (2004) 125.
- [36] B. Bhushan, L. Paquet, J. Spain, J. Hawari, *Appl. Environ. Microbiol.* 69 (2003) 5216.
- [37] S. Trott, S.F. Nishino, J. Hawari, J.C. Spain, *Appl. Environ. Microbiol.* 69 (2003) 1871.
- [38] J. Hawari, S. Deschamps, C. Beaulieu, L. Paquet, A. Halasz, *Water Res.* 38 (2004) 4055.
- [39] R. Bakhtiar, S. Bulusu, *Rapid Commun. Mass Spectrom.* 9 (1995) 1391.
- [40] K. Srinivasan, M.G. Bartlett, *Rapid Commun. Mass Spectrom.* 14 (2000) 624.
- [41] S.J. Gaskell, *J. Mass Spectrom.* 32 (1997) 677.
- [42] Capitosol FAQ <http://www.cydexinc.com/faq-01.html>, Cydex, Overland Park, KS, 2004.
- [43] T. Reemtsma, *J. Chromatogr. A* 1000 (2003) 477.
- [44] Solvent data base Louisiana State University, 2004, <http://macro.lsu.edu/howto/solvents>.

ORIGINAL ARTICLE

Effect of iron(III), humic acids and anthraquinone-2,6-disulfonate on biodegradation of cyclic nitramines by *Clostridium* sp. EDB2

B. Bhushan, A. Halasz and J. Hawari

Biotechnology Research Institute, National Research Council of Canada, Montreal, Quebec, Canada

KeywordsAQDS, biodegradation, *Clostridium* sp., Fe(III), HMX, humic acids, RDX.**Correspondence**

Jalal Hawari, Biotechnology Research Institute,
National Research Council of Canada, 6100
Royalmount Avenue, Montreal, Quebec H4P
2R2, Canada.
E-mail: jalal.hawari@nrc.ca

2005/0484: received 5 May 2005, revised and
accepted 11 July 2005

doi:10.1111/j.1365-2672.2005.02819.x

Abstract

Aims: To determine the biodegradation of cyclic nitramines by an anaerobic marine bacterium, *Clostridium* sp. EDB2, in the presence of Fe(III), humic acids (HA) and anthraquinone-2,6-disulfonate (AQDS).

Methods and Results: An obligate anaerobic bacterium, *Clostridium* sp. EDB2, degraded RDX and HMX, and produced similar product distribution including nitrite, methylenedinitramine, nitrous oxide, ammonium, formaldehyde, formic acid and carbon dioxide. Carbon (C) and nitrogen (N) mass balance for RDX products were 87% and 82%, respectively, and for HMX were 88% and 74%, respectively. Bacterial growth and biodegradation of RDX and HMX were stimulated in the presence of Fe(III), HA and AQDS suggesting that strain EDB2 utilized Fe(III), HA and AQDS as redox mediators to transfer electrons to cyclic nitramines.

Conclusions: Strain EDB2 demonstrated a multidimensional approach to degrade RDX and HMX: first, direct degradation of the chemicals; second, indirect degradation by reducing Fe(III) to produce reactive-Fe(II); third, indirect degradation by reducing HA and AQDS which act as electron shuttles to transfer electrons to the cyclic nitramines.

Significance and Impact of the Study: The present study could be helpful in determining the fate of cyclic nitramine energetic chemicals in the environments rich in Fe(III) and HA.

Introduction

Environmental contamination of soil, sediments and groundwater, with RDX (hexahydro-1,3,5-trinitro-1,3,5-triazine) and HMX (octahydro-1,3,5,7-tetranitro-1,3,5,7-tetrazocine), is a worldwide problem. The Departments of Defense (DoD) and Energy (DoE), USA, alone have over 21 000 contaminated sites and most of them are contaminated with explosives (Talley and Sleeper 1997). The Department of Defense Canada has an estimated 103 training sites and three open burning/open detonation (OB/OD) sites which are potentially contaminated with RDX, HMX and 2,4,6-trinitrotoluene (TNT) (Thiboutot *et al.* 1998). There are countless number of explosives-contaminated sites around the world which remain classified and statistically not available. Several reports have

confirmed that RDX and HMX are toxic, and cause adverse effects on biological systems, environment and human health (Levine *et al.* 1990; Yinon 1990; Talmage *et al.* 1999; Gong *et al.* 2002; Kucukardali *et al.* 2003; Hoek 2004). United States Environmental Protection Agency (USEPA) has recommended a lifetime health advisory for RDX (Etnier and Hartley 1990) and HMX (McLellan *et al.* 1988). Consequently, the cleanup of explosive(s)-contaminated sites is a matter of growing concern among environmental protection groups.

Bioremediation of cyclic nitramines such as RDX and HMX, with very little water solubility of 40.0 and 6.6 mg l⁻¹, respectively (Groom *et al.* 2003), has always been a challenging task. Microbial degradation and augmentation of natural attenuation are the most reliable cost-effective methods for *in situ* remediation. Previous

reports have mainly highlighted the role of zero-valent iron, Fe(0), in augmenting the biodegradation of RDX (Scherer *et al.* 2000; Oh *et al.* 2001; Wildman and Alvarez 2001); however, no literature is available on the use of Fe(III), HA and/or AQDS, frequently encountered in the environment, in accelerating biodegradation of cyclic nitramines.

In marine and freshwater environments, Fe(II)-minerals and humic substances have been shown to accelerate abiotic transformation of organic pollutants (Schwarzenbach *et al.* 1990; Curtis and Reinhard 1994). In our previous studies, we found that Halifax sediments, collected from a shipwreck site near Halifax harbour in Canada, contained a high amount of insoluble iron mainly Fe(III) and Fe(II) (40 g kg⁻¹ sediment) as determined with X-ray photo-spectroscopy, and a significant amount of organic carbon content (16 g kg⁻¹ sediment) (Bhushan *et al.* 2004; Zhao *et al.* 2004a). In the present study, we explored the possibility of whether microbially reduced iron minerals, humic acids (HA) and its analogue anthraquinone-2,6-disulphonate (AQDS) can help enhance biodegradation of RDX and HMX. Enhanced degradation under laboratory conditions may help understand and thus strategies can be devised to accelerate the natural attenuation of these chemicals in marine and estuarine environments.

Materials and methods

Chemicals

Commercial grade RDX, HMX (chemical purity >99% for both explosives), [UL-¹⁴C]RDX (chemical purity >98%, radiochemical purity 97% and specific radioactivity 28.7 µCi mmol⁻¹) and [UL-¹⁴C]HMX (chemical purity >94%, radiochemical purity 91% and specific radioactivity 101.0 µCi mmol⁻¹) were provided by the Defense Research and Development Canada (DRDC), Valcartier, Quebec. Hexahydro-1-nitroso-3,5-dinitro-1,3,5-triazine (MNX) and 4-nitro-2,4-diazabutanal (NDAB) were obtained from SRI International (Menlo Park, CA). Hexahydro-1,3,5-trinitroso-1,3,5-triazine (TNX) was synthesized according to the method described by Brockman *et al.* (1949). Methylenedinitramine (MEDINA) was obtained from the Rare Chemical Department of Aldrich, Oakville, Ontario, Canada.

Ferrozine, Fe₂O₃ (hematite), α-FeOOH (goethite), anthraquinone-2,6-disulfonate (AQDS), HCHO, HCOOH and NADH were purchased from Sigma Chemicals, Canada. Humic acid (HA), purchased from Aldrich, Oakville, Ontario, Canada, was washed with deionized water three times to remove soluble impurities. Nitrous oxide (N₂O) was purchased from Scott Specialty Gases,

Sarnia, Ontario, Canada. All other chemicals were of highest purity grade.

Media composition

Medium M1 was composed of (per litre): peptone 8 g, yeast extract 4 g, NaCl 10 g and glucose 6 g. Medium M2 was composed of (per litre): NaCl 10.0 g, NaHCO₃ 2.5 g, NaH₂PO₄ 0.6 g, KCl 0.2 g and NH₄Cl 0.5 g. Ingredients were mixed in hot water and pH was adjusted to 7.0 with 1 N NaOH. One litre of M2 medium was bubbled with N₂ : CO₂ (80 : 20) for 45 min. After autoclaving at 121°C for 20 min, we added filter-sterilized solutions of glucose 4.5 g, peptone 1.0 g, trace elements 10 ml and vitamin mixture 10 ml. The composition of trace elements and vitamin mixture were the same as reported (Lovley *et al.* 1984). For making solid agar slants or plates of medium M1 or M2, 1.8% (w/v) agar powder (Difco) was added to the respective medium.

Reduction of Fe(III) and AQDS by growing culture and resting cells of strain EDB2

Strain EDB2, isolated from a marine sediment in our previous study (Bhushan *et al.* 2004), was grown in medium M2 containing either 50 mmol l⁻¹ Fe(III)-citrate or 1.0 mmol l⁻¹ AQDS under anaerobic conditions. Bacterial growth was determined in terms of total cell count following staining with 0.01% acridine orange as described previously (Hobbie *et al.* 1977) by using an epifluorescent microscope (Leitz Wetzlar, Germany). For Fe(III) and AQDS reduction assay, cells (10 mg wet biomass/ml) were incubated with either 10 mmol l⁻¹ Fe(III)-citrate or 1 mmol l⁻¹ AQDS in the presence of NADH. The reduction of AQDS to AH₂QDS was measured at A_{450nm} (Lovley *et al.* 1996), whereas reduction of Fe(III) to Fe(II) was determined by Ferrozine method (Stookey 1970).

Biotransformation assays

Biotransformation assays were performed in 6-ml air-tight glass vials under strict anaerobic conditions by purging the aqueous phase and the head space with argon for 20 min. Each assay vial contained, in 1 ml of assay mixture, either RDX (50 µmol l⁻¹) or HMX (30 µmol l⁻¹), NADH (150 µmol l⁻¹), resting cells preparation (5 mg wet biomass/ml) and potassium phosphate buffer (50 mmol l⁻¹, pH 7.0). Reactions were performed at 30°C. Three different controls were prepared by omitting either resting cells, NADH or both from the assay mixture. Residual NADH was measured as described before (Bhushan *et al.* 2003). Samples from the liquid and the gas phase in the vials were analysed

(described below) for the residual compound and its products.

Effect of Fe(III), HA and AQDS on bacterial growth and biodegradation of cyclic nitramines

Variable concentrations of Fe(III) (10–40 mmol l⁻¹), HA (0.1–2.0 mg ml⁻¹) and AQDS (0.1–2.0 mmol l⁻¹) were added separately to the medium M1 containing either RDX (150 µmol l⁻¹) or HMX (55 µmol l⁻¹) in serum bottles. After inoculation of the medium with strain EDB2, the disappearance of RDX and HMX was followed over time with HPLC. Microbial reduction of AQDS to AH₂QDS was marked by the gradual appearance of orange colour that was measured at A_{450nm} (Lovley *et al.* 1996), whereas bacterial growth was measured by direct cell counts as described above. Reduction of Fe(III) was estimated by Ferrozine method (Stookey 1970). Data were compared with a parallel control experiment with strain EDB2 but without any of the Fe(III), HA or AQDS. Parallel abiotic (without strain EDB2) control experiments with Fe(III), HA or AQDS were also performed to account for the abiotic degradation of RDX and HMX.

Effect of Fe(III), HA and AQDS on mineralization of radio-labelled cyclic nitramines

Mineralization experiments were performed under anaerobic conditions in 20-ml glass vials sealed with Teflon-coated butyl rubber stopper under an atmosphere of nitrogen. Microcosms were prepared in 5.0 ml of medium M1 containing Fe(III), HA or AQDS at a concentration of 25 mmol l⁻¹, 1 mg ml⁻¹ or 1.0 mmol l⁻¹, respectively, and inoculated with 1 ml of bacterial culture (approximately 2 × 10⁸ cells ml⁻¹). Radio-labelled [UL-¹⁴C]RDX (33 µg ml⁻¹ medium equivalent to 50118 dpm) or [UL-¹⁴C]HMX (16 µg ml⁻¹ medium equivalent to 54310 dpm) was added to the microcosms through the rubber septum. A glass tube, placed inside the microcosm, containing 0.5 ml of 0.5 mol l⁻¹ KOH was used as ¹⁴CO₂ trap. Corresponding abiotic controls (without bacterial culture) were also prepared. Evolution of ¹⁴CO₂ was determined in terms of dpm counts in KOH solution using a liquid scintillation counter (Packard, Tri-Carb 4530, model 2100 TR, Packard Instruments Company, Meriden, CT).

Abiotic degradation of cyclic nitramines by microbially reduced HA, AH₂QDS and iron minerals

Reduced HA was prepared by growing EDB2 cells in medium M1, containing HA (1 mg ml⁻¹), for 4 days at 30°C under anaerobic conditions (N₂ : CO₂; 80 : 20).

After stationary growth phase, HgCl₂ (2.5 mmol l⁻¹) was added to the medium to kill the bacterial cells. The black precipitate thus obtained was allowed to settle at the bottom, liquid phase was removed aseptically from the top using a syringe. The precipitate was dried under argon atmosphere and used for determining its reactivity against RDX and HMX (see below).

AH₂QDS was produced by microbial reduction of AQDS. Strain EDB2 was grown in medium M1 supplemented with 1 mmol l⁻¹ AQDS. Production of AH₂QDS was followed at A_{450nm} until the stationary phase (~OD 0.97) was obtained. Bacterial cells were removed by filtration through sterile 0.22-µm pore filter (Millipore, Bedford, MA), and the sterile AH₂QDS thus obtained, was stored under anaerobic conditions (argon atmosphere). RDX (20 µmol l⁻¹) or HMX (20 µmol l⁻¹) was incubated with 1 ml of AH₂QDS under anaerobic conditions at 30°C for different time intervals. Residual cyclic nitramine was measured with HPLC (described below).

Reduced biogenic iron minerals were prepared by adding either soluble- (i.e., ferric-citrate) or insoluble- (i.e., hematite or goethite) Fe(III) to the medium M2 at a concentration of 50 mmol l⁻¹. Generation of Fe(II) was followed over time as a function of growth of strain EDB2. The Fe(II) was estimated by the Ferrozine method (Stookey 1970) following extraction with 0.5 N HCl. For X-ray diffraction (XRD) analysis of reduced iron, cells were grown in medium M2 supplemented with 100 mmol l⁻¹ ferric citrate for 4 days at 30°C under anaerobic (N₂ : CO₂; 80 : 20) and stationary conditions. Iron(III) was completely reduced to dark brown precipitates settled at the bottom. The liquid phase was removed with sterile syringe by piercing through the septum. The reduced iron precipitate thus obtained was dried under argon atmosphere and stored under argon until analysed. XRD-phase analyses were performed and analysed by CAMET Research Inc., Goleta, CA. The dried iron precipitate samples were grounded in agate mortar prior to probing in a wide angle powder diffractometer using Cu Kα radiation (8.1 keV) with a diffracted beam monochromator.

Siderite (FeCO₃), obtained by strain EDB2-mediated reduction of Fe(III)-citrate, and the black precipitate of reduced iron mineral, obtained by bacterial reduction of goethite (α-FeOOH), were prepared as described above except that HgCl₂ (2.5 mmol l⁻¹) was added to the medium to kill the bacterial cells before isolating the reduced precipitate. Reactions of reduced substrates (i.e., HA or iron, each 1 mg ml⁻¹) with RDX (20 µmol l⁻¹) or HMX (20 µmol l⁻¹) were conducted in PBS (50 mmol l⁻¹, pH 7.0) at 30°C under anaerobic conditions with argon in headspace. The procedure and conditions were same as described above for biotransformation assays.

Analytical procedures

RDX, HMX and their degradation products such as nitroso intermediates, methylenedinitramine, NO_2^- , NH_4^+ , HCHO, HCOOH and N_2O were analysed with LC–UV, LC–MS or GC as previously reported (Hawari *et al.* 2001; Halasz *et al.* 2002).

Results

Biodegradation of cyclic nitramines by strain EDB2

An obligate anaerobic bacterium *Clostridium* strain EDB2 was isolated from a marine sediment which demonstrated chemotaxis response towards RDX and HMX and degraded both energetic chemicals (Bhushan *et al.* 2004). In the present study, a time course with intact resting cells showed that the disappearance of both RDX and HMX was accompanied by the concomitant release of nitrite, nitrous oxide and HCHO (Fig. 1a,b). After 4 h of reaction, each reacted RDX molecule consumed 0.9 ± 0.1 (mean \pm SD; $n = 3$) NADH molecule, and produced 0.7 molecules of nitrite, 0.2 molecules of MEDINA, 1.4 molecules of nitrous oxide, 0.6 molecules of ammonium, 1.8 molecules of formaldehyde and 0.6

molecule of formic acid (Table 1). Of the total three carbons in each RDX molecule, 2.4 were recovered as formaldehyde and formic acid; whereas of the total six nitrogen atoms in each RDX molecule, 4.1 were recovered as nitrite, nitrous oxide and ammonium. The total carbon and nitrogen mass balance were determined as 87% and 82%, respectively (Table 1).

On the other hand, each reacted HMX molecule consumed 1.1 ± 0.1 (mean \pm SD; $n = 3$) NADH molecule, and produced 0.8 molecules of nitrite, 0.1 molecules of MEDINA, 1.7 molecules of nitrous oxide, 1.3 molecules of ammonium, 2.6 molecules of formaldehyde and 0.8 molecules of formic acid (Table 1). Of the total four carbons in each HMX molecule, 3.4 were recovered as formaldehyde and formic acid, whereas of the total eight nitrogen atoms, 5.5 were recovered as nitrite, nitrous oxide and ammonium. The carbon and nitrogen mass balance were determined as 88% and 74%, respectively (Table 1).

In addition to the above products, we also detected traces of nitroso intermediates from RDX such as MNX, hexahydro-1,3-dinitroso-5-nitro-1,3,5-triazine (DNX) and hexahydro-1,3,5-trinitroso-1,3,5-triazine (TNX), whereas HMX produced a trace amount of mononitroso-intermediate, octahydro-1-nitroso-3,5,7-trinitro-1,3,5,7-tetrazocine. None of the nitroso-intermediates from either RDX or HMX persisted and disappeared after the complete removal of RDX or HMX from the medium.

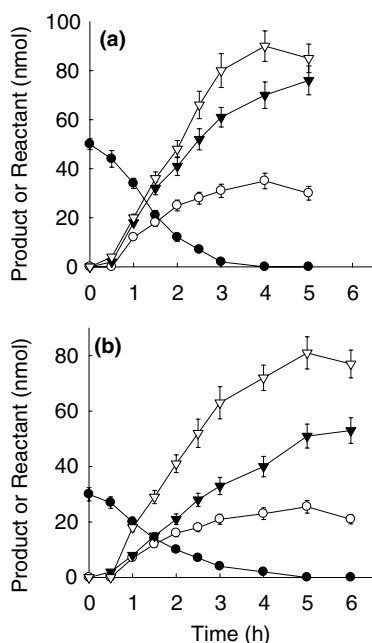


Figure 1 Time course of biotransformation of RDX (a) and HMX (b) by intact resting cells of strain EDB2 using NADH as electron donor at pH 7.0 and 30°C. Symbols for both figures, RDX or HMX (●), nitrite (○), nitrous oxide (▼) and formaldehyde (▽). Data are mean \pm SD ($n = 3$). Some error bars are not visible because of their small size.

Effect of Fe(III), HA and AQDS on bacterial growth and biodegradation of cyclic nitramines

When strain EDB2 was grown in medium M2 under anaerobic conditions in the presence of either Fe(III), AQDS or HA, all three chemicals stimulated bacterial growth compared to the control (Fig. 2). Furthermore, we found that intact resting cells of strain EDB2 reduced Fe(III) citrate and AQDS using NADH as an electron donor (data not shown).

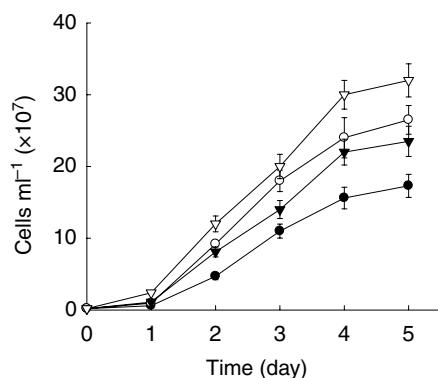
In growing culture, HA (1 mg ml^{-1}), AQDS (1 mmol l^{-1}) and Fe(III) (25 mmol l^{-1}) enhanced the biotransformation of RDX in medium M1 compared to the control (Fig. 3a). We found that RDX ($150 \mu\text{mol l}^{-1}$) was completely removed in 5 days in the presence of HA, and in 8 days in the presence of either Fe(III) or AQDS, as compared to 10 days in the absence of these chemicals (Fig. 3a). On the other hand, mineralization of RDX was higher in the presence of either HA, AQDS or Fe(III) as compared to that in the absence of these chemicals (Fig. 3b). Of the initial $150 \mu\text{mol l}^{-1}$ of $[\text{UL-}^{14}\text{C}]\text{RDX}$, about $54\text{--}60 \mu\text{mol l}^{-1}$ was mineralized to $^{14}\text{CO}_2$ in the presence of either HA, AQDS or Fe(III) compared to the control without these chemicals which showed $42 \mu\text{mol l}^{-1}$ mineralization (Fig. 3b).

Table 1 Product stoichiometry and mass balance determined after 4 and 5 h reaction of strain EDB2 with RDX and HMX, respectively

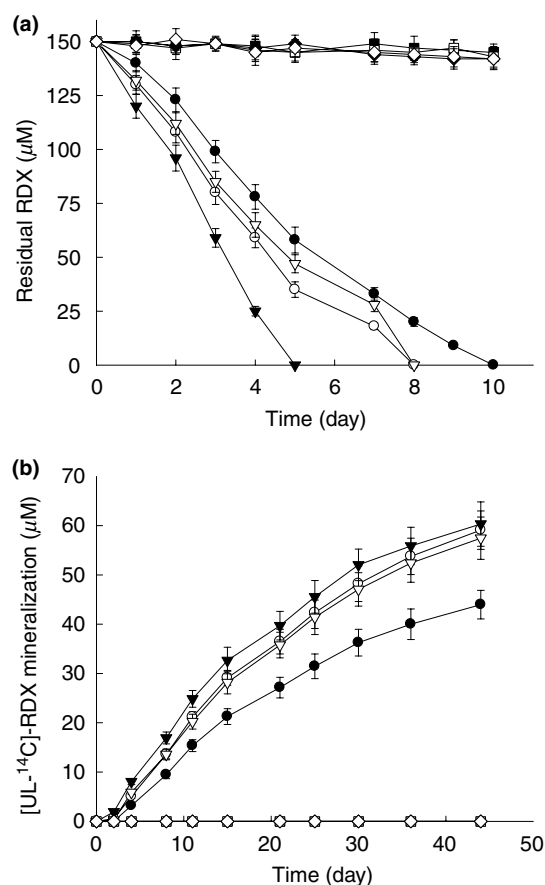
Reactant/ product	RDX				HMX			
	Amount (nmol)	Molar ratio of products per reacted RDX molecule	% Nitrogen recovery	% Carbon recovery	Amount (nmol)	Molar ratio of products per reacted HMX molecule	% Nitrogen recovery	% Carbon recovery
1. RDX/HMX	50	1.0	100	100	30	1.0	100	100
2. Nitrite	35	0.7	11.7	NA	25	0.8	10.0	NA
3. MEDINA*	10	0.2	13.3	6.7	3	0.1	5.0	2.5
4. Nitrous oxide	70	1.4	46.7	NA	52	1.7	42.5	NA
5. Ammonium	30	0.6	10.0	NA	39	1.3	16.3	NA
6. Formaldehyde	91	1.8	NA	60.0	78	2.6	NA	65.0
7. Formic acid	30	0.6	NA	20.0	23	0.8	NA	20.0
Total mass balance			81.7	86.7			73.8	87.5

NA, not applicable.

*Methylenedinitramine.

**Figure 2** Growth of strain EDB2 in medium M2 in the presence of Fe(III) citrate (▽), AQDS (○), humic acids (▼) and control without any of these chemical (●) at pH 7.0 and 30°C under anaerobic conditions. Data are mean \pm SD ($n = 2$). Some error bars are not visible because of their small size.

On the other hand, addition of either Fe(III), HA or AQDS to medium M1 enhanced biotransformation of HMX at various levels (Fig. 4a). In the presence of Fe(III), HMX ($55 \mu\text{mol l}^{-1}$) was completely removed from the growth medium within 5 days of incubation compared to the control which took 11 days to degrade the chemical (Fig. 4a). Mineralization of HMX was also enhanced in the presence of either Fe(III), HA or AQDS (Fig. 4b). Of the initial $55 \mu\text{mol l}^{-1}$ of $[\text{UL-}^{14}\text{C}]\text{HMX}$, about $12 \mu\text{mol l}^{-1}$ was mineralized to $^{14}\text{CO}_2$ in the presence of Fe(III) compared to the control without Fe(III) which showed only $2.8 \mu\text{mol l}^{-1}$ of mineralization after 45 days of incubation (Fig. 4b). Abiotic controls containing either Fe(III), HA or AQDS did not react with either RDX or HMX in the absence of strain EDB2.

**Figure 3** Biotransformation (a) and mineralization (b) of RDX by growing culture of strain EDB2 in medium M1 in the presence of Fe(III) citrate (▽), humic acids (▼), AQDS (○) and medium without additive (●). Abiotic controls, iron (■), humic acids (□), AQDS (◆) and medium without additive (◇). Data are mean \pm SD ($n = 2$). Some error bars are not visible because of their small size.

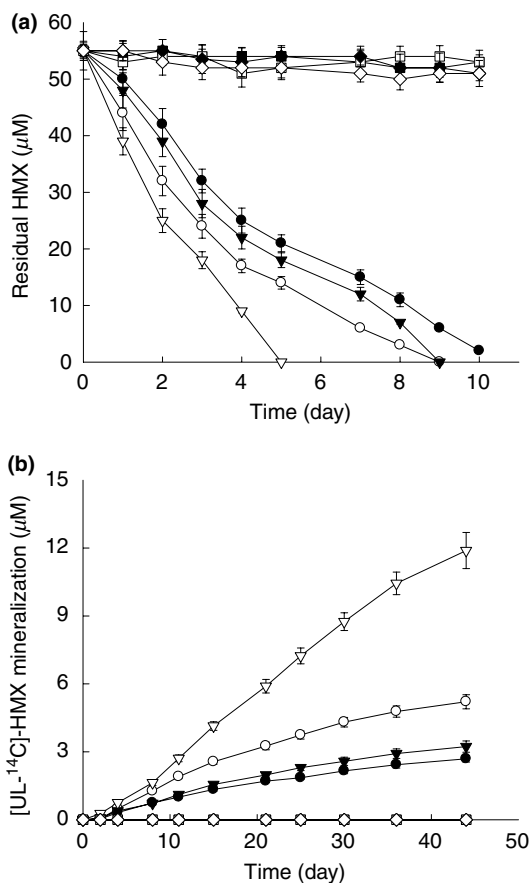


Figure 4 Biotransformation (a) and mineralization (b) of HMX by growing culture of strain EDB2 in medium M1 in the presence of Fe(III) citrate (▽), humic acids (▼), AQDS (○) and medium without additive (●). Abiotic controls, iron (■), humic acids (□), AQDS (◆) and medium without additive (◇). Data are mean \pm SD ($n = 2$). Some error bars are not visible because of their small size.

Degradation of cyclic nitramines by microbially reduced HA, AH₂QDS and iron minerals

Strain EDB2 reduced AQDS to AH₂QDS as a function of its growth. At stationary growth phase (after 4 days) all of the AQDS (1 mmol l^{-1}) was converted to AH₂QDS with $\text{OD}_{450\text{nm}}$ 0.97 (Fig. 5). We found that cell-free AH₂QDS transformed RDX and HMX at rates of 0.5 ± 0.05 and $0.3 \pm 0.02 \text{ nmol h}^{-1} \mu\text{mol AH}_2\text{QDS}^{-1}$ (Table 2). On the other hand, cell-free reduced HA also transformed RDX and HMX at rates of 0.7 ± 0.1 and $0.2 \pm 0.02 \text{ nmol h}^{-1} \text{ mg dry HA}^{-1}$ (Table 2).

To understand why the presence of Fe(III) enhanced biodegradation, we prepared cell-free precipitate of microbially reduced iron and determined its reactivity towards RDX and HMX (see experimental section). X-ray diffraction analysis showed that the reduced iron precipitate was of biogenic siderite (FeCO_3). The latter, abiotically

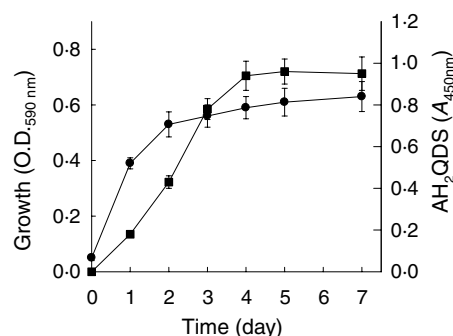


Figure 5 Reduction of AQDS to AH₂QDS (■) in medium M1 by the growing culture of strain EDB2 (●). Data are mean \pm SD ($n = 3$). Some error bars are not visible because of their small size.

Table 2 Abiotic degradation of RDX and HMX by microbially reduced iron, humic acids and AH₂QDS

Microbially reduced chemical	Rate of degradation [$\text{nmol h}^{-1} (\text{mg reduced chemical})^{-1}$]	
	RDX	HMX
1. Siderite	0.5 ± 0.1	0.4 ± 0.04
2. Goethite	0.3 ± 0.05	0.2 ± 0.02
3. Hematite	0.4 ± 0.1	0.1 ± 0.01
4. Humic acids	0.7 ± 0.1	0.2 ± 0.02
5. AH ₂ QDS*	0.5 ± 0.05	0.3 ± 0.02

*Rate of transformation in terms of $\text{nmol h}^{-1} (\mu\text{mol AH}_2\text{QDS})^{-1}$.

Data are mean \pm SD ($n = 3$).

cally transformed RDX and HMX at rates of 0.5 ± 0.1 and $0.4 \pm 0.04 \text{ nmol h}^{-1} \text{ mg dry mineral}^{-1}$, respectively (Table 2). On the other hand, insoluble forms of Fe(III) such as goethite ($\alpha\text{-FeOOH}$) and hematite (Fe_2O_3) were also reduced to Fe(II) by strain EDB2 as determined by the Ferrozine method (Stookey 1970). We found that goethite, reduced by strain EDB2, transformed RDX and HMX at rates of 0.3 ± 0.05 and $0.2 \pm 0.02 \text{ nmol h}^{-1} \text{ mg dry mineral}^{-1}$, respectively, whereas reduced hematite also transformed RDX and HMX at rates of 0.4 ± 0.1 and $0.1 \pm 0.01 \text{ nmol h}^{-1} \text{ mg dry mineral}^{-1}$, respectively (Table 2), compared to the non-reduced iron minerals which did not react with any of the two cyclic nitramines. In control experiments, the free Fe(II) solution ($20 \text{ mmol l}^{-1} \text{ FeSO}_4$) did not react with either RDX or HMX under abiotic conditions for up to 22 days.

Discussion

We demonstrated that *Clostridium* sp. EDB2 degraded cyclic nitramines, RDX and HMX. The products (i.e., nitrite and nitroso intermediates) obtained from RDX

and HMX revealed that both chemicals were degraded via two different pathways that occurred simultaneously, i.e., first, initial N-denitration, and second, initial reduction of nitro groups to nitroso groups. The concomitant release of N_2O and HCHO from RDX and HMX is indicative of ring opening and decomposition of the respective molecule. The products and pathways of degradation were closely similar to those reported earlier with other *Clostridium* spp. For instance, *Cl. bifermentans* HAW 1 degraded RDX and HMX either via initial N-denitration or via initial reduction to corresponding nitroso intermediates (Zhao *et al.* 2003, 2004b), whereas Zhang and Hughes (2003) reported biodegradation of RDX with *Cl. acetobutylicum* via sequential reduction of all the three nitro groups.

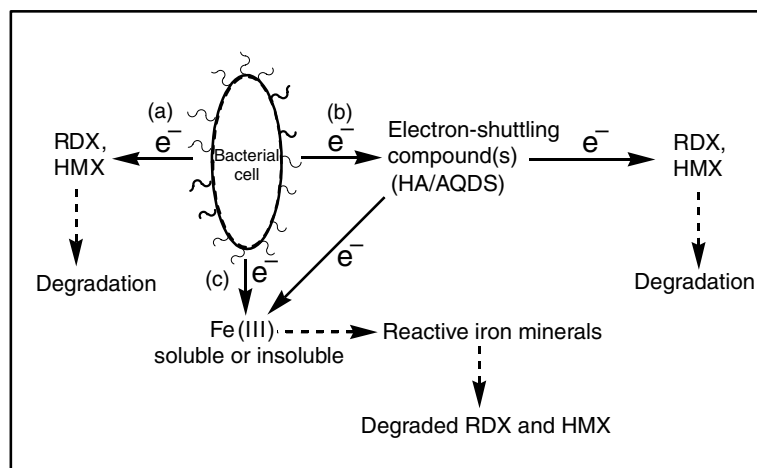
Interestingly, we found that Fe(III), AQDS and HA stimulated the growth of strain EDB2 suggesting that strain EDB2 utilized these chemicals as terminal electron acceptors. This finding is in accordance with the previous studies which also reported that Fe(III) stimulated the growth of fermentative bacteria, *Cl. beijerinckii* (Dobbin *et al.* 1999) and *Cl. butyricum* EG3 (Park *et al.* 2001), by acting as an electron sink. On the other hand, resting cells of strain EDB2 also reduced Fe(III) and AQDS indicating the involvement of a membrane-linked reductase enzyme(s). Furthermore, the presence of Fe(III), AQDS and HA in the growth medium enhanced the biodegradation of RDX and HMX by strain EDB2. In accordance with our findings, the Fe(II)-bearing minerals such as siderite, goethite and hematite have been shown to be reactive towards nitroaromatic compounds and polyhalogenated alkanes (Elsner *et al.* 2004). Analogously, the present study also suggested that iron-reducing bacteria present in the sediment environments might produce reactive biogenic iron minerals. The latter could react with cyclic-nitramines abiotically (as shown above) to accelerate their *in situ* degradation.

Recently, Gregory *et al.* (2004) reported that RDX did not react with freely suspended Fe(II) alone; however, Fe(II) bound to magnetite abiotically transformed RDX to produce NH_4^+ , N_2O and HCHO. Furthermore, only 10% of RDX was mineralized to CO_2 , which indicated that efficient mineralization cannot be achieved under abiotic conditions. The finding of Gregory *et al.* (2004) is in accordance with our present observation that free Fe(II) (as $FeSO_4$) did not react with either RDX or HMX for up to 22 days of incubation, however, Fe(II) bound to the siderite, hematite and goethite did react with both energetic chemicals.

It is evident that strain EDB2 first biotransformed RDX and HMX to produce HCHO, which then underwent bio-conversion to CO_2 . For instance, when we incubated growing cells of strain EDB2 with radio-labelled $H^{14}CHO$ under similar conditions as those used for RDX or HMX, we found 40% mineralization of $H^{14}CHO$ to $^{14}CO_2$ in 4 days (data not shown). As shown above, the nonreduced Fe(III), HA and AQDS did not react with either RDX or HMX suggesting an indirect involvement of the three chemicals in accelerating the biodegradation process. In a subsequent experiment (Table 2), we found that microbially reduced iron, HA and AH_2QDS abiotically reacted with RDX and HMX to eventually produce HCHO, a source of CO_2 , and thereby indirectly accelerated the mineralization process.

Taken together, strain EDB2 demonstrated a multidimensional approach to degrade RDX and HMX (Fig. 6): first, directly by coming in contact with the two cyclic nitramines; second, by reducing Fe(III), the most abundant electron acceptor in marine and freshwater sediments, to produce biogenic Fe(II), which is reactive towards cyclic nitramines; and third, by reducing electron shuttles such as HA and AQDS, which act as electron shuttles to transfer electrons to the cyclic nitramines. In all the three cases, product distribution was similar

Figure 6 Schematic representation of strategies used by strain EDB2 to degrade RDX and HMX via different routes. (a) Cyclic nitramines degraded by direct interaction with strain EDB2. (b) Electron-shuttle compounds (HA/AQDS), reduced by strain EDB2, abiotically degraded cyclic nitramines. (c) Iron minerals, reduced by strain EDB2, abiotically degraded cyclic nitramines. Solid arrows indicate direction of flow of electrons.



because the cyclic nitramines were degraded either via initial N-denitration or via initial reduction of nitro groups to nitroso groups prior to ring cleavage and decomposition. The above properties render strain EDB2 suitable for accelerating the (bio)remediation of cyclic nitramine explosives in iron(III)- and HA-rich environments such as marine sediments.

As microbial reduction of iron and humic substances occurs on a large-scale in subsurface environments such as sediments, estuaries and groundwater (Lonergan *et al.* 1996; Benz *et al.* 1998; Coates *et al.* 1998; Vargas *et al.* 1998), such environments would be ideal for accelerating the cleanup of cyclic nitramine energetic chemicals. To our knowledge, this is the first report that states the use of Fe(III)- and HA-reducing bacterium to accelerate bioremediation of cyclic nitramines in Fe(III)- and HA-rich environments.

Acknowledgements

We gratefully acknowledge the Office of Naval Research (Award N000140310269), USA, and the DoD/DoE/EPA, SERDP (project ER 1431), USA, for financial support. We also thank the Department of National Defense, Val Bélair, Canada, for their support. We sincerely acknowledge the analytical and technical support of L. Paquet, A. Corriveau and C. Beaulieu. Drs J.S. Zhao, D. Fournier and F. M. Rivera are acknowledged for helpful discussions. We thank the editor and two anonymous reviewers for their useful comments.

References

- Benz, M., Schink, B. and Brune, A. (1998) Humic acid reduction by *Propionibacterium freudenreichii* and other fermenting bacteria. *Appl Environ Microbiol* **64**, 4507–4512.
- Bhushan, B., Trott, S., Spain, J.C., Halasz, A., Paquet, L. and Hawari, J. (2003) Biotransformation of hexahydro-1,3,5-trinitro-1,3,5-triazine (RDX) by a rabbit liver cytochrome P450: insight into the mechanism of RDX biodegradation by *Rhodococcus* sp. DN22. *Appl Environ Microbiol* **69**, 1347–1351.
- Bhushan, B., Halasz, A., Thiboutot, S., Ampleman, G. and Hawari, J. (2004) Chemotaxis-mediated biodegradation of cyclic nitramine explosives RDX, HMX, and CL-20 by *Clostridium* sp. EDB2. *Biochem Biophys Res Commun* **316**, 516–521.
- Brockman, F.J., Downing, D.C. and Wright, G. F. (1949) Nitrolysis of hexamethylenetetramine. *Can J Res* **27B**, 469–474.
- Coates, J.D., Ellis, D.J., Blunt-Harris, E.L., Gaw, C.V., Roden, E.E. and Lovley, D.R. (1998) Recovery of humic-reducing bacteria from a diversity of environments. *Appl Environ Microbiol* **64**, 1504–1509.
- Curtis, G.P. and Reinhard, M. (1994) Reductive dehalogenation of hexachloroethane, carbon tetrachloride, and bromoform by anthrahydroquinone disulfonate and humic acid. *Environ Sci Technol* **28**, 2393–2401.
- Dobbin, P.S., Carter, J.P., Garcia-Salamanca, S.J.C., von Hobe, M., Powell, A.K. and Richardson, D.J. (1999) Dissimilatory Fe(III) reduction by *Clostridium beijerinckii* isolated from freshwater sediment using Fe(III) maltol enrichment. *FEMS Microbiol Lett* **176**, 131–138.
- Elsner, M., Schwarzenbach, R.P. and Haderlein, S.B. (2004) Reactivity of Fe(II)-bearing minerals toward reductive transformation of organic contaminants. *Environ Sci Technol* **38**, 799–807.
- Etnier, E.L. and Hartley, W.R. (1990) Comparison of water quality criterion and lifetime health advisory for hexahydro-1,3,5-trinitro-1,3,5-triazine (RDX). *Regul Toxicol Pharmacol* **11**, 118–122.
- Gong, P., Hawari, J., Thiboutot, S., Ampleman, G. and Sunahara, G.I. (2002) Toxicity of octahydro-1,3,5,7-tetranitro-1,3,5,7-tetrazocine (HMX) to soil microbes. *Bull Environ Contam Toxicol* **69**, 97–103.
- Gregory, K.B., Larese-Casanova, P., Parkin, G.F. and Scherer, M.M. (2004) Abiotic transformation of hexahydro-1,3,5-trinitro-1,3,5-triazine by Fe(II) bound to magnetite. *Environ Sci Technol* **38**, 1408–1414.
- Groom, C.A., Halasz, A., Paquet, L., D'Cruz, P. and Hawari, J. (2003) Cyclodextrin-assisted capillary electrophoresis for determination of the cyclic nitramine explosives RDX, HMX and CL-20: comparison with high-performance liquid chromatography. *J Chromatogr A* **999**, 17–22.
- Halasz, A., Spain, J.C., Paquet, L., Beaulieu, C. and Hawari, J. (2002) Insights into the formation and degradation of methylenedinitramine during the incubation of RDX with anaerobic sludge. *Environ Sci Technol* **36**, 633–638.
- Hawari, J., Halasz, A., Beaudet, S., Paquet, L., Ampleman, G. and Thiboutot, S. (2001) Biotransformation routes of octahydro-1,3,5,7-tetranitro-1,3,5,7-tetrazocine by municipal anaerobic sludge. *Environ Sci Technol* **35**, 70–75.
- Hobbie, J.E., Daley, R.J. and Jasper, S. (1977) Use of nucleopore filters for counting bacteria by fluorescence microscopy. *Appl Environ Microbiol* **33**, 1225–1228.
- Hoek, B. (2004) Military explosives and health: organic energetic compound syndrome? *Med Confl Surviv* **20**, 326–333.
- Kucukardali, Y., Acar, H.V., Ozkan, S., Nalbant, S., Yazgan, Y., Atasoy, E.M., Keskin, O., Naz, A. *et al.* (2003) Accidental oral poisoning caused by RDX (cyclonite): a report of 5 cases. *J Intensive Care Med* **18**, 42–46.
- Levine, B.S., Furedi, E.M., Gordon, D.E., Barkley, J.J. and Lish, P.M. (1990) Toxic interactions of the munitions compounds TNT and RDX in F344 rats. *Fundam Appl Toxicol* **15**, 373–380.
- Lonergan, D.J., Jenter, H.L., Coates, J.D., Phillips, E.J., Schmidt, T.M. and Lovley, D.R. (1996) Phylogenetic analysis of dissimilatory Fe(III)-reducing bacteria. *J Bacteriol* **178**, 2402–2408.

- Lovley, D.R., Greening, R.C. and Ferry, J.G. (1984) Rapidly growing rumen methanogenic organism that synthesizes coenzyme M and has a high affinity for formate. *Appl Environ Microbiol* **48**, 81–87.
- Lovley, D.R., Coates, J.D., Blunt-Harris, E.L., Phillips, E.J.P. and Woodward, J.C. (1996) Humic substances as electron acceptors for microbial respiration. *Nature* **382**, 445–448.
- McLellan, W., Hartley, W.R. and Brower, M. (1988) *Health advisory for octahydro-1,3,5,7-tetranitro-1,3,5,7-tetrazocine, Technical Report PB90-273533*. Washington, DC: Office of Drinking Water, U.S. Environmental Protection Agency.
- Oh, B.T., Just, C.L. and Alvarez, P.J. (2001) Hexahydro-1,3,5-trinitro-1,3,5-triazine mineralization by zero-valent iron and mixed anaerobic cultures. *Environ Sci Technol* **35**, 4341–4346.
- Park, H.S., Kim, B.H., Kim, H.S., Kim, H.J., Kim, G.T., Kim, M., Chang, I.S., Park, Y.K. *et al.* (2001) A novel electrochemically active and Fe(III)-reducing bacterium phylogenetically related to *Clostridium butyricum* isolated from a microbial fuel cell. *Anaerobe* **7**, 297–306.
- Scherer, M.M., Richter, S., Valentine, R.L. and Alvarez, P.J. (2000) Chemistry and microbiology of permeable reactive barriers for *in situ* groundwater clean up. *Crit Rev Microbiol* **26**, 221–264.
- Schwarzenbach, R.P., Stierli, R., Lanz, K. and Zeyer, J. (1990) Quinone and iron porphyrin mediated reduction of nitroaromatic compounds in homogeneous aqueous solution. *Environ Sci Technol* **24**, 1566–1574.
- Stookey, L. (1970) Ferrozine-a new spectrophotometric reagent for iron. *Anal Chem* **42**, 779–781.
- Talley, J.W. and Sleeper, P.M. (1997) Roadblocks to the implementation of biotreatment strategies. *Ann NY Acad Sci* **829**, 16–29.
- Talmage, S.S., Opresko, D.M., Maxwell, C.J., Welsh, C.J.E., Cretella, F.M., Reno, P.H. and Daniel, F.B. (1999) Nitroaromatic munition compounds: environment effects and screening values. *Rev Environ Contam Toxicol* **161**, 1–156.
- Thiboutot, S., Ampleman, G., Gagnon, A., Marois, A., Jenkins, T.F., Walsh, M.E., Thorne, P.G. and Ranney, T.A. (1998) Characterization of anti-tank firing ranges at CFB Valcartier. *Report DREV-R-9809*. WATC Wainwright and CFAD Dundurn, Quebec.
- Vargas, M., Kashefi, K., Blunt-Harris, E.L. and Lovley, D.R. (1998) Microbiological evidence for Fe(III) reduction on early Earth. *Nature* **395**, 65–67.
- Wildman, M.J. and Alvarez, P.J. (2001) RDX degradation using an integrated Fe(0)-microbial treatment approach. *Water Sci Technol* **43**, 25–33.
- Yinon, J. (1990) *Toxicity and Metabolism of Explosives*. pp. 145–170. Boca Raton, FL: CRC Press.
- Zhang, C. and Hughes, J.B. (2003) Biodegradation pathways of hexahydro-1,3,5-trinitro-1,3,5-triazine (RDX) by *Clostridium acetobutylicum* cell-free extract. *Chemosphere* **50**, 665–671.
- Zhao, J.S., Paquet, L., Halasz, A. and Hawari, J. (2003) Metabolism of hexahydro-1,3,5-trinitro-1,3,5-triazine through initial reduction to hexahydro-1-nitroso-3,5-dinitro-1,3,5-triazine followed by denitration in *Clostridium bifermentans* HAW-1. *Appl Microbiol Biotechnol* **63**, 187–193.
- Zhao, J.S., Greer, C.W., Thiboutot, S., Ampleman, G. and Hawari, J. (2004a) Biodegradation of the nitramine explosives hexahydro-1,3,5-trinitro-1,3,5-triazine and octahydro-1,3,5,7-tetranitro-1,3,5,7-tetrazocine in cold marine sediment under anaerobic and oligotrophic conditions. *Can J Microbiol* **50**, 91–96.
- Zhao, J.S., Paquet, L., Halasz, A., Manno, D. and Hawari, J. (2004b) Metabolism of octahydro-1,3,5,7-tetranitro-1,3,5,7-tetrazocine by *Clostridium bifermentans* HAW-1 and several other H₂-producing fermentative anaerobic bacteria. *FEMS Microbiol Lett* **237**, 65–72.

Degradation of CL-20 by white-rot fungi

Diane Fournier, Fanny Monteil-Rivera, Annamaria Halasz,
Manish Bhatt, Jalal Hawari *

Biotechnology Research Institute, National Research Council of Canada, Environmental Chemistry Group,
6100 Royalmount Avenue, Montreal, Que., Canada H4P 2R2

Received 22 March 2005; received in revised form 16 June 2005; accepted 23 June 2005

Available online 19 August 2005

Abstract

In previous studies, we found that the emerging energetic chemical, CL-20 ($C_6H_6N_{12}O_{12}$, 2,4,6,8,10,12-hexanitro-2,4,6,8,10,12-hexaazaisowurtzitane), can be degraded following its initial denitration using both aerobic and anaerobic bacteria. The C and N mass balances were not determined due to the absence of labeled starting compounds. The present study describes the degradation of the emerging contaminant by *Phanerochaete chrysosporium* using ring-labeled [^{15}N]-CL-20 and [^{14}C]-CL-20. Ligninolytic cultures degraded CL-20 with the release of nitrous oxide (N_2O) in amounts corresponding to 45% of the nitrogen content of CL-20. When ring-labeled [^{15}N]-CL-20 was used, both $^{14}N^{14}NO$ and $^{15}N^{14}NO$ were observed, likely produced from $-NO_2$ and $N-NO_2$, respectively. The incubation of uniformly labeled [^{14}C]-CL-20 with fungi led to the production of $^{14}CO_2$ (>80%). Another ligninolytic fungus, *Irpex lacteus*, was also able to degrade CL-20, but as for *P. chrysosporium*, no early intermediates were observed. When CL-20 was incubated with manganese peroxidase (MnP), we detected an intermediate with a $[M-H]^-$ mass ion at 345 Da (or 351 and 349 Da when using ring-labeled and nitro-labeled [^{15}N]-CL-20, respectively) matching a molecular formula of $C_6H_6N_{10}O_8$. The intermediate was thus tentatively identified as a doubly denitrated CL-20 product. The concomitant release of nitrite ions (NO_2^-) with CL-20 degradation by MnP also supported the occurrence of an initial denitration prior to cleavage and decomposition.

© 2005 Elsevier Ltd. All rights reserved.

Keywords: CL-20; Degradation; Nitramine; *Phanerochaete chrysosporium*; Fungi

1. Introduction

The environmental fate and impact of the emerging energetic chemical CL-20, $C_6H_6N_{12}O_{12}$ (compound 1, Fig. 1) are not well defined. Preliminary toxicological studies indicated that CL-20 is not acutely toxic to the

marine bacteria *Vibrio fischeri*, freshwater green algae *Selenastrum capricornutum*, terrestrial higher plants (perennial ryegrass and alfalfa), and indigenous soil microorganisms (Gong et al., 2004). However, the polycyclic nitramine has significant lethal and sublethal effects on the earthworm *Eisenia andrei* (Robidoux et al., 2004). At lower doses, the toxicity of the nitramine was more important in a sandy soil than in an organic rich soil (Robidoux et al., 2004), a phenomenon explained by the favored sorption of CL-20 to soil organic fraction (Balakrishnan et al., 2004a).

* Corresponding author. Tel.: +1 514 496 6267; fax: +1 514 496 6265.

E-mail address: jalal.hawari@cnrc-nrc.gc.ca (J. Hawari).

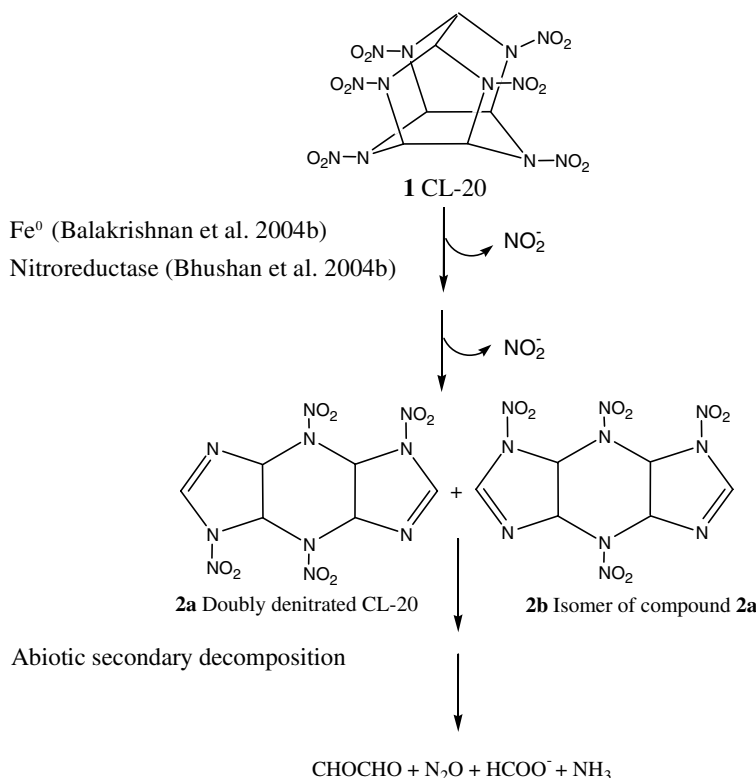


Fig. 1. Structure of CL-20 (**1**) and CL-20 denitration products (**2a** and **2b**) observed during treatment with Fe^0 (Balakrishnan et al., 2004b) or with nitroreductase (Bhushan et al., 2004b).

While two aerobic RDX-degrading strains (*Rhodococcus* sp. DN22 and *Rhodococcus rhodochrous* 11Y) failed to degrade CL-20 (unpublished data), several aerobic and anaerobic microorganisms degraded the energetic compound (Trott et al., 2003; Bhushan et al., 2003, 2004a; Karakaya et al., 2004). CL-20 was found to transform via an N-denitration mechanism, as confirmed by the detection of nitrite ions (NO_2^-) and putative doubly denitrated CL-20 intermediates (compound **2a** and its isomer **2b**, Fig. 1) during treatment with nitroreductase (Bhushan et al., 2004b). The proposed denitrated intermediates have also been observed when reacting CL-20 with zero valent iron (Balakrishnan et al., 2004b). In the biotic like in the abiotic processes, compound **2a** and its isomer **2b** degraded into the end-products nitrous oxide (N_2O), formate (HCOO^-), ammonia (NH_3), and glyoxal (CHOCHO) (Fig. 1).

Despite the important progresses that have been achieved in the understanding of CL-20 degradation pathways, the fate of carbons from the emerging chemical is not thoroughly known. In the present study, we assessed the ability of the ligninolytic white-rot fungi, *Phanerochaete chrysosporium* and *Irpex lacteus*, to degrade CL-20. For the first time, the carbon mass balance was determined using the radiotracer ^{14}C -CL-20.

P. chrysosporium and *I. lacteus* are lignin degraders that synthesize nonspecific enzymes such as lignin peroxidase (LiP), manganese peroxidase (MnP), and other critical metabolic components such as oxidases, reductases, hydrogen peroxide, veratryl alcohol, oxalate, and quinones (Kersten et al., 1985; Stahl and Aust, 1995). Due to the complex nature of fungal metabolic chemistry, we used MnP to get insight into the degradation mechanism.

2. Material and methods

2.1. Chemicals

2,4,6,8,10,12-Hexanitro-2,4,6,8,10,12-hexaazaisowurtzitane (ϵ -CL-20), ring-labeled ^{15}N -CL-20, nitro-labeled ^{15}N -[CL-20], and uniformly labeled ^{14}C -CL-20 (chemical purity > 97%, specific activity of 0.75 mCi/g) were provided by A.T.K. Thiokol Propulsion (Brigham City, UT). $[1,2-^{14}\text{C}]$ -glyoxal (chemical purity > 99%, specific activity of 56 mCi/mmol) was from American Radio-labeled Chemicals, Inc. (St. Louis, MO). All other chemicals used in this study were of reagent grade.

2.2. Bio-transformation of CL-20 in liquid culture by *P. chrysosporium* and *I. lacteus*

P. chrysosporium strain ATCC 24725 and *I. lacteus* (obtained from Dr. V. Sasek, Institute of Microbiology, Prague, Czech Republic) were maintained on YPD plates, and were cultivated in a modified Kirk's nitrogen-limited medium (pH 4.5) as previously described (Fournier et al., 2004). Kirk's modified medium contains a carbon source (10 g/l glucose) and a limited source of nitrogen (1.2 mM ammonium tartrate), which are enough to promote the initial development of fungal mycelia and induce the production of ligninolytic enzymes (the medium is referred below as the N-limited mineral medium). Bio-transformation experiments were performed in the N-limited mineral medium (10 ml in 125 ml serum bottle) inoculated with 2×10^6 fungal spores. CL-20 (stock solution of approximately 15000 mg l^{-1} , prepared in acetone) was added to the spore suspension. Heat-killed fungal spores were incubated with CL-20 as controls for possible abiotic degradation. The bottles were sealed with Teflon coated serum septa and aluminum caps. The cultures were incubated statically in the dark at $37 \pm 2^\circ\text{C}$ (for *P. chrysosporium*) and $20 \pm 2^\circ\text{C}$ for *I. lacteus*, and were aerated every 3–4 days.

2.3. Mineralization of CL-20 and glyoxal with fungi

Mineralization experiments were performed by adding the radiotracer [^{14}C]-CL-20 (0.048 μCi , 162.6 nmol) or [^{14}C]-glyoxal (0.288 μCi , 3100 nmol) to *P. chrysosporium* spore suspensions. Formation of $^{14}\text{CO}_2$ was monitored as described previously (Fournier et al., 2004). Once again, the microcosms were aerated every 3–4 days.

2.4. Bio-transformation of CL-20 with MnP

MnP from a high potential fermentation strain of *Nemalotoma frowardii* was purchased from Jena Bioscience GmbH (Jena, Germany). The MnP reactions were performed in 6 ml vials in a total of 2 ml: sodium malonate (50 mM, pH 4.5), MnCl_2 (1 mM), H_2O_2 (0.33 mM), MnP (3 U) and CL-20 (38 mg l^{-1} using the above-described stock solution). CL-20 was present at a concentration superior to its aqueous solubility (Monteil-Rivera et al., 2004) in an attempt to generate sufficient amounts of reaction intermediates to allow detection. The vials were sealed with Teflon coated serum septa and aluminum caps. Reactions were carried out at $37 \pm 2^\circ\text{C}$ under agitation at 150 rpm.

2.5. Analytical techniques

After sampling the headspace for N_2O analysis (Fournier et al., 2004), the liquid phase of fungal cul-

tures or enzymatic reaction were sacrificed by adding one equivalent volume of acidified acetonitrile (0.25 ml of concentrated H_2SO_4 per liter of acetonitrile) to one volume of reaction mixture. Whole fungal cultures were submitted to sonication at 20°C for 18 h. In all cases, the resulting solution was then filtered through a $0.45 \mu\text{m}$ membrane (Millipore PTFE), the first 3 ml being discarded. CL-20 was analyzed by HPLC connected to a photodiode array (PDA), as described previously (Monteil-Rivera et al., 2004). Analyses of nitrate (NO_3^-), formate (HCOO^-), glycolate ($\text{HOCH}_2\text{COO}^-$), ammonia (NH_3), and glyoxal (HCOHCO) were also performed as previously described (Balakrishnan et al., 2004b). Intermediate products of CL-20 were analyzed using a Bruker Esquire 3000 plus ion trap spectrometer (Bruker-Daltonics, Boston, MA, USA) equipped with an Agilent 1100 HPLC system (Agilent, Waldbronn, Germany). The atmospheric electrospray source was operated in negative mode using nitrogen as a drying gas (15.0 psi), at a flow rate of 5 l/min and a temperature of 150°C . The capillary voltage was set at 4000 V with an end plate offset of -500 V . The scanning mass to charge range was 40–550 m/z . Details on the LC-MS set up can be found in Hawari et al. (2004). Nitrite (NO_2^-) was analyzed using the photometric US EPA Method 354.1 (US EPA, 1979).

3. Results and discussion

3.1. Bio-transformation of CL-20 by fungi

Degradation of CL-20 added to spores suspension of *P. chrysosporium* was monitored for up to 8 days. Fig. 2A shows the disappearance of CL-20 in the presence of growing or heat-killed fungal cultures. In heat-killed controls the initial amount of CL-20 (85 nmol) remained stable during all the incubation period. The degradation with active *P. chrysosporium* started after a lag phase of 2 days (Fig. 2A). After 5 days of incubation, CL-20 was totally depleted from the culture medium. The formation of N_2O started after 3 days of incubation (Fig. 2A). On the seventh day, the ratio of N_2O over CL-20 degraded indicated that 45% of the nitrogen content of CL-20 was transformed into nitrous oxide. When ring-labeled [^{15}N]-CL-20 was used in degradation experiments, the GC/MS analysis of N_2O showed the presence of both $^{14}\text{N}^{14}\text{NO}$ and $^{15}\text{N}^{14}\text{NO}$, likely produced from peripheral nitro ($-\text{NO}_2$) and the nitramine ($\text{N}-\text{NO}_2$) groups, respectively. No nitrite ions (NO_2^-) were detected, but when *P. chrysosporium* was cultivated with NaNO_2 as the sole nitrogen source, the growth of the mycelia was observed with the concomitant production of N_2O . It should be noted that no growth and no N_2O production were observed in the absence of either CL-20 or NaNO_2 . No CL-20 intermediary metabolites were

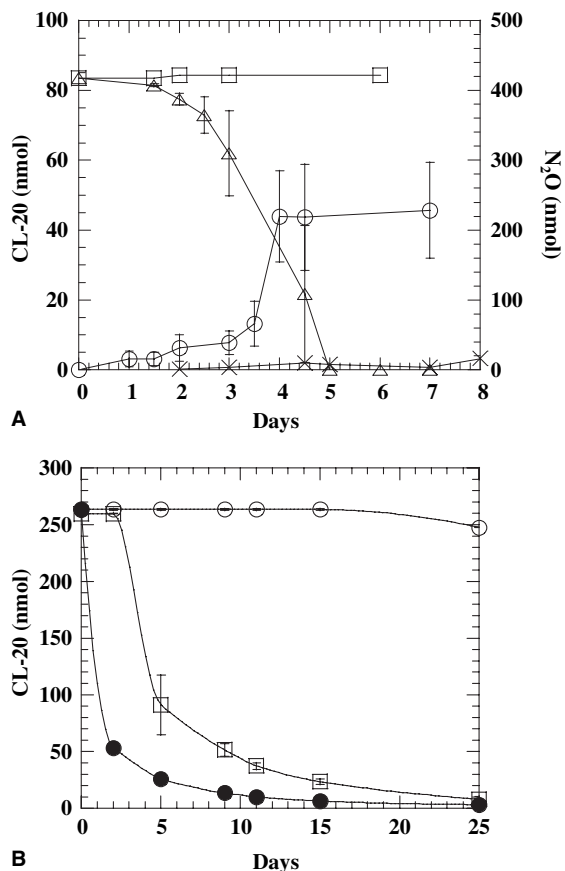


Fig. 2. (A) Degradation of CL-20 (83 nmol) (Δ) and N₂O production (○) by growing cultures of *Phanerochaete chrysosporium*. CL-20 (□) and N₂O (×) amounts observed with heat-killed spores of *P. chrysosporium*. Bars indicate standard deviation from duplicate experiments. (B) Degradation of CL-20 (260 nmol) by 7 days-old *P. chrysosporium* (●), *I. lacteus* (□), or noninoculated cultures (○).

detected, probably because they were readily transformed in the culture supernatant, via the action of ligninolytic enzymes such as LiP or MnP.

With the hope to generate detectable amounts of intermediary metabolites, *P. chrysosporium* and another white-rot fungus *I. lacteus* were pre-grown for 7 days prior to the addition of higher amounts of CL-20 than used above (260 nmol). Cultures were sampled twice a day for LC/MS analysis. As depicted in Fig. 2B, degradation of CL-20 by *P. chrysosporium* started without any lag phase. After 25 days of incubation at 37 °C, CL-20 was totally depleted from the culture medium, but the analysis of the liquid phase on LC/MS did not show any intermediates. When incubated at 20 °C, *I. lacteus* also degraded CL-20 but after a lag phase of 3–4 days. This lag phase can be due to the slower growth and or slower ligninolytic enzymes production by *I. lac-*

teus compared to *P. chrysosporium*. As observed with *P. chrysosporium*, *I. lacteus* was able to remove almost all the nitramine after 25 days of incubation (Fig. 2B), but once again, no CL-20 intermediates were detected.

3.2. CL-20 carbon mass balance

Mineralization experiments were conducted by adding uniformly labeled [¹⁴C]-CL-20 to *P. chrysosporium* cultures. As depicted in Fig. 3, the production of CO₂ began after 5 days of incubation, reaching 80% of CO₂ after 78 days, showing that almost 5C of the total 6C atoms of CL-20 mineralized into CO₂.

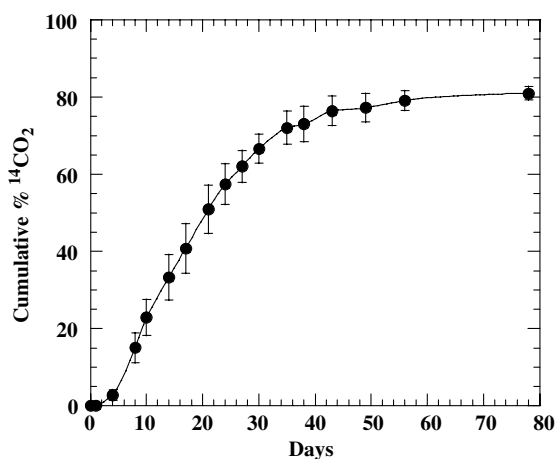


Fig. 3. Liberation of ¹⁴CO₂ from [¹⁴C]-CL-20 (0.048 μCi, 162.6 nmol) added to spores suspensions of *Phanerochaete chrysosporium* prepared in N-limited medium. Bars indicate standard deviation from triplicate experiments.

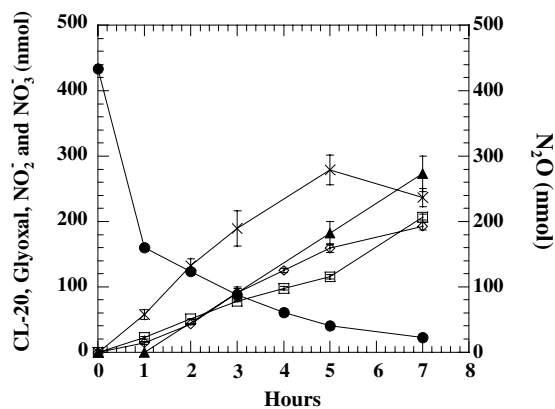


Fig. 4. Bio-transformation of CL-20 (●) with the MnP from *Nematotoma frowardii* and formation of the metabolites NO₂⁻ (×), NO₃⁻ (▲), N₂O (◇) and glyoxal (□). Bars indicate standard deviation from triplicate experiments.

The observation of N_2O ($^{14}\text{N}^{14}\text{NO}$ from nitro group) and CO_2 indicate that *P. chrysosporium* catalyzes ring cleavage of CL-20 via denitration, nitrite ions which were not detected, being likely assimilated by fungi cultivated under nitrogen-limited conditions. Because no

early intermediates were observed during the incubation of CL-20 with the whole fungi, despite the high CL-20 starting concentrations, the widely studied ligninolytic enzyme MnP was used with the hope to detect such metabolites.

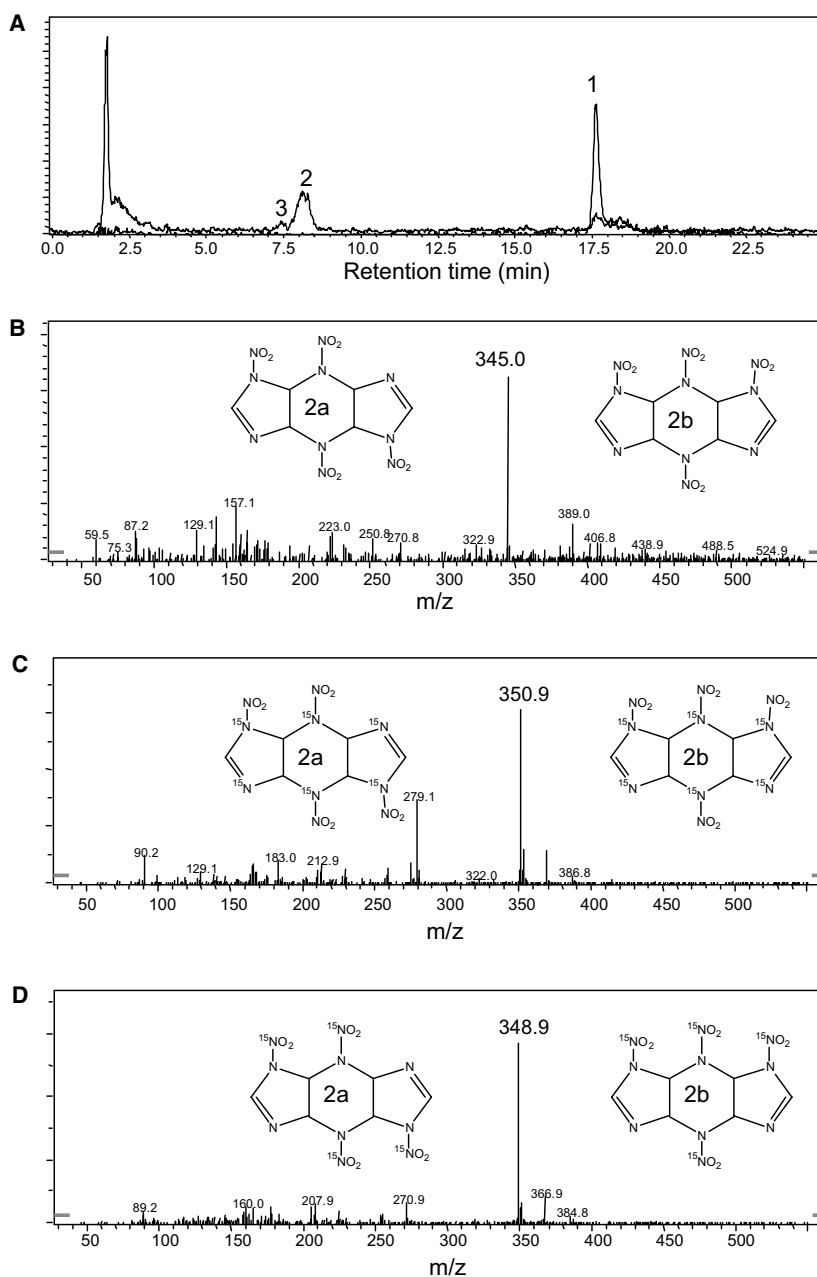


Fig. 5. (A) LC-MS extracted ion chromatograms (m/z 500 and 345) of CL-20 (1) and its initial intermediates (2 and 3) observed after 2 h of incubation of CL-20 with MnP. (B) LC-MS (ES-) mass spectrum and proposed structural formula of the two doubly denitrated isomers from CL-20 (**2a** and **2b**). (C) LC-MS (ES-) mass spectrum and proposed structural formula of the two doubly denitrated isomers from uniformly ring-labeled ^{15}N -[CL-20]. (D) LC-MS (ES-) mass spectrum and proposed structural formula of the two doubly denitrated isomers from nitro-labeled ^{15}N -[CL-20].

3.3. Transformation of CL-20 with MnP—insights into the degradation mechanism

In previous studies, MnP was found to degrade the nitramine RDX (Stahl et al., 2001), its ring cleavage product 4-nitro-2,4-diazabutanal (NDAB) (Fournier et al., 2004), and the TNT metabolite aminodinitrotoluene (Stahl and Aust, 1995; Fritsche et al., 2000). MnP oxidizes Mn^{2+} ions into highly reactive Mn^{3+} ions, which are stabilized by a fungal-produced chelating agent such as oxalate. Chelated Mn^{3+} ions oxidize a broad variety of chemicals via one-electron transfer reactions. The ligninolytic enzyme MnP is produced by almost all white-rot fungi, and all MnPs described so far appear to follow the same classical catalytic cycle as detailed by Hofrichter (2002). Therefore it was assumed that MnP from different basidiomycetes would attack CL-20 in a similar way. In the present study, we used to bio-transform CL-20, a commercial MnP purified from *N. frowardii*, another ligninolytic white-rot fungus.

MnP catalyzed the degradation of CL-20 (Fig. 4) and rendered possible the detection of two LC/MS peaks, each showing a $[M-H]^-$ mass ion at 345 Da (Fig. 5A, peaks 2 and 3), after 1 h of incubation. These peaks showed similar chromatographic and mass data to the ones detected during the degradation of CL-20 using Fe^0 (Balakrishnan et al., 2004b) or nitroreductase (Bhushan et al., 2004b). Each of the two LC/MS peaks matched a molecular formula of $C_6H_6N_{10}O_8$ and was tentatively identified as one of the two isomers of the doubly denitrated CL-20 molecule (Fig. 5B, 2a and 2b). The use of ring-labeled $[^{15}N]$ -CL-20 and nitro-labeled $[^{15}N]$ -CL-20 respectively revealed the presence of LC/MS peaks showing a $[M-H]^-$ mass ion at 351 Da (an increase of 6 Da representing the 6 ^{15}N atoms, Fig. 5C) and a $[M-H]^-$ mass ion at 349 Da (an increase of 4 Da representing 4 $^{15}NO_2$ groups, Fig. 5D) in agreement with the formation of the doubly denitrated CL-20 intermediate and its isomer. Significant amounts of nitrite (NO_2^-) were formed concomitantly with CL-20 removal (Fig. 4), supporting the occurrence of an initial denitration process as observed with Fe^0 (Balakrishnan et al., 2004b). The amount of NO_2^- (280 nmol) was maximal after 5 h of incubation. Considering the oxidative conditions produced by the MnP system, NO_2^- ions were probably oxidized into NO_3^- ions, as demonstrated by the appearance of the latter after 1 h of incubation. When whole fungi were incubated with CL-20, the nitrite ions released were likely assimilated, allowing the growth of the fungal mycelia. Nitrous oxide (N_2O) was also produced during the degradation of CL-20 with MnP (Fig. 4). The amounts of N_2O increased linearly to a maximum of 200 nmol, giving a ratio N_2O over CL-20 of 8%. The ratio obtained with growing fungi was much higher (45%) and better

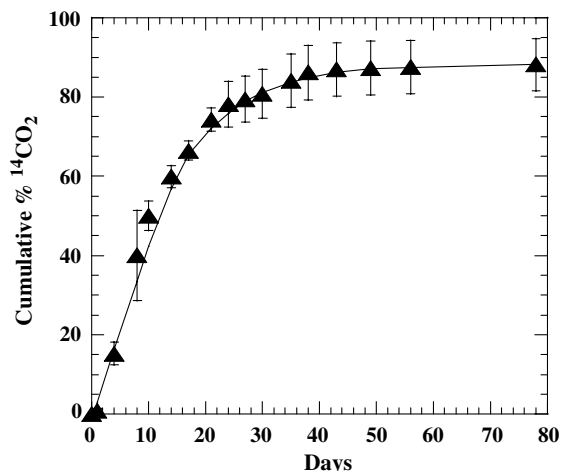


Fig. 6. Liberation of $^{14}CO_2$ from $[^{14}C]$ -glyoxal added to spores of *Phanerochaete chrysosporium* in N-limited medium. Bars indicate standard deviation from triplicate experiments.

reflects the complex nature of *P. chrysosporium* metabolism. Several assays aiming at the detection of ammonia (NH_3) were not successful because of the presence of important analytical interferences, even after an extensive washing of the commercial MnP to remove excess salts.

No formate ($HCOO^-$) was produced but a significant amount of glyoxal was detected (Fig. 4). One mole of removed CL-20 ($C_6H_6N_{12}O_{12}$) gave 0.5 mol of glyoxal ($C_2H_2O_2$). The formation of glyoxal as a CL-20 product is environmentally significant since the di-aldehyde is known to be toxic (Shangari et al., 2003). The degradability of glyoxal was then investigated, using either pure MnP or *P. chrysosporium*. When incubated with MnP, the di-aldehyde remained intact after more than 18 h of incubation (result not shown). However, *P. chrysosporium* was able to mineralize 88% of the radio-labeled glyoxal added (liberated as $^{14}CO_2$) (Fig. 6), thus indicating that the compound would not persist in the presence of white-rot fungi. The mineralization of glyoxal may be based on the participation of the metalloenzyme glyoxal oxidase that functions as an extracellular factory for production of hydrogen peroxide (Whittaker et al., 1996).

4. Conclusion

This study demonstrates that the white-rot fungi *P. chrysosporium* and *I. lacteus* can efficiently decompose CL-20 under aerobic conditions. For the first time, the use of uniformly labeled $[^{14}C]$ -CL-20 indicates that *P. chrysosporium* could effectively (>80%) mineralize the nitramine, as determined by the release of $^{14}CO_2$. The use of pure MnP provided several evidences supporting

the occurrence of an initial denitration step on CL-20 prior to ring cleavage and decomposition. The detection of glyoxal as a CL-20 metabolite and its mineralization by *P. chrysosporium* indicate that the di-aldehyde is a CL-20 product but that it would not persist in the presence of white-rot fungi. This study demonstrates that CL-20 would not be persistent in environments that favor the growth of ligninolytic fungi.

Acknowledgements

The authors wish to thank Alain Corriveau, Zorana Radovich-Hrapovich, Dominic Manno, and Chantale Beaulieu for their technical assistance. We also thank Thiokol Propulsion (Brigham City, UT) for providing CL-20, ring-labeled and nitro-labeled [^{15}N]-CL-20, and uniformly-labeled [^{14}C]-CL-20. We are grateful to the U.S. Strategic Environmental Research and Development Program (SERDP CP-1256) and to Defense Research and Development Canada (DRDC), Valcartier, Canada for financial support.

References

- Balakrishnan, V.K., Monteil-Rivera, F., Gautier, M., Hawari, J., 2004a. Sorption and stability of the polycyclic nitramine explosive CL-20 in soil. *J. Environ. Qual.* 33, 1362–1368.
- Balakrishnan, V.K., Monteil-Rivera, F., Halasz, A., Corbeanu, A., Hawari, J., 2004b. Decomposition of the polycyclic nitramine explosive, CL-20, by Fe^0 . *Environ. Sci. Technol.* 38, 6861–6866.
- Bhushan, B., Paquet, L., Spain, J.C., Hawari, J., 2003. Biotransformation of 2,4,6,8,10,12-hexanitro-2,4,6,8,10,12-hexaazaisowurtzitane (CL-20) by denitrifying *Pseudomonas* sp. strain FA1. *Appl. Environ. Microbiol.* 69, 5216–5221.
- Bhushan, B., Halasz, A., Thiboutot, S., Ampleman, G., Hawari, J., 2004a. Chemotaxis-mediated biodegradation of cyclic nitramine explosives RDX HMX and CL-20 by *Clostridium* sp. EDB2. *Biochem. Biophys. Res. Co.* 316, 816–821.
- Bhushan, B., Halasz, A., Hawari, J., 2004b. Nitroreductase catalyzed biotransformation of CL-20. *Biochem. Biophys. Res. Co.* 322, 271–276.
- Fournier, D., Halasz, A., Spain, J., Spanggord, R.J., Bottaro, J.C., Hawari, J., 2004. Biodegradation of the hexahydro-1,3,5-trinitro-1,3,5-triazine ring cleavage product 4-nitro-2,4-diazabutanol (NDAB) by *Phanerochaete chrysosporium*. *Appl. Environ. Microbiol.* 70, 1123–1128.
- Fritzsche, W., Scheibner, K., Herre, A., Hofrichter, M., 2000. Fungal degradation of explosives: TNT and related nitroaromatic compounds, book chapter. In: Spain, J.C., Hughes, J.B., Knackmuss, H.-J. (Eds.), *Biodegradation of Nitroaromatic Compounds and Explosives*. CRC Press, Boca Raton, FL, pp. 213–237.
- Gong, P., Sunahara, G.I., Rocheleau, S., Dodard, S.G., Robidoux, P.Y., Hawari, J., 2004. Preliminary ecotoxicological characterization of a new energetic substance, CL-20. *Chemosphere* 56, 653–658.
- Hawari, J., Deschamps, S., Beaulieu, C., Paquet, L., Halasz, A., 2004. Photodegradation of CL-20: insights into the mechanisms of initial reactions and environmental fate. *Water Res.* 38, 4044–4064.
- Hofrichter, M., 2002. Review: lignin conversion by manganese peroxidase (MnP). *Enzyme Microb. Tech.* 30, 454–466.
- Karakaya, P., Sidhoum, M., Christodoulatos, C., 2004. Biokinetic study for degradation of CL-20 with *Phanerochaete chrysosporium* (ATCC-24725). In: *Proceedings of the West Coast Conference on Soils, Sediments and Water*, March 15–18, San Diego, CA.
- Kersten, P.J., Tien, M., Kalyanaraman, B., Kirk, T.K., 1985. The ligninase of *Phanerochaete chrysosporium* generates cation radicals from methoxybenzenes. *J. Biol. Chem.* 260, 2609–2612.
- Monteil-Rivera, F., Paquet, L., Deschamps, S., Balakrishnan, V.K., Beaulieu, C., Hawari, J., 2004. Physico-chemical measurements of CL-20 for environmental applications. Comparison with RDX and HMX. *J. Chromatogr. A* 1025, 125–132.
- Robidoux, P.Y., Sunahara, G.I., Savard, K., Berthelot, Y., Leduc, F., Dodard, S., Martel, M., Gong, P., Hawari, J., 2004. Acute and chronic toxicity of the new explosive CL-20 to the earthworm (*Eisenia andrei*) exposed to amended natural soils. *Environ. Toxicol. Chem.* 23, 1026–1034.
- Shangari, N., Bruce, W.R., Poon, R., O'Brien, P.J., 2003. Toxicity of glyoxals—role of oxidative stress, metabolic detoxification and thiamine deficiency. *Biochem. Soc. Trans.* 31, 1390–1393.
- Stahl, J.D., Aust, S.D., 1995. Biodegradation of 2,4,6-trinitrotoluene by the white rot fungus *Phanerochaete chrysosporium*. In: Spain, J.C. (Ed.), *Biodegradation of Nitroaromatic Compounds*. Plenum Press, New York, pp. 117–133.
- Stahl, J.D., Van Aken, B., Cameron, M.D., Aust, S.D., 2001. Hexahydro-1,3,5-trinitro-1,3,5-triazine (RDX) biodegradation in liquid and solid-state matrices by *Phanerochaete chrysosporium*. *Bioremed. J.* 5, 13–25.
- Trott, S., Nishino, S.F., Hawari, J., Spain, J.C., 2003. Biodegradation of the nitramine explosive, CL-20. *Appl. Environ. Microbiol.* 69, 1871–1874.
- US Environmental Protection Agency, 1979. Method 354.1 for chemical analysis of water and wastes. Nitrogen-Nitrite. Environmental monitoring and support laboratory office of research and development, Cincinnati, OH.
- Whittaker, M.M., Kersten, P.J., Nakamura, N., Sanders-Loehr, J., Schweizer, E.S., Whittaker, J.W., 1996. Glyoxal oxidase from *Phanerochaete chrysosporium* is a new radical-copper oxidase. *J. Biol. Chem.* 271, 681–687.